Advanced Structured Materials

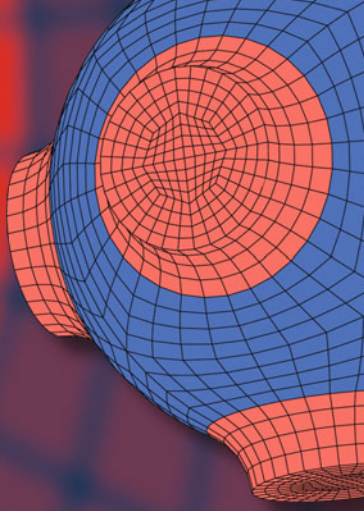

Ivan Argatov
Gennady Mishuris

Contact Mechanics of Articular Cartilage Layers

Asymptotic models

Springer

Advanced Structured Materials

Volume 50

More information about this series at http://www.springer.com/series/8611

Ivan Argatov · Gennady Mishuris

Contact Mechanics of Articular Cartilage Layers

Asymptotic Models

Springer

Ivan Argatov
Department of Mathematics
Aberystwyth University
Aberystwyth, Ceredigion
UK

Gennady Mishuris
Department of Mathematics
Aberystwyth University
Aberystwyth, Ceredigion
UK

ISSN 1869-8433 ISSN 1869-8441 (electronic)
Advanced Structured Materials
ISBN 978-3-319-20082-8 ISBN 978-3-319-20083-5 (eBook)
DOI 10.1007/978-3-319-20083-5

Library of Congress Control Number: 2015941864

Springer Cham Heidelberg New York Dordrecht London

Printed on acid-free paper

Springer International Publishing AG Switzerland is part of Springer Science+Business Media (www.springer.com)

To Alina and Wiktoria

Preface

This book is based on research results developed during our Marie Curie project devoted to asymptotic modeling of articular contact. Over the past two decades, articular contact mechanics has developed significantly in response to the increasing demand from orthopedics. While significant progress has been achieved in the mathematical modeling of the contact interaction between articular cartilage layers, we realized when writing the plan of the book that many of those results, obtained in the isotropic case, could be generalized for the case of transverse isotropy. The latter is of paramount importance in contact biomechanics, because many biological tissues like articular cartilage should be modeled as transversely isotropic material. Correspondingly, this plan required that many of the lacunae found in existing theory be filled in and allowed us to correct some misprints and omissions. Overall, our aim was to create a compendium of knowledge on asymptotic models for contact interactions of thin elastic/viscoelastic/biphasic layers.

Generally speaking, this book is about mathematical models for unilateral contact problems (with a priori unknown contact area) involving thin linearly deformable layers bonded to rigid bodies (called substrates) which transfer an externally applied compressive load. Particular attention is paid to analysis of the contact pressure distribution between the layers as well as to the relation between the contact force and the contact approach between the substrates.

From a methodological point of view, the book implements a unified asymptotic approach focused on deriving approximate analytical solutions, which are presented in the form of simplified mathematical models, called asymptotic models. Though we make use of rigorous mathematical methods, we tried to avoid excessive technical details of the asymptotic analysis in order to simplify the presentation of the book's material for a broader audience. With the same purpose we adopt unified notation across the different chapters.

The asymptotic technique we employ to model the deformation response of thin layers is generally known in the literature as a perturbation algorithm originally credited to Gol'denveizer [1]. The development of asymptotic methods in contact problems for thin elastic layers originates in the works of Aleksandrov [2], Koiter [3], Alblas and Kuipers [4], and others, although the majority of research papers

were devoted to the two-dimensional and axisymmetric cases. The application of asymptotic methods in articular contact problems was initiated by Ateshian et al. [5] and later developed by Wu et al. [6–8] and others.

In principle, analytical solutions are widely viewed as benchmark solutions for numerical methods. At the same time, asymptotic models have an importance of their own: they not only provide insights into the qualitative behavior of numerical solutions to the multiparametric problem under consideration, but also can expand our understanding of more realistic simulation models.

This book is organized into nine chapters. Each chapter is self-consistent, can be read independently, and is supplied with a comprehensive reference list. Chapters 1–4 present asymptotic analysis of the frictionless unilateral contact problems for thin elastic and viscoelastic layers in a form accessible to a general engineering audience. A specific character of deformation models for articular cartilage is discussed in Chap. 5, where a linear biphasic theory is outlined in detail. In Chap. 6, we generalize the asymptotic deformation model of Ateshian et al. [5] for the case of transverse isotropy and study the contact problems for thin bonded biphasic layers. Asymptotic modeling methodology for tibio-femoral contact is presented in Chap. 7, based on the asymptotic models constructed in the previous chapters. Some features reflecting the real structure of articular cartilage such as inhomogeneity are considered in Chap. 8, again from a general point of view and under a simplifying assumption of elastic deformation behavior. Finally, some sensitivity analysis issues for the asymptotic models of articular contact are addressed in Chap. 9.

This monograph is recommended for biomechanics researchers dealing with different aspects of articular contact as well as for Ph.D. students enrolled in contact mechanics and biomechanics courses.

Acknowledgments

The authors would like to thank the Department of Mathematics at Aberystwyth University for providing excellent academic facilities throughout the duration of the project project that eventually led to this book. The support of the European Commission via the grants FP7, PEOPLE, Marie Curie IE project “OA AM” No. 253055 (2010–2012) and FP7, PEOPLE, Marie Curie IRSES project “TAMER” No. 610547 (2014–2018) is gratefully acknowledged. We also thank Miss Nina Hämäläinen for preparation of the figures and Mr. Oliver Bain for proofreading the manuscript.

Aberystwyth
April 2015

Ivan Argatov
Gennady Mishuris

References

1. Gol'denveizer, A.L.: Derivation of an approximate theory of bending of a plate by the method of asymptotic integration of the equations of the theory of elasticity. J. Appl. Math. Mech. **26**, 1000–1025 (1962)
2. Aleksandrov, V.M.: On the approximate solution of a certain type of integral equation. J. Appl. Math. Mech. **26**, 1410–1424 (1962)
3. Koiter, W.T.: Solutions of some elasticity problems by asymptotic methods. In: Applications of the theory of functions to continuum mechanics (Muskhelishvili, N.I., ed.), pp. 15–31. Int. Symp., Tbilisi, USSR 1963. Moscow, Nauka (1965)
4. Alblas, J.B., Kuipers, M.: On the two-dimensional problem of a cylindrical stamp pressed into a thin elastic layer. Acta Mech. **9**, 292–311 (1970)
5. Ateshian, G.A., Lai, W.M., Zhu, W.B., Mow, V.C.: An asymptotic solution for the contact of two biphasic cartilage layers. J. Biomech. **27**, 1347–1360 (1994)
6. Wu, J.Z., Herzog, W., Ronsky, J.: Modeling axi-symmetrical joint contact with biphasic cartilage layers—an asymptotic solution. J. Biomech. **29**, 1263–1281 (1996)
7. Wu, J.Z., Herzog, W., Epstein, M.: An improved solution for the contact of two biphasic cartilage layers. J. Biomech. **30**, 371–375 (1997)
8. Wu, J. Z., Herzog, W., Epstein, M.: Evaluation of the finite element software ABAQUS for biomechanical modelling of biphasic tissues. J. Biomech. **31**, 165–169 (1997)

Contents

Chapter 1
Deformation of a Thin Bonded Transversely Isotropic Elastic Layer

Abstract In this chapter we study frictionless contact problems for a thin transversely isotropic elastic layer bonded to a rigid substrate and indented by a smooth absolutely rigid punch under the assumption that the layer thickness is relatively small compared to the characteristic size of the contact area. We apply a perturbation technique to obtain asymptotic solutions of different degrees of accuracy and formulate simple mathematical models (called asymptotic models) to describe the deformational behavior of a bonded compressible elastic layer in the thin-layer approximation. In particular, the effects of unilateral contact interaction (with a priori unknown contact area) and the tangential displacements at the contact interface (taken into account in formulating the contact condition) are considered. It is shown that the case of an incompressible layer requires special consideration.

1.1 Deformation Problem Formulation

The constitutive equations for a homogeneous transversely isotropic elastic material, based in the Cartesian coordinate system (x_1, x_2, x_3), where the Ox_1x_2 plane coincides with the plane of elastic symmetry, has the following form [10, 23, 36]:

$$\begin{aligned}
\varepsilon_{11} &= \frac{1}{E_1}(\sigma_{11} - \nu_{12}\sigma_{22}) - \frac{\nu_{31}}{E_3}\sigma_{33}, & \varepsilon_{23} &= \frac{1}{2G_{13}}\sigma_{23},\\
\varepsilon_{22} &= \frac{1}{E_1}(-\nu_{12}\sigma_{11} + \sigma_{22}) - \frac{\nu_{31}}{E_3}\sigma_{33}, & \varepsilon_{13} &= \frac{1}{2G_{13}}\sigma_{13},\\
\varepsilon_{33} &= -\frac{\nu_{31}}{E_3}(\sigma_{11} + \sigma_{22}) + \frac{1}{E_3}\sigma_{33}, & \varepsilon_{12} &= \frac{1}{2G_{12}}\sigma_{12}.
\end{aligned} \tag{1.1}$$

Here, E and E' are Young's moduli in the plane of transverse isotropy and in the direction normal to it, respectively, ν and ν' are Poisson's ratios characterizing the lateral strain response in the plane of transverse isotropy to a stress acting parallel or normal to it, respectively, G' is the shear elastic modulus in planes normal to the plane of transverse isotropy, and $G = E/[2(1+\nu)]$ is the in-plane shear modulus.

I. Argatov and G. Mishuris, *Contact Mechanics of Articular Cartilage Layers*,
Advanced Structured Materials 50, DOI 10.1007/978-3-319-20083-5_1

By inverting the equations of Hooke's law (1.1), the stress-strain relationships can be written in the matrix form as follows [13]:

$$\begin{pmatrix}\sigma_{11}\\ \sigma_{22}\\ \sigma_{33}\\ \sigma_{23}\\ \sigma_{13}\\ \sigma_{12}\end{pmatrix} = \begin{bmatrix} A_{11} & A_{12} & A_{13} & 0 & 0 & 0\\ A_{12} & A_{11} & A_{13} & 0 & 0 & 0\\ A_{13} & A_{13} & A_{33} & 0 & 0 & 0\\ 0 & 0 & 0 & 2A_{44} & 0 & 0\\ 0 & 0 & 0 & 0 & 2A_{44} & 0\\ 0 & 0 & 0 & 0 & 0 & 2A_{66}\end{bmatrix} \begin{pmatrix}\varepsilon_{11}\\ \varepsilon_{22}\\ \varepsilon_{33}\\ \varepsilon_{23}\\ \varepsilon_{13}\\ \varepsilon_{12}\end{pmatrix}. \tag{1.2}$$

For a transversely isotropic material, only five independent elastic constants A_{11}, A_{12}, A_{13}, A_{33}, and A_{44} are needed to describe its deformational behavior, since $2A_{66} = A_{11} - A_{12}$. These five elastic moduli are expressed in terms of the engineering elastic constants (E, E', ν, ν', and G') by the formulas

$$A_{11} = \frac{E\left(1 - \frac{E}{E'}\nu'^2\right)}{(1+\nu)\left(1 - \nu - \frac{2E}{E'}\nu'^2\right)}, \quad A_{12} = \frac{E\left(\nu + \frac{E}{E'}\nu'^2\right)}{(1+\nu)\left(1 - \nu - \frac{2E}{E'}\nu'^2\right)},$$

$$A_{13} = \frac{E\nu'}{1 - \nu - \frac{2E}{E'}\nu'^2}, \quad A_{33} = \frac{E'(1-\nu)}{1 - \nu - \frac{2E}{E'}\nu'^2}, \quad A_{44} = G'. \tag{1.3}$$

The equations of equilibrium for the elastic medium are

$$\frac{\partial \sigma_{i1}}{\partial x_1} + \frac{\partial \sigma_{i2}}{\partial x_2} + \frac{\partial \sigma_{i3}}{\partial x_3} = 0, \quad i = 1, 2, 3. \tag{1.4}$$

The components of strain are given in terms of the displacements as

$$\varepsilon_{ij} = \frac{1}{2}\left(\frac{\partial u_i}{\partial x_j} + \frac{\partial u_j}{\partial x_i}\right), \quad i, j = 1, 2, 3. \tag{1.5}$$

Equations (1.2), (1.4), and (1.5) constitute the governing equations of the classical (linear) theory of elasticity [23, 29].

Let the in-plane (tangential or horizontal) displacement vector and the vertical (normal or out of the plane of isotropy) displacement be denoted by $\mathbf{v}$ and w, respectively, such that the overall displacement vector is represented as $\mathbf{u} = (\mathbf{v}, w)$.

In what follows, we will denote the two-dimensional Cartesian coordinate system (x_1, x_2) in the plane of the layer by $\mathbf{y} = (y_1, y_2)$ (called the in-plane coordinates), while the normal coordinate will be denoted as z, such that $\mathbf{x} = (\mathbf{y}, z)$.

The substitution of the strain-displacement relations (1.5) into the equations of Hooke's law (1.2) gives the stress-displacement relationships

$$\begin{aligned}
\sigma_{11} &= A_{11}\frac{\partial v_1}{\partial y_1} + A_{12}\frac{\partial v_2}{\partial y_2} + A_{13}\frac{\partial w}{\partial z}, \quad \sigma_{23} = A_{44}\Big(\frac{\partial w}{\partial y_2} + \frac{\partial v_2}{\partial z}\Big),\\
\sigma_{22} &= A_{12}\frac{\partial v_1}{\partial y_1} + A_{11}\frac{\partial v_2}{\partial y_2} + A_{13}\frac{\partial w}{\partial z}, \quad \sigma_{13} = A_{44}\Big(\frac{\partial w}{\partial y_1} + \frac{\partial v_1}{\partial z}\Big),\\
\sigma_{33} &= A_{13}\frac{\partial v_1}{\partial y_1} + A_{13}\frac{\partial v_2}{\partial y_2} + A_{33}\frac{\partial w}{\partial z}, \quad \sigma_{12} = A_{66}\Big(\frac{\partial v_1}{\partial y_2} + \frac{\partial v_2}{\partial y_1}\Big).
\end{aligned} \tag{1.6}$$

Thus, by substituting the above equations into the equilibrium equations (1.4), one obtains the following Lamé equations:

$$\begin{aligned}
A_{66}\Delta_y\mathbf{v} + (A_{11} - A_{66})\nabla_y\nabla_y\cdot\mathbf{v} + A_{44}\frac{\partial^2\mathbf{v}}{\partial z^2} + (A_{13} + A_{44})\frac{\partial}{\partial}\nabla_y w = \mathbf{0},\\
A_{44}\Delta_y w + A_{33}\frac{\partial^2 w}{\partial z^2} + (A_{13} + A_{44})\frac{\partial}{\partial z}\nabla_y\cdot\mathbf{v} = 0.
\end{aligned} \tag{1.7}$$

Here, $\nabla_y = (\partial/\partial y_1, \partial/\partial y_2)$ and $\Delta_y = \nabla_y\cdot\nabla_y$ are the in-plane Hamilton and Laplace operators, respectively, while the scalar product is denoted by a dot.

Now, let us consider a thin elastic layer of uniform thickness, h, ideally bondedto a rigid substrate (see Fig. 1.1). At the bottom surface of the layer, $z = h$, the following boundary conditions hold:

$$\mathbf{v}\big|_{z=h} = \mathbf{0}, \quad w\big|_{z=h} = 0. \tag{1.8}$$

We assume that the layer is loaded by a normal load, p, with no tangential tractions (see Fig. 1.1), so that the corresponding boundary conditions on the upper surface of the layer are

$$\sigma_{13}\big|_{z=0} = \sigma_{23}\big|_{z=0} = 0, \quad \sigma_{33}\big|_{z=0} = -p. \tag{1.9}$$

In light of the stress-displacement relations (1.6), Eq. (1.9) can be rewritten as

$$\frac{\partial w}{\partial y_1} + \frac{\partial v_1}{\partial z}\bigg|_{z=0} = 0, \quad \frac{\partial w}{\partial y_2} + \frac{\partial v_2}{\partial z}\bigg|_{z=0} = 0, \tag{1.10}$$

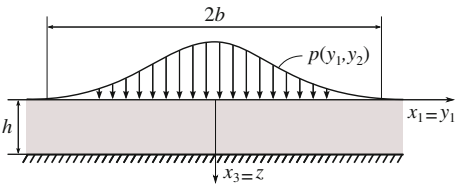

Fig. 1.1 An elastic layer of uniform thickness bonded to a rigid substrate and loaded by a normal load. In contact problems, the load function $p(\mathbf{y})$ has a finite support (with a characteristic length b)

$$A_{13}\frac{\partial v_1}{\partial y_1} + A_{13}\frac{\partial v_2}{\partial y_2} + A_{33}\frac{\partial w}{\partial z}\bigg|_{z=0} = -p. \tag{1.11}$$

We assume that p is a sufficiently smooth given function of the in-plane coordinates (y_1, y_2), defined on the whole upper surface of the layer.

The problem (1.7)–(1.11) is seen often in mechanical applications and later will be employed to model the contact interactions involving thin elastic layers.

1.2 Perturbation Analysis of the Deformation Problem

Assuming now that the elastic layer is relatively thin, we require that

$$h = \varepsilon h_*, \tag{1.12}$$

where ε is a small positive parameter, and h_* is independent of ε, having the order of magnitude of a characteristic length, b, of the external normal load distribution (see Fig. 1.1). For example, in the case when the load $p(\mathbf{y})$ is distributed over an elliptical area with semi-axes a and b such that $b \le a$, the minor semi-axis can be taken as the characteristic length.

To proceed, we first introduce the dimensionless in-plane coordinates

$$\boldsymbol{\eta} = (\eta_1, \eta_2), \quad \eta_i = \frac{y_i}{h_*}, \quad i = 1, 2, \tag{1.13}$$

and the so-called "stretched" dimensionless normal coordinate

$$\zeta = \frac{1}{\varepsilon}\frac{z}{h_*}. \tag{1.14}$$

Substituting the coordinate changes (1.13) and (1.14) into the Lamé equations (1.7), we introduce the small parameter into the problem equations:

$$\varepsilon^2\big(A_{66}\Delta_\eta \mathbf{v} + (A_{11} - A_{66})\nabla_\eta\nabla_\eta\cdot\mathbf{v}\big) + \varepsilon(A_{13} + A_{44})\nabla_\eta\frac{\partial w}{\partial\zeta} + A_{44}\frac{\partial^2\mathbf{v}}{\partial\zeta^2} = \mathbf{0},$$

$$\varepsilon^2 A_{44}\Delta_\eta w + \varepsilon(A_{13} + A_{44})\nabla_\eta\cdot\frac{\partial\mathbf{v}}{\partial\zeta} + A_{33}\frac{\partial^2 w}{\partial\zeta^2} = 0. \tag{1.15}$$

Correspondingly, the boundary conditions (1.10) and (1.11) become

$$\varepsilon\nabla_\eta w + \frac{\partial\mathbf{v}}{\partial\zeta}\bigg|_{\zeta=0} = \mathbf{0}, \tag{1.16}$$

$$A_{13}\nabla_\eta\cdot\mathbf{v}+\varepsilon^{-1}A_{33}\frac{\partial w}{\partial\zeta}\bigg|_{\zeta=0}=-h_*p. \tag{1.17}$$

Using the perturbation algorithm [16], we construct an approximate solution to the system (1.15)–(1.17) in the form of asymptotic expansions

$$\mathbf{v}=\varepsilon\mathbf{v}^0(\boldsymbol{\eta},\zeta)+\varepsilon^2\mathbf{v}^1(\boldsymbol{\eta},\zeta)+\varepsilon^3\mathbf{v}^2(\boldsymbol{\eta},\zeta)+\dots, \tag{1.18}$$

$$w=\varepsilon w^0(\boldsymbol{\eta},\zeta)+\varepsilon^2 w^1(\boldsymbol{\eta},\zeta)+\varepsilon^3 w^2(\boldsymbol{\eta},\zeta)+\dots, \tag{1.19}$$

where the successive coefficients of the powers of ε are assumed to be independent of ε. Note also that the absence of the zeroth-order terms in the above series is suggested by the only non-homogeneous equation (1.17).

The substitution of the expansions (1.18) and (1.19) into Eqs. (1.15)–(1.17) results in a set of equations that must be satisfied for arbitrary ε, and thus, the successive powers must be zero. For more details we refer to [7, 26, 27]. Note also that the perturbation technique [16] was widely used for deriving the transmission conditions for thin elastic interfaces [9, 20, 22, 24, 25].

Consequently, we arrive at a series of problems that begins with the pair

$$A_{44}\frac{\partial^2\mathbf{v}^0}{\partial\zeta^2}=\mathbf{0},\quad \zeta\in(0,1),\quad \frac{\partial\mathbf{v}^0}{\partial\zeta}\bigg|_{\zeta=0}=\mathbf{0},\quad \mathbf{v}^0\big|_{\zeta=1}=\mathbf{0}; \tag{1.20}$$

$$A_{33}\frac{\partial^2 w^0}{\partial\zeta^2}=0,\quad \zeta\in(0,1),\quad A_{33}\frac{\partial w^0}{\partial\zeta}\bigg|_{\zeta=0}=-h_*p,\quad w^0\big|_{\zeta=1}=0. \tag{1.21}$$

From (1.20), it immediately follows that $\mathbf{v}^0(\boldsymbol{\eta},\zeta)\equiv\mathbf{0}$, and therefore we get $w^1(\boldsymbol{\eta},\zeta)\equiv 0$. On the other hand, the problem (1.21) implies that

$$w^0(\boldsymbol{\eta},\zeta)=\frac{h_*p}{A_{33}}(1-\zeta). \tag{1.22}$$

Thus, for the first non-trivial term of the expansion (1.18), we have the problem

$$A_{44}\frac{\partial^2\mathbf{v}^1}{\partial\zeta^2}=-(A_{13}+A_{44})\nabla_\eta\frac{\partial w^0}{\partial\zeta}=\frac{A_{13}+A_{44}}{A_{33}}h_*\nabla_\eta p,\quad \zeta\in(0,1),$$

$$\frac{\partial\mathbf{v}^1}{\partial\zeta}\bigg|_{\zeta=0}=-\nabla_\eta w^0\big|_{\zeta=0}=-\frac{h_*}{A_{33}}\nabla_\eta p,\quad \mathbf{v}^1\big|_{\zeta=1}=\mathbf{0}.$$

From here, it follows after simple calculations that

$$\mathbf{v}^1(\boldsymbol{\eta},\zeta)=\frac{1}{A_{33}}\left(\frac{1}{2}\left(1+\frac{A_{13}}{A_{44}}\right)(1-\zeta)^2-\frac{A_{13}}{A_{44}}(1-\zeta)\right)h_*\nabla_\eta p. \tag{1.23}$$

The second non-trivial term of the expansion (1.19) satisfies the problem

$$A_{33}\frac{\partial^2 w^2}{\partial\zeta^2} = -(A_{13}+A_{44})\nabla_\eta\cdot\frac{\partial\mathbf{v}^1}{\partial\zeta} - A_{44}\Delta_\eta w^0, \quad \zeta\in(0,1),$$

$$A_{33}\frac{\partial w^2}{\partial\zeta}\Big|_{\zeta=0} = -A_{13}\nabla_\eta\cdot\mathbf{v}^1\big|_{\zeta=0}, \quad w^2\big|_{\zeta=1} = 0,$$

which, in light of (1.22), gives

$$w^2(\boldsymbol{\eta},\zeta) = \frac{A_{13}}{A_{33}^2}\left\{\frac{1}{2}(1-\zeta) - \frac{A_{13}+A_{44}}{2A_{44}}(1-\zeta)^2 + \frac{A_{13}+2A_{44}}{6A_{44}}(1-\zeta)^3\right\}h_*\Delta_\eta p. \tag{1.24}$$

We do not consider the problem for $\mathbf{v}^2(\boldsymbol{\eta},\zeta)$ (it can be easily shown that $\mathbf{v}^2(\boldsymbol{\eta},\zeta)\equiv\mathbf{0}$), because the two-term asymptotic approximations for the stress components are given by

$$\begin{aligned}
h_*\sigma_{11} &\simeq A_{13}\frac{\partial w^0}{\partial\zeta} + \varepsilon^2\Big(A_{11}\frac{\partial v_1^1}{\partial\eta_1} + A_{12}\frac{\partial v_2^1}{\partial\eta_2} + A_{13}\frac{\partial w^2}{\partial\zeta}\Big),\\
h_*\sigma_{22} &\simeq A_{13}\frac{\partial w^0}{\partial\zeta} + \varepsilon^2\Big(A_{12}\frac{\partial v_1^1}{\partial\eta_1} + A_{11}\frac{\partial v_2^1}{\partial\eta_2} + A_{13}\frac{\partial w^2}{\partial\zeta}\Big),\\
h_*\sigma_{33} &\simeq A_{33}\frac{\partial w^0}{\partial\zeta} + \varepsilon^2\Big(A_{13}\nabla_\eta\cdot\mathbf{v}^1 + A_{33}\frac{\partial w^2}{\partial\zeta}\Big),\\
h_*(\sigma_{13}\mathbf{e}_1+\sigma_{23}\mathbf{e}_2) &\simeq \varepsilon A_{44}\Big(\nabla_\eta w^0 + \frac{\partial\mathbf{v}^1}{\partial\zeta}\Big),\\
h_*\sigma_{12} &\simeq \frac{\varepsilon^2}{2}(A_{11}-A_{12})\nabla_\eta\cdot\mathbf{v}^1.
\end{aligned} \tag{1.25}$$

As can be seen from (1.25), the in-plane components of strain ε_{ij} $(i,j=1,2)$ are of the order $O(\varepsilon^2)$ while in the main asymptotic term, due to (1.22), the strain out of the plane, ε_{33}, is constant across the layer thickness. These findings are consistent with the phenomenological hypotheses used for thin compressible elastic foundations [18, 37].

According to (1.22) and (1.24), the normal (vertical) and tangential (horizontal) displacements of the surface points of the elastic layer are given by

$$w\big|_{\zeta=0} \simeq \varepsilon\frac{h_*p}{A_{33}} + \varepsilon^3\frac{h_*A_{13}(A_{44}-A_{13})}{3A_{33}^2A_{44}}\Delta_\eta p, \tag{1.26}$$

$$\mathbf{v}\big|_{\zeta=0} \simeq \varepsilon^2 \frac{h_*(A_{44} - A_{13})}{2A_{33}A_{44}} \nabla_\eta p. \tag{1.27}$$

Recall that $\Delta_\eta p$ is the Laplacian of the load distribution. It can be shown that the next term in the asymptotic expansion (1.26) will contain the second iteration of the Laplace operator, i.e., $\Delta_\eta^2 p = \Delta_\eta \Delta_\eta p$. That is why the outlined perturbation algorithm provides an approximate solution under the condition that p is a relatively smooth function defined on the whole upper surface.

Finally, note that in the isotropic case formulas (1.26) and (1.27), as a consequence of (1.12), (1.13), take the form

$$w\big|_{z=0} \simeq \frac{f_0(\nu)}{E} hp(\mathbf{y}) + \frac{f_1(\nu)}{E} h^3 \Delta_y p(\mathbf{y}), \tag{1.28}$$

$$\mathbf{v}\big|_{z=0} \simeq \frac{f_2(\nu)}{E} h^2 \nabla_y p(\mathbf{y}), \tag{1.29}$$

where E and ν are Young's modulus and Poisson's ratio, respectively, while $f_0(\nu)$, $f_1(\nu)$, and $f_2(\nu)$ are given by

$$f_0(\nu) = \frac{(1+\nu)(1-2\nu)}{1-\nu}, \qquad f_1(\nu) = \frac{\nu(1+\nu)(1-4\nu)}{3(1-\nu)^2}, \qquad f_2(\nu) = \frac{(1+\nu)(1-4\nu)}{2(1-\nu)}. \tag{1.30}$$

Observe (see also Fig. 1.2) that $f_0(0.5) = 0$ in the incompressible case, wherein the main asymptotic term in formula (1.28) vanishes.

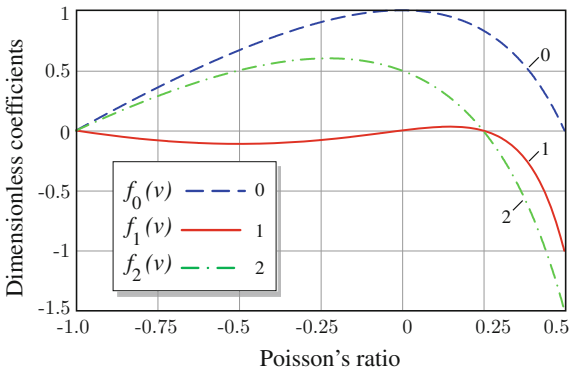

Fig. 1.2 Variation of the dimensionless coefficients (1.30) in the asymptotic formulas (1.28) and (1.29) for the isotropic case

1.3 Contact Problem Formulation for a Thin Elastic Layer

Let us consider the so-called unilateral contact problem for a thin bonded elastic layer and a frictionless rigid punch (see Fig. 1.3). To frame our discussion, we assume that, in the unloading configuration, the punch is bounded by the surface

$$z = -\varphi(\mathbf{y})$$

and has the shape of an elliptic paraboloid (parabolic punch)

$$\varphi(\mathbf{y}) = \frac{y_1^2}{2R_1} + \frac{y_2^2}{2R_2}. \tag{1.31}$$

Here, R_1 and R_2 are the radii of curvature of the principal normal cross-sections of the punch surface at its vertex, and $\varphi(\mathbf{y})$ is called the shape function.

The contact interface is assumed to be frictionless so that

$$\sigma_{13}(\mathbf{y}, 0) = \sigma_{23}(\mathbf{y}, 0) = 0. \tag{1.32}$$

If under the action of an external load, F, the punch receives some displacement, δ_0, then the punch surface becomes

$$z = \delta_0 - \varphi(\mathbf{y}).$$

The Signorini boundary condition of unilateral contact [12, 34, 35], that the surface points of the layer do not penetrate into the punch, reads as

$$\begin{gathered} w(\mathbf{y}, 0) - \delta_0 + \varphi(\mathbf{y}) \geq 0, \qquad \sigma_{33}(\mathbf{y}, 0) \leq 0, \\ \big[w(\mathbf{y}, 0) - \delta_0 + \varphi(\mathbf{y})\big]\sigma_{33}(\mathbf{y}, 0) = 0, \end{gathered} \tag{1.33}$$

which can be rewritten in the following form:

$$\begin{aligned} &\sigma_{33}(\mathbf{y}, 0) \leq 0, \\ \sigma_{33}(\mathbf{y}, 0) < 0 \quad &\Rightarrow \quad w(\mathbf{y}, 0) = \delta_0 - \varphi(\mathbf{y}), \\ \sigma_{33}(\mathbf{y}, 0) = 0 \quad &\Rightarrow \quad w(\mathbf{y}, 0) \geq \delta_0 - \varphi(\mathbf{y}). \end{aligned} \tag{1.34}$$

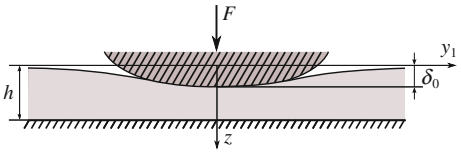

Fig. 1.3 Contact interaction of an elastic layer with an absolutely rigid punch in the deformed configuration

An important characteristic of the contact interaction is the contact pressure distribution beneath the punch

$$p(\mathbf{y}) = -\sigma_{33}(\mathbf{y}, 0), \quad \mathbf{y} \in \omega, \tag{1.35}$$

where ω is the contact area, which is not known a priori.

According to the last two relations in (1.33), the contact pressure should be positive inside ω and vanish on the contour Γ of the domain ω, so that

$$p(\mathbf{y}) > 0, \quad \mathbf{y} \in \omega, \quad p(\mathbf{y}) = 0, \quad \mathbf{y} \in \Gamma. \tag{1.36}$$

The above requirement will be called the positiveness condition.

In addition to (1.36), the boundary condition (1.34) implies that

$$w(\mathbf{y}, 0) = \delta_0 - \varphi(\mathbf{y}), \quad \mathbf{y} \in \omega. \tag{1.37}$$

We emphasize that the contour Γ is unknown and should be determined in the process of solving the contact problem.

The equilibrium equation for the punch-layer-substrate system is

$$\iint\limits_{\omega} p(\mathbf{y})\, d(\mathbf{y}) = F, \tag{1.38}$$

where F is the external load acting on the punch (contact force).

Further, it should be noted that the contact condition (1.37) simplifies the geometrical aspects of the contact interaction since it does not take into account the tangential displacements of the surface points of the elastic layer, which occur even under the normal loading (see Fig. 1.4).

The refined unilateral contact condition can be obtained from (1.33) by replacing the first inequality in (1.33) with the following [21]:

$$w(\mathbf{y}, 0) - \delta_0 + \varphi\big(y_1 + v_1(\mathbf{y}, 0),\, y_2 + v_2(\mathbf{y}, 0)\big) \geq 0. \tag{1.39}$$

Here, v_i $(i = 1, 2)$ are the tangential displacements of the surface point $(\mathbf{y}, 0)$.

According to (1.39), the following equation holds within the contact area:

$$w(\mathbf{y}, 0) = \delta_0 - \varphi(\mathbf{y} + \mathbf{v}(\mathbf{y}, 0)), \quad \mathbf{y} \in \omega.$$

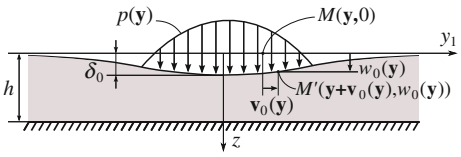

Fig. 1.4 Tangential displacements of the surface points under normal loading

We assume that both the normal and tangential displacements are very small compared to the characteristic size of the contact area. In this case, the above nonlinear equation can be replaced by the first-order linearized contact condition

$$w(\mathbf{y}, 0) = \delta_0 - \varphi(\mathbf{y}) - \nabla_y \varphi(\mathbf{y}) \cdot \mathbf{v}(\mathbf{y}, 0), \quad \mathbf{y} \in \omega. \tag{1.40}$$

The refined contact condition (1.40) was used in a number of studies [3, 6, 14, 15].

To solve the contact problem (1.36), (1.40) requires that we find the contact pressure distribution $p(\mathbf{y})$, positive over the contact area ω and vanishing on its contour Γ, such that the resulting normal and tangential displacements $w(\mathbf{y}, 0)$ and $\mathbf{v}(\mathbf{y}, 0)$ satisfy Eq. (1.40) within ω, while outside it the linearized inequality obtained from the unilateral boundary condition (1.39) must hold.

1.4 Asymptotic Solution of the Contact Problem for a Thin Bonded Compressible Elastic Layer

To study the asymptotic behavior of the solution to the contact problem (1.7), (1.8), (1.32), and (1.33) when $\varepsilon \to 0$, in addition to (1.12) we will assume that

$$\delta_0 = \varepsilon \delta_0^*, \quad R_1 = \varepsilon^{-1} R_1^*, \quad R_2 = \varepsilon^{-1} R_2^*, \tag{1.41}$$

where δ_0^*, R_1^*, and R_2^* are independent of ε and comparable with h_*. Note that, following [4], the geometric parameters of the problem having the dimension of length (that is h, δ_0, R_1, and R_2) are scaled in such a way that the elastic layer thickness will be small compared to the characteristic length of the contact area.

In light of (1.41), the boundary contact condition (1.33) takes the form

$$w\big|_{\zeta=0} = \varepsilon\big(\delta_0^* - \varphi^*(\boldsymbol{\eta})\big), \quad \boldsymbol{\eta} \in \omega^*, \tag{1.42}$$

where ω^* is the contact area in the stretched coordinates (1.13), and we have introduced the notation

$$\varphi^*(\boldsymbol{\eta}) = h_*^2\big((2R_1^*)^{-1}\eta_1^2 + (2R_2^*)^{-1}\eta_2^2\big). \tag{1.43}$$

Following [4, 16], the so-called inner asymptotic expansion for the solution of the contact problem is represented in the form of series (1.18) and (1.19). Applying the perturbation algorithm described in Sect. 1.2, the displacement field under the punch can be obtained in the following form:

$$\mathbf{v} \simeq -\varepsilon^2 \nabla_\eta \varphi^*(\boldsymbol{\eta}) \left(\frac{1}{2}\left(1 + \frac{A_{13}}{A_{44}}\right)(1-\zeta)^2 - \frac{A_{13}}{A_{44}}(1-\zeta) \right), \tag{1.44}$$

$$w \simeq \varepsilon\big(\delta_0^* - \varphi^*(\boldsymbol{\eta})\big)(1-\zeta) + \varepsilon^3 \Delta_\eta \varphi^*(\boldsymbol{\eta}) \Big\{ \frac{A_{13}(A_{13}+A_{44})}{2A_{33}A_{44}} \zeta(1-\zeta) - \frac{A_{13}(A_{13}+2A_{44})}{6A_{33}A_{44}} \zeta(1-\zeta)(2-\zeta) \Big\}. \tag{1.45}$$

Correspondingly, the contact pressure density is given by

$$p \simeq \frac{A_{33}}{h_*}\big(\delta_0^* - \varphi^*(\boldsymbol{\eta})\big) - \varepsilon^2 \frac{A_{13}(A_{13}-A_{44})}{3A_{44}h_*} \Delta_\eta \varphi^*(\boldsymbol{\eta}). \tag{1.46}$$

The higher-order terms of the asymptotic expansions (1.18) and (1.19) satisfy the recurrence equations

$$A_{44}\frac{\partial^2 \mathbf{v}^k}{\partial \zeta^2} = -(A_{13}+A_{44})\nabla_\eta \frac{\partial w^{k-1}}{\partial \zeta} - A_{66}\Delta_\eta \mathbf{v}^{k-2} - (A_{11}-A_{66})\nabla_\eta \nabla_\eta \cdot \mathbf{v}^{k-2}, \tag{1.47}$$

$$A_{33}\frac{\partial^2 w^k}{\partial \zeta^2} = -(A_{13}+A_{44})\nabla_\eta \cdot \frac{\partial \mathbf{v}^{k-1}}{\partial \zeta} - A_{44}\Delta_\eta w^{k-2}, \quad k = 2, 3, \ldots, \tag{1.48}$$

with the boundary conditions

$$\frac{\partial \mathbf{v}^k}{\partial \zeta}\Big|_{\zeta=0} = -\nabla_\eta w^{k-1}\big|_{\zeta=0}, \quad \mathbf{v}^k\big|_{\zeta=1} = \mathbf{0}, \tag{1.49}$$

$$w^k\big|_{\zeta=0} = 0, \quad w^k\big|_{\zeta=1} = 0. \tag{1.50}$$

In the special case (1.43), when the punch shape function is quadratic, we have $\Delta_\eta \varphi^*(\boldsymbol{\eta}) \equiv \text{const}$. Hence, the function $w^2(\boldsymbol{\eta}, \zeta)$ does not depend on the in-plane coordinates (η_1, η_2), while $\mathbf{v}^1(\boldsymbol{\eta}, \zeta)$ is a linear function of η_1 and η_2. In light of (1.47)–(1.50), this implies that the other terms in the expansions (1.18) and (1.19) do not contribute to the asymptotic solution (1.44) and (1.45).

The substitution of the approximations for the displacement field (1.44), (1.45) into formulas (1.25) yields approximations for the stress components. In particular, for the normal stress and the out-of-plane shear stresses, we obtain

$$h_*\sigma_{33} \simeq -A_{33}\big(\delta_0^* - \varphi^*(\boldsymbol{\eta})\big) + \varepsilon^2 \Delta_\eta \varphi^*(\boldsymbol{\eta}) \Big(\frac{A_{13}(2A_{13}+A_{44})}{6A_{44}} - \frac{A_{13}}{2}(1-\zeta^2) \Big), \tag{1.51}$$

$$h_*(\sigma_{13}\mathbf{e}_1 + \sigma_{23}\mathbf{e}_2) \simeq -\varepsilon A_{13} \nabla_\eta \varphi^*(\boldsymbol{\eta}) \zeta. \tag{1.52}$$

Note that by substituting $\zeta = 0$ into (1.51), we recover formula (1.46). In the case of an isotropic material, formulas (1.51) and (1.52) were obtained in [4, 5].

Thus, in light of the positiveness requirement (1.36), formula (1.46) implies that the leading asymptotics of the contact pressure distribution should be written as

$$p \simeq \frac{A_{33}}{h_*}\big(\delta_0^* - \varphi^*(\boldsymbol{\eta})\big)_+, \tag{1.53}$$

where $(t)_+ = (t + |t|)/2$ is the positive part function, and $\varphi^*(\boldsymbol{\eta})$ is given by (1.43).

Furthermore, Eqs. (1.43) and (1.51) yield

$$-h_*\sigma_{33} \simeq A_{33}\left(\delta_0^* - \frac{h_*^2\eta_1^2}{2R_1^*} - \frac{h_*^2\eta_2^2}{2R_2^*}\right) - \varepsilon^2\frac{h_*^2(R_1^* + R_2^*)}{R_1^*R_2^*}\,\frac{A_{13}(A_{44} - A_{13})}{3A_{44}}.$$

Now, based on the above formula, we find that the second-order asymptotic approximation for the contact pressure density is given by

$$p \simeq \frac{A_{33}}{h}\left(\delta_\varepsilon - \frac{y_1^2}{2R_1} - \frac{y_2^2}{2R_2}\right)_+, \tag{1.54}$$

where we have introduced the notation

$$\delta_\varepsilon = \delta_0 - \frac{h^2(R_1 + R_2)}{R_1R_2}\,\frac{A_{13}(A_{44} - A_{13})}{3A_{33}A_{44}}. \tag{1.55}$$

Formula (1.54) implies that the contact area ω is bounded by an ellipse with the semi-axes

$$a = \sqrt{2R_1\delta_\varepsilon}, \quad b = \sqrt{2R_2\delta_\varepsilon}. \tag{1.56}$$

In the case of an isotropic elastic layer, formulas (1.54)–(1.56) were obtained by Alexandrov and Pozharskii [2] by another method.

1.5 Asymptotic Models for the Beformation Response of a Thin Bonded Compressible Elastic Layer

In this section we generalize the results of asymptotic analysis by formulating simple mathematical models (called asymptotic models) to describe the deformational behavior of a bonded compressible elastic layer in the thin-layer approximation.

1.5.1 Zeroth-Order Asymptotic Model for the Contact Problem

In contact problems, an important role is played by the normal displacement of the surface points

$$w_0(\mathbf{y}) = w(\mathbf{y}, 0), \tag{1.57}$$

which, following the terminology of Barber [8], will be called the local indentation.

In the case of a thin bonded transversally isotropic elastic layer, according to (1.12), (1.13) and (1.26), we have

$$w_0 \simeq \frac{h}{A_{33}} p + \frac{h^3 A_{13}(A_{44} - A_{13})}{3A_{33}^2 A_{44}} \Delta_y p. \tag{1.58}$$

By neglecting the second term on the right-hand side of the above equation and substituting the obtained result into the contact condition (1.37), we obtain

$$\frac{h}{A_{33}} p(\mathbf{y}) = \delta_0 - \varphi(\mathbf{y}), \quad \mathbf{y} \in \omega. \tag{1.59}$$

Under the assumption of unilateral contact between the punch and the layer, the contact area ω is determined by the positiveness condition (1.36) and depends on the punch shape function $\varphi(\mathbf{y})$. Formally, the leading-order (i.e., the zeroth-order) asymptotic solution to the problem (1.36), (1.59) is given by Eq. (1.53), which after recovering the original notation by (1.12), (1.41), and (1.42), takes the form

$$p(\mathbf{y}) = \frac{A_{33}}{h} \big(\delta_0 - \varphi(\mathbf{y})\big)_+. \tag{1.60}$$

In the case of a parabolic punch (1.31), the contact area is elliptical, with semi-axes a and b such that $a/b = \sqrt{R_1/R_2}$ and

$$a = \sqrt{2R_1\delta_0}, \quad b = \sqrt{2R_2\delta_0}, \tag{1.61}$$

so that formula (1.60) can be rewritten as

$$p(\mathbf{y}) = p_0 \left(1 - \frac{y_1^2}{a^2} - \frac{y_2^2}{b^2}\right)_+ \tag{1.62}$$

with the maximum contact pressure

$$p_0 = A_{33} \frac{\delta_0}{h}. \tag{1.63}$$

Integrating the contact pressure density (1.62) over the contact area and taking into account Eqs. (1.61) and (1.63), we obtain the force-displacement relationship

$$F = \frac{\pi}{h} \sqrt{R_1 R_2} A_{33} \delta_0^2. \tag{1.64}$$

Thus, for a thin compressible elastic layer, the contact pressure beneath the punch in the leading asymptotic term is proportional to the local indentation [see Eqs. (1.37) and (1.59)]. The fact that the deformation response of a thin compressible layer resembles that of a Winkler elastic foundation with the modulus

$$k = \frac{A_{33}}{h} \tag{1.65}$$

was first rigorously established by Aleksandrov [1] in the case of a thin bonded isotropic layer, where formula (1.65) reduces to

$$k = \frac{E(1-\nu)}{(1+\nu)(1-2\nu)h}. \tag{1.66}$$

Note that contact problems for a Winkler foundation were considered in [18, 31, 32]. In the framework of the zeroth-order asymptotic model, indentation problems were studied in [8, 17] and [28], where formulas (1.66) and (1.65) were recovered in the isotropic and transversely isotropic cases, respectively.

Note also that in the axisymmetric case (when $R_1 = R_2$) the obtained solution (1.61)–(1.64) reduces to the result obtained by Ning et al. [28] for a spherical punch based on Johnson's simplifying hypothesis [18] that plane sections remain planar after compression.

1.5.2 Asymptotic Model for the Pasternak Foundation

As the Winkler foundation model assumes that the contact pressure is merely proportional to the local indentation, i.e.,

$$p(\mathbf{y}) = kw_0(\mathbf{y}), \tag{1.67}$$

it can be represented by the mechanical model of a layer of closely spaced, independent, linear springs (see Fig. 1.5). At the same time, it is well-known that real foundations may exhibit considerable interaction among their constitutive elements. To overcome the inherent deficiency of the Winkler model, several phenomenological models of elastic foundations have been proposed [11, 37, 38].

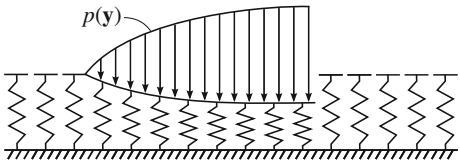

Fig. 1.5 Winkler's foundation model, which for a discontinuous loading predicts the correspondingdiscontinuous local indentation

In particular, the two-parameter model for the deformational behavior of soils proposed by Pasternak [30] assumes the existence of shear interaction between the spring elements and is regarded [19] as mechanically the most logical extension of the Winkler model (1.67), and analytically as the next higher approximation. The response function for the Pasternak model is given by

$$p(\mathbf{y}) = k_P w_0(\mathbf{y}) - G_P \Delta_y w_0(\mathbf{y}), \tag{1.68}$$

where k_P and G_P are the foundation constants.

The Pasternak foundation can be constructed by connecting a layer of the Winkler spring elements to a surface layer of vertically incompressible elements which deform in transverse shear only [33].

It is noteworthy that the phenomenological approach has a disadvantage in that the parameters k_P and G_P are difficult to determine [38].

On the other hand, in the case of a thin bonded compressible elastic layer, the asymptotic formula (1.46) yields the following response function:

$$p(\mathbf{y}) \simeq \frac{A_{33}}{h} w_0(\mathbf{y}) - \frac{A_{13}(A_{44} - A_{13})}{3A_{44}} h \Delta_y w_0(\mathbf{y}). \tag{1.69}$$

Now, comparing Eqs. (1.68) and (1.69), we obtain the relations

$$k_P = \frac{A_{33}}{h}, \quad G_P = \frac{A_{13}(A_{44} - A_{13})}{3A_{44}} h. \tag{1.70}$$

In the case of an isotropic material, we have

$$k_P = \frac{E(1-\nu)}{(1+\nu)(1-2\nu)h}, \quad G_P = \frac{E\nu(1-4\nu)h}{3(1+\nu)(1-2\nu)^2}. \tag{1.71}$$

Observe that for $\nu \in (0.25, 0.5)$, formula $(1.71)_2$ produces a negative value for the parameter G_P. Hence, formulas (1.71) can provide the foundation constants for the Pasternak model (1.68) when the layer material is sufficiently compressible.

1.5.3 Refined Contact Model with Allowance for Tangential Displacements on the Contact Interface

Let us consider the unilateral contact problem for a frictionless rigid punch in the shape of an elliptic paraboloid (1.31), formulated by the refined contact condition (1.40), which can be rewritten as

$$w_0(\mathbf{y}) + \nabla_y \varphi(\mathbf{y}) \cdot \mathbf{v}_0(\mathbf{y}) = \delta_0 - \varphi(\mathbf{y}). \tag{1.72}$$

Here, w_0 and $\mathbf{v}_0$ are the normal and tangential displacements of the surface points of the elastic layer on the contact interface.

In the framework of the first-order asymptotic model, we have

$$w_0 = \frac{h}{A_{33}} p, \tag{1.73}$$

$$\mathbf{v}_0 = \frac{A_{44} - A_{13}}{2A_{33}A_{44}} h^2 \nabla_y p. \tag{1.74}$$

Recall that the above equations are obtained from formulas (1.26) and (1.27).

Substituting (1.73) and (1.74) into Eq. (1.72), we arrive at the equation

$$\frac{h}{A_{33}} p(\mathbf{y}) + \frac{A_{44} - A_{13}}{2A_{33}A_{44}} h^2 \nabla_y \varphi(\mathbf{y}) \cdot \nabla_y p(\mathbf{y}) = \delta_0 - \varphi(\mathbf{y}), \quad \mathbf{y} \in \omega. \tag{1.75}$$

Here, ω is the contact area which should be determined with the help of the positiveness condition (1.35) imposed on the contact pressure $p(\mathbf{y})$.

In the case of a parabolic punch (1.31), the solution of Eq. (1.75) can be represented in the form

$$p(\mathbf{y}) = p_0 \left(1 - \frac{y_1^2}{a^2} - \frac{y_2^2}{b^2}\right) \tag{1.76}$$

with unknown parameters p_0, a, and b.

The substitution of (1.31) and (1.76) into Eq. (1.75) gives

$$\frac{h}{A_{33}} p_0 \left(1 - \frac{y_1^2}{a^2} - \frac{y_2^2}{b^2}\right) - \frac{(A_{44} - A_{13})h^2}{A_{33}A_{44}} \left(\frac{y_1^2}{R_1 a^2} + \frac{y_2^2}{R_2 b^2}\right) = \delta_0 - \frac{y_1^2}{2R_1} - \frac{y_2^2}{2R_2}.$$

From here it immediately follows that

$$\begin{aligned} p_0 &= A_{33} \frac{\delta_0}{h}, \\ a &= \sqrt{2R_1\delta_0} \left(1 + \frac{(A_{44} - A_{13})}{A_{44}} \frac{h}{R_1}\right)^{1/2}, \\ b &= \sqrt{2R_2\delta_0} \left(1 + \frac{(A_{44} - A_{13})}{A_{44}} \frac{h}{R_2}\right)^{1/2}. \end{aligned} \tag{1.77}$$

Finally, taking into account the relation $F = (\pi/2)abp_0$ between the maximum contact pressure p_0 and the contact force F, we get

$$F \simeq \frac{\pi}{h} \sqrt{R_1 R_2} A_{33} \delta_0^2 \left(1 + \frac{(A_{44} - A_{13})}{A_{44}} \frac{h}{R}\right), \tag{1.78}$$

where $R = 2R_1R_2/(R_1 + R_2)$ is the harmonic mean of the curvature radii R_1 and R_2. Note also that in writing Eq. (1.78), we have neglected the terms of order $O((h/R)^2)$.

In the case of isotropic material, $(A_{44} - A_{13})/A_{44} = (1 - 4\nu)/(1 - 2\nu)$, and, as can be seen from Eqs. (1.77) and (1.78), the effect of tangential displacements increases when the material becomes more incompressible.

References

1. Aleksandrov, V.M.: On the approximate solution of a certain type of integral equation. J. Appl. Math. Mech. **26**, 1410–1424 (1962)
2. Alexandrov, V.M., Pozharskii, D.A.: Three-Dimensional Contact Problems. Kluwer, Dordrecht (2001)
3. Argatov, I.I.: Approximate solution of an axisymmetric contact problem with allowance for tangential displacements on the contact surface. J. Appl. Mech. Tech. Phys. **45**, 118–123 (2004)
4. Argatov, I.I.: Pressure of a paraboloidal die on a thin elastic layer. Doklady Phys. **50**, 524–528 (2005)
5. Argatov, I.I.: Asymptotic Models of Elastic Contact [in Russian]. Nauka, St Petersburg (2005)
6. Argatov, I.I., Mishuris, G.S.: Axisymmetric contact problem for a biphasic cartilage layer with allowance for tangential displacements on the contact surface. Eur. J. Mech. A/Solids **29**, 1051–1064 (2010)
7. Argatov, I., Mishuris, G.: Asymptotic Methods in Mechanics, [Electronic Edition]. Aberystwyth University, Ceredigion (2011)
8. Barber, J.R.: Contact problems for the thin elastic layer. Int. J. Mech. Sci. **32**, 129–132 (1990)
9. Benveniste, Y., Miloh, T.: Imperfect soft and stiff interfaces in two-dimensional elasticity. Mech. Mater. **33**, 309–323 (2001)
10. Bigoni, D.: Nonlinear Solid Mechanics. Bifurcation Theory and Material Instability. Cambridge University Press, Cambridge (2012)
11. Dutta, S.C., Roy, R.: A critical review on idealization and modeling for interaction among soil-foundation-structure system. Comput. Struct. **80**, 1579–1594 (2002)
12. Duvaut, G., Lions, J.-L.: Les inéquations en mécanique et en physique. Dunod, Paris (1972)
13. Elliott, H.A.: Three-dimensional stress distributions in hexagonal aeolotropic crystals. Math. Proc. Camb. Phil. Soc. **44**, 522–533 (1948)
14. Galanov, B.A.: Approximate solution to some problems of elastic contact of two bodies. Mech. Solids **16**, 61–67 (1981)
15. Georgiadis, L.M.: Tangential-displacement effects in the wedge indentation of an elastic half-space—an integral-equation approach. Comput. Mech. **21**, 347–352 (1998)
16. Gol'denveizer, A.L.: Derivation of an approximate theory of bending of a plate by the method of asymptotic integration of the equations of the theory of elasticity. J. Appl. Math. Mech. **26**, 1000–1025 (1962)
17. Jaffar, M.J.: Asymptotic behaviour of thin elastic layers bonded and unbonded to a rigid foundation. Int. J. Mech. Sci. **31**, 229–235 (1989)
18. Johnson, K.L.: Contact Mechanics. Cambridge University Press, Cambridge (1985)
19. Kerr, A.D.: Elastic and viscoelastic foundation models. J. Appl. Mech. Trans. ASME **31**, 491–498 (1964)
20. Klarbring, A., Movchan, A.B.: Asymptotic modelling of adhesive joints. Mech. Mater. **28**, 137–145 (1998)
21. Kravchuk, A.S.: On the Hertz problem for linearly and nonlinearly elastic bodies of finite dimensions. J. Appl. Math. Mech. **41**, 320–328 (1977)
22. Lebon, F., Rizzoni, R.: Asymptotic analysis of a thin interface: the case involving similar rigidity. Int. J. Eng. Sci. **48**, 473–486 (2010)
23. Lekhnitskii, S.G.: Theory of Elasticity of an Anisotropic Body. Mir publishing, Moscow (1981)

24. Mishuris, G.: Mode III interface crack lying at thin nonhomogeneous anisotropic interface. Asymptotics near the crack tip. In: Movchan, A.B. (ed.) IUTAM Symposium on Asymptotics, Singularities and Homogenisation in Problems of Mechanics, pp. 251–260. Kluwer (2003)
25. Mishuris, G.: Imperfect transmission conditions for a thin weakly compressible interface. 2D problems. Arch. Mech. **56**, 103–115 (2004)
26. Movchan, A.B., Movchan, N.V.: Mathematical Modeling of Solids with Nonregular Boundaries. CRC-Press, Boca Raton (1995)
27. Nayfeh, A.H.: Introduction to Perturbation Techniques. Wiley, New York (1993)
28. Ning, X., Lovell, M., Slaughter, W.S.: Asymptotic solutions for axisymmetric contact of a thin, transversely isotropic elastic layer. Wear **260**, 693–698 (2006)
29. Novozhilov, V.V.: Theory of Elasticity. Pergamon Press, New York (1961)
30. Pasternak, P.L.: On a New Method of Analysis of an Elastic Foundation by Means of Two-Constants [in Russian]. Gosudarstvennoe Izdatelstvo Literatury po Stroitelstvu i Arkhitekture, Moscow (1954)
31. Popov, V.L., Heß, M.: Methode Der Dimensionsreduktion in Der Kontaktmechanik Und Reibung [in German]. Springer, Berlin (2013)
32. Popov, V.L., Hess, M.: Method of dimensionality reduction in contact mechanics and friction: a users handbook. I. Axially-symmetric contacts. Facta Universitati. Ser. Mech. Eng. **12**, 1–14 (2014)
33. Selvadurai, A.P.S.: Elastic Analysis of Soil-Foundation Interaction. Elsevier, Amsterdam (1979)
34. Shillor, M., Sofonea, M., Telega, J.J.: Models and Analysis of Quasistatic Contact: Variational Methods. Springer, Berlin (2004)
35. Signorini, A.: Questioni di elasticità non linearizzata e semilinearizzata. Rend. Mat. e Appl. **18**, 95–139 (1959)
36. Ting, T.C.T.: Anisotropic Elasticity. Oxford University Press, Oxford (1996)
37. Vlasov, V.Z., Leontyev, N.N.: Beams, Plates and Shells on Elastic Foundation [in Russian]. Fizmatgiz, Moscow (1960). English translation, Israel Program for Scientific Translations, Jerusalem (1966)
38. Wang, Y.H., Tham, L.G., Cheung, Y.K.: Beams and plates on elastic foundations: a review. Prog. Struct. Eng. Mater. **7**, 174–182 (2005)

Chapter 2
Asymptotic Analysis of the Contact Problem for Two Bonded Elastic Layers

Abstract The first part of the chapter deals with the distributional asymptotic analysis of the contact problem of frictionless unilateral interaction of two bonded elastic layers. The case of incompressible layer materials is thoroughly treated in the second part of the chapter, beginning in Sect. 2.4.

2.1 Contact Problem Formulation

In this section we formulate the problem of frictionless unilateral contact between two uniform transversely isotropic elastic layers bonded to rigid substrates. In the case of substrates shaped like elliptic paraboloids, the general expression for the gap function is derived. The boundary conditions of unilateral contact are considered in detail, including the refined contact condition with allowance for tangential displacements on the contact interface. The contact problem is formulated as an integral equation over the contact area, which in turn should be determined by the positiveness condition imposed on the contact pressure.

2.1.1 Geometry of Surfaces in Contact

Let us consider two thin elastic layers ($n = 1, 2$), each of uniform thickness h_n, ideally bonded to rigid substrates with slightly curved surfaces (see Fig. 2.1). Introducing the Cartesian coordinate system (y_1, y_2, z), we write out the equations of the surfaces of the coating layers ($n = 1, 2$) in the form

$$z = (-1)^n \varphi_n(\mathbf{y}), \tag{2.1}$$

assuming that in the undeformed state the thin layer/substrate systems occupy domains $z \le -\varphi_1(\mathbf{y})$ and $z \ge \varphi_2(\mathbf{y})$.

In particular, it is of great practical interest to consider the case of substrates shaped like paraboloids

I. Argatov and G. Mishuris, *Contact Mechanics of Articular Cartilage Layers*,
Advanced Structured Materials 50, DOI 10.1007/978-3-319-20083-5_2

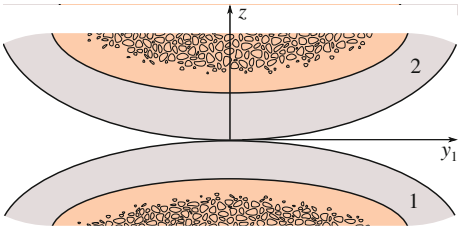

Fig. 2.1 Contact of two thin elastic layers in the initial undeformed configuration

$$\varphi_n(\mathbf{y}) = k_{11}^{(n)} y_1^2 + 2k_{12}^{(n)} y_1 y_2 + k_{22}^{(n)} y_2^2, \tag{2.2}$$

where the coefficients $k_{11}^{(n)}$, $k_{12}^{(n)}$, and $k_{22}^{(n)}$ have the dimension of reciprocal length.

The initial gap between the two surfaces is given by the gap function

$$\varphi(\mathbf{y}) = \varphi_1(\mathbf{y}) + \varphi_2(\mathbf{y}). \tag{2.3}$$

Correspondingly, in the case (2.2), we have

$$\varphi(\mathbf{y}) = k_{11} y_1^2 + 2k_{12} y_1 y_2 + k_{22} y_2^2, \tag{2.4}$$

where

$$k_{11} = k_{11}^{(1)} + k_{11}^{(2)}, \quad k_{12} = k_{12}^{(1)} + k_{12}^{(2)}, \quad k_{22} = k_{22}^{(1)} + k_{22}^{(2)}.$$

Now, let $R_1^{(n)}$ and $R_2^{(n)}$ be the principal radii of curvature of the surface of the n-th layer at its apex, such that the n-th layer surface can then be expressed as

$$\varphi_n(\mathbf{y}) = \frac{(y_1^n)^2}{2R_1^{(n)}} + \frac{(y_2^n)^2}{2R_2^{(n)}}, \tag{2.5}$$

where the directions of the local coordinate axes y_1^n and y_2^n coincide with the principal curvature directions.

The transformation of the coordinates (y_1^n, y_2^n) to the common set of axes (y_1, y_2) inclined at the angle β_n to the axis y_1^n is given by

$$y_1^n = y_1 \cos\beta_n - y_2 \sin\beta_n, \quad y_2^n = y_1 \sin\beta_n + y_2 \cos\beta_n. \tag{2.6}$$

Hence, in light of (2.5) and (2.6), the coefficients on the right-hand side of (2.2) can be expressed as

$$2k_{11}^{(n)} = \kappa_1^{(n)} \cos^2\beta_n + \kappa_2^{(n)} \sin^2\beta_n, \quad 2k_{22}^{(n)} = \kappa_1^{(n)} \sin^2\beta_n + \kappa_2^{(n)} \cos^2\beta_n,$$

$$2k_{12}^{(n)} = \left(\kappa_2^{(n)} - \kappa_1^{(n)}\right) \sin\beta_n \cos\beta_n,$$

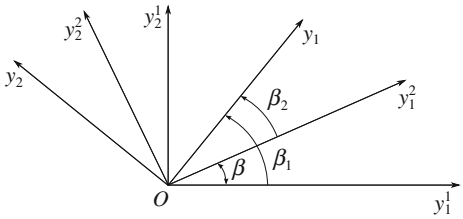

Fig. 2.2 Coordinate systems involved in determining the initial gap between the contacting surfaces

where $\kappa_1^{(n)}$ and $\kappa_2^{(n)}$ are the principal curvatures, i.e.,

$$\kappa_1^{(n)} = \frac{1}{R_1^{(n)}}, \quad \kappa_2^{(n)} = \frac{1}{R_2^{(n)}}.$$

Now, by a suitable choice of the coordinate axes (y_1, y_2), we can make k_{12} zero in (2.4). For instance, let us choose the angle β_1 in such a way that

$$\left(\kappa_2^{(1)} - \kappa_1^{(1)}\right) \sin 2\beta_1 + \left(\kappa_2^{(2)} - \kappa_1^{(2)}\right) \sin 2\beta_2 = 0. \tag{2.7}$$

Taking into account that (see Fig. 2.2)

$$\beta = \beta_1 - \beta_2, \tag{2.8}$$

from Eq. (2.7), we readily find

$$\tan 2\beta_1 = \frac{\left(\kappa_2^{(2)} - \kappa_1^{(2)}\right) \sin 2\beta}{\kappa_2^{(1)} - \kappa_1^{(1)} + \left(\kappa_2^{(2)} - \kappa_1^{(2)}\right) \cos 2\beta}. \tag{2.9}$$

Thus, the parabolic gap function (2.4) takes the simplest form

$$\varphi(\mathbf{y}) = k_1 y_1^2 + k_2 y_2^2, \tag{2.10}$$

where the coefficients k_1 and k_2 are evaluated by the formulas

$$\begin{aligned} 2k_1 &= \kappa_1^{(1)} \cos^2 \beta_1 + \kappa_2^{(1)} \sin^2 \beta_1 + \kappa_1^{(2)} \cos^2 \beta_2 + \kappa_2^{(2)} \sin^2 \beta_2, \\ 2k_2 &= \kappa_1^{(1)} \sin^2 \beta_1 + \kappa_2^{(1)} \cos^2 \beta_1 + \kappa_1^{(2)} \sin^2 \beta_2 + \kappa_2^{(2)} \cos^2 \beta_2. \end{aligned} \tag{2.11}$$

From the above equations, it follows that

$$\begin{aligned} 2(k_1 + k_2) &= \kappa_1^{(1)} + \kappa_2^{(1)} + \kappa_1^{(2)} + \kappa_2^{(2)}, \\ 2(k_1 - k_2) &= \left(\kappa_1^{(1)} - \kappa_2^{(1)}\right) \cos 2\beta_1 + \left(\kappa_1^{(2)} - \kappa_2^{(2)}\right) \cos 2\beta_2. \end{aligned} \tag{2.12}$$

Note [19, 20] that by taking into account (2.12), Eq. (2.11) can be rewritten as

$$\begin{aligned} 2k_1 &= \left(\kappa_1^{(1)} + \kappa_2^{(1)} + \kappa_1^{(2)} + \kappa_2^{(2)}\right) \sin^2 \frac{\tau}{2}, \\ 2k_2 &= \left(\kappa_1^{(1)} + \kappa_2^{(1)} + \kappa_1^{(2)} + \kappa_2^{(2)}\right) \cos^2 \frac{\tau}{2}, \end{aligned} \tag{2.13}$$

where τ is an auxiliary parameter given by $\cos\tau = (k_2 - k_1)/(k_2 + k_1)$. From Eq. (2.13), it follows that the coefficients k_1 and k_2 have the same sign, explaining why the equidistant curves $k_1 y_1^2 + k_2 y_2^2 = const$ are concentric ellipses.

Finally, it should be underlined that since the angle β, as well as the curvatures $\kappa_1^{(n)}$ and $\kappa_2^{(n)}$ $(n = 1, 2)$, are supposed to be known, we can evaluate the angle β_1 from Eq. (2.9), and after that Eq. (2.8) will yield $\beta_2 = \beta_1 - \beta$. Equation (2.12) will then give k_1 and k_2, the parameters of the gap function $\varphi(\mathbf{y})$ (see Eq. (2.10)).

2.1.2 Unilateral Contact Conditions

We consider the contact interaction of the elastic layers as a normal load F is applied to the substrates, producing their (vertical) contact approach δ_0 (see Fig. 2.3).

Before deformation, the gap between the layer surfaces was given by Eq. (2.10), which can be rewritten as

$$\varphi(\mathbf{y}) = \frac{y_1^2}{2R_1} + \frac{y_2^2}{2R_2}, \tag{2.14}$$

where $R_1 = 1/(2k_1)$ and $R_2 = 1/(2k_2)$, for k_1 and k_2 given by (2.13). In what follows, we may assume that $R_1 \geq R_2$.

If the surface point $\mathrm{M}'(\mathbf{y}', z')$ of the first layer (laying in the domain $z \leq -\varphi_1(\mathbf{y})$) and the surface point $\mathrm{M}''(\mathbf{y}'', z'')$ of the second layer (laying in the domain $z \geq \varphi_2(\mathbf{y})$) coincide after deformation (see Fig. 2.4), the following relations hold true [20]:

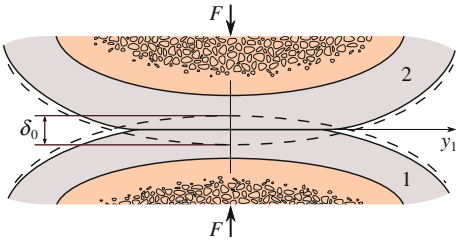

Fig. 2.3 Schematic diagram for the frictionless contact interaction of elastic layers 1 and 2 under an external load F, which implies the corresponding contact approach δ_0 along the axis of the force direction

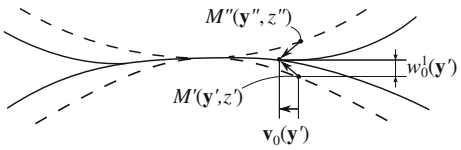

Fig. 2.4 Schematic diagram of the elastic contact interaction with allowance for tangential displacements on the contact interface

$$\mathbf{y}' + \mathbf{v}_0^{(1)}(\mathbf{y}') = \mathbf{y}'' + \mathbf{v}_0^{(2)}(\mathbf{y}''), \tag{2.15}$$

$$\varphi_2(\mathbf{y}'') + w_0^{(2)}(\mathbf{y}'') = -\big(\varphi_1(\mathbf{y}') + w_0^{(1)}(\mathbf{y}')\big) + \delta_0. \tag{2.16}$$

Here, $w_0^n(\mathbf{y})$ $(n = 1, 2)$ are the absolute values of the vertical displacements of the surface points of the n-th elastic layer (the normal displacements are assumed to be measured positive into each layer), $\mathbf{v}_0^n(\mathbf{y})$ $(n = 1, 2)$ are the tangential displacements of the surface points, and the relations $z' = -\varphi_1(\mathbf{y}')$ and $z'' = \varphi_2(\mathbf{y}'')$ were taken into account in writing Eq. (2.16).

From Eq. (2.15), it follows that

$$\mathbf{y}'' = \mathbf{y}' + \mathbf{v}_0^{(1)}(\mathbf{y}') - \mathbf{v}_0^{(2)}(\mathbf{y}''). \tag{2.17}$$

Now, identifying the coordinates $\mathbf{y}'$ and $\mathbf{y}''$ when evaluating the displacements of the contact points M′ and M″, we reduce Eq. (2.16) to a more simple form

$$\varphi_2\big(\mathbf{y} + \mathbf{v}_0^{(1)} - \mathbf{v}_0^{(2)}\big) + w_0^{(2)} + \varphi_1(\mathbf{y}) + w_0^{(1)} = \delta_0, \tag{2.18}$$

where $\mathbf{y} \in \omega$, and ω is the contact area. To simplify the notation, we dropped the primes on the left-hand side of Eq. (2.18).

The next simplifying step consists of linearizing Eq. (2.18). In this way, by taking Eq. (2.3) into account, we replace the above nonlinear contact condition by the linearized condition of frictionless contact

$$w_0^{(1)}(\mathbf{y}) + w_0^{(2)}(\mathbf{y}) = \delta_0 - \varphi(\mathbf{y}) - \nabla_y \varphi_2(\mathbf{y}) \cdot \big(\mathbf{v}_0^{(1)}(\mathbf{y}) - \mathbf{v}_0^{(2)}(\mathbf{y})\big), \tag{2.19}$$

where $\mathbf{y} \in \omega$, and the dot denotes the scalar product.

We note here that the choice of numbering of the elastic layers should assume that the modulus of the gradient $|\nabla_y \varphi_2(\mathbf{y})|$ is in a sense greater than $|\nabla_y \varphi_1(\mathbf{y})|$, or in other words, the surface of layer 1 (master surface) is assumed to be flatter than the surface of layer 2.

Observe that the refined contact condition (2.19) reduces to (1.40) in the case of a single elastic layer in contact with a punch, when $\varphi_1(\mathbf{y}) \equiv 0$ (the surface of the layer is flat) and $\varphi_2(\mathbf{y}) = \varphi(\mathbf{y})$, while $w_0^{(2)}(\mathbf{y}) \equiv 0$ and $\mathbf{v}_0^{(2)}(\mathbf{y}) \equiv 0$ (the punch is absolutely rigid).

Finally, by neglecting the effect of tangential displacements, we reduce Eq. (2.19) to the classical contact condition

$$w_0^{(1)}(\mathbf{y}) + w_0^{(2)}(\mathbf{y}) = \delta_0 - \varphi(\mathbf{y}), \quad \mathbf{y} \in \omega. \tag{2.20}$$

As negative stresses are not allowed at the contact interface, the contour Γ of the contact area ω is determined from the positiveness condition that the contact pressure $p(\mathbf{y})$ is positive inside ω and vanishes at its boundary, that is

$$p(\mathbf{y}) > 0, \quad \mathbf{y} \in \omega, \quad p(\mathbf{y}) = 0, \quad \mathbf{y} \in \Gamma. \tag{2.21}$$

Consequently, according to Newton's third law we have

$$p(\mathbf{y}) = -\sigma_{33}^{(1)}(\mathbf{y}, 0) = -\sigma_{33}^{(2)}(\mathbf{y}, 0),$$

where $\sigma_{33}^{(n)}$ $(n = 1, 2)$ is the normal stress in the n-th layer.

2.1.3 Governing Integral Equation

According to the principle of superposition, the contact problem (2.20), (2.21) can be recast as a Fredholm integral equation of the first kind with the kernel being a combination of the layer surface vertical displacements resulting from a normal point force. The corresponding Green's function problem for an elastic layer subjected to a point force applied to its surface is conveniety treated by the two-dimensional Fourier transform technique [6, 24].

By applying the standard Fourier transformation, the local indentation of the n-th elastic layer $(n = 1, 2)$ can be expressed in the form

$$w_0^{(n)}(\mathbf{y}) = \frac{1}{2\pi\theta_n} \iint_{-\infty}^{+\infty} \hat{p}(\alpha_1, \alpha_2) \frac{\mathscr{L}_n(\alpha h_n)}{\alpha} e^{-i(\alpha_1 y_1 + \alpha_2 y_2)} d\alpha_1 d\alpha_2, \tag{2.22}$$

where θ_n is a dimensional elastic constant, h_n is the thickness of the n-th layer, $\alpha = \sqrt{\alpha_1^2 + \alpha_2^2}$, and $\hat{p}(\alpha_1, \alpha_2)$ denotes the transform of the contact pressure, i.e.,

$$\hat{p}(\alpha_1, \alpha_2) = \frac{1}{2\pi} \iint_{-\infty}^{+\infty} p(y_1, y_2) e^{i(\alpha_1 y_1 + \alpha_2 y_2)} dy_1 dy_2. \tag{2.23}$$

In the case of a transversely isotropic elastic layer bonded to a flat rigid substrate, in accordance with the known solution [11], the kernel function is as follows:

$$\theta = \frac{A_{11}A_{33} - A_{13}^2}{(\gamma_1 + \gamma_2)A_{11}}, \tag{2.24}$$

$$\mathscr{L}(\lambda) = 1 + \frac{2\big[m_+(\gamma_1 e^{-2\lambda_1} + \gamma_2 e^{-2\lambda_2}) - \gamma_- m_- e^{-2\lambda_1 - 2\lambda_2} - 4\gamma_1\gamma_2 e^{-\lambda_1 - \lambda_2}\big]}{8\gamma_1\gamma_2 e^{-\lambda_1 - \lambda_2} + \gamma_- m_-(1 + e^{-2\lambda_1 - 2\lambda_2}) - \gamma_+ m_+(e^{-2\lambda_1} + e^{-2\lambda_2})}. \tag{2.25}$$

Here, γ_1 and γ_2 are the roots of the bi-quadratic equation

$$\gamma^4 A_{11}A_{44} - \gamma^2\big[A_{11}A_{33} - A_{13}(A_{13} + 2A_{44})\big] + A_{33}A_{44} = 0, \tag{2.26}$$

and we have employed the following notation:

$$\lambda_1 = \frac{\lambda}{\gamma_1}, \quad \lambda_2 = \frac{\lambda}{\gamma_2}, \quad \gamma_+ = \gamma_1 + \gamma_2, \quad \gamma_- = \gamma_1 - \gamma_2, \tag{2.27}$$

$$m_+ = m_2\gamma_1 + m_1\gamma_2, \quad m_- = m_2\gamma_1 - m_1\gamma_2,$$

$$m_1 = \frac{A_{11}\gamma_1^2 - A_{44}}{A_{13} + A_{44}}, \quad m_2 = \frac{A_{11}\gamma_2^2 - A_{44}}{A_{13} + A_{44}}.$$

Note that θ_n and $\mathscr{L}_n(\lambda)$ are obtained from (2.24) and (2.25) by suitable selection of the n-th layer elastic parameters.

In the case of a bonded isotropic layer, we have $\gamma_1 = \gamma_2 = 1$ and Eqs. (2.24), (2.25) for the kernel function reduce as follows [25]:

$$\theta = \frac{E}{2(1 - \nu^2)}, \tag{2.28}$$

$$\mathscr{L}(\lambda) = \frac{2\kappa \sinh 2\lambda - 4\lambda}{2\kappa \cosh 2\lambda + 1 + \kappa^2 + 4\lambda^2}. \tag{2.29}$$

Here, E is Young's modulus, ν is Poisson's ratio, $\kappa = 3 - 4\nu$ is Kolosov's constant.

The function $\mathscr{L}(\lambda)$ defined by formula (2.29), being continuous and positive for $\lambda \in (0, +\infty)$, satisfies the following asymptotic relations:

$$\begin{aligned} &\mathscr{L}(\lambda) = \mathscr{A}\lambda + O(\lambda^3), \quad \lambda \to 0; \\ &\mathscr{L}(\lambda) = 1 + O(\lambda^2 e^{-2\lambda}), \quad \lambda \to \infty. \end{aligned} \tag{2.30}$$

For the function $\mathscr{L}(\lambda)$ given by (2.25), the first asymptotic relation (2.30) can be checked directly, while the asymptotic remainder in the second relation can be easily replaced with $O(e^{-c_1\lambda})$, where c_1 is some positive constant. On the basis of these properties for each function $\mathscr{L}_n(\lambda)$, it can be shown [25] that the kernel

$$K_n(\mathbf{y}) = \int_0^{+\infty}\!\!\int \frac{\mathscr{L}_n(s)}{s} \cos\frac{s_1 y_1}{h_n} \cos\frac{s_2 y_2}{h_n}\, ds_1 ds_2, \tag{2.31}$$

where $s = \sqrt{s_1^2 + s_2^2}$, decreases at infinity as rapidly as $e^{-c_2 h_n^{-1}|\mathbf{y}|}$ for some $c_2 > 0$.

Note also that by changing the integration variables in (2.31), we obtain

$$K_n(\mathbf{y}) = h_n \int_0^{+\infty}\!\!\int \frac{\mathscr{L}_n(h_n\alpha)}{\alpha} \cos\alpha_1 y_1 \cos\alpha_2 y_2\, d\alpha_1 d\alpha_2, \tag{2.32}$$

where $\alpha = \sqrt{\alpha_1^2 + \alpha_2^2}$.

Now, using Eqs. (2.23) and (2.31), we rewrite Eq. (2.22) in the form

$$w_0^{(n)}(\mathbf{y}) = \frac{1}{\pi^2 h_n \theta_n} \iint_\omega p(\mathbf{y}') K_n(y_1 - y_1', y_2 - y_2')\, d\mathbf{y}', \tag{2.33}$$

where the contact pressure density $p(\mathbf{y})$ vanishing outside the contact area ω has already been taken into account.

Thus, substituting the expressions (2.33) ($n = 1, 2$) into the contact condition (2.20), and recalling (2.32), we arrive at the following integral equation:

$$\frac{1}{\pi^2 h\theta} \iint_\omega p(\mathbf{y}') K(y_1 - y_1', y_2 - y_2')\, d\mathbf{y}' = \delta_0 - \varphi(\mathbf{y}). \tag{2.34}$$

Here we have introduced the notation

$$h = h_1 + h_2, \quad \theta = \frac{\theta_1\theta_2}{\theta_1 + \theta_2}, \tag{2.35}$$

$$K(\mathbf{y}) = \int_0^{+\infty}\!\!\int \frac{\mathscr{L}(s)}{s} \cos\frac{s_1 y_1}{h} \cos\frac{s_2 y_2}{h}\, ds_1 ds_2, \tag{2.36}$$

$$\mathscr{L}(s) = \frac{\theta}{\theta_1}\mathscr{L}_1\Big(\frac{h_1}{h}s\Big) + \frac{\theta}{\theta_2}\mathscr{L}_2\Big(\frac{h_2}{h}s\Big). \tag{2.37}$$

Equation (2.34) represents the governing integral equation of the frictionless contact problem for two elastic layers bonded to slightly curved rigid substrates, where the substrate shapes are taken into account through the gap function $\varphi(\mathbf{y})$, and the curvature effect on the integral operator on the right-hand side is neglected.

2.2 Distributional Asymptotic Analysis

In this section, we develop an alternative for the perturbation approach to the contact problem in the thin-layer approximation considered in Sects. 1.2 and 1.4. It is assumed that the joint layer thickness h is small compared to the characteristic length of the contact area ω. Correspondingly, we require that

$$h = \varepsilon h_*, \quad \delta_0 = \varepsilon \delta_0^*, \quad R_1 = \varepsilon^{-1} R_1^*, \quad R_2 = \varepsilon^{-1} R_2^*, \tag{2.38}$$

where δ_0^*, R_1^*, and R_2^* are comparable with h_*, all being independent of ε. Note that we follow the same notation as in the previous chapter, wherever possible.

2.2.1 *Moment Asymptotic Expansion for the Integral Operator of the Frictionless Contact Problem for a Thin Elastic Layer*

A key point of the distributional asymptotic analysis is to make use of a large positive dimensionless parameter

$$\Lambda = \frac{1}{\varepsilon} \tag{2.39}$$

contained in the kernel (2.36) as a consequence of (2.37) and $(2.38)_1$. For this purpose, it is convenient to introduce dimensionless variables

$$\boldsymbol{\eta} = (\eta_1, \eta_2), \quad \eta_i = h_*^{-1} y_i, \quad i = 1, 2. \tag{2.40}$$

Substituting expressions (2.38) and (2.40) into Eq. (2.34), we readily obtain

$$\iint\limits_{\omega_*} p_*(\boldsymbol{\eta}') k\big(\Lambda(\eta_1 - \eta_1'), \Lambda(\eta_2 - \eta_2')\big)\, d\boldsymbol{\eta}' = \frac{\pi^2 \theta}{\Lambda^2 h_*} \big(\delta_0^* - \varphi^*(\boldsymbol{\eta})\big), \tag{2.41}$$

where we have introduced the notation

$$p_*(\boldsymbol{\eta}) = p(h_* \eta_1, h_* \eta_2), \tag{2.42}$$

$$k(\boldsymbol{\xi}) = \int\limits_0^{+\infty}\!\!\int \frac{\mathscr{L}(s)}{s} \cos s_1 \xi_1 \cos s_2 \xi_2 \, ds_1 ds_2, \tag{2.43}$$

$$\varphi^*(\boldsymbol{\eta}) = h_*^2 \big((2R_1^*)^{-1} \eta_1^2 + (2R_2^*)^{-1} \eta_2^2\big). \tag{2.44}$$

Following Argatov [7], we apply the so-called distributional asymptotic approach developed by Estrada and Kanwal [10]. Before proceeding, let us clarify the notation used. Let $\boldsymbol{\alpha} = (\alpha_1, \alpha_2)$ be a multi-index of nonnegative integers and $|\boldsymbol{\alpha}| = \alpha_1 + \alpha_2$, then for any $\boldsymbol{\eta} \in \mathbb{R}^2$ we put $\boldsymbol{\eta}^{\alpha} = \eta_1^{\alpha_1}\eta_2^{\alpha_2}$ and define

$$\mathbf{D}^{\alpha} f(\boldsymbol{\eta}) = \frac{\partial^{|\alpha|} f(\eta_1, \eta_2)}{\partial \eta_1^{\alpha_1} \partial \eta_2^{\alpha_2}}, \quad \mathbf{D}^0 f(\boldsymbol{\eta}) = f(\boldsymbol{\eta}).$$

We also employ the standard notation $\boldsymbol{\alpha}! = \alpha_1!\alpha_2!$ for the multi-index α, where $\alpha_1!$ denotes the factorial of α_1.

The moment asymptotic expansion can be written as follows [10]:

$$k(\Lambda\boldsymbol{\eta}) \sim \sum_{|\alpha|=0}^{\infty} \frac{(-1)^{|\alpha|}\mu_{\alpha}\mathbf{D}^{\alpha}\delta(\boldsymbol{\eta})}{\boldsymbol{\alpha}!\Lambda^{|\alpha|+2}}, \quad \Lambda \to \infty. \tag{2.45}$$

Here, $\mu_{\alpha} = \mu_{\alpha_1\alpha_2}$ are the moments of the generalized function $k(\boldsymbol{\xi})$ given by

$$\mu_{\alpha} = \left\langle k(\boldsymbol{\xi}), \boldsymbol{\xi}^{\alpha} \right\rangle = \iint_{-\infty}^{+\infty} k(\boldsymbol{\xi})\xi_1^{\alpha_1}\xi_2^{\alpha_2} d\xi_1 d\xi_2. \tag{2.46}$$

The asymptotic expansion (2.45) is valid in several important spaces of distributions (see, e.g., [10, 26]). In particular, it holds for distributions of rapid decay at infinity, and in particular, for the kernel (2.36).

The interpretation of the asymptotic relation (2.45) is in the distributional sense. This means that the asymptotic formula

$$\langle k(\Lambda\boldsymbol{\eta}), \phi(\boldsymbol{\eta})\rangle = \sum_{|\alpha|=0}^{N} \frac{\mu_{\alpha}\mathbf{D}^{\alpha}\phi(\mathbf{0})}{\boldsymbol{\alpha}!\Lambda^{|\alpha|+2}} + O(\Lambda^{-N-3}), \quad \Lambda \to \infty, \tag{2.47}$$

holds true for any $\phi(\boldsymbol{\eta})$ from the corresponding space of test functions.

For the kernel function (2.36), the application of (2.46) yields the moments

$$\begin{aligned}\mu_{\alpha} &= \iint_{-\infty}^{+\infty} \xi_1^{\alpha_1}\xi_2^{\alpha_2} \iint_{0}^{+\infty} \frac{\mathscr{L}(s)}{s} \cos s_1\xi_1 \cos s_2\xi_2 \, ds_1 ds_2 d\xi_1 d\xi_2 \\ &= \frac{1}{4} \iint_{-\infty}^{+\infty} \frac{\mathscr{L}(s)}{s} \prod_{j=1}^{2} \int_{-\infty}^{+\infty} \xi_j^{\alpha_j} \cos s_j\xi_j \, d\xi_j ds_1 ds_2. \end{aligned} \tag{2.48}$$

Using the well-known representation for Dirac's delta function

$$\delta(s_j) = \frac{1}{\pi} \int_0^{+\infty} \cos s_j \xi_j \, d\xi_j, \tag{2.49}$$

we find from Eq. (2.48), after integration by parts, that

$$\mu_{2k,2n-2k} = (-1)^n \pi^2 \iint_{-\infty}^{+\infty} \frac{\mathscr{L}(s)}{s} \delta^{(2k)}(s_1) \delta^{(2n-2k)}(s_2) \, ds_1 ds_2, \tag{2.50}$$

where $k = 0, 1, \ldots, n$ and $n \in \mathbb{N} \cup \{0\}$, and

$$\mu_\alpha = 0, \quad |\alpha| = 2n - 1, \quad n \in \mathbb{N};$$

$$\mu_\alpha = 0, \quad \alpha_1 = 2k - 1, \quad \alpha_2 = 2n - 2k + 1, \quad |\alpha| = 2n, \quad k = 1, 2, \ldots, n.$$

Now, by recalling the definition of the two-dimensional Dirac delta function $\delta(s_1, s_2) = \delta(s_1)\delta(s_2)$ and substituting the expansion

$$\frac{\mathscr{L}(s)}{s} = \mathscr{A}(1 + m_1 s^2 + m_2 s^4 + \ldots) \tag{2.51}$$

into Eq. (2.50), we find

$$\begin{aligned} \mu_{2k,2n-2k} &= (-1)^n \pi^2 \mathscr{A} m_n \iint_{-\infty}^{+\infty} (s_1^2 + s_2^2) \delta^{(2k)}(s_1) \delta^{(2n-2k)}(s_2) \, ds_1 ds_2 \\ &= (-1)^n \pi^2 \mathscr{A} m_n C_n^k 2^n k!(n-k)!, \end{aligned} \tag{2.52}$$

where C_n^k are binomial coefficients given by

$$C_n^k = \frac{n!}{k!(n-k)!}.$$

Then, from relations (2.45) and (2.52), where we may set $m_0 = 1$, we find

$$k(\Lambda \boldsymbol{\eta}) \sim \sum_{n=0}^{\infty} (-1)^n \pi^2 \mathscr{A} \frac{m_n}{\Lambda^{2n+2}} \sum_{k=0}^{n} C_n^k \frac{\partial^{2n} \delta(\boldsymbol{\eta})}{\partial \eta_1^{2k} \partial \eta_2^{2n-2k}}. \tag{2.53}$$

Correspondingly, substituting the moment asymptotic expansion (2.53) into the left-hand side of Eq. (2.41), we obtain

$$\iint\limits_{\omega_*} p_*(\boldsymbol{\xi})k\big(\Lambda(\boldsymbol{\eta}-\boldsymbol{\xi})\big)\,d\boldsymbol{\xi} \sim \sum_{n=0}^{\infty}(-1)^n\pi^2\mathscr{A}\frac{m_n}{\Lambda^{2n+2}}\sum_{k=0}^{n}C_n^k\frac{\partial^{2n}p_*(\boldsymbol{\eta})}{\partial\eta_1^{2k}\partial\eta_2^{2n-2k}}. \quad (2.54)$$

To simplify the right-hand side of (2.54), we recall that

$$\Delta_\eta^n \equiv \left(\frac{\partial^2}{\partial\eta_1^2}+\frac{\partial^2}{\partial\eta_2^2}\right)^n = \sum_{k=0}^{n}C_n^k\frac{\partial^{2n}}{\partial\eta_1^{2k}\partial\eta_2^{2n-2k}}.$$

Hence, by the above formula, we have

$$\frac{\Lambda^2 h_*}{\pi^2\theta}\iint\limits_{\omega_*} p_*(\boldsymbol{\eta}')k\big(\Lambda(\boldsymbol{\eta}-\boldsymbol{\eta}')\big)\,d\boldsymbol{\eta}' \sim \frac{\mathscr{A}h_*}{\theta}\sum_{n=0}^{\infty}(-1)^n\frac{m_n}{\Lambda^{2n}}\Delta_\eta^n p_*(\boldsymbol{\eta}). \quad (2.55)$$

Note that the above integral operator is normalized by the factor $\Lambda^2 h_*/(\pi^2\theta)$, such that the left-hand side of (2.55) represents the local indentation normalized by Λ when stretching the normal coordinate (see, in particular, (2.38) and (2.41)).

2.2.2 Asymptotic Solution of the Contact Problem for Slightly Curved Thin Compressible Elastic Layers

Using the notation (2.39) and the asymptotic expansions (2.55), we rewrite the governing integral equation (2.41) in the form

$$\frac{\mathscr{A}h_*}{\theta}\sum_{n=0}^{\infty}(-1)^n\varepsilon^{2n}m_n\Delta_\eta^n p_*(\boldsymbol{\eta}) \sim \delta_0^* - \varphi^*(\boldsymbol{\eta}). \quad (2.56)$$

The solution to Eq. (2.56) can be represented in the form of an asymptotic series in powers of ε as follows:

$$p_*(\boldsymbol{\eta}) \sim p_*^0(\boldsymbol{\eta}) + \varepsilon^2 p_*^1(\boldsymbol{\eta}) + \varepsilon^4 p_*^2(\boldsymbol{\eta}) + \dots . \quad (2.57)$$

The substitution of the asymptotic expansion (2.57) into Eq. (2.56) yields the following system of equations for the successive evaluation of its coefficients:

$$\frac{\mathscr{A}h_*}{\theta}m_0 p_*^0(\boldsymbol{\eta}) = \delta_0^* - \varphi^*(\boldsymbol{\eta}),$$

$$\sum_{j=0}^{k}(-1)^{k-j}m_{k-j}\Delta_\eta^{k-j}p_*^j(\boldsymbol{\eta}) = 0, \quad k = 1, 2, \dots .$$

It then follows that

$$p_*^0(\boldsymbol{\eta}) = \frac{\theta}{\mathscr{A}h_*}\big(\delta_0^* - \varphi^*(\boldsymbol{\eta})\big), \tag{2.58}$$

$$p_*^k(\boldsymbol{\eta}) = -\sum_{j=0}^{k-1}(-1)^{k-j} m_{k-j}\Delta_\eta^{k-j} p_*^j(\boldsymbol{\eta}), \quad k = 1, 2, \ldots . \tag{2.59}$$

We further note that formula (2.59) can be rewritten in the form

$$p_*^k(\boldsymbol{\eta}) = (-1)^k \frac{\theta}{\mathscr{A}h_*} M_k \Delta_\eta^k f_*(\boldsymbol{\eta}), \quad k = 0, 1, 2, \ldots, \tag{2.60}$$

where in light of (2.58) we have $M_0 = 1$ and $f_*(\boldsymbol{\eta}) = \delta_0^* - \varphi^*(\boldsymbol{\eta})$.

To evaluate the coefficients M_k introduced in (2.60), we consider the expansion reciprocal to (2.51), that is

$$\frac{s}{\mathscr{L}(s)} = \frac{1}{\mathscr{A}}(1 + M_1 s^2 + M_2 s^4 + \ldots). \tag{2.61}$$

It is easily proved by induction that for any positive integer k the recurrence relation that facilitates the calculation of the coefficients M_k in (2.61) from the coefficients of the the expansion (2.51) has the form

$$M_k = -\sum_{j=0}^{k-1} m_{k-j} M_j, \quad k = 1, 2, \ldots .$$

Alternatively, the above formula can be directly recovered from (2.59) and (2.60).

Thus, the constructed inner asymptotic expansion (2.57)–(2.59) is similar to the solution obtained earlier by Vorovich et al. [25].

Finally, in the case of the parabolic punch (2.14), we get by simple calculation

$$p_*^1(\boldsymbol{\eta}) = \frac{\theta m_1 h_*}{\mathscr{A}}\Big(\frac{1}{R_1^*} + \frac{1}{R_2^*}\Big), \quad p_*^k(\boldsymbol{\eta}) \equiv 0, \quad k = 2, 3, \ldots . \tag{2.62}$$

Upon substituting (2.58) and (2.62) into (2.57), our final result is

$$p_*(\boldsymbol{\eta}) \sim \frac{\theta}{\mathscr{A}h_*}\left(\delta_0^* + \varepsilon^2 2m_1\frac{h_*^2}{R^*} - h_*^2\Big(\frac{\eta_1^2}{2R_1^*} + \frac{\eta_2^2}{2R_2^*}\Big)\right), \tag{2.63}$$

where $R^* = 2R_1^*R_2^*/(R_1^* + R_2^*)$ is the harmonic mean of R_1^* and R_2^*.

2.2.3 Comparison of the Results Obtained by the Perturbation and Distributional Asymptotic Methods

Let us consider the case of a single layer in contact with a rigid punch, so that $\theta_2^{-1} = 0$, $\theta = \theta_1$, and $h = h_1$. According to the asymptotic expansion (2.55) (see also Eq. (2.56)), the local indentation of the elastic layer, i.e., the normal displacement of the surface points, is expressed by

$$w_0(\mathbf{y}) \sim \frac{\mathscr{A}h}{\theta} \sum_{n=0}^{\infty} (-1)^n m_n h^{2n} \Delta_y^n p(\mathbf{y}), \tag{2.64}$$

where $\mathscr{A}$ and m_n are dimensionless coefficients in the series expansion (2.51) for the kernel function $\mathscr{L}(s)/s$.

Formula (2.64) can be rewritten in the form

$$w_0(\mathbf{y}) \sim h \sum_{n=0}^{\infty} (-1)^n \mathscr{M}_n h^{2n} \Delta_y^n p(\mathbf{y}), \tag{2.65}$$

where $\mathscr{M}_n$ are dimensional coefficients in the expansion

$$\begin{aligned} \frac{\mathscr{L}(s)}{\theta s} &= \frac{\mathscr{A}}{\theta}(1 + m_1 s^2 + m_2 s^4 + \ldots) \\ &= \mathscr{M}_0 + \mathscr{M}_1 s^2 + \mathscr{M}_2 s^4 + \ldots . \end{aligned} \tag{2.66}$$

In particular, from (2.65), it follows that

$$w_0(\mathbf{y}) \simeq \mathscr{M}_0 h p(\mathbf{y}) - \mathscr{M}_1 h^3 \Delta_y p(\mathbf{y}). \tag{2.67}$$

On the other hand, based on the perturbation algorithm [14] in Sect. 1.2 (see formula (1.26)), we obtained the asymptotic expansion

$$w_0(\mathbf{y}) \simeq \frac{h}{A_{33}} p(\mathbf{y}) - \frac{h^3 A_{13}(A_{13} - A_{44})}{3A_{33}^2 A_{44}} \Delta_y p(\mathbf{y}). \tag{2.68}$$

By comparing (2.67) and (2.68), we arrive at the following relations, whose validity should be checked:

$$\mathscr{M}_0 = \frac{1}{A_{33}}, \quad \mathscr{M}_1 = \frac{A_{13}(A_{13} - A_{44})}{3A_{33}^2 A_{44}}. \tag{2.69}$$

Expanding the function (2.25) into a Maclaurin series, we find

$$\mathscr{A} = \frac{A_{44}(\gamma_1 - \gamma_2)^2(\gamma_1 + \gamma_2)}{\gamma_1^2\gamma_2^2\big[A_{11}(\gamma_1^2 + \gamma_2^2) - 2(A_{13} + 2A_{44})\big]}, \tag{2.70}$$

where γ_1 and γ_2 are the roots of the characteristic equation (2.26).

In order to establish the equality between A_{33}^{-1} and $\mathscr{M}_0 = \theta^{-1}\mathscr{A}$, where θ and $\mathscr{A}$ are given by (2.24) and (2.70), we make use of Vieta's theorem for the bi-quadratic equation (2.26) and the formulas

$$\gamma_1^2\gamma_2^2 = \frac{A_{33}}{A_{11}}, \quad \gamma_1^2 + \gamma_2^2 = \frac{A_{11}A_{33} - A_{13}(A_{13} + 2A_{44})}{A_{11}A_{44}},$$

$$\big(\gamma_1^2 - \gamma_2^2\big)^2 = \frac{(A_{11}A_{33} - A_{13}^2)(A_{11}A_{13} - 4A_{13}A_{44} - 4A_{44}^2 - A_{13}^2)}{A_{11}^2A_{44}^2}.$$

The check of the second equality in (2.69) is more tedious, because the expression for m_1, and correspondingly for $\mathscr{M}_1$, is much more cumbersome and is not written here for brevity.

2.3 Boundary-Layer Problem in the Compressible Case

Both the perturbation technique and the distributional asymptotic method provide approximate solutions, which are valid inside the contact area but do not describe the true solution near its contour, where a special approximate solution of the boundary-layer type should be constructed. In this section, the case of compressible layer materials is considered.

2.3.1 Variation of the Contact Area

The leading-order asymptotic approximation (2.58) for the contact pressure distribution density, i.e.,

$$p_*^0(\boldsymbol{\eta}) = \frac{\theta}{\mathscr{A}h_*}\big(\delta_0^* - \varphi^*(\boldsymbol{\eta})\big)_+, \tag{2.71}$$

determines the main approximation ω_*^0 to the sought-for contact area ω_* (in the dimensionless coordinates (2.40)).

It is obvious from Eq. (2.44) that the domain ω_*^0, which corresponds to the density (2.71), is elliptic. The major semiaxis and the eccentricity of the contour Γ_*^0 of the domain ω_*^0 will be denoted by a_* and e. By simple calculations we find

$$a_* = \frac{1}{h_*}\sqrt{2\delta_0^* R_1^*}, \quad e^2 = 1 - \frac{R_2^*}{R_1^*}. \tag{2.72}$$

Following the asymptotic procedure introduced by Aleksandrov [2], we consider the behavior of the integral (2.34) and its density in the neighborhood of the unknown contour Γ_* of the domain ω_*.

In light of (2.41), the integral equation (2.34) now takes the form

$$\iint\limits_{\omega_*} p_*(\boldsymbol{\xi}) k\big(\varepsilon^{-1}(\boldsymbol{\eta} - \boldsymbol{\xi})\big)\, d\boldsymbol{\xi} = \varepsilon^2 \frac{\pi^2 \theta}{h_*}\big(\delta_0^* - \varphi^*(\boldsymbol{\eta})\big). \tag{2.73}$$

Suppose $\eta_1 = f_1^*(s)$, $\eta_2 = f_2^*(s)$ is a natural parametrization of the contour Γ_*^0. We will assume that when traveling along Γ_*^0 in the direction of increasing s-coordinate, the region ω_*^0 enclosed by Γ_*^0 remains on the left. Then, the unit vector of the inward (with respect to the domain ω_*^0) normal to the contour Γ_*^0 is

$$\mathbf{n}^0(s) = -f_2^{*\prime}(s)\mathbf{e}_1 + f_1^{*\prime}(s)\mathbf{e}_2, \tag{2.74}$$

where the prime denotes differentiation with respect to s.

In a small neighborhood, $\Xi_\varepsilon^*(s)$, of the contour Γ_*^0, we introduce the local system of coordinates (s, n), associated with the Cartesian coordinates (η_1, η_2) by the formulas

$$\eta_1 = f_1^*(s) + n n_1^0(s), \quad \eta_2 = f_2^*(s) + n n_2^0(s), \tag{2.75}$$

where $\mathbf{n}^0(s) = \big(n_1^0(s), n_2^0(s)\big)$ is given by (2.74), and n is the distance (taking the sign into account) along the inward normal to the contour Γ_*^0.

Further, let us assume that the contour Γ_* of the contact area ω_* in the local coordinates is described by the equation

$$n = \Upsilon_\varepsilon^*(s), \tag{2.76}$$

where $\Upsilon_\varepsilon^*(s)$ is a function to be determined. We set

$$\Upsilon_\varepsilon^*(s) = \varepsilon \Upsilon^*(s). \tag{2.77}$$

In the neighborhood $\Xi_\varepsilon^*(s)$ of the point s, where $|\boldsymbol{\xi} - \boldsymbol{\eta}(s)| = O(\sqrt{\varepsilon}\rho^*(s))$ and $\rho^*(s) = \big[f_2^{*\prime\prime}(s) f_1^{*\prime}(s) - f_1^{*\prime\prime}(s) f_2^{*\prime}(s)\big]^{-1}$ is the radius of curvature of contour Γ_*^0 at the point s, we make in the integral (2.73) the following change of variables:

$$\xi_1 = f_1^{*\prime}(s) + n' n_1^0(s), \quad \xi_2 = f_2^{*\prime}(s) + n' n_2^0(s).$$

Next we introduce the so-called "fast" variables

$$\nu = \varepsilon^{-1} n, \quad \nu' = \varepsilon^{-1} n', \quad \sigma' = \varepsilon^{-1}(s' - s), \tag{2.78}$$

keeping the scale for the s-coordinate along Γ_*^0 unchanged. From now on, the "slow" variable s is considered to be fixed.

Thus, in the neighborhood $\Xi_\varepsilon^*(s)$, when $\varepsilon \to 0$, the following relations hold:

$$f_j^*(s') = f_j^*(s) + \varepsilon\sigma' f_j^{*\prime}(s) + O(\varepsilon^2), \quad n_j^0(s') = n_j^0(s) + O(\varepsilon), \quad j = 1, 2,$$

$$|\boldsymbol{\xi} - \boldsymbol{\eta}(s)| = \varepsilon\sqrt{(\sigma')^2 + (\nu - \nu')^2} + O(\varepsilon^2), \quad \rho^*(s') = \rho^*(s) + O(\varepsilon),$$

$$\Upsilon^*(s') = \Upsilon^*(s) + O(\varepsilon), \quad \frac{D(\xi_1, \xi_2)}{D(s', n')} = 1 - \frac{\varepsilon\nu'}{\rho^*(s + \varepsilon\sigma')} = 1 + O(\varepsilon).$$

Note, finally, that the above formulas are valid for any smooth contour Γ_*.

2.3.2 Boundary-Layer Integral Equation

Separating the principal asymptotic terms according to the previous formulas, we take the limit

$$\lim_{\varepsilon \to 0} k\big(\varepsilon^{-1}(\boldsymbol{\eta} - \boldsymbol{\xi})\big) = k\Big(\sigma' f_1^{*\prime}(s) + (\nu - \nu')n_1^0(s), \\ \sigma' f_2^{*\prime}(s) + (\nu - \nu')n_2^0(s)\Big). \tag{2.79}$$

By invoking the formulas (see Eq. (2.74))

$$f_1^{*\prime}(s) = \cos\psi, \quad f_2^{*\prime}(s) = \sin\psi, \quad n_1^0(s) = -\sin\psi, \quad n_2^0(s) = \cos\psi, \tag{2.80}$$

where ψ provides an angular parameterization to the ellipse Γ_*^0, it can be shown directly that the right-hand side of the relation (2.79) is equal to $k(\sigma', \nu' - \nu)$.

Indeed, in light of (2.43), we have

$$k(\boldsymbol{\xi}) = \frac{1}{4} \iint_{-\infty}^{+\infty} \frac{\mathscr{L}(s)}{s} e^{\mathrm{i}(s_1\xi_1 + s_2\xi_2)} ds_1 ds_2, \tag{2.81}$$

and by making the substitutions

$$s_1 = t_1 \cos\psi - t_2 \sin\psi, \quad s_2 = t_1 \sin\psi + t_2 \cos\psi,$$

$$\frac{D(s_1, s_2)}{D(t_1, t_2)} = 1, \quad s \equiv \sqrt{s_1^2 + s_2^2} = \sqrt{t_1^2 + t_2^2} \equiv t,$$

we find that the representation (2.81) can be written in the form

$$k(\boldsymbol{\xi}) = \frac{1}{4} \iint_{-\infty}^{+\infty} \frac{\mathscr{L}(t)}{t} \cos\bigl[\xi_1(t_1 \cos\psi - t_2 \sin\psi) + \xi_2(t_1 \sin\psi + t_2 \cos\psi)\bigr]\, dt_1 dt_2, \tag{2.82}$$

provided that $t^{-1}\mathscr{L}(t)$ is an even function for $t \in (-\infty, +\infty)$.

Thus, from Eqs. (2.79), (2.80), and (2.82) it follows immediately that

$$\lim_{\varepsilon \to 0} k(\varepsilon^{-1}(\boldsymbol{\eta} - \boldsymbol{\xi})) = k(\sigma', \nu' - \nu), \tag{2.83}$$

while on the other hand, we see on the right-hand side of Eq. (2.73) that

$$\delta_0^* - \varphi^*(\boldsymbol{\eta}) = h_*^2\bigl[\varepsilon\nu b_1^*(s) + \varepsilon^2\nu^2 b_2^*(s)\bigr], \tag{2.84}$$

where

$$\begin{aligned} b_1^*(s) &= -\frac{f_1^*(s)n_1^0(s)}{R_1^*} - \frac{f_2^*(s)n_2^0(s)}{R_2^*}, \\ 2b_2^*(s) &= -\frac{n_1^0(s)^2}{R_1^*} - \frac{n_2^0(s)^2}{R_2^*}. \end{aligned} \tag{2.85}$$

Hence, by approximating the contact pressure density as $p_\varepsilon^*(\boldsymbol{\xi}) \sim q_\varepsilon^*(s, \nu')$ in the neighborhood $\Xi_\varepsilon^*(s)$ of the boundary of the contact area (see, for example, [3]) and letting $\varepsilon \to 0$ in light of Eqs. (2.73), (2.75)–(2.78), (2.83) and (2.84), we arrive at the following integral equation:

$$\int_{\Upsilon^*(s)}^{+\infty} q^{**}(s, \nu') M(\nu' - \nu)\, d\nu' = \pi\theta h_* b_1^*(s)\nu. \tag{2.86}$$

Here, $q^{**}(s, \nu) = \varepsilon^{-1} q_\varepsilon^*(s, \nu)$, and we have introduced the notation

$$M(t) = \frac{1}{\pi} \int_{-\infty}^{+\infty} k(\sigma', t)\, d\sigma'.$$

Observe that the s-coordinate is present in Eq. (2.86) as a parameter.

Making use of formula (2.49), we represent the above formula in the form

$$M(t) = \int_0^{+\infty} \frac{\mathscr{L}(u)}{u} \cos ut \, du. \tag{2.87}$$

Finally, in addition to Eq. (2.86), which the boundary-layer solution $q^{**}(s, \nu)$ must satisfy, it is necessary to obey the contact pressure positivity condition (2.21). Hence, the function $\Upsilon^*(s)$ satisfies the equation

$$q^{**}(s, \Upsilon^*(s)) = 0. \tag{2.88}$$

Otherwise, we would contradict the assumption that the contact must be made over the whole domain ω_*.

2.3.3 Aleksandrov's Approximation

We note that the integral equation (2.86) is of the Wiener–Hopf type [23] and can be solved in closed form (see, in particular, [1, 5]). However, since a simple factorization for the function $w^{-1}\mathscr{L}(w)$ of the complex variable $w = u + \mathrm{i}\nu$ is not available, it is not possible to obtain the exact solution of Eq. (2.86) in a simple form. Thus, the approximate version of the Wiener–Hopf method has to be used. Confining our considerations to the first-order approximation, we replace the function $\mathscr{L}(u)$ by the following simple algebraic approximation [3]:

$$\tilde{\mathscr{L}}(u) = u \frac{\sqrt{u^2 + B^2}}{u^2 + C}. \tag{2.89}$$

It can easily be shown that the functions $u^{-1}\mathscr{L}(u)$ and $u^{-1}\tilde{\mathscr{L}}(u)$ satisfy Koiter's conditions [18] that they should have the same limits for s tending to zero and infinity, provided that the following relation holds:

$$\frac{B}{C} = \mathscr{A}. \tag{2.90}$$

In addition, following Aleksandrov [3], we select the constants B and C in such a manner that

$$\lim_{u \to 0} \frac{d^2}{du^2} \left(\frac{u}{\mathscr{L}(u)} - \frac{u}{\tilde{\mathscr{L}}(u)} \right) = 0.$$

From here it immediately follows that

$$\frac{m_1}{\mathscr{A}} = \frac{C}{2B^3} - \frac{1}{B}, \tag{2.91}$$

where (see formula (2.51))

$$\mathscr{A} = \lim_{u\to 0} \frac{\mathscr{L}(u)}{u}, \quad m_1 = \frac{1}{2\mathscr{A}} \lim_{u\to 0} \frac{d^2}{du^2} \frac{\mathscr{L}(u)}{u}. \tag{2.92}$$

From (2.24), (2.66), and (2.70), we have

$$\mathscr{A} = \frac{A_{11}A_{33} - A_{13}^2}{(\gamma_1 + \gamma_2)A_{11}A_{33}}, \quad m_1 = \frac{A_{13}(A_{13} - A_{44})}{3A_{33}A_{44}},$$

where γ_1 and γ_2 are the roots of the characteristic equation (2.26).

At the same time, Eqs. (2.90) and (2.91) yield the following formulas (cf. [12]):

$$B = \frac{1}{\mathscr{A} + \sqrt{\mathscr{A}^2 + 2m_1}}, \quad C = \frac{1}{\mathscr{A}\left[\mathscr{A} + \sqrt{\mathscr{A}^2 + 2m_1}\right]}.$$

Recall that $\mathscr{A}$ and m_1 are defined by (2.92).

In the case of isotropic layer bonded to a rigid foundation (see formula (2.29)), we have

$$\mathscr{A} = \frac{1 - 2\nu}{2(1 - \nu)^2},$$

where ν is Poisson's ratio of the layer material. From the above, it is readily seen (see also Fig. 2.5) that the asymptotic constant $\mathscr{A}$ approaches zero when the material becomes incompressible.

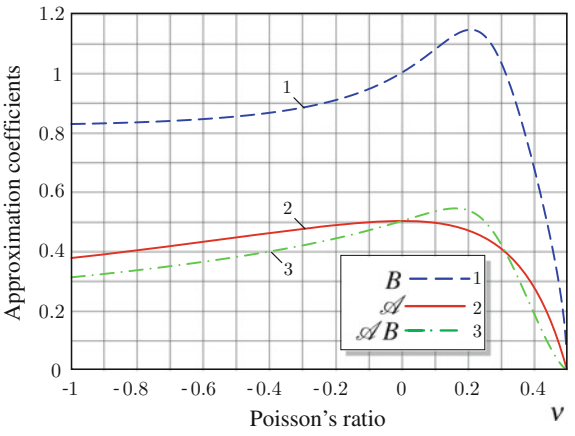

Fig. 2.5 Variation of the approximation coefficients in the isotropic case

Let us consider a Wiener–Hopf integral equation of the first kind

$$\int_0^{+\infty} \varphi(\tau')\tilde{M}(\tau' - \tau)\, d\tau' = \psi(\tau), \quad 0 \le \tau < \infty, \tag{2.93}$$

with the kernel

$$\tilde{M}(\tau) = \int_0^{+\infty} \frac{\tilde{\mathscr{L}}(u)}{u} \cos u\tau\, du, \tag{2.94}$$

where the kernel function $\tilde{\mathscr{L}}(u)$ is given by (2.89).

It can be shown [5, 25] that for the right-hand sides of Eq. (2.93)

$$\psi_0(\tau) = 1, \quad \psi_1(\tau) = \tau, \quad \psi_2(\tau) = \tau^2,$$

the corresponding special solutions are, respectively,

$$\varphi_0(\tau) = \frac{1}{\mathscr{A}} \operatorname{erf}\sqrt{B\tau} + \frac{e^{-B\tau}}{\sqrt{\pi \mathscr{A} \tau}}, \tag{2.95}$$

$$\varphi_1(\tau) = \frac{\tau}{\mathscr{A}} \operatorname{erf}\sqrt{B\tau} - \frac{e^{-B\tau}}{\sqrt{\pi B\tau}}\left(1 - \frac{\tau}{\mathscr{A}} - \frac{1}{2\sqrt{\mathscr{A}B}}\right), \tag{2.96}$$

$$\varphi_2(\tau) = \left(\frac{\tau^2}{\mathscr{A}} + \frac{1}{\mathscr{A}B^2} - \frac{2}{B}\right) \operatorname{erf}\sqrt{B\tau} - \frac{e^{-B\tau}}{\sqrt{\pi B\tau}}\left(\frac{1}{B} - \frac{3}{4B\sqrt{\mathscr{A}B}} + \frac{\tau}{2\mathscr{A}B} - \frac{\tau^2}{\mathscr{A}}\right). \tag{2.97}$$

Here, $\operatorname{erf}(x)$ is the error function, which is defined as

$$\operatorname{erf}(x) = \frac{2}{\sqrt{\pi}} \int_0^x e^{-t^2} dt.$$

The above solutions are illustrated in Fig. 2.6. Observe that after the normalization these functions depend on the dimensionless elastic constants $\mathscr{A}$ and B via their product $\mathscr{A}B$, while the dependence on the coordinate τ comes as $B\tau$.

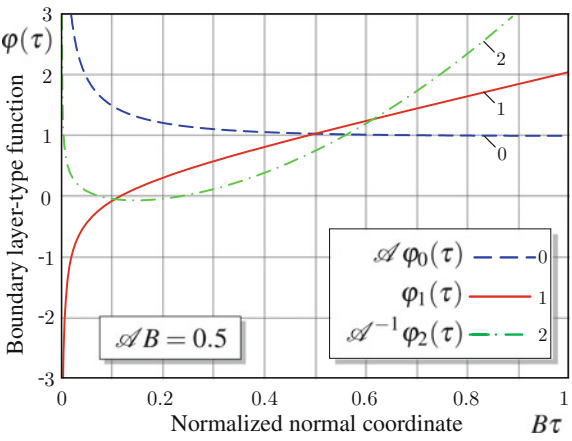

Fig. 2.6 Aleksandrov's approximate boundary layer-type solutions (2.95)–(2.97)

2.3.4 Boundary-Layer in the Compressible Case

We replace $\mathscr{L}(s)$ in the integral (2.87) by $\tilde{\mathscr{L}}(s)$, substitute the corresponding kernel $\tilde{M}(t)$ defined by (2.94) into Eq. (2.86), and implement in the resulting equation a change of variables

$$\nu = \Upsilon^*(s) + \tau, \quad \nu' = \Upsilon^*(s) + \tau'.$$

In this way the integral equation (2.86) can be transformed into the form

$$\int_0^{+\infty} \tilde{q}^{**}(s, \Upsilon^*(s) + \tau')\tilde{N}(\tau' - \tau)\, d\tau' = \pi\theta h_* b_1^*(s)(\Upsilon^*(s) + \tau). \tag{2.98}$$

In the case (2.89), make use of Aleksandrov's results [3] (see, in particular, formulas (2.95) and (2.96)), thus producing the solution to Eq. (2.98) in the form

$$\frac{\tilde{q}^{**}(s, \Upsilon^*(s) + \tau)}{\theta h_* b_1^*(s)} = \frac{\tau}{\mathscr{A}} \operatorname{erf}\sqrt{B\tau} - \frac{1}{\sqrt{\pi B\tau}} e^{-B\tau}\left(1 - \frac{\sqrt{C}}{2B} - \frac{\tau}{\mathscr{A}}\right) + \frac{\Upsilon^*(s)}{\mathscr{A}} \operatorname{erf}\sqrt{B\tau} + \frac{\Upsilon^*(s)}{\sqrt{\pi\mathscr{A}\tau}} e^{-B\tau}. \tag{2.99}$$

Since, in light of (2.88), the function (2.99) must satisfy Eq. (2.88), the boundary layer is found to be

$$\tilde{q}^{**}(s, \nu) = \frac{\theta h_* b_1^*(s)}{\mathscr{A}} \left\{ \nu \operatorname{erf}\sqrt{B(\nu - \Upsilon^*(s))} \right.$$

$$+\sqrt{\frac{\nu-\Upsilon^*(s)}{\pi B}}\exp\bigl(-B[\nu-\Upsilon^*(s)]\bigr)\Bigr\}, \tag{2.100}$$

provided that

$$\Upsilon^*(s)=\sqrt{\frac{\mathscr{A}}{B}}-\frac{1}{2B}. \tag{2.101}$$

Note that in the axisymmetric case the obtained boundary layer (2.100) is essentially similar to the leading term of the asymptotics for the contact pressure density constructed in [25] (see formula (49.11)). The resultant of the contact pressure (with the boundary layer taken into account) was evaluated in [8]. It is also worth noting [3] that the relations (2.90) and (2.91) are necessary for the correct matching between the boundary-layer solution (2.100) and the inner asymptotic solution (2.71).

2.4 Incompressible Transversely Isotropic Elastic Material

The generalized Hooke's law (1.1), establishing a linear relationship between components of the stress tensor $\boldsymbol{\sigma}$, and components of the tensor of infinitesimal strains $\boldsymbol{\varepsilon}$, can be written in the tensor form

$$\boldsymbol{\varepsilon}=\mathbf{S}:\boldsymbol{\sigma} \tag{2.102}$$

or alternatively in the matrix form as follows [21]:

$$\begin{pmatrix}\varepsilon_{11}\\ \varepsilon_{22}\\ \varepsilon_{33}\\ \varepsilon_{23}\\ \varepsilon_{13}\\ \varepsilon_{12}\end{pmatrix}=\begin{bmatrix}S_{1111} & S_{1221} & S_{1331} & 0 & 0 & 0\\ S_{1221} & S_{1111} & S_{1331} & 0 & 0 & 0\\ S_{1331} & S_{1331} & S_{3333} & 0 & 0 & 0\\ 0 & 0 & 0 & 2S_{2233} & 0 & 0\\ 0 & 0 & 0 & 0 & 2S_{2233} & 0\\ 0 & 0 & 0 & 0 & 0 & 2S_{1122}\end{bmatrix}\begin{pmatrix}\sigma_{11}\\ \sigma_{22}\\ \sigma_{33}\\ \sigma_{23}\\ \sigma_{13}\\ \sigma_{12}\end{pmatrix}. \tag{2.103}$$

Here, S_{ijkl} are the components of the fourth-rank compliance tensor. For a transversely isotropic material the compliance matrix involves only five independent entries, so that $2S_{1122}=S_{1111}-S_{1221}$, while S_{1111}, S_{1221}, S_{1331}, S_{3333}, and S_{2233} are expressed in terms of engineering elastic constants by the formulas

$$S_{1111}=\frac{1}{E},\quad S_{1221}=-\frac{\nu}{E},\quad S_{1331}=-\frac{\nu'}{E'},\quad S_{3333}=\frac{1}{E'},\quad S_{2233}=\frac{1}{4G'}, \tag{2.104}$$

where E and E' are Young's moduli in the plane of transverse isotropy and in the direction normal to it, ν and ν' are Poisson's ratios characterizing the lateral strain response in the plane of transverse isotropy to a stress acting parallel or normal to

it, G' is the shear modulus in planes normal to the plane of transverse isotropy. We note also that the in-plane shear modulus is given by $G = E/[2(1+\nu)]$.

2.4.1 Stress-Strain Relations for Incompressible Material

Recall that a solid's resistance to all-round compression is characterized by the bulk modulus, K. For a homogeneous anisotropic material occupying a volume V, the bulk modulus is defined as the ratio of the small hydrostatic pressure increase, Δp, to the resulting relative decrease of the volume, $\Delta V/V$.

Since under the assumption of small deformations, $\Delta V/V = \varepsilon_{11} + \varepsilon_{22} + \varepsilon_{33}$, by substituting $\sigma_{11} = \sigma_{22} = \sigma_{33} = -\Delta p$ into Eq. (2.103), we readily obtain

$$\frac{1}{K} = 2S_{1111} + 2S_{1221} + 4S_{1331} + S_{3333}.$$

In terms of the stiffnesses, the bulk modulus is given by

$$K = \frac{A_{33}(A_{11} + A_{12}) - 2A_{13}^2}{A_{11} + A_{12} - 4A_{13} + 2A_{33}},$$

where A_{ij} are determined by formulas (1.3).

According to (2.104), the above formula can be recast in terms of the engineering constants as

$$K = \left(\frac{2(1-\nu)}{E} + \frac{1-4\nu'}{E'} \right)^{-1}, \tag{2.105}$$

which in the isotropic case reduces to

$$K = \frac{E}{3(1-2\nu)}.$$

If the material is incompressible, then the bulk modulus is infinite. At the same time, the incompressibility condition

$$\varepsilon_{11} + \varepsilon_{22} + \varepsilon_{33} = 0 \tag{2.106}$$

must be satisfied for arbitrary stress $\boldsymbol{\sigma}$ satisfying the equilibrium equations.

As was shown by Itskov and Aksel [15], the incompressibility condition (2.106) written in the form $\mathbf{I} : \boldsymbol{\varepsilon} = 0$, where $\mathbf{I}$ is the second-order identity tensor, implies that $\mathbf{S} : \mathbf{I} = \mathbf{0}$. The last tensor equation, in the general case, imposes 6 additional constrains on the compliance tensor $\mathbf{S}$. In the case of transverse isotropy, only two of these incompressibility conditions are not identically satisfied.

For the compliance matrix to be positive definite, it is required that

$$E > 0, \quad E' > 0, \quad G' > 0, \quad \nu^2 \leq 1,$$

and

$$\nu'^2 \leq \frac{E'(1-\nu)}{2E}. \tag{2.107}$$

By considering the special case of a hydrostatic loading, when $\sigma_{11} = \sigma_{22} = \sigma_{33} = p$ and $\sigma_{23} = \sigma_{13} = \sigma_{12} = 0$, it can be easily verified that the incompressibility condition (2.106) is achieved if

$$\frac{2}{E} - \frac{2\nu}{E} - \frac{4\nu'}{E'} + \frac{1}{E'} = 0. \tag{2.108}$$

Following [13], we eliminate the Poisson's ratio ν between (2.107) and (2.108) to get $(\nu' - 0.5)^2 \leq 0$, from which it immediately follows that $\nu' = 0.5$. Now, substituting this value into Eq. (2.108), we obtain $\nu = 1 - 0.5(E/E')$.

Thus, for an incompressible transversely isotropic material only 3 material constants remain independent and the following relations hold [13, 15]:

$$\nu' = \frac{1}{2}, \quad \nu = 1 - \frac{E}{2E'}. \tag{2.109}$$

These relations determine the incompressibility limit. Consequently, the condition of positive definiteness of the compliance tensor reduces to

$$E < 4E'. \tag{2.110}$$

It should be emphasized that whereas the stress-strain relations for compressible materials can be obtained through the direct inversion of Hooke's law (2.103), leading to $\boldsymbol{\sigma} = \mathbf{C} : \boldsymbol{\varepsilon}$ with the stiffness tensor $\mathbf{C} = \mathbf{S}^{-1}$, for incompressible materials the constitutive relation is given by

$$\boldsymbol{\sigma} = \mathbf{C} : \boldsymbol{\varepsilon} - p\mathbf{I}, \tag{2.111}$$

where evaluation of the super-symmetric fourth-order elasticity tensor $\mathbf{C}$ requires a special procedure developed in [15].

In the matrix form, Eq. (2.111) can be rewritten as

$$\begin{pmatrix} \sigma_{11} \\ \sigma_{22} \\ \sigma_{33} \\ \sigma_{23} \\ \sigma_{13} \\ \sigma_{12} \end{pmatrix} = \begin{bmatrix} a_{11} & a_{12} & a_{13} & 0 & 0 & 0 \\ a_{12} & a_{11} & a_{13} & 0 & 0 & 0 \\ a_{13} & a_{13} & a_{33} & 0 & 0 & 0 \\ 0 & 0 & 0 & 2a_{44} & 0 & 0 \\ 0 & 0 & 0 & 0 & 2a_{44} & 0 \\ 0 & 0 & 0 & 0 & 0 & 2a_{66} \end{bmatrix} \begin{pmatrix} \varepsilon_{11} \\ \varepsilon_{22} \\ \varepsilon_{33} \\ \varepsilon_{23} \\ \varepsilon_{13} \\ \varepsilon_{12} \end{pmatrix} - \begin{pmatrix} p \\ p \\ p \\ 0 \\ 0 \\ 0 \end{pmatrix}, \tag{2.112}$$

where, according to Itskov and Aksel [15], we have

$$a_{11} = \frac{4E'(2E + E')}{9(4E' - E)}, \quad a_{33} = \frac{4}{9}E', \quad a_{12} = \frac{2E'(2E' - 5E)}{9(4E' - E)},$$

$$a_{13} = -\frac{2}{9}E', \quad a_{44} = G', \quad a_{66} = G. \tag{2.113}$$

As a consequence of $(2.109)_2$, the in-plane shear modulus is given by

$$G = \frac{EE'}{4E' - E}. \tag{2.114}$$

Thus, for an incompressible transversely isotropic material, the number of independent material constants is equal to 3, and E, E', and G' can be taken, for instance.

Note also that according to $(2.109)_2$ and (2.110), the in-plane Poisson's ratio satisfies the inequality $\nu > -1$.

In the isotropic case, when $E = E'$, $G = G'$, and $\nu = \nu'$, Eqs. (2.109) and (2.114) imply that $\nu = 0.5$ and $G = E/3$. Consequently, Eq. (2.113) yield $a_{11} = a_{33} = 4E/9$ and $a_{12} = a_{13} = -2E/9$. Taking into account the incompressibility condition (2.106), we represent the stress-strain relations as follows, where no summation is implied by the repeated index:

$$\sigma_{ii} = 2G\varepsilon_{ii} - p, \quad \sigma_{ij} = 2G\varepsilon_{ij}, \quad i \neq j, \quad i, j = 1, 2, 3. \tag{2.115}$$

Notice that Eq. (2.115) represent a usual form of the constitutive relations for isotropic incompressible material [9, 28].

Finally, the unknown hydrostatic pressure parameter p in the constitutive law (2.112) should be determined from the incompressibility condition (2.106).

2.4.2 *Isotropically Compressible Transversely Isotropic Materials*

Note that for an incompressible material under a uniform hydrostatic pressure not only the trace of the strain tensor is equal to zero, but also the deviatoric part of the strain tensor vanishes. Following [15], we consider anisotropic materials which under a uniform hydrostatic pressure exhibit strictly isotropic volumetric response. In this case, the bulk modulus, K, of such an isotropically compressible material is independent of the stress state and represents its intrinsic property.

For an isotropically compressible transversely isotropic material, the number of independent material constants is equal to 4, while E, E', G', and K can be taken, in this instance. As a result, the following relations hold [15]:

$$\nu' = \frac{1}{2} - \frac{E'}{6K}, \quad \nu = 1 - \frac{E}{2}\Big(\frac{1}{E'} + \frac{1}{3K}\Big), \quad G = \frac{E'E}{4E' - E - \dfrac{E'E}{3K}}.$$

Correspondingly, the constitutive relations can be written in the form

$$\begin{pmatrix} \sigma_{11} \\ \sigma_{22} \\ \sigma_{33} \\ \sigma_{23} \\ \sigma_{13} \\ \sigma_{12} \end{pmatrix} = \begin{bmatrix} c_{11} & c_{12} & c_{13} & 0 & 0 & 0 \\ c_{12} & c_{11} & c_{13} & 0 & 0 & 0 \\ c_{13} & c_{13} & c_{33} & 0 & 0 & 0 \\ 0 & 0 & 0 & 2c_{44} & 0 & 0 \\ 0 & 0 & 0 & 0 & 2c_{44} & 0 \\ 0 & 0 & 0 & 0 & 0 & 2c_{66} \end{bmatrix} \begin{pmatrix} \varepsilon_{11} \\ \varepsilon_{22} \\ \varepsilon_{33} \\ \varepsilon_{23} \\ \varepsilon_{13} \\ \varepsilon_{12} \end{pmatrix} - \begin{pmatrix} p \\ p \\ p \\ 0 \\ 0 \\ 0 \end{pmatrix}, \tag{2.116}$$

$$p = -K(\varepsilon_{11} + \varepsilon_{22} + \varepsilon_{33}), \tag{2.117}$$

where, according to Itskov and Aksel [15], c_{ij} are given by

$$\begin{aligned} c_{11} &= \frac{1}{3D}\Big(\frac{2}{E'} + \frac{1}{E} - \frac{1}{3K}\Big), \quad c_{33} = \frac{1}{3D}\Big(\frac{4}{E} - \frac{1}{E'} - \frac{1}{3K}\Big), \\ c_{12} &= \frac{1}{6D}\Big(\frac{2}{E} - \frac{5}{E'} + \frac{1}{3K}\Big), \quad c_{13} = \frac{1}{6D}\Big(\frac{1}{E'} - \frac{4}{E} + \frac{1}{3K}\Big), \\ D &= \frac{3}{4E'}\Big(\frac{4}{E} - \frac{1}{E'}\Big) - \frac{1}{6K}\Big(\frac{1}{E'} + \frac{2}{E}\Big) + \frac{1}{36K^2}. \end{aligned} \tag{2.118}$$

Thus, for isotropically compressible materials, the case of weak compressibility can be treated as the limit as $E'/K \to 0$.

2.5 Deformation of a Thin Incompressible Transversely Isotropic Elastic Layer Bonded to a Rigid Substrate

Let us consider a thin transversely isotropic elastic layer of uniform thickness, h, ideally bonded to a rigid substrate and loaded by a normal load, q, (see Fig. 2.7).

According to the perturbation analysis performed in Sect. 1.2, the leading-order asymptotic approximation for the displacement field is given by the following formulas (see Eqs. (1.18), (1.19), (1.22)–(1.24)):

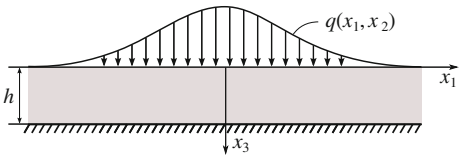

Fig. 2.7 An elastic layer of uniform thickness bonded to a rigid substrate and carrying a normal load

$$\mathbf{v} \simeq \varepsilon^2 \left(\frac{A_{13}+A_{44}}{2A_{33}}(1-\zeta)^2 - \frac{A_{13}}{A_{33}}(1-\zeta) \right) \frac{h_*}{A_{44}} \nabla_\eta q, \tag{2.119}$$

$$w \simeq \varepsilon \frac{h_* q}{A_{33}}(1-\zeta) + \varepsilon^3 \left\{ \frac{A_{13}(A_{13}+2A_{44})}{6A_{33}^2}(1-\zeta)^3 - \frac{A_{13}(A_{13}+A_{44})}{2A_{33}^2}(1-\zeta)^2 + \frac{A_{13}A_{44}}{2A_{33}^2}(1-\zeta) \right\} \frac{h_*}{A_{44}} \Delta_\eta q. \tag{2.120}$$

For any transversely isotropic material, we have

$$\frac{A_{13}}{A_{33}} = \frac{E\nu'}{E'(1-\nu)}.$$

When the material approaches the incompressible limit, the right-hand side of the above relation tends to 1 (see Eq. (2.109)), while the ratio A_{44}/A_{33} vanishes. Hence, formulas (2.119) and (2.120) reduce to the following:

$$\mathbf{v} \simeq \varepsilon^2 \left(\frac{1}{2}(1-\zeta)^2 - (1-\zeta) \right) \frac{h_*}{a_{44}} \nabla_\eta q, \tag{2.121}$$

$$w \simeq \varepsilon^3 \left\{ \frac{1}{6}(1-\zeta)^3 - \frac{1}{2}(1-\zeta)^2 \right\} \frac{h_*}{a_{44}} \Delta_\eta q. \tag{2.122}$$

Note that $a_{44} = A_{44}$ is the out-of-plane shear modulus.

2.5.1 *Perturbation Analysis of the Deformation Problem for a Thin Incompressible Elastic Layer*

From another point of view, the problem under consideration can be formulated based on the constitutive relation (2.112). Indeed, the equilibrium equations yield

$$a_{66}\Delta_y \mathbf{v} + (a_{11}-a_{66})\nabla_y \nabla_y \cdot \mathbf{v} + a_{44}\frac{\partial^2 \mathbf{v}}{\partial z^2} + (a_{13}+a_{44})\frac{\partial}{\partial z}\nabla_y w - \nabla_y p = \mathbf{0},$$

$$a_{44}\Delta_y w + a_{33}\frac{\partial^2 w}{\partial z^2} + (a_{13}+a_{44})\frac{\partial}{\partial z}\nabla_y \cdot \mathbf{v} - \frac{\partial p}{\partial z} = 0, \tag{2.123}$$

and the incompressibility condition is

$$\nabla_y \cdot \mathbf{v} + \frac{\partial w}{\partial z} = 0. \tag{2.124}$$

In the case of the elastic layer bonded to a rigid substrate, the boundary conditions at the layer bottom surface are

$$\mathbf{v}\big|_{z=h} = \mathbf{0}, \quad w\big|_{z=h} = 0, \tag{2.125}$$

while at the upper surface, under the assumption of normal loading, we have

$$\sigma_{13}\big|_{z=0} = \sigma_{23}\big|_{z=0} = 0, \quad \sigma_{33}\big|_{z=0} = -q.$$

The last boundary conditions can be rewritten as

$$\nabla_y w + \frac{\partial \mathbf{v}}{\partial z}\bigg|_{z=0} = \mathbf{0}, \tag{2.126}$$

$$a_{13}\nabla_y \cdot \mathbf{v} + a_{33}\frac{\partial w}{\partial z} - p\bigg|_{z=0} = -q. \tag{2.127}$$

Assuming that the elastic layer is relatively thin and $h = \varepsilon h_*$, we introduce the stretched normal coordinate

$$\zeta = \varepsilon^{-1} h_*^{-1} z$$

and the dimensionless in-plane coordinates

$$\boldsymbol{\eta} = (\eta_1, \eta_2), \quad \eta_i = h_*^{-1} y_i, \quad i = 1, 2.$$

Correspondingly, the system of equations (2.123), (2.124) with the boundary conditions (2.125)–(2.127) takes the form

$$\varepsilon^{-2} a_{44}\frac{\partial^2 \mathbf{v}}{\partial \zeta^2} + \varepsilon^{-1}(a_{13} + a_{44})\nabla_\eta \frac{\partial w}{\partial \zeta} + a_{66}\Delta_\eta \mathbf{v} + (a_{11} - a_{66})\nabla_\eta \nabla_\eta \cdot \mathbf{v} - h_* \nabla_\eta p = \mathbf{0}, \tag{2.128}$$

$$\varepsilon^{-2} a_{33}\frac{\partial^2 w}{\partial \zeta^2} + \varepsilon^{-1}\left((a_{13} + a_{44})\nabla_\eta \cdot \frac{\partial \mathbf{v}}{\partial \zeta} - h_* \frac{\partial p}{\partial \zeta}\right) + a_{44}\Delta_\eta w = 0, \tag{2.129}$$

$$\varepsilon^{-1}\frac{\partial w}{\partial \zeta} + \nabla_\eta \cdot \mathbf{v} = 0, \tag{2.130}$$

$$\mathbf{v}\big|_{\zeta=1} = \mathbf{0}, \quad w\big|_{\zeta=1} = 0, \tag{2.131}$$

$$\varepsilon^{-1}\frac{\partial \mathbf{v}}{\partial \zeta} + \nabla_\eta w\bigg|_{\zeta=0} = \mathbf{0}, \tag{2.132}$$

$$\frac{1}{h_*}\left(\varepsilon^{-1}a_{33}\frac{\partial w}{\partial \zeta}+a_{13}\nabla_\eta\cdot\mathbf{v}\right)-p\Big|_{\zeta=0}=-q. \tag{2.133}$$

In light of (2.119), (2.120), and (2.133), the asymptotic ansatz for the solution to the system (2.128)–(2.133) is represented in the form

$$\mathbf{v}\simeq\varepsilon^2\mathbf{v}^1(\boldsymbol{\eta},\zeta), \tag{2.134}$$

$$w\simeq\varepsilon^3 w^2(\boldsymbol{\eta},\zeta), \tag{2.135}$$

$$p\simeq q+\varepsilon^2 p^2(\boldsymbol{\eta},\zeta). \tag{2.136}$$

Substituting (2.134)–(2.136) into Eq. (2.128)–(2.133), we arrive at the problem

$$a_{44}\frac{\partial^2\mathbf{v}^1}{\partial\zeta^2}=h_*\nabla_\eta q,\quad \zeta\in(0,1),\quad \mathbf{v}^1\big|_{\zeta=1}=\mathbf{0},\quad \frac{\partial\mathbf{v}^1}{\partial\zeta}\Big|_{\zeta=0}=\mathbf{0}; \tag{2.137}$$

$$a_{33}\frac{\partial^2 w^2}{\partial\zeta^2}=-(a_{13}+a_{44})\nabla_\eta\cdot\frac{\partial\mathbf{v}^1}{\partial\zeta}+h_*\frac{\partial p^2}{\partial\zeta},\quad \zeta\in(0,1), \tag{2.138}$$

$$w^2\big|_{\zeta=1}=0,\quad a_{33}\frac{\partial w^2}{\partial\zeta}+a_{13}\nabla_\eta\cdot\mathbf{v}^1-h_*p^2\Big|_{\zeta=0}=0, \tag{2.139}$$

$$\frac{\partial w^2}{\partial\zeta}+\nabla_\eta\cdot\mathbf{v}^1=0,\quad \zeta\in(0,1). \tag{2.140}$$

From (2.137), it immediately follows that

$$\mathbf{v}^1(\boldsymbol{\eta},\zeta)=-\frac{h_*}{2a_{44}}(1-\zeta^2)\nabla_\eta q(\boldsymbol{\eta}). \tag{2.141}$$

Now, integrating Eq. (2.138), we get

$$a_{33}\frac{\partial w^2}{\partial\zeta}=-(a_{13}+a_{44})\nabla_\eta\cdot\mathbf{v}^1+h_*p^2+C_2, \tag{2.142}$$

where C_2 is an integration constant, which may depend on η_1 and η_2.

By taking into account (2.140) and (2.141), we rewrite Eq. (2.142) in the form

$$\begin{aligned}h_*p^2&=-C_2+(a_{13}+a_{44}-a_{33})\nabla_\eta\cdot\mathbf{v}^1\\&=-C_2-\frac{a_{13}+a_{44}-a_{33}}{2a_{44}}(1-\zeta^2)h_*\Delta_\eta q(\boldsymbol{\eta}).\end{aligned} \tag{2.143}$$

Again, making use of Eqs. (2.140) and (2.141), we transform the boundary condition $(2.139)_2$ into

$$h_* p^2\big|_{\zeta=0} = (a_{13} - a_{33})\nabla_\eta \cdot \mathbf{v}^1\big|_{\zeta=0} = -\frac{a_{13} - a_{33}}{2a_{44}} h_* \Delta_\eta q(\boldsymbol{\eta}). \tag{2.144}$$

From (2.143) and (2.144), it follows that

$$C_2 = a_{44}\nabla_\eta \cdot \mathbf{v}^1\big|_{\zeta=0} = -\frac{h_*}{2}\Delta_\eta q(\boldsymbol{\eta}). \tag{2.145}$$

Hence, the substitution of (2.145) into Eq. (2.143) yields

$$p^2 = \frac{\Delta_\eta q(\boldsymbol{\eta})}{2a_{44}}\big(a_{44} - (a_{44} + a_{13} - a_{33})(1 - \zeta^2)\big). \tag{2.146}$$

Finally, in light of (2.141), (2.145), and (2.146), Eq. (2.142) takes the form

$$\frac{\partial w^2}{\partial \zeta} = \frac{h_*}{2a_{44}}(1 - \zeta^2)\Delta_\eta q(\boldsymbol{\eta}), \tag{2.147}$$

which after integration (with the boundary condition $(2.139)_1$ at the bottom layer surface taken into account) becomes

$$w^2(\boldsymbol{\eta}, \zeta) = -\frac{h_*}{6a_{44}}(1 - \zeta)^2(2 + \zeta)\Delta_\eta q(\boldsymbol{\eta}). \tag{2.148}$$

It is easy to see that formulas (2.141) and (2.148) completely agree with (2.121) and (2.122), respectively, which are obtained from (2.119) and (2.120) for the compressible layer by passing to the incompressible limit.

Thus, the displacements of the surface points of the bonded incompressible elastic layer can be approximated by the following leading-order asymptotic formulas:

$$\mathbf{v}\big|_{\zeta=0} \simeq -\varepsilon^2 \frac{h_*}{2a_{44}}\nabla_\eta q(\boldsymbol{\eta}), \tag{2.149}$$

$$w\big|_{\zeta=0} \simeq -\varepsilon^3 \frac{h_*}{3a_{44}}\Delta_\eta q(\boldsymbol{\eta}). \tag{2.150}$$

After recovering the dimensional coordinates, these relations take the form

$$\mathbf{v}\big|_{z=0} \simeq -\frac{h^2}{2a_{44}}\nabla_y q(\mathbf{y}), \tag{2.151}$$

$$w\big|_{z=0} \simeq -\frac{h^3}{3a_{44}}\Delta_y q(\mathbf{y}). \tag{2.152}$$

We note that the two-term asymptotic approximation for the hydrostatic pressure is given by formulas (2.136) and (2.146).

Finally, we observe that the case of a practically incompressible elastic layer (weakly compressible layer) requires special consideration [22].

2.5.2 Local Indentation of a Thin Weakly Compressible Elastic Layer

Following Mishuris [22], we briefly consider the case of a weakly compressible material, where

$$\frac{G'}{K} \ll 1. \tag{2.153}$$

Excluding the hydrostatic pressure p from Eqs. (2.116) and (2.117), we obtain

$$\begin{pmatrix} \sigma_{11} \\ \sigma_{22} \\ \sigma_{33} \\ \sigma_{23} \\ \sigma_{13} \\ \sigma_{12} \end{pmatrix} = \begin{bmatrix} C_{11} & C_{12} & C_{13} & 0 & 0 & 0 \\ C_{12} & C_{11} & C_{13} & 0 & 0 & 0 \\ C_{13} & C_{13} & C_{33} & 0 & 0 & 0 \\ 0 & 0 & 0 & 2C_{44} & 0 & 0 \\ 0 & 0 & 0 & 0 & 2C_{44} & 0 \\ 0 & 0 & 0 & 0 & 0 & 2C_{66} \end{bmatrix} \begin{pmatrix} \varepsilon_{11} \\ \varepsilon_{22} \\ \varepsilon_{33} \\ \varepsilon_{23} \\ \varepsilon_{13} \\ \varepsilon_{12} \end{pmatrix}, \tag{2.154}$$

where we have introduced the notation (with the coefficients c_{ij} given by (2.118))

$$C_{1j} = c_{1j} + K, \quad j = 1, 2, 3, \quad C_{33} = c_{33} + K, \quad C_{44} = G', \quad C_{66} = G.$$

Observe that the form of constitutive equation (2.154) for isotropically compressible materials is similar to that of Eq. (1.2) for compressible materials. Therefore, the following asymptotic approximations hold (see Sect. 1.2):

$$\mathbf{v}_0 \simeq -\varepsilon^2 \frac{h_*(C_{13} - C_{44})}{2C_{33}C_{44}} \nabla_\eta p, \tag{2.155}$$

$$w_0 \simeq \varepsilon \frac{h_* p}{C_{33}} - \varepsilon^3 \frac{h_* C_{13}(C_{13} - C_{44})}{3C_{33}^2 C_{44}} \Delta_\eta p. \tag{2.156}$$

Recall that the in-plane coordinates (η_1, η_2) are dimensionless (see Eq. (1.13)).

Thus, in light of (2.153), the elastic constants entering formulas (2.155), (2.156) can be expanded as

$$\frac{C_{13} - C_{44}}{C_{33}C_{44}} = \frac{1}{G'} - \frac{2E' + 3G'}{3G'K} + O\left(\frac{E'^2}{G'K^2}\right),$$

$$\frac{1}{C_{33}} = \frac{1}{K} - \frac{4E'}{9K^2} + O\left(\frac{E'^2}{K^3}\right), \tag{2.157}$$

$$\frac{C_{13}(C_{13} - C_{44})}{C_{33}^2 C_{44}} = \frac{1}{G'} - \frac{4E' + 3G'}{3G'K} + O\left(\frac{E'^2}{G'K^2}\right). \tag{2.158}$$

Let L be a characteristic length of the contact area, so that $\varepsilon = h/L$ and $h = \varepsilon h^*$. Thus, following three cases can then occur:

(1) Compressible layer when $(h/L)^2 \ll G'/K$ or, equivalently, $K \ll G'(L/h)^2$;
(2) Weakly compressible layer when $G'/K \sim (h/L)^2$;
(3) Practically incompressible layer when $G'/K \ll (h/L)^2$.

In the first and third cases, respectively, the first or second term in the asymptotic formula (2.156) becomes dominant. In the second case, both terms on the right-hand side of (2.156) are equally important.

Finally, we would like to emphasize that in the case of a thin elastic layer, the effect of incompressibility depends on the degree of its thinness.

2.6 Boundary-Layer Problem in the Incompressible Case

The case of incompressible materials requires a special consideration. In this section, the Wiener–Hopf method will be applied to the corresponding boundary-layer integral equation with a polynomial right-hand side.

2.6.1 Transformation of the Governing Integral Equation

In light of (2.22), Eq. (2.34) can be rewritten in the form

$$\frac{h}{\pi^2\theta} \iint\limits_{\omega} p(\mathbf{y}') K_*(y_1 - y_1', y_2 - y_2')\, d\mathbf{y}' = \mathscr{W}_0(\mathbf{y}), \tag{2.159}$$

where we have introduced the notation

$$K_*(\mathbf{y}) = \iint\limits_0^{+\infty} \frac{\mathscr{L}(s)}{s^3} \cos\frac{s_1 y_1}{h} \cos\frac{s_2 y_2}{h}\, ds_1 ds_2,$$

$$\mathscr{W}_0(\mathbf{y}) = \frac{1}{2\pi} \iint\limits_{-\infty}^{+\infty} \frac{1}{\alpha^2} \sum_{n=1}^{2} \hat{w}_0^{(n)}(\alpha_1, \alpha_2) e^{-i(\alpha_1 y_1 + \alpha_2 y_2)} d\alpha_1 d\alpha_2. \tag{2.160}$$

Recall that the kernel function $\mathscr{L}(s)$ is given by (2.37), and $\hat{w}_0^{(n)}(\alpha_1, \alpha_2)$ denotes the Fourier transform of the local indentation of the n-th elastic layer.

In the contact problem, the sum of the local indentation functions $w_0^{(1)}(\mathbf{y})$ and $w_0^{(2)}(\mathbf{y})$, whose Fourier transforms appear in (2.160), is known only inside the contact area ω according to the contact condition (2.20), whereas outside ω the normal surface displacements $w_0^{(n)}(\mathbf{y})$ are determined by the contact pressure density $p(\mathbf{y})$, which is not given a priori, even in the case of fixed contact area. Thus, the right-hand side of Eq. (2.159) is also unknown.

By definition (see formula (2.160)), we can represent the right-hand side of the governing integral equation (2.159) in the form

$$\mathscr{W}_0(\mathbf{y}) = \mathscr{W}_0^1(\mathbf{y}) + \mathscr{W}_0^0(\mathbf{y}), \tag{2.161}$$

where $\mathscr{W}_0^0(\mathbf{y})$ is a harmonic function, and $\mathscr{W}_0^1(\mathbf{y})$ satisfies the problem

$$-\Delta_y \mathscr{W}_0^1(\mathbf{y}) = \delta_0 - \varphi(\mathbf{y}), \quad \mathbf{y} \in \omega; \quad \mathscr{W}_0^1(\mathbf{y}) = 0, \quad \mathbf{y} \in \Gamma. \tag{2.162}$$

Denoting by $C_0(s)$ an arbitrary function of the arc length coordinate s along the contour Γ_*, we have

$$\Delta_\eta \mathscr{W}_0^0(h_*\boldsymbol{\eta}) = 0, \quad \boldsymbol{\eta} \in \omega_*; \quad \mathscr{W}_0^0(h_*\boldsymbol{\eta}) = C_0(s), \quad s \in \Gamma_*, \tag{2.163}$$

where ω_* is the contact area in the dimensionless coordinates (2.40).

Note that as

$$-\int\limits_{-\infty}^{+\infty}\int\left(\frac{\partial^2 v}{\partial y_1^2} + \frac{\partial^2 v}{\partial y_2^2}\right) e^{i(\alpha_1 y_1 + \alpha_2 y_2)} dy_1 dy_2 = (\alpha_1^2 + \alpha_2)\hat{v}(\alpha_1, \alpha_2),$$

Equation (2.159) can be regarded as the result of application of the inverse Laplace operator $-\Delta_\eta^{-1}$ to the original governing integral equation (2.34).

2.6.2 Boundary-Layer Integral Equation

Performing the same analysis as in Sects. 2.3.1 and 2.3.2, but differing in that the local coordinates (s, n) are introduced in a small neighborhood of the contour Γ_*, we arrive at the following integral equation:

$$\int\limits_0^{+\infty} q^{**}(s, \nu') M_*(\nu' - \nu)\, d\nu' = \pi\theta h_* C_0(s). \tag{2.164}$$

Here, $q^{**}(s,\nu)=\varepsilon^{-1}q_\varepsilon^*(s,\nu)$, and the kernel is given by

$$M_*(t)=\int_0^{+\infty}\frac{\mathscr{L}(u)}{u^3}\cos ut\,du. \tag{2.165}$$

Let us consider Eq. (2.164) with a special right-hand side

$$\int_0^{+\infty}\phi_j(\tau)M_*(\tau-t)\,dt=t^j,\quad 0<t<\infty, \tag{2.166}$$

where $j=0,1,2,\ldots$

Recall (in particular, see formula (2.66)) that in the incompressible case, the function $\mathscr{L}(u)$ satisfies the following asymptotic relationships:

$$\mathscr{L}(u)=\mu_1u^3+\mu_2u^5+O(u^7),\quad u\to 0, \tag{2.167}$$

$$\mathscr{L}(u)=1+O(e^{-c_1u}),\quad u\to\infty. \tag{2.168}$$

The dimensionless coefficients μ_k are given by

$$\mu_k=\theta\mathscr{M}_k, \tag{2.169}$$

where the dimensional quantities $\mathscr{M}_k$ are introduced in (2.66).

Therefore, Eq. (2.166) possesses a solution such that

$$\phi_j(t)\sim\omega_jt^{-3/2},\quad t\to 0, \tag{2.170}$$

$$\phi_j(t)=O(t^j),\quad t\to\infty. \tag{2.171}$$

Let us reformulate the problem (2.166) into the distribution type formulation. Specifically, by introducing a small parameter $\varepsilon>0$, we consider the problem

$$\int_0^{\infty}\phi_j^\varepsilon(\tau)M_*(\tau-t)\,dt=t^je^{-\varepsilon t},\quad 0<t<\infty, \tag{2.172}$$

and will pass to the limit $\varepsilon\to 0$ later. We omit, where clarity permits, the subscript and superscript in ϕ_j^ε, using the common notation ϕ and clarifying where necessary.

Consequently,, we will look for a solution to Eq. (2.172) satisfying the following assumption at infinity:

$$\phi(t)=O(t^j)e^{-\varepsilon t},\quad t\to\infty. \tag{2.173}$$

Under the assumptions made, we extend by zero the definition of the function $\phi(t)$ for $t \in (-\infty, 0)$ and apply the Fourier transformation to Eq. (2.173), obtaining the following classical Wiener–Hopf type equation as a result:

$$\overline{\phi}_+(s)\overline{M}_*(s) = r_-(s) + b_j \frac{1}{(\mathrm{i}s - \varepsilon)^{1+j}}. \tag{2.174}$$

Here an overbar denotes the Fourier transform, $b_0 = -1$, $b_1 = 1$, $b_2 = -2$, and

$$\overline{\phi}_+(s) = \int_{-\infty}^{+\infty} \phi(t) e^{\mathrm{i}st} dt = \int_0^{\infty} \phi(t) e^{\mathrm{i}st} dt$$

is the analytic function in the upper half plane behaving at infinity as

$$\overline{\phi}_+(\mathrm{i}\xi) = O(\xi^{1/2}), \quad \xi \to \infty, \tag{2.175}$$

Note that, when writing (2.175), we take the condition (2.170) into account.

From (2.165), we directly compute

$$\overline{M}_*(s) = \frac{\pi}{s^3} \mathscr{L}(s), \tag{2.176}$$

and thus $\overline{M}_*(s)$ is bounded at zero, while from (2.173), we only conclude that

$$\overline{\phi}_+(s) = O\left(\frac{1}{(s + \mathrm{i}\varepsilon)^{1+j}}\right), \quad s \to -\mathrm{i}\varepsilon. \tag{2.177}$$

We now assume that $\varepsilon \to 0$ and transform Eq. (2.174) into the equivalent form

$$\overline{\phi}_+(s) L_*(s) N(s) = r_-(s) + \frac{\tilde{b}_j}{(s + \mathrm{i}0)^{1+j}}, \tag{2.178}$$

where $\tilde{b}_0 = \mathrm{i}$, $\tilde{b}_1 = -1$, $\tilde{b}_2 = -2\mathrm{i}$, and

$$L_*(s) = \frac{\pi}{(s^2 + A^2)\sqrt{s^2 + B^2}}, \tag{2.179}$$

$$N(s) = \frac{\mathscr{L}(s)(s^2 + A^2)\sqrt{s^2 + B^2}}{s^3}. \tag{2.180}$$

It can easily be checked that $N(s)$ is an even function, and is always positive along the real axis, while for any positive values of A and B it satisfies the condition

$$N(s) = 1 + O(s^{-2}), \quad s \to \pm\infty. \tag{2.181}$$

Thus, the function (2.180) allows for factorization along the real axis in the form

$$N(s) = \frac{N_+(s)}{N_-(s)},$$

where

$$N_\pm(s) = \exp\left\{\frac{1}{2\pi \mathrm{i}} \int_{-\infty}^{\infty} \frac{\log N(t)}{t - s} dt\right\}, \quad \pm \Im s > 0.$$

The functions $N_\pm(s)$ possess the following asymptotic representations:

$$N_\pm(s) = 1 - \frac{1}{\mathrm{i}\pi s} \int_0^\infty \log N(t) dt + o(s^{-1}), \quad \pm \mathrm{i}s \to \infty, \tag{2.182}$$

$$N_\pm(s) = \exp\left\{\frac{1}{\pi} \int_0^\infty \arg N(t) \frac{dt}{t}\right\} + O(s), \quad s \to 0. \tag{2.183}$$

We now introduce the notation

$$L_*^\pm(s) = \frac{\sqrt{\pi}}{(A \mp \mathrm{i}s)\sqrt{B \mp \mathrm{i}s}}, \tag{2.184}$$

so that the Wiener–Hopf equation (2.178) can be rewritten in the equivalent form

$$\overline{\phi}_+(s) L_*^+(s) N_+(s) = F_-(s)\left(r_-(s) + \frac{\tilde{b}_j}{(s + \mathrm{i}0)^{1+j}}\right), \tag{2.185}$$

where

$$F_-(s) = \frac{N_-(s)}{L_*^-(s)}. \tag{2.186}$$

In light of (2.182)–(2.184), we have

$$F_-(s) = O(1), \quad s \to 0; \quad F_-(s) \sim (\mathrm{i}s)^{3/2}, \quad s \to -\mathrm{i}\infty. \tag{2.187}$$

Note that the branch cuts in the respective square roots are taken along the imaginary axis from the points $-\mathrm{i}$ to $+\infty$ and from $+\mathrm{i}$ to $-\infty$ for the functions $L_*^+(s)$ and $L_*^-(s)$, respectively. Thus, the function $F_-(s)$ is analytic in the neighbourhood of the zero point and can be expanded in the Taylor series as follows:

$$F_-(s) = \sum_{k=0}^{j} F_-^{(k)}(0) \frac{s^k}{k!} + O(s^{k+1}), \quad s \to 0. \tag{2.188}$$

Finally, we transform Eq. (2.185) to the form

$$\overline{\phi}_+(s)L_*^+(s)N_+(s) = F_-(s)\overline{r}_-(s) + \frac{\tilde{b}_j}{(s+\mathrm{i}0)^{1+j}}\left(F_-(s) - \sum_{k=0}^{j} F_-^{(k)}(0)\frac{s^k}{k!}\right) + \frac{\tilde{b}_j}{(s+\mathrm{i}0)^{1+j}}\sum_{k=0}^{j} F_-^{(k)}(0)\frac{s^k}{k!}. \tag{2.189}$$

The left-hand side of this equation is an analytic function in the upper half-plane having a pole at the point $s = 0$. The right-hand side of (2.189) consists of three terms where the first two are analytic functions in the lower half-plane. Finally, the third term is a plus function having a pole at the point $s = 0$.

Taking into account the assumed behavior of the sought for solution, we can write it in the form

$$\overline{\phi}_+(s) = \frac{\tilde{b}_j}{(s+\mathrm{i}0)^{1+j}L_*^+(s)N_+(s)}\sum_{k=0}^{j} F_-^{(k)}(0)\frac{s^k}{k!}, \tag{2.190}$$

$$\overline{r}_-(s) = -\frac{\tilde{b}_j}{(s+\mathrm{i}0)^{1+j}F_-(s)}\left(F_-(s) - \sum_{k=0}^{j} F_-^{(k)}(0)\frac{s^k}{k!}\right). \tag{2.191}$$

Note that $\overline{r}_-(s)$ is analytic in the lower half plane containing the real axis and the common analyticity strip $0 < \operatorname{Im} s < \chi$, for some positive χ.

2.6.3 Special Solutions of the Boundary-Layer Integral Equation

For further analysis, it is crucial to consider an auxiliary function

$$\Phi_j(t) = \frac{1}{2\pi}\int_{-\infty}^{+\infty} \frac{e^{-\mathrm{i}st}ds}{(s+\mathrm{i}0)^{j+1}L_*^+(s)N_+(s)}. \tag{2.192}$$

Here it is worth mentioning that the functions $\Phi_j(t)$, $j = 0, 1, 2, \ldots$, enjoy a recurrent property

$$\Phi_j'(t) = -\mathrm{i}\Phi_{j-1}(t), \quad \Phi_j(t) = \mathrm{i}\Phi_{j+1}'(t). \tag{2.193}$$

We continue by analyzing the asymptotic behavior of $\Phi_j(t)$ at zero and infinity. Note that the function $1/[L_*^+(s)N_+(s)]$ is analytic near the zero point, and thus

$$\frac{1}{L_*^+(s)N_+(s)} = \sum_{k=0}^{j} C_k^{(0)} s^k + O(s^{j+1}), \quad s \to 0.$$

This allows us to consider the following representation of the function $\Phi_j(t)$, suitable for large values of the variable t:

$$\Phi_j(t) = \frac{1}{2\pi} \int_{-\infty}^{\infty} \left(\frac{1}{L_*^+(s)N_+(s)} - \sum_{k=0}^{j} C_k^{(0)} s^k \right) \frac{e^{-\mathrm{i}st} ds}{(s+\mathrm{i}0)^{j+1}} + \sum_{k=0}^{j} C_k^{(0)} P_{j-k}(t). \tag{2.194}$$

The polynomials $P_m(t)$ are given by the formula

$$P_m(t) = \frac{1}{2\pi} \int_{-\infty}^{\infty} \frac{e^{-\mathrm{i}st} ds}{(s+\mathrm{i}0)^{m+1}}, \quad m = 0, 1, 2, \ldots. \tag{2.195}$$

In particular, it immediately follows that

$$P_0(t) = -\mathrm{i}, \quad P_1(t) = -t, \quad P_2(t) = \frac{\mathrm{i}t^2}{2},$$

and thus formula (2.194) yields

$$\Phi_j(t) = \sum_{k=0}^{j} C_k^{(0)} P_{j-k}(t) + o(1), \quad t \to \infty. \tag{2.196}$$

To investigate the asymptotic behavior of the function $\Phi_j(t)$ near the point $t = 0$, we observe that

$$\frac{1}{L_*^+(s)N_+(s)} = -\mathrm{i}s \left(C_0^{(\infty)} (-\mathrm{i}s)^{1/2} + C_1^{(\infty)} (-\mathrm{i}s)^{-1/2} \right) + O\left((-\mathrm{i}s)^{-1/2}\right), \tag{2.197}$$

as $-\mathrm{i}s \to +\infty$. Correspondingly, as $t \to 0$, we arrive at the following estimate:

$$\Phi_j(t) = \frac{-\mathrm{i}}{2\pi} \int_{-\infty}^{\infty} \frac{(C_0^{(\infty)} (-\mathrm{i}s)^{1/2} + C_1^{(\infty)} (-\mathrm{i}s)^{-1/2}) e^{-\mathrm{i}st}}{(s+\mathrm{i}0)^j} ds + O(1). \tag{2.198}$$

Here the integration pass should be further deformed to impart a classical sense to the Fourier transform.

As a result, we obtain the asymptotic relationships

$$\Phi_0(t) = \frac{\mathrm{i}}{2\sqrt{\pi}} C_0^{(\infty)} t^{-3/2} - \frac{\mathrm{i}}{\sqrt{\pi}} C_1^{(\infty)} t^{-1/2} + O(1), \quad t \to 0, \tag{2.199}$$

$$\Phi_1(t) = -\frac{1}{\sqrt{\pi}} C_0^{(\infty)} t^{-1/2} + O(1), \quad t \to 0, \tag{2.200}$$

$$\Phi_2(t) = O(1), \quad t \to 0, \tag{2.201}$$

where we have used the identity

$$\frac{1}{2\pi} \int_{-\infty}^{\infty} (-\mathrm{i}s)^{-1/2} e^{-\mathrm{i}st}\, ds = \frac{1}{\sqrt{\pi}} t^{-1/2}. \tag{2.202}$$

We are now ready to return to the general solution (2.190) and consider three cases $j = 0, 1, 2$ separately.

The case $j = 0$. Due to the fact that $\tilde{b}_0 = \mathrm{i}$, the respective solution takes the form

$$\phi_0(t) = \mathrm{i} F_-(0) \Phi_0(t), \tag{2.203}$$

and based on the results presented above for the asymptotic behavior of the function $\Phi_j(t)$ at infinity (see (2.194)), we conclude that

$$\phi_0(t) = \frac{F_-(0)}{N_+(0) L_*^+(0)} + o(1), \quad t \to \infty. \tag{2.204}$$

In light of (2.167), (2.179), and (2.180), formula (2.204) can be recast as

$$\phi_0(t) = \frac{1}{\mu_1} + o(1), \quad t \to \infty. \tag{2.205}$$

Note that in the isotropic incompressible case (2.29), we have

$$\mathscr{L}(u) = \frac{\sinh 2u - 2u}{\cosh 2u + 1 + 2u^2} \tag{2.206}$$

and (see also formula (2.167))

$$\mathscr{L}(u) = \frac{2}{3} u^3 - \frac{6}{5} u^5 + O(u^7), \quad u \to 0.$$

Thus, $\mu_1 = 2/3$, and the asymptotic formula (2.205) agrees with the corresponding result obtained by Aleksandrov [4].

On the other hand, taking into account the asymptotic behavior (2.199) of the function $\Phi_0(t)$ at the zero point, we readily see that

$$\phi_0(t) \sim -\frac{F_-(0)}{2\sqrt{\pi}} C_0^{(\infty)} t^{-3/2}, \quad t \to 0.$$

Considering (2.180), (2.186) and (2.197), the above formula takes the form

$$\phi_0(t) \sim -\frac{A\sqrt{B}N_-(0)}{2\pi^{3/2}} t^{-3/2}, \quad t \to 0. \tag{2.207}$$

The case $j = 1$. Now, since $\tilde{b}_1 = -1$, Eq. (2.189) has the following solution:

$$\overline{\phi}_+(s) = -\frac{F_-(0) + sF'_-(0)}{(s + \mathrm{i}0)^2 L_*^+(s) N_+(s)}. \tag{2.208}$$

As a result, we obtain

$$\phi_1(t) = -F_-(0)\Phi_1(t) - F'_-(0)\Phi_0(t). \tag{2.209}$$

The case $j = 2$. Finally, we have $\tilde{b}_2 = -2\mathrm{i}$ and the solution to the problem takes the form

$$\overline{\phi}_+(s) = -\mathrm{i}\frac{2F_-(0) + 2sF'_-(0) + s^2F''_-(0)}{(s + \mathrm{i}0)^3 L_*^+(s) N_+(s)}.$$

As a result, we see that

$$\phi_2(t) = -2\mathrm{i}F_-(0)\Phi_2(t) - 2\mathrm{i}F'_-(0)\Phi_1(t) - \mathrm{i}F''_-(0)\Phi_0(t). \tag{2.210}$$

Formulas (2.203), (2.209), and (2.210) provide solutions to Eq. (2.166) with special right-hand sides $\psi^j(t) = t^j$ for $j = 0, 1, 2$, respectively.

2.6.4 *Solution of the Boundary-Layer Integral Equation with a Polynomial Right-Hand Side*

We now consider Eq. (2.164), where the right-hand side is a linear combination of the polynomials t^0, t^1, and t^2. That is

$$\int_0^{+\infty} \phi(\tau) M_*(\tau - t)\, dt = \sum_{k=0}^{2} c_k t^k, \quad 0 < t < \infty. \tag{2.211}$$

According to (2.190), a solution to Eq. (2.211) can be represented in the form

$$\phi(t) = \Omega(t)t^{-3/2}, \quad 0 < t < \infty. \tag{2.212}$$

Formula (2.212) will give a finite-energy solution, if $\Omega(0) = 0$ and $\Omega(t)$ has a local derivative (near zero) belonging to the Holder class. In other words, $\Omega \sim \omega_0 t^{1+\alpha}$ as $t \to 0$, where $0 < \alpha < 1$ defines the Holder class, or equivalently

$$\phi(t) \sim \omega_0 t^{\alpha-1/2}, \quad t \to 0. \tag{2.213}$$

Therefore, in order to satisfy the asymptotic condition (2.213), one of the constants c_0, c_1, and c_2 in (2.211) should be a linear combination of the other two. In light of (2.211), the regularity condition (2.213) takes form

$$c_0\phi_0(t) + c_1\phi_1(t) + c_2\phi_2(t) = O(t^{-1/2}), \quad t \to 0. \tag{2.214}$$

Now taking into account Eqs. (2.203), (2.209), and (2.210), we conclude that the asymptotic condition (2.214) is equivalent to the following:

$$c_0F_-(0) + ic_1F'_-(0) - c_2F''_-(0) = 0. \tag{2.215}$$

Here, $F_-(0)$, $F'_-(0)$ and $F''_-(0)$ are the values of the function (2.186) and its two successive derivatives at zero (see formula (2.188)).

Thus, it is clear that Eq. (2.164) has a finite-energy solution if

$$C_0(s) \equiv 0, \tag{2.216}$$

where s is the arc length coordinate along the contour Γ_*.

2.6.5 *Approximate Solution of the Boundary-Layer Integral Equation*

Following Aleksandrov [4], we look for a solution in its approximate form, assuming $N(s) \equiv 1$. The function $\Phi_j(t)$ simplifies as follows:

$$\Phi_j(t) = \frac{1}{2\pi\sqrt{\pi}} \int_{-\infty}^{\infty} \frac{(A - is)\sqrt{B - is}}{(s + i0)^{j+1}} e^{-ist} ds. \tag{2.217}$$

Note that it is enough to construct the function $\Phi_2(t)$, while $\Phi_0(t)$ and $\Phi_1(t)$ could be evaluated using the recurrence relationships between them (2.193).

We apply Cauchy's residue theorem to evaluate the Bromwich contour integral of (2.217). It is readily seen that the integrand function has a pole at $s = 0$ of the order $j + 1$ and a branch point at $s = -\mathrm{i}B$. In this way, we find

$$\begin{aligned}
\mathrm{i}\sqrt{\pi}\Phi_0(t) &= A\sqrt{B} + \frac{e^{-Bt}}{\pi}\big(A\psi_1(t) - \psi_0(t)\big),\\
-\sqrt{\pi}\Phi_1(t) &= \sqrt{B} + \frac{A}{2\sqrt{B}} + A\sqrt{B}t - \frac{e^{-Bt}}{\pi}\big(A\psi_2(t) - \psi_1(t)\big),\\
\mathrm{i}\sqrt{\pi}\Phi_2(t) &= \sqrt{B}\left(\frac{A-4B}{8B^2} - \left(1 + \frac{A}{2B}\right)t - \frac{At^2}{2}\right) - \frac{e^{-Bt}}{\pi}\big(A\psi_3(t) - \psi_2(t)\big),
\end{aligned} \tag{2.218}$$

where we have introduced the notation

$$\psi_n(t) = \int_0^\infty \frac{e^{-t\xi}\sqrt{\xi}}{(\xi + B)^n}\, d\xi.$$

In particular, we have

$$\begin{aligned}
\psi_0(t) &= \frac{\sqrt{\pi}}{2t^{3/2}},\\
\psi_1(t) &= \frac{\sqrt{\pi}}{\sqrt{t}} - \pi\sqrt{B}e^{Bt}\,\mathrm{erfc}\,(\sqrt{Bt}),\\
\psi_2(t) &= -\sqrt{\pi}\sqrt{t} + \frac{\pi(1+2Bt)}{2\sqrt{B}}e^{Bt}\,\mathrm{erfc}\,(\sqrt{Bt}),\\
\psi_3(t) &= \frac{\sqrt{\pi}\sqrt{t}(2Bt+1)}{4B} - \frac{\pi}{8B^{3/2}}e^{Bt}(4B^2t^2 + 4Bt - 1)\,\mathrm{erfc}\,(\sqrt{Bt}).
\end{aligned} \tag{2.219}$$

Furthermore, in light of (2.184), the formula

$$F_-(s) = \frac{1}{L_*^-(s)}$$

simplifies to

$$F_-(s) = \frac{1}{\sqrt{\pi}}(A + is)\sqrt{B + is}.$$

It now follows that

$$F_-(0) = \frac{1}{\sqrt{\pi}} A\sqrt{B},$$
$$F'_-(0) = \frac{i}{2\sqrt{\pi}\sqrt{B}}(A + 2B),$$
$$F''_-(0) = \frac{1}{4\sqrt{\pi}B\sqrt{B}}(A - 4B), \tag{2.220}$$

while correspondingly, the regularity condition (2.215) takes the form

$$Ac_0 - c_1\frac{A + 2B}{2B} + c_2\frac{4B - A}{4B^2} = 0. \tag{2.221}$$

Further, taking into account formulas (2.203), (2.209), (2.210) and (2.218)–(2.220), we obtain

$$\begin{aligned}
\phi_0(t) &= \frac{A^2 B}{\pi}\,\mathrm{erf}\,(\sqrt{Bt}) + \frac{A\sqrt{B}e^{-Bt}}{2\pi^{3/2}t^{3/2}}(2At - 1),\\
\phi_1(t) &= \frac{A^2 Bt}{\pi}\,\mathrm{erf}\,(\sqrt{Bt}) + \frac{e^{-Bt}}{4\pi^{3/2}\sqrt{B}t^{3/2}}(4A^2Bt^2 - 2A^2t + A + 2B),\\
\phi_2(t) &= \frac{(A^2B^2t - A^2 - 2B^2)}{\pi B}\,\mathrm{erf}\,(\sqrt{Bt})\\
&\quad + \frac{e^{-Bt}}{8\pi^{3/2}B^{3/2}t^{3/2}}\big(8A^2B^2t^3 - 4A^2Bt^2 - 2A^2t + A - 16B^2t - 4B\big).
\end{aligned} \tag{2.222}$$

Observe that following Aleksandrov [4], we can select the coefficients A and B in the approximate kernel function

$$\tilde{\mathscr{L}}(s) = \frac{s^3}{(s^2 + A^2)\sqrt{s^2 + B^2}} \tag{2.223}$$

in such a way that (cf. formula (2.167))

$$\tilde{\mathscr{L}}(s) = \mu_1 s^3 + \mu_2 s^5 + O(s^7), \quad s \to 0. \tag{2.224}$$

By simple calculations, we find

$$A^2 = \frac{1}{\mu_1 B}, \tag{2.225}$$

where the coefficient B is determined as a positive root of the cubic equation

$$2\mu_1^2 B^3 + 2\mu_2 B^2 + \mu_1 = 0. \tag{2.226}$$

Therefore, in light of (2.223) and (2.224), for the function $N(s)$ defined by (2.180), the following asymptotic formula holds true:

$$N(s) = 1 + O(s^4), \quad s \to 0. \tag{2.227}$$

Note that in the isotropic incompressible case (2.206), Eq. (2.226) is equivalent to $20B^3 - 54B^2 + 15 = 0$, which has one negative and two positive roots $B_1 = 0.597219$ and $B_2 = 2.588024$. By formula (2.225), we calculate $A_1 = 1.584816$ and $A_2 = 0.761310$. The errors of the corresponding approximations (2.223) to the kernel function (2.206) do not exceed 14 % and 20 %, respectively, for all $0 \le s < +\infty$.

2.7 Leading-Order Asymptotic Solution of the Contact Problem for Incompressible Layers

In the incompressible case, the process of solving the contact problem by asymptotic methods reduces to that of solving the so-called resulting problem for the leading-order asymptotic solution. In this section, the resulting boundary value problem (later called asymptotic model) is formulated, including the governing differential equation and the corresponding boundary condition.

2.7.1 Governing Differential Equation

According to (2.67) and (2.152), the local indentation of a thin bonded incompressible elastic layer can be approximated by

$$w_0^{(n)}(\mathbf{y}) \simeq -\mathscr{M}_1^{(n)} h_n^3 \Delta_y p(\mathbf{y}), \tag{2.228}$$

where

$$\mathscr{M}_1^{(n)} = \frac{1}{3a_{44}^{(n)}}$$

and $a_{44}^{(n)} = G'_n$ is the out-of-plane shear modulus of the n-th elastic layer.

Substituting the asymptotic representations (2.228), $n = 1, 2$, into the contact condition (2.20), we arrive at the equation

$$-\left(\mathscr{M}_1^{(1)} h_1^3 + \mathscr{M}_1^{(2)} h_2^3\right) \Delta_y p(\mathbf{y}) = \delta_0 - \varphi(\mathbf{y}), \quad \mathbf{y} \in \omega. \tag{2.229}$$

Let us introduce the notation

$$\mathscr{M}_1 = \mathscr{M}_1^{(1)} \frac{h_1^3}{h^3} + \mathscr{M}_1^{(2)} \frac{h_2^3}{h^3}, \tag{2.230}$$

where $h = h_1 + h_2$ is the joint thickness. Then, we can rewrite Eq. (2.229) as follows:

$$-\mathscr{M}_1 h^3 \Delta_y p(\mathbf{y}) = \delta_0 - \varphi(\mathbf{y}), \quad \mathbf{y} \in \omega. \tag{2.231}$$

Recall that the elastic constant $\mathscr{M}_1^{(n)}$ is introduced by the expansion

$$\frac{\mathscr{L}_n(s)}{\theta_n s} = \mathscr{M}_1^{(n)} s^2 + O(s^4), \quad s \to 0,$$

where $\mathscr{L}_n(s)$ is the kernel function of the n-th layer. From here it follows that

$$\frac{\theta}{\theta_n} \mathscr{L}_n\Big(\frac{h_n}{h} s\Big) = \theta \mathscr{M}_1^{(n)} \frac{h_n^3}{h^3} s^3 + O(s^5), \quad s \to 0.$$

By substituting the above expansion into formula (2.37), we derive the following asymptotic expansion for the compound kernel function:

$$\frac{\mathscr{L}(s)}{\theta s} = \Big(\mathscr{M}_1^{(1)} \frac{h_1^3}{h^3} + \mathscr{M}_1^{(2)} \frac{h_2^3}{h^3}\Big) s^2 + O(s^4), \quad s \to 0.$$

It is readily seen that the latter formula is consistent with the definition (2.230) of the compound elastic constant $\mathscr{M}_1$.

The governing equation (2.231) should be supplemented by the appropriate boundary conditions at the contour Γ of the contact area ω.

2.7.2 Boundary Condition in the Case of Fixed Contact Area

By introducing the dimensionless coordinates (2.40) into the governing integral equation (2.159), and recollecting the notation $\Lambda = \varepsilon^{-1}$, we have

$$\frac{h_*^3}{\pi^2 \theta \Lambda} \iint\limits_{\omega_*} p_*(\boldsymbol{\xi}) k_*\big(\Lambda(\boldsymbol{\eta} - \boldsymbol{\xi})\big)\, d\boldsymbol{\xi} = \mathscr{W}_0^*(\boldsymbol{\eta}), \tag{2.232}$$

where $p_*(\boldsymbol{\eta}) = p(h_*\boldsymbol{\eta})$ and $\mathscr{W}_0^*(\boldsymbol{\eta}) = \mathscr{W}_0(h_*\boldsymbol{\eta})$.

Applying the distributional asymptotic analysis (see Sect. 2.2.1), in light of the asymptotic expansion (2.167) for the kernel function $\mathscr{L}(s)$, we find that

$$k_*(\Lambda\boldsymbol{\eta}) \sim \frac{\pi^2\mu_1}{\Lambda^2}\delta(\boldsymbol{\eta}) - \frac{\pi^2\mu_2}{\Lambda^4}\Delta_\eta\delta(\boldsymbol{\eta}) + \ldots, \quad \Lambda \to \infty, \tag{2.233}$$

where $\mu_k = \theta\mathscr{M}_k$, and $\delta(\boldsymbol{\eta})$ is the two-dimensional Dirac delta function.

Therefore, substituting the asymptotic approximation (2.233) into Eq. (2.232), we obtain

$$h^3\mathscr{M}_1 p(\mathbf{y}) - h^5\mathscr{M}_2\Delta_y p(\mathbf{y}) + \ldots = \mathscr{W}_0(\mathbf{y}). \tag{2.234}$$

To leading asymptotic order we have

$$h^3\mathscr{M}_1 p(\mathbf{y}) \simeq \mathscr{W}_0(\mathbf{y}). \tag{2.235}$$

We are now in a position to derive the leading order asymptotic model in the case of fixed contact area. Taking into account relations (2.161)–(2.163) and (2.216), we conclude that the function $\mathscr{W}_0(\mathbf{y})$ should satisfy the problem

$$-\Delta_y\mathscr{W}_0(\mathbf{y}) = \delta_0 - \varphi(\mathbf{y}), \quad \mathbf{y} \in \omega; \quad \mathscr{W}_0(\mathbf{y}) = 0, \quad \mathbf{y} \in \Gamma. \tag{2.236}$$

On the other hand, by substituting the representation $\mathscr{W}_0(\mathbf{y}) \simeq h^3\mathscr{M}_1 p(\mathbf{y})$, which is none other than (2.235), into Eq. (2.236), we arrive at the following problem:

$$-h^3\mathscr{M}_1\Delta_y p(\mathbf{y}) = \delta_0 - \varphi(\mathbf{y}), \quad \mathbf{y} \in \omega, \tag{2.237}$$

$$p(\mathbf{y}) = 0, \quad \mathbf{y} \in \Gamma. \tag{2.238}$$

It is readily seen that Eq. (2.237) is identical to the governing differential equation (2.231), while Eq. (2.238) represents the sought for boundary condition.

It is interesting to note that the leading order asymptotic model (2.237), (2.238) provides the so-called [4] degenerate solution, which vanishes at the boundary of the contact area even for a punch with a sharp edge, whereas, generally speaking, the original solution has a square root singularity.

2.7.3 Boundary Conditions in the Case of Unilateral Contact

We now revisit the boundary-layer problem considered in Sect. 2.6.2, taking into account the fact that in light of (2.216), the right-hand side of the governing integral equation (2.159) now satisfies the boundary-value problem (2.236).

Considering the behavior of the function $\mathscr{W}_0(\mathbf{y})$ near the contour Γ in the fast dimensionless coordinates (see, in particular, Eqs. (2.40) and (2.78)), we have

$$\mathscr{W}_0(h_*\boldsymbol{\eta}) = \varepsilon\nu B_1^*(s) + \varepsilon^2\nu^2 B_2^*(s) + \ldots, \quad \nu \to 0^+, \quad s \in \Gamma, \tag{2.239}$$

where we have introduced the notation

$$B_1^*(s) = h_* \frac{\partial \mathscr{W}_0}{\partial n}(\mathbf{y}), \quad B_2^*(s) = \frac{h_*^2}{2} \frac{\partial^2 \mathscr{W}_0}{\partial n^2}(\mathbf{y}), \quad \mathbf{y} \in \Gamma.$$

Taking into account only the leading term in (2.239), we arrive at the boundary-layer integral equation

$$\int_0^{+\infty} q^{**}(s, \nu') M_*(\nu' - \nu)\, d\nu' = \pi\theta h_* B_1^*(s)\nu. \tag{2.240}$$

In the unilateral contact problem (see (2.21)), the solution of Eq. (2.240) should vanish at the contact area contour, i.e.,

$$q^{**}(s, 0) = 0, \quad s \in \Gamma.$$

On the other hand, according to (2.166), we have $q^{**}(s, \nu) = \pi\theta h_* B_1^*(s)\phi_1(\nu)$, while, due to (2.200) and (2.209), this function possesses a singularity at $\nu = 0$ unless $B_1^*(s) = 0$ for all $s \in \Gamma$. In other words, as a consequence of (2.235) and (2.239), the obtained result represents the second boundary condition

$$\frac{\partial p}{\partial n}(\mathbf{y}) = 0, \quad \mathbf{y} \in \Gamma, \tag{2.241}$$

that should be added to the problem (2.237), (2.238) in the case of unilateral contact with unknown contact area ω. Note that Eq. (2.241) is called [17, 27] the zero-pressure-gradient condition.

References

1. Alblas, J.B., Kuipers, M.: On the two-dimensional problem of a cylindrical stamp pressed into a thin elastic layer. Acta Mech. **9**, 292–311 (1970)
2. Aleksandrov, V.M.: The solution of a type of two-dimensional integral equations. J. Appl. Math. Mech. **28**, 714–717 (1964)
3. Aleksandrov, V.M.: Asymptotic solution of the contact problem for a thin elastic layer. J. Appl. Math. Mech. **33**, 49–63 (1969)
4. Aleksandrov, V.M.: Asymptotic solution of the axisymmetric contact problem for an elastic layer of incompressible material. J. Appl. Math. Mech. **67**, 589–593 (2003)
5. Aleksandrov, V.M., Babeshko, V.A.: Contact problems for an elastic strip of small thickness. Izv. Akad. Nauk SSSR. Ser. Mekhanika. **2**, 95–107 (1965). [in Russian]
6. Alexandrov, V.M., Pozharskii, D.A.: Three-Dimensional Contact Problems. Kluwer, Dordrecht (2001)
7. Argatov, I.I.: Pressure of a punch in the form of an elliptic paraboloid on a thin elastic layer. Acta Mech. **180**, 221–232 (2005)

8. Argatov, I.I.: Pressure of a paraboloidal die on a thin elastic layer. Dokl. Phys. **50**, 524–528 (2005)
9. Chadwick, R.S.: Axisymmetric indentation of a thin incompressible elastic layer. SIAM J. Appl. Math. **62**, 1520–1530 (2002)
10. Estrada, R., Kanwal, R.P.: A distributional theory for asymptotic expansions. Proc. R. Soc. Lond. A **428**, 399–430 (1990)
11. Fabrikant, V.I.: Elementary solution of contact problems for a transversely isotropic elastic layer bonded to a rigid foundation. Z. Angew. Math. Phys. **57**, 464–490 (2006)
12. Fabrikant, V.I.: Numerical methods of solution of contact problems in layered media. Int. J. Comput. Meth. Eng. Sci. Mech. **12**, 84–95 (2011)
13. Garcia, J.J., Altiero, N.J., Haut, R.C.: An approach for the stress analysis of transversely isotropic biphasic cartilage under impact load. J. Biomech. Eng. **120**, 608–613 (1998)
14. Gol'denveizer, A.L.: Derivation of an approximate theory of bending of a plate by the method of asymptotic integration of the equations of the theory of elasticity. J. Appl. Math. Mech. **26**, 1000–1025 (1962)
15. Itskov, M., Aksel, N.: Elastic constants and their admissible values for incompressible and slightly compressible anisotropic materials. Acta Mech. **157**, 81–96 (2002)
16. Johnson, K.L.: Contact Mechanics. Cambridge Univ. Press, Cambridge, UK (1985)
17. Hlaváček, M.: A note on an asymptotic solution for the contact of two biphasic cartilage layers in a loaded synovial joint at rest. J. Biomech. **32**, 987–991 (1999)
18. Koiter, W.T.: Solutions of some elasticity problems by asymptotic methods. In: Applications of the theory of functions to continuum mechanics. Muskhelishvili, N.I. (ed.), pp. 15–31. International Symposium Tbilisi, USSR 1963. Moscow, Nauka (1965)
19. Leibenzon, L.S.: Course in the Theory of Elasticity. Gostekhizdat, Moscow-Leningrad (1947)
20. Love, A.E.H.: A Treatise on the Mathematical Theory of Elasticity. Dover, New York (1944)
21. Mehrabadi, M.M., Cowin, S.C.: Eigentensors of linear anisotropic elastic materials. Quart. J. Mech. Appl. Math. **43**, 15–41 (1990)
22. Mishuris, G.: Imperfect transmission conditions for a thin weakly compressible interface. 2D problems. Arch. Mech. **56**, 103–115 (2004)
23. Noble, B.: Methods Based on the Wiener-Hopf Technique for the Solution of Partial Differential Equations. Pergamon Press, New York (1958)
24. Sneddon, I.N.: Fourier Transforms. Dover, New York (1995)
25. Vorovich, I.I., Aleksandrov, V.M., Babeshko, V.A.: Non-classical Mixed Problems of the Theory of Elasticity. Nauka, Moscow (1974). [in Russian]
26. Wong, R.: Distributional derivation of an asymptotic expansion. Proc. Amer. Math. Soc. **80**, 266–270 (1980)
27. Wu, J.Z., Herzog, W.: On the pressure gradient boundary condition for the contact of two biphasic cartilage layers. J. Biomech. **33**, 1331–1332 (2000)
28. Yang, F.: Indentation of an incompressible elastic film. Mech. Mater. **30**, 275–286 (1998)

Chapter 3
Unilateral Frictionless Contact of Thin Bonded Incompressible Elastic Layers

Abstract This chapter is devoted to solving contact problems for thin bonded incompressible transversely isotropic elastic layers in the thin-layer approximation, based on the leading-order asymptotic model developed in Chap. 2.

3.1 Asymptotic Model for the Frictionless Contact of Thin Bonded Incompressible Layers

In this section we summarize the results of the asymptotic analysis performed in Sects. 2.5 and 2.7, by formulating a leading-order asymptotic model to describe (in the thin-layer approximation) the frictionless contact interaction of two incompressible elastic layers bonded to rigid substrates.

3.1.1 Leading-Order Asymptotic Model for the Unilateral Contact

We will continue use of previous notation, wherever possible, and consider two thin transversally isotropic elastic layers of uniform thicknesses h_1 and h_2 ideally bonded to rigid substrates (see Fig. 3.1). Let $\varphi(\mathbf{y})$ and δ_0 denote the gap between the layer surfaces before deformation and the contact approach of the rigid substrates under the external normal load, respectively.

According to the asymptotic analysis performed in the previous chapter in the incompressible case (see, in particular, Sect. 2.7), the contact pressure density, $p(\mathbf{y})$, which is assumed to be positive, should satisfy the differential equation

I. Argatov and G. Mishuris, *Contact Mechanics of Articular Cartilage Layers*,
Advanced Structured Materials 50, DOI 10.1007/978-3-319-20083-5_3

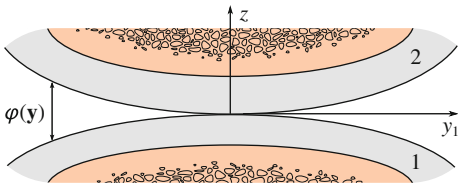

Fig. 3.1 Contact of two thin elastic layers in the initial undeformed configuration, with the variable gap function $\varphi(\mathbf{y})$ measured along the common normal axis z

$$-\left(\frac{h_1^3}{3G_1'}+\frac{h_2^3}{3G_2'}\right)\Delta_y p(\mathbf{y})=\delta_0-\varphi(\mathbf{y}),\quad \mathbf{y}\in\omega. \tag{3.1}$$

Here, $\Delta_y=\partial^2/\partial y_1^2+\partial^2/\partial y_2^2$ is the Laplace operator, G_n' is the out-of-plane shear modulus of the nth layer ($n=1,2$), $\mathbf{y}=(y_1,y_2)$ are the in-plane Cartesian coordinates, and ω is the contact area, which is not given a priori.

In the case of unilateral contact, the contact area should be determined in the process of solving Eq. (3.1) with respect to the following boundary conditions:

$$p(\mathbf{y})=0,\quad \frac{\partial p}{\partial n}(\mathbf{y})=0,\quad \mathbf{y}\in\Gamma. \tag{3.2}$$

Here, $\partial/\partial n$ is the normal derivative at the contour Γ of the domain ω.

For simplicity, we introduce the following notation:

$$m=\left(\frac{h_1^3}{3G_1'}+\frac{h_2^3}{3G_2'}\right)^{-1}. \tag{3.3}$$

Finally, denoting by F the total external load applied to the substrates, which produces the contact approach δ_0, we write out the equilibrium equation

$$\iint\limits_{\omega} p(\mathbf{y})\,d\mathbf{y}=F. \tag{3.4}$$

Equations (3.1), (3.2), and (3.4) constitute the leading-order asymptotic model of the unilateral contact for thin bonded incompressible elastic layers. We should note that, as was shown in [16], the error of the leading-order asymptotic model based on the zero-pressure-gradient condition for the contact pressure across the contact contour, which was used in [7, 8, 17, 18], increases as the ratio of the diameter of the contact area to the layer thickness decreases.

3.1.2 Elliptical Contact of Thin Bonded Incompressible Elastic Layers

Let the gap function be represented by an elliptic paraboloid

$$\varphi(\mathbf{y}) = \frac{y_1^2}{2R_1} + \frac{y_2^2}{2R_2}. \tag{3.5}$$

In this case, the exact solution to the boundary-value problem (3.1) and (3.2) can be obtained in the following form [8]:

$$p(\mathbf{y}) = p_0\left(1 - \frac{y_1^2}{a^2} - \frac{y_2^2}{b^2}\right)^2. \tag{3.6}$$

Here, p_0 is the maximum contact pressure, while a and b are the semi-axes of the elliptical contact area ω.

By substituting (3.6) into Eq. (3.1), and taking into account relations (3.3) and (3.5), one arrives at the following system of algebraic equations [8]:

$$\delta_0 = \frac{4p_0}{m}\left(\frac{1}{a^2} + \frac{1}{b^2}\right), \tag{3.7}$$

$$\frac{1}{2R_1} = \frac{4p_0}{ma^2}\left(\frac{3}{a^2} + \frac{1}{b^2}\right), \quad \frac{1}{2R_2} = \frac{4p_0}{mb^2}\left(\frac{1}{a^2} + \frac{3}{b^2}\right). \tag{3.8}$$

Let s denote the aspect ratio of the contact area, i.e.,

$$s = \frac{b}{a}, \tag{3.9}$$

then, from Eq. (3.8) it immediately follows that

$$s^2 = \sqrt{\left(\frac{R_1 - R_2}{6R_1}\right)^2 + \frac{R_2}{R_1}} - \frac{(R_1 - R_2)}{6R_1}. \tag{3.10}$$

Now, Eqs. (3.7) and $(3.8)_1$ yield

$$a^2 = \frac{2(3s^2+1)}{s^2+1} R_1\delta_0, \tag{3.11}$$

$$p_0 = \frac{s^2(3s^2+1)}{2(s^2+1)^2} m R_1\delta_0^2. \tag{3.12}$$

Then, substitution of the contact pressure distribution (3.6) into the equilibrium equation (3.4) gives $F = (\pi/3)p_0ab$, where, as a result of (3.9), (3.11), and (3.12), we obtain the following equation [4]:

$$F = \frac{\pi m}{3}\frac{s^3(3s^2+1)^2}{(s^2+1)^3}R_1^2\delta_0^3. \tag{3.13}$$

Observe that the force-displacement relationship (3.13) depends on both radii R_1 and R_2 (see Eq. (3.10)). A compound geometric characteristic of the gap between the contact surfaces can be introduced, for instance, through the arithmetic mean $(R_1 + R_2)/2$ or the geometric mean $\sqrt{R_1R_2}$ as well as through the harmonic mean $2R_1R_2/(R_1 + R_2)$. As, with regard to the articular contact, the radii R_1 and R_2 do not differ much, the corresponding scaling dimensionless factor should not deviate overly from a constant value for $s \approx 1$. It can be checked that the geometric mean $\sqrt{R_1R_2}$, as a geometric characteristic of the initial gap, provides the best result among the mentioned variants. Thus, we rewrite Eq. (3.13) in the form

$$F = \frac{2\pi}{3}c_F(s)mR_1R_2\delta_0^3, \tag{3.14}$$

where m is given by (3.3), and we have introduced the notation

$$c_F(s) = \frac{s(3s^2+1)(s^2+3)}{2(s^2+1)^3}. \tag{3.15}$$

Note that the coefficient $c_F(s)$ is normalized to be $c_F(1) = 1$ (see Fig. 3.2).

We finally note that another approximate solution was obtained by Hlaváček [16], using the averaging method originally developed by Matthewson [21].

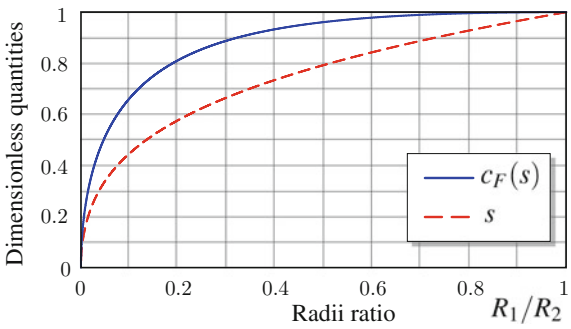

Fig. 3.2 The dimensionless quantities s and $c_F(s)$ as functions of the curvature radii ratio R_1/R_2, based on Eqs. (3.10) and (3.15)

3.1.3 Similarity Analysis of the Contact Problem for Thin Bonded Incompressible Elastic Layers

Let the gap between contacting layers before deformation be described by a homogeneous function, $\varphi_d(\mathbf{y})$, of degree d, which for any rational variable $\lambda > 0$ has the property

$$\varphi_d(\lambda \mathbf{y}) = \lambda^d \varphi_d(\mathbf{y}). \tag{3.16}$$

Following Borodich [9, 10], we introduce a similarity transformation of one solution to the problem into another. We assume that for a value of the contact force F the solution of the contact problem (3.1), (3.2), and (3.4) under the similarity condition (3.16) is given by the contact pressure function $p(\mathbf{y})$, the contact approach quantity δ_0, and the contact region ω bounded by the contour Γ.

Then, for any positive contact force F', the solution of the boundary value contact problem is given by

$$p'(\mathbf{y}) = \lambda^{-(2+d)} p(\lambda \mathbf{y}),$$

$$\delta_0' = \lambda^{-d} \delta_0, \tag{3.17}$$

$$F' = \lambda^{-(4+d)} F, \tag{3.18}$$

where $\lambda = (F/F')^{1/(4+d)}$, and the contact regions ω and ω' change according to the homothetic transformation

$$\left[(y_1, y_2) \in \omega'\right] \Longleftrightarrow \left[(\lambda y_1, \lambda y_2) \in \omega\right].$$

From (3.17) and (3.18), it follows that

$$\frac{F}{F'} = \left(\frac{\delta_0}{\delta_0'}\right)^{(4+d)/d}. \tag{3.19}$$

For the parabolic gap function (3.5), i.e., for $d = 2$, we find that $(4 + d)/d = 3$ and formula (3.19) agrees with Eq. (3.14).

3.2 Axisymmetric Refined Contact Problem for Thin Bonded Incompressible Elastic Layers, with Allowance for Tangential Displacements on the Contact Interface

As was shown in Sect. 1.5.3, in the contact problem for a compressible elastic layer, the effect of tangential displacements increases when the material becomes more incompressible. Our emphasis here will be on the issues involved in the analytical modeling.

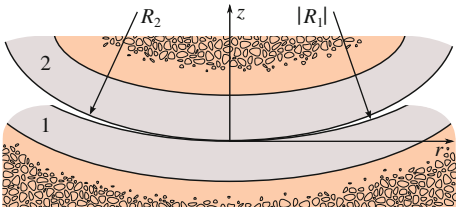

Fig. 3.3 Thin incompressible elastic layers bonded to rigid substrates shaped like bodies of revolution in the unloading configuration. The surface of layer 1 is concave and $R_1 < 0$

3.2.1 *Refined Formulation of the Axisymmetric Contact Problem*

We consider two thin incompressible linear elastic layers attached to rigid substrates shaped like bodies of revolution (see Fig. 3.3). Introducing the cylindrical coordinate system, we write the equations of the layer surfaces (before loading) in the form

$$z = (-1)^n \varphi_n(r).$$

In the particular case of the contacting surfaces shaped like paraboloids of revolution, we have

$$\varphi_n(r) = \frac{r^2}{2R_n}, \quad n = 1, 2, \tag{3.20}$$

where R_n is the curvature radius of the nth layer surface at its apex.

The initial gap between the layer surfaces, $\varphi(r) = \varphi_1(r) + \varphi_2(r)$, is given by

$$\varphi(r) = \frac{r^2}{2R}, \tag{3.21}$$

where we have introduced the notation $R^{-1} = R_1^{-1} + R_2^{-1}$.

We denote the axial approach of the contacting bodies by δ_0. Then the linearized refined contact condition, which takes into account the tangential displacements at the contact interface, can be written as follows (see Eq. (2.19)):

$$w_0^{(1)}(r) + w_0^{(2)}(r) = \delta_0 - \varphi(r) - \frac{d\varphi_2(r)}{dr}\left(\mathbf{v}_0^{(1)}(r) - \mathbf{v}_0^{(2)}(r)\right), \quad r \le a. \tag{3.22}$$

Here, $w_0^{(n)}(r)$ and $v_0^{(n)}(r)$ are the normal (vertical) and the tangential (horizontal in the radial direction) displacements of the surface points of the nth layer, a is the radius of the contact area, and it is assumed that $|R_2| \le |R_1|$, i.e., the surface of layer 1 is assumed to be flatter than the surface of layer 2.

According to the perturbation analysis presented in Sect. 2.5, the displacements $w_0^{(n)}(r)$ and $v_0^{(n)}(r)$ can be approximated by the leading-order asymptotic formulas written in the cylindrical coordinates as follows:

$$w_0^{(n)}(r) = -\frac{h_n^3}{3G_n'}\frac{1}{r}\frac{d}{dr}\left(r\frac{dp(r)}{dr}\right), \tag{3.23}$$

$$v_0^{(n)}(r) = -\frac{h_n^2}{2G_n'}\frac{dp(r)}{dr}. \tag{3.24}$$

Here, $p(r)$ is the contact pressure, h_n and G_n' are the thickness and the out-of-plane shear modulus of the nth layer, respectively.

In light of formulas (3.20) and (3.21), Eq. (3.22) takes the form

$$w_0^{(1)}(r) + w_0^{(2)}(r) + \frac{r}{R_2}\left(\mathbf{v}_0^{(1)}(r) - \mathbf{v}_0^{(2)}(r)\right) = \delta_0 - \varphi(r), \quad r \le a. \tag{3.25}$$

Now, substituting the expressions (3.23) and (3.24) into the above relation, we arrive at the following governing differential equation:

$$\frac{1}{r}\frac{d}{dr}\left(r\frac{dp(r)}{dr}\right) + \varkappa_2 r\frac{dp(r)}{dr} = m(Cr^2 - \delta_0). \tag{3.26}$$

Here we have introduced the auxiliary notation

$$m = \left(\frac{h_1^3}{3G_1'} + \frac{h_2^3}{3G_2'}\right)^{-1}, \quad C = \frac{1}{2R}, \tag{3.27}$$

$$\varkappa_2 = \frac{m}{R_2}\left(\frac{h_1^2}{2G_1'} - \frac{h_2^2}{2G_2'}\right). \tag{3.28}$$

The radius, a, of the circular contact area is determined from the condition that the contact pressure is positive

$$p(r) > 0, \quad r < a,$$

and vanishes at the contour of the contact area, i.e.,

$$p(a) = 0. \tag{3.29}$$

Moreover, in the case of the contact problem for incompressible elastic layers, a smooth transition of the surface normal stresses from the contact region $r < a$ to the outside region $r > a$ is additionally assumed, and the following boundary condition is imposed (see, in particular, Sect. 2.7.3 and [8, 11, 17]):

$$\left.\frac{dp(r)}{dr}\right|_{r=a} = 0. \tag{3.30}$$

From the physical point of view, the contact pressure at the center of the circular contact area must satisfy the regularity condition

$$\left.\frac{dp(r)}{dr}\right|_{r=0} = 0. \tag{3.31}$$

The equilibrium equation for the whole system is

$$2\pi \int_0^a p(\rho)\rho\, d\rho = F, \tag{3.32}$$

where F denotes the external load applied to the substrates.

In the case where $\varkappa_2 = 0$, the contact problem under consideration coincides with that studied by Barber [8] and Jaffar [17]. Here we address the question of when accounting for the additional term in Eq. (3.26) is important for applications.

3.2.2 Equation for the Contact Approach

Integrating Eq. (3.26) with respect to r, we obtain

$$r\frac{dp(r)}{dr} + \varkappa_2 \int_0^r \rho^2 \frac{dp(\rho)}{d\rho}\, d\rho = m\left(C\frac{r^4}{4} - \delta_0\frac{r^2}{2}\right) + D_1. \tag{3.33}$$

The constant of integration D_1 vanishes in accordance with the regularization condition (3.31) at the center of the contact area.

To simplify the above equation, we transform the second integral using integration by parts as follows:

$$\int_0^r \rho^2 \frac{dp(\rho)}{d\rho}\, d\rho = r^2 p(r) - 2\int_0^r p(\rho)\rho\, d\rho.$$

Therefore, Eq. (3.33) takes the form

$$\frac{dp(r)}{dr} + \varkappa_2\left(rp(r) - \frac{2}{r}\int_0^r p(\rho)\rho\, d\rho\right) = m\left(C\frac{r^3}{4} - \delta_0\frac{r}{2}\right). \tag{3.34}$$

Now, substituting the value $r = a$ into the above equation and taking into account the boundary conditions (3.29), (3.30) at the contour of the contact area, we obtain

$$-\frac{2\varkappa_2}{a}\int_0^a p(\rho)\rho\,d\rho = m\left(C\frac{a^3}{4} - \delta_0\frac{a}{2}\right).$$

Finally, in light of formula (3.32), the above equation takes the form

$$\delta_0 = C\frac{a^2}{2} + \frac{2\varkappa_2}{m}\frac{F}{\pi a^2}. \tag{3.35}$$

We underline that either δ_0 or F is known a priori, but not both simultaneously, while in the unilateral contact problem the contact radius a is also unknown.

3.2.3 Equation for the Contact Radius

We now return to Eq. (3.34), which after integration with respect to variable r takes the following form:

$$p(r) + \varkappa_2\left\{\int_0^r p(\rho)\rho\,d\rho - 2\int_0^r \frac{1}{\rho}\int_0^\rho p(\xi)\xi\,d\xi d\rho\right\} = m\left(C\frac{r^4}{16} - \delta_0\frac{r^2}{4}\right) + D_2. \tag{3.36}$$

Changing the order of integration in the second integral, we see that

$$\int_0^r \frac{1}{\rho}\int_0^\rho p(\xi)\xi\,d\xi d\rho = \int_0^r p(\rho)\rho\ln\frac{r}{\rho}\,d\rho. \tag{3.37}$$

Then, taking into account the above formula, we rewrite Eq. (3.36) in the form

$$p(r) + \varkappa_2\left\{\int_0^r p(\rho)\rho\,d\rho - 2\int_0^r p(\rho)\rho\ln\frac{r}{\rho}\,d\rho\right\} = m\left(C\frac{r^4}{16} - \delta_0\frac{r^2}{4}\right) + D_2. \tag{3.38}$$

By using the boundary condition (3.29) at $r = a$, the constant of integration can be evaluated as a function of the contact radius a as follows:

$$D_2 = \frac{m}{4}\delta_0 a^2 - \frac{m}{16}Ca^4 + \frac{\varkappa_2}{2\pi}F - 2\varkappa_2 \int_0^a p(\rho)\rho \ln\frac{a}{\rho}\, d\rho. \tag{3.39}$$

Further, multiplying both sides of Eq. (3.38) by r and integrating over the contact interval, we obtain

$$\frac{F}{2\pi} + \varkappa_2\left\{\int_0^a \rho \int_0^\rho p(\xi)\xi\, d\xi d\rho - 2\int_0^a \rho \int_0^\rho p(\xi)\xi \ln\frac{\rho}{\xi}\, d\xi d\rho\right\} = m\left(C\frac{a^6}{96} - \delta_0\frac{a^4}{16}\right) + \frac{a^2}{2}D_2,$$

and proceed by changing the order of integration to find

$$\frac{F}{2\pi} + \varkappa_2\left\{\frac{1}{2}\int_0^a p(\xi)\xi\left(a^2-\xi^2\right)d\xi - \int_0^a p(\xi)\xi\left(a^2\ln\frac{a}{\xi} - \frac{1}{2}\left(a^2-\xi^2\right)\right)d\xi\right\} = m\left(C\frac{a^6}{96} - \delta_0\frac{a^4}{16}\right) + \frac{a^2}{2}D_2.$$

Now, taking into account formulas (3.32) and (3.39), we rewrite the above equation as

$$F + \varkappa_2\left(\frac{a^2}{2}F - 2\pi\int_0^a p(\rho)\rho^3\, d\rho\right) = \pi m\left(\delta_0\frac{a^4}{8} - C\frac{a^6}{24}\right),$$

and employ Eq. (3.35) to exclude δ_0 and obtain

$$\frac{\pi m}{48}Ca^6 = F + \varkappa_2\left(\frac{a^2}{4}F - 2\pi\int_0^a p(\rho)\rho^3\, d\rho\right). \tag{3.40}$$

For further convenience we rewrite Eq. (3.40) in the equivalent form

$$\frac{\pi m}{48}Ca^6 = F + \varkappa_2\left(\frac{a^2}{4}F + \frac{\pi}{2}\int_0^a \rho^4\frac{dp(\rho)}{d\rho}\, d\rho\right). \tag{3.41}$$

Note that Eq. (3.41) was obtained by integrating by parts the integral in Eq. (3.40), while taking into account the boundary condition (3.29).

3.2.4 Contact Pressure

We return to Eq. (3.26) to consider the contact pressure $p(r)$, and introduce a new dependent variable $y(r)$ via the formula

$$y(r) = r\frac{dp(r)}{dr}. \tag{3.42}$$

Using the substitution (3.42), we represent Eq. (3.26) in the form

$$\frac{1}{r}\frac{dy(r)}{dr} + \varkappa_2 y(r) = m(Cr^2 - \delta_0). \tag{3.43}$$

The general solution of the homogeneous equation

$$\frac{dy_0(r)}{dr} + \varkappa_2 r y_0(r) = 0,$$

corresponding to Eq. (3.43), has the form

$$y_0(r) = C_0 \exp\Big(-\frac{\varkappa_2}{2}r^2\Big).$$

By applying Lagrange's method of variation of parameters, and taking into account the contact pressure regularity condition (3.31), we obtain the corresponding particular solution of Eq. (3.43) in the form

$$y(r) = m\exp\Big(-\frac{\varkappa_2}{2}r^2\Big)\int\limits_0^r \exp\Big(\frac{\varkappa_2}{2}\xi^2\Big)\xi(C\xi^2 - \delta_0)\,d\xi. \tag{3.44}$$

Now, recalling Eq. (3.44), the sought-for contact pressure distribution can be obtained by integration of Eq. (3.42), with respect to the boundary condition (3.29). In this way, we derive the formula

$$p(r) = \frac{m}{\varkappa_2}\left\{\frac{C}{2}(r^2 - a^2) + \left(\frac{2C}{\varkappa_2} + \delta_0\right)g\Big(a^2\varkappa_2; \frac{r}{a}\Big)\right\}, \tag{3.45}$$

where we have introduced the notation

$$g(\varepsilon_2; \rho) = \int\limits_\rho^1 \frac{1}{x}\left(1 - \exp\Big(\frac{\varepsilon_2}{2}\xi^2\Big)\right)dx. \tag{3.46}$$

Note that, according to (3.27) and (3.28), the quantity $\varepsilon_2 = a^2\varkappa_2$ is dimensionless.

3.2.5 Approximate Equation for the Radius of the Contact Area

In the case where the parameter $\varkappa_2$, having the dimension L^{-2} (with L being the dimension of length), in its dimensionless form ε_2 (i.e., being multiplied by the contact radius squared), is reasonably small, an approximate solution to the problem can be obtained in the following way.

Let us introduce the generalized polar moments of inertia of the contact pressure by means of the formula

$$F_n = 2\pi \int_0^a p(\rho)\rho^{2n+1} d\rho. \tag{3.47}$$

Thus, Eq. (3.40) can be rewritten as

$$\frac{\pi m}{48} C a^6 = F_0 + \varkappa_2 \left(\frac{a^2}{4} F_0 - F_1 \right). \tag{3.48}$$

By taking into account formula (3.39), we can represent Eq. (3.38) in the form

$$p(r) + 2\varkappa_2 \left\{ \int_0^a p(\rho)\rho \ln \frac{a}{\rho} d\rho - \int_0^r p(\rho)\rho \ln \frac{r}{\rho} d\rho - \frac{1}{2} \int_r^a p(\rho)\rho \, d\rho \right\}$$
$$= \frac{mC}{16}(a^2 - r^2)^2 + (a^2 - r^2)\frac{\varkappa_2 F_0}{2\pi a^2}. \tag{3.49}$$

The following formulas can be verified by direct calculations using obvious changes of the integration variable:

$$2\pi \int_0^a \rho^{2n+1} \int_r^a p(\rho)\rho \, d\rho dr = \frac{F_{n+1}}{2(n+1)}, \tag{3.50}$$

$$2\pi \int_0^a r^{2n+1} \int_0^r p(\rho)\rho \ln \frac{r}{\rho} d\rho dr = \frac{2\pi a^{2n+2}}{2(n+1)} \int_0^a p(\rho)\rho \ln \frac{a}{\rho} d\rho$$
$$- \frac{a^{2n+2}}{4(n+1)^2} F_0 + \frac{1}{4(n+1)^2} F_{n+1}, \tag{3.51}$$

$$2\pi \int_0^a r^{2n+1} \int_0^a p(\rho)\rho \ln \frac{a}{\rho}\, d\rho dr = \frac{2\pi a^{2n+2}}{2(n+1)} \int_0^a p(\rho)\rho \ln \frac{a}{\rho}\, d\rho. \tag{3.52}$$

We now multiply the both sides of Eq. (3.49) by $2\pi r^{2n+1}$ and integrate the obtained relation with respect to r. Following, taking into account formulas (3.50)–(3.52), we arrive at the following equation:

$$F_n = \frac{\pi m C a^{2n+6}}{8(n+1)(n+2)(n+3)} - \varkappa_2 \left\{ \frac{a^{2n+2}}{2(n+1)^2(n+2)} F_0 - \frac{(n+2)}{2(n+1)^2} F_{n+1} \right\}. \tag{3.53}$$

In particular, for $n = 1$, the above formula takes the form

$$F_1 = \frac{\pi m C a^8}{192} - \varkappa_2 \left\{ \frac{a^4}{24} F_0 - \frac{3}{8} F_2 \right\}. \tag{3.54}$$

Neglecting the last term on the right-hand side of (3.54), we derive the zeroth-order approximate relation

$$F_1 \simeq \frac{\pi m C a^8}{192}, \tag{3.55}$$

and by substituting the expression (3.55) into the right-hand side of Eq. (3.48), we obtain the following approximate equation for the radius of the contact area:

$$\frac{\pi m}{48} C \left(a^6 + \frac{\varkappa_2}{4} a^8 \right) \simeq F \left(1 + \frac{\varkappa_2 a^2}{4} \right). \tag{3.56}$$

By perturbation analysis, we find that

$$a \simeq \left(\frac{48F}{\pi m C} \right)^{1/6} \left(1 - \frac{\varkappa_2}{8} \left(\frac{48F}{\pi m C} \right)^{1/3} \right). \tag{3.57}$$

It must be emphasized that Eqs. (3.56) and (3.57) take into account only the first-order correction to the effect of tangential displacements on the contact area.

In principle, the approximate equation for a can be made more accurate by employing the iterative process based upon formula (3.53). For example, by making use of formulas (3.54) and (3.53), for $n = 2$, we derive

$$F_1 \simeq \frac{\pi m C}{192} a^8 - \frac{\varkappa_2}{24} \left\{ a^4 F + \frac{3\pi m C}{160} a^{10} \right\}. \tag{3.58}$$

It is readily seen that formula (3.58) refines the first-order approximation (3.55), by means of the second order terms, and leads to

$$\frac{\pi m}{48} C \left(a^6 + \frac{\varkappa_2}{4} a^8 + \frac{3\varkappa_2^2}{80} a^{10} \right) \simeq F + \frac{\varkappa_2}{4} a^2 F + \frac{\varkappa_2^2}{24} a^4 F.$$

This equation effectively allows us to incorporate the second-order term into the first-order asymptotic formula (3.57).

3.2.6 Approximate Solution

Let us introduce a dimensionless parameter

$$\varepsilon_2 = a^2 \varkappa_2, \tag{3.59}$$

then Eq. (3.35) can be rewritten as

$$\mathscr{D}_0 = \varepsilon_2 + \frac{1}{12\varepsilon_2} \mathscr{F}, \tag{3.60}$$

where $\mathscr{D}_0$ and $\mathscr{F}$ are the dimensionless contact approach and force defined by

$$\mathscr{D}_0 = \frac{2\varkappa_2 \delta_0}{C}, \quad \mathscr{F} = \frac{48\varkappa_2^3 F}{\pi m C}. \tag{3.61}$$

Further, by substituting the exact solution for the contact pressure (3.45) into Eq. (3.41), we arrive at the equation

$$\mathscr{F} = 12\big[(4 + \mathscr{D}_0)\big(2\exp(-\varepsilon_2/2) + \varepsilon_2 - 2\big) - \varepsilon_2\big],$$

which can, by virtue of Eq. (3.60), be transformed as follows:

$$\mathscr{F} = \frac{12\varepsilon_2\big[(4 + \varepsilon_2)\exp(-\varepsilon_2/2) - 4 + \varepsilon_2\big]}{1 - \exp(-\varepsilon_2/2)}. \tag{3.62}$$

Finally, using (3.62), we exclude $\mathscr{F}$ from Eq. (3.60) to get

$$\mathscr{D}_0 = \frac{2\big(2\exp(-\varepsilon_2/2) + \varepsilon_2 - 2\big)}{1 - \exp(-\varepsilon_2/2)}. \tag{3.63}$$

It is interesting that there are simple but yet quite accurate approximations for the right-hand side of Eqs. (3.62) and (3.63). Namely, we replace those equations with the following:

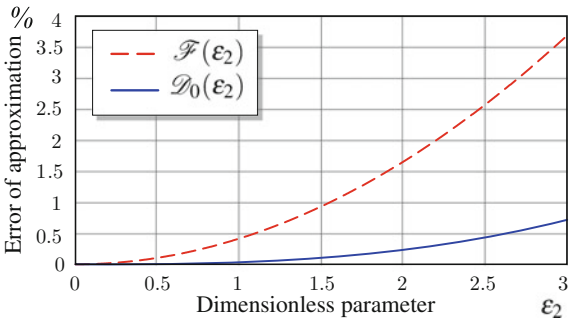

Fig. 3.4 The relative errors of the approximations provided by formulas (3.64) and (3.65) for Eqs. (3.62) and (3.63), respectively

$$\mathscr{F} \simeq \varepsilon_2^3, \tag{3.64}$$

$$\mathscr{D}_0 \simeq \varepsilon_2 + \frac{\varepsilon_2^2}{12}. \tag{3.65}$$

Note that formula (3.64) represents the zeroth-order approximation, while formula (3.65) was obtained from (3.60) after the substitution of the approximation (3.64).

From (3.64) and (3.65), it immediately follows that

$$\mathscr{D}_0 \simeq \mathscr{F}^{1/3} + \frac{\mathscr{F}^{2/3}}{12}. \tag{3.66}$$

The accuracy of these simple approximations is illustrated by Fig. 3.4. Note that the accuracy of the approximate displacement-force relation (3.66) is the same as that of formula (3.65). It is also noteworthy that for the zeroth-order approximation $\mathscr{D}_0 \simeq \varepsilon_2$, the relative error $\dfrac{\varepsilon_2 - \mathscr{D}_0}{\mathscr{D}_0} \cdot 100\,\%$ increases almost linearly with increasing ε_2 reaching the value of $-8\,\%$ at $\varepsilon_2 = 1$, for example. Finally, note that the first-order approximation

$$\mathscr{F} \simeq \varepsilon_2^3 - \frac{\varepsilon_2^5}{240},$$

which is obtained by expanding the right-hand side of Eq. (3.62) in a Maclaurin series, has a negligible error (for instance, only $-0.2\,\%$ at $\varepsilon_2 = 3$).

The problem of the approximation of the contact pressure density is more difficult. First, we rewrite the exact solution (3.45) as

$$\frac{\varkappa_2^2}{mC} p(r) = \frac{\varepsilon_2}{2}(\rho^2 - 1) + \left(2 + \frac{\mathscr{D}_0}{2}\right) g(\varepsilon_2; \rho), \tag{3.67}$$

where the function $g(\varepsilon_2; \rho)$ is defined by formula (3.46).

In the limit case, when the effect of tangential displacements is completely neglected, Eq. (3.67) reduces to the formula

$$\frac{\varkappa_2^2}{mC} p_0(\rho) = \frac{\varepsilon_2^2}{16}(1-\rho^2)^2, \tag{3.68}$$

or equivalently

$$p_0(r) = \frac{mC}{16}(a^2 - r^2)^2. \tag{3.69}$$

Observe that formula (3.68), considered as an approximation for the exact solution (3.67), has some error (negative) in the center of the contact area (see Fig. 3.5) as well as near the contour of the contact area (where the relative error is positive).

By expanding the right-hand side of Eq. (3.67) in a Maclaurin series, we derive the following first-order approximation:

$$\frac{\varkappa_2^2}{mC} p_1(\rho) = \frac{\varepsilon_2^2}{16}(1-\rho^2)^2\Big(1 + \frac{\varepsilon_2}{36}(1 - -4\rho^2)\Big). \tag{3.70}$$

The accuracy of this approximation is illustrated by Fig. 3.6 for three values of the parameter ε_2.

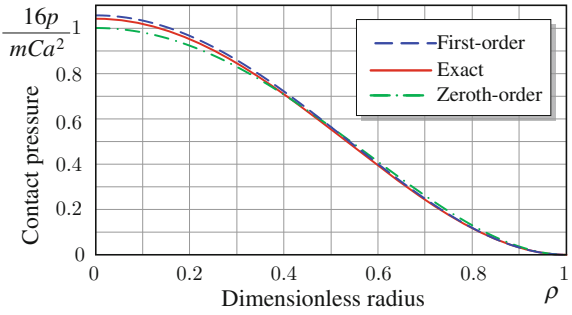

Fig. 3.5 Functions $p(\rho)$ (exact solution (3.67)), $p_0(\rho)$ (zeroth-order approximation (3.68)), and $p_1(\rho)$ (first-order approximation (3.70)) normalized by the multiplier $16\varepsilon_2^{-2}\varkappa_2^2(mC)^{-1}$

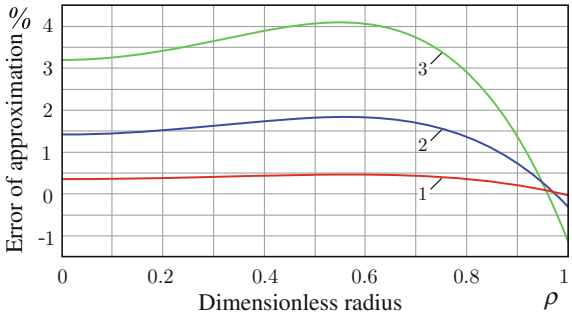

Fig. 3.6 The relative error of the first-order approximation (3.70) for the contact pressure. *Lines 1, 2,* and *3* correspond to $\varepsilon_2 = 1$, 2, and 3, respectively

3.3 Refined Contact Model for a Thin Bonded Incompressible Elastic Layer with the Effect of Tangential Displacements

In this section we consider a generalization of the contact problem studied in Sect. 3.2 by relaxing the constraint of axisymmetry. In order to simplify this study, we consider the problem of contact interaction between a thin incompressible layer and a rigid punch, the case, where the effect of tangential displacements is strongest.

3.3.1 Refined Formulation of the Contact Problem

Let us consider the unilateral contact problem (see Fig. 3.7) for a thin bonded incompressible elastic layer and a frictionless rigid punch in the shape of an elliptic paraboloid

$$\varphi(\mathbf{y}) = \frac{y_1^2}{2R_1} + \frac{y_2^2}{2R_2}. \tag{3.71}$$

According to the analysis performed in Sect. 2.1.2 (see also [3, 13, 15]), the linearized contact condition takes the form

$$w_0(\mathbf{y}) = \delta_0 - \varphi(\mathbf{y}) - \nabla_y \varphi(\mathbf{y}) \cdot \mathbf{v}_0(\mathbf{y}). \tag{3.72}$$

Here, $w_0(\mathbf{y})$ is the normal displacement of the surface points of the elastic layer on the contact interface (which is called the local indentation of the elastic layer), $\mathbf{v}_0(\mathbf{y})$ is the corresponding tangential displacement vector, and δ_0 is the punch's normal displacement (contact approach to the substrate).

Based on the perturbation analysis presented in Sect. 2.5, the displacements $\mathbf{v}_0(\mathbf{y})$ and $w_0(\mathbf{y})$ can be approximated by the leading-order asymptotic formulas

$$w_0(\mathbf{y}) = -\frac{h^3}{3G'} \Delta_y p(\mathbf{y}), \tag{3.73}$$

$$\mathbf{v}_0(\mathbf{y}) = -\frac{h^2}{2G'} \nabla_y p(\mathbf{y}), \tag{3.74}$$

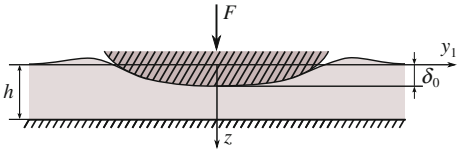

Fig. 3.7 A thin incompressible viscoelastic layer indented by a rigid punch

where $p(\mathbf{y})$ is the contact pressure, h and G' are the thickness and the out-of-plane shear modulus of the transversely isotropic elastic layer.

The contact area, ω, is determined by the condition that the contact pressure is positive

$$p(\mathbf{y}) > 0, \quad \mathbf{y} \in \omega, \tag{3.75}$$

and vanishes at the contour of the contact area, i.e.,

$$p(\mathbf{y}) = 0, \quad \mathbf{y} \in \Gamma. \tag{3.76}$$

In addition to the boundary condition above, following [8, 11, 17] (see also Sect. 2.7.3), we assume a smooth transition of the contact pressure $p(\mathbf{y})$ as the point of observation $\mathbf{y}$ approaches the contour Γ, i.e.,

$$\frac{\partial p}{\partial n}(\mathbf{y}) = 0, \quad \mathbf{y} \in \Gamma. \tag{3.77}$$

Here, $\partial/\partial n$ is the normal derivative directed outward from ω.

Denoting by F the external load applied to the punch, we write out the equilibrium equation

$$\iint\limits_{\omega} p(\mathbf{y})\, d\mathbf{y} = F. \tag{3.78}$$

By substituting the expressions (3.73) and (3.74) for the elastic displacements into the refined contact condition (3.72), we derive the governing differential equation

$$\Delta_y p(\mathbf{y}) = m\big(\varphi(\mathbf{y}) - \delta_0\big) - \chi \nabla_y \varphi(\mathbf{y}) \cdot \nabla_y p(\mathbf{y}), \tag{3.79}$$

where we have introduced the notation

$$m = \frac{3G'}{h^3}, \quad \chi = \frac{3}{2h}. \tag{3.80}$$

The refined contact problem consists in finding δ_0, $p(\mathbf{y})$, and ω which satisfy Eqs. (3.75)–(3.79) for given $\varphi(\mathbf{y})$ and F.

3.3.2 Approximate Solution for the Contact Pressure

In the case $\chi = 0$, the problem we are considering was studied in Sect. 3.1.2 (see also [5, 8]) and a closed-form solution was obtained with elliptical contact area. Based on this solution, we construct an approximation for the solution of Eq. (3.79), assuming that the dimensional parameter χ is relatively small.

Regarding the contour Γ as a perturbation of an ellipse, we look for the contact pressure in the following form:

$$p(\mathbf{y}) = p_0\big(\Xi(\mathbf{y}) + \chi\xi(\mathbf{y})\big)^2. \tag{3.81}$$

Here, p_0 is a constant coefficient representing the maximum contact pressure, $\Xi(\mathbf{y})$ and $\xi(\mathbf{y})$ are polynomials defined as

$$\Xi(\mathbf{y}) = 1 - B_1 y_1^2 - B_2 y_2^2, \quad \xi(\mathbf{y}) = A_{11} y_1^4 + A_{12} y_1^2 y_2^2 + A_{22} y_2^4. \tag{3.82}$$

Observe that the first term in parentheses on the right-hand side of (3.81) represents the closed-form solution for the limit problem ($\chi = 0$), while the second term is introduced to account for the effect of tangential displacements introduced by the last term on the right-hand side of Eq. (3.79).

It is important to emphasize that, in light of the boundary condition (3.76), the solution (3.81) assumes that the contact area ω is close to the ellipse $\Xi(\mathbf{y}) = 0$, and the contour Γ is determined by the equation

$$\Xi(\mathbf{y}) + \chi\xi(\mathbf{y}) = 0. \tag{3.83}$$

At the same time, as $\nabla_y \psi(\mathbf{y})^2 = 2\psi(\mathbf{y})\nabla_y \psi(\mathbf{y})$ for any differentiable scalar function $\psi(\mathbf{y})$, the contact pressure density (3.81) also satisfies the boundary condition (3.77) on the ellipse (3.83).

Furthermore, by straightforward calculations, we find

$$\begin{aligned}
&\frac{1}{p_0}\nabla_y p(\mathbf{y}) = 2\big(\Xi(\mathbf{y}) + \chi\xi(\mathbf{y})\big)\big(\nabla_y \Xi(\mathbf{y}) + \chi\nabla_y \xi(\mathbf{y})\big),\\
&\frac{1}{2p_0}\Delta_y p(\mathbf{y}) = \Xi(\mathbf{y})\Delta_y \Xi(\mathbf{y}) + |\nabla_y \Xi(\mathbf{y})|^2\\
&\qquad\qquad + \chi\big[\xi(\mathbf{y})\Delta_y \Xi(\mathbf{y}) + \Xi(\mathbf{y})\Delta_y \xi(\mathbf{y}) + 2\nabla_y \Xi(\mathbf{y}) \cdot \nabla_y \xi(\mathbf{y})\big]\\
&\qquad\qquad + \chi^2\big(\xi(\mathbf{y})\Delta_y \xi(\mathbf{y}) + |\nabla_y \xi(\mathbf{y})|^2\big),
\end{aligned} \tag{3.84}$$

where

$$\nabla_y \Xi(\mathbf{y}) = -2(B_1 y_1, B_2 y_2), \quad \Delta_y \Xi(\mathbf{y}) = -2(B_1 + B_2), \tag{3.85}$$

$$\nabla_y \xi(\mathbf{y}) = 2(2A_{11} y_1^3 + A_{12} y_1 y_2^2, A_{12} y_1^2 y_2 + 2A_{22} y_2^3),$$

$$\Delta_y \xi(\mathbf{y}) = 2(6A_{11} + A_{12}) y_1^2 + 2(A_{12} + 6A_{22}) y_2^2.$$

Now, substituting the above relations into (3.84) and neglecting the terms of order χ^2, we obtain

$$\frac{1}{2p_0}\Delta_y p(\mathbf{y}) \simeq P_0 + P_1 y_1^2 + P_2 y_2^2 + P_{11} y_1^4 + P_{12} y_1^2 y_2^2 + P_{22} y_2^4, \tag{3.86}$$

where

$$\begin{aligned}
P_0 &= -4(B_1 + B_2),\\
P_1 &= 4\big[B_1(3B_1 + B_2) + \chi(6A_{11} + A_{12})\big],\\
P_2 &= 4\big[B_2(B_1 + 3B_2) + \chi(A_{12} + 6A_{12})\big],\\
P_{11} &= -4\chi\big[(15B_1 + B_2)A_{11} + B_1 A_{12}\big],\\
P_{12} &= -24\chi\big[B_2 A_{11} + (B_1 + B_2)A_{12} + A_{22}B_1\big],\\
P_{22} &= -4\chi\big[(B_1 + 15B_2)A_{22} + B_2 A_{12}\big].
\end{aligned}$$

Formula (3.86) allows us to calculate the result of the substitution of the approximation (3.81) into the left-hand side of Eq. (3.79). Alternatively, when substituting the approximation (3.81) into the right-hand side of Eq. (3.79), under the assumption that χ is relatively small, we make use of the following approximate relation:

$$\chi \nabla_y \varphi(\mathbf{y}) \cdot \nabla_y p(\mathbf{y}) \simeq 2\chi p_0 \Xi(\mathbf{y}) \nabla_y \varphi(\mathbf{y}) \cdot \nabla_y \Xi(\mathbf{y}). \tag{3.87}$$

Hence, in light of (3.71), (3.85), and (3.87), we obtain

$$\begin{aligned}
m\big(\varphi(\mathbf{y}) - \delta_0\big) - \chi \nabla_y \varphi(\mathbf{y}) \cdot \nabla_y p(\mathbf{y}) = Q_0 + Q_1 y_1^2 + Q_2 y_2^2\\
+ Q_{11} y_1^4 + Q_{12} y_1^2 y_2^2 + Q_{22} y_2^4,
\end{aligned} \tag{3.88}$$

where

$$Q_0 = -m\delta_0, \quad Q_1 = \frac{m}{2R_1} + \frac{4\chi p_0}{R_1} B_1, \quad Q_2 = \frac{m}{2R_2} + \frac{4\chi p_0}{R_2} B_2,$$

$$Q_{11} = -\frac{4\chi p_0}{R_1} B_1^2, \quad Q_{12} = -4\chi p_0 B_1 B_2 \Big(\frac{1}{R_1} + \frac{1}{R_2}\Big), \quad Q_{22} = -\frac{4\chi p_0}{R_2} B_2^2.$$

The right-hand sides of Eqs. (3.86) and (3.88) are represented by fourth-order polynomials with 6 coefficients that lead to the following system:

$$\begin{aligned}
4p_0(B_1 + B_2) &= m\delta_0,\\
4p_0\big[B_1(3B_1 + B_2) + \chi(6A_{11} + A_{12})\big] &= \frac{m}{2R_1} + \frac{4\chi p_0}{R_1} B_1,\\
4p_0\big[B_2(B_1 + 3B_2) + \chi(A_{12} + 6A_{22})\big] &= \frac{m}{2R_2} + \frac{4\chi p_0}{R_2} B_2,
\end{aligned} \tag{3.89}$$

and

$$\begin{aligned}(15B_1 + B_2)A_{11} + B_1A_{12} &= \frac{B_1^2}{R_1},\\ B_2A_{11} + (B_1 + B_2)A_{12} + A_{22}B_1 &= \frac{1}{6}\Big(\frac{1}{R_1} + \frac{1}{R_2}\Big)B_1B_2,\\ (B_1 + 15B_2)A_{22} + B_2A_{12} &= \frac{B_2^2}{R_2}.\end{aligned} \tag{3.90}$$

Thus, the contact pressure density (3.81) satisfies Eq. (3.79) up to terms of order χ^2, provided its coefficients p_0, B_1, B_2, A_{11}, A_{12}, and A_{22} are determined as a solution of the system of algebraic equations (3.89) and (3.90).

3.3.3 Asymptotic Solution of the Resulting Algebraic Problem

The subsystem (3.90), regarded as a system of three linear algebraic equations with respect to A_{11}, A_{12}, and A_{22}, yields

$$A_{11} = B_1^2\frac{\Delta_1(B_1, B_2)}{\Delta(B_1, B_2)}, \quad A_{12} = \frac{\Delta_{12}(B_1, B_2)}{\Delta(B_1, B_2)}, \quad A_{22} = B_2^2\frac{\Delta_2(B_1, B_2)}{\Delta(B_1, B_2)}, \tag{3.91}$$

where

$$\begin{aligned}\Delta &= 90R_1R_2(B_1 + B_2)(B_1^2 + 14B_1B_2 + B_2^2),\\ \Delta_1 &= 6B_1^2R_2 + B_2^2(75R_2 - 9R_1) + B_1B_2(89R_2 - R_1),\\ \Delta_{12} &= B_1B_2\big[3B_1^2(5R_1 + 3R_2) + 3B_2^2(3R_1 + 5R_2) + 136B_1B_2(R_1 + R_2)\big],\\ \Delta_2 &= B_1^2(75R_1 - 9R_2) + 6B_2^2R_1 + B_1B_2(89R_1 - R_2).\end{aligned}$$

Now, substituting (3.91) into Eq. (3.89), we arrive at the following system of nonlinear algebraic equations with respect to p_0, B_1, and B_2:

$$\begin{aligned}4p_0(B_1 + B_2) &= m\delta_0,\\ B_1(3B_1 + B_2) &= \frac{m}{8R_1p_0} + \chi f_1(B_1, B_2),\\ B_2(B_1 + 3B_2) &= \frac{m}{8R_2p_0} + \chi f_2(B_1, B_2).\end{aligned} \tag{3.92}$$

The new quantities $f_1(B_1, B_2)$ and $f_2(B_1, B_2)$ are given by

$$\begin{aligned}f_1(B_1, B_2) &= B_1(9B_1 + B_2)\frac{\Delta_1(B_1, B_2)}{\Delta(B_1, B_2)},\\ f_2(B_1, B_2) &= B_2(B_1 + 9B_2)\frac{\Delta_2(B_1, B_2)}{\Delta(B_1, B_2)}.\end{aligned}$$

To solve the system (3.92), we first convert it to the form

$$\begin{aligned} p_0 &= \frac{m\delta_0}{4(B_1+B_2)},\\ 3B_1^2+B_1B_2 &= \frac{B_1+B_2}{2R_1\delta_0}+\chi f_1(B_1,B_2),\\ B_1B_2+3B_2^2 &= \frac{B_1+B_2}{2R_2\delta_0}+\chi f_2(B_1,B_2). \end{aligned} \tag{3.93}$$

We will consider the last two equations in (3.93) independently of the first one and set

$$B_i \simeq B_i^0+\chi B_i^1, \quad i=1,2, \tag{3.94}$$

where B_1^0 and B_2^0 represent the solution to the limit problem such that

$$B_1^0=\frac{R_1-R_2}{6(\beta_0^2-1)R_1R_2\delta_0}, \quad B_2^0=\beta_0^2B_1^0, \quad \frac{\beta_0^2(1+3\beta_0^2)}{3+\beta_0^2}=\frac{R_1}{R_2}. \tag{3.95}$$

Thus, substituting the approximations (3.94) into Eq. (3.93) and neglecting the terms of order χ^2, we arrive at the following linear algebraic system with respect to the asymptotic corrections B_1^1 and B_2^1:

$$\begin{aligned} \Big(6B_1^0+B_2^0-\frac{1}{2R_1\delta_0}\Big)B_1^1+\Big(B_1^0-\frac{1}{2R_1\delta_0}\Big)B_2^1 &= f_1(B_1^0,B_2^0),\\ \Big(B_2^0-\frac{1}{2R_2\delta_0}\Big)B_1^1+\Big(B_1^0+6B_2^0-\frac{1}{2R_2\delta_0}\Big)B_2^1 &= f_2(B_1^0,B_2^0). \end{aligned}$$

From here it immediately follows that

$$B_i^1=\frac{\Delta_i^1(B_1^0,B_2^0)}{\Delta^1(B_1^0,B_2^0)}, \quad i=1,2, \tag{3.96}$$

where

$$\begin{aligned} \Delta_1^1 &= \Big(B_1^0+6B_2^0-\frac{1}{2R_2\delta_0}\Big)f_1(B_1^0,B_2^0)-\Big(B_1^0-\frac{1}{2R_1\delta_0}\Big)f_2(B_1^0,B_2^0),\\ \Delta_2^1 &= \Big(6B_1^0+B_2^0-\frac{1}{2R_1\delta_0}\Big)f_2(B_1^0,B_2^0)-\Big(B_2^0-\frac{1}{2R_2\delta_0}\Big)f_1(B_1^0,B_2^0),\\ \Delta^1 &= 6(B_1^0+B_2^0)^2+24B_1^0B_2^0-\frac{B_1^0}{2\delta_0}\Big(\frac{5}{R_2}+\frac{1}{R_1}\Big)-\frac{B_2^0}{2\delta_0}\Big(\frac{5}{R_1}+\frac{1}{R_2}\Big). \end{aligned}$$

Formulas (3.94) and (3.96) give the first-order asymptotic approximations for the coefficients B_1 and B_2, provided the contact displacement δ_0 is known. After that, formulas (3.91) allow evaluation of the coefficients A_{11}, A_{12}, and A_{22}, while the first equation (3.93) yields the maximum contact pressure p_0.

3.3.4 Approximation for the Contact Area

Recall that the contour Γ of the contact area ω is defined by (3.83), which as a consequence of (3.82) can be rewritten as

$$\chi A_{22} y_2^4 - \big(B_2 - \chi A_{12} y_1^2\big) y_2^2 + 1 - B_1 y_1^2 + \chi A_{11} y_1^4 = 0. \tag{3.97}$$

It is clear that the domain ω is symmetric with respect to the coordinate axes, and the upper arc of Γ is described by the equation

$$y_2 = Y(y_1), \quad |y_1| \le \frac{d_1}{2}, \tag{3.98}$$

where $Y(y_1)$ and d_1 are given by

$$Y(y_1) = \sqrt{\frac{2\big(1 - B_1 y_1^2 + \chi A_{11} y_1^4\big)}{B_2 - \chi A_{12} y_1^2 + \sqrt{D_2(y_1)}}}, \quad d_1 = \frac{2\sqrt{2}}{\sqrt{B_1 + \sqrt{B_1^2 - 4\chi A_{11}}}},$$

$$D_2(y_1) = \big(B_2 - \chi A_{12} y_1^2\big)^2 - 4\chi A_{22}\big(1 - B_1 y_1^2 + \chi A_{11} y_1^4\big).$$

Observe that d_1 has a geometrical meaning as the diameter of the contact area ω in the direction of the y_1-axis.

The obtained formulas allow us to calculate the double integral (3.78) as follows:

$$\begin{aligned} F &= p_0 \iint\limits_{\omega} \big(\Xi(\mathbf{y}) + \chi\xi(\mathbf{y})\big)^2 d\mathbf{y} \\ &= 4p_0 \int\limits_0^{d_1/2} dy_1 \int\limits_0^{Y(y_1)} \big(\Xi(\mathbf{y}) + \chi\xi(\mathbf{y})\big)^2 dy_2, \end{aligned}$$

thus implicitly connecting the contact force F and the contact displacement δ_0.

3.3.5 Equation for the Contact Force

We now return to the governing differential equation (3.79). Following [19], we multiply both sides by $\varphi(\mathbf{y})$ and integrate over the contact domain ω. In this way, we obtain

$$\iint_{\omega} \varphi(\mathbf{y})\Delta_y p(\mathbf{y})\,d\mathbf{y} = m \iint_{\omega} \big(\varphi(\mathbf{y}) - \delta_0\big)\varphi(\mathbf{y})\,d\mathbf{y} - \chi \iint_{\omega} \varphi(\mathbf{y})\nabla_y\varphi(\mathbf{y}) \cdot \nabla_y p(\mathbf{y})\,d\mathbf{y}. \tag{3.99}$$

Second, making use of the second Green's formula

$$\iint_{\omega} \big(u(\mathbf{y})\Delta_y v(\mathbf{y}) - v(\mathbf{y})\Delta_y u(\mathbf{y})\big)d\mathbf{y} = \int_{\Gamma} \Big(u(\mathbf{y})\frac{\partial v}{\partial n}(\mathbf{y}) - v(\mathbf{y})\frac{\partial u}{\partial n}(\mathbf{y})\Big)ds_y,$$

we transform the left-hand side of Eq. (3.99) to the form

$$\iint_{\omega} \varphi(\mathbf{y})\Delta_y p(\mathbf{y})\,d\mathbf{y} = \iint_{\omega} p(\mathbf{y})\Delta_y\varphi(\mathbf{y})\,d\mathbf{y} + \int_{\Gamma} \Big(\varphi(\mathbf{y})\frac{\partial p}{\partial n}(\mathbf{y}) - p(\mathbf{y})\frac{\partial \varphi}{\partial n}(\mathbf{y})\Big)ds_y.$$

Thus, taking into account the homogeneous boundary conditions (3.76) and (3.77), we find

$$\iint_{\omega} \varphi(\mathbf{y})\Delta_y p(\mathbf{y})\,d\mathbf{y} = \Big(\frac{1}{R_1} + \frac{1}{R_2}\Big)F, \tag{3.100}$$

irrespective of the shape of ω.

Third, the first integral on the right-hand side of Eq. (3.99) can be calculated directly:

$$\iint_{\omega} \varphi(\mathbf{y})^2 d\mathbf{y} - \delta_0 \iint_{\omega} \varphi(\mathbf{y})\,d\mathbf{y} = \frac{1}{4}\Big(\frac{\mathscr{I}_{40}(\omega)}{R_1^2} + \frac{2\mathscr{I}_{22}(\omega)}{R_1 R_2} + \frac{\mathscr{I}_{04}(\omega)}{R_2^2}\Big) - \frac{\delta_0}{2}\Big(\frac{\mathscr{I}_{20}(\omega)}{R_1} + \frac{\mathscr{I}_{02}(\omega)}{R_2}\Big). \tag{3.101}$$

Here we have introduced the notation

$$\mathscr{I}_{kl}(\omega) = \iint_{\omega} y_1^k y_2^l d\mathbf{y}. \tag{3.102}$$

Fourth, the last term on the right-hand side of Eq. (3.99) can be evaluated with the help of the first Green's formula

$$\iint_{\omega} \nabla_y u(\mathbf{y}) \cdot \nabla_y v(\mathbf{y})\, d\mathbf{y} = -\iint_{\omega} u(\mathbf{y}) \Delta_y v(\mathbf{y})\, d\mathbf{y} + \int_{\Gamma} u(\mathbf{y}) \frac{\partial v}{\partial n}(\mathbf{y})\, ds_y$$

and the differential identity

$$\varphi(\mathbf{y}) \nabla_y \varphi(\mathbf{y})^2 = \frac{1}{2} \nabla_y \varphi(\mathbf{y})^2.$$

Taking into account the boundary condition (3.76), we obtain

$$\iint_{\omega} \varphi(\mathbf{y}) \nabla_y \varphi(\mathbf{y}) \cdot \nabla_y p(\mathbf{y})\, d\mathbf{y} = -\frac{1}{2} \iint_{\omega} p(\mathbf{y}) \Delta_y \varphi(\mathbf{y})^2 d\mathbf{y}, \tag{3.103}$$

where

$$\Delta_y \varphi(\mathbf{y})^2 = \frac{1}{R_1}\Big(\frac{3}{R_1} + \frac{1}{R_2}\Big) y_1^2 + \frac{1}{R_2}\Big(\frac{1}{R_1} + \frac{3}{R_2}\Big) y_2^2.$$

Now, collecting formulas (3.99)–(3.101) and (3.103), we arrive at the relation

$$\begin{aligned} \frac{R_1 + R_2}{R_1 R_2} F = {} & \frac{m}{4}\left(\frac{\mathscr{I}_{40}(\omega)}{R_1^2} + \frac{2\mathscr{I}_{22}(\omega)}{R_1 R_2} + \frac{\mathscr{I}_{04}(\omega)}{R_2^2}\right) \\ & - \frac{m\delta_0}{2}\left(\frac{\mathscr{I}_{20}(\omega)}{R_1} + \frac{\mathscr{I}_{02}(\omega)}{R_2}\right) \\ & + \frac{\chi}{2} \iint_{\omega} p(\mathbf{y}) \Delta_y \varphi(\mathbf{y})^2 d\mathbf{y}. \end{aligned} \tag{3.104}$$

We emphasize that this equation is an exact consequence of the governing differential equation (3.79). In order to derive from it the force-displacement relation we still need to calculate the last integral in (3.104). However, as we are considering the first-order asymptotic model, it will be sufficient to solve this problem with an accuracy of the order $O(\chi^2)$.

Again following [19], we multiply both sides of Eq. (3.79) by $\varphi(\mathbf{y})^2$ and integrate them over the contact domain ω. Using once more the second Green's formula and taking into account the homogeneous boundary conditions (3.76) and (3.77), we find

$$\iint_{\omega} p(\mathbf{y}) \Delta_y \varphi(\mathbf{y})^2 d\mathbf{y} = m \iint_{\omega} \big(\varphi(\mathbf{y}) - \delta_0\big) \varphi(\mathbf{y})^2 d\mathbf{y} + O(\chi). \tag{3.105}$$

Finally, from (3.104) and (3.105), it follows that

$$\begin{aligned}\frac{4(R_1+R_2)}{mR_1R_2}F \simeq{}& \frac{\mathscr{I}_{40}(\omega)}{R_1^2}+\frac{2\mathscr{I}_{22}(\omega)}{R_1R_2}+\frac{\mathscr{I}_{04}(\omega)}{R_2^2}\\ &+\frac{\chi}{4}\left(\frac{\mathscr{I}_{60}(\omega)}{R_1^3}+\frac{3\mathscr{I}_{42}(\omega)}{R_1^2R_2}+\frac{3\mathscr{I}_{24}(\omega)}{R_1R_2^2}+\frac{\mathscr{I}_{06}(\omega)}{R_2^3}\right)\\ &-\delta_0\left\{2\left(\frac{\mathscr{I}_{20}(\omega)}{R_1}+\frac{\mathscr{I}_{02}(\omega)}{R_2}\right)\right.\\ &\left.+\frac{\chi}{2}\left(\frac{\mathscr{I}_{40}(\omega)}{R_1^2}+\frac{2\mathscr{I}_{22}(\omega)}{R_1R_2}+\frac{\mathscr{I}_{04}(\omega)}{R_2^2}\right)\right\},\end{aligned}\tag{3.106}$$

where $\mathscr{I}_{kl}(\omega)$ are the moments of the contact area ω defined by formula (3.102).

3.3.6 Variation of the Contact Area

We now recast Eq. (3.97) for the contour Γ of the contact area ω in the form

$$1-B_1y_1^2-B_2y_2^2+\chi\left(A_{11}y_1^4+A_{12}y_1^2y_2^2+A_{22}y_2^4\right)=0,\tag{3.107}$$

and consider the contour Γ as a variation of the ellipse γ defined by the equation

$$1-B_1y_1^2-B_2y_2^2=0,\tag{3.108}$$

which can also be parameterized by the equations

$$y_1=b_1\cos\tau,\quad y_2=b_2\sin\tau.$$

Here, $\tau\in(0,2\pi]$ is a parameter, b_1 and b_2 are the semi-axes of the ellipse (3.108) such that

$$b_1^2=\frac{1}{B_1},\quad b_2^2=\frac{1}{B_2}.$$

In the neighborhood of γ we introduce a local coordinate system (τ,n), where n is the signed distance to the ellipse (3.108) measured along the outward normal

$$\mathbf{n}(\tau)=\frac{1}{\sqrt{b_1^2\sin^2\tau+b_2^2\cos^2\tau}}(b_2\cos\tau,b_1\sin\tau).$$

Thus, the unknown boundary Γ of the contact domain ω can be described in the local coordinates by a parametric equation (see Fig. 3.8)

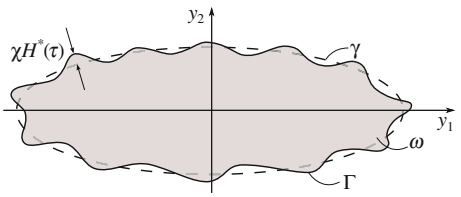

Fig. 3.8 Schematic representation of the contact domain ω with the contour Γ, which is considered as a variation of the elliptic contour γ

$$n = \chi H^*(\tau), \tag{3.109}$$

so that the parametrization in the Cartesian coordinate system is as follows:

$$y_1 = b_1 \cos\tau + \chi H^*(\tau) \frac{b_2 \cos\tau}{\sqrt{b_1^2 \sin^2\tau + b_2^2 \cos^2\tau}},$$
$$y_2 = b_2 \sin\tau + \chi H^*(\tau) \frac{b_1 \sin\tau}{\sqrt{b_1^2 \sin^2\tau + b_2^2 \cos^2\tau}}.$$

Substituting the above equations into Eq. (3.107) and neglecting the terms of the order $O(\chi^2)$, we obtain

$$H^*(\tau) = \frac{b_1 b_2 \left(A_{11} b_1^4 \cos^4\tau + A_{12} b_1^2 b_2^2 \cos^2\tau \sin^2\tau + A_{22} b_2^4 \sin^4\tau\right)}{2\sqrt{b_1^2 \sin^2\tau + b_2^2 \cos^2\tau}}. \tag{3.110}$$

This obtained result allows us to approximately calculate the integral characteristics (3.102) of the contact area ω as follows:

$$\mathscr{I}_{kl}(\omega) \simeq \iint\limits_{B_1 y_1^2 + B_2 y_2^2 < 1} y_1^k y_2^l d\mathbf{y} + \chi \int\limits_0^{2\pi} y_1(\tau)^k y_2(\tau)^l H^*(\tau)\, ds_\tau.$$

Here, $y_1(\tau)$ and $y_2(\tau)$ are the coordinates of the point τ on the ellipse (3.108), that is $y_1(\tau) = b_1 \cos\tau$ and $y_2(\tau) = b_2 \sin\tau$, while the differential of the arc length is given by $ds_\tau = \sqrt{b_1^2 \sin^2\tau + b_2^2 \cos^2\tau}\, d\tau$.

In this way, we obtain

$$\begin{aligned} \mathscr{I}_{20}(\omega) &\simeq \frac{\pi}{4} b_1^3 b_2 \left(1 + \frac{\chi}{4}\left(5A_{11} b_1^4 + A_{12} b_1^2 b_2^2 + A_{22} b_2^4\right)\right), \\ \mathscr{I}_{02}(\omega) &\simeq \frac{\pi}{4} b_1 b_2^3 \left(1 + \frac{\chi}{4}\left(A_{11} b_1^4 + A_{12} b_1^2 b_2^2 + 5A_{22} b_2^4\right)\right) \end{aligned} \tag{3.111}$$

for the second-order moments and

$$\begin{aligned}
\mathscr{I}_{40}(\omega) &\simeq \frac{\pi}{8} b_1^5 b_2 \Big(1 + \frac{\chi}{16}\big(35A_{11}b_1^4 + 5A_{12}b_1^2b_2^2 + 3A_{22}b_2^4\big)\Big),\\
\mathscr{I}_{22}(\omega) &\simeq \frac{\pi}{24} b_1^3 b_2^3 \Big(1 + \frac{3\chi}{16}\big(5A_{11}b_1^4 + 3A_{12}b_1^2b_2^2 + 5A_{22}b_2^4\big)\Big),\\
\mathscr{I}_{04}(\omega) &\simeq \frac{\pi}{8} b_1 b_2^5 \Big(1 + \frac{\chi}{16}\big(3A_{11}b_1^4 + 5A_{12}b_1^2b_2^2 + 35A_{22}b_2^4\big)\Big).
\end{aligned} \tag{3.112}$$

for the fourth-order moments of the contact domain ω.

Finally, as the sixth-order moments of ω enter Eq. (3.106) along with the factor χ, we can make use of the zeroth-order approximations

$$\begin{Bmatrix} \mathscr{I}_{60}(\omega) \\ \mathscr{I}_{42}(\omega) \\ \mathscr{I}_{24}(\omega) \\ \mathscr{I}_{06}(\omega) \end{Bmatrix} \simeq \frac{\pi b_1 b_2}{64} \begin{Bmatrix} 5b_1^6 \\ b_1^4 b_2^2 \\ b_1^2 b_2^4 \\ 5b_2^6 \end{Bmatrix}. \tag{3.113}$$

Note that in numerically solving the moments of the contact area $\mathscr{I}_{kl}(\omega)$ can be evaluated directly based on the definition (3.102).

3.3.7 *Comparison with the Solution of the Axisymmetric Problem*

In the axisymmetric case (see Fig. 3.9), formula (3.81) simplifies to

$$p(\mathbf{y}) = p_0\big(1 - B_1 r^2 + \chi A_{11} r^4\big)^2, \tag{3.114}$$

where $r = \sqrt{y_1^2 + y_2^2}$ is the polar radius.

Correspondingly, Eqs. (3.89) and (3.90) take the form

$$8p_0B_1 = m\delta_0, \quad 16p_0(B_1^2 + 2\chi A_{11}) = \frac{m}{2R} + \frac{4\chi p_0}{R} B_1,$$

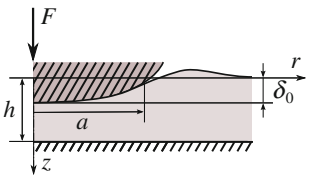

Fig. 3.9 Axisymmetric contact of a parabolic punch with a bonded incompressible elastic layer

$$A_{11} = \frac{B_1}{18R}. \tag{3.115}$$

From here it immediately follows that

$$B_1 = \frac{1}{4\delta_0 R} + \frac{5\chi}{36R}. \tag{3.116}$$

Note that, because formula $(3.95)_1$ does not allow a direct passage to the limit $R_2 = R_1$ and $\beta_0 = 1$, it should be transformed with the help of Eq. $(3.95)_3$ as follows:

$$B_1^0 = \frac{\beta_0^2 + 1}{2R_1\delta_0(\beta_0^2 + 3)}.$$

Further, formula (3.114) assumes that the contact area is circular with radius a determined from the equation

$$\chi A_{11} a^4 - B_1 a^2 + 1 = 0.$$

In light of (3.115) and (3.116), this equation yields

$$a^2 \simeq 4R\delta_0 - \frac{4\chi}{3} R\delta_0^2.$$

The same results can be obtained from the asymptotic formula (3.65) as a consequence of (3.59) and $(3.61)_1$, provided the relation $\varkappa_2 = \chi / R$ is taken into account.

We note that the established asymptotic method can be used for solving the two-dimensional refined unilateral contact problem for a thin orthotropic incompressible elastic strip, thus generalizing the asymptotic solutions obtained in [1, 2, 12, 20].

Finally, observe that the asymptotic models developed in this section can be applied not only for articular contact, but also, for example, in studying the heel resting problem [14] and other bone-soft tissue contact problems [22].

References

1. Alblas, J.B., Kuipers, M.: On the two dimensional problem of a cylindrical stamp pressed into a thin elastic layer. Acta Mech. **9**, 292–311 (1970)
2. Aleksandrov, V.M.: Two problems with mixed boundary conditions for an elastic orthotropic strip. J. Appl. Math. Mech. **70**, 128–138 (2006)
3. Argatov, I.I.: Approximate solution of an axisymmetric contact problem with allowance for tangential displacements on the contact surface. J. Appl. Mech. Tech. Phys. **45**, 118–123 (2004)
4. Argatov, I.I.: Development of an asymptotic modeling methodology for tibio-femoral contact in multibody dynamic simulations of the human knee joint. Multibody Syst. Dyn. **28**, 3–20 (2012)
5. Argatov, I., Mishuris, G.: Frictionless elliptical contact of thin viscoelastic layers bonded to rigid substrates. Appl. Math. Model. **35**, 3201–3212 (2011)

6. Argatov, I., Mishuris, G.: Elliptical contact of thin biphasic cartilage layers: Exact solution for monotonic loading. J. Biomech. **44**, 759–761 (2011)
7. Ateshian, G.A., Lai, W.M., Zhu, W.B., Mow, V.C.: An asymptotic solution for the contact of two biphasic cartilage layers. J. Biomech. **27**, 1347–1360 (1994)
8. Barber, J.R.: Contact problems for the thin elastic layer. Int. J. Mech. Sci. **32**, 129–132 (1990)
9. Borodich, F.M.: Similarity in the problem of contact between elastic bodies. J. Appl. Math. Mech. **47**, 519–521 (1983)
10. Borodich, F.M.: The Hertz-type and adhesive contact problems for depth-sensing indentation. Adv. Appl. Mech. **47**, 225–366 (2014)
11. Chadwick, R.S.: Axisymmetric indentation of a thin incompressible elastic layer. SIAM J. Appl. Math. **62**, 1520–1530 (2002)
12. Erbaş, B., Yusufoğlu, E., Kaplunov, J.: A plane contact problem for an elastic orthotropic strip. J. Eng. Math. **70**, 399–409 (2011)
13. Galanov, B.A.: Approximate solution to some problems of elastic contact of two bodies. Mech. Solids **16**, 61–67 (1981)
14. Gefen, A.: The biomechanics of heel ulcers. J. Tissue Viabil. **19**, 124–131 (2010)
15. Georgiadis, L.M.: Tangential-displacement effects in the wedge indentation of an elastic half-space—an integral-equation approach. Comput. Mech. **21**, 347–352 (1998)
16. Hlaváček, M.: Elliptical contact on elastic incompressible coatings. Eng. Mech. **15**, 249–261 (2008)
17. Jaffar, M.J.: Asymptotic behaviour of thin elastic layers bonded and unbonded to a rigid foundation. Int. J. Mech. Sci. **31**, 229–235 (1989)
18. Johnson, K.L.: Contact Mechanics. Cambridge Univ. Press, Cambridge, UK (1985)
19. Koroleva, A.A., Rogosin, S.V., Mishuris, G.S.: Analysis of the unilateral contact problem for biphasic cartilage layers with an elliptic contact zone and accounting for the tangential displacements. arXiv preprint arXiv:1503.06206 (2015)
20. Malits, P.: Plane contact problem for a thin incompressible strip. Q. J. Mech. Appl. Math. **65**, 313–332 (2012)
21. Matthewson, M.J.: Axi-symmetric contact on thin compliant coatings. J. Mech. Phys. Solids **29**, 89–113 (1981)
22. Portnoy, S., Vuillerme, N., Payan, Y., Gefen, A.: Clinically oriented real-time monitoring of the individual's risk for deep tissue injury. Med. Biol. Eng. Comput. **49**, 473–483 (2011)

Chapter 4
Frictionless Contact of Thin Viscoelastic Layers

Abstract The chapter begins with an introduction to linear viscoelastic theory, and then proceeds to a generalization of the elastic leading-order asymptotic models for the viscoelastic case, based on the correspondence principle. In Sect. 4.2, we consider the main features of the analytical technique for solving unilateral contact problems for a viscoelastic foundation. The axisymmetric contact problem for a thin bonded incompressible viscoelastic layer is analyzed in Sect. 4.3 and in the refined formulation accounting for tangential displacements in Sect. 4.4. Finally, in Sect. 4.5 we solve the problem of frictionless contact for thin incompressible viscoelastic layers bonded to rigid substrates shaped like elliptic paraboloids.

4.1 Deformation of a Thin Viscoelastic Layer

In this section we consider a general correspondence principle for quasi-static deformation of viscoelastic materials and apply it in the case of a thin transversely isotropic layer based on the developed leading-order asymptotic solution.

4.1.1 Viscoelastic Constitutive Laws

Various mathematical models have been developed to describe the deformational material properties of time-dependent materials [17, 24]. Recall that according to the Boltzmann superposition principle [11], the constitutive relation for a viscoelastic anisotropic material can be written in the form of the Stieltjes integral

$$\sigma_{ij}(t) = \int_0^{\infty} \varepsilon_{kl}(t-s)\, dG_{ijkl}(s). \tag{4.1}$$

Here, $G_{ijkl}(t)$ are components of a fourth order tensor, which are called the relaxation functions. It is assumed that $G_{ijkl}(t) = 0$ for $-\infty < t < 0$, and thus the constitutive law (4.1) is invariant with respect to arbitrary shifts in the time scale.

I. Argatov and G. Mishuris, *Contact Mechanics of Articular Cartilage Layers*,
Advanced Structured Materials 50, DOI 10.1007/978-3-319-20083-5_4

From the symmetry of the stress and strain tensors, it immediately follows that $G_{ijkl}(t) = G_{jikl}(t) = G_{ijlk}(t)$. The relaxation functions are presumably positive and decreasing at positive times, being discontinuous at time zero [22]. In particular, transversely isotropic materials are describable by five independent relaxation functions, which can have different time dependence.

Usually it is assumed that strains $\varepsilon_{ij}(t)$ are continuous for $t \geq 0$ and may have a step discontinuity at $t = 0$, while $\varepsilon_{ij}(t) = 0$ for $t < 0$. Assuming additionally the continuity of the first derivatives of the relaxation functions $G_{ijkl}(t)$ for $0 \leq t < \infty$, we can rewrite Eq. (4.1) in the form

$$\sigma_{ij}(t) = G_{ijkl}(0)\varepsilon_{kl}(t) + \int_0^t \varepsilon_{kl}(t-s)\frac{dG_{ijkl}}{ds}(s)\,ds. \tag{4.2}$$

The above form of the constitutive law exposes the instantaneous elastic reaction of the viscoelastic material with the instantaneous elastic moduli $G_{ijkl}(0)$.

After integration by parts, Eq. (4.2) takes the form

$$\sigma_{ij}(t) = G_{ijkl}(t)\varepsilon_{kl}(0) + \int_0^t G_{ijkl}(t-\tau)\dot{\varepsilon}_{kl}(\tau)\,d\tau, \tag{4.3}$$

where the differentiation with respect to the time variable t is denoted by a dot.

Further, the above relation can be generalized for the whole history, provided that $\varepsilon_{ij}(t) \to 0$ as $t \to -\infty$, as follows:

$$\sigma_{ij}(t) = \int_{-\infty}^t G_{ijkl}(t-\tau)\dot{\varepsilon}_{kl}(\tau)\,d\tau. \tag{4.4}$$

The inverse constitutive law has the form

$$\varepsilon_{ij}(t) = \int_{-\infty}^t J_{ijkl}(t-\tau)\dot{\sigma}_{kl}(\tau)\,d\tau, \tag{4.5}$$

where $J_{ijkl}(t)$ are the creep functions such that $J_{ijkl}(t) = 0$ for $-\infty < t < 0$, and $J_{ijkl}(t) = J_{jikl}(t) = J_{ijlk}(t)$. It is assumed that the creep functions are continuous and possess continuous first derivatives on the interval $0 \leq t < \infty$.

Now, taking the Fourier transform of (4.4), we find

$$\hat{\sigma}_{ij}(\omega) = G^*_{ijkl}(\omega)\hat{\varepsilon}_{kl}(\omega), \tag{4.6}$$

where the circumflex refers to the corresponding Fourier transformed quantity, which is a complex-valued function of the angular frequency ω. In particular, by definition, we have

$$\hat{G}_{ijkl}(\omega) = \int_{-\infty}^{\infty} G_{ijkl}(t) \exp(-\mathrm{i}\omega t)\, dt, \tag{4.7}$$

where i is the imaginary unit such that $\mathrm{i}^2 = -1$.

Since the Fourier transform of the derivative $d\varepsilon_{kl}(t)/dt$ is given by $\mathrm{i}\omega\hat{\varepsilon}_{kl}(\omega)$, the application of the convolution property yields the following representation for the complex elastic moduli:

$$G^*_{ijkl}(\omega) = \mathrm{i}\omega\hat{G}_{ijkl}(\omega). \tag{4.8}$$

In the same way, the Fourier transform of Eq. (4.5) results in the relation

$$\hat{\varepsilon}_{ij}(\omega) = J^*_{ijkl}(\omega)\hat{\sigma}_{kl}(\omega), \tag{4.9}$$

where $J^*_{ijkl}(\omega)$ are the complex elastic compliances such that

$$J^*_{ijkl}(\omega) = \mathrm{i}\omega\hat{J}_{ijkl}(\omega). \tag{4.10}$$

Note that Eqs. (4.4) and (4.5) represent the stress-strain relations in the relaxation and creep integral forms, respectively, while Eqs. (4.6) and (4.9) represent the constitutive relations in the frequency domain.

4.1.2 Correspondence Principle for a Viscoelastic Layer

To set up the following analysis, we consider the quasi-static deformation of a linear anisotropic viscoelastic layer bonded to a rigid substrate (see Fig. 4.1).

The stress-strain relationship is given by either (4.4) or (4.5), while the linearized strain-displacement relations are

$$\varepsilon_{ij} = \frac{1}{2}\left(\frac{\partial u_i}{\partial x_j} + \frac{\partial u_j}{\partial x_i}\right), \tag{4.11}$$

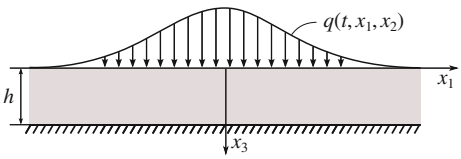

Fig. 4.1 A viscoelastic layer bonded to a rigid substrate and loaded by a normal load variable in time

where u_1, u_2, and u_3 denote the Cartesian components of the displacement vector $\mathbf{u}$.

The equations of equilibrium in the absence of body forces take the form

$$\frac{\partial \sigma_{i1}}{\partial x_1} + \frac{\partial \sigma_{i2}}{\partial x_2} + \frac{\partial \sigma_{i3}}{\partial x_3} = 0, \quad i = 1, 2, 3. \tag{4.12}$$

In the case of the viscoelastic layer bonded to a rigid base, the following displacement boundary conditions hold:

$$u_i\big|_{x_3=h} = 0, \quad i = 1, 2, 3. \tag{4.13}$$

Assuming that the layer is loaded by a normal distributed load, $q(t, x_1, x_2)$, we impose the following traction boundary conditions on the upper layer surface:

$$\sigma_{13}\big|_{x_3=0} = \sigma_{23}\big|_{x_3=0} = 0, \quad \sigma_{33}\big|_{x_3=0} = -q(t, x_1, x_2). \tag{4.14}$$

Moreover, the following initial conditions must be met:

$$u_i(t, \mathbf{x}) = \varepsilon_{ij}(t, \mathbf{x}) = \sigma_{ij}(t, \mathbf{x}) = 0, \quad -\infty < t < 0. \tag{4.15}$$

Thus, the deformation problem consists in finding field histories for the displacement vector $\mathbf{u}$, the strain tensor $\boldsymbol{\varepsilon}$, and the stress tensor $\boldsymbol{\sigma}$ which for the known relaxation tensor $\mathbf{G}$ (or the creep tensor $\mathbf{J}$) and the prescribed surface load density $q(t, x_1, x_2)$ satisfy Eqs. (4.4) (or (4.5)), (4.11)–(4.15).

Among the above equations, only the viscoelastic constitutive equations (4.4) and (4.5) contain products of time-dependent quantities. Therefore, applying the Fourier transform to Eqs. (4.11)–(4.15), the obtained relations in the frequency domain will not differ from their elastic counterparts. Correspondingly, the Fourier transform of Eqs. (4.4) and (4.5) leads to Eqs. (4.6) and (4.9), respectively, which relate the Fourier transforms of stresses and strains and are analogous to the generalized Hooke's law $\sigma_{ij} = C_{ijkl}\varepsilon_{kl}$, where C_{ijkl} are elastic moduli.

Thus, the transforms $\hat{\mathbf{u}}$, $\hat{\boldsymbol{\varepsilon}}$, and $\hat{\boldsymbol{\sigma}}$ satisfy what is formally an elasticity problem. The correspondence principle [17, 22] states that if a solution to some linear elasticity problem for an elastic solid characterized by elastic moduli C_{ijkl} is known, then the solution to the corresponding deformation problem for a linearly viscoelastic material, characterized by relaxation functions $G_{ijkl}(t)$, can be obtained by replacing the real elastic moduli C_{ijkl} in the elastic solution with the complex moduli $G^*_{ijkl}(\omega)$ of the viscoelastic material, and then employing an inverse Fourier transform back to the time domain from the frequency domain.

We emphasize that usually the correspondence principle involving Laplace transform is usually used to solve boundary-value problems for viscoelastic materials. In this case, for example, Eq. (4.4) is transformed to the Laplace domain as follows:

$$\tilde{\sigma}_{ij}(s) = s\tilde{G}_{ijkl}(s)\tilde{\varepsilon}_{kl}(s). \tag{4.16}$$

Here, s is the transformation variable, and tildes denote Laplace transforms, i.e.,

$$\tilde{G}_{ijkl}(s) = \int_0^\infty G_{ijkl}(t) \exp(-st)\, dt.$$

Observe that, in contrast to Eq. (4.6), on the right-hand side of Eq. (4.16) there is an extra multiplier of the transformed variable, which was previously absorbed into the definition of the complex elastic moduli $G^*_{ijkl}(\omega)$ (see Eq. (4.8)). Hence, if an elastic solution is known, according to the correspondence principle, the corresponding viscoelastic solution may be obtained by replacing each elastic material characteristics appearing in the elastic solution by its s-multiplied Laplace transform, and transforming back to the time domain.

It is also worth noting [17] that the Fourier transform of a transient viscoelastic response function represents a dynamic response function (in a harmonic loading) which is itself measurable experimentally.

4.1.3 Deformation of a Thin Compressible Transversely Isotropic Viscoelastic Layer Bonded to a Rigid Base

According to the perturbation analysis performed in Sect. 1.2 (see, for example, formula (1.58)), the leading-order asymptotic solution for the quasi-static local indentation of a compressible elastic layer of thickness h is given by

$$\begin{aligned} w_0(t, \mathbf{y}) &\equiv u_3(t, y_1, y_2, 0) \\ &\simeq \frac{h}{A_{33}} q(t, \mathbf{y}). \end{aligned} \tag{4.17}$$

In the isotropic case the elastic constant A_{33} is equal to $\lambda + 2\mu$ (with λ and μ being Lamé's constants) and is called the aggregate elastic modulus [1, 15]. Recall that while Young's modulus, E', is determined from a uniaxial loading testing in the x_3-direction, the aggregate elastic modulus A_{33} is determined under a uniaxial confined strain testing condition with the only non-zero strain component ε_{33}. In the case of transversely isotropic materials, we call A_{33} the longitudinal aggregate elastic modulus and introduce a new notation

$$E'_A = A_{33}. \tag{4.18}$$

For a transversely isotropic viscoelastic material, we can introduce the longitudinal (axial) aggregate relaxation modulus, $E'_A(t)$. This function can be experimentally measured in the confined compression test (see Fig. 4.2), which models a one-dimensional deformation problem in the x_3-direction, where the normal strains ε_{11}, ε_{22}, and all shear strains vanish.

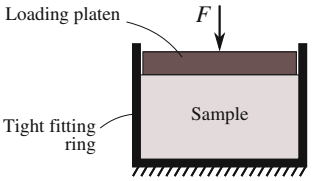

Fig. 4.2 Confined compression testing configuration for measuring the aggregate creep modulus of a viscoelastic material using a cylindrical sample placed in a confining chamber of ring form

In the displacement-controlled confined compression test [13], where the axis of material symmetry coincides with the axis of geometrical symmetry, the stress-strain relation (with the convention of positive compressive stress) has the form

$$\begin{aligned}\sigma_{33}(t) &= \varepsilon_{33}(0)E'_A(t) + \int_0^t E'_A(t-\tau)\dot{\varepsilon}_{33}(\tau)\,d\tau \\ &= \int_{0^-}^t E'_A(t-\tau)\dot{\varepsilon}_{33}(\tau)\,d\tau, \end{aligned} \tag{4.19}$$

where the lower integration limit 0^- indicates that the integration starts at infinitesimally negative time in order to include the strain discontinuity at time zero.

Thus, the introduced above material characteristic $E'_A(t)$ represents the material response for unit-step deformation loading $\varepsilon_{33}(t) = \mathscr{H}(t)$, where $\mathscr{H}(t)$ is the Heaviside step function such that $\mathscr{H}(t) = 0$ for $t < 0$ and $\mathscr{H}(t) = 1$ for $t \geq 0$.

In the load-controlled testing configuration for the confined compression test, the inverse relation can be written as

$$\begin{aligned}\varepsilon_{33}(t) &= \int_{0^-}^t J'_A(t-\tau)\dot{\sigma}_{33}(\tau)\,d\tau \\ &= \sigma_{33}(0)J'_A(t) + \int_0^t J'_A(t-\tau)\dot{\sigma}_{33}(\tau)\,d\tau, \end{aligned} \tag{4.20}$$

where the function $J'_A(t)$ represents the creep response of the viscoelastic material in confined compression under application of a step normal stress of unit magnitude.

In what follows, the material characteristics $J'_A(t)$ will be called the longitudinal (axial) aggregate creep compliance. Since the creep compliance represents the strain history resulting from a step stress $\sigma_{33}(t) = \mathscr{H}(t)$ (see, e.g., formula (4.20)), by substituting the function $J'_A(t)$ into Eq. (4.19), we obtain

$$\mathscr{H}(t) = J'_A(0)E'_A(t) + \int_0^t E'_A(t-\tau)\frac{dJ'_A(\tau)}{d\tau}\,d\tau. \tag{4.21}$$

From (4.21), it immediately follows that

$$J'_A(0) = \frac{1}{E'_A(0)}. \tag{4.22}$$

Note also that Eq. (4.21) can be recast equivalently as

$$\int_0^t E'_A(t-\tau)J'_A(\tau)\,d\tau = t. \tag{4.23}$$

In the Laplace domain, the interrelation between the relaxation and creep functions, which is represented by Eq. (4.23), results in the relation

$$s^2\tilde{E}'_A(s)\tilde{J}'_A(s) = 1. \tag{4.24}$$

Thus, by applying the viscoelastic correspondence principle, in light of the notation (4.18), Eq. (4.17) yields

$$\tilde{w}_0(s,\mathbf{y}) = \frac{h}{s\tilde{E}'_A(s)}\tilde{q}(s,\mathbf{y}),$$

where tildes denote Laplace transforms.

Taking into account (4.24), we rewrite the above equation in the form

$$\tilde{w}_0(s,\mathbf{y}) = hs\tilde{J}'_A(s)\tilde{q}(s,\mathbf{y}). \tag{4.25}$$

Finally, performing the inverse transform, we find

$$w_0(t,\mathbf{y}) = h\int_{0^-}^t J'_A(t-\tau)\frac{\partial q}{\partial\tau}(\tau,\mathbf{y})\,d\tau. \tag{4.26}$$

Equation (4.26) represents the leading-order asymptotic model for a thin bonded compressible transversely isotropic viscoelastic layer.

4.1.4 Deformation of a Thin Bonded Incompressible Transversely Isotropic Viscoelastic Layer

According to the perturbation analysis performed in Sect. 2.5 (see, in particular, formula (2.152)), the leading-order asymptotic solution for the quasi-static local indentation of an incompressible elastic layer of thickness h is given by

$$\begin{aligned} w_0(t,\mathbf{y}) &\equiv u_3(t,y_1,y_2,0) \\ &\simeq -\frac{h^3}{3a_{44}}\Delta_y q(t,\mathbf{y}), \end{aligned} \tag{4.27}$$

where the elastic constant a_{44} coincides with the out-of-plane shear modulus G', i.e.,

$$a_{44} = G'. \tag{4.28}$$

For a transversely isotropic viscoelastic material, we introduce the out-of-plane relaxation modulus in shear, $G'(t)$. This material characteristic represents the material response for unit-step deformation loading $\varepsilon_{31}(t) = \mathscr{H}(t)$ (or $\varepsilon_{32}(t) = \mathscr{H}(t)$), and thus the corresponding stress-strain relations are as follows:

$$\begin{aligned} \sigma_{3i}(t) &= 2\varepsilon_{3i}(0)G'(t) + 2\int_0^t G'(t-\tau)\dot{\varepsilon}_{3i}(\tau)\,d\tau \\ &= 2\int_{0^-}^t G'(t-\tau)\dot{\varepsilon}_{3i}(\tau)\,d\tau, \quad i = 1,2. \end{aligned} \tag{4.29}$$

The inverse relations are given by

$$\begin{aligned} 2\varepsilon_{3i}(t) &= \int_{0^-}^t J'(t-\tau)\dot{\sigma}_{3i}(\tau)\,d\tau \\ &= \sigma_{3i}(0)J'(t) + \int_0^t J'(t-\tau)\dot{\sigma}_{3i}(\tau)\,d\tau. \end{aligned} \tag{4.30}$$

Here, $J'(t)$ is the out-of-plane creep compliance in shear, which represents the deformation response of the viscoelastic material under application of a step out-of-plane shear stress of unit magnitude.

For the relaxation modulus $G'(t)$ and the creep compliance $J'(t)$, relations similar to (4.21)–(4.24) hold true. In particular, for their Laplace transforms we have

$$s^2\tilde{G}'(s)\tilde{J}'(s) = 1, \tag{4.31}$$

while, analogously to (4.22), their instantaneous values are inversely reciprocal

$$J'(0) = \frac{1}{G'(0)}, \tag{4.32}$$

so that at zero-plus time an elastic material response prevails.

Thus, by applying the viscoelastic correspondence principle, in light of (4.28), Eq. (4.27) yields

$$\tilde{w}_0(s, \mathbf{y}) = -\frac{h^3}{3s\tilde{G}'(s)} \Delta_y \tilde{q}(s, \mathbf{y}).$$

Taking into account (4.31), we rewrite the above equation in the form

$$\tilde{w}_0(s, \mathbf{y}) = -\frac{h^3}{3} s\tilde{J}'(s) \Delta_y \tilde{q}(s, \mathbf{y}), \tag{4.33}$$

which after performing the inverse transform takes the final form

$$w_0(t, \mathbf{y}) = -\frac{h^3}{3} \int_{0^-}^{t} J'(t - \tau) \Delta_y \frac{\partial q}{\partial \tau}(\tau, \mathbf{y})\, d\tau. \tag{4.34}$$

Equation (4.34) represents the leading-order asymptotic model for a thin incompressible isotropic viscoelastic layer bonded to a rigid base.

4.2 Axisymmetric Contact of Thin Compressible Viscoelastic Layers

This section presents closed-form solutions for the contact pressure induced by the frictionless contact interaction of two thin compressible transversely isotropic viscoelastic layers bonded to rigid substrates. It is assumed that inertial effects are negligible, and the contact interaction is quasi-static.

4.2.1 Contact Problem Formulation

Consider axisymmetric frictionless contact interaction between two thin compressible viscoelastic layers of thicknesses h_1 and h_2 bonded to rigid substrates shaped like bodies of revolution. Introducing the cylindrical coordinate system, we write the equations of the layer surfaces (in the undeformed state) in the form

$$z = (-1)^n \varphi_n(r), \quad n = 1, 2.$$

Denoting the contact approach of the substrates by $\delta_0(t)$, we write the unilateral contact non-penetration condition (see Sect. 2.1.2) as follows:

$$\delta_0(t) - \left(w_0^{(1)}(t,r) + w_0^{(2)}(t,r)\right) \le \varphi(r). \tag{4.35}$$

Here, $w_0^{(n)}(t,r)$ is the vertical displacement (local indentation) of the surface points of the nth layer, and $\varphi(r)$ is the initial gap function defined by

$$\varphi(r) = \varphi_1(r) + \varphi_2(r).$$

According to Eq. (4.26), the local indentation of a thin bonded compressible transversely isotropic viscoelastic layer can be approximated as

$$w_0^{(n)}(t,r) = h_n \int_{0^-}^{t} J_A'^{(n)}(t-\tau)\frac{\partial p}{\partial \tau}(\tau,r)\,d\tau. \tag{4.36}$$

Here, $p(t,r)$ is the contact pressure distribution, $J_A'^{(n)}(t)$ is the axial aggregate creep compliance of the nth layer, $t = 0$ is the initial time of contact, while the lower integration limit 0^- denotes the infinitesimally negative time moment to account for the pressure discontinuity at zero.

Under the assumption, for example, that the gap function $\varphi(r)$ is positive and convex, the contact area $\omega(t)$ will be a circle of radius $a(t)$. The contact area is determined by the condition that the contact pressure is positive inside $\omega(t)$ and vanishes at the contour of the contact area, that is

$$p(t,r) > 0, \quad r < a(t), \quad p(t,a(t)) = 0. \tag{4.37}$$

Outside the contact area (for $r > a(t)$), in light of the unilateral contact condition (4.35), the following inequality must be satisfied:

$$\delta_0(t) - \varphi(r) < w_0^{(1)}(t,r) + w_0^{(2)}(t,r).$$

In the thin-layer approximation, the in-plane deformational interaction in a thin compressible elastic layer is neglected (as in the Winkler foundation model), the above condition reduces to

$$\delta_0(t) - \varphi(r) < 0, \quad r > a(t). \tag{4.38}$$

The equilibrium equation for the whole system is

$$2\pi \int_0^{a(t)} p(t,\rho)\rho\,d\rho = F(t), \tag{4.39}$$

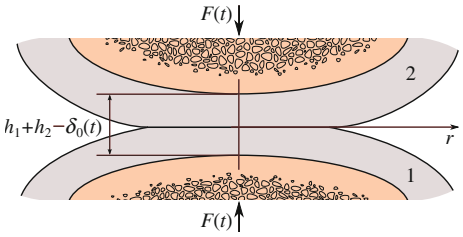

Fig. 4.3 Schematic diagram for the contact interaction of bonded viscoelastic layers under variable external load $F(t)$ in the current deformed configuration corresponding to the time moment t

where $F(t)$ denotes the external load (see Fig. 4.3).

By substituting the asymptotic approximations (4.36) into (4.35), we arrive at the following equation for the contact pressure:

$$\sum_{n=1}^{2} h_n \int_{0-}^{t} J_A^{\prime(n)}(t-\tau)\frac{\partial p}{\partial \tau}(\tau, r)\, d\tau = \delta_0(t) - \varphi(r)\mathscr{H}(t), \quad r \le a(t). \tag{4.40}$$

Observe that, by introducing the Heaviside function factor $\mathscr{H}(t)$, Eq. (4.40) takes into account the zero initial conditions for $t < 0$ and assumes that contact deformation is applied in a step manner at time $t = 0$.

The contact problem thus consists in finding histories $\delta_0(t)$, $a(t)$, $p(t, r)$ which, for given $\varphi(r)$, known $J_A^{\prime(n)}(t)$, $n = 1, 2$, and prescribed $F(t)$, satisfy (4.35)–(4.40).

4.2.2 Axial Aggregate Relaxation and Creep Functions

Let E'_{A0} be the instantaneous axial (longitudinal) aggregate elastic modulus of a transversely isotropic viscoelastic layer, i.e., $E'_{A0} = E'_A(0)$. By letting

$$E'_A(t) = E'_{A0}\Psi'_A(t), \tag{4.41}$$

we introduce the corresponding normalized relaxation function $\Psi'(t)$ such that

$$\Psi'_A(0) = 1. \tag{4.42}$$

Now, taking into account the relation between the relaxation and creep functions in the Laplace domain (4.24), we may introduce the associated creep function $\Phi'_A(t)$ of the viscoelastic layer material as

$$J'_A(t) = \frac{1}{E'_{A0}}\Phi'_A(t), \tag{4.43}$$

so that the following relation holds true:

$$s^2\tilde{\Psi}'_A(s)\tilde{\Phi}'_A(s) = 1. \tag{4.44}$$

The above equation allows one to determine $\Phi'_A(t)$, given $\Psi'_A(t)$, or vice versa.

Further, consider an integral operator

$$\int_{0^-}^{t} \Phi'_A(t-\tau)\frac{\partial u}{\partial \tau}(\tau)\,d\tau = v(t), \tag{4.45}$$

where $u(t) = 0$ for $t < 0$, so that $u(0^-) = 0$.

In light of (4.44), Eq. (4.45) can be inverted to yield

$$u(t) = \int_{0^-}^{t} \Psi'_A(t-\tau)\frac{\partial v}{\partial \tau}(\tau)\,d\tau. \tag{4.46}$$

Hence, for any function $u(t)$, we have

$$u(t) = \int_{0^-}^{t} \Phi'_A(t-\tau)\frac{\partial}{\partial \tau}\int_{0^-}^{\tau} \Psi'_A(\tau-\theta)\frac{\partial u}{\partial \theta}(\theta)\,d\theta d\tau. \tag{4.47}$$

Note also that for any time moment $\tau_1 \in (0, +\infty)$, the identity (4.47) can be generalized as follows [9, 23]:

$$u(t) = u(\tau_1) + \int_{\tau_1}^{t} \Psi'_A(t-\tau)\frac{\partial}{\partial \tau}\int_{\tau_1}^{\tau} \Phi'_A(\tau-\theta)\frac{\partial u}{\partial \theta}(\theta)\,d\theta d\tau. \tag{4.48}$$

Formulas (4.47) and (4.48) also hold true in the case when $\Phi'_A(t)$ and $\Psi'_A(t)$ are exchanged as well as for $\tau_1(t)$ being a function of time.

4.2.3 Instantaneous Contact

Following [7], we transform the governing equation (4.40) into the form

$$\frac{h}{E'_{A0}}\int_{0^-}^{t} \Phi_\alpha(t-\tau)\frac{\partial p}{\partial \tau}(\tau, r)\,d\tau = \delta_0(t) - \varphi(r)\mathscr{H}(t), \quad r \le a(t), \tag{4.49}$$

where $h = h_1 + h_2$ is the joint thickness, E'_{A0} and $\Phi_\alpha(t)$ are the equivalent aggregate instantaneous axial elastic modulus and the compound creep function, respectively, given by

$$\Phi_\alpha(t) = \alpha_1 \Phi_A^{\prime(1)}(t) + \alpha_2 \Phi_A^{\prime(2)}(t), \tag{4.50}$$

$$\alpha_1 = \frac{h_1 E_{A0}^{\prime(2)}}{h_1 E_{A0}^{\prime(2)} + h_2 E_{A0}^{\prime(1)}}, \quad \alpha_2 = \frac{h_2 E_{A0}^{\prime(1)}}{h_1 E_{A0}^{\prime(2)} + h_2 E_{A0}^{\prime(1)}}, \tag{4.51}$$

$$E'_{A0} = \frac{(h_1 + h_2) E_{A0}^{\prime(1)} E_{A0}^{\prime(2)}}{h_1 E_{A0}^{\prime(2)} + h_2 E_{A0}^{\prime(1)}}, \tag{4.52}$$

where $\Phi_A^{\prime(n)}(t)$ is the normalized axial aggregate creep function and $E_{A0}^{\prime(n)} = E_A^{\prime(n)}(0)$ is the instantaneous axial aggregate elastic modulus of the nth layer.

Observe that formula (4.52) determines the equivalent modulus in such a way that $\alpha_1 + \alpha_2 = 1$ (see Eq. (4.51)), and so $\Phi_\alpha(0) = 1$.

We consider the compressive loading histories which are discontinuous at the initial time $t = 0$, such that $F(t) = 0$ for $t < 0$ with $F(0^+) > 0$, where

$$F(0^+) = \lim_{t \to 0^+} F(t).$$

We emphasize that the asymptotic model (4.49) assumes that the contacting viscoelastic layers are relatively thin, meaning that the radius $a(0^+)$ of the instantaneous contact area $\omega(0^+)$, corresponding to the instantaneous value of the contact force $F(0^+)$, is much larger than the thicknesses of the contacting layers h_1 and h_2, so that the underlying assumption of the asymptotic analysis holds true.

Now, considering an infinitesimally positive time t in Eq. (4.49), we arrive at the equation of instantaneous contact

$$\frac{h}{E'_{A0}} p(0^+, r) = \delta_0(0^+) - \varphi(r), \tag{4.53}$$

where we have taken into account the normalization condition $\Phi_\alpha(0) = 1$.

According to (4.37), the contact area $\omega(0^+)$ coincides with the domain where the right-hand side of Eq. (4.53) is positive, and so

$$p(0^+, r) = \frac{E'_{A0}}{h} \big(\delta_0(0^+) - \varphi(r)\big)_+, \tag{4.54}$$

where $(x)_+ = (x + |x|)/2$ is the positive part function.

As a result, the instantaneous contact radius is determined from the equation

$$\delta_0(0^+) = \varphi(a(0^+)), \tag{4.55}$$

whereas, in turn, the instantaneous contact approach, $\delta_0(0^+)$, is determined by the instantaneous contact force $F(0^+)$ from the equilibrium equation

$$\frac{h}{\pi E'_{A0}} F(0^+) = a(0^+)^2 \delta_0(0^+) - 2 \int_0^{a(0^+)} \varphi(\rho)\rho \, d\rho. \tag{4.56}$$

Note also that Eq. (4.54) can be rewritten as

$$p(0^+, r) = \frac{E'_{A0}}{h} \big(\delta_0(0^+) - \varphi(r)\big) \mathscr{H}\big(a(0^+) - r\big). \tag{4.57}$$

Based on physical considerations for non-conforming contact, it is reasonable to assume that $\varphi(r)$, $r \in (0, +\infty)$, is a positive, continuous and differentiable function with a piecewise continuous second derivative $\varphi''(r)$ such that $\varphi(0^+) = 0$ (normalization condition for the contact approach), $\varphi'(0^+) = 0$ (condition of smoothness of the contact surfaces), and $\varphi'(r) > 0$ for $r > 0$ (condition that the gap is an increasing function). In such a case, Eqs. (4.55) and (4.56) will have unique solutions.

4.2.4 Monotonically Increasing Contact Area

Let us first consider the case when $\omega(\tau) \subset \omega(t)$ for any time moments $\tau, t \in (0, t_m)$ such that $\tau < t$ (see Fig. 4.4). In other words, the contact radius $a(t)$ is assumed to be a monotonically increasing function of the time-like variable t.

In light of (4.20), Eq. (4.49) can be rewritten as

$$p(0^+, r)\Phi_\alpha(t) + \int_0^t \Phi_\alpha(t - \tau)\dot{p}(\tau, r) \, d\tau = \frac{E'_{A0}}{h} \big(\delta_0(t) - \varphi(r)\mathscr{H}(t)\big). \tag{4.58}$$

Now, integrating by parts, we reduce Eq. (4.58) to the following form:

$$\Phi_\alpha(0)p(t, r) + \int_0^t \dot{\Phi}_\alpha(t - \tau)p(\tau, r) \, d\tau = \frac{E'_{A0}}{h} \big(\delta_0(t) - \varphi(r)\mathscr{H}(t)\big). \tag{4.59}$$

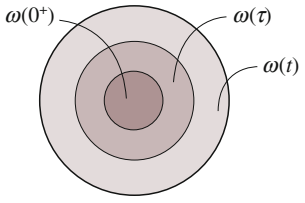

Fig. 4.4 Variation in time of the contact area in the case of monotonically increasing contact radius ($0^+ < \tau < t$), where $\omega(0^+)$ is the instantaneous contact area

Recall [11] that the relaxation moduli $J_A^{\prime(1)}(t)$ and $J_A^{\prime(2)}(t)$ must be strictly monotonically increasing functions. This implies that the derivative $\dot{\Phi}_\alpha(t)$ is strictly positive for $t \in (0, +\infty)$. Thus, in the case of monotonically increasing contact area, according to (4.37) and (4.38), the contact area $\omega(t)$ coincides with the domain where the right-hand side of Eq. (4.59) is positive.

Indeed, since negative pressure is not allowed due to (4.37), the left-hand side of Eq. (4.59) is positive inside the contact area $\omega(t)$. This implies that $\omega(t)$ is a subset of the domain, where the right-hand side Eq. (4.59) is positive. However, due to (4.38), the intersection of this last set with the absolute complement of $\omega(t)$ is empty. Hence, in the case when the viscoelastic layers are not initially deformed outside the monotonically increasing contact area $\omega(t)$ (i.e., the gap between the layers is determined by the function $\varphi(r)$ defined according to the undeformed configuration), the positiveness condition of the right-hand side of Eq. (4.59) determines the location of the contact area $\omega(t)$.

Thus, the governing integral equation (4.49) can be rewritten in the form

$$\frac{h}{E'_{A0}} \int_{0^-}^{t} \Phi_\alpha(t-\tau) \frac{\partial p}{\partial \tau}(\tau, r)\, d\tau = \big(\delta_0(t) - \varphi(r)\mathscr{H}(t)\big)_+, \tag{4.60}$$

or as follows:

$$\frac{h}{E'_{A0}} \int_{0^-}^{t} \Phi_\alpha(t-\tau) \frac{\partial p}{\partial \tau}(\tau, r)\, d\tau = \big(\delta_0(t) - \varphi(r)\mathscr{H}(t)\big)\mathscr{H}\big(a(t) - r\big). \tag{4.61}$$

Under the assumptions imposed upon the gap function $\varphi(r)$ in Sect. 4.2.3, we find that the contact area is circular, and the contact radius $a(t)$ is related to the contact approach $\delta_0(t)$ by the formula

$$a(t) = \varphi^{-1}\big(\delta_0(t)\big), \tag{4.62}$$

where $\varphi^{-1}(x)$ is the inverse function for $x = \varphi(r)$.

Integrating both sides of Eq. (4.60) over the contact domain and taking into account (4.39), we obtain

$$\frac{h}{E'_{A0}} \int_{0^-}^{t} \Phi_\alpha(t-\tau) \dot{F}(\tau)\, d\tau = \pi a(t)^2 \delta_0(t) - 2\pi \mathscr{H}(t) \int_0^{a(t)} \varphi(\rho)\rho\, d\rho.$$

Note that, formally speaking, $\delta_0(t)$ and $a(t)$ are histories such that $\delta_0(t) = 0$ and $a(t) = 0$ for $t < 0$. That is why the above equation can be simplified as follows:

$$\frac{h}{E'_{A0}}\int_{0^-}^{t}\Phi_\alpha(t-\tau)\dot{F}(\tau)\,d\tau=\pi a(t)^2\delta_0(t)-2\pi\int_0^{a(t)}\varphi(\rho)\rho\,d\rho. \tag{4.63}$$

As a result of (4.62), the right-hand side of Eq. (4.63) can be represented by

$$g\big(\delta_0(t)\big)=\pi\delta_0(t)\varphi^{-1}\big(\delta_0(t)\big)^2-2\pi\int_0^{\varphi^{-1}(\delta_0(t))}\varphi(\rho)\rho\,d\rho. \tag{4.64}$$

Therefore, from (4.63) and (4.64), it follows that

$$\delta_0(t)=g^{-1}\left(\frac{h}{E'_{A0}}\int_{0^-}^{t}\Phi_\alpha(t-\tau)\dot{F}(\tau)\,d\tau\right), \tag{4.65}$$

where $g^{-1}(y)$ is the inverse function for $y=g(x)$ given by

$$g(x)=\pi x\varphi^{-1}(x)^2-2\pi\int_0^{\varphi^{-1}(x)}\varphi(\rho)\rho\,d\rho.$$

Further, by inverting Eq. (4.63), we obtain the force-displacement relationship

$$F(t)=\frac{E'_{A0}}{h}\int_{0^-}^{t}\Psi_\alpha(t-\tau)\frac{dg\big(\delta_0(\tau)\big)}{d\tau}\,d\tau. \tag{4.66}$$

Here, $\Psi_\alpha(t)$ is the compound relaxation function defined by

$$\tilde{\Psi}_\alpha(s)=\frac{\tilde{\Psi}_A'^{(1)}(s)\tilde{\Psi}_A'^{(2)}(s)}{\alpha_1\tilde{\Psi}_A'^{(2)}(s)+\alpha_2\tilde{\Psi}_A'^{(1)}(s)}, \tag{4.67}$$

while $\tilde{\Psi}_A'^{(1)}(s)$ and $\tilde{\Psi}_A'^{(2)}(s)$ are the Laplace transforms of the relaxation functions $\Psi_A'^{(1)}(t)$ and $\Psi_A'^{(2)}(t)$ for the viscoelastic layers. Observe that by normalization,

$$\Psi_\alpha(0)=1, \tag{4.68}$$

and that, according to the initial value theorem for Laplace transforms, we have

$$\Psi_\alpha(0^+)=\lim_{s\to\infty}s\tilde{\Psi}_\alpha(s).$$

Now, taking into account (4.67), we obtain

$$\Psi_\alpha(0^+) = \lim_{s\to\infty} \frac{s\tilde{\Psi}_A'^{(1)}(s)s\tilde{\Psi}_A'^{(2)}(s)}{\alpha_1 s\tilde{\Psi}_A'^{(2)}(s) + \alpha_2 s\tilde{\Psi}_A'^{(1)}(s)}$$
$$= \frac{\Psi_A'^{(1)}(0^+)\Psi_A'^{(2)}(0^+)}{\alpha_1\Psi_A'^{(2)}(0^+) + \alpha_2\Psi_A'^{(1)}(0^+)}.$$

The normalization condition (4.68) for the compound relaxation function is readily established by making use of Eqs. (4.42) and (4.51).

In the case of a parabolic gap function, when

$$\varphi(r) = \frac{r^2}{2R}, \tag{4.69}$$

we have $\varphi^{-1}(x) = \sqrt{2Rx}$ and $g^{-1}(y) = \sqrt{(\pi R)^{-1}y}$, and

$$g(x) = 2\pi Rx^2 - 2\pi \int_0^{\sqrt{2Rx}} \frac{\rho^2}{2R}\rho\, d\rho$$
$$= \pi Rx^2.$$

Therefore, Eqs. (4.62), (4.65)–(4.73) can be concretized, respectively, as follows:

$$a(t) = \sqrt{2R\delta_0(t)}, \tag{4.70}$$

$$\delta_0(t) = \left(\frac{h}{\pi RE'_{A0}}\int_{0^-}^{t} \Phi_\alpha(t-\tau)\dot{F}(\tau)\, d\tau\right)^{1/2}, \tag{4.71}$$

$$F(t) = \frac{\pi RE'_{A0}}{h}\int_{0^-}^{t} \Psi_\alpha(t-\tau)\frac{d}{d\tau}\delta_0(\tau)^2\, d\tau. \tag{4.72}$$

Observe that, in the case of the increasing contact area, the relation between the contact radius $a(t)$ and the contact approach $\delta_0(t)$ has the form of the corresponding elastic solution (see Eq. (4.70)), and is general in nature [12, 18, 23].

4.2.5 Monotonically Increasing Contact Area: Contact Pressure

As the right-hand side of the integral equation (4.61) makes sense for all $r \geq 0$, we can write out its solution in the form

$$p(t,r) = \frac{E'_{A0}}{h} \int_{0^-}^{t} \Psi_\alpha(t-\tau) \frac{\partial}{\partial \tau} \Big\{ \big[\delta_0(\tau) - \varphi(r)\mathscr{H}(\tau)\big] \mathscr{H}\big(a(\tau) - r\big) \Big\} \, d\tau, \quad (4.73)$$

where $\delta_0(t)$ and $a(t)$ are known functions, since they are determined from the function $F(t)$ by formulas (4.62) and (4.65).

In the case of the parabolic gap (4.69) and as a result of (4.70), Eq. (4.73) reduces to

$$p(t,r) = \frac{E'_{A0}}{2Rh} \int_{0^-}^{t} \Psi_\alpha(t-\tau) \frac{\partial}{\partial \tau} \Big\{ \big(a(\tau)^2 - r^2 \mathscr{H}(\tau)\big) \mathscr{H}\big(a(\tau) - r\big) \Big\} \, d\tau, \quad (4.74)$$

where according to (4.70) and (4.71), we have

$$a(t) = \left(\frac{4hR}{\pi E'_{A0}} \int_{0^-}^{t} \Phi_\alpha(t-\tau) \dot{F}(\tau) \, d\tau \right)^{1/4}.$$

Note that Eq. (4.73) can be further simplified by integration by parts. Alternatively, the obtained result can be explained as follows. If the point of observation r belongs to the instantaneous contact area $\omega(0^+)$, then it is clear that $r < a(\tau)$ for any $\tau \in (0, t_m)$, and formula (4.73) reduces to

$$p(t,r) = \frac{E'_{A0}}{h} \int_{0^-}^{t} \Psi_\alpha(t-\tau) \frac{\partial}{\partial \tau} \big[\delta_0(\tau) - \varphi(r)\mathscr{H}(\tau)\big] \, d\tau, \quad r \leq a(0^+),$$

which is equivalent to

$$\begin{aligned} p(t,r) = {} & \frac{E'_{A0}}{h} \Psi_\alpha(t) \big(\delta_0(0^+) - \varphi(r)\big) \\ & + \frac{E'_{A0}}{h} \int_{0}^{t} \Psi_\alpha(t-\tau) \dot{\delta}_0(\tau) \, d\tau, \quad r \leq a(0^+). \end{aligned} \quad (4.75)$$

Now, if the point r lies outside of $\omega(0^+)$, then it is known a priori that $p(\tau, r) \equiv 0$ for $\tau \in (0, t_*(r))$, where $t_*(r)$ is the time when the contour of the contact area first reaches the point r. The quantity is determined by the equation

$$\delta_0(t_*) = \varphi(r), \tag{4.76}$$

so that

$$t_*(r) = \delta_0^{-1}(\varphi(r)), \quad r > a(0^+).$$

Thus, since $\mathscr{H}(a(\tau) - r) = 0$ for $\tau \in (0, t_*(r))$, formula (4.73) can be recast as

$$\begin{aligned} p(t,r) &= \frac{E'_{A0}}{h} \int\limits_{t_*(r)}^{t} \Psi_\alpha(t-\tau) \frac{\partial}{\partial \tau} \big[\delta_0(\tau) - \varphi(r)\mathscr{H}(\tau)\big]\, d\tau \\ &= \frac{E'_{A0}}{h} \int\limits_{t_*(r)}^{t} \Psi_\alpha(t-\tau)\dot{\delta}_0(\tau)\, d\tau, \quad r > a(0^+). \end{aligned} \tag{4.77}$$

Finally, extending the definition of the function $t_*(r)$ to the whole contact area by assuming that $t_*(r) = 0$ for $0 \le r \le a(0^+)$, we combine the two formulas (4.75) and (4.77) into one as follows:

$$\begin{aligned} p(t,r) = {} & \frac{E'_{A0}}{h} \Psi_\alpha(t) \big(\delta_0(0^+) - \varphi(r)\big) \mathscr{H}\big(a(0^+) - r\big) \\ & + \frac{E'_{A0}}{h} \int\limits_{t_*(r)}^{t} \Psi_\alpha(t-\tau)\dot{\delta}_0(\tau)\, d\tau. \end{aligned} \tag{4.78}$$

Here, in light of (4.76), we have

$$t_*(r) = \begin{cases} 0, & r \le a(0^+), \\ \delta_0^{-1}(\varphi(r)), & r > a(0^+). \end{cases}$$

The first term on the right-hand side of (4.78) is caused by the instantaneous indentation, while the second term reflects the subsequent creep effect.

4.2.6 Case of Stepwise Loading

Let us now assume that

$$F(t) = F_0 \mathscr{H}(t). \tag{4.79}$$

Then, in the case of a parabolic gap function (4.69), Eq. (4.71) yields

$$\delta_0(t) = \left(\frac{hF_0}{\pi R E'_{A0}} \Phi_\alpha(t) \right)^{1/2} \mathscr{H}(t), \tag{4.80}$$

where the Heaviside function factor may be dropped, as $\Phi_\alpha(t) = 0$ for $t < 0$, by definition of the compound creep function.

It is clear that for a monotonically increasing function $\Phi_\alpha(t)$, the function $\delta_0(t)$ determined by the above equation will also be monotonically increasing. Hence, as the contact approach $\delta_0(t)$ and the contact radius $a(t)$ are related by a monotonic function (see Eq. (4.70)), the circular contact domain $\omega(t)$ will be monotonically increasing as well.

Further, if the point of observation r belongs to the instantaneous contact domain $\omega(0^+)$, then Eq. (4.75) for $t > 0$ and $r \le a(0^+)$ yields

$$\frac{h}{E'_{A0}} p(t,r) = \Psi_\alpha(t)\big(\delta_0(0^+) - \varphi(r)\big) + \int_0^t \Psi_\alpha(t-\tau)\dot{\delta}_0(\tau)\, d\tau, \tag{4.81}$$

where, in light of (4.80), we have

$$\delta_0(0^+) = \left(\frac{hF_0\Phi_\alpha(0)}{\pi R E'_{A0}}\right)^{1/2}, \tag{4.82}$$

$$\dot{\delta}(\tau) = \frac{hF_0}{2\pi R E'_{A0}} \frac{1}{\delta_0(\tau)} \frac{d\Phi_\alpha(\tau)}{d\tau}. \tag{4.83}$$

Now, if the point r lies outside of the instantaneous contact area $\omega(0^+)$, i.e., $r > a(0^+)$, then by formula (4.77) we obtain

$$\frac{h}{E'_{A0}} p(t,r) = \int_{t_*(r)}^t \Psi_\alpha(t-\tau)\dot{\delta}_0(\tau)\, d\tau. \tag{4.84}$$

Here, $t_*(r)$ is the time moment when the contour of the contact zone first reaches the point r and is determined by Eq. (4.76), which in the case of a parabolic gap takes the form

$$\delta_0(t_*) = \frac{r^2}{2R}. \tag{4.85}$$

Finally, according to (4.80), Eq. (4.85) is reduced to the following equation:

$$\Phi_\alpha(t_*) = \frac{\pi E'_{A0}}{4F_0} \frac{r^4}{hR}.$$

From here it follows that

$$t_*(r) = \Phi_\alpha^{-1}\left(\frac{\pi E'_{A0} r^4}{4F_0 hR}\right),$$

where $\Phi_\alpha^{-1}(x) = t$ is the inverse function with respect to $\Phi_\alpha(t) = x$.

Now, in light of (4.82), Eqs. (4.80) and (4.70) can be rewritten in the form

$$\delta_0(t) = \delta_0(0^+)\left(\frac{\Phi_\alpha(t)}{\Phi_\alpha(0)}\right)^{1/2}, \tag{4.86}$$

$$a(t) = a(0^+)\left(\frac{\Phi_\alpha(t)}{\Phi_\alpha(0)}\right)^{1/4}, \tag{4.87}$$

where $\delta_0(0^+)$ is given by (4.82), and

$$a(0^+) = \left(\frac{4RhF_0}{\pi E'_{A0}}\Phi_\alpha(0)\right)^{1/4}.$$

Observe that the solution (4.86), (4.87) agrees with the solution obtained by Naghieh et al. [20] in the axisymmetric isotropic case.

We underline that formulas (4.80), (4.82), (4.83), (4.85)–(4.87) are valid for the case of the parabolic gap function (4.69), while Eqs. (4.81) and (4.84) have a more general character.

4.2.7 Monotonically Decreasing Contact Area

Following [9], we consider the case when $t > t_m$ (see Fig. 4.5) and the contact radius $a(t)$ is monotonically decreasing.

Let us rewrite (4.49) in the form

$$\frac{h}{E'_{A0}}\int_{0^-}^{t}\Phi_\alpha(t-\tau)\frac{\partial p}{\partial \tau}(\tau, r)\,d\tau = w_0(t, r), \tag{4.88}$$

where

$$w_0(t, r) = \delta_0(t) - \varphi(r)\mathscr{H}(t), \quad r \le a(t). \tag{4.89}$$

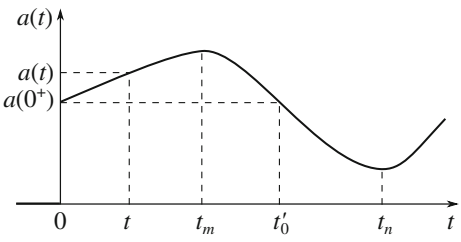

Fig. 4.5 A stepwise non-monotonic history of the contact radius variation

Now we can invert the relation (4.88) and write out the obtained result in the form

$$p(t,r) = \frac{E'_{A0}}{h}\int\limits_{0^-}^{t_m} \Psi_\alpha(t-\tau)\frac{\partial w_0}{\partial \tau}(\tau,r)\,d\tau + \frac{E'_{A0}}{h}\int\limits_{t_m}^{t} \Psi_\alpha(t-\tau)\frac{\partial w_0}{\partial \tau}(\tau,r)\,d\tau. \tag{4.90}$$

Since the contact pressure is already known on the interval $t \in (0, t_m)$, the first term on the right-hand side of Eq. (4.90) is known, and

$$w_0(t,r) = \frac{h}{E'_{A0}}\int\limits_{0^-}^{t} \Phi_\alpha(t-\tau)\frac{\partial p}{\partial \tau}(\tau,r)\,d\tau, \quad t \in (0,t_m),$$

where the contact pressure density $p(t,r)$ is given by formula (4.73). Thus, by substituting (4.73) into the above equation and making use of the identity (4.47), which is valid also for the compound relaxation and creep functions, we obtain

$$\begin{aligned} w_0(t,r) &= \big[\delta_0(t) - \varphi(r)\mathscr{H}(t)\big]\mathscr{H}\big(a(t)-r\big), \\ &= \big[\delta_0(t) - \varphi(r)\mathscr{H}(t)\big]\mathscr{H}\big(\delta_0(t)-\varphi(r)\big), \\ &= \big(\delta_0(t) - \varphi(r)\mathscr{H}(t)\big)_+, \quad t \in (0^-, t_m), \end{aligned} \tag{4.91}$$

where $(x)_+ = (x + |x|)/2$ is the positive part function.

On the other hand, the second term on the right-hand side of Eq. (4.90) inside the contact area is determined by the gap function according to (4.89).

Thus, in light of (4.89) and (4.91), Eq. (4.90) can be further transformed into

$$p(t,r) = \frac{E'_{A0}}{h}\int\limits_{0^-}^{t_m} \Psi_\alpha(t-\tau)\frac{\partial}{\partial \tau}\big(\delta_0(\tau) - \varphi(r)\mathscr{H}(\tau)\big)_+\,d\tau + \frac{E'_{A0}}{h}\int\limits_{t_m}^{t} \Psi_\alpha(t-\tau)\dot{\delta}_0(\tau)\,d\tau, \quad r < a(t). \tag{4.92}$$

Note that the function $\delta_0(\tau)$, $\tau \in (t_m, t)$, in the second integral on the right-hand side of (4.92), is not known and should be determined together with the function $a(\tau)$, $\tau \in (t_m, t)$. We recall that during the process of contact interaction, the contact approach $\delta_0(t)$ and the contact radius $a(t)$ are related by Eq. (4.63), which is insufficient to determine the two functions. The missing equation is obtained by satisfying the positiveness condition of the right-hand side of Eq. (4.92), that in fact determines the location of the contact area $\omega(t)$.

At the time moment $t = t_0'$ (see Fig. 4.5), the decreasing contact area enters the instantaneous contact area $r < a(0^+)$, which is formed as the result of instantaneous elastic deformation. Hence, on the time interval $t \in (t_0', t_n)$, the right-hand side of Eq. (4.88) can first be solved by the application of the inverse transform in time [9]. In this way, we calculate the contact pressure

$$p(t,r) = \frac{E'_{A0}}{h}\left(\int\limits_{0^-}^{t} \Psi_\alpha(t-\tau)\frac{\partial}{\partial\tau}\big[\delta_0(\tau) - \varphi(r)\mathscr{H}(\tau)\big]\,d\tau \right)_+, \tag{4.93}$$

and, correspondingly, the contact radius is given by

$$a(t) = \varphi^{-1}\left(\delta_0(0^+) + \frac{1}{\Psi_\alpha(t)} \int\limits_{0^-}^{t} \Psi_\alpha(t-\tau)\dot{\delta}_0(\tau)\,d\tau \right)_+. \tag{4.94}$$

Finally, we emphasize that formulas (4.93) and (4.94) hold true only on the time interval $t \in (t_0', t_n)$, where t_n is the extremum of the contact radius $a(t)$ (see Fig. 4.5).

4.2.8 Case of Stepwise Displacement-Controlled Loading

We now consider the situation where the contact approach is applied in a stepwise manner at the initial moment and then held constant for the rest of the contact interaction, i.e., $\delta_0(t) = \delta_0\mathscr{H}(t)$, where δ_0 is constant over time.

According to the governing integral equation (4.49), we have

$$\frac{h}{E'_{A0}} \int\limits_{0^-}^{t} \Phi_\alpha(t-\tau)\frac{\partial p}{\partial\tau}(\tau,r)\,d\tau = (\delta_0 - \varphi(r))\mathscr{H}(t), \quad r \le a(t). \tag{4.95}$$

By the same argument as that in Sect. 4.2.3, it can be easily shown that the contact radius $a(t) = \text{const}$, and is determined by the equation $\varphi(a) = \delta_0$.

Hence, Eq. (4.95) yields

$$p(t,r) = \frac{E'_{A0}}{h} \int\limits_{0^-}^{t} \Psi_\alpha(t-\tau)\frac{\partial}{\partial\tau}\big[\big(\delta_0 - \varphi(r)\big)_+\mathscr{H}(\tau)\big]\,d\tau,$$

from which it immediately follows that

$$p(t,r) = \frac{E'_{A0}}{h}\,\Psi_\alpha(t)\big(\delta_0 - \varphi(r)\big)_+.$$

Thus, in the case of stepwise displacement-controlled loading, the contact area remains constant, while the contact pressure relaxes as a function of time.

4.3 Axisymmetric Contact of Thin Incompressible Viscoelastic Layers: Monotonically Increasing Contact Area

In this section, we obtain closed-form solutions for the contact pressure induced by the frictionless contact interaction of two thin incompressible transversely isotropic viscoelastic layers bonded to rigid substrates.

4.3.1 Formulation of the Contact Problem

We now consider an axisymmetric contact between two thin linear viscoelastic layers firmly attached to rigid substrates shaped like bodies of revolution. Introducing the cylindrical coordinate system, we write the equations of the layer surfaces (before loading) in the form $z = (-1)^n \varphi_n(r)$ $(n = 1, 2)$. The gap function is defined in the undeformed configuration (see Fig. 4.6) as follows:

$$\varphi(r) = \varphi_1(r) + \varphi_2(r).$$

Denoting the contact approach of the substrates by $\delta_0(t)$, we write out the linearized unilateral non-penetration condition in the form

$$\delta_0(t) - \left(w_0^{(1)}(t, r) + w_0^{(2)}(t, r)\right) \le \varphi_1(r) + \varphi_2(r). \tag{4.96}$$

According to Eq. (4.34), the vertical displacement of the boundary points of the nth thin layer, $w_0^{(n)}(t, r)$, is expressed through the contact pressure $p(t, r)$ as follows:

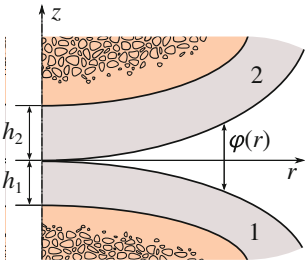

Fig. 4.6 Two viscoelastic layers bonded to axisymmetric rigid substrates in the undeformed configuration

$$w_0^{(n)}(t,r) = -\frac{h_n^3}{3}\int\limits_{0^-}^{t} J'^{(n)}(t-\tau)\Delta\frac{\partial p}{\partial \tau}(\tau,r)\,d\tau. \tag{4.97}$$

Here, h_n is the thickness of the nth layer, $J'^{(n)}(t)$ is the out-of-plane shear creep compliance, and Δ is the Laplace operator, which in the axisymmetric case is given by the following formula:

$$\Delta p = \frac{1}{r}\frac{\partial}{\partial r}\left(r\frac{\partial p}{\partial r}\right). \tag{4.98}$$

The equality in the contact condition (4.96) determines the contact radius $a(t)$. In other words, the following equation holds within the contact area:

$$w_0^{(1)}(t,r) + w_0^{(2)}(t,r) = \delta_0(t) - \varphi(r), \quad r \le a(t). \tag{4.99}$$

Substituting the expressions for the displacements $w_0^{(1)}(t,r)$ and $w_0^{(2)}(t,r)$ given by formula (4.97) into Eq. (4.99), and taking into account (4.98), we represent the contact condition in the form

$$-\sum_{n=1}^{2}\frac{h_n^3}{3}\int\limits_{0^-}^{t} J'^{(n)}(t-\tau)\frac{1}{r}\frac{\partial}{\partial r}\left(r\frac{\partial^2 p}{\partial r\partial \tau}(\tau,r)\right)d\tau = \delta_0(t) - \varphi(r)\mathscr{H}(t), \tag{4.100}$$

where $\mathscr{H}(t)$ is the Heaviside function introduced in the usual way, $\mathscr{H}(t) = 0$ for $t < 0$ and $\mathscr{H}(t) = 1$ for $t \ge 0$.

By letting

$$J'^{(n)}(t) = \frac{1}{G_0'^{(n)}}\Phi'^{(n)}(t), \tag{4.101}$$

where $G_0'^{(n)} = 1/J'^{(n)}(0^+)$ is the instantaneous out-of-plane shear elastic modulus of the nth layer, we introduce the corresponding normalized creep function $\Phi'^{(n)}(t)$.

Furthermore, the compound creep function, $\Phi_\beta(t)$, and the equivalent instantaneous shear elastic modulus, G_0', can be defined as follows:

$$\Phi_\beta(t) = \beta_1\Phi'^{(1)}(t) + \beta_2\Phi'^{(2)}(t), \tag{4.102}$$

$$G_0' = \frac{(h_1+h_2)^3 G_0'^{(1)} G_0'^{(2)}}{h_1^3 G_0'^{(2)} + h_2^3 G_0'^{(1)}}, \tag{4.103}$$

$$\beta_1 = \frac{h_1^3 G_0'^{(2)}}{h_1^3 G_0'^{(2)} + h_2^3 G_0'^{(1)}}, \quad \beta_2 = \frac{h_2^3 G_0'^{(1)}}{h_1^3 G_0'^{(2)} + h_2^3 G_0'^{(1)}}. \tag{4.104}$$

Observe that formula (4.103) determines the equivalent modulus in such a way that $\beta_1 + \beta_2 = 1$ (see Eq. (4.104)) and thus, $\Phi_\beta(0) = 1$.

We proceed by introducing an auxiliary notation

$$m = \frac{3G_0'}{h^3}, \tag{4.105}$$

where $h = h_1 + h_2$ is the joint thickness.

Then, taking into account (4.101)–(4.105), we rewrite Eq. (4.100) as

$$\int_{0^-}^{t} \Phi_\beta(t-\tau)\frac{1}{r}\frac{\partial}{\partial r}\Big(r\frac{\partial^2 p}{\partial r\,\partial\tau}(\tau, r)\Big)\,d\tau = m\big(\varphi(r)\mathscr{H}(t) - \delta_0(t)\big). \tag{4.106}$$

The above equation is used to find the contact pressure $p(t, r)$, while the contact radius $a(t)$ is determined from the condition that the contact pressure is positive and vanishes at the contour of the contact area, i.e.,

$$p(t, r) > 0, \quad r < a(t), \quad p(t, a(t)) = 0. \tag{4.107}$$

In the case of contact problems for thin incompressible layers (see Sect. 2.7.3 and [8, 10, 14]), we additionally assume a smooth transition of the contact stresses from the contact region $r < a(t)$ to the outside region $r > a(t)$ that is

$$\frac{\partial p}{\partial r}(t, r)\bigg|_{r=a(t)} = 0. \tag{4.108}$$

Furthermore, from the physical point of view, the contact pressure between the contacting smoothly curved surfaces should satisfy the regularity condition at the center of the contact area that the even extension $p(t, x)$, $x \in (-a(t), a(t))$, of the contact pressure density is continuously differentiable. Thus, the following boundary condition is additionally imposed:

$$\frac{\partial p}{\partial r}p(t, r)\bigg|_{r=0} = 0. \tag{4.109}$$

Finally, the equilibrium equation for the whole system is given by

$$2\pi \int_0^{a(t)} p(t, \rho)\rho\,d\rho = F(t), \tag{4.110}$$

where $F(t)$ denotes the external axial load. We consider the loading histories which are discontinuous at the initial time $t = 0$ such that $F(t) = 0$ for $t < 0$ and $F(t) > 0$

for $t \geq 0$, as the asymptotic model is not capable of describing the contact interaction when the contact radius is smaller or comparable with the layer thicknesses.

Note also that for non-decreasing loads when $dF(t)/dt \geq 0$, the contact radius is expected to increase monotonously, that is $da(t)/dt > 0$. This condition must be checked a posteriori.

Following [3], we derive a general solution for the axisymmetric contact problem for thin incompressible viscoelastic layers formulated by Eq. (4.106), in the case of an arbitrary joint geometry and under the assumption of increasing loading.

4.3.2 Equation for the Contact Approach

Integrating Eq. (4.106) with respect to r, we find

$$\int_{0^-}^{t} \Phi_\beta(t-\tau)\frac{\partial^2 p}{\partial r \partial \tau}(\tau, r)\, d\tau = m\left(\frac{\mathscr{H}(t)}{r}\int_0^r \varphi(\rho)\rho\, d\rho - \frac{r}{2}\delta_0(t)\right), \tag{4.111}$$

where the constant of integration vanishes due to the regularity condition (4.109).

After substituting the value $r = a(t)$ into the above equation and taking into account the boundary conditions (4.107) and (4.108), we transform this equation into the following:

$$\delta_0(t) = \frac{2}{a(t)^2}\int_0^{a(t)} \varphi(\rho)\rho\, d\rho. \tag{4.112}$$

Equation (4.112) connects the contact approach $\delta_0(t)$ and the unknown contact radius $a(t)$ of the circular contact area.

4.3.3 Equation for the Radius of the Contact Area

Upon integration with respect to r and changing the order of integration, Eq. (4.111) takes the form

$$\int_{0^-}^{t} \Phi_\beta(t-\tau)\frac{\partial p}{\partial \tau}(\tau, r)\, d\tau = m\left(\mathscr{H}(t)\int_0^r \varphi(\rho)\rho \ln\frac{r}{\rho}\, d\rho - \frac{r^2}{4}\delta_0(t)\right) + D_2(t). \tag{4.113}$$

By using the boundary condition (4.107), the constant of integration $D_2(t)$ can be obtained as a function of the contact radius $a(t)$ in the form

$$D_2(t) = \frac{m}{4}\,\delta_0(t)a(t)^2 - m\mathscr{H}(t)\int_0^{a(t)} \varphi(\rho)\rho \ln\frac{a(t)}{\rho}\,d\rho. \tag{4.114}$$

We now multiply both sides of Eq. (4.113) by r and integrate over the contact interval $(0, a(t))$. After changing the order of integration and taking account of (4.110) and (4.114), we obtain

$$\frac{1}{\pi m}\int_{0^-}^{t} \Phi_\beta(t-\tau)\dot{F}(\tau)\,d\tau = \delta_0(t)\frac{a(t)^4}{8} - \frac{\mathscr{H}(t)}{2}\int_0^{a(t)} \varphi(\rho)\rho(a(t)^2-\rho^2)\,d\rho. \tag{4.115}$$

Finally, in light of (4.112), the above equation can be simplified to

$$\frac{\pi m}{4}\mathscr{H}(t)\int_0^{a(t)} \varphi(\rho)\rho\big(2\rho^2 - a(t)^2\big)\,d\rho = \int_{0^-}^{t} \Phi_\beta(t-\tau)\dot{F}(\tau)\,d\tau. \tag{4.116}$$

Equation (4.116) connects the unknown radius of the contact area $a(t)$ and the prescribed contact load $F(t)$.

4.3.4 Example: General Paraboloid of Revolution

Let us assume that the gap between the layer surfaces is described by the formula

$$\varphi(r) = Cr^\lambda, \tag{4.117}$$

where C and λ are constants.

Then, Eqs. (4.112) and (4.116) take the form

$$\delta_0(t) = \frac{2C}{\lambda+2}\,a(t)^\lambda, \tag{4.118}$$

$$\frac{\pi m\lambda C a(t)^{\lambda+4}}{4(\lambda+2)(\lambda+4)} = f(t), \tag{4.119}$$

where we have introduced the notation

$$f(t) = \int_{0^-}^{t} \Phi_\beta(t-\tau)\dot{F}(\tau)\,d\tau. \tag{4.120}$$

It is readily seen that Eq. (4.119) allows us to determine the contact radius $a(t)$ as follows:

$$a(t) = \Big(\frac{4(\lambda+2)(\lambda+4)}{\pi m\lambda C} f(t)\Big)^{1/(\lambda+4)}. \tag{4.121}$$

By substituting the obtained solution (4.121) into Eq. (4.118), we derive the following formula for the contact approach:

$$\delta_0(t) = \frac{2C}{\lambda+2}\Big(\frac{4(\lambda+2)(\lambda+4)}{\pi m\lambda C} f(t)\Big)^{\lambda/(\lambda+4)}. \tag{4.122}$$

We recall that formula (4.120) can be rewritten as

$$f(t) = \Phi_\beta(t)F(0^+) + \int_{0}^{t} \Phi_\beta(t-\tau)\dot{F}(\tau)\,d\tau. \tag{4.123}$$

Since we consider monotonic loading (i.e., the contact force function $F(t)$ does not decrease with time), the utilized mathematical model of contact shows (see, in particular, Eqs. (4.121) and (4.123)) that the contact radius $a(t)$ will also be increasing.

4.3.5 Contact Pressure Distribution

By taking formula (4.114) into account, we can rewrite Eq. (4.113) as follows:

$$\int_{0^-}^{t} \Phi_\beta(t-\tau)\frac{\partial p}{\partial \tau}(\tau, r)\,d\tau = \frac{m}{4}\,\delta_0(t)\big(a(t)^2 - r^2\big) - m\mathscr{H}(\tau)\Theta\big(a(t), r\big), \quad r \le a(t). \tag{4.124}$$

The new notation $\Theta(a, r)$ is given by

$$\Theta(a, r) = \int_{0}^{a} \varphi(\rho)\rho \ln\frac{a}{\rho}\,d\rho - \int_{0}^{r} \varphi(\rho)\rho \ln\frac{r}{\rho}\,d\rho,$$

and in the special case (4.117), we have

$$\Theta(a,r)=\frac{C}{(\lambda+2)^2}\big(a^{\lambda+2}-r^{\lambda+2}\big).$$

For an arbitrary $r>0$, formula (4.124) can be generalized to

$$\int_{0^-}^{t}\Phi_\beta(t-\tau)\frac{\partial p}{\partial\tau}(\tau,r)\,d\tau=\frac{m}{4}\,\delta_0(t)\big(a(t)^2-r^2\big)_+ - m\mathscr{H}(\tau)\Theta\big(a(t),r\big)\mathscr{H}\big(a(t)-r\big). \quad (4.125)$$

Therefore, by inverting Eq. (4.125), we obtain

$$p(t,r)=m\int_{0^-}^{t}\Psi_\beta(t-\tau)\frac{\partial}{\partial\tau}\left\{\left[\frac{1}{4}\,\delta_0(\tau)\big(a(\tau)^2-r^2\big) - \mathscr{H}(\tau)\Theta\big(a(\tau),r\big)\right]\mathscr{H}\big(a(\tau)-r\big)\right\}d\tau. \quad (4.126)$$

Here, $\Psi_\beta(t)$ is the corresponding compound relaxation function determined by its Laplace transform

$$\tilde{\Psi}_\beta(s)=\frac{1}{s^2\tilde{\Phi}_\beta(s)}. \quad (4.127)$$

Formula (4.126) is the sought-for general solution of Eq. (4.124). Note also that, since

$$\tilde{\Phi}_\beta(s)=\beta_1\tilde{\Phi}'^{(1)}(s)+\beta_2\tilde{\Phi}'^{(2)}(s)$$

and

$$\tilde{\Phi}'^{(n)}(s)=\frac{1}{s^2\tilde{\Psi}'^{(n)}(s)},$$

where $\tilde{\Psi}'^{(n)}(s)$ is the Laplace transform of the normalized relaxation function in out-of-plane shear $\Psi'^{(n)}(t)$ for the nth layer, formula (4.127) can be rewritten as

$$\tilde{\Psi}_\beta(s)=\frac{\tilde{\Psi}'^{(1)}(s)\tilde{\Psi}'^{(2)}(s)}{\beta_1\tilde{\Psi}'^{(2)}(s)+\beta_2\tilde{\Psi}'^{(1)}(s)} \quad (4.128)$$

while the coefficients β_1 and β_2 are given by (4.104).

4.3.6 Example: Paraboloid of Revolution

This is a special case of the more general situation considered in Sect. 4.3.4, where

$$\varphi(r) = \frac{r^2}{2R}$$

and R is a positive constant.

So, making use of the substitution $C = (2R)^{-1}$ and $\lambda = 2$, we have reduced Eqs. (4.118), (4.121), and (4.122) respectively to the following relations:

$$\delta_0(t) = \frac{a(t)^2}{4R}, \tag{4.129}$$

$$a(t) = \left(\frac{96R}{\pi m} f(t)\right)^{1/6}, \tag{4.130}$$

$$\delta_0(t) = \frac{1}{2R}\left(\frac{12R}{\pi m} f(t)\right)^{1/3}. \tag{4.131}$$

where the quantity $f(t)$ is related to the contact load $F(t)$ through Eq. (4.120).

Furthermore, in light of (4.126) and (4.129), the contact pressure is given by

$$p(t,r) = \frac{m}{32R} \int_{0^-}^{t} \Psi_\beta(t-\tau) \frac{\partial}{\partial \tau} \left\{ \left(a(\tau)^2 - r^2\right)_+^2 \mathscr{H}(\tau) \right\} d\tau. \tag{4.132}$$

Observe that, as we are considering the case of a stepwise loading, the function $\delta_0(\tau)$ can be replaced with $\delta_0(\tau)\mathscr{H}(\tau)$ in (4.126) in order to simplify the integrand in (4.132). Note also that the effect of the multiplier $\mathscr{H}\big(a(\tau) - r\big)$ is introduced through the the positive part function $(x)_+ = (x + |x|)/2$.

4.4 Axisymmetric Refined Contact Problem for a Thin Bonded Incompressible Viscoelastic Layer with Allowance for Tangential Displacements on the Contact Surface

In this section, the frictionless unilateral axisymmetric contact problem for a thin incompressible viscoelastic layer indented by a rigid punch is considered. The refined linearized contact condition, which takes into account both the radial and tangential displacements of the boundary points of the viscoelastic layer, is imposed and an

approximate analytical solution is constructed under the assumption that the contact area increases with time under a non-decreasing external loading.

4.4.1 Refined Formulation of the Contact Problem

We consider a thin incompressible transversely isotropic linear viscoelastic layer indented by a punch shaped like a body of revolution. Introducing the cylindrical coordinate system, we write the equation of the punch surface (before loading) in the form $z = -\varphi(r)$, so that the punch occupies a convex domain $z \le -\varphi(r)$ whereas it is in contact with the plane $z = 0$ at a single point chosen as the origin of the coordinate system (r, z).

In the case of the punch shaped like a paraboloid of revolution, we have

$$\varphi(r) = \frac{r^2}{2R}, \tag{4.133}$$

where R is the curvature radius of the punch surface at its apex.

We denote the vertical displacement of the punch by $\delta_0(t)$ (see Fig. 4.7). The refined unilateral contact condition that the surface points of the viscoelastic layer (under loading) do not penetrate into the punch can be written as follows [16]:

$$w_0(t, r) \ge \delta_0(t) - \varphi\big(r + v_0(t, r)\big). \tag{4.134}$$

According to the perturbation analysis carried out in Sect. 2.5 and the elastic-viscoelastic correspondence principle formulated in Sect. 4.1.2, the leading-order asymptotic approximations for the vertical and the radial horizontal displacements of the boundary points of the viscoelastic layer, $w_0(t, r)$ and $v_0(t, r)$, in the cylindrical coordinates can be expressed as follows:

$$w_0(t, r) = -\frac{h^3}{3} \int_{0^-}^{t} J'(t - \tau) \Delta \frac{\partial p}{\partial \tau}(\tau, r)\, d\tau, \tag{4.135}$$

$$v_0(t, r) = -\frac{h^2}{2} \int_{0^-}^{t} J'(t - \tau) \frac{\partial^2 p}{\partial r \partial \tau}(\tau, r)\, d\tau. \tag{4.136}$$

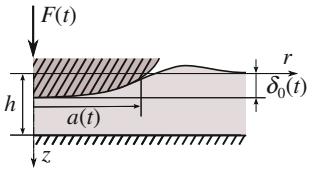

Fig. 4.7 A thin incompressible viscoelastic layer indented by a rigid punch

Here, h is the thickness of the viscoelastic layer, $J'(t)$ is the out-of-plane shear creep compliance, and Δ is the Laplacian, which in the axisymmetric case is defined by

$$\Delta p = \frac{1}{r}\frac{\partial}{\partial r}\Big(r\frac{\partial p}{\partial r}\Big).$$

The equality in relation (4.134) determines the contact area, and the following equation holds within the contact interval:

$$w_0(t,r) - \delta_0(t) + \varphi\big(r + v_0(t,r)\big) = 0, \quad r \le a(t). \tag{4.137}$$

We assume that the tangential displacement $v_0(t,r)$ is small compared to the contact radius $a(t)$. In this case, the nonlinear equation (4.137) can be replaced by the following linearized contact condition (see also Sect. 1.3):

$$w_0(t,r) - \delta_0(t) + \varphi(r) + \frac{d\varphi(r)}{dr}v_0(t,r) = 0, \quad r \le a(t).$$

In light of formula (4.133), the above equation takes the form

$$w_0(t,r) + \frac{r}{R}v_0(t,r) = \delta_0(t) - \frac{r^2}{2R}, \quad r \le a(t). \tag{4.138}$$

Substituting the expressions (4.135) and (4.136) into Eq. (4.138), we write the governing integral equation in the following form ($r \le a(t)$):

$$\frac{h^3}{3}\int\limits_{0^-}^{t} J'(t-\tau)\frac{\partial}{\partial\tau}\left\{\frac{1}{r}\frac{\partial}{\partial r}\Big(r\frac{\partial p}{\partial r}(\tau,r)\Big) + \frac{3r}{2hR}\frac{\partial p}{\partial r}(\tau,r)\right\}d\tau = \varphi(r)\mathscr{H}(t) - \delta_0(t). \tag{4.139}$$

Here, $\mathscr{H}(t)$ is the Heaviside function introduced in the standard way such that $\mathscr{H}(t) = 0$ for $t < 0$ and $\mathscr{H}(t) = 1$ for $t \ge 0$.

By letting

$$J'(t) = \frac{1}{G_0'}\Phi(t), \tag{4.140}$$

where $G_0' = 1/J'(0^+)$ is the instantaneous out-of-plane shear elastic modulus of the viscoelastic layer, we introduce the corresponding normalized creep function $\Phi(t)$.

To simplify our formulas, for any function of time and position, $q(t,r)$, we introduce the notation

$$\mathscr{K}q(\tau,r) = \int\limits_{0^-}^{t}\Phi(t-\tau)\frac{\partial q}{\partial\tau}(\tau,r)\,d\tau. \tag{4.141}$$

Therefore, the operator equation $\mathscr{K}q(\tau,r) = Q(t,r)$ can be inverted to obtain $q(t,r) = \mathscr{K}^{-1}Q(\tau,r)$, where

$$\mathscr{K}^{-1}Q(\tau,r) = \int_{0^-}^{t} \Psi(t-\tau)\frac{\partial Q}{\partial \tau}(\tau,r)\,d\tau \tag{4.142}$$

and $\Psi(t)$ denotes the normalized relaxation function in out-of-plane shear.

Thus, in light of (4.133) and (4.141), Eq. (4.139) can be written in the form

$$\mathscr{K}\left\{\frac{1}{r}\frac{\partial}{\partial r}\left(r\frac{\partial p}{\partial r}(\tau,r)\right) + \varkappa r\frac{\partial p}{\partial r}(\tau,r)\right\} = m\big(Cr^2\mathscr{H}(t) - \delta_0(t)\big), \tag{4.143}$$

where $\varkappa$, m, and C are dimensional constants given by

$$\varkappa = \frac{3}{2hR}, \quad m = \frac{3G_0'}{h^3}, \quad C = \frac{1}{2R}. \tag{4.144}$$

Equation (4.143) is used to find the contact pressure density $p(t,r), 0 \le r \le a(t)$. The radius of the contact area $a(t)$ is determined from the condition that the contact pressure is positive and vanishes at the contour of the contact area, that is

$$p(t,r) > 0, \quad r < a(t); \quad p(t,a(t)) = 0. \tag{4.145}$$

In the case of a thin incompressible layer, we additionally assume a smooth transition of the contact pressure from the contact region $r < a(t)$ to the outside region $r > a(t)$, i.e., the following zero-pressure-gradient boundary condition is imposed (see Sect. 2.7.3 and [1, 10]):

$$\left.\frac{\partial p(t,r)}{\partial r}\right|_{r=a(t)} = 0. \tag{4.146}$$

Moreover, from the physical point of view, the contact pressure under an axisymmetric blunt punch should satisfy the regularity condition

$$\left.\frac{\partial p(t,r)}{\partial r}\right|_{r=0} = 0. \tag{4.147}$$

Finally, the equilibrium equation for the whole system is

$$2\pi\int_0^{a(t)} p(t,\rho)\rho\,d\rho = F(t), \tag{4.148}$$

where $F(t)$ denotes the external load such that $F(t) = 0$ for $t < 0$ and $F(t) > 0$ for $t \geq 0$ with $F(0^+) > 0$.

For non-decreasing loads, when $dF(t)/dt \geq 0$, the contact area increases monotonically, i.e., the following monotonicity condition holds [25]:

$$\frac{da(t)}{dt} > 0, \quad t \in (0, +\infty). \tag{4.149}$$

This condition must be checked a posteriori.

It can be seen from formulas (4.135) and (4.136) that the tangential displacement $v_0(t, r)$ is an order of magnitude greater than the normal displacement $w_0(t, r)$, due to the multipliers h^2 and h^3, respectively. Thus, the formulation of the contact problem without the tangential displacement contradicts with the notion of neglecting terms that could contribute significantly in certain configurations. This begs the question of whether and how the tangential displacements influence the parameters of the contact pressure distribution. It is clear that the inclusion of the tangential displacements makes the contact problem formulation more precise, at the cost of increased difficulty in solving, and requires a much more elaborate approach in finding an analytical solution.

4.4.2 Equation for the Punch Displacement

Integrating Eq. (4.143) with respect to r, we obtain

$$\mathscr{K}\left\{r\frac{\partial p(\tau, r)}{\partial r} + \varkappa \int_0^r \rho^2 \frac{\partial p(\tau, \rho)}{\partial \rho}\, d\rho\right\} = \frac{m}{4}\left(Cr^4 - 2\delta_0(t) r^2\right), \tag{4.150}$$

where the constant of integration $D_1(t)$ vanishes in accordance with the regularization condition (4.147) at $r = 0$.

We transform the second integral in (4.150) by integration by parts

$$\int_0^r \rho^2 \frac{\partial p(\tau, \rho)}{\partial \rho}\, d\rho = r^2 p(\tau, r) - 2\int_0^r p(\tau, \rho)\rho\, d\rho.$$

Thus, Eq. (4.150) becomes

$$\mathscr{K}\left\{\frac{\partial p(\tau, r)}{\partial r} + \varkappa\left(rp(\tau, r) - \frac{2}{r}\int_0^r p(\tau, \rho)\rho\, d\rho\right)\right\} = \frac{m}{4}\left(Cr^3 - 2\delta_0(t) r\right). \tag{4.151}$$

Substituting the value $r = a(t)$ into the above equation and taking into account the corresponding boundary conditions (4.145) and (4.146), we obtain

$$-\frac{2\varkappa}{a(t)}\mathscr{K}\int_0^{a(t)} p(\tau,\rho)\rho\,d\rho = \frac{m}{4}\big(Ca(t)^3 - 2\delta_0(t)a(t)\big). \tag{4.152}$$

Further, by definition (4.141), we have

$$\begin{aligned}\mathscr{K}\int_0^{a(t)} p(\tau,\rho)\rho\,d\rho &= \int_{0^-}^{t}\Phi(t-\tau)\frac{\partial}{\partial\tau}\int_0^{a(t)} p(\tau,\rho)\rho\,d\rho d\tau\\ &= \int_{0^-}^{t}\Phi(t-\tau)\frac{\partial}{\partial\tau}\int_0^{a(\tau)} p(\tau,\rho)\rho\,d\rho d\tau,\end{aligned}$$

where the monotonicity condition (4.149) was taken into account.

Thus, Eq. (4.152) reduces to

$$-\frac{2\varkappa}{a(t)}\mathscr{K}\int_0^{a(\tau)} p(\tau,\rho)\rho\,d\rho = \frac{m}{4}\big(Ca(t)^3 - 2\delta_0(t)a(t)\big), \tag{4.153}$$

and, as a consequence of (4.148), takes the form

$$\delta_0(t) = C\frac{a(t)^2}{2} + \frac{2\varkappa}{m}\frac{1}{\pi a(t)^2}\mathscr{K}F(\tau). \tag{4.154}$$

Equation (4.154) connects the unknown contact radius, the unknown punch displacement $\delta_0(t)$, and the contact load $F(t)$.

4.4.3 Equation for the Radius of Contact Area

We now return to Eq. (4.151) and integrate with respect to r to obtain

$$\begin{aligned}\mathscr{K}\left\{p(\tau,r) + \varkappa\left(\int_0^r p(\tau,\rho)\rho\,d\rho - 2\int_0^r\frac{1}{\rho}\int_0^\rho p(\tau,\xi)\xi\,d\xi d\rho\right)\right\}\\ = \frac{m}{16}\big(Cr^4 - 4\delta_0(t)r^2\big) + D_2(t).\end{aligned} \tag{4.155}$$

Changing the order of integration in the second integral, we arrive at the formula

$$\int_0^r \frac{1}{\rho} \int_0^\rho p(\tau, \xi)\xi \, d\xi d\rho = \int_0^r p(\tau, \rho)\rho \ln \frac{r}{\rho} \, d\rho.$$

Then, taking into account the above formula, we rewrite Eq. (4.155) in the form

$$\mathscr{K}\left\{p(\tau, r) + \varkappa\left(\int_0^r p(\tau, \rho)\rho \, d\rho - 2\int_0^r p(\tau, \rho)\rho \ln \frac{r}{\rho} \, d\rho\right)\right\} = \frac{m}{16}\left(Cr^4 - 4\delta_0(t)r^2\right) + D_2(t). \quad (4.156)$$

By using the boundary condition (4.145), the constant of integration in the above equation can be evaluated as follows:

$$D_2(t) = \frac{m}{4}\delta_0(t)a(t)^2 - \frac{m}{16}Ca(t)^4 + \frac{\varkappa}{2\pi}\mathscr{K}F(\tau) - 2\varkappa\mathscr{K}\int_0^{a(\tau)} p(\tau, \rho)\rho \ln \frac{a(t)}{\rho} \, d\rho. \quad (4.157)$$

Further, by multiplying both sides of Eq. (4.156) by r and integrating over the current contact interval $(0, a(t))$, we obtain

$$\frac{1}{2\pi}\mathscr{K}F(\tau) + \varkappa\mathscr{K}\left\{\int_0^{a(t)} \rho \int_0^\rho p(\tau, \xi)\xi \, d\xi d\rho - 2\int_0^{a(t)} \rho \int_0^\rho p(\tau, \xi)\xi \ln \frac{\rho}{\xi} \, d\xi d\rho\right\} = m\left(C\frac{a(t)^6}{96} - \delta_0(t)\frac{a(t)^4}{16}\right) + \frac{a(t)^2}{2}D_2(t), \quad (4.158)$$

and by changing the order of integration, we obtain

$$\frac{1}{2\pi}\mathscr{K}F(\tau) + \varkappa\mathscr{K}\left\{\frac{1}{2}\int_0^{a(\tau)} p(\tau, \xi)\xi\left(a(t)^2 - \xi^2\right) d\xi - \int_0^{a(\tau)} p(\tau, \xi)\xi\left(a(t)^2 \ln \frac{a(t)}{\xi} - \frac{1}{2}\left(a(t)^2 - \xi^2\right)\right) d\xi\right\}$$

$$= m\left(C\frac{a(t)^6}{96} - \delta_0(t)\frac{a(t)^4}{16}\right) + \frac{a(t)^2}{2}D_2(t).$$

In light of (4.148) and (4.157), we reduce the above equation to the form

$$\mathscr{K}F(\tau) + \varkappa\mathscr{K}\left(\frac{a(t)^2}{2}F(\tau) - 2\pi\int_0^{a(\tau)} p(\tau,\rho)\rho^3\,d\rho\right)$$
$$= \pi m\left(\delta_0(t)\frac{a(t)^4}{8} - C\frac{a(t)^6}{24}\right).$$

Finally, taking into account Eq. (4.154), we obtain

$$\frac{\pi m}{48}Ca(t)^6 = \mathscr{K}F(\tau)$$
$$+ \varkappa\mathscr{K}\left(\frac{a(t)^2}{4}F(\tau) - 2\pi\int_0^{a(\tau)} p(\tau,\rho)\rho^3\,d\rho\right). \qquad (4.159)$$

Since we consider a monotonic loading (the function $F(t)$ does not decrease with time), the function $a(t)$ will also be increasing.

4.4.4 Contact Pressure

Returning to Eq. (4.143), we introduce a new dependent variable $y(t,r)$ such that

$$y(t,r) = r\frac{\partial p(t,r)}{\partial r}. \qquad (4.160)$$

Using the substitution (4.160), we can represent Eq. (4.143) in the form

$$\mathscr{K}\left(\frac{1}{r}\frac{\partial y(\tau,r)}{\partial r} + \varkappa y(t,r)\right) = mf(t,r), \qquad (4.161)$$

where

$$f(t,r) = \big(Cr^2 - \delta_0(t)\big)\mathscr{H}\big(a(t) - r\big). \qquad (4.162)$$

By applying the Laplace transform to both sides of Eq. (4.161), we obtain

$$s\tilde{\Phi}(s)\left(\frac{1}{r}\frac{d\tilde{y}}{dr} + \varkappa\tilde{y}\right) = m\tilde{f}(s,r), \qquad (4.163)$$

where the tilde denotes the time Laplace transform and s is the Laplace transform variable. Note that all these functions should be analytic in the half-plane $\Re s > 0$.

The general solution to the homogeneous equation corresponding to Eq. (4.163) has the form

$$\tilde{y}_0(s, r) = C_0(s) \exp\Big(-\frac{\varkappa}{2} r^2\Big), \tag{4.164}$$

where $C_0(s)$ is an integration variable.

Now, applying Lagrange's method of variation of parameters, and taking into account the regularity condition (4.147), now given by

$$\tilde{y}(s, r) = O(r^2), \quad r \to 0, \tag{4.165}$$

we obtain the following particular solution of Eq. (4.163), which is valid for arbitrary $r \geq 0$:

$$\tilde{y}(s, r) = m \exp\Big(-\frac{\varkappa}{2} r^2\Big) \int_0^r \exp\Big(\frac{\varkappa}{2} \xi^2\Big) \frac{\xi \tilde{f}(s, \xi)}{s \tilde{\Phi}(s)} \, d\xi. \tag{4.166}$$

Under the assumption of monotonic loading and as a result of increasing contact radius $a(t)$, we compute the Laplace transform of the right hand-side of Eq. (4.161) as follows:

$$\tilde{f}(s, r) = \begin{cases} \dfrac{Cr^2}{s} - \tilde{\delta}_0(s), & 0 \leq r \leq a_0, \\ \dfrac{Cr^2}{s} \exp\big(-s t_*(r)\big) - \displaystyle\int_{t_*(r)}^{\infty} \exp(-st) \delta_0(t) \, dt, & r \geq a_0. \end{cases} \tag{4.167}$$

Here, $a_0 = a(0^+)$ is the radius of the instantaneous contact area, and $t_*(r)$ is the time when the contour of the contact area first reaches the point r.

If we denote by $t = a^{-1}(r)$ the inverse to the function $r = a(t)$, then we have

$$t_*(r) = \begin{cases} 0, & 0 \leq r \leq a_0, \\ a^{-1}(r), & a_0 \leq r. \end{cases} \tag{4.168}$$

We note that the solution to Eq. (4.161) is different from zero only in the domain $\Omega_0 \bigcup \Omega_+$, as illustrated on Fig. 4.8. This problem must be considered separately for

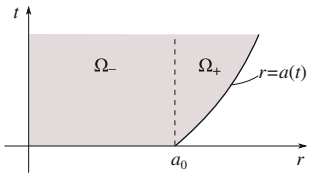

Fig. 4.8 Support domain of the solution to Eq. (4.161)

each domain. We finally note that when the parameter $\varkappa$ in its dimensionless form is reasonably small, an approximate equation for the contact radius can be derived from Eq. (4.159). For more details we refer to [5, 19].

4.5 Elliptical Contact of Thin Bonded Incompressible Viscoelastic Layers: Monotonically Increasing Contact Area

In this section, an exact solution for the frictionless unilateral contact problem for two thin incompressible transversely isotropic viscoelastic layers bonded to rigid substrates is obtained in the framework of the leading-order asymptotic model, under the assumption of a monotonically increasing contact area.

4.5.1 Formulation of the Contact Problem

Consider two thin viscoelastic layers of uniform thicknesses h_1 and h_2, ideally bonded to rigid substrates, and touching at a single point in the undeformed configuration (see Fig. 4.9). Let $\varphi(\mathbf{y})$ denote the gap between the layer surfaces before deformation. Here, following Argatov and Mishuris [6, 7], we consider a special case, where the gap function is represented by an elliptic paraboloid

$$\varphi(\mathbf{y}) = \frac{y_1^2}{2R_1} + \frac{y_2^2}{2R_2}, \tag{4.169}$$

and R_1 and R_2 are positive constants having dimensions of length.

Let $\delta_0(t)$ and $w_0^{(n)}(t, \mathbf{y})$ denote, respectively, the contact approach of the rigid substrates under external loading and the corresponding local indentation of the nth layer. Then, inside the contact area, $\omega(t)$, which is assumed to be a function of the time variable t, we impose the contact condition

$$w_0^{(1)}(t, \mathbf{y}) + w_0^{(2)}(t, \mathbf{y}) = \delta_0(t) - \varphi(\mathbf{y}), \quad \mathbf{y} \in \omega(t). \tag{4.170}$$

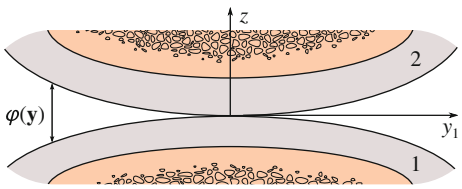

Fig. 4.9 Contact of two thin viscoelastic layers in the initial undeformed configuration, with the variable initial gap function $\varphi(\mathbf{y})$ measured along the common normal axis z

In the case of unilateral contact, the contact pressure between the viscoelastic layers, $p(\mathbf{y})$, is assumed to be positive inside the contact area $\omega(t)$ and to satisfy the following boundary conditions (see Sect. 2.7.3 and [1, 10, 14]):

$$p(t,\mathbf{y}) = 0, \quad \frac{\partial p}{\partial n}(t,\mathbf{y}) = 0, \quad \mathbf{y} \in \Gamma(t). \tag{4.171}$$

Here, $\partial/\partial n$ is the normal derivative at the contour $\Gamma(t)$ of the domain $\omega(t)$.

According to Eq. (4.34), the vertical displacement of the surface points of the nth layer of a thin bonded incompressible transversely isotropic viscoelastic layer can be approximated by

$$w_0^{(n)}(t,r) = -\frac{h_n^3}{3}\int\limits_{0-}^{t} J'^{(n)}(t-\tau)\Delta_y \frac{\partial p}{\partial \tau}(\tau,\mathbf{y})\,d\tau, \tag{4.172}$$

where $J'^{(n)}(t)$ is the out-of-plane creep compliance in shear of the nth layer.

By substituting the asymptotic approximations (4.172) into (4.170), we arrive at the governing integro-differential equation

$$-\sum_{n=1}^{2}\frac{h_n^3}{3}\int\limits_{0-}^{t} J'^{(n)}(t-\tau)\Delta_y \frac{\partial p}{\partial \tau}(\tau,\mathbf{y})\,d\tau = \delta_0(t) - \varphi(\mathbf{y})\mathscr{H}(t), \tag{4.173}$$

where $\mathbf{y} \in \omega(t)$, and the Heaviside function factor $\mathscr{H}(t)$ takes into account the zero initial conditions for $t < 0$.

Finally, denoting the external load applied to the substrates by $F(t)$, we write out the equilibrium equation

$$F(t) = \iint\limits_{\omega(t)} p(t,\mathbf{y})\,d\mathbf{y}. \tag{4.174}$$

The unilateral contact problem under consideration thus consists in finding histories $\delta_0(t)$, $\omega(t)$, $p(t,\mathbf{y})$ which, for given $\varphi(\mathbf{y})$, known $J'^{(n)}(t)$, $n = 1, 2$, and prescribed $F(t)$, satisfy (4.171), (4.173), and (4.174).

We retain the notation used in Sect. 4.3 and rewrite Eq. (4.173) as

$$-\int\limits_{0-}^{t} \Phi_\beta(t-\tau)\Delta_y \frac{\partial p}{\partial \tau}(\tau,\mathbf{y})\,d\tau = m\big(\delta_0(t) - \varphi(\mathbf{y})\mathscr{H}(t)\big). \tag{4.175}$$

Here, $\Phi_\beta(t)$ is the normalized ($\Phi_\beta(0) = 1$) compound creep function and m is a dimensional constant given by (4.102)–(4.105).

Following [6, 7], we derive an exact solution of the contact problem for thin bonded incompressible viscoelastic layers, which is formulated by Eqs. (4.171) and

(4.175) in the case of an elliptic gap (4.169), under the monotonicity condition for the contact area, that is $\omega(t_1) \subset \omega(t_2)$ for $t_1 \le t_2$.

4.5.2 General Solution for the Case of Elliptical Contact

Let us rewrite Eq. (4.175) in the form

$$\Delta_y \mathscr{P}(t, \mathbf{y}) = m\big(\varphi(\mathbf{y})\mathscr{H}(t) - \delta_0(t)\big), \quad \mathbf{y} \in \omega(t), \tag{4.176}$$

where we have introduced the notation

$$\mathscr{P}(t, \mathbf{y}) = \int_{0-}^{t} \Phi_\beta(t-\tau)\frac{\partial p}{\partial \tau}(\tau, \mathbf{y})\, d\tau. \tag{4.177}$$

As a consequence of (4.171), the function $\mathscr{P}(t, \mathbf{y})$ must satisfy the following boundary conditions:

$$\mathscr{P}(t, \mathbf{y}) = 0, \quad \mathbf{y} \in \Gamma(t), \quad \frac{\partial \mathscr{P}}{\partial n}(t, \mathbf{y}) = 0, \quad \mathbf{y} \in \Gamma(t). \tag{4.178}$$

In the case (4.169), the right-hand side of Eq. (4.176) is a quadratic polynomial in the variables y_1 and y_2, and we set

$$\mathscr{P}(t, \mathbf{y}) = \mathscr{P}_0(t)\left(1 - \frac{y_1^2}{a(t)^2} - \frac{y_2^2}{b(t)^2}\right)^2, \quad \mathbf{y} \in \omega(t). \tag{4.179}$$

It is simple to verify that the function (4.179) satisfies the boundary conditions (4.178) exactly.

The representation (4.179) assumes that the contour $\Gamma(t)$ is an ellipse with the semi-axes $a(t)$ and $b(t)$. Moreover, for $\mathbf{y} \notin \omega(t)$, we should have $\mathscr{P}(t, \mathbf{y}) = 0$. Thus, the function $\mathscr{P}(t, \mathbf{y})$ determined by (4.179) for $\mathbf{y} \in \omega(t)$ can be extended on the entire plane of variable $\mathbf{y} = (y_1, y_2)$ by the multiplication of the right-hand side of (4.179) by the factor $\mathscr{H}\big(1 - y_1^2/a(t)^2 - y_2^2/b(t)^2\big)$, that is

$$\mathscr{P}(t, \mathbf{y}) = \mathscr{P}_0(t)\Xi(t, \mathbf{y})^2\mathscr{H}\big(\Xi(t, \mathbf{y})\big), \quad \mathbf{y} \in \mathbb{R}^2, \tag{4.180}$$

where we have introduced the notation

$$\Xi(t, \mathbf{y}) = 1 - \frac{y_1^2}{a(t)^2} - \frac{y_2^2}{b(t)^2}. \tag{4.181}$$

Substituting (4.180) into Eq. (4.176), we obtain after some calculation the following system of algebraic equations:

$$\delta_0(t) = \frac{4\mathscr{P}_0(t)}{m}\left(\frac{1}{a(t)^2} + \frac{1}{b(t)^2}\right), \tag{4.182}$$

$$\frac{1}{2R_1} = \frac{4\mathscr{P}_0(t)}{ma(t)^2}\left(\frac{3}{a(t)^2} + \frac{1}{b(t)^2}\right), \tag{4.183}$$

$$\frac{1}{2R_2} = \frac{4\mathscr{P}_0(t)}{mb(t)^2}\left(\frac{1}{a(t)^2} + \frac{3}{b(t)^2}\right). \tag{4.184}$$

The form of the ellipse $\Gamma(t)$ can be characterized by its aspect ratio s, defined as follows:

$$s = \frac{b(t)}{a(t)}. \tag{4.185}$$

From Eqs. (4.183) and (4.184), it immediately follows that

$$\frac{R_2}{R_1} = \frac{s^2(3s^2+1)}{3+s^2}, \tag{4.186}$$

and it is readily seen that Eq. (4.186) can be reduced to a quadratic equation for s^2

$$3s^4 + \left(1 - \frac{R_2}{R_1}\right)s^2 - \frac{3R_2}{R_1} = 0.$$

In this way we immediately obtain

$$s^2 = \sqrt{\left(\frac{R_1 - R_2}{6R_1}\right)^2 + \frac{R_2}{R_1}} - \frac{(R_1 - R_2)}{6R_1}. \tag{4.187}$$

Further, in light of (4.183)–(4.185), Eq. (4.182) takes the form

$$\delta_0(t) = \frac{a(t)^2}{2R_1}\frac{(s^2+1)}{(3s^2+1)}. \tag{4.188}$$

From Eq. (4.183) it follows that

$$\mathscr{P}_0(t) = \frac{ma(t)^4}{8R_1}\frac{s^2}{(3s^2+1)}. \tag{4.189}$$

As a consequence of (4.177), the contact force $F(t)$ satisfies the equation

$$\int_{0-}^{t} \Phi_\beta(t-\tau)\frac{dF(\tau)}{d\tau}\,d\tau = \frac{\pi m}{24R_1}\frac{s^3}{(3s^2+1)}a(t)^6. \tag{4.190}$$

Thus, the major semi-axis $a(t)$ of the contact domain $\omega(t)$ can be determined as a function of time t in the following way:

$$a(t) = \left[\frac{24R_1}{\pi m}\frac{(3s^2+1)}{s^3}\right]^{1/6}\left(\int_{0-}^{t} \Phi_\beta(t-\tau)\frac{dF(\tau)}{d\tau}\,d\tau\right)^{1/6}. \tag{4.191}$$

Then, formulas (4.188) and (4.189) allow us to determine the quantities $\delta_0(t)$ and $\mathscr{P}_0(t)$, respectively.

Let us denote by $\Psi_\beta(t)$ the normalized compound relaxation function for the viscoelastic incompressible layers defined by formula (4.127) or, equivalently, by formula (4.128).

Then, according to Eqs. (4.177) and (4.180), the contact pressure distribution is given by

$$p(t,\mathbf{y}) = \int_{0-}^{t} \Psi_\beta(t-\tau)\frac{\partial}{\partial\tau}\left\{\mathscr{P}_0(\tau)\Xi(\tau,\mathbf{y})^2\mathscr{H}\big(\Xi(\tau,\mathbf{y})\big)\right\}d\tau. \tag{4.192}$$

The application of integration by parts to (4.192) yields

$$\begin{aligned} p(t,\mathbf{y}) = {} & \mathscr{P}_0(t)\Xi(t,\mathbf{y})^2 \\ & - \int_{0^+}^{t} \frac{\partial\Psi_\beta}{\partial\tau}(t-\tau)\mathscr{P}_0(\tau)\Xi(\tau,\mathbf{y})^2\mathscr{H}\big(\Xi(\tau,\mathbf{y})\big)d\tau. \end{aligned} \tag{4.193}$$

Recall that $\Psi_\beta(0) = 1$, and formula (4.193) assumes that $p(t,\mathbf{y}) = 0$ for $\mathbf{y} \notin \omega(t)$.

Denoting by $t_*(\mathbf{y})$ the time when the contour of the contact zone first reaches the point $\mathbf{y}$, we rewrite formula (4.193) as follows:

$$p(t,\mathbf{y}) = \mathscr{P}_0(t)\Xi(t,\mathbf{y})^2 - \int_{t_*(\mathbf{y})}^{t} \frac{\partial\Psi_\beta}{\partial\tau}(t-\tau)\mathscr{P}_0(\tau)\Xi(\tau,\mathbf{y})^2 d\tau. \tag{4.194}$$

The quantity $t_*(\mathbf{y})$ is determined by the equation

$$a(t_*)^2 = y_1^2 + s^{-2}y_2^2. \tag{4.195}$$

Substituting the expression (4.191) into Eq. (4.195), we arrive at the equation

$$\int_{0-}^{t_*} \Phi_\beta(t_* - \tau)\frac{dF(\tau)}{d\tau}\,d\tau = \frac{\pi m}{24R_1}\frac{s^3}{(3s^2+1)}\left(y_1^2 + \frac{y_2^2}{s^2}\right)^3. \tag{4.196}$$

We note that formula (4.194) assumes that $t_*(\mathbf{y}) = 0$ for the points of the instantaneous contact area $\omega(0^+)$. In the following, the quantity $t_*(\mathbf{y})$ will be called the time-to-contact for the point $\mathbf{y}$.

4.5.3 Case of Stepwise Loading

Assuming that

$$F(t) = F_0\mathscr{H}(t), \tag{4.197}$$

and using Eqs. (4.188) and (4.191), we find that

$$\delta_0(t) = \delta_0(0^+)\left(\frac{\Phi_\alpha(t)}{\Phi_\alpha(0)}\right)^{1/3}\mathscr{H}(t), \tag{4.198}$$

$$a(t) = a(0^+)\left(\frac{\Phi_\alpha(t)}{\Phi_\alpha(0)}\right)^{1/6}\mathscr{H}(t), \tag{4.199}$$

$$\mathscr{P}_0(t) = \mathscr{P}_0(0^+)\left(\frac{\Phi_\alpha(t)}{\Phi_\alpha(0)}\right)^{2/3}\mathscr{H}(t), \tag{4.200}$$

where

$$\delta_0(0^+) = \left(\frac{3}{\pi m R_1^2}\right)^{1/3}\frac{(s^2+1)}{s(3s^2+1)^{2/3}}\left(F_0\Phi_\beta(0)\right)^{1/3}, \tag{4.201}$$

$$a(0^+) = \left[\frac{\pi m}{24R_1}\frac{s^3}{(3s^2+1)}\right]^{-1/6}\left(F_0\Phi_\beta(0)\right)^{1/6}, \tag{4.202}$$

$$\mathscr{P}_0(0^+) = \left(\frac{9m}{\pi^2 R_1}\right)^{1/3}\frac{s^2}{s^2(3s^2+1)^{1/3}}\left(F_0\Phi_\beta(0)\right)^{2/3}. \tag{4.203}$$

Equation (4.202) determines the major semi-axis of the instantaneous contact domain $\omega(0^+)$. For $\mathbf{y}$ lying outside $\omega(0^+)$, the quantity $t_*(\mathbf{y})$ satisfies Eq. (4.195). From Eqs. (4.202) and (4.195), it follows that

$$t_*(\mathbf{y}) = \Phi_\beta^{-1}\left(\frac{\Phi_\beta(0)}{a^6(0^+)}\left(y_1 + \frac{y_2^2}{s^2}\right)^2\right), \tag{4.204}$$

where $\Phi_\beta^{-1}(x) = t$ is the inverse function with respect to $\Phi_\beta(t) = x$.

4.5.4 Axisymmetric Contact Problem for Incompressible Coatings: Case of Stepwise Loading

Axisymmetric indentation problems for a viscoelastic layer have been considered in papers [20, 21] for the special cases of the Maxwell model and the standard viscoelastic solid model. Now, let us set $R_1 = R_2 = R$. Consequently, we obtain $s = 1$, and Eqs. (4.201)–(4.203), respectively, take the form

$$\delta_0(0^+) = \left(\frac{3}{2\pi m R_1^2}\right)^{1/3}\left(F_0\Phi_\beta(0)\right)^{1/3}, \tag{4.205}$$

$$a(0^+) = \left(\frac{\pi m}{96R_1}\right)^{-1/6}\left(F_0\Phi_\beta(0)\right)^{1/6}, \tag{4.206}$$

$$\mathscr{P}_0(0^+) = \left(\frac{18m}{\pi^2 R_1}\right)^{1/3}\left(F_0\Phi_\beta(0)\right)^{2/3}. \tag{4.207}$$

According to (4.194), the axisymmetric contact pressure distribution is given by the following formula (cf. Sect. 4.3.6):

$$p(r,t) = \Psi_\beta(0)\mathscr{P}_0(t)\left(1 - \frac{r^2}{a(t)^2}\right)^2 - \int\limits_{t_*(r)}^{t} \frac{\partial\Psi_\beta}{\partial\tau}(t-\tau)\mathscr{P}_0(\tau)\left(1 - \frac{r^2}{a(\tau)^2}\right)^2 d\tau. \tag{4.208}$$

Here, $r = \sqrt{y_1^2 + y_2^2}$ is the radial coordinate, and in light of (4.204), the time-to-contact for all points on the circle of radius $r > a(0^+)$ is given by

$$t_*(r) = \Phi_\beta^{-1}\left(\frac{\Phi_\beta(0)}{a(0^+)^6}r^6\right). \tag{4.209}$$

Formulas (4.205)–(4.209) are valid for the stepwise loading (4.197). In the general case of the axisymmetric contact problem, the solution can be easily derived using formulas (4.188), (4.191), (4.194), and (4.196) with $s = 1$ and $y_1^2 + y_2^2 = r^2$.

4.5.5 Case of Incompressible Layers Following the Maxwell Model

Recall that the Maxwell model is represented by the series combination of an elastic spring and a dashpot, and can be characterized by the following normalized creep and relaxation functions:

$$\Phi'^{(n)}(t) = 1 + \frac{t}{\tau_0^{(n)}}, \quad \Psi'^{(n)}(t) = \exp\Big(-\frac{t}{\tau_0^{(n)}}\Big), \tag{4.210}$$

where $\tau_0^{(n)}$ is the relaxation time of the viscoelastic material of the nth layer. Note that the concept of the relaxed state for the Maxwell model is not applicable.

According to (4.102), the normalized compound creep function is given by

$$\Phi_\beta(t) = 1 + \frac{t}{\tau_0},$$

where τ_0 is defined by the formula

$$\frac{1}{\tau_0} = \frac{\beta_1}{\tau_0^{(1)}} + \frac{\beta_2}{\tau_0^{(2)}}$$

for β_1 and β_2 given by (4.104).

Correspondingly, in light of (4.210), the normalized compound relaxation function is simply

$$\Psi_\beta(t) = \exp\Big(-\frac{t}{\tau_0}\Big),$$

which agrees with formula (4.128).

Taking into account that $p(t, \mathbf{y}) = 0$ for $t < 0$, we can rewrite Eq. (4.175) as

$$\Delta_y p(t, \mathbf{y}) + \frac{1}{\tau_0}\int_0^t \Delta_y p(\tau, \mathbf{y})\, d\tau = m\big(\varphi(\mathbf{y})\mathscr{H}(t) - \delta_0(t)\big). \tag{4.211}$$

We observe that Eq. (4.211) coincides with the governing integral equation derived as a result of asymptotic analysis in [1] for describing the short-time contact of thin biphasic cartilage layers.

In light of (4.210), formula (4.194) takes the form

$$p(t, \mathbf{y}) = \mathscr{P}_0(t)\Xi(t, \mathbf{y})^2 - \frac{1}{\tau_0}\int_{t_*(\mathbf{y})}^t \mathscr{P}_0(\tau)\Xi(\tau, \mathbf{y})^2 \exp\Big(-\frac{t-\tau}{\tau_0}\Big)\, d\tau, \tag{4.212}$$

where the factor $\Xi(t, \mathbf{y})$ is given by formula (4.181), and where $\mathscr{P}_0(t)$, $a(t)$, and $b(t)$ satisfy Eqs. (4.182)–(4.184). Apart from the notation, formula (4.212) coincides with the solution obtained in [6].

4.5.6 Force-Displacement Relationship

Excluding $a(t)$ from (4.190) and (4.188), we arrive at the following equation [4]:

$$F(t) = \frac{2\pi}{3} c_F(s) m R_1 R_2 \int_{0-}^{t} \Psi_\beta(t-\tau) \frac{d}{d\tau} \left(\delta_0(\tau)^3\right) d\tau. \tag{4.213}$$

Here, $c_F(s)$ is dimensionless factor, which depends on the aspect ratio of the contact area $s = b/a$ (see formula (4.187)) and is given by

$$c_F(s) = \frac{s(3s^2+1)(s^2+3)}{2(s^2+1)^3}.$$

We note that Eq. (4.213) is valid for the contact interaction that consists of a monotonic loading phase. Thus, it can be applied to modeling contact forces in impact situations, whereas the case of repetitive loading requires a special further consideration.

References

1. Ateshian, G.A., Lai, W.M., Zhu, W.B., Mow, V.C.: An asymptotic solution for the contact of two biphasic cartilage layers. J. Biomech. **27**, 1347–1360 (1994)
2. Argatov, I.I.: Asymptotic modeling of the impact of a spherical indenter on an elastic half-space. Int. J. Solids Struct. **45**, 5035–5048 (2008)
3. Argatov, I.: A general solution of the axisymmetric contact problem for biphasic cartilage layers. Mech. Res. Comm. **38**, 29–33 (2011)
4. Argatov, I.I.: Development of an asymptotic modeling methodology for tibio-femoral contact in multibody dynamic simulations of the human knee joint. Multibody Syst. Dyn. **28**, 3–20 (2012)
5. Argatov, I.I., Mishuris, G.S.: Axisymmetric contact problem for a biphasic cartilage layer with allowance for tangential displacements on the contact surface. Eur. J. Mech. A/Solids **29**, 1051–1064 (2010)
6. Argatov, I., Mishuris, G.: Elliptical contact of thin biphasic cartilage layers: exact solution for monotonic loading. J. Biomech. **44**, 759–761 (2011)
7. Argatov, I., Mishuris, G.: Frictionless elliptical contact of thin viscoelastic layers bonded to rigid substrates. Appl. Math. Model. **35**, 3201–3212 (2011)
8. Barber, J.R.: Contact problems for the thin elastic layer. Int. J. Mech. Sci. **32**, 129–132 (1990)

9. Belokon', A.V., Vorovich, I.I.: Contact problems of the linear theory of viscoelasticity ignoring friction and cohesion forces [in Russian]. Izv. Akad. Nauk SSSR. MTT [Mechanics of Solids], **6**, 63–73 (1973)
10. Chadwick, R.S.: Axisymmetric indentation of a thin incompressible elastic layer. SIAM J. Appl. Math. **62**, 1520–1530 (2002)
11. Christensen, R.M.: Theory of Viscoelasticity. Academic Press, New York (1982)
12. Graham, G.A.C.: The contact problem in the linear theory of viscoelasticity. Int. J. Eng. Sci. **3**, 27–46 (1965)
13. Hoang, S.K., Abousleiman, Y.N.: Poroviscoelasticity of transversely isotropic cylinders under laboratory loading conditions. Mech. Res. Commun. **37**, 298–306 (2010)
14. Jaffar, M.J.: Asymptotic behaviour of thin elastic layers bonded and unbonded to a rigid foundation. Int. J. Mech. Sci. **31**, 229–235 (1989)
15. Korhonen, R.K., Laasanen, M.S., Töyräs, J., Rieppo, J., Hirvonen, J., Helminen, H.J., Jurvelin, J.S.: Comparison of the equilibrium response of articular cartilage in unconfined compression, confined compression and indentation. J. Biomech. **35**, 903–909 (2002)
16. Kravchuk, A.S.: On the Hertz problem for linearly and nonlinearly elastic bodies of finite dimensions. J. Appl. Math. Mech. **41**, 320–328 (1977)
17. Lakes, R.S.: Viscoelastic Materials. Cambridge University Press, Cambridge (2009)
18. Lee, E.H., Radok, J.R.M.: The contact problem for viscoelastic bodies. J. Appl. Mech. **27**, 438–444 (1960)
19. Mishuris, G., Argatov, I.: Exact solution to a refined contact problem for biphasic cartilage layers. In: Nithiarasu, P., Löhner, R. (eds.) Proceedings of the 1st International Conference on Mathematical and Computational Biomedical Engineering—CMBE2009, pp. 151–154. Swanseak, UK, June 29–July 1 2009
20. Naghieh, G.R., Jin, Z.M., Rahnejat, H.: Contact characteristics of viscoelastic bonded layers. Appl. Math. Model. **22**, 569–581 (1998)
21. Naghieh, G.R., Rahnejat, H., Jin, Z.M.: Characteristics of frictionless contact of bonded elastic and viscoelastic layered solids. Wear **232**, 243–249 (1999)
22. Pipkin, A.C.: Lectures on Viscoelastic Theory. Springer, New York (1986)
23. Ting, T.C.T.: Contact problems in the linear theory of viscoelasticity. J. Appl. Mech. **35**, 248–254 (1968)
24. Tschoegl, N.W.: Time dependence in material properties: an overview. Mech. Time-Depend. Mat. **1**, 3–31 (1997)
25. Wu, J.Z., Herzog, W., Epstein, M.: An improved solution for the contact of two biphasic cartilage layers. J. Biomech. **30**, 371–375 (1997)

Chapter 5
Linear Transversely Isotropic Biphasic Model for Articular Cartilage Layer

Abstract In Sect. 5.1, we develop a linear biphasic theory for the case of a transversely isotropic elastic solid matrix with transverse isotropy of permeability. In Sects. 5.2 and 5.3, we consider the linear biphasic models of confined and unconfined compression, respectively, for the biphasic stress relaxation and the biphasic creep tests. Finally, in Sect. 5.4 we outline the biphasic poroviscoelastic model, which accounts for the inherent viscoelasticity of the solid matrix.

5.1 Linear Biphasic Model

In this section we introduce the linear biphasic theory, which models articular cartilage as a binary mixture of an intrinsically incompressible elastic matrix (skeleton) and an inviscid (i.e., dissipationless) incompressible fluid. We also present and discuss the formulation of the governing differential equations along with the different types of boundary conditions.

5.1.1 Linear Biphasic Theory

According to the biphasic theory of Mow et al. [60], articular cartilage is modeled as a biphasic mixture consisting of a solid phase (representing collagen, proteoglycans, chrondrocytes, and other quantitatively minor glycoproteins) and a fluid phase (representing mobile interstitial fluid and dissolved electrolytes). The fluid phase typically ranges between 65 and 90 % of the articular cartilage tissue by weight [8].

Note also that various biphasic and poroelastic models were used to describe the deformation behavior of bone [20], skin [62], polymeric and silk hydrogels [16, 42], and arterial walls [40]. An overview of computational models for the mechanical behavior of articular cartilage was given in [27, 49, 76].

Let the fluid volume fraction (porosity) be denoted by $\phi_{\mathrm{f}} = V_{\mathrm{f}}/V$, and the solid volume fraction be $\phi_{\mathrm{s}} = V_{\mathrm{s}}/V$, where $V_{\mathrm{f}} + V_{\mathrm{s}} = V$, so that

I. Argatov and G. Mishuris, *Contact Mechanics of Articular Cartilage Layers*,
Advanced Structured Materials 50, DOI 10.1007/978-3-319-20083-5_5

$$\phi_{\mathrm{f}} + \phi_{\mathrm{s}} = 1. \tag{5.1}$$

The continuity equation for a biphasic medium is

$$\nabla \cdot (\phi_{\mathrm{f}} \mathbf{v}^{\mathrm{f}} + \phi_{\mathrm{s}} \mathbf{v}^{\mathrm{s}}) = 0, \tag{5.2}$$

where $\mathbf{v}^{\mathrm{f}}$ and $\mathbf{v}^{\mathrm{s}}$ are solid and fluid velocities, ∇ is the gradient operator.

Under quasi-static conditions, and in the absence of body forces, the momentum equations for each phase are given by

$$\begin{aligned} \nabla \cdot \boldsymbol{\sigma}^{\mathrm{s}} - \boldsymbol{\pi}^{\mathrm{f}} &= \mathbf{0}, \\ \nabla \cdot \boldsymbol{\sigma}^{\mathrm{f}} + \boldsymbol{\pi}^{\mathrm{f}} &= \mathbf{0}, \end{aligned} \tag{5.3}$$

where $\boldsymbol{\pi}^{\mathrm{f}}$ is the momentum exchange between the phases due to frictional drag of relative fluid flow through the porous-permeable solid matrix. In articular cartilage, it has been shown [35] that this momentum exchange term creates a frictional drag several orders of magnitude greater than the viscous shear stress within the interstitial fluid due to the viscosity of the fluid. The internal fluid viscosity can usually be neglected except for very small layers of very permeable materials [11].

Thus, neglecting the frictional dissipation between the fluid particles, the interstitial water is assumed to be inviscid, and the fluid phase stress is given by

$$\boldsymbol{\sigma}^{\mathrm{f}} = -\phi_{\mathrm{f}} p \mathbf{I}. \tag{5.4}$$

Here, p is the fluid pressure, $\mathbf{I}$ is the identity tensor.

The single pore-fluid flow is governed by the local interaction force per unit volume defined as follows [12, 55, 65]:

$$\boldsymbol{\pi}^{\mathrm{f}} = -\mathbf{K} \cdot (\mathbf{v}^{\mathrm{f}} - \mathbf{v}^{\mathrm{s}}). \tag{5.5}$$

Here, $\mathbf{K}$ represents a hydraulic resistivity (or inverse permeability) tensor, which is related to the permeability tensor, $\mathbf{k}$, through

$$\mathbf{K} = \phi_{\mathrm{f}}^2 \mathbf{k}^{-1}, \tag{5.6}$$

and apparently depends on the deformable pore structure and the interstitial fluid properties [58, 59, 67]. Note also that the permeability of the tissue decreases when the pore volume decreases [24, 33].

Generally, $\mathbf{k}$ is a positive definite and symmetric tensor. For a transversely isotropic skeleton, if $x_3 = 0$ is the plane of isotropy, the matrix of the permeability tensor takes the form

$$\mathbf{k} = \begin{pmatrix} k_1 & 0 & 0 \\ 0 & k_1 & 0 \\ 0 & 0 & k_3 \end{pmatrix}.$$

As was shown in [25], the transverse isotropy of permeability in articular cartilage is caused by its microstructural anisotropy. In particular, the permeability is greater in the direction parallel to the collagen fibres than the orthogonal.

In the isotropic case [44], $\mathbf{K} = K\mathbf{I}$, where K is the diffusion coefficient and is related to the permeability coefficient of the solid matrix, k, by $k = \phi_{\mathrm{f}}^2/K$.

The stress-strain relation for the solid matrix is assumed to have the form

$$\boldsymbol{\sigma}^{\mathrm{s}} = -\phi_{\mathrm{s}} p\mathbf{I} + \boldsymbol{\sigma}^{\mathrm{e}}, \tag{5.7}$$

where $\boldsymbol{\sigma}^{\mathrm{e}}$ is the effective (or elastic) stress of the solid matrix. Note that the concept of effective stress was originally formulated by Terzaghi [74] in a geotechnical consolidation problem, presuming that the effective soil stress is determined by the total stress minus the excess pore pressure.

Thus, under these assumptions the total stress in the biphasic material, which is defined as the sum

$$\boldsymbol{\sigma} = \boldsymbol{\sigma}^{\mathrm{s}} + \boldsymbol{\sigma}^{\mathrm{f}}, \tag{5.8}$$

in light of (5.4) and (5.7) is given by

$$\boldsymbol{\sigma} = -p\mathbf{I} + \boldsymbol{\sigma}^{\mathrm{e}}, \tag{5.9}$$

while from (5.3) it follows that

$$\nabla \cdot \boldsymbol{\sigma} = \mathbf{0}. \tag{5.10}$$

For an anisotropic linearly elastic material, the effective stress $\boldsymbol{\sigma}^{\mathrm{e}}$ is related to the infinitesimal strain tensor of the solid matrix, $\boldsymbol{\varepsilon}$, by Hooke's law

$$\boldsymbol{\sigma}^{\mathrm{e}} = \mathbf{C} : \boldsymbol{\varepsilon},$$

where $\mathbf{C}$ is a fourth-order stiffness tensor, and the strain tensor is given by

$$\boldsymbol{\varepsilon} = \frac{1}{2}\left(\nabla\mathbf{u} + \nabla\mathbf{u}^{\mathsf{T}}\right), \tag{5.11}$$

where $\mathbf{u}$ is the displacement vector of the solid phase. Note also that the solid velocity is

$$\mathbf{v}^{\mathrm{s}} = \frac{\partial \mathbf{u}}{\partial t}, \tag{5.12}$$

where t is a time variable.

Following Cohen et al. [19], we assume that the solid-phase material is transversely isotropic, so that

$$\begin{pmatrix} \sigma^{\mathrm{e}}_{11} \\ \sigma^{\mathrm{e}}_{22} \\ \sigma^{\mathrm{e}}_{33} \\ \sigma^{\mathrm{e}}_{23} \\ \sigma^{\mathrm{e}}_{13} \\ \sigma^{\mathrm{e}}_{12} \end{pmatrix} = \begin{bmatrix} A^{\mathrm{s}}_{11} & A^{\mathrm{s}}_{12} & A^{\mathrm{s}}_{13} & 0 & 0 & 0 \\ A^{\mathrm{s}}_{12} & A^{\mathrm{s}}_{11} & A^{\mathrm{s}}_{13} & 0 & 0 & 0 \\ A^{\mathrm{s}}_{13} & A^{\mathrm{s}}_{13} & A^{\mathrm{s}}_{33} & 0 & 0 & 0 \\ 0 & 0 & 0 & 2A^{\mathrm{s}}_{44} & 0 & 0 \\ 0 & 0 & 0 & 0 & 2A^{\mathrm{s}}_{44} & 0 \\ 0 & 0 & 0 & 0 & 0 & 2A^{\mathrm{s}}_{66} \end{bmatrix} \begin{pmatrix} \varepsilon_{11} \\ \varepsilon_{22} \\ \varepsilon_{33} \\ \varepsilon_{23} \\ \varepsilon_{13} \\ \varepsilon_{12} \end{pmatrix}, \tag{5.13}$$

where A^{s}_{11}, A^{s}_{12}, A^{s}_{13}, A^{s}_{33}, and A^{s}_{44} are five independent elastic constants of the solid skeleton.

The substitution of (5.4), (5.5), and (5.7) into Eq. (5.3) yields

$$-\phi_{\mathrm{s}} \nabla p + \nabla \cdot \boldsymbol{\sigma}^{\mathrm{e}} + \mathbf{K} \cdot (\mathbf{v}^{\mathrm{f}} - \mathbf{v}^{\mathrm{s}}) = \mathbf{0}, \tag{5.14}$$

$$-\phi_{\mathrm{f}} \nabla p - \mathbf{K} \cdot (\mathbf{v}^{\mathrm{f}} - \mathbf{v}^{\mathrm{s}}) = \mathbf{0}, \tag{5.15}$$

whereas the substitution of (5.9) into Eq. (5.10) gives

$$-\nabla p + \nabla \cdot \boldsymbol{\sigma}^{\mathrm{e}} = \mathbf{0}. \tag{5.16}$$

Observe [55] that in the equations above, the vector $\mathbf{v}^{\mathrm{f}} - \mathbf{v}^{\mathrm{s}}$ represents the seepage velocity, describing the fluid motion relative to the deforming solid matrix. Moreover, relating this vector only to the fluid part of the mixture, the so-called relative fluid flux (or filter velocity), $\mathbf{w}^{\mathrm{f}}$, can be defined by the formula

$$\mathbf{w}^{\mathrm{f}} = \phi_{\mathrm{f}} (\mathbf{v}^{\mathrm{f}} - \mathbf{v}^{\mathrm{s}}). \tag{5.17}$$

Then, introducing the relative fluid flux into Eq. (5.15) according to its definition (5.17) and taking into account the relation (5.6) between the hydraulic resistivity tensor $\mathbf{K}$ and the permeability tensor $\mathbf{k}$, we arrive at the equation

$$\mathbf{w}^{\mathrm{f}} = -\mathbf{k} \cdot \nabla p, \tag{5.18}$$

which can be interpreted [10] as Darcy's law relative to the motion of the solid matrix.

As a result of (5.1) and (5.17), the continuity equation (5.2) can be recast as

$$\nabla \cdot (\mathbf{v}^{\mathrm{s}} + \mathbf{w}^{\mathrm{f}}) = 0,$$

which after the substitution of (5.12) and (5.18) is reduced to the equation

$$\frac{\partial}{\partial t} \nabla \cdot \mathbf{u} = \nabla \cdot (\mathbf{k} \cdot \nabla p), \tag{5.19}$$

where $\nabla \cdot \mathbf{u}$ is the dilatation of the solid matrix. It is important to note that Eqs. (5.16) and (5.19) can be solved independently of Eq. (5.18).

Observe [19] that the linear transversely isotropic biphasic model requires altogether seven constitutional parameters: five elastic constants (Young's moduli and Poisson's ratios in the transverse plane and out-of-plane, E_1^s, ν_{12}^s and E_3^s, ν_{31}^s, respectively, and the out-of-plane shear modulus, G_{13}^s) and two permeability coefficients k_1 and k_3, which are called the axial (in-plane) and transverse (out-of-plane) permeability coefficients, respectively.

Finally, it should be emphasized [57] that in addition to its mechanical response, articular cartilage also exhibits complex electrochemical phenomena due to the charged nature of its solid phase and the electrolytes dissolved in the interstitial water. A number of constitutive theories [31, 37, 45] for charged-hydrated soft tissues like articular cartilage have been developed using the multiphasic approach (see comprehensive review by Mow and Guo [57]), and a generalized correspondence principle for the equilibrium deformational behavior in the framework of the triphasic model was introduced [52, 53].

5.1.2 Boundary and Initial Conditions

Following Barry and Holmes [10], we consider the most common boundary conditions applicable to thin fluid-saturated porous layers. We assume that a biphasic layer is firmly attached to a rigid impermeable substrate, on the bottom of the layer, $x_3 = h$, in which case the boundary conditions become

$$\mathbf{u}\big|_{x_3=h} = \mathbf{0}, \tag{5.20}$$

$$\left.\frac{\partial p}{\partial x_3}\right|_{x_3=h} = 0. \tag{5.21}$$

On the upper surface, $x_3 = 0$, a number of different boundary conditions may be formulated depending on the problem setting. If the porous layer is in contact with a porous filter, then the boundary condition

$$p\big|_{x_3=0} = 0 \tag{5.22}$$

is imposed on the top surface.

If the layer is pressed against an impermeable punch, then

$$\left.\frac{\partial p}{\partial x_3}\right|_{x_3=0} = 0. \tag{5.23}$$

Further, the normal stress balance under a rigid punch $\sigma_{33}\big|_{x_3=0} = -q$ gives

$$-p + A^{\mathrm{s}}_{13}\frac{\partial u_1}{\partial x_1} + A^{\mathrm{s}}_{13}\frac{\partial u_2}{\partial x_2} + A^{\mathrm{s}}_{33}\frac{\partial u_3}{\partial x_3}\bigg|_{x_3=0} = -q, \tag{5.24}$$

where q is the load distribution on the top surface transferred by the punch. Note that the left-hand side of Eq. (5.24) represents the normal total stress σ_{33}.

For the frictionless contact, the tangential stresses σ_{31} and σ_{32} are zero, so that

$$\frac{\partial u_1}{\partial x_3} + \frac{\partial u_3}{\partial x_1}\bigg|_{x_3=0} = 0, \quad \frac{\partial u_2}{\partial x_3} + \frac{\partial u_3}{\partial x_2}\bigg|_{x_3=0} = 0. \tag{5.25}$$

In an idealized situation, the normal load q would be a known function of variables t, x_1, x_2. However, if the surface load is transferred from a punch, then within the contact area, ω, the contact condition is formulated as

$$u_3\big|_{x_3=0} = \delta_0(t) - \varphi(x_1, x_2), \quad (x_1, x_2) \in \omega, \tag{5.26}$$

where $\delta_0(t)$ is the normal displacement of the punch, $\varphi(x_1, x_2)$ is the punch shape function (defining the initial gap between the contacting surfaces).

Before continuing, we observe that the punch equilibrium implies that

$$\iint_{\omega} q(t, \mathbf{y})\, d\mathbf{y} = F(t), \tag{5.27}$$

where $F(t)$ is an applied external force.

In the case of frictionless contact between two biphasic layers, based on the results of Hou et al. [35] for porous layers saturated with inviscid interstitial fluids, Ateshian et al. [6] formulated the following interface boundary conditions:

$$[\![p]\!] = 0, \quad [\![\mathbf{u}\cdot\mathbf{n}]\!] = \mathbf{0}, \quad [\![\mathbf{w}^{\mathrm{f}}\cdot\mathbf{n}]\!] = \mathbf{0}, \quad [\![\sigma_N^{(n)}]\!] = 0, \tag{5.28}$$

$$\boldsymbol{\sigma}_T^{(n)} = 0. \tag{5.29}$$

Here, $\mathbf{n}$ is the normal unit vector on the contact interface, $[\![\cdot]\!]$ denotes the jump across the interface of the quantity within the brackets (e.g., $[\![p]\!] = p_+ - p_-$, where p_+ and p_- are the limit values of p at the two opposite sides of the interface), $\sigma_N^{(n)}$ and $\boldsymbol{\sigma}_T^{(n)}$ are the normal and tangential components of the total stress vector $\boldsymbol{\sigma}^{(n)} = \boldsymbol{\sigma}\cdot\mathbf{n}$, such that $\sigma_N^{(n)} = \boldsymbol{\sigma}^{(n)}\cdot\mathbf{n}$ and $\boldsymbol{\sigma}_T^{(n)} = \boldsymbol{\sigma}^{(n)} - \sigma_N^{(n)}\mathbf{n}$.

Note that the interface boundary conditions (5.28) simply state that the fluid pressure, p, the normal component of the solid displacement vector, $\mathbf{u}\cdot\mathbf{n}$, the normal component of the relative fluid flow, $\mathbf{w}^{\mathrm{f}}\cdot\mathbf{n}$, and the normal component of the total stress vector, $\sigma_N^{(n)}$, must be continuous across the interface.

Finally, we consider the usual initial conditions that the displacement vector, $\mathbf{u}$, the relative fluid flux, $\mathbf{w}^{\mathrm{f}}$, and the fluid pressure, p, are zero before the external load is applied, i.e.,

$$\mathbf{u} = \mathbf{0}, \quad \mathbf{w}^{\mathrm{f}} = \mathbf{0}, \quad p = 0, \quad -\infty < t < 0, \tag{5.30}$$

throughout the biphasic medium.

5.1.3 *Equivalent Elastic Material Properties of a Transversely Isotropic Biphasic Material for the Instantaneous Response*

It is known [23] that during short-duration impact events, articular cartilage can be considered as an elastic material. Moreover, it has been shown that the instantaneous response of a biphasic material is equivalent to that of an incompressible elastic material [5–7]. Following Garcia et al. [29], we introduce the elastic properties of the equivalent transversely isotropic incompressible elastic material, which can be used to model its instantaneous response.

In the biphasic model (see Eq. (5.8)), the total stresses in a biphasic material are defined as

$$\sigma_{ij} = \sigma_{ij}^{\mathrm{s}} + \sigma_{ij}^{\mathrm{f}}, \tag{5.31}$$

where σ_{ij}^{s} are the stresses in the solid matrix, σ_{ij}^{f} are the stresses in the fluid phase.

The stresses in the fluid phase are equal to the pressure in the fluid, p, averaged over the whole volume, i.e.,

$$\sigma_{ij}^{\mathrm{f}} = -\phi_{\mathrm{f}}\, p\delta_{ij}, \tag{5.32}$$

where ϕ_{f} is the volume fraction of the fluid phase, δ_{ij} is the Kroneker delta.

At the same time, the stresses in the solid matrix are determined in terms of the effective stresses, σ_{ij}^{e}, as

$$\sigma_{ij}^{\mathrm{s}} = -\phi_{\mathrm{s}}\, p\delta_{ij} + \sigma_{ij}^{\mathrm{e}}, \tag{5.33}$$

where $\phi_{\mathrm{s}} = 1 - \phi_{\mathrm{f}}$ is the volume fraction of the solid phase.

From (5.31)–(5.33), it follows that the total stresses in the biphasic tissue can be decomposed as

$$\sigma_{ij} = -p\delta_{ij} + \sigma_{ij}^{\mathrm{e}}. \tag{5.34}$$

It should be emphasized that, since both the fluid and the material forming the skeleton are assumed to be incompressible, the strains in the biphasic tissue are due to the effective stresses. Thus, the strains in the tissue are given by

$$\begin{aligned}
\varepsilon_{11} &= \frac{1}{E_1^{\mathrm{s}}}(\sigma_{11}^{\mathrm{e}} - \nu_{12}^{\mathrm{s}}\sigma_{22}^{\mathrm{e}}) - \frac{\nu_{31}^{\mathrm{s}}}{E_3^{\mathrm{s}}}\sigma_{33}^{\mathrm{e}}, & \varepsilon_{23} &= \frac{1}{2G_{13}^{\mathrm{s}}}\sigma_{23}^{\mathrm{e}},\\
\varepsilon_{22} &= \frac{1}{E_1^{\mathrm{s}}}(-\nu_{12}^{\mathrm{s}}\sigma_{11}^{\mathrm{e}} + \sigma_{22}^{\mathrm{e}}) - \frac{\nu_{31}^{\mathrm{s}}}{E_3^{\mathrm{s}}}\sigma_{33}^{\mathrm{e}}, & \varepsilon_{13} &= \frac{1}{2G_{13}^{\mathrm{s}}}\sigma_{13}^{\mathrm{e}},\\
\varepsilon_{33} &= -\frac{\nu_{31}^{\mathrm{s}}}{E_3^{\mathrm{s}}}(\sigma_{11}^{\mathrm{e}} + \sigma_{22}^{\mathrm{e}}) + \frac{1}{E_3^{\mathrm{s}}}\sigma_{33}^{\mathrm{e}}, & \varepsilon_{12} &= \frac{1}{2G_{12}^{\mathrm{s}}}\sigma_{12}^{\mathrm{e}},
\end{aligned} \tag{5.35}$$

where E_1^{s} and E_3^{s} are Young's moduli of the solid matrix in the plane of transverse isotropy and in the orthogonal direction, respectively, ν_{12}^{s} and ν_{31}^{s} are Poisson's ratios characterizing the lateral strain response in the plane of transverse isotropy to a stress acting parallel or normal to it, respectively, G_{13}^{s} is the shear modulus in planes normal to the plane of transverse isotropy, and $G_{12}^{\mathrm{s}} = E_1^{\mathrm{s}}/[2(1+\nu_{12}^{\mathrm{s}})]$ is the in-plane shear modulus.

For a transversely isotropic material, the incompressibility condition is attained if its Poisson's ratios are as follows [29, 39]:

$$\nu_{31} = \frac{1}{2}, \quad \nu_{12} = 1 - \frac{E_1}{2E_3}. \tag{5.36}$$

Let the three independent constants of the equivalent incompressible elastic material be denoted by E_1, E_3, and G_{13}, while its Poisson's ratios are given by (5.36).

Observe [7] that upon sudden loading of a biphasic tissue, the interstitial fluid does not have sufficient time to leave the tissue, except at permeable boundaries. At time $t = 0^+$, the matrix pores change shape but not volume. Thus, it is assumed [29] that the general stress field in a transversely isotropic biphasic material at time zero can be decomposed into the pressure in the fluid and the effective stresses in the solid skeleton according to Eq. (5.34), in such a way that the fluid pressure at time zero is

$$p = -\alpha\sigma_{kk}. \tag{5.37}$$

Here, $\sigma_{kk} = \sigma_{11} + \sigma_{22} + \sigma_{33}$ is the trace of the total stress tensor, and α is a dimensionless parameter, to be determined.

Thus, on one hand, the deformation of a biphasic material at time zero is given by Eq. (5.35), where in light of the hypothesis (5.37) we have

$$\sigma_{ij}^{\mathrm{e}} = \sigma_{ij} - \alpha\sigma_{kk}\delta_{ij}. \tag{5.38}$$

On the other hand, the same deformation must be equal to the deformation of the equivalent incompressible tissue under the total stress field σ_{ij}. This means, first, that the shear moduli G_{12}^{s} and G_{13}^{s} should be the same for the solid skeleton and the equivalent incompressible elastic material, and in particular,

$$G_{13} = G_{13}^{\mathrm{s}}, \tag{5.39}$$

since the inviscid interstitial fluid sustains only pressure.

Therefore, applying the decomposition (5.38) to normal stresses, one arrives at a homogeneous system of linear algebraic equations with respect to σ_{11}, σ_{22}, and σ_{33}, with the coefficients depending on E_1, E_3, and α. As was shown in [29], this system is satisfied for any combination of the normal stresses, if the equivalent elastic moduli are given by

$$\begin{aligned} E_1 &= \frac{E_1^{\mathrm{s}}\left[1-4\nu_{31}^{\mathrm{s}}+2(1-\nu_{12}^{\mathrm{s}})(E_3^{\mathrm{s}}/E_1^{\mathrm{s}})\right]}{1+\left(1-\nu_{12}^{\mathrm{s}2}\right)(E_3^{\mathrm{s}}/E_1^{\mathrm{s}})-2\nu_{31}^{\mathrm{s}}(1+\nu_{12}^{\mathrm{s}})-\nu_{31}^{\mathrm{s}2}(E_1^{\mathrm{s}}/E_3^{\mathrm{s}})}, \\ E_3 &= \frac{E_3^{\mathrm{s}}\left[1-4\nu_{31}^{\mathrm{s}}+2(1-\nu_{12}^{\mathrm{s}})(E_3^{\mathrm{s}}/E_1^{\mathrm{s}})\right]}{2(1-\nu_{12}^{\mathrm{s}})(E_3^{\mathrm{s}}/E_1^{\mathrm{s}})-4\nu_{31}^{\mathrm{s}2}}. \end{aligned} \tag{5.40}$$

Note that the corresponding decomposition parameter α depends on the applied stresses σ_{11}, σ_{22}, and σ_{33}.

Thus, the instantaneous response of any transversely isotropic biphasic tissue is equivalent to that of an incompressible transversely isotropic elastic material with the material constants ν_{12}, ν_{31}, G_{13}, E_1, and E_3, given by (5.36), (5.39), and (5.40).

We note that in the isotropic case, the equivalent elastic material will also be isotropic, with Poisson's ratio $\nu = 0.5$ and the shear modulus $G = G_{\mathrm{s}}$, where G_{s} is the shear modulus of the elastic skeleton. As a consequence of the relations $E_1^{\mathrm{s}} = E_3^{\mathrm{s}} = 2(1+\nu_{\mathrm{s}})G_{\mathrm{s}}$ and $\nu_{12}^{\mathrm{s}} = \nu_{31}^{\mathrm{s}} = \nu_{\mathrm{s}}$, Eq. (5.40) yield the same result $E_1 = E_3 = 3G_{\mathrm{s}}$, irrespective of the value of the Poisson's ratio ν_{s} of the skeleton.

Note also that if the elastic constants of the elastic skeleton satisfy the incompressibility condition (5.36), then Eq. (5.40) give $E_1 = E_1^{\mathrm{s}}$ and $E_3 = E_3^{\mathrm{s}}$, respectively, when successively taking the limits $\nu_{31}^{\mathrm{s}} \to 0.5$ (with ν_{12}^{s} fixed) and after that as $\nu_{12}^{\mathrm{s}} \to 1 - E_1^{\mathrm{s}}/(2E_3^{\mathrm{s}})$, and vice-versa.

5.1.4 Axisymmetric Biphasic Model

Let us consider a biphasic material with the axis of symmetry oriented along the z axis of an (r, θ, z) cylindrical coordinate system. The constitutive equations (5.13) for the effective stresses of the solid matrix are as follows:

$$\begin{aligned} \sigma_{rr}^{\mathrm{e}} &= A_{11}^{\mathrm{s}}\varepsilon_{rr} + A_{12}^{\mathrm{s}}\varepsilon_{\theta\theta} + A_{13}^{\mathrm{s}}\varepsilon_{zz}, \\ \sigma_{\theta\theta}^{\mathrm{e}} &= A_{12}^{\mathrm{s}}\varepsilon_{rr} + A_{11}^{\mathrm{s}}\varepsilon_{\theta\theta} + A_{13}^{\mathrm{s}}\varepsilon_{zz}, \\ \sigma_{zz}^{\mathrm{e}} &= A_{13}^{\mathrm{s}}\varepsilon_{rr} + A_{13}^{\mathrm{s}}\varepsilon_{\theta\theta} + A_{33}^{\mathrm{s}}\varepsilon_{zz}, \\ \sigma_{rz}^{\mathrm{e}} &= 2A_{44}^{\mathrm{s}}\varepsilon_{rz}. \end{aligned} \tag{5.41}$$

The strain-displacement relations (5.11) become

$$\varepsilon_{rr} = \frac{\partial u_r}{\partial r}, \quad \varepsilon_{\theta\theta} = \frac{u_r}{r}, \quad \varepsilon_{zz} = \frac{\partial u_z}{\partial z}, \quad \varepsilon_{rz} = \frac{1}{2}\Big(\frac{\partial u_r}{\partial z} + \frac{\partial u_z}{\partial r}\Big), \tag{5.42}$$

where u_r and u_z denote the radial and axial displacements.

The equilibrium equations (5.10), which are written with respect to the total stress

$$\boldsymbol{\sigma} = -p\mathbf{I} + \boldsymbol{\sigma}^{\mathrm{e}},$$

now reduce to the following equations of equilibrium:

$$\begin{aligned} -\frac{\partial p}{\partial r} + \frac{1}{r}\frac{\partial (r\sigma^{\mathrm{e}}_{rr})}{\partial r} - \frac{\sigma^{\mathrm{e}}_{\theta\theta}}{r} + \frac{\partial \sigma^{\mathrm{e}}_{rz}}{\partial z} = 0, \\ -\frac{\partial p}{\partial z} + \frac{1}{r}\frac{\partial (r\sigma^{\mathrm{e}}_{rz})}{\partial r} + \frac{\partial \sigma^{\mathrm{e}}_{zz}}{\partial z} = 0. \end{aligned} \tag{5.43}$$

Correspondingly, Eq. (5.19) takes the form

$$\frac{\partial}{\partial t}\left(\frac{\partial u_r}{\partial r} + \frac{u_r}{r} + \frac{\partial u_z}{\partial z}\right) = \frac{1}{r}\frac{\partial}{\partial r}\Big(rk_1\frac{\partial p}{\partial r}\Big) + \frac{\partial}{\partial z}\Big(k_3\frac{\partial p}{\partial z}\Big), \tag{5.44}$$

where k_1 and k_3 are the in-plane and out-of-plane permeability coefficients, while the relative fluid flux can be expressed as

$$\mathbf{w}^{\mathrm{f}} = -k_1\frac{\partial p}{\partial r}\mathbf{e}_r - k_3\frac{\partial p}{\partial z}\mathbf{e}_z, \tag{5.45}$$

with the radial and axial unit coordinate vectors $\mathbf{e}_r$ and $\mathbf{e}_z$, respectively.

5.2 Confined Compression of a Biphasic Material

In this section, we outline a linear confined compression biphasic model. In particular, the biphasic stress relaxation and the biphasic creep tests in confined compression are considered.

5.2.1 Confined Compression Problem

In the confined compression test, a cylindrical plug of biphasic material is constrained in a confining chamber with impermeable rigid walls, and is subjected to a compressive load, $F(t)$, via a porous loading plate (see Fig. 5.1). Observe that the non-linear confined compression problem has been considered in a number of publications [8, 9, 62].

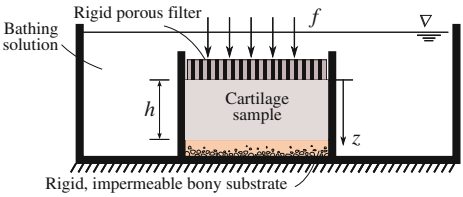

Fig. 5.1 Schematic of the confined compression configuration [52]

In the cylindrical coordinate system, the boundary conditions on the lateral surface are

$$w_r^{\mathrm{f}}\big|_{r=a} = 0, \quad \sigma_{rz}\big|_{r=a} = \sigma_{r\theta}\big|_{r=a} = 0, \quad u_r\big|_{r=a} = 0, \tag{5.46}$$

where w_r^{f} is the transverse (in-plane) relative fluid flux, σ_{rz} and $\sigma_{r\theta}$ are out-of-plane and in-plane total shear stresses, and u_r is the radial displacement of the solid matrix.

The boundary conditions at the bottom surface, $z = h$, are as follows:

$$w_z^{\mathrm{f}}\big|_{z=h} = 0, \quad \sigma_{zr}\big|_{z=h} = \sigma_{z\theta}\big|_{z=h} = 0. \quad u_z\big|_{z=h} = 0, \tag{5.47}$$

Here, w_z^{f} and u_z are the vertical relative fluid flux and the vertical displacement of the solid matrix, respectively.

Meanwhile, the boundary conditions at the top surface, $z = 0$, have the form

$$p\big|_{z=0} = 0, \quad \sigma_{zr}\big|_{z=0} = \sigma_{z\theta}\big|_{z=0} = 0, \tag{5.48}$$

where p is the interstitial fluid pressure.

Observe that the boundary condition $(5.48)_1$ describes the free-draining porous interface, where no resistance to fluid movement is assumed at the interface between the porous loading plate and the sample surface.

For the stress relaxation test, the additional boundary condition at the top is

$$u_z\big|_{z=0} = w(t), \tag{5.49}$$

where $w(t)$ is a specified displacement of the loading plate.

For example, the ramp displacement is defined as

$$w(t) = \begin{cases} V_0 t, & 0 \le t \le t_0, \\ V_0 t_0, & t_0 \le t, \end{cases} \tag{5.50}$$

and V_0, t_0 are given constants.

On the other hand, for creep, the boundary condition is

$$\sigma_{zz}\big|_{z=0} = -\frac{F(t)}{A}, \tag{5.51}$$

where $F(t)$ is a specified external load acting on the porous loading plate, and $A = \pi a^2$ is the sample cross-sectional area.

For example, if the load is applied instantaneously, then

$$F(t) = F_0 \mathscr{H}(t), \tag{5.52}$$

where $\mathscr{H}(t)$ is the Heaviside step function.

The experimental setup of the confined compression test for articular cartilage represents a one-dimensional problem in the axial direction, so that

$$u_r = u_\theta = 0, \quad \varepsilon_{rr} = \varepsilon_{\theta\theta} = 0, \quad w_r^{\mathrm{f}} = w_\theta^{\mathrm{f}} = 0, \tag{5.53}$$

while all non-trivial variables are dependent on t and z only.

Note that the assumptions $(5.53)_1$ and $(5.53)_2$ dictate that the rigid confining chamber prevents any lateral deformation. Therefore, the axial total stress is

$$\sigma_{zz} = -p + H_A \varepsilon_{zz}, \tag{5.54}$$

where H_A is the confined compression equilibrium modulus (aggregate elastic modulus) of the solid matrix given by

$$H_A = A_{33}^{\mathrm{s}}. \tag{5.55}$$

Hence, taking into account the free-draining condition $(5.48)_1$, the traction boundary condition (5.51) can be reduced to the following:

$$H_A \frac{\partial u_z}{\partial z}\Big|_{z=0} = -f(t). \tag{5.56}$$

Here, $f(t)$ is the applied compressive stress, i.e.,

$$f(t) = \frac{F(t)}{A}. \tag{5.57}$$

Finally, to complete the confined compression problem formulation, we assume the usual initial conditions (5.30).

5.2.2 Governing Equation of the Confined Compression Model

Under the assumptions made in the confined compression model, the only equilibrium differential equation $(5.43)_2$ takes the form

$$-\frac{\partial p}{\partial z}+\frac{\partial \sigma_{zz}^{\mathrm{e}}}{\partial z}=0, \tag{5.58}$$

where, in light of (5.53) and (5.54), we have

$$\sigma_{zz}^{\mathrm{e}}=H_A\varepsilon_{zz}. \tag{5.59}$$

Integrating Eq. (5.59) with respect to the coordinate z, we arrive at the equation

$$-p+\sigma_{zz}^{\mathrm{e}}=\sigma_{zz}(t). \tag{5.60}$$

Here, $\sigma_{zz}(t)$ is the integration constant (being a function of the time variable t only).

Now, comparing Eqs. (5.54) and (5.60), we find that the total normal stress, $\sigma_{zz}(t)$, is uniform through the depth of the biphasic sample.

Further, since all non-trivial variables are dependent on t and z only, the equilibrium equation (5.44) for the fluid phase after integration with respect to the coordinate z reduces to

$$\frac{\partial u_z}{\partial t}=k_3\frac{\partial p}{\partial z}, \tag{5.61}$$

where k_3 is the axial permeability coefficient.

Now, collecting Eqs. (5.59)–(5.61), we arrive at the governing equation

$$\frac{\partial u_z}{\partial t}=k_3\frac{\partial}{\partial z}\left(H_A\frac{\partial u_z}{\partial z}\right), \tag{5.62}$$

which for a homogeneous biphasic material simplifies to a Fourier equation

$$\frac{\partial u_z}{\partial t}=k_3H_A\frac{\partial^2 u_z}{\partial z^2}. \tag{5.63}$$

Equation (5.63) is supplemented by the homogeneous initial condition

$$u_z(0,z)=0$$

and the boundary condition at the bottom surface

$$u_z(t,h)=0.$$

For stress relaxation, the general boundary condition at the top surface is

$$u_z(t,0)=w(t), \tag{5.64}$$

where $w(t)$ is the prescribed surface displacement as a function of time, while for creep, in light of (5.56), we have

$$\frac{\partial u_z}{\partial z}(t,0) = -\frac{f(t)}{H_A}, \tag{5.65}$$

where $f(t)$ is the prescribed compressive stress as a function of time.

Note that the second-order parabolic partial differential equation (5.62) was solved in [26] using a semi-analytical approach based on the finite difference and Laplace transform methods. The effect of the depth-dependent aggregate modulus on articular cartilage stress-relaxation in confined compression was studied in [75].

5.2.3 Biphasic Stress Relaxation in Confined Compression

The following formula [64] gives the general solution to the problem (5.63) and (5.64):

$$u_z(t,z) = w(t)\left(1-\frac{z}{h}\right) - \sum_{n=1}^{\infty} \frac{2}{\pi n} \sin\left(\pi n \frac{z}{h}\right)\left(\mathscr{K}_n w\right)(t). \tag{5.66}$$

Here we have introduced the notation

$$\left(\mathscr{K}_n w\right)(t) = \int_{0^-}^{t} \exp\left(-\frac{n^2(t-\tau)}{\tau_R'}\right)\dot{w}(\tau)\,d\tau, \tag{5.67}$$

where τ_R' is the characteristic relaxation time in confined compression defined by

$$\tau_R' = \frac{h^2}{\pi^2 k_3 H_A}. \tag{5.68}$$

Recall that the lower integration limit 0^- in the integral operator above indicates that the integration in (5.67) starts at infinitesimally negative time so as to include the displacement discontinuity at time zero.

The strain of the solid matrix can be simply obtained from the relationship

$$\varepsilon_{zz} = \frac{\partial u_z}{\partial z}.$$

Then according to Eq. (5.60), we have

$$p = H_A \varepsilon_{zz} - \sigma_{zz}(t), \tag{5.69}$$

from which we can determine the total normal stress, in light of the free-draining boundary condition $(5.48)_1$, as follows:

$$\sigma_{zz}(t) = H_A \varepsilon_{zz}\big|_{z=0}.$$

The interstitial hydrostatic pressure can be expressed in the form

$$p(t,z) = \frac{2H_A}{h}\sum_{n=1}^{\infty}\Big[1-\cos\Big(\pi n\frac{z}{h}\Big)\Big]\big(\mathscr{K}_n w\big)(t). \tag{5.70}$$

The corresponding stress relaxation response in confined compression is then given by

$$\sigma_{zz}(t) = -H_A\frac{w(t)}{h} - \frac{2H_A}{h}\sum_{n=1}^{\infty}\big(\mathscr{K}_n w\big)(t). \tag{5.71}$$

In the case of constant strain rate compression in the loading phase $t \in (0, t_0)$, followed by the hold period $t \in (t_0, +\infty)$, formula (5.50) yields

$$\dot{w}(t) = \begin{cases} V_0, & 0 \le t \le t_0, \\ 0, & t_0 \le t. \end{cases}$$

Therefore, in the case of ramp displacement (5.50), the integral (5.67), which appears on the right-hand sides of (5.66), (5.70), and (5.71), is evaluated as

$$\begin{aligned} \big(\mathscr{K}_n w\big)(t) &= \frac{V_0\tau_R'}{n^2}\Big(1-\exp\Big(-\frac{n^2 t}{\tau_R'}\Big)\Big), \quad 0 \le t < t_0, \\ \big(\mathscr{K}_n w\big)(t) &= \frac{V_0\tau_R'}{n^2}\exp\Big(-\frac{n^2 t}{\tau_R'}\Big)\Big(\exp\Big(\frac{n^2 t_0}{\tau_R'}\Big)-1\Big), \quad t_0 \le t. \end{aligned}$$

Now, taking into account the above formulas and the identity

$$\sum_{n=1}^{\infty}\frac{1}{n^2} = \frac{\pi^2}{6},$$

we arrive at the following formulas [60]:

$$\sigma_{zz}(t) = -H_A\frac{V_0 t}{h} - \frac{V_0 h}{3k_3} + \frac{2V_0 h}{\pi^2 k_3}\sum_{n=1}^{\infty}\frac{1}{n^2}\exp\Big(-\frac{n^2 t}{\tau_R'}\Big) \tag{5.72}$$

for $0 \le t < t_0$, and

$$\sigma_{zz}(t) = -H_A\frac{V_0 t_0}{h} + \frac{2V_0 h}{\pi^2 k_3}\sum_{n=1}^{\infty}\frac{1}{n^2}\left\{\exp\Big(-\frac{n^2 t}{\tau_R'}\Big) - \exp\Big(-\frac{n^2(t-t_0)}{\tau_R'}\Big)\right\} \tag{5.73}$$

for $t \ge t_0$.

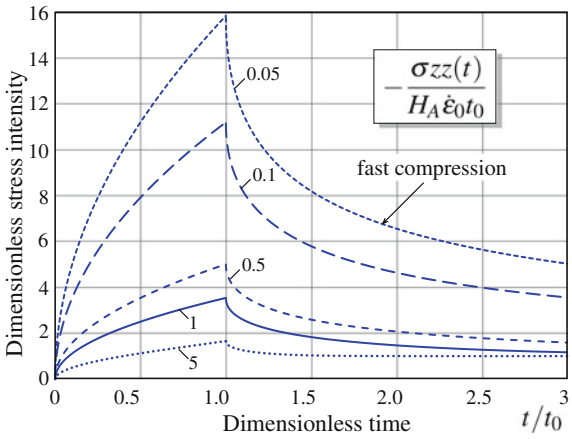

Fig. 5.2 The effect of t_0/τ_R' on the stress-relaxation time history in response to a ramped displacement. (The values taken by t_0/τ_R' are indicated on the figure.) Note the limit value 1 as $t \to \infty$ in all cases due to the normalization

According to Eqs. (5.72) and (5.73), the effect of t_0/τ_R' on the dimensionless stress-relaxation time history $-\sigma_{zz}(t)/[H_A \dot{\varepsilon}_0 t_0]$, where $\dot{\varepsilon}_0 = V_0/h$, is shown in Fig. 5.2.

Equations (5.72) and (5.73) can be used for determining the aggregate modulus, H_A, and the constant axial permeability coefficient, k_3, from the stress relaxation experiment by fitting the theoretical solution on to the experimental curve for the measured total normal stress [69].

5.2.4 Biphasic Creep in Confined Compression

The following formula [64] gives the general solution to the problem (5.63) and (5.65):

$$u_z(t,z) = \frac{2k_3}{h} \sum_{n=1}^{\infty} \cos\left(\frac{\pi(2n-1)z}{2h}\right) \left(\mathcal{N}_n f\right)(t). \tag{5.74}$$

Here we have introduced the notation

$$\left(\mathcal{N}_n f\right)(t) = \int_0^t \exp\left(-(2n-1)^2 \frac{(t-\tau)}{\tau_R''}\right) f(\tau)\, d\tau, \tag{5.75}$$

where τ_R' is the characteristic time having the meaning of a retardation time in confined compression defined as

$$\tau_R'' = \frac{4h^2}{\pi^2 k_3 H_A}. \tag{5.76}$$

Thus, the nominal sample-average strain (surface-to-surface strain), which is calculated from the distance $h - u_z(t,0)$ between the loading platens, is

$$\frac{u_z(t,0)}{h} = \frac{2k_3}{h^2}\sum_{n=1}^{\infty}\big(\mathscr{N}_n f\big)(t). \tag{5.77}$$

Taking into account the constitutive equation (5.60) and the boundary conditions $(5.48)_1$ and (5.56), we find that the total normal stress in the biphasic sample is

$$\sigma_{zz}(t) = -f(t).$$

Hence, Eq. (5.69) allows evaluation of the interstitial hydrostatic pressure via

$$p = H_A\varepsilon_{zz} + f(t). \tag{5.78}$$

Evaluating the strain of the solid matrix according to formula (5.74) and substituting the obtained result into Eq. (5.78), we find

$$p(t,z) = f(t) - \frac{\pi k_3 H_A}{h^2}\sum_{n=1}^{\infty}(2n-1)\sin\Big(\frac{\pi(2n-1)z}{2h}\Big)\big(\mathscr{N}_n f\big)(t). \tag{5.79}$$

For a creep experiment, where a constant external load, F_0, is applied instantaneously, the following loading law holds true (see Eq. (5.57)):

$$f(t) = f_0\mathscr{H}(t). \tag{5.80}$$

Here, $\mathscr{H}(t)$ is the Heaviside step function, $f_0 = F_0/A$ is the constant compressive stress, and A is the cross-sectional area of the biphasic sample.

Correspondingly, formula (5.77) yields the following result [14]:

$$\frac{u_z(t,0)}{h} = \frac{f_0}{H_A}\left\{1 - \frac{8}{\pi^2}\sum_{n=1}^{\infty}\frac{1}{(2n-1)^2}\exp\Big(-(2n-1)^2\frac{t}{\tau_R''}\Big)\right\}. \tag{5.81}$$

Note that in writing (5.81), we used the identity

$$\sum_{n=1}^{\infty}\frac{1}{(2n-1)^2} = \frac{\pi^2}{8}.$$

In the same way, in the case (5.80), formula (5.79) is rearranged to obtain

$$p(t,z) = \frac{4f_0}{\pi}\sum_{n=1}^{\infty}\frac{1}{2n-1}\sin\Big(\frac{\pi(2n-1)z}{2h}\Big)\exp\Big(-(2n-1)^2\frac{t}{\tau_R''}\Big). \tag{5.82}$$

In writing (5.82), the following identity was used (see, e.g., [30], formula (1.442.1)):

$$\sum_{n=1}^{\infty} \frac{\sin(2n-1)\zeta}{2n-1} = \frac{\pi}{4}, \quad 0 < \zeta < \pi. \tag{5.83}$$

By substituting $z = h$ into Eq. (5.82), we readily obtain

$$p(t,h) = \frac{4f_0}{\pi} \sum_{k=0}^{\infty} \frac{(-1)^k}{2k+1} \exp\left(-(2k+1)^2 \frac{t}{\tau_R''}\right). \tag{5.84}$$

Note also [69] that the interstitial fluid pressure at the impermeable interface, $z = h$, can be represented by the formula

$$p(t,h) = H_A\left(\varepsilon_{zz}\big|_{z=h} - \varepsilon_{zz}\big|_{z=0}\right),$$

where ε_{zz} is the strain of the solid matrix, $\varepsilon_{zz} = \partial u_z/\partial z$, while the displacement u_z is taken from (5.74) for creep and from (5.66) for stress relaxation.

Correspondingly, the so-called fluid load support

$$\frac{W^p}{W} = \frac{p(t,h)}{f(t)}$$

is evaluated as follows [63]:

$$\frac{W^p}{W} = \left(\frac{\partial u}{\partial z}\Big|_{z=0} - \frac{\partial u}{\partial z}\Big|_{z=h}\right) \Big/ \frac{\partial u}{\partial z}\Big|_{z=0}.$$

In the stepwise creep test, according to (5.80) and (5.84), we have

$$\frac{W^p}{W} = \frac{4}{\pi} \sum_{k=0}^{\infty} \frac{(-1)^k}{2k+1} \exp\left(-(2k+1)^2 \frac{t}{\tau_R''}\right).$$

Therefore, as a consequence of (5.83), the above formula yields the maximum value

$$\frac{W^p}{W}\Big|_{t=0} = 1.$$

It should be noted [63] that in real creep testing configurations, there exists a delay in pressurization due to the impedance of the pressure transducer in measuring the pressure $p(t,h)$. Namely, the greater the compliance of the pressure transducer, the greater the delay in the interstitial fluid pressurization achieving the peak value of W^p/W.

Equation (5.81) is commonly used in determining the aggregate modulus, H_A, and the constant axial permeability coefficient, k_3, from the confined compression creep experiment by fitting the theoretical solution on to the experimental curve for the nominal sample-average strain. It should be mentioned that for improved mechanical characterization of articular cartilage, testing experiments may involve multiple-step ramp loading [50] as well as an alternating sequence of stress relaxation and creep transients [17].

Finally, observe [13] that the presence of a gap between the loading plate and the confining chamber walls, which is necessary to guarantee a correct plate movement, allows flow exudation and tissue extrusion around the plate, thus leading to underestimation of H_A and overestimation of k_3.

5.2.5 *Dynamic Behavior of a Biphasic Material Under Cyclic Compressive Loading in Confined Compression*

Let us now consider the following loading history for cyclic compressive confined compression [70, 73]:

$$f(t) = f_0(1 - \cos \omega t)\mathscr{H}(t). \tag{5.85}$$

Here, f_0 is the median magnitude of the applied cyclic stress, and ω is the loading angular frequency. Recall that $\omega/(2\pi)$ is the loading frequency measured in hertz.

First of all, using integration by parts and the identity (see, e.g., [30], formula (1.444.6))

$$\sum_{n=1}^{\infty} \frac{\cos(2n-1)\zeta}{(2n-1)^2} = \frac{\pi}{4}\Big(\frac{\pi}{2} - \zeta\Big), \quad 0 < \zeta < \pi,$$

we transform formulas (5.74) and (5.79) as follows:

$$u_z(t,z) = \frac{h}{H_A}\Big\{ f(t)\Big(1 - \frac{z}{h}\Big) - \frac{8}{\pi^2}\sum_{n=1}^{\infty} \frac{1}{(2n-1)^2} \cos\Big(\frac{\pi(2n-1)z}{2h}\Big)\big(\mathscr{M}_n f\big)(t)\Big\}, \tag{5.86}$$

$$p(t,z) = \frac{4}{\pi}\sum_{n=1}^{\infty} \frac{1}{2n-1} \sin\Big(\frac{\pi(2n-1)z}{2h}\Big)\big(\mathscr{M}_n f\big)(t). \tag{5.87}$$

Here we have introduced the notation

$$\big(\mathscr{M}_n f\big)(t) = \int_{0^-}^{t} \exp\Big(-(2n-1)^2 \frac{(t-\tau)}{\tau_R''}\Big) \dot{f}(\tau)\, d\tau. \tag{5.88}$$

As usual, the notation 0^- in the lower limit of the integral above means that

$$\int_{0^-}^{t} e^{-a_n(t-\tau)}\dot{f}(\tau)\,d\tau = f(0^+)e^{-a_n t} + \int_{0}^{t} e^{-a_n(t-\tau)}\dot{f}(\tau)\,d\tau,$$

where $f(0^+)$ is the limit of the function $f(t)$ when the independent variable t approaches 0 from the right.

Since $f(0) = 0$ for the function defined by formula (5.85), we have

$$\dot{f}(\tau) = \omega f_0 \mathscr{H}(t)\sin\omega t,$$

so that Eqs. (5.86) and (5.87) yield

$$\begin{aligned} u_z(t,z) = \frac{f_0 h}{H_A}\Bigg\{ & (1-\cos\omega t)\Big(1-\frac{z}{h}\Big) \\ & - \frac{8}{\pi^2}\sin\omega t \sum_{n=1}^{\infty} \frac{\omega a_n}{(2n-1)^2(a_n^2+\omega^2)} \cos\Big(\frac{\pi(2n-1)z}{2h}\Big) \\ & + \frac{8}{\pi^2}\cos\omega t \sum_{n=1}^{\infty} \frac{\omega^2}{(2n-1)^2(a_n^2+\omega^2)} \cos\Big(\frac{\pi(2n-1)z}{2h}\Big) \\ & - \frac{8}{\pi^2}\sum_{n=1}^{\infty} \frac{\omega^2}{(2n-1)^2(a_n^2+\omega^2)} \exp(-a_n t)\cos\Big(\frac{\pi(2n-1)z}{2h}\Big)\Bigg\} \end{aligned} \tag{5.89}$$

for the vertical displacement of the solid matrix and

$$\begin{aligned} p(t,z) = \frac{4f_0}{\pi}\Bigg\{ & \sin\omega t \sum_{n=1}^{\infty} \frac{\omega a_n}{(2n-1)(a_n^2+\omega^2)} \sin\Big(\frac{\pi(2n-1)z}{2h}\Big) \\ & - \cos\omega t \sum_{n=1}^{\infty} \frac{\omega^2}{(2n-1)(a_n^2+\omega^2)} \sin\Big(\frac{\pi(2n-1)z}{2h}\Big) \\ & + \sum_{n=1}^{\infty} \frac{\omega^2}{(2n-1)(a_n^2+\omega^2)} \exp(-a_n t)\sin\Big(\frac{\pi(2n-1)z}{2h}\Big)\Bigg\} \end{aligned} \tag{5.90}$$

for the interstitial fluid pressure, where we have introduced the notation

$$a_n = \frac{(2n-1)^2}{\tau_R''}.$$

It can be checked that Eqs. (5.89) and (5.90) coincide with the corresponding results obtained by Suh et al. [73], apart from notation.

5.3 Unconfined Compression of a Biphasic Material

In this section, the unconfined compression biphasic model is developed. In particular, the biphasic stress relaxation and the biphasic creep tests in unconfined compression are studied.

5.3.1 Unconfined Compression Problem

In the axisymmetric unconfined compression test, a thin cylindrical disk of biphasic material is compressed between two smooth (frictionless) and impermeable rigid platens (see Fig. 5.3). Therefore, the material is free to expand radially, and free fluid flow is enabled across the lateral cylindrical surface.

In the cylindrical coordinate system, the boundary conditions on the lateral surface are

$$p\big|_{r=a} = 0, \quad \sigma_{rz}\big|_{r=a} = \sigma_{r\theta}\big|_{r=a} = \sigma_{rr}\big|_{r=a} = 0. \tag{5.91}$$

Here, p is the interstitial fluid pressure, σ_{rz} and $\sigma_{r\theta}$ are shear stresses, σ_{rr} is the radial normal stress.

The boundary conditions at the bottom surface, $z = h$, are

$$w_z^{\mathrm{f}}\big|_{z=h} = 0, \quad \sigma_{zr}\big|_{z=h} = \sigma_{z\theta}\big|_{z=h} = 0, \quad u_z\big|_{z=h} = 0, \tag{5.92}$$

where w_z^{f} and u_z are the vertical relative fluid flux and the vertical displacement of the solid matrix, respectively.

At the top surface, $z = 0$, we have the following boundary conditions:

$$w_z^{\mathrm{f}}\big|_{z=0} = 0, \quad \sigma_{zr}\big|_{z=0} = \sigma_{z\theta}\big|_{z=0} = 0, \quad u_z\big|_{z=0} = w(t). \tag{5.93}$$

Here, $w(t)$ is the vertical displacement of the upper platen.

Again, we can consider either the creep test (load-controlled) or the stress-relaxation test (displacement-controlled) in unconfined compression. For the stress-relaxation experiment, $w(t)$ is a prescribed function of time.

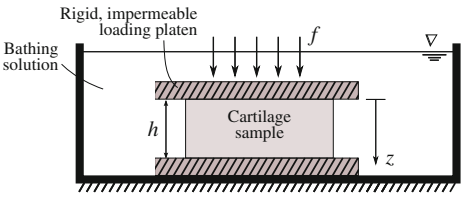

Fig. 5.3 Schematic of the unconfined compression configuration [52]. The articular cartilage sample has to be stripped off from the subchondral bone and cut into a perfect cylinder

Following Armstrong et al. [5] and Cohen et al. [19], we assume the radial displacement of the solid skeleton, u_r, the fluid relative radial velocity, w_r^{f}, and the fluid pressure, p, to be of the form

$$u_r = u_r(t, r), \quad w_r^{\mathrm{f}} = w_r^{\mathrm{f}}(t, r), \quad p = p(t, r). \tag{5.94}$$

Moreover, the axial strain, ε_{zz}, is assumed to be uniform throughout the sample, i.e.,

$$\varepsilon_{zz} = \varepsilon(t), \tag{5.95}$$

where $\varepsilon(t)$ is a time-dependent function.

Hence, in light of the assumption (5.95), the integration of the equation

$$\varepsilon_{zz} = \frac{\partial u_z}{\partial z}$$

with the boundary conditions $(5.92)_3$ and $(5.93)_3$ taken into account yields

$$\varepsilon(t) = -\frac{w(t)}{h}, \tag{5.96}$$

$$u_z(t, z) = -\varepsilon(t)(h - z). \tag{5.97}$$

According to (5.94), (5.95), and (5.97), the only nonzero strain components are

$$\varepsilon_{rr} = \frac{\partial u_r}{\partial r}, \quad \varepsilon_{\theta\theta} = \frac{u_r}{r}, \quad \varepsilon_{zz} = \varepsilon,$$

and, correspondingly, Eq. (5.41) yield the following nonzero effective stresses:

$$\begin{aligned}
\sigma_{rr}^{\mathrm{e}} &= A_{11}^{\mathrm{s}} \frac{\partial u_r}{\partial r} + A_{12}^{\mathrm{s}} \frac{u_r}{r} + A_{13}^{\mathrm{s}} \varepsilon, \\
\sigma_{\theta\theta}^{\mathrm{e}} &= A_{12}^{\mathrm{s}} \frac{\partial u_r}{\partial r} + A_{11}^{\mathrm{s}} \frac{u_r}{r} + A_{13}^{\mathrm{s}} \varepsilon, \\
\sigma_{zz}^{\mathrm{e}} &= A_{13}^{\mathrm{s}} \frac{\partial u_r}{\partial r} + A_{13}^{\mathrm{s}} \frac{u_r}{r} + A_{33}^{\mathrm{s}} \varepsilon.
\end{aligned} \tag{5.98}$$

The substitution of (5.98) into the equilibrium equations for the solid matrix (5.43) results in the differential equation

$$-\frac{\partial p}{\partial r} + A_{11}^{\mathrm{s}} \left(\frac{\partial^2 u_r}{\partial r^2} + \frac{1}{r} \frac{\partial u_r}{\partial r} - \frac{u_r}{r^2} \right) = 0, \tag{5.99}$$

while Eq. (5.44) takes the form

$$\frac{\partial}{\partial t}\left(\frac{\partial u_r}{\partial r}+\frac{u_r}{r}+\varepsilon\right)=\frac{1}{r}\frac{\partial}{\partial r}\left(rk_1\frac{\partial p}{\partial r}\right), \tag{5.100}$$

where k_1 is the transverse (in-plane) permeability coefficient.

Finally, the relative fluid flux (5.45), in light of (5.94), is given by

$$\mathbf{w}^{\mathrm{f}}=-k_1\frac{\partial p}{\partial r}\mathbf{e}_r, \tag{5.101}$$

where $\mathbf{e}_r$ is the radial unit vector.

Equations (5.99)–(5.101), with the boundary conditions (5.91)–(5.93) and the zero initial conditions, constitute the unconfined compression problem.

It has been established [57] that the incorporation of a transverse isotropy for material properties into the linear biphasic theory improves its predictive power in unconfined compression analysis [19].

5.3.2 *Solution of the Unconfined Compression Problem*

Let us first turn to Eq. (5.100). Taking into account that

$$\frac{\partial u_r}{\partial r}+\frac{u_r}{r}=\frac{1}{r}\frac{\partial}{\partial r}(ru_r),$$

we can integrate Eq. (5.100) once with respect to the radial coordinate to get

$$\frac{\partial p}{\partial r}=\frac{1}{k_1}\frac{\partial}{\partial t}\left(u_r+\frac{\varepsilon}{2}r\right), \tag{5.102}$$

where the integration constant vanishes due to the regularity condition at the center of the sample, $r=0$.

Therefore, Eqs. (5.99) and (5.102) yield the following equation [19]:

$$\frac{\partial^2 u_r}{\partial r^2}+\frac{1}{r}\frac{\partial u_r}{\partial r}-\frac{u_r}{r^2}=\frac{1}{A^{\mathrm{s}}_{11}k_1}\frac{\partial}{\partial t}\left(u_r+\frac{\varepsilon}{2}r\right). \tag{5.103}$$

Recall that the boundary conditions $(5.91)_2$ are formulated in terms of the components of the total stress tensor

$$\boldsymbol{\sigma}=-p\mathbf{I}+\boldsymbol{\sigma}^{\mathrm{e}}. \tag{5.104}$$

Hence, as a consequence of the constitutive equation (5.98), the boundary conditions (5.91) become

$$p\big|_{r=a} = 0, \quad A^{\mathrm{s}}_{11}\frac{\partial u_r}{\partial r} + A^{\mathrm{s}}_{12}\frac{u_r}{r} + A^{\mathrm{s}}_{13}\varepsilon\,\Big|_{r=a} = 0. \tag{5.105}$$

To simplify our treatment of the problem, we introduce dimensionless variables

$$\rho = \frac{r}{a}, \quad U = \frac{u_r}{a}, \quad \tau = \frac{A^{\mathrm{s}}_{11}k_1}{a^2}t, \quad P = \frac{p}{A^{\mathrm{s}}_{11}}. \tag{5.106}$$

Then, Eqs. (5.102)–(5.105) take the form

$$\frac{\partial P}{\partial \rho} = \frac{\partial}{\partial \tau}\Big(U + \frac{\varepsilon}{2}\rho\Big), \tag{5.107}$$

$$\frac{\partial^2 U}{\partial \rho^2} + \frac{1}{\rho}\frac{\partial U}{\partial \rho} - \frac{U}{\rho^2} = \frac{\partial}{\partial \tau}\Big(U + \frac{\varepsilon}{2}\rho\Big), \tag{5.108}$$

$$P\big|_{\rho=1} = 0, \quad \frac{\partial U}{\partial \rho} + \alpha_{12}\frac{U}{\rho} + \alpha_{13}\varepsilon\,\Big|_{\rho=1} = 0, \tag{5.109}$$

where we have introduced the notation

$$\alpha_{12} = \frac{A^{\mathrm{s}}_{12}}{A^{\mathrm{s}}_{11}}, \quad \alpha_{13} = \frac{A^{\mathrm{s}}_{13}}{A^{\mathrm{s}}_{11}}. \tag{5.110}$$

Now, let $\tilde{P}(s)$, $\tilde{U}(s)$, and $\tilde{\varepsilon}(s)$ denote the Laplace transforms with respect to the dimensionless time τ. Taking into account the zero initial conditions, the Laplace transformation of Eqs. (5.107)–(5.109) leads to the system

$$\frac{\partial \tilde{P}}{\partial \rho} = s\Big(\tilde{U} + \frac{\tilde{\varepsilon}}{2}\rho\Big), \tag{5.111}$$

$$\frac{\partial^2 \tilde{U}}{\partial \rho^2} + \frac{1}{\rho}\frac{\partial \tilde{U}}{\partial \rho} - \frac{\tilde{U}}{\rho^2} = s\Big(\tilde{U} + \frac{\tilde{\varepsilon}}{2}\rho\Big), \tag{5.112}$$

$$\tilde{P}\big|_{\rho=1} = 0, \quad \frac{\partial \tilde{U}}{\partial \rho} + \alpha_{12}\frac{\tilde{U}}{\rho} + \alpha_{13}\tilde{\varepsilon}\,\Big|_{\rho=1} = 0. \tag{5.113}$$

The general solution of Eq. (5.112) can be represented in the form

$$\tilde{U} = -\frac{\tilde{\varepsilon}}{2}\rho + \tilde{U}_0, \tag{5.114}$$

where $\tilde{U}_0$ is the general solution of the homogeneous equation corresponding to Eq. (5.112), i.e.,

$$\frac{\partial^2 \tilde{U}_0}{\partial \rho^2} + \frac{1}{\rho}\frac{\partial \tilde{U}_0}{\partial \rho} - \left(s + \frac{1}{\rho^2}\right)\tilde{U}_0 = 0. \tag{5.115}$$

Making use of the change of the independent variable $\rho = \rho'/\sqrt{s}$, Eq. (5.115) can be reduced to the modified Bessel's equation. In this way, taking into account the regularity condition at $\rho = 0$, we obtain

$$\tilde{U}_0 = C_0 I_1(\sqrt{s}\rho), \tag{5.116}$$

where C_0 is an arbitrary function of the Laplace transform parameter s. This integration constant (with respect to the variable ρ) should be determined from the boundary condition $(5.113)_2$, which in light of (5.114) becomes

$$\frac{\partial \tilde{U}_0}{\partial \rho} + \alpha_{12}\frac{\tilde{U}_0}{\rho}\bigg|_{\rho=1} = \frac{\tilde{\varepsilon}}{2}(1 + \alpha_{12} - 2\alpha_{13}).$$

By substituting the expression (5.116) into the above equation and taking into account the identity $I_1'(x) = I_0(x) - (1/x)I_1(x)$ for the modified Bessel functions of the first kind, we find

$$C_0 = \frac{(1 + \alpha_{12} - 2\alpha_{13})\tilde{\varepsilon}(s)}{2\left[\sqrt{s}I_0(\sqrt{s}) - (1 - \alpha_{12})I_1(\sqrt{s})\right]}. \tag{5.117}$$

Collecting formulas (5.114)–(5.117), we obtain

$$\tilde{U} = -\frac{\tilde{\varepsilon}}{2}\rho\left(1 - \frac{(1 + \alpha_{12} - 2\alpha_{13})I_1(\sqrt{s}\rho)}{\sqrt{s}\rho\left(I_0(\sqrt{s}) - (1 - \alpha_{12})\dfrac{I_1(\sqrt{s})}{\sqrt{s}}\right)}\right). \tag{5.118}$$

We now calculate the Laplace transform of the dimensionalized pressure, $\tilde{P}$, from Eq. (5.111), which as a result of (5.114) can be rewritten as

$$\frac{\partial \tilde{P}}{\partial \rho} = s\tilde{U}_0.$$

The integration of the above equation with respect to ρ, in light of the identity $I_0'(x) = I_1(x)$, yields

$$\tilde{P} = C_0\sqrt{s}I_0(\sqrt{s}\rho) + C_1,$$

where C_1 is an arbitrary function of s. By satisfying the boundary condition $(5.113)_1$, we immediately get $C_1 = -C_0\sqrt{s}I_0(\sqrt{s})$ and

$$\tilde{P} = C_0\sqrt{s}\left(I_0(\sqrt{s}\rho) - I_0(\sqrt{s})\right), \tag{5.119}$$

where C_0 is given by (5.117).

Finally, we consider the force response of the biphasic sample

$$F(t) = -2\pi \int_0^a \sigma_{zz}(t, r) r \, dr, \tag{5.120}$$

where, in light of (5.98) and (5.104), the out-of-plane normal total stress is given by

$$\sigma_{zz} = -p + A^{\mathrm{s}}_{13} \frac{\partial u_r}{\partial r} + A^{\mathrm{s}}_{13} \frac{u_r}{r} + A^{\mathrm{s}}_{33} \varepsilon. \tag{5.121}$$

In terms of the dimensionless variables (5.106), Eq. (5.120) takes the form

$$\mathscr{F}(\tau) = -2 \int_0^1 \left(-P + \alpha_{13} \left(\frac{\partial U}{\partial \rho} + \frac{U}{\rho} \right) + \alpha_{33} \varepsilon \right) \rho \, d\rho, \tag{5.122}$$

where we have introduced the notation

$$\mathscr{F}(\tau) = \frac{F(t)}{\pi a^2 A^{\mathrm{s}}_{11}}, \tag{5.123}$$

$$\alpha_{33} = \frac{A^{\mathrm{s}}_{33}}{A^{\mathrm{s}}_{11}}. \tag{5.124}$$

After application of the Laplace transform, Eq. (5.122) becomes

$$\tilde{\mathscr{F}}(s) = -2 \int_0^1 \left(-\tilde{P} + \alpha_{13} \left(\frac{\partial \tilde{U}}{\partial \rho} + \frac{\tilde{U}}{\rho} \right) + \alpha_{33} \tilde{\varepsilon} \right) \rho \, d\rho. \tag{5.125}$$

Now, taking into account Eqs. (5.114), (5.117), (5.119) and formulas

$$I_0'(x) = I_1(x), \quad x I_1'(x) = x I_0(x) - I_1(x),$$

the integral (5.125) becomes

$$\tilde{\mathscr{F}}(s) = -\frac{\gamma_1 I_0(\sqrt{s}) - \gamma_2 \dfrac{I_1(\sqrt{s})}{\sqrt{s}}}{I_0(\sqrt{s}) - \gamma_0 \dfrac{I_1(\sqrt{s})}{\sqrt{s}}} \tilde{\varepsilon}(s), \tag{5.126}$$

where we have also introduced the notation

$$\begin{aligned}\gamma_0 &= 1-\alpha_{12},\\ \gamma_1 &= \frac{1}{2}(1+\alpha_{12}+2\alpha_{33}-4\alpha_{13}),\\ \gamma_2 &= \alpha_{33}(1-\alpha_{12})+1+\alpha_{12}-4\alpha_{13}+2\alpha_{13}^2.\end{aligned} \tag{5.127}$$

Formulas (5.126) and (5.127) coincide with the corresponding results given by Cohen et al. [19], up to the notation. In the isotropic case, we have

$$\alpha_{12}=\alpha_{13}=\frac{\lambda_s}{H_A},\quad \alpha_{33}=1,\quad \gamma_0=\frac{2\mu_s}{H_A},\quad \gamma_1=\frac{3\mu_s}{H_A},\quad \gamma_2=\frac{8\mu_s^2}{H_A^2},$$

where λ_s, μ_s, and H_A are the Lamé elastic constants and the aggregate elastic modulus of the solid skeleton, respectively, and the original results of Armstrong et al. [5] are immediately recovered.

5.3.3 Unconfined Compression Model

Following [3], we rewrite Eq. (5.126) in the form

$$\tilde{\mathscr{F}}(s)=-s\tilde{\varepsilon}(s)\tilde{\mathscr{K}}(s), \tag{5.128}$$

where we have introduced the notation

$$\tilde{\mathscr{K}}(s)=\frac{\gamma_1 I_0(\sqrt{s})-\gamma_2\dfrac{I_1(\sqrt{s})}{\sqrt{s}}}{s\left(I_0(\sqrt{s})-\gamma_0\dfrac{I_1(\sqrt{s})}{\sqrt{s}}\right)}. \tag{5.129}$$

By applying the convolution theorem to Eq. (5.128), we obtain

$$\mathscr{F}(\tau)=-\int_{0^-}^{\tau}\frac{d\varepsilon(\tau')}{d\tau'}\mathscr{K}(\tau-\tau')\,d\tau', \tag{5.130}$$

where $\mathscr{K}(\tau)=\mathscr{L}^{-1}\{\tilde{\mathscr{K}}(s)\}$ is the original function of $\tilde{\mathscr{K}}(s)$, and $\tau=0^-$ is the dimensionless time moment just preceding the initial moment of loading $\tau=0$. In deriving Eq. (5.130), we have used the formula

$$\mathscr{L}^{-1}\{s\tilde{\varepsilon}(s)\}=\frac{d\varepsilon(\tau)}{d\tau}+\varepsilon(0^+)\delta(\tau),$$

where $\delta(\tau)$ is the Dirac function.

Following [5], we calculate the inverse Laplace transform by using the residue theorem (see, e.g., [46, 48]) to find

$$\mathscr{K}(\tau) = \frac{2\gamma_1 - \gamma_2}{2 - \gamma_0} + \sum_{n=1}^{\infty} \frac{2(\gamma_2 - \gamma_0\gamma_1)}{\alpha_n^2 - \gamma_0(2 - \gamma_0)} e^{-\alpha_n^2 \tau}, \tag{5.131}$$

where α_n are the roots of the transcendental equation

$$J_0(x) - \gamma_0 \frac{J_1(x)}{x} = 0, \tag{5.132}$$

in which $J_0(x)$ and $J_1(x)$ are Bessel functions of the first kind.

The inverse relation for Eq. (5.130) can be represented by

$$\varepsilon(\tau) = -\int_{0^-}^{\tau} \frac{d\mathscr{F}(\tau')}{d\tau'} \mathscr{M}(\tau - \tau')\, d\tau', \tag{5.133}$$

where $\mathscr{M}(\tau) = \mathscr{L}^{-1}\{\tilde{\mathscr{M}}(s)\}$, and $\tilde{\mathscr{M}}(s)$ is defined by the formula

$$\tilde{\mathscr{M}}(s) = \frac{I_0(\sqrt{s}) - \gamma_0 \dfrac{I_1(\sqrt{s})}{\sqrt{s}}}{s\left(\gamma_1 I_0(\sqrt{s}) - \gamma_2 \dfrac{I_1(\sqrt{s})}{\sqrt{s}}\right)}. \tag{5.134}$$

Again making use of the residue theorem, we obtain

$$\mathscr{M}(\tau) = \frac{2 - \gamma_0}{2\gamma_1 - \gamma_2} - \sum_{n=1}^{\infty} \frac{2(\gamma_2 - \gamma_0\gamma_1)}{\gamma_1^2 \beta_n^2 + \gamma_2(\gamma_2 - 2\gamma_1)} e^{-\beta_n^2 \tau}, \tag{5.135}$$

where β_n are the roots of the transcendental equation

$$J_0(x) - \frac{\gamma_2}{\gamma_1} \frac{J_1(x)}{x} = 0. \tag{5.136}$$

The short-time asymptotic approximation for the kernel $\mathscr{K}(\tau)$, as can also be found for $\mathscr{M}(\tau)$, can be obtained by evaluating the Laplace inverse of $\tilde{\mathscr{K}}(s)$ as $s \to \infty$. For this purpose, we apply the following well known asymptotic expansion (see, e.g., [30], formula (8.451.5)):

$$I_n(z) = \frac{e^z}{\sqrt{2\pi z}} \left\{1 + \frac{(1 - 4n^2)}{8z} + O(z^{-2})\right\}.$$

By making use of the above asymptotic formula, we expand the right-hand sides of (5.129) and (5.134) in terms of $1/\sqrt{s}$. As a result, we arrive at the following asymptotic expansions:

$$\mathscr{K}(\tau) = \gamma_1 - \frac{2}{\sqrt{\pi}}(\gamma_2 - \gamma_0\gamma_1)\sqrt{\tau} + O(\tau), \quad \tau \to 0^+, \tag{5.137}$$

$$\mathscr{M}(\tau) = \frac{1}{\gamma_1} + \frac{2}{\sqrt{\pi}}\frac{(\gamma_2 - \gamma_0\gamma_1)}{\gamma_1^2}\sqrt{\tau} + O(\tau), \quad \tau \to 0^+. \tag{5.138}$$

The asymptotic approximations (5.137) and (5.138) can be used in evaluating unconfined impact compression tests where the impact duration is relatively small compared to the so-called [5] gel diffusion time for the biphasic material $t_{\mathrm{g}} = a^2/(H_A k_1)$, which is the time taken for a cylindrical biphasic sample of radius a to reach equilibrium in unconfined stepwise compression.

Further, let us introduce the notation

$$\mathscr{K}_0 = \mathscr{K}(0), \quad \mathscr{M}_0 = \mathscr{M}(0).$$

In light of (5.137) and (5.138), we have

$$\mathscr{K}_0 = \gamma_1, \quad \mathscr{M}_0 = \frac{1}{\gamma_1}. \tag{5.139}$$

Hence, the following identities hold true:

$$\begin{aligned} \frac{2\gamma_1 - \gamma_2}{2 - \gamma_0} + \sum_{n=1}^{\infty} \frac{2(\gamma_2 - \gamma_0\gamma_1)}{\alpha_n^2 - \gamma_0(2 - \gamma_0)} &= \gamma_1, \\ \frac{2 - \gamma_0}{2\gamma_1 - \gamma_2} - \sum_{n=1}^{\infty} \frac{2(\gamma_2 - \gamma_0\gamma_1)}{\gamma_1^2\beta_n^2 + \gamma_2(\gamma_2 - 2\gamma_1)} &= \frac{1}{\gamma_1}. \end{aligned} \tag{5.140}$$

Using Eq. (5.140), we can rewrite the kernel functions (5.131) and (5.135) as

$$\begin{aligned} \mathscr{K}(\tau) &= \mathscr{K}_0 - \sum_{n=1}^{\infty} \frac{2(\gamma_2 - \gamma_0\gamma_1)}{\alpha_n^2 - \gamma_0(2 - \gamma_0)}\left(1 - e^{-\alpha_n^2\tau}\right), \\ \mathscr{M}(\tau) &= \mathscr{M}_0 + \sum_{n=1}^{\infty} \frac{2(\gamma_2 - \gamma_0\gamma_1)}{\gamma_1^2\beta_n^2 + \gamma_2(\gamma_2 - 2\gamma_1)}\left(1 - e^{-\beta_n^2\tau}\right), \end{aligned} \tag{5.141}$$

and then introduce the normalized kernel functions

$$K(t) = \frac{1}{\mathscr{K}_0}\mathscr{K}\left(\frac{A_{11}^{\mathrm{s}} k_1}{a^2}t\right), \quad M(t) = \frac{1}{\mathscr{M}_0}\mathscr{M}\left(\frac{A_{11}^{\mathrm{s}} k_1}{a^2}t\right), \tag{5.142}$$

so that, in light of (5.106) and (5.139)–(5.142), we have

$$K(t) = 1 - \sum_{n=1}^{\infty} \mathscr{A}_n \left(1 - \exp\left(-\frac{t}{\rho_n}\right)\right), \tag{5.143}$$

$$M(t) = 1 + \sum_{n=1}^{\infty} \mathscr{B}_n \left(1 - \exp\left(-\frac{t}{\tau_n}\right)\right), \tag{5.144}$$

where we have introduced the notation

$$\mathscr{A}_n = \frac{2(\gamma_2 - \gamma_0\gamma_1)}{\gamma_1\left[\alpha_n^2 - \gamma_0(2 - \gamma_0)\right]}, \quad \mathscr{B}_n = \frac{2\gamma_1(\gamma_2 - \gamma_0\gamma_1)}{\gamma_1^2\beta_n^2 + \gamma_2(\gamma_2 - 2\gamma_1)}, \tag{5.145}$$

$$\rho_n = \frac{a^2}{\alpha_n^2 A_{11}^{\mathrm{s}} k_1}, \quad \tau_n = \frac{a^2}{\beta_n^2 A_{11}^{\mathrm{s}} k_1}. \tag{5.146}$$

Note that, by analogy with the viscoelastic model, the functions $K(t)$ and $M(t)$ may be called the normalized biphasic relaxation function and the normalized biphasic creep function for unconfined compression, respectively. Note also that the sequences $\rho_1 > \rho_2 > \ldots$ and $\tau_1 > \tau_2 > \ldots$, which are defined by formulas (5.146), represent the discrete relaxation and retardation spectra, respectively.

In the dimensional form, Eqs. (5.130) and (5.133) can be recast as follows (see formulas (5.96), (5.106), and (5.123)):

$$F(t) = \frac{\pi a^2 E_3}{h} \int_{0^-}^{t} K(t - t')\dot{w}(t')\, dt', \tag{5.147}$$

$$w(t) = \frac{h}{\pi a^2 E_3} \int_{0^-}^{t} M(t - t')\dot{F}(t')\, dt'. \tag{5.148}$$

Here we have introduced the notation

$$E_3 = A_{11}^{\mathrm{s}} \mathscr{K}_0 = \frac{A_{11}^{\mathrm{s}}}{\mathscr{M}_0},$$

which according to Eqs. (5.110), (5.124), (5.127), and (5.139), has the form

$$E_3 = \frac{1}{2}\left(A_{11}^{\mathrm{s}} + A_{12}^{\mathrm{s}} + 2A_{33}^{\mathrm{s}} - 4A_{13}^{\mathrm{s}}\right). \tag{5.149}$$

Note that the elastic constant E_3 defined by formula (5.149) coincides with the out-of-plane Young's modulus of the equivalent (for instantaneous response) transversely isotropic incompressible elastic material given by formula $(5.40)_2$.

In terms of the technical elastic constants, formulas (5.127) yield

$$\gamma_0 = \frac{1 - \nu_{12}^{\mathrm{s}} - 2\nu_{31}^{\mathrm{s}2} n_1}{1 - \nu_{31}^{\mathrm{s}2} n_1}, \tag{5.150}$$

$$\frac{\gamma_2}{\gamma_1} = \frac{2\left\{\left[1 - 4\nu_{31}^{\mathrm{s}}(1 - \nu_{12}^{\mathrm{s}}\nu_{31}^{\mathrm{s}})\right] n_1 + (1 - \nu_{12}^{\mathrm{s}})^2 - \nu_{31}^{\mathrm{s}2}(1 - 4\nu_{31}^{\mathrm{s}}) n_1^2\right\}}{\left(1 - n_1 \nu_{31}^{\mathrm{s}2}\right)\left[(1 - 4\nu_{31}^{\mathrm{s}}) n_1 + 2(1 - \nu_{12}^{\mathrm{s}})\right]}, \tag{5.151}$$

where we have introduced the notation

$$n_1 = \frac{E_1^{\mathrm{s}}}{E_3^{\mathrm{s}}}.$$

Finally, we note that in light of (5.150), Eq. (5.132) coincides with the corresponding equation derived in [19].

5.3.4 Biphasic Stress Relaxation in Unconfined Compression

For an imposed step displacement, i.e.,

$$w(t) = w_0 \mathscr{H}(t),$$

where $\mathscr{H}(t)$ is the Heaviside step function, by formula (5.147) we have

$$F(t) = \pi a^2 E_3 \frac{w_0}{h} K(t), \tag{5.152}$$

for $K(t)$ and E_3 given by (5.143) and (5.149).

Following Cohen et al. [19], we consider the ratio of the peak load intensity (F_{peak}, at $t \to 0^+$) to the one at equilibrium (F_{eq}, at $t \to +\infty$), which in light of the relations $K(0) = 1$ and $K(+\infty) = 1 - \sum_{n=1}^{\infty} \mathscr{A}_n$ takes the form

$$\frac{F_{\mathrm{peak}}}{F_{\mathrm{eq}}} = \frac{\gamma_1(2 - \gamma_0)}{2\gamma_1 - \gamma_2}. \tag{5.153}$$

We note that in writing the above equation we have used the first identity (5.140).

In the isotropic case, the right-hand side of (5.153) reduces to $3/[2(1 + \nu_{\mathrm{s}})]$, which is a strictly decreasing function of Poisson's ratio ν_{s} and for positive ν_{s} attains a maximum value of 1.5 at $\nu_{\mathrm{s}} = 0$, as shown by Armstrong et al. [5].

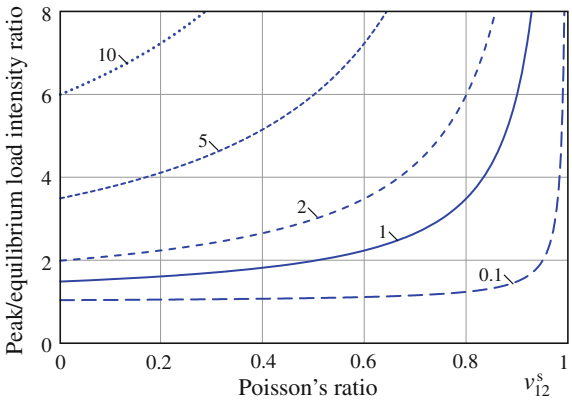

Fig. 5.4 The effect of ν_{12}^{s} and E_1^s/E_3^s on the peak to equilibrium ratio of the load intensity in the stress-relaxation response to a step displacement. (The values taken by E_1^s/E_3^s are indicated on the figure)

Taking into account formulas (5.110), (5.124), and (5.127), we rewrite Eq. (5.153) in the following form [19]:

$$\frac{F_{\text{peak}}}{F_{\text{eq}}} = \frac{2(1-\nu_{12}^{s}) + (1-4\nu_{31}^{s})E_1^s/E_3^s}{2\big(1-\nu_{12}^{s}-2\nu_{31}^{s2}E_1^s/E_3^s\big)}. \tag{5.154}$$

For the particular case of $\nu_{31}^{s} = 0$, the maximum values of the load intensity ratio are depicted in Fig. 5.4 for different values of E_1^s/E_3^s and $\nu_{12}^{s} \in (0, 1.0)$. Note the high values that this ratio can attain (much greater than the maximum value 1.5 for the ratio $F_{\text{peak}}/F_{\text{eq}} = 3/[2(1+\nu)]$ in the isotropic case for $\nu = 0$).

For an imposed ramp displacement, i.e.,

$$w(t) = \begin{cases} V_0 t, & 0 \le t \le t_0, \\ V_0 t_0, & t_0 \le t, \end{cases}$$

when a constant strain rate $-V_0/h$ is maintained until time t_0, the general solution (3.49) yields

$$F(t) = \pi a^2 E_3 \frac{V_0}{h}\left\{\frac{(2\gamma_1-\gamma_2)}{\gamma_1(2-\gamma_0)}t + \sum_{n=1}^{\infty}\mathscr{A}_n\rho_n\big(1-e^{-t/\rho_n}\big)\right\} \tag{5.155}$$

for $0 \le t \le t_0$, and for $t \ge t_0$ gives

$$F(t) = \pi a^2 E_3 \frac{V_0}{h}\left\{\frac{(2\gamma_1-\gamma_2)}{\gamma_1(2-\gamma_0)}t_0 + \sum_{n=1}^{\infty}\mathscr{A}_n\rho_n\big(e^{-(t-t_0)/\rho_n}-e^{-t/\rho_n}\big)\big)\right\}. \tag{5.156}$$

Note that at equilibrium (as $t \to \infty$), the load intensity will be

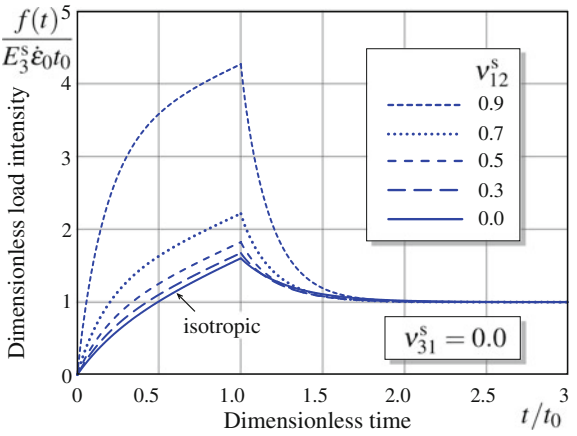

Fig. 5.5 The effect of ν_{12}^s on the stress-relaxation time history in response to a ramped displacement, when $E_1^s/E_3^s = 5$ and $t_0/t_g = 1$

$$F_{eq} = \pi a^2 E_3 \frac{(2\gamma_1 - \gamma_2)}{\gamma_1(2-\gamma_0)} \frac{V_0 t_0}{h},$$

which in light of (5.110), (5.124), and (5.127), reduces to

$$F_{eq} = \pi a^2 E_3^s \frac{V_0 t_0}{h}. \tag{5.157}$$

The characteristic relaxation time in unconfined compression can be defined by

$$\tau_R' = \frac{a^2}{\alpha_1^2 A_{11}^s k_1}, \tag{5.158}$$

where α_1 is the first root of the transcendental equation (5.132).

For the special case in which $\nu_{31}^s = 0$, $E_1^s/E_3^s = 5$, and the ratio of the ramp time to the gel diffusion time, $t_g = a^2/(A_{11}^s k_1)$ (cf. formula (5.158)), is $t_0/t_g = 1$, the effect of ν_{12}^s on the dimensionless stress-relaxation time history $f(t)/[E_3^s \dot{\varepsilon}_0 t_0]$, where $f(t) = F(t)/[\pi a^2]$ and $\dot{\varepsilon}_0 = V_0/h$, is shown in Fig. 5.5. Also, according to Cohen et al. [19], Fig. 5.6 illustrates the effect of the ratio t_0/t_g on the stress relaxation time history for the special case of $\nu_{12}^s = 0.3$, $\nu_{31}^s = 0$, and $E_1^s/E_3^s = 5$.

We also note an alternative representation for $F(t)$ in the loading stage, similar to the one obtained in [19], which follows from the direct inverse Laplace transform of Eq. (5.128) for $\tilde{\varepsilon}(s) = -(V_0 t_g/h)s^{-2}$. Then, for $0 \le t \le t_0$ we have

$$F(t) = \pi a^2 E_3 \frac{V_0}{h} \left\{ \frac{(2\gamma_1 - \gamma_2)}{\gamma_1(2-\gamma_0)} t + \frac{\gamma_2 - \gamma_0\gamma_1}{4\gamma_1(2-\gamma_0)^2} - \sum_{n=1}^{\infty} \mathscr{A}_n \rho_n e^{-t/\rho_n} \right\}.$$

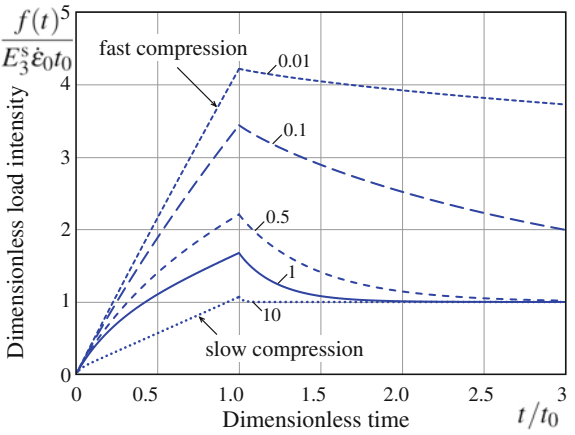

Fig. 5.6 The effect of t_0/t_g on the stress-relaxation time history in response to a ramped displacement, when $\nu_{12}^s = 0.3$, $\nu_{31}^s = 0.0$, and $E_1^s/E_3^s = 5$. (The values taken by t_0/t_g are indicated on the figure)

Equations (5.155) and (5.156) can be used in determining the material properties from the unconfined stress relaxation experiment, by fitting the theoretical solution on to the experimental curve for the total normal stress [19, 32].

5.3.5 *Biphasic Creep in Unconfined Compression*

For an imposed step loading, $F(t) = F_0 \mathscr{H}(t)$, we obtain from formula (5.148) that

$$w(t) = \frac{hF_0}{\pi a^2 E_3} M(t), \tag{5.159}$$

where $M(t)$ and E_3 are given by (5.144) and (5.149).

Taking into account Eqs. $(5.140)_2$ and $(5.145)_2$, we find

$$M(t) = \frac{\gamma_2 + 2\gamma_1^2 - \gamma_1(\gamma_0 + \gamma_2)}{\gamma_1(2\gamma_1 - \gamma_2)} - \sum_{n=1}^{\infty} \mathscr{B}_n \exp\left(-\frac{t}{\tau_n}\right), \tag{5.160}$$

where γ_0, γ_1, γ_2 and $\mathscr{B}_n$, τ_n are given by (5.127) and $(5.145)_2$, $(5.146)_2$, respectively.

The characteristic retardation time in unconfined compression can be defined by

$$\tau_R'' = \frac{a^2}{\beta_1^2 A_{11}^s k_1},$$

where β_1 is the first root of the transcendental equation (5.136).

In the isotropic case, formulas (5.159) and (5.160) reduce to the solution originally obtained by Armstrong et al. [5].

Equations (5.159) and (5.160) are used in determining the biphasic materials properties from the unconfined compression creep experiment by fitting the theoretical solution with the experimental curve for the nominal strain [5, 47].

Observe that the deformation response is characterized by an instantaneous jump

$$w(0^+) = \frac{hF_0}{\pi a^2 E_3}$$

followed by a decreasing slope until equilibrium is reached, where

$$w(+\infty) = \frac{hF_0}{\pi a^2 E_3^{\mathrm{s}}}.$$

Note that the identity

$$E_3 = \frac{\gamma_1(2\gamma_1 - \gamma_2)}{\gamma_2 + 2\gamma_1^2 - \gamma_1(\gamma_0 + \gamma_2)} E_3^{\mathrm{s}}$$

can be directly proved using the expressions (5.110), (5.124), (5.127), and (5.149).

In the isotropic case, when the deformation behavior of the solid phase is described by two elastic constants E_{s} and ν_{s}, the equilibrium response of biphasic material in unconfined and confined compression allows us to evaluate the Young's modulus E_{s} and the aggregate modulus H_A. Thus, taking into account that

$$H_A = \frac{1 - \nu_{\mathrm{s}}}{(1 + \nu_{\mathrm{s}})(1 - 2\nu_{\mathrm{s}})} E_{\mathrm{s}},$$

the following formula for Poisson's ratio can be derived [43]:

$$\nu_{\mathrm{s}} = \frac{1}{4}\left(\frac{E_{\mathrm{s}}}{H_A} - 1 + \sqrt{\left(\frac{E_{\mathrm{s}}}{H_A} - 1\right)\left(\frac{E_{\mathrm{s}}}{H_A} - 9\right)}\right).$$

Finally, note that platen/specimen friction influences the mechanical response of articular cartilage in unconfined compression [5, 71, 77]. In particular, the peak reaction forces in unconfined stress-relaxation experiments exceed the corresponding maximum values predicted analytically. Consequently, the frictional effect becomes more significant for specimens with large aspect (diameter/height) ratios.

5.3.6 Cyclic Compressive Loading in Unconfined Compression

It is well known that the long-term creep and relaxation tests, typically used for determining viscoelastic and biphasic/poroelastic properties, are not appropriate for rapidly assessing the dynamic biomechanical properties of biological tissues like

articular cartilage. For in vivo measurements of tissue viability, Appleyard et al. [1] developed a dynamic indentation instrument, which employs a single-frequency (20 Hz) sinusoidal oscillatory waveform superimposed on a carrier load.

Following Li et al. [51], we assume that a biphasic tissue sample is subjected to a cyclic displacement input

$$w(t) = [w_0(1 - \cos \omega t) + w_1]\mathscr{H}(t), \tag{5.161}$$

where w_1/h is the prestrain resulting from the initial deformation applied to the sample to create the desired preload, w_0 is the displacement amplitude, i.e., w_0/h is equal to one-half the peak-to-peak cyclic strain input superimposed on the prestrain, and $\omega = 2\pi f$ is the angular frequency, f being the loading frequency.

Differentiating (5.161), we obtain

$$\frac{dw(t)}{dt} = \mathscr{H}(t) w_0 \omega \sin \omega t + w_1 \delta(t). \tag{5.162}$$

Substituting expression (5.162) into Eq. (5.147), we arrive, after some algebra, at the following stress output:

$$\frac{F(t)}{\pi a^2} = \frac{E_3}{h}\left\{ w_1 K(t) + w_0 \left(\frac{2\gamma_1 - \gamma_2}{\gamma_1(2 - \gamma_0)} + \sum_{n=1}^{\infty} \frac{\rho_n^2 \omega^2 \mathscr{A}_n}{1 + \rho_n^2 \omega^2} \exp\left(-\frac{t}{\rho_n}\right)\right)\right.$$
$$\left. - w_0\left[K_1(\omega)\cos \omega t - K_2(\omega) \sin \omega t\right]\right\}. \tag{5.163}$$

Here we have introduced the notation

$$K_1(\omega) = 1 - \sum_{n=1}^{\infty} \frac{\mathscr{A}_n}{1 + \rho_n^2 \omega^2}, \tag{5.164}$$

$$K_2(\omega) = \sum_{n=1}^{\infty} \frac{\rho_n \omega \mathscr{A}_n}{1 + \rho_n^2 \omega^2}. \tag{5.165}$$

To assign a physical meaning to the introduced functions $K_1(\omega)$ and $K_2(\omega)$, let us compare the oscillating part of the input strain, that is $-(w_0/h)\cos \omega t$, with the corresponding oscillating part of the compressive stress, which is equal to $-E_3(w_0/h)\left[K_1(\omega)\cos \omega t - K_2(\omega)\sin \omega t\right]$. By analogy with the viscoelastic model, we obtain that $K_1(\omega)$ and $K_2(\omega)$ represent, respectively, the apparent relative storage and loss moduli. Correspondingly, the apparent loss angle, $\delta(\omega)$, can be introduced by the formula

$$\tan \delta(\omega) = \frac{K_2(\omega)}{K_1(\omega)}. \tag{5.166}$$

The apparent loss angle $\delta(\omega)$ describes the phase difference between the displacement input and force output.

In the case of load-controlled compression, following Suh et al. [73], we will assume that the tissue sample is subjected to a cyclic compressive loading

$$F(t) = [F_0(1 - \cos\omega t) + F_1]\mathscr{H}(t), \tag{5.167}$$

where F_0 is the force amplitude, and F_1 is the initial preload.

After substitution of the expression (5.167) into Eq. (5.148), we finally obtain the following resulting strain output:

$$\frac{w(t)}{h} = \frac{1}{\pi a^2 E_3}\left\{F_1 M(t) + F_0\left(\frac{\gamma_1(2-\gamma_0)}{2\gamma_1 - \gamma_2} - \sum_{n=1}^{\infty}\frac{\tau_n^2\omega^2\mathscr{B}_n}{1+\tau_n^2\omega^2}\exp\left(-\frac{t}{\tau_n}\right)\right)\right.$$
$$\left. - F_0\big[M_1(\omega)\cos\omega t + M_2(\omega)\sin\omega t\big]\right\}, \tag{5.168}$$

where we have introduced the notation

$$M_1(\omega) = 1 + \sum_{n=1}^{\infty}\frac{\mathscr{B}_n}{1+\tau_n^2\omega^2}, \tag{5.169}$$

$$M_2(\omega) = \sum_{n=1}^{\infty}\frac{\tau_n\omega\mathscr{B}_n}{1+\tau_n^2\omega^2}. \tag{5.170}$$

Note that $M_1(\omega)$ and $M_2(\omega)$ have physical meanings of the apparent relative storage and loss compliances, respectively.

5.3.7 Displacement-Controlled Unconfined Compression Test

Following Argatov [3], we consider an unconfined compression test with the upper plate displacement specified according to the equation

$$w(t) = w_0 \sin\omega t, \quad t \in (0, \pi/\omega). \tag{5.171}$$

The maximum displacement, w_0, will be achieved at the time moment $t_m = \pi/(2\omega)$. The moment of time $t = \tilde{t}'_M$, when the contact force $F(t)$ vanishes, determines the duration of the contact. The contact force itself can be evaluated according to Eqs. (5.147) and (5.171) as follows:

$$F(t) = \frac{\pi a^2 E_3}{h} w_0 \omega \int_0^t K(t-\tau) \cos \omega\tau \, d\tau. \tag{5.172}$$

According to Eq. (5.172), the contact force at the moment of maximum displacement is given by

$$F(t_m) = \frac{\pi a^2 E_3}{h} w_0 \tilde{K}_1(\omega), \tag{5.173}$$

where we have introduced the notation

$$\tilde{K}_1(\omega) = \omega \int_0^{\pi/(2\omega)} K(\tau) \sin \omega\tau \, d\tau. \tag{5.174}$$

By analogy with the viscoelastic case [2, 4], the quantity $\tilde{K}_1(\omega)$ will be called the reduced incomplete apparent storage modulus.

Substituting the expression (5.143) into the right-hand side of Eq. (5.174), we obtain

$$\tilde{K}_1(\omega) = 1 - \sum_{n=1}^{\infty} \frac{\mathscr{A}_n}{1+\rho_n^2\omega^2} - \sum_{n=1}^{\infty} \frac{\rho_n \omega \mathscr{A}_n}{1+\rho_n^2\omega^2} \exp\Big(-\frac{\pi}{2\omega\rho_n}\Big). \tag{5.175}$$

Now, taking into consideration Eqs. (5.164) and (5.175), we may conclude that the difference between the reduced apparent storage modulus $K_1(\omega)$ and the reduced incomplete apparent storage modulus $\tilde{K}_1(\omega)$ is relatively small at low frequencies. To be more precise, the difference $K_1(\omega) - \tilde{K}_1(\omega)$ is positive and of order $O\big(\omega\rho_1 \exp(-\pi/(2\omega\rho_1))\big)$ as $\omega \to 0$, where ρ_1 is the maximum relaxation time.

In the high frequency limit, the upper limit of the integral (5.174) tends to zero as ω increases. Thus, the behavior of $\tilde{K}_1(\omega)$ as $\omega \to +\infty$ will depend on the behavior of $K(t)$ as $t \to 0$. According to (5.137), as $\omega \to \infty$, we have

$$\tilde{K}_1(\omega) = 1 - \frac{2s_{1/2}}{\sqrt{\pi}} \frac{(\gamma_2 - \gamma_0\gamma_1)}{\gamma_1} \sqrt{\frac{A_{11}^{\mathrm{s}} k_1}{a^2}} \frac{1}{\sqrt{\omega}} + O(\omega^{-1}), \tag{5.176}$$

where $s_{1/2} = \int_0^{\pi/2} \sqrt{x} \sin x \, dx$.

On the other hand, due to the asymptotic formula (5.176), the following limit relation holds true: $\lim K_1(\omega) = 1$ as $\omega \to \infty$. Thus, we conclude that $\tilde{K}_1(\omega) \simeq K_1(\omega)$ for $\omega \to \infty$ as well as $\tilde{K}_1(\omega) \simeq K_1(\omega)$ for $\omega \to 0$. In other words, the reduced incomplete apparent storage modulus $\tilde{K}_1(\omega)$ obeys both asymptotic behaviors of the reduced apparent storage modulus $K_1(\omega)$.

5.3.8 Force-Controlled Unconfined Compression Test

Consider now an unconfined compression test where the external force is as specified by the equation

$$F(t) = F_0 \sin \omega t, \quad t \in (0, \pi/\omega). \tag{5.177}$$

The maximum contact force, F_0, will be achieved at the time moment $t_M = \pi/(2\omega)$. The moment of time $t'_M = \pi/\omega$, when the contact force $F(t)$ vanishes, determines the duration of the compression test. According to Eqs. (5.148) and (5.177), the upper plate displacement can be evaluated as follows:

$$w(t) = \frac{h}{\pi a^2 E_3} F_0 \omega \int_0^t M(t-\tau) \cos \omega\tau \, d\tau. \tag{5.178}$$

Due to Eq. (5.178), the displacement at the moment of maximum contact force is given by

$$w(t_M) = \frac{h}{\pi a^2 E_3} F_0 \tilde{M}_1(\omega), \tag{5.179}$$

where we have introduced the notation

$$\tilde{M}_1(\omega) = \omega \int_0^{\pi/(2\omega)} M(\tau) \sin \omega\tau \, d\tau. \tag{5.180}$$

By analogy with the viscoelastic case [2, 4], the quantity $\tilde{M}_1(\omega)$ will be called the reduced incomplete apparent storage compliance.

Substituting the expression (5.138) into the right-hand side of Eq. (5.180), we obtain

$$\tilde{M}_1(\omega) = 1 + \sum_{n=1}^{\infty} \frac{\mathscr{B}_n}{1+\tau_n^2\omega^2} + \sum_{n=1}^{\infty} \frac{\tau_n \omega \mathscr{B}_n}{1+\tau_n^2\omega^2} \exp\Big(-\frac{\pi}{2\omega\tau_n}\Big). \tag{5.181}$$

Using the same method as for $\tilde{K}_1(\omega)$, it can be shown that the incomplete apparent storage compliance $\tilde{M}_1(\omega)$ obeys both asymptotic behaviors of the apparent storage compliance $M_1(\omega)$, that is $\tilde{M}_1(\omega) \simeq M_1(\omega)$ for $\omega \to 0$ along with $\tilde{M}_1(\omega) \simeq M_1(\omega)$ for $\omega \to \infty$.

5.4 Biphasic Poroviscoelastic (BPVE) Model

In this section, the biphasic poroviscoelastic model is briefly outlined. The confined and unconfined compression tests as well as the torsion test are considered.

5.4.1 Linear Biphasic Poroviscoelastic Theory

The biphasic theory was extended by Mak [54] to account for the inherent viscoelasticity of the solid matrix, by replacing the effective stresses (5.13) in the constitutive equation (5.7) with viscoelastic constitutive relations in the hereditary integral form. Therefore, for a transversely isotropic material, we have

$$\begin{aligned}
\sigma_{11}^{\mathrm{VE}} &= B_{11}^{\mathrm{s}} * \varepsilon_{11} + B_{12}^{\mathrm{s}} * \varepsilon_{22} + B_{13}^{\mathrm{s}} * \varepsilon_{33}, \quad & \sigma_{23}^{\mathrm{VE}} &= 2B_{44}^{\mathrm{s}} * \varepsilon_{23}, \\
\sigma_{22}^{\mathrm{VE}} &= B_{12}^{\mathrm{s}} * \varepsilon_{11} + B_{11}^{\mathrm{s}} * \varepsilon_{22} + B_{13}^{\mathrm{s}} * \varepsilon_{33}, \quad & \sigma_{13}^{\mathrm{VE}} &= 2B_{44}^{\mathrm{s}} * \varepsilon_{13}, \\
\sigma_{33}^{\mathrm{VE}} &= B_{13}^{\mathrm{s}} * \varepsilon_{11} + B_{13}^{\mathrm{s}} * \varepsilon_{22} + B_{33}^{\mathrm{s}} * \varepsilon_{33}, \quad & \sigma_{12}^{\mathrm{VE}} &= 2B_{66}^{\mathrm{s}} * \varepsilon_{12},
\end{aligned} \tag{5.182}$$

where the $*$ sign denotes the Stieltjes integral, i.e.,

$$B_{kl}^{\mathrm{s}} * \varepsilon_{ij} = \int_{-\infty}^{t} B_{kl}^{\mathrm{s}}(t-\tau)\, d\varepsilon_{ij}(\tau). \tag{5.183}$$

For simplicity's sake, following [68], we assume that the deformation behavior of the solid phase is governed by a single reduced stress-relaxation function, $\psi(t)$, which is usually assumed to be in the following form proposed by Fung [28]:

$$\psi(t) = 1 + \int_{0}^{\infty} S(\tau) e^{-t/\tau} d\tau, \tag{5.184}$$

where

$$S(\tau) = \begin{cases} \dfrac{c}{\tau}, & \tau_1 \le \tau \le \tau_2, \\ 0, & \tau < \tau_1, \quad \tau > \tau_2. \end{cases} \tag{5.185}$$

We note (see, e.g., [38, 49]) that the relaxation spectrum (5.185) with constant amplitude over a range of frequencies $\tau \in (\tau_1, \tau_2)$, which was originally introduced by Neubert [61], has least sensitivity to strain rate, which has been believed to be the case for some biological tissues [28].

The function $S(\tau)$ defines a continuous relaxation spectrum, where the parameter c is a proportionality constant for the amplitude of the spectrum $S(\tau)$. The width of the spectrum is defined by the time constants τ_1 and τ_2, which govern the fast and slow relaxation phenomena, respectively.

Note that at initial times after loading and at equilibrium, respectively, we have

$$\psi(0) = 1 + c \ln \frac{\tau_2}{\tau_1}, \quad \psi(+\infty) = 1. \tag{5.186}$$

Therefore, under the above assumptions, the relaxation functions $B^{\mathrm{s}}_{kl}(t)$ can be represented as

$$B^{\mathrm{s}}_{kl}(t) = B^{\mathrm{s}\infty}_{kl}\psi(t), \tag{5.187}$$

where $B^{\mathrm{s}\infty}_{kl} = B^{\mathrm{s}}_{kl}(+\infty)$ are the equilibrium elastic moduli, while the instantaneous elastic moduli, $B^{\mathrm{s}0}_{kl} = B^{\mathrm{s}}_{kl}(0)$, are given by

$$B^{\mathrm{s}0}_{kl} = B^{\mathrm{s}\infty}_{kl}\Big(1 + c\ln\frac{\tau_2}{\tau_1}\Big). \tag{5.188}$$

The viscoelastic parameters c, τ_1, τ_2 are material properties of the solid skeleton that need to be determined from experimental data. The confined and unconfined compression problems for a BPVE material were considered in [34, 36, 54, 68].

Thus, the constitutive equations for the solid matrix in the biphasic poroviscoelastic (BPVE) theory have the form

$$\boldsymbol{\sigma}^{\mathrm{s}} = -\phi_{\mathrm{s}}p\mathbf{I} + \boldsymbol{\sigma}^{\mathrm{VE}}, \tag{5.189}$$

where p is the pressure of the fluid phase, $\mathbf{I}$ is the identity tensor, and the components of the stress tensor $\boldsymbol{\sigma}^{\mathrm{VE}}$ are given by (5.182).

The reduced stress-relaxation function (5.184) and (5.185) can be represented by

$$\psi(t) = 1 + c\Big[E_1\Big(\frac{t}{\tau_2}\Big) - E_1\Big(\frac{t}{\tau_1}\Big)\Big], \tag{5.190}$$

where $E_1(x)$ is the exponential integral function, i.e.,

$$E_1(x) = \int_0^1 \frac{1}{\xi}\exp\Big(-\frac{x}{\xi}\Big)d\xi.$$

Observe [68] that, if the width of the relaxation spectrum reduces to zero, i.e., $\tau_1 \to \tau_2$, the reduced relaxation function (5.190) becomes $\psi(t) = 1$. It is also readily seen that the intrinsic viscoelastic effect diminishes as $c \to 0$. Thus, for the limiting cases $c \to 0$ or $\tau_1 \to \tau_2$, and the BPVE theory reduces to the linear biphasic theory.

Note also that for the sake of numerical efficiency the discrete form of the relaxation function

$$\psi(t) = 1 + \sum_i C_i \exp\Big(-\frac{t}{\tau_i}\Big)$$

has also been used for articular cartilage [21, 72]. Multiple discrete spectrums (different sets of C_i and τ_i) can be used to fit the experimental data for the short-term, mid-term and long-term responses [49].

We finally note [57] that the inclusion of intrinsic matrix viscoelastic properties for the solid matrix in the biphasic theory [54] improved the prediction in the unconfined compression case [68] as well as the material property determination [36, 66].

5.4.2 *Confined Compression of a Biphasic Poroviscoelastic Material*

Under the idealized conditions of the confined compression experiment described in Sect. 5.2.1, the displacement of the solid matrix and the fluid movement occur only in the axial direction, and the governing differential equation (5.63) of the biphasic model should be replaced with the following [54, 68]:

$$\int_{-\infty}^{t} B_{33}^{\mathrm{s}}(t-\tau)\frac{\partial}{\partial\tau}\left(\frac{\partial^2 u_z}{\partial z^2}\right)d\tau = \frac{1}{k_3}\frac{\partial u_z}{\partial t}. \tag{5.191}$$

Here, $u_z(t, z)$ is the axial displacement of the solid phase, k_3 is the axial permeability, and $B_{33}^{\mathrm{s}}(t)$ is the axial aggregate relaxation modulus of the solid phase.

For creep, the initial and boundary conditions are

$$u_z(t, z) = 0, \quad -\infty < t < 0, \tag{5.192}$$

$$\int_{-\infty}^{t} B_{33}^{\mathrm{s}}(t-\tau)\frac{\partial}{\partial\tau}\left(\frac{\partial u_z}{\partial z}\right)d\tau\Bigg|_{z=0} = -\sigma(t)\mathscr{H}(t), \tag{5.193}$$

$$u_z\big|_{z=h} = 0, \tag{5.194}$$

where $\sigma(t)$ is the applied compressive stress (see Eq. (5.63)).

Following [54, 68], we put

$$B_{33}^{\mathrm{s}}(t) = H_A\psi(t), \tag{5.195}$$

where $H_A = B_{33}^{\mathrm{s}\infty}$ is the equilibrium aggregate elastic modulus, and $\psi(t)$ is the reduced stress-relaxation function given by (5.184) and (5.185).

To solve the problem (5.191)–(5.194), we introduce dimensionless quantities

$$\zeta = \frac{z}{h}, \quad \tau = \alpha_1 t, \quad \tau_i' = \alpha_1\tau_i, \quad i = 1, 2, \quad \alpha_1 = \frac{H_A k_3}{h^2} \tag{5.196}$$

and apply the Laplace transform to Eqs. (5.191), (5.193), and (5.194) with respect to the dimensionless time variable τ. In this way, remembering that the Laplace

transform of the function $\psi(\tau/\alpha_1)$ (see Eqs. (5.184) and (5.185)) is given by

$$\tilde{\psi}(s) = \frac{1}{s}\left(1 + c \ln \frac{1 + s\tau_2'}{1 + s\tau_1'}\right), \tag{5.197}$$

we arrive at the problem

$$\begin{aligned} \frac{\partial^2 \tilde{u}_z}{\partial \zeta^2} - f(s)\tilde{u}_z = 0, \qquad \zeta \in (0,1), \\ \frac{\partial \tilde{u}_z}{\partial \zeta}\Big|_{\zeta=0} = -\frac{h}{H_A}\frac{f(s)\tilde{\sigma}(s)}{s}, \quad \tilde{u}_z\big|_{\zeta=1} = 0, \end{aligned} \tag{5.198}$$

where we have introduced the notation

$$f(s) = \frac{1}{\tilde{\psi}(s)}. \tag{5.199}$$

From (5.198), we readily obtain

$$\tilde{u}_z = \frac{h\tilde{\sigma}(s)\sqrt{f(s)}}{H_A s}\frac{\sinh\left[\sqrt{f(s)}(1-\zeta)\right]}{\cosh\sqrt{f(s)}}. \tag{5.200}$$

In the case where a constant external load, F_0, is applied instantaneously, we have $\sigma(t) = \sigma_0 \mathscr{H}(t)$, where $\sigma_0 = F_0/A$ with A being the sample cross-sectional area, and $\tilde{\sigma}(s) = \sigma_0/s$, so that formula (5.200) reduces to the fallowing [54, 68]:

$$\tilde{u}_z = \frac{h\sigma_0}{H_A}\frac{\sqrt{f(s)}\sinh\left[\sqrt{f(s)}(1-\zeta)\right]}{s^2\cosh\sqrt{f(s)}}.$$

An asymptotic approximation of the surface displacement $u_z|_{z=0}$ for small times after loading can be obtained by evaluating the inverse Laplace transform as $s \to \infty$, when $f(s) \sim s/\alpha_2$, for a constant α_2. Taking into account (5.197), (5.199) and the relation $\tau_2'/\tau_1' = \tau_2/\tau_1$ (see Eq. $(5.196)_3$), we get

$$\alpha_2 = 1 + c \ln \frac{\tau_2}{\tau_1}.$$

Thus, the short-time asymptotic approximation for the nominal sample-average strain is given by the following formula [54, 68]:

$$\frac{u_z(t,0)}{h} \simeq \frac{2\sigma_0}{H_A}\sqrt{\frac{\alpha_1}{\pi\alpha_2}}t.$$

Note that $\alpha_2 = \psi(0)$ (see Eqs. (5.184) and (5.185)). This dimensionless parameter characterizes the intrinsic solid matrix viscoelastic effects. Observe also [68] that

larger values of α_2, reflecting increased effects of matrix viscoelasticity, or lower values of α_1, and reflecting a low value of the solid matrix permeability, will have the same effect in reducing the early creep response.

5.4.3 Unconfined Compression of a BPVE Material

In the framework of the BPVE theory, the unconfined compression problem (considered previously in Sect. 5.3.1) differs in essence via the constitutive equations (5.98), which now take the form

$$\begin{aligned}
\sigma_{rr}^{\mathrm{VE}} &= B_{11}^{\mathrm{s}} * \frac{\partial u_r}{\partial r} + B_{12}^{\mathrm{s}} * \frac{u_r}{r} + B_{13}^{\mathrm{s}} * \varepsilon, \\
\sigma_{\theta\theta}^{\mathrm{VE}} &= B_{12}^{\mathrm{s}} * \frac{\partial u_r}{\partial r} + B_{11}^{\mathrm{s}} * \frac{u_r}{r} + B_{13}^{\mathrm{s}} * \varepsilon, \\
\sigma_{zz}^{\mathrm{VE}} &= B_{13}^{\mathrm{s}} * \frac{\partial u_r}{\partial r} + B_{13}^{\mathrm{s}} * \frac{u_r}{r} + B_{33}^{\mathrm{s}} * \varepsilon.
\end{aligned} \tag{5.201}$$

The equilibrium equation of the solid matrix (5.99) now has the form

$$-\frac{\partial p}{\partial r} + B_{11}^{\mathrm{s}} * \left(\frac{\partial^2 u_r}{\partial r^2} + \frac{1}{r}\frac{\partial u_r}{\partial r} - \frac{u_r}{r^2} \right) = 0.$$

We recall that the boundary conditions (5.91)–(5.93) are formulated in terms of the components of the total stress tensor

$$\boldsymbol{\sigma} = -p\mathbf{I} + \boldsymbol{\sigma}^{\mathrm{VE}}. \tag{5.202}$$

To solve this problem, let us first introduce the dimensionless variables

$$\rho = \frac{r}{a}, \quad U = \frac{u_r}{a},$$

where we have refrained from using the variables t and p in the non-dimensionalization. Secondly, we apply the Laplace transform with respect to the time variable t, denoting by a tilde the transformed quantities. We then introduce auxiliary notation

$$\tilde{P} = \frac{\tilde{p}}{\bar{B}_{11}^{\mathrm{s}}(s)}, \quad \alpha_{12} = \frac{\bar{B}_{12}^{\mathrm{s}}(s)}{\bar{B}_{11}^{\mathrm{s}}(s)}, \quad \alpha_{13} = \frac{\bar{B}_{13}^{\mathrm{s}}(s)}{\bar{B}_{11}^{\mathrm{s}}(s)}, \quad \alpha_{33} = \frac{\bar{B}_{33}^{\mathrm{s}}(s)}{\bar{B}_{11}^{\mathrm{s}}(s)}, \tag{5.203}$$

$$f(s) = \frac{a^2 s}{k_1 \bar{B}_{11}^{\mathrm{s}}(s)}, \quad \bar{B}_{kl}^{\mathrm{s}}(s) = s\tilde{B}_{kl}^{\mathrm{s}}(s). \tag{5.204}$$

In this case, the biphasic unconfined compression problem (5.111)–(5.113) is replaced with the following:

$$\frac{\partial \tilde{P}}{\partial \rho} = f(s)\Big(\tilde{U} + \frac{\tilde{\varepsilon}}{2}\rho\Big),$$

$$\frac{\partial^2 \tilde{U}}{\partial \rho^2} + \frac{1}{\rho}\frac{\partial \tilde{U}}{\partial \rho} - \frac{\tilde{U}}{\rho^2} = f(s)\Big(\tilde{U} + \frac{\tilde{\varepsilon}}{2}\rho\Big),$$

$$\tilde{P}\big|_{\rho=1} = 0, \quad \frac{\partial \tilde{U}}{\partial \rho} + \alpha_{12}(s)\frac{\tilde{U}}{\rho} + \alpha_{13}(s)\tilde{\varepsilon}\,\Big|_{\rho=1} = 0.$$

In the same way as was done in Sect. 5.3.2, we find

$$\tilde{U} = -\frac{\tilde{\varepsilon}(s)}{2}\rho\left(1 - \frac{(1+\alpha_{12}(s)-2\alpha_{13}(s))\dfrac{I_1(\sqrt{f(s)}\rho)}{\sqrt{f(s)}\rho}}{I_0(\sqrt{f(s)}) - (1-\alpha_{12}(s))\dfrac{I_1(\sqrt{f(s)})}{\sqrt{f(s)}}}\right), \tag{5.205}$$

$$\tilde{p} = \frac{(1+\alpha_{12}(s)-2\alpha_{13}(s))\tilde{\varepsilon}(s)\big[I_0(\sqrt{f(s)}\rho) - I_0(\sqrt{f(s)})\big]}{2\left(I_0(\sqrt{f(s)}) - (1-\alpha_{12}(s))\dfrac{I_1(\sqrt{f(s)})}{\sqrt{f(s)}}\right)}. \tag{5.206}$$

We now consider the force response of the BPVE sample

$$F(t) = -2\pi\int_0^a \sigma_{zz}(t,r)r\,dr, \tag{5.207}$$

where, as a result of (5.201) and (5.202), the normal total stress is given by

$$\sigma_{zz}(t,r) = -p + B_{13}^{\mathrm{s}} * \left(\frac{\partial u_r}{\partial r} + \frac{u_r}{r}\right) + B_{33}^{\mathrm{s}} * \varepsilon.$$

Upon application of the Laplace transform to Eq. (5.207), rewritten in terms of the dimensionless variables (5.203), we obtain

$$\frac{\tilde{F}(s)}{\pi a^2 \bar{B}_{11}^{\mathrm{s}}(s)} = -2\int_0^1 \left(-\tilde{P} + \alpha_{13}(s)\Big(\frac{\partial \tilde{U}}{\partial \rho} + \frac{\tilde{U}}{\rho}\Big) + \alpha_{33}(s)\tilde{\varepsilon}\right)\rho\,d\rho.$$

Taking into account formulas (5.205) and (5.206), and performing the integration in the above equation, we arrive at formula (5.126), where the coefficients γ_0, γ_1, and γ_2 are evaluated by Eq. (5.127), where α_{12}, α_{13}, and α_{33} are as given by (5.203).

Finally, note that the instantaneous axial modulus E_3, in light of (5.149), is

$$E_3 = \frac{1}{2}\left(B_{11}^{s0} + B_{12}^{s0} + 2B_{33}^{s0} - 4B_{13}^{s0}\right),$$

where $B_{kl}^{s0} = B_{kl}^{s}(0)$ are the instantaneous elastic moduli of the solid matrix.

We can thus hypothesize that the instantaneous response of a transversely isotropic biphasic poroviscoelastic tissue is equivalent to that of an incompressible transversely isotropic elastic material with the material constants given by formulas (5.36), (5.39), and (5.40), where ν_{12}^{s}, ν_{31}^{s}, G_{13}^{s}, E_1^{s}, and E_3^{s} are regarded as instantaneous elastic material properties of the poroviscoelastic matrix.

Observe that the deformation response of a biphasic or BPVE sample depends on how it is tested. In particular, while only the aggregate relaxation modulus $B_{33}^{s}(t)$ governs the behavior of a sample tested in confined compression, all four relaxation moduli $B_{11}^{s}(t)$, $B_{12}^{s}(t)$, $B_{13}^{s}(t)$, and $B_{33}^{s}(t)$ have significant influence on the deformation behavior of a BPVE sample tested in unconfined compression.

Finally, we note [34] that the failure to account for either anisotropy or viscoelasticity of the articular cartilage matrix could result in flawed predictions of the tissue deformation under general external loading.

5.4.4 Torsion of a Biphasic Poroviscoelastic Material

We consider a cylindrical sample of a BPVE material of radius a and height h subjected to a torque T (see Fig. 5.7). Let θ denotes the angle of torsional displacement imposed on the upper surface of the sample to achieve a specified shear strain, γ. Between these geometrical parameters, the following relation takes place:

$$\gamma = \vartheta a. \tag{5.208}$$

Here, $\vartheta = \theta/h$ is the so-called twist, defined as the angle of rotation per unit length along the axis of the sample.

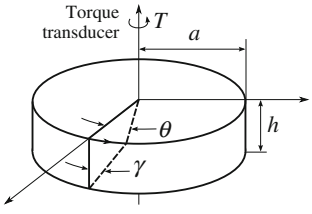

Fig. 5.7 Schematic of the pure torsional shear testing configuration

The components of the in-plane displacement vector are $u_r = 0$ and $u_\theta = \vartheta r z$, and so the only nonzero component of strain is

$$\varepsilon_{z\theta} = \frac{1}{2}\vartheta r. \tag{5.209}$$

The torque is given by

$$T = 2\pi \int_0^a r^2 \sigma_{z\theta}\, dr, \tag{5.210}$$

where according to (5.182) and (5.202) the total shear stress $\sigma_{z\theta}$ is related to the shear strain component $\varepsilon_{z\theta}$ as follows:

$$\sigma_{z\theta} = 2 \int_{-\infty}^{t} B_{44}^{\mathrm{s}}(t-\tau) \frac{\partial \varepsilon_{z\theta}}{\partial \tau}(\tau)\, d\tau. \tag{5.211}$$

Therefore, the substitution of (5.209) and (5.211) into Eq. (5.210) yields

$$T(t) = I_{\mathrm{p}} \int_{-\infty}^{t} B_{44}^{\mathrm{s}}(t-\tau) \frac{\partial \vartheta}{\partial \tau}(\tau)\, d\tau, \tag{5.212}$$

where $I_{\mathrm{p}} = \pi a^4/2$ is the polar moment of inertia of the sample's cross section area.

Furthermore, introducing the so-called shear stress

$$\tau = \frac{aT}{I_{\mathrm{p}}},$$

which is defined as maximum shear stress in the sample, and taking into account (5.208), we can rewrite Eq. (5.212) in terms of the shear strain as follows:

$$\tau(t) = \int_{-\infty}^{t} B_{44}^{\mathrm{s}}(t-t') \frac{\partial \gamma}{\partial t'}(t')\, dt'. \tag{5.213}$$

Now, assuming that the employed herein viscoelastic material of the solid phase is described by the Fung model [28], we represent the above equation in the form

$$\tau(t) = B_{44}^{\mathrm{s}\infty} \int_{-\infty}^{t} \psi(t-t') \frac{\partial \gamma}{\partial t'}(t')\, dt', \tag{5.214}$$

where $B_{44}^{s\infty}$ is the equilibrium out-of-plane shear modulus, and $\psi(t)$ is the reduced relaxation function given by (5.184) and (5.185), i.e.,

$$\psi(t) = 1 + c \int_{\tau_1}^{\tau_2} \frac{1}{\tau} \exp\Big(-\frac{t}{\tau}\Big) d\tau. \tag{5.215}$$

Following Iatridis et al. [38], we now outline the main shear testing protocols.

Stress-relaxation behavior. In the stress-relaxation experiments, the sample is subjected to a ramping phase, where the strain increases linearly at a constant strain rate, followed by a relaxation phase, where the shear strain is held constant, i.e.,

$$\gamma(t) = \begin{cases} \dfrac{\gamma_0}{t_0} t, & 0 \le t \le t_0, \\ \gamma_0, & t_0 \le t, \end{cases}$$

where γ_0 and t_0 are given constants.

For the ramping phase ($0 \le t \le t_0$), we have

$$\tau(t) = \frac{B_{44}^{s\infty}\gamma_0}{t_0}\big[t + c_1 F_1(t, \tau_1, \tau_2)\big],$$

where (with $E_i(x)$ being the exponential integral)

$$F_1(t, \tau_1, \tau_2) = \tau_2\big(1 - e^{-t/\tau_2}\big) - \tau_1\big(1 - e^{-t/\tau_1}\big) - t\big[E_i(t/\tau_1) - E_i(t/\tau_2)\big],$$

$$E_i(x) = \int_x^{\infty} \frac{\exp(-\xi)}{\xi}\, d\xi.$$

For the stress-relaxation phase, the solution is given in terms of the shifted time parameter $\hat{t} = t - t_0$ in the following form [38]:

$$\tau(t) = \frac{B_{44}^{s\infty}\gamma_0}{t_0}\big[t_0 + c_1 G_1(t, \hat{t}, \tau_1, \tau_2)\big],$$

where

$$\begin{aligned} G_1(t, \hat{t}, \tau_1, \tau_2) = {} & \tau_2\big(e^{-\hat{t}/\tau_2} - e^{-t/\tau_2}\big) - \tau_1\big(e^{-\hat{t}/\tau_1} - e^{-t/\tau_1}\big) \\ & - \big\{\hat{t}\big[E_i(\hat{t}/\tau_2) - E_i(\hat{t}/\tau_1)\big] - t\big[E_i(t/\tau_2) - E_i(t/\tau_1)\big]\big\}. \end{aligned}$$

Creep behavior. Let us introduce the out-of-plane creep compliance in shear of the solid matrix, $J_{44}^{s}(t)$, which governs the deformation response of the solid phase under application of a step out-of-plane shear stress of unit magnitude. Hence, the

inverse relation for (5.213) is given by

$$\gamma(t) = \int_{0^-}^{t} J_{44}^{\mathrm{s}}(t-t')\frac{\partial \tau}{\partial t'}(t')\,dt'. \tag{5.216}$$

For a given relaxation modulus $B_{44}^{\mathrm{s}}(t)$, the corresponding creep compliance can be evaluated via its Laplace transform

$$\tilde{J}_{44}^{\mathrm{s}}(s) = \frac{1}{s^2\tilde{B}_{44}^{\mathrm{s}}(s)}. \tag{5.217}$$

Let us now introduce the reduced creep function, $\varphi(t)$, by the formula

$$J_{44}^{\mathrm{s}}(t) = J_{44}^{\mathrm{s}\infty}\varphi(t), \tag{5.218}$$

where $J_{44}^{\mathrm{s}\infty} = J_{44}^{\mathrm{s}}(+\infty)$ is the equilibrium compliance. Since the reduced stress-relaxation function is defined by $\psi(t) = B_{44}^{\mathrm{s}}(t)/B_{44}^{\mathrm{s}\infty}$, where $B_{44}^{\mathrm{s}\infty}$ is the equilibrium modulus such that $B_{44}^{\mathrm{s}\infty} = 1/J_{44}^{\mathrm{s}\infty}$, the following normalization conditions hold:

$$\psi(+\infty) = 1, \quad \varphi(+\infty) = 1.$$

The Fung reduced creep function $\varphi(t)$ corresponding to the reduced relaxation function $\psi(t)$ given by Eq. (5.218) can be obtained by employment of the Laplace transform and Eq. (5.217), that is

$$\tilde{\psi}(s)\tilde{\varphi}(s) = \frac{1}{s^2},$$

where the Laplace transform $\tilde{\psi}(s)$ is given by formula (5.197).

According to Dortmans et al. [22], the following formula holds:

$$\begin{aligned}\varphi(t) = 1 &- \frac{(\tau_c-\tau_2)(\tau_c-\tau_1)}{c\tau_c(\tau_2-\tau_1)}e^{-t/\tau_c} \\ &- c\int_{\tau_1}^{\tau_2} e^{-t/\tau}\frac{1}{\tau}\frac{1}{\left(1+c\ln\dfrac{\tau_2-\tau}{\tau-\tau_1}\right)^2+\pi^2c^2}\,d\tau,\end{aligned} \tag{5.219}$$

where we have used the notation

$$\tau_c = \frac{\tau_2 e^{1/c}-\tau_1}{e^{1/c}-1}.$$

In the creep experiment, a constant torque, T_0, is applied instantaneously, i.e., $T(t) = T_0\mathscr{H}(t)$ and $\tau(t) = \tau_0\mathscr{H}(t)$, where $\tau_0 = aT_0/I_\mathrm{p}$. Therefore, by formulas (5.216) and (5.218), we obtain

$$\gamma(t) = \tau_0 J_{44}^{\mathrm{s}\infty}\varphi(t),$$

where $\varphi(t)$ is given by (5.219).

Steady sinusoidal behavior. If the sample is subjected to a dynamic frequency sweep, the sinusoidal shear strain input is given by

$$\gamma = \gamma_0 e^{\mathrm{i}\omega t},$$

where γ_0 (rad) is the peak shear strain, ω (rad/s) is the angular frequency, and i is the imaginary unit equal to the square root of -1.

In the absence of inertial forces, the corresponding shear stress output will be

$$\tau = \tau_0 e^{\mathrm{i}\omega t},$$

where τ_0 is a complex quantity.

The ratio of the amplitudes τ_0 and γ_0 determines the reduced complex elastic shear modulus, ψ^*, such that

$$\tau_0 = B_{44}^{\mathrm{s}\infty}\psi^*\gamma_0.$$

The reduced complex modulus ψ^* is comprised of real and imaginary parts, i.e.,

$$\psi^* = \psi_1 + \mathrm{i}\psi_2,$$

which defines as the reduced storage, ψ_1, and loss, ψ_2, modulus, respectively.

The reduced storage and loss moduli as functions of angular frequency are evaluated as follows [38]:

$$\psi_1(\omega) = 1 + \frac{c}{2}\ln\frac{1+(\omega\tau_2)^2}{1+(\omega\tau_1)^2},$$

$$\psi_2(\omega) = c\left\{\tan^{-1}(\omega\tau_2) - \tan^{-1}(\omega\tau_1)\right\}.$$

The torsional shear configuration shown in Fig. 5.7 has been used to study equilibrium and dynamic shear moduli as well as the characterization of the stress-relaxation behavior of articular cartilage. Note also [15] that other types of shear testing (for instance, single-lap test) may be important in determining the capacity of cartilage to repair.

It is also noteworthy that under a small shear strain no volumetric changes or pressure gradients occur in a cylindrical sample of BPVE material, and therefore no interstitial fluid flow is induced. Thus, shear tests under infinitesimal strain enable

evaluation of the intrinsic viscoelastic, flow-independent properties of the collagen-proteoglycan solid matrix [18, 41].

Finally, we note that a finite element formulation for describing the large deformation response of biphasic materials in torsion was presented in [56], with a specific focus on the consideration of nonlinear coupling between torsional deformation and fluid pressurization in articular cartilage.

References

1. Appleyard, R.C., Swain, M.V., Khanna, S., Murrell, G.A.C.: The accuracy and reliability of a novel handheld dynamic indentation probe for analysing articular cartilage. Phys. Med. Biol. **46**, 541–550 (2001)
2. Argatov, I.: Sinusoidally-driven flat-ended indentation of time-dependent materials: Asymptotic models for low and high rate loading. Mech. Mater. **48**, 56–70 (2012)
3. Argatov, I.: Sinusoidally-driven unconfined compression test for a biphasic tissue. arXiv preprint arXiv:1207.4679 (2012)
4. Argatov, I., Daniels, A.U., Mishuris, G., Ronken, S., Wirz, D.: Accounting for the thickness effect in dynamic spherical indentation of a viscoelastic layer: application to non-destructive testing of articular cartilage. Eur. J. Mech. A/Solids **37**, 304–317 (2013)
5. Armstrong, C.G., Lai, W.M., Mow, V.C.: An analysis of the unconfined compression of articular cartilage. J. Biomech. Eng. **106**, 165–173 (1984)
6. Ateshian, G.A., Ellis, B.J., Weiss, J.A.: Equivalence between short-time biphasic and incompressible elastic material responses. J. Biomech. Eng. **129**, 405–412 (2007)
7. Ateshian, G.A., Lai, W.M., Zhu, W.B., Mow, V.C.: An asymptotic solution for the contact of two biphasic cartilage layers. J. Biomech. **27**, 1347–1360 (1994)
8. Ateshian, G.A., Warden, W.H., Kim, J.J., Grelsamer, R.P., Mow, V.C.: Finite deformation biphasic material properties of bovine articular cartilage from confined compression experiments. J. Biomech. **30**, 1157–1164 (1997)
9. Barry, S.I., Aldis, G.K.: Comparison of models for flow induced deformation of soft biological tissue. J. Biomech. **23**, 647–654 (1990)
10. Barry, S.I., Holmes, M.: Asymptotic behaviour of thin poroelastic layers. IMA J. Appl. Math. **66**, 175–194 (2001)
11. Barry, S.I., Mercer, G.N.: Flow and deformation in poroelasticity—i unusual exact solutions. Math. Comp. Model. **30**, 23–29 (1999)
12. Biot, M.A.: Theory of finite deformations of porous solids. Indiana Univ. Math. J. **21**, 597–620 (1972)
13. Boschetti, F., Pennati, G., Gervaso, F., Peretti, G.M., Dubini, G.: Biomechanical properties of human articular cartilage under compressive loads. Biorheology **41**, 159–166 (2004)
14. Buschmann, M.D.: Numerical conversion of transient to harmonic response functions for linear viscoelastic materials. J. Biomech. **30**, 197–202 (1997)
15. Chen, A.C., Klisch, S.M., Bae, W.C., Temple, M.M., McGowan, K.B., Gratz, K.R., Schumacher, B.L., Sah, R.L.: Mechanical characterization of native and tissue-engineered cartilage. In: de Ceuninck, F., Sabatini, M., Pastoureau, Ph (eds.) Cartilage and Osteoarthritis, pp. 157–190. Humana Press, Totowa, NJ (2004)
16. Chen, X., Dunn, A.C., Sawyer, W.G., Sarntinoranont, M.: A biphasic model for micro-indentation of a hydrogel-based contact lens. J. Biomech. Eng. **129**, 156–163 (2007)
17. Chin, H.C., Khayat, G., Quinn, T.M.: Improved characterization of cartilage mechanical properties using a combination of stress relaxation and creep. J. Biomech. **44**, 198–201 (2011)
18. Cohen, N.P., Foster, R.J., Mow, V.C.: Composition and dynamics of articular cartilage: structure, function, and maintaining healthy state. J. Orthop. Sports Phys. Ther. **28**, 203–215 (1998)

19. Cohen, B., Lai, W.M., Mow, V.C.: A transversely isotropic biphasic model for unconfined compression of growth plate and chondroepiphysis. J. Biomech. Eng. **120**, 491–496 (1998)
20. Cowin, S.C.: Bone poroelasticity. J. Biomech. **32**, 217–238 (1999)
21. DiSilvestro, M.R., Suh, J.-K.F.: A cross-validation of the biphasic poroviscoelastic model of articular cartilage in unconfined compression, indentation, and confined compression. J. Biomech. **34**, 519–525 (2001)
22. Dortmans, L.J.M.G., van de Ven, A.A.F., Sauren, A.A.H.J.: A note on the reduced creep function corresponding to the quasi-linear visco-elastic model proposed by Fung. J. Biomech. Eng. **116**, 373–375 (1994)
23. Eberhardt, A.W., Keer, L.M., Lewis, J.L., Vithoontien, V.: An analytical model of joint contact. J. Biomech. Eng. **112**, 407–413 (1990)
24. Ehlers, W., Markert, B.: On the viscoelastic behaviour of fluid-saturated porous materials. Granular Matter **2**, 153–161 (2000)
25. Federico, S., Herzog, W.: On the anisotropy and inhomogeneity of permeability in articular cartilage. Biomech. Model. Mechanobiol. **7**, 367–378 (2008)
26. Federico, S., Grillo, A., Giaquinta, G., Herzog, W.: A semi-analytical solution for the confined compression of hydrated soft tissue. Meccanica **44**, 197–205 (2009)
27. Freutel, M., Schmidt, H., Dürselen, L., Ignatius, A., Galbusera, F.: Finite element modeling of soft tissues: material models, tissue interaction and challenges. Clin. Biomech. **29**, 363–372 (2014)
28. Fung, Y.C.: Biomechanics: Mechanical Properties of Living Tissues. Springer-Verlag, New York (1981)
29. Garcia, J.J., Altiero, N.J., Haut, R.C.: An approach for the stress analysis of transversely isotropic biphasic cartilage under impact load. J. Biomech. Eng. **120**, 608–613 (1998)
30. Gradshteyn, I.S., Ryzhik, I.M.: Table of Integrals, Series, and Products. Academic, New York (1980)
31. Gu, W.Y., Lai, W.M., Mow, V.C.: A mixture theory for charged hydrated soft tissues containing multi-electrolytes: passive transport and swelling behaviors. J. Biomech. Eng. **120**, 169–180 (1998)
32. Hatami-Marbini, H., Etebu, E.: An experimental and theoretical analysis of unconfined compression of corneal stroma. J. Biomech. **46**, 1752–1758 (2013)
33. Higginson, G.R., Litchfield, M.R., Snaith, J.: Load-deformation-time characteristics of articular cartilage. Int. J. mech. Sci. **18**, 481–486 (1976)
34. Hoang, S.K., Abousleiman, Y.N.: Poroviscoelasticity of transversely isotropic cylinders under laboratory loading conditions. Mech. Res. Commun. **37**, 298–306 (2010)
35. Hou, J.S., Mow, V.C., Lai, W.M., Holmes, M.H.: An analysis of the squeeze-film lubrication mechanism for articular cartilage. J. Biomech. **25**, 247–259 (1992)
36. Huang, C.-Y., Mow, V.C., Ateshian, G.A.: The role of flow-independent viscoelasticity in the biphasic tensile and compressive responses of articular cartilage. J. Biomech. Eng. **123**, 410–417 (2001)
37. Huyghe, J.M., Janssen, J.D.: Quadriphasic mechanics of swelling incompressible porous media. Int. J. Eng. Sci. **35**, 793–802 (1997)
38. Iatridis, J.C., Setton, L.A., Weidenbaum, M., Mow, V.C.: The viscoelastic behavior of the non-degenerate human lumbar nucleus pulposus in shear. J. Biomech. **30**, 1005–1013 (1997)
39. Itskov, M., Aksel, N.: Elastic constants and their admissible values for incompressible and slightly compressible anisotropic materials. Acta Mech. **157**, 81–96 (2002)
40. Johnson, M., Tarbell, J.M.: A biphasic, anisotropic model of the aortic wall. J. Biomech. Eng. **123**, 52–57 (2000)
41. Knecht, S., Vanwanseele, B., Stüssi, E.: A review on the mechanical quality of articular cartilage—Implications for the diagnosis of osteoarthritis. Clin. Biomech. **21**, 999–1012 (2006)
42. Kluge, J.A., Rosiello, N.C., Leisk, G.G., Kaplan, D.L., Dorfmann, A.L.: The consolidation behavior of silk hydrogels. J. Mech. Behav. Biomed. Mater. **3**, 278–289 (2010)
43. Korhonen, R.K., Laasanen, M.S.: Töyräs, J., Rieppo, J., Hirvonen, J., Helminen, H.J., Jurvelin, J.S.: Comparison of the equilibrium response of articular cartilage in unconfined compression, confined compression and indentation. J. Biomech. **35**, 903–909 (2002)

44. Lai, W.M., Mow, V.C.: Drug-induced compression of articular cartilage during a permeation experiment. Biorheology **17**, 111–123 (1980)
45. Lai, W.M., Hou, J.S., Mow, V.C.: A triphasic theory for the swelling and deformational behaviors of articular cartilage. J. Biomech. Eng. **113**, 245–258 (1991)
46. Lavrentyev, M.A., Shabat, B.V.: Methods of Complex Variable Functions. Nauka, Moscow (1987) (in Russian)
47. Leipzig, N.D., Athanasiou, K.A.: Unconfined creep compression of chondrocytes. J. Biomech. **38**, 77–85 (2005)
48. LePage, W.R.: Complex Variables and the Laplace Transform for Engineers. McGraw-Hill, New York (1961)
49. Li, L.P., Ahsanizadeh, S.: Computational modelling of articular cartilage. In: Jin, Z. (ed.) Computational Modelling of Biomechanics and Biotribology in the Musculoskeletal System: Biomaterials and Tissues, pp. 205–243. Woodhead Publications, Cambridge (2014)
50. Li, L.P., Korhonen, R.K., Iivarinen, J., Jurvelin, J.S., Herzog, W.: Fluid pressure driven fibril reinforcement in creep and relaxation tests of articular cartilage. Med. Eng. Phys. **30**, 182–189 (2008)
51. Li, S., Patwardhan, A.G., Amirouche, F.M.L., Havey, R., Meade, K.P.: Limitations of the standard linear solid model of intervertebral discs subject to prolonged loading and low-frequency vibration in axial compression. J. Biomech. **28**, 779–790 (1995)
52. Lu, X.L., Mow, V.C.: Biomechanics of articular cartilage and determination of material properties. Med. Sci. Sports Exerc. **40**, 193–199 (2008)
53. Lu, X.L., Miller, C., Chen, F.H., Guo, X.E., Mow, V.C.: The generalized triphasic correspondence principle for simultaneous determination of the mechanical properties and proteoglycan content of articular cartilage by indentation. J. Biomech. **40**, 2434–2441 (2006)
54. Mak, A.F.: The apparent viscoelastic behavior of articular cartilage—the contributions from the intrinsic matrix viscoelasticity and interstitial fluid flows. J. Biomech. Eng. **108**, 123–130 (1986)
55. Markert, B.: A constitutive approach to 3-d nonlinear fluid flow through finite deformable porous continua. Transport Porous Med. **70**, 427–450 (2007)
56. Meng, X.N., LeRoux, M.A., Laursen, T.A., Setton, L.A.: A nonlinear finite element formulation for axisymmetric torsion of biphasic materials. Int. J. Solids Struct. **39**, 879–895 (2002)
57. Mow, V.C., Guo, X.E.: Mechano-electrochemical properties of articular cartilage: their inhomogeneities and anisotropies. Annu. Rev. Biomed. Eng. **4**, 175–209 (2002)
58. Mow, V.C., Lai, W.M.: Recent developments in synovial joint biomechanics. SIAM Rev. **22**, 275–317 (1980)
59. Mow, V.C., Holmes, M.H., Lai, W.M.: Fluid transport and mechanical properties of articular cartilage: a review. J. Biomech. **17**, 377–394 (1984)
60. Mow, V.C., Kuei, S.C., Lai, W.M., Armstrong, C.G.: Biphasic creep and stress relaxation of articular cartilage in compression: theory and experiments. J. Biomech. Eng. **102**, 73–84 (1980)
61. Neubert, H.K.P.: A simple model representing internal damping in solid materials. Aeronaut. Quart. **14**, 187–210 (1963)
62. Oomens, C.W.J., Van Campen, D.H., Grootenboer, H.J.: A mixture approach to the mechanics of skin. J. Biomech. **20**, 877–885 (1987)
63. Park, S., Krishnan, R., Nicoll, S.B., Ateshian, G.A.: Cartilage interstitial fluid load support in unconfined compression. J. Biomech. **36**, 1785–1796 (2003)
64. Polyanin, A.D.: Handbook of Linear Partial Differential Equations for Engineers and Scientists. Chapman and Hall/CRC Press, Boca Raton, London (2002)
65. Peña, E., Del Palomar, A.P., Calvo, B., Martínez, M.A., Doblaré, M.: Computational modelling of diarthrodial joints. Physiological, pathological and pos-surgery simulations. Arch. Comput. Methods. Eng. **14**, 47–91 (2007)
66. Raghunathan, S., Evans, D., Sparks, J.L.: Poroviscoelastic modeling of liver biomechanical response in unconfined compression. Ann. Biomed. Eng. **38**, 1789–1800 (2010)
67. Reynaud, B., Quinn, T.M.: Anisotropic hydraulic permeability in compressed articular cartilage. J. Biomech. **39**, 131–137 (2006)

68. Setton, L.A., Zhu, W., Mow, V.C.: The biphasic poroviscoelastic model for articular cartilage: theory and experiment. J. Biomech. **26**, 581–592 (1993)
69. Soltz, M.A., Ateshian, G.A.: Experimental verification and theoretical prediction of interstitial fluid pressurization at an impermeable contact interface in confined compression. J. Biomech. **31**, 927–934 (1998)
70. Soltz, M.A., Ateshian, G.A.: Interstitial fluid pressurization during confined compression cyclical loading of articular cartilage. Ann. Biomed. Eng. **28**, 150–159 (2000)
71. Spilker, R.L., Suh, J.K., Mow, V.C.: Effects of friction on the unconfined compressive response of articular cartilage: a finite element analysis. J. Biomech. Eng. **112**, 138–146 (1990)
72. Suh, J.-K., Bai, S.: Finite element formulation of biphasic poroviscoelastic model for articular cartilage. J. Biomech. Eng. **120**, 195–201 (1998)
73. Suh, J.-K., Li, Z., Woo, S.L.-Y.: Dynamic behavior of a biphasic cartilage model under cyclic compressive loading. J. Biomech. **28**, 357–364 (1995)
74. Terzaghi, K.: Theoretical Soil Mechanics. Wiley, New York (1942)
75. Wang, C.C.-B., Hung, C.T., Mow, V.C.: An analysis of the effects of depth-dependent aggregate modulus on articular cartilage stress-relaxation behavior in compression. J. Biomech. **34**, 75–84 (2001)
76. Wilson, W., Van Donkelaar, C.C., Van Rietbergen, R., Huiskes, R.: The role of computational models in the search for the mechanical behavior and damage mechanisms of articular cartilage. Med. Eng. Phys. **27**, 810–826 (2005)
77. Wu, J.Z., Dong, R.G., Schopper, A.W.: Analysis of effects of friction on the deformation behavior of soft tissues in unconfined compression tests. J. Biomech. **37**, 147–155 (2004)

Chapter 6
Contact of Thin Biphasic Layers

Abstract In Sect. 6.1, a three-dimensional deformation problem for an articular cartilage layer is studied in the framework of the linear biphasic model. The articular cartilage bonded to subchondral bone is modeled as a transversely isotropic biphasic material consisting of a solid phase and a fluid phase. In Sect. 6.2, the same problem is reconsidered with the effect of inherent viscoelasticity of the solid matrix taken into account. The frictionless unilateral contact problem for the articular cartilage layers is considered in Sect. 6.3. It is assumed that the subchondral bones are rigid and shaped like elliptic paraboloids. The obtained short-time leading-order asymptotic solution is valid for monotonically increasing loading conditions.

6.1 Deformation of a Thin Bonded Biphasic Layer

In this section, the short-time leading-order asymptotic solution of the deformation problem for a thin transversely isotropic biphasic layer bonded to a rigid impermeable substrate and subjected to a normal load is constructed. Also, the long-term response of the biphasic layer under constant load is briefly discussed.

6.1.1 Deformation Problem Formulation

Let us consider a thin transversely isotropic biphasic layer of uniform thickness, h, ideally bonded to a rigid impermeable substrate and loaded by a normal time dependent load, q, (see Fig. 6.1). In the following, the two-dimensional Cartesian coordinate system (x_1, x_2) in the plane of the biphasic layer will be denoted by $\mathbf{y} = (y_1, y_2)$, so that $\mathbf{x} = (\mathbf{y}, z)$, where z is the normal coordinate. Also, the displacement vector of the solid matrix is represented as $\mathbf{u} = (\mathbf{v}, w)$, where $\mathbf{v}$ and w are the in-plane displacement vector and the normal displacement, respectively.

The system of governing differential equations (5.16)–(5.19) for a biphasic medium can now be rewritten as

I. Argatov and G. Mishuris, *Contact Mechanics of Articular Cartilage Layers*,
Advanced Structured Materials 50, DOI 10.1007/978-3-319-20083-5_6

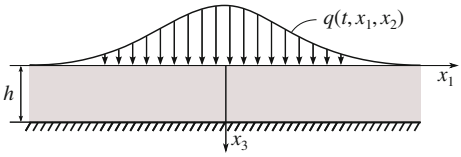

Fig. 6.1 A biphasic layer bonded to a rigid impermeable substrate and supporting a time-dependent normal load

$$A^{\mathrm{s}}_{66}\Delta_y \mathbf{v} + (A^{\mathrm{s}}_{11} - A^{\mathrm{s}}_{66})\nabla_y \nabla_y \cdot \mathbf{v} + A^{\mathrm{s}}_{44}\frac{\partial^2 \mathbf{v}}{\partial z^2} + (A^{\mathrm{s}}_{13} + A^{\mathrm{s}}_{44})\frac{\partial}{\partial z}\nabla_y w = \nabla_y p,$$

$$A^{\mathrm{s}}_{44}\Delta_y w + A^{\mathrm{s}}_{33}\frac{\partial^2 w}{\partial z^2} + (A^{\mathrm{s}}_{13} + A^{\mathrm{s}}_{44})\frac{\partial}{\partial z}\nabla_y \cdot \mathbf{v} = \frac{\partial p}{\partial z}, \quad (6.1)$$

$$\frac{\partial}{\partial t}\left(\nabla_y \cdot \mathbf{v} + \frac{\partial w}{\partial z}\right) = k_1 \Delta_y p + k_3 \frac{\partial^2 p}{\partial z^2}, \quad (6.2)$$

$$\mathbf{w}^{\mathrm{f}} = -k_1 \nabla_y p - k_3 \frac{\partial p}{\partial z}\mathbf{e}_3. \quad (6.3)$$

Here, $\nabla_y = (\partial/\partial y_1)\mathbf{e}_1 + (\partial/\partial y_2)\mathbf{e}_2$ and $\Delta_y = \nabla_y \cdot \nabla_y$ are the in-plane Hamilton and Laplace operators, respectively, while the scalar product is denoted by a dot.

At the bottom surface of the biphasic layer, $z = h$, the boundary conditions (5.20) and (5.21) now take the form

$$\mathbf{v}\big|_{z=h} = \mathbf{0}, \quad w\big|_{z=h} = 0, \quad \left.\frac{\partial p}{\partial z}\right|_{z=h} = 0.$$

As on the upper surface, $z = 0$, the layer is assumed to be loaded only by a variable distributed normal load q, the traction boundary conditions

$$\sigma_{33}\big|_{z=0} = -q, \quad \sigma_{13}\big|_{z=0} = \sigma_{23}\big|_{z=0} = 0$$

can be rewritten as follows (see Eqs. (5.24) and (5.25)):

$$-p + A^{\mathrm{s}}_{13}\nabla_y \cdot \mathbf{v} + A^{\mathrm{s}}_{33}\left.\frac{\partial w}{\partial z}\right|_{z=0} = -q, \quad (6.4)$$

$$\nabla_y w + \left.\frac{\partial \mathbf{v}}{\partial z}\right|_{z=0} = \mathbf{0}.$$

Moreover, assuming that the normal load q is transferred from an impermeable punch, we require that

$$\left.\frac{\partial p}{\partial z}\right|_{z=0} = 0,$$

that is no fluid flow takes place across the contact interface.

Equations (6.1)–(6.3) along with the above boundary conditions and the zero initial conditions (see Eq. (5.30))

$$\mathbf{v} = \mathbf{0}, \quad w = 0, \quad p = 0, \quad \mathbf{w}^{\mathrm{f}} = \mathbf{0}, \quad -\infty < t < 0,$$

constitute the deformation problem for a thin biphasic layer.

6.1.2 *Perturbation Analysis of the Deformation Problem: Short-Time Asymptotic Solution*

Assuming that the biphasic layer is relatively thin, we set

$$h = \varepsilon h_*, \tag{6.5}$$

where ε is a small positive parameter, h_* is independent of ε and has the order of magnitude of a characteristic length in the plane of the layer.

Now, we introduce the dimensionless in-plane coordinates

$$\boldsymbol{\eta} = (\eta_1, \eta_2), \quad \eta_i = \frac{y_i}{h_*}, \quad i = 1, 2, \tag{6.6}$$

and the stretched dimensionless normal coordinate

$$\zeta = \varepsilon^{-1} \frac{z}{h_*}. \tag{6.7}$$

Also, following Ateshian et al. [7], the governing equations are non-dimensionalized using non-dimensional variables

$$\tau = \frac{k_3 A_{33}^{\mathrm{s}}}{h^2} t, \quad \mathbf{V} = \frac{\mathbf{v}}{h}, \quad W = \frac{w}{h}, \quad P = \frac{p}{A_{44}^{\mathrm{s}}}, \quad Q = \frac{q}{A_{44}^{\mathrm{s}}}. \tag{6.8}$$

Observe that as a consequence of (6.5), the first formula above can be simply rewritten as $\tau = \varepsilon^{-2}(k_3 A_{33}^{\mathrm{s}}/h_*^2)t$, so that a finite interval for the fast variable τ corresponds to a very short interval for the time variable t. Correspondingly, the approximate solution obtained below represents the short-time asymptotics.

Therefore, the system of differential equations (6.1)–(6.3) with the corresponding boundary and initial conditions takes the form

$$\frac{\partial^2 \mathbf{V}}{\partial \zeta^2} + \varepsilon\Big((1 + \beta_{13})\nabla_\eta \frac{\partial W}{\partial \zeta} - \nabla_\eta P\Big) + \varepsilon^2\big(\beta_{66}\Delta_\eta \mathbf{V} + (\beta_{11} - \beta_{66})\nabla_\eta \nabla_\eta \cdot \mathbf{V}\big) = \mathbf{0},$$

$$\beta_{33}\frac{\partial^2 W}{\partial\zeta^2}-\frac{\partial P}{\partial\zeta}+\varepsilon(1+\beta_{13})\nabla_\eta\cdot\frac{\partial\mathbf{V}}{\partial\zeta}+\varepsilon^2\Delta_\eta W=0, \tag{6.9}$$

$$\beta_{33}\frac{\partial^2 W}{\partial\tau\partial\zeta}-\frac{\partial^2 P}{\partial\zeta^2}+\varepsilon\beta_{33}\frac{\partial}{\partial\tau}\nabla_\eta\cdot\mathbf{V}-\varepsilon^2\kappa_1\Delta_\eta P=0,$$

$$\mathbf{V}\big|_{\zeta=1}=\mathbf{0},\quad W\big|_{\zeta=1}=0,\quad \frac{\partial P}{\partial\zeta}\bigg|_{\zeta=1}=0,$$

$$Q-P+\varepsilon\beta_{13}\nabla_\eta\cdot\mathbf{V}+\beta_{33}\frac{\partial W}{\partial\zeta}\bigg|_{\zeta=0}=0, \tag{6.10}$$

$$\frac{\partial\mathbf{V}}{\partial\zeta}+\varepsilon\nabla_\eta W\bigg|_{\zeta=0}=\mathbf{0},\quad \frac{\partial P}{\partial\zeta}\bigg|_{\zeta=0}=0,$$

$$\mathbf{V}=\mathbf{0},\quad W=0,\quad P=0,\quad -\infty<\tau<0.$$

Here we have introduced the notation

$$\beta_{11}=\frac{A^{\mathrm{s}}_{11}}{A^{\mathrm{s}}_{44}},\quad \beta_{13}=\frac{A^{\mathrm{s}}_{13}}{A^{\mathrm{s}}_{44}},\quad \beta_{33}=\frac{A^{\mathrm{s}}_{33}}{A^{\mathrm{s}}_{44}},\quad \beta_{66}=\frac{A^{\mathrm{s}}_{66}}{A^{\mathrm{s}}_{44}},\quad \kappa_1=\frac{k_1}{k_3}. \tag{6.11}$$

Following Ateshian et al. [7], the asymptotic ansatz for the solution to the system (6.9) and (6.10) is represented in the form

$$\begin{aligned} P&=P^0+\varepsilon^2P^1+\cdots,\\ \mathbf{V}&=\varepsilon\mathbf{V}^0+\cdots,\\ W&=\varepsilon^2W^0+\cdots, \end{aligned} \tag{6.12}$$

where only non-vanishing leading asymptotic terms are included. Note that this asymptotic ansatz is particularly motivated by the only nonhomogeneous equation (6.4) in the deformation problem under consideration.

Substituting the asymptotic expressions (6.12) into Eq. (6.9) and the boundary conditions (6.10), after collecting terms of like order, we obtain

$$P^0\equiv Q \tag{6.13}$$

and arrive at the following problems:

$$\frac{\partial^2\mathbf{V}^0}{\partial\zeta^2}=\nabla_\eta Q,\quad \zeta\in(0,1),\quad \frac{\partial\mathbf{V}^0}{\partial\zeta}\bigg|_{\zeta=0}=\mathbf{0},\quad \mathbf{V}^0\big|_{\zeta=1}=\mathbf{0}; \tag{6.14}$$

$$\begin{aligned}
\beta_{33}\frac{\partial^2 W^0}{\partial\zeta^2}-\frac{\partial P^1}{\partial\zeta}&=-(1+\beta_{13})\nabla_\eta\cdot\frac{\partial\mathbf{V}^0}{\partial\zeta},\quad \zeta\in(0,1),\\
\beta_{33}\frac{\partial^2 W^0}{\partial\tau\partial\zeta}-\frac{\partial^2 P^1}{\partial\zeta^2}&=\kappa_1\Delta_\eta Q-\beta_{33}\frac{\partial}{\partial\tau}\nabla_\eta\cdot\mathbf{V}^0,\quad \zeta\in(0,1),
\end{aligned}\tag{6.15}$$

$$\begin{aligned}
W^0\big|_{\zeta=1}=0,\quad \left.\frac{\partial P^1}{\partial\zeta}\right|_{\zeta=1}&=0,\\
-P^1+\beta_{33}\left.\frac{\partial W^0}{\partial\zeta}\right|_{\zeta=0}=-\beta_{13}\nabla_\eta\cdot\mathbf{V}^0\big|_{\zeta=0},\quad \left.\frac{\partial P^1}{\partial\zeta}\right|_{\zeta=0}&=0.
\end{aligned}\tag{6.16}$$

By direct integration of the ordinary boundary-value problem (6.14), we find

$$\mathbf{V}^0=-\frac{1}{2}(1-\zeta^2)\nabla_\eta Q.\tag{6.17}$$

The substitution of (6.17) into (6.15) and (6.16) yields

$$\begin{aligned}
\beta_{33}\frac{\partial^2 W^0}{\partial\zeta^2}-\frac{\partial P^1}{\partial\zeta}&=-(1+\beta_{13})\zeta\Delta_\eta Q,\quad \zeta\in(0,1),\\
\beta_{33}\frac{\partial^2 W^0}{\partial\tau\partial\zeta}-\frac{\partial^2 P^1}{\partial\zeta^2}&=\kappa_1\Delta_\eta Q+\frac{\beta_{33}}{2}(1-\zeta^2)\frac{\partial}{\partial\tau}\Delta_\eta Q,\quad \zeta\in(0,1),
\end{aligned}\tag{6.18}$$

$$\begin{aligned}
W^0\big|_{\zeta=1}=0,\quad \left.\frac{\partial P^1}{\partial\zeta}\right|_{\zeta=1}&=0,\\
\beta_{33}\frac{\partial W^0}{\partial\zeta}-P^1\Big|_{\zeta=0}=\frac{\beta_{13}}{2}\Delta_\eta Q,\quad \left.\frac{\partial P^1}{\partial\zeta}\right|_{\zeta=0}&=0.
\end{aligned}\tag{6.19}$$

The exact solution of this resulting problem (6.18) and (6.19) can be determined via the Laplace transform method (see, e.g., [19, 20]).

6.1.3 Solution of the Resulting Ordinary Boundary-Value Problem

We proceed by first remarking that, along with the coordinate system $(\mathbf{y}, z)$ where the coordinate center is placed at the contact interface and the z axis is directed into the layer, another coordinate system is commonly used with its coordinate center placed at the bottom surface of the layer (see Fig. 6.2). In this case we have

$$\bar{z}=h-z,\quad \bar{\mathbf{y}}=-\mathbf{y},\tag{6.20}$$

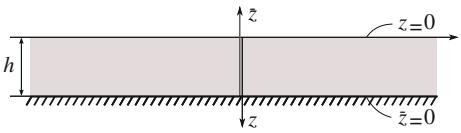

Fig. 6.2 A biphasic layer of uniform thickness bonded to a rigid impermeable substrate: Two systems of coordinates

where $\bar{z}$ and $\bar{\mathbf{y}}$ are the new normal and in-plane coordinates.

Moreover, since the normal axis has changed direction to its opposite, the normal displacements should be related by

$$\bar{W}(t, \bar{\mathbf{y}}, \bar{z}) = -W(t, \mathbf{y}, z). \tag{6.21}$$

The coordinate transformation (6.20) and (6.21) must be taken into account when comparing the obtained results with other studies.

Making use of (6.20) and (6.21), we transform the problem (6.18) and (6.19) to

$$\begin{aligned} \beta_{33}\frac{\partial^2 \bar{W}^0}{\partial \bar{\zeta}^2} - \frac{\partial P^1}{\partial \bar{\zeta}} &= (1+\beta_{13})(1-\bar{\zeta})\Delta_\eta Q, \quad \bar{\zeta} \in (0,1), \\ \beta_{33}\frac{\partial^2 \bar{W}^0}{\partial \tau \partial \bar{\zeta}} - \frac{\partial^2 P^1}{\partial \bar{\zeta}^2} &= \kappa_1 \Delta_\eta Q + \frac{\beta_{33}}{2}\bar{\zeta}(2-\bar{\zeta})\frac{\partial}{\partial \tau}\Delta_\eta Q, \quad \bar{\zeta} \in (0,1), \end{aligned} \tag{6.22}$$

$$\begin{aligned} \bar{W}^0\big|_{\bar{\zeta}=0} = 0, \quad \left.\frac{\partial P^1}{\partial \bar{\zeta}}\right|_{\bar{\zeta}=0} = 0, \\ \beta_{33}\frac{\partial \bar{W}^0}{\partial \bar{\zeta}} - P^1\Big|_{\bar{\zeta}=1} = \frac{\beta_{13}}{2}\Delta_\eta Q, \quad \left.\frac{\partial P^1}{\partial \bar{\zeta}}\right|_{\bar{\zeta}=1} = 0. \end{aligned} \tag{6.23}$$

Now, let $\tilde{\bar{W}}^0$, $\tilde{P}^1$, and $\tilde{Q}$ denote the Laplace transforms of $\bar{W}^0$, P^1, and Q, respectively, with respect to the dimensionless time variable τ, and s be the Laplace transform parameter.

Taking into account the zero initial conditions, the Laplace transformation of Eqs. (6.22) and (6.23) leads to the system

$$\begin{aligned} \beta_{33}\frac{\partial^2 \tilde{\bar{W}}^0}{\partial \bar{\zeta}^2} - \frac{\partial \tilde{P}^1}{\partial \bar{\zeta}} &= (1+\beta_{13})(1-\bar{\zeta})\Delta_\eta \tilde{Q}, \quad \bar{\zeta} \in (0,1), \\ s\beta_{33}\frac{\partial \tilde{\bar{W}}^0}{\partial \bar{\zeta}} - \frac{\partial^2 \tilde{P}^1}{\partial \bar{\zeta}^2} &= \kappa_1 \Delta_\eta \tilde{Q} + s\beta_{33}\frac{\bar{\zeta}}{2}(2-\bar{\zeta})\Delta_\eta \tilde{Q}, \quad \bar{\zeta} \in (0,1), \end{aligned} \tag{6.24}$$

$$\begin{aligned} \tilde{\bar{W}}^0\big|_{\bar{\zeta}=0} = 0, \quad \left.\frac{\partial \tilde{P}^1}{\partial \bar{\zeta}}\right|_{\bar{\zeta}=0} = 0, \\ \beta_{33}\frac{\partial \tilde{\bar{W}}^0}{\partial \bar{\zeta}} - \tilde{P}^1\Big|_{\bar{\zeta}=1} = \frac{\beta_{13}}{2}\Delta_\eta \tilde{Q}, \quad \left.\frac{\partial \tilde{P}^1}{\partial \bar{\zeta}}\right|_{\bar{\zeta}=1} = 0. \end{aligned} \tag{6.25}$$

The homogeneous differential system corresponding to Eq. (6.24) has the characteristic equation $\lambda^4 - s\lambda^2 = 0$, with three roots $\lambda_{1,2} = 0$, $\lambda_{3,4} = \pm\sqrt{s}$, and its general solution is given by

$$\begin{aligned} \tilde{\bar{W}}_0^0 &= C_0 + C_1 \cosh\sqrt{s}\bar{\zeta} + C_2 \sinh\sqrt{s}\bar{\zeta}, \\ \tilde{P}_0^1 &= C_3 + \beta_{33}\sqrt{s}\big(C_1 \sinh\sqrt{s}\bar{\zeta} + C_2 \cosh\sqrt{s}\bar{\zeta}\big), \end{aligned}$$

where $C_0, \ldots, C_3$ are arbitrary functions of the Laplace transform parameter s.

A particular solution of the system (6.24), which does not necessarily satisfy the boundary conditions (6.25), can be found by the method of undetermined coefficients in the form

$$\begin{aligned} \tilde{\bar{W}}_1^0 &= \left(\frac{1}{s\beta_{33}}\big(1 + \kappa_1 + \beta_{13} - \beta_{33}\big)\bar{\zeta} + \frac{\bar{\zeta}^2}{2} - \frac{\bar{\zeta}^3}{6}\right)\Delta_\eta \tilde{Q}, \\ \tilde{P}_1^1 &= (\beta_{33} - 1 - \beta_{13})\left(\bar{\zeta} - \frac{\bar{\zeta}^2}{2}\right)\Delta_\eta \tilde{Q}. \end{aligned}$$

Now, substituting the expressions

$$\tilde{\bar{W}}^0 = \tilde{\bar{W}}_0^0 + \tilde{\bar{W}}_1^0, \quad \tilde{P}^1 = \tilde{P}_0^1 + \tilde{P}_1^1$$

into the system of boundary conditions (6.25), we derive a system of four linear algebraic equations for determining C_0, C_1, C_2, and C_3 as follows:

$$\begin{aligned} C_0 = -C_1 = -\frac{1}{\beta_{33}s}\big(1 + \beta_{13} - \beta_{33}\big)\Delta_\eta \tilde{Q}, \quad C_2 = \frac{\cosh\sqrt{s}}{\sinh\sqrt{s}}C_0, \\ C_3 = \left(\frac{1}{2} + \frac{1}{s}\big(1 + \kappa_1 + \beta_{13} - \beta_{33}\big)\right)\Delta_\eta \tilde{Q}. \end{aligned}$$

Collecting the above formulas, we thus obtain

$$\begin{aligned} \tilde{\bar{W}}^0 &= \Delta_\eta \tilde{Q}\left\{\frac{\delta_1}{\beta_{13}s}\left(1 - \frac{\sinh\sqrt{s}(1-\bar{\zeta})}{\sinh\sqrt{s}}\right) + \frac{\bar{\zeta}^2}{2}\left(1 - \frac{\bar{\zeta}}{3}\right) + \frac{\delta_0}{\beta_{13}s}\bar{\zeta}\right\}, \\ \tilde{P}^1 &= \Delta_\eta \tilde{Q}\left\{\delta_1\left(\frac{\cosh\sqrt{s}(1-\bar{\zeta})}{\sqrt{s}\sinh\sqrt{s}} + \bar{\zeta}\left(1 - \frac{\bar{\zeta}}{2}\right)\right) + \frac{1}{2} + \frac{\delta_0}{s}\right\}, \end{aligned}$$

where, for simplicity, we have introduced the auxiliary notation

$$\delta_0 = 1 + \kappa_1 + \beta_{13} - \beta_{33}, \quad \delta_1 = \beta_{33} - 1 - \beta_{13}. \tag{6.26}$$

By performing the inverse Laplace transform using the residue theorem, we get

$$\begin{aligned}\bar{W}^0 = {} & \Delta_\eta Q(\tau)\frac{\bar{\zeta}^2}{2}\Big(1 - \frac{\bar{\zeta}}{3}\Big) + \frac{(\delta_1 + \delta_0\bar{\zeta})}{\beta_{33}}\int_0^\tau \Delta_\eta Q(\tau')\,d\tau' \\ & - \frac{\delta_1}{\beta_{33}}\int_0^\tau \Delta_\eta Q(\tau')\Big\{1 - \bar{\zeta} \\ & + \frac{2}{\pi}\sum_{n=1}^{\infty}(-1)^n\frac{\sin\pi n(1-\bar{\zeta})}{n}e^{-\pi^2 n^2(\tau-\tau')}\Big\}d\tau',\end{aligned} \tag{6.27}$$

$$\begin{aligned}P^1 = {} & \Delta_\eta Q(\tau)\Big(\frac{1}{2} + \delta_1\bar{\zeta}\Big(1 - \frac{\bar{\zeta}}{2}\Big)\Big) + \delta_0\int_0^\tau \Delta_\eta Q(\tau')\,d\tau' \\ & + \delta_1\int_0^\tau \Delta_\eta Q(\tau')\Big\{1 + 2\sum_{n=1}^{\infty}(-1)^n\cos\pi n(1-\bar{\zeta})e^{-\pi^2 n^2(\tau-\tau')}\Big\}d\tau'.\end{aligned} \tag{6.28}$$

Note that in the isotropic case we have $\delta_0 = 0$ and $\delta_1 = 1$, i.e.,

$$1 + \kappa_1 + \beta_{13} - \beta_{33} = 0, \quad \beta_{33} - 1 - \beta_{13} = 1,$$

and formulas (6.27) and (6.28) agree with the leading-order asymptotic solution originally obtained by Ateshian et al. [7].

6.1.4 Displacements of the Solid Matrix

By recovering the dimensional variables (see, in particular, Eqs. (6.6)–(6.8), (6.11), (6.12), (6.17), (6.20), (6.21), and (6.27)), we arrive at the following leading-order asymptotic approximations for the in-plane (tangential) and out-of-plane (normal) displacements:

$$\mathbf{v} \simeq -\frac{h^2}{2A_{44}^{\mathrm{s}}}\Big(1 - \frac{z^2}{h^2}\Big)\nabla_y q(t, \mathbf{y}),$$

$$
\begin{aligned}
w \simeq & -\frac{h^3}{3A^{\mathrm{s}}_{44}}\Delta_y q(t,\mathbf{y})\Big(1-\frac{z}{h}\Big)^2\Big(1+\frac{z}{2h}\Big) \\
& - hk_1\int_0^t \Delta_y q(t',\mathbf{y})\,dt'\Bigg(1-\frac{\big[(k_1+k_3)A^{\mathrm{s}}_{44}+k_3\big(A^{\mathrm{s}}_{13}-A^{\mathrm{s}}_{33}\big)\big]}{k_1A^{\mathrm{s}}_{44}}\frac{z}{h}\Bigg) \\
& + \frac{hk_3\big(A^{\mathrm{s}}_{33}-A^{\mathrm{s}}_{44}-A^{\mathrm{s}}_{13}\big)}{A^{\mathrm{s}}_{44}}\Bigg\{\frac{z}{h}\int_0^t \Delta_y q(t',\mathbf{y})\,dt' \\
& + \frac{2}{\pi}\sum_{n=1}^{\infty}\frac{(-1)^n}{n}\sin\pi n\frac{z}{h}\int_0^t \Delta_y q(t',\mathbf{y})\exp\Big(-\pi^2n^2\frac{k_3A^{\mathrm{s}}_{33}}{h^2}(t-t')\Big)dt'\Bigg\}.
\end{aligned}
$$

According to the derived solution, the displacements of the surface points of the bonded thin biphasic layer are

$$
\mathbf{v}\big|_{z=0} \simeq -\frac{h^2}{2A^{\mathrm{s}}_{44}}\nabla_y q(t,\mathbf{y}), \tag{6.29}
$$

$$
w\big|_{z=0} \simeq -\frac{h^3}{3A^{\mathrm{s}}_{44}}\Delta_y q(t,\mathbf{y}) - hk_1\int_0^t \Delta_y q(\tau,\mathbf{y})\,d\tau. \tag{6.30}
$$

The leading-order asymptotic relations (6.29) and (6.30) derived for the so-called local indentation will be used to formulate asymptotic models for the unilateral frictionless contact interaction between thin bonded biphasic layers.

6.1.5 Interstitial Fluid Pressure and Relative Fluid Flux

In light of (6.6)–(6.8), $(6.12)_1$, (6.13), and (6.28), we obtain

$$
\begin{aligned}
p \simeq & \, q(t,\mathbf{y}) + \frac{h^2\big(A^{\mathrm{s}}_{44}+2A^{\mathrm{s}}_{33}-2A^{\mathrm{s}}_{13}\big)}{6A^{\mathrm{s}}_{44}}\Delta_y q(t,\mathbf{y}) + k_1A^{\mathrm{s}}_{33}\int_0^t \Delta_y q(t',\mathbf{y})\,dt' \\
& - \frac{2h^2}{\pi^2}\frac{\big(A^{\mathrm{s}}_{33}-A^{\mathrm{s}}_{44}-A^{\mathrm{s}}_{13}\big)}{A^{\mathrm{s}}_{44}}\sum_{n=1}^{\infty}\frac{(-1)^n}{n^2}\cos\pi n\frac{z}{h} \\
& \times\int_{0^-}^t \Delta_y\dot{q}(t',\mathbf{y})\exp\Big(-\pi^2n^2\frac{k_3A^{\mathrm{s}}_{33}}{h^2}(t-t')\Big)dt'.
\end{aligned} \tag{6.31}
$$

Recall that the lower integration limit 0^- in the last integral in (6.31) allows consideration of the load discontinuity at time zero.

We now introduce the dimensionless variables (6.6)–(6.8) into Eq. (6.3), and obtain

$$\mathbf{w}^{\mathrm{f}} = -\frac{k_1 A^{\mathrm{s}}_{44}}{h_*}\nabla_\eta P - \frac{k_3 A^{\mathrm{s}}_{44}}{\varepsilon h_*}\frac{\partial P}{\partial \zeta}\mathbf{e}_3.$$

As a result of $(6.12)_1$, we state the following asymptotic formulas

$$w^{\mathrm{f}}_1\mathbf{e}_1 + w^{\mathrm{f}}_2\mathbf{e}_2 \simeq -\frac{k_1 A^{\mathrm{s}}_{44}}{h_*}\big(\nabla_\eta Q + \varepsilon^2\nabla_\eta P^1\big),$$
$$w^{\mathrm{f}}_3 \simeq -\varepsilon\frac{k_3 A^{\mathrm{s}}_{44}}{h_*}\frac{\partial P^1}{\partial \zeta}.$$

The in-plane and out-of-plane components of the relative fluid flux can be evaluated by differentiating the asymptotic expansion (6.31).

6.1.6 Stresses in the Solid and Fluid Phases

As a consequence of (6.8) and (6.12), the above asymptotic analysis yields the following leading-order asymptotic formulas for the solid matrix strains:

$$\begin{gathered}\varepsilon_{11} \simeq \varepsilon^2\frac{\partial V^0_1}{\partial \eta_1}, \quad \varepsilon_{22} \simeq \varepsilon^2\frac{\partial V^0_2}{\partial \eta_2}, \quad \varepsilon_{33} \simeq \varepsilon^2\frac{\partial W^0}{\partial \zeta},\\ \varepsilon_{12} \simeq \frac{\varepsilon^2}{2}\left(\frac{\partial V^0_1}{\partial \eta_2} + \frac{\partial V^0_2}{\partial \eta_1}\right), \quad \varepsilon_{13} \simeq \frac{\varepsilon}{2}\frac{\partial V^0_1}{\partial \zeta}, \quad \varepsilon_{23} \simeq \frac{\varepsilon}{2}\frac{\partial V^0_2}{\partial \zeta}.\end{gathered} \tag{6.32}$$

Substituting these asymptotic approximations into Eq. (5.13), we can evaluate the effective stresses σ^{e}_{ij} in the solid matrix. After that, in light of (5.1) and (5.7), the stresses in the solid matrix can be approximately evaluated by the formula

$$\boldsymbol{\sigma}^{\mathrm{s}} = -(1-\phi_{\mathrm{f}})p\mathbf{I} + \boldsymbol{\sigma}^{\mathrm{e}},$$

where ϕ_{f} is the porosity of the solid matrix (fluid volume fraction), and the stresses in the fluid phase are defined by the following formula (see Eq. (5.4)):

$$\boldsymbol{\sigma}^{\mathrm{f}} = -\phi_{\mathrm{f}}\,p\mathbf{I}.$$

In particular, according to (5.13), (6.17), and (6.32), we obtain

$$\sigma^{\mathrm{e}}_{31}\mathbf{e}_1 + \sigma^{\mathrm{e}}_{32}\mathbf{e}_2 \simeq z\nabla_y q(t,\mathbf{y}), \tag{6.33}$$

from which it follows that the maximum shear stress in a thin bonded biphasic layer under distributed normal loading is achieved at the bonding interface, $z = h$, at the location of maximum gradient $|q(t, \mathbf{y})|$.

Observe [7] that, as the dominant terms in the deformations and stresses are the lowest-order quantities, the normal strains and effective stresses as well as the in-plane shear strain and effective stress, ε_{12} and σ^{e}_{12}, are $O(\varepsilon^2)$, while the out-of-plane strains and effective shear stresses are $O(\varepsilon)$ (see Eq. (6.32)).

In light of $(6.12)_1$, the hydrostatic pressure is $O(1)$ and is significantly larger than the effective normal stresses. Also, as its lowest-order term is $O(\varepsilon)$, the shear stresses σ^{s}_{3i} $(i = 1, 2)$ in the solid phase, which are equal to the effective shear stresses σ^{e}_{3i} $(i = 1, 2)$, are one order of magnitude greater than the effective normal stresses.

We emphasize (see, e.g., [7]) that this order of magnitude analysis has major implications on how a thin layer of biphasic tissue (e.g., articular cartilage) supports distributed compressive load under the bonding condition.

Finally, let us now introduce the in-plane typical length scale, L, such that $\varepsilon = h/L$. (Note that, as a consequence of (6.5), we simply have $L = h_*$.) In contact problem [7], L refers to the characteristic length of the contact area. Then, the first formula (6.8) can be rewritten as

$$\tau = \frac{t}{\mathscr{T}_3},$$

where $\mathscr{T}_3 = h^2/(k_3 A^{\mathrm{s}}_{33})$ is the typical vertical diffusion time within the biphasic layer [8]. On the other hand, formula $(6.8)_1$ can be rewritten as

$$\tau = \varepsilon^{-2} \frac{k_3 A^{\mathrm{s}}_{33}}{L^2} t,$$

which shows that the dimensionless time variable τ is introduced by stretching the dimensionless time variable $(k_3 A^{\mathrm{s}}_{33}/L^2)t$.

We thus underline that formulas (6.29) and (6.30) present the leading-order asymptotic solution, which is valid for short times only.

6.1.7 *Long-Term (Equilibrium) Response of a Thin Bonded Biphasic Layer Under Constant Loading*

To begin, we assume that the normal load distribution q has a finite support and does not depend on the time variable t. Following [7], we consider the equilibrium (long-term, when $t/\mathscr{T}_3 \gg 1$) response of a thin bonded layer of biphasic material after the relative motion of the interstitial fluid has ceased and the fluid pressure has vanished. In this case the system of governing differential equations (6.1) and (6.2) reduces to that for a single phase *compressible* elastic layer with material properties coinciding with those of the solid matrix.

The corresponding asymptotic solution was derived in Sect. 1.2 and the leading asymptotic terms are summarized below (see Eqs. (1.22) and (1.23))

$$\mathbf{v} \simeq \frac{h^2}{A^{\mathrm{s}}_{33}}\left\{\frac{1}{2}\left(1+\frac{A^{\mathrm{s}}_{13}}{A^{\mathrm{s}}_{44}}\right)\left(1-\frac{z}{h}\right)^2-\frac{A^{\mathrm{s}}_{13}}{A^{\mathrm{s}}_{44}}\left(1-\frac{z}{h}\right)\right\}\nabla_y q(\mathbf{y}),$$
$$w \simeq \frac{h}{A^{\mathrm{s}}_{33}}\left(1-\frac{z}{h}\right)q(\mathbf{y}).$$

Finally, we observe [7] that during the biphasic creep process, the short-time asymptotic solution gradually evolves into the equilibrium (long-term) asymptotic solution, which has drastically different characteristics.

6.2 Deformation of a Thin Transversely Isotropic Biphasic Poroelastic Layer Bonded to a Rigid Impermeable Substrate

In this section, the short-time leading-order asymptotic solution of the deformation problem for a thin biphasic poroelastic (BPVE) layer is constructed. The main result of the section (see Sect. 6.2.3) is an approximate formula for the local indentation of a thin bonded BPVE layer.

6.2.1 Deformation Problem Formulation

In this section, we follow the problem formulation given in detail in Sect. 6.1, with the sole difference being that the total stresses within a thin biphasic poroviscoelastic (BPVE) layer are determined by the constitutive relations

$$\begin{aligned}
\sigma_{11} &= -p + B^{\mathrm{s}}_{11} * \varepsilon_{11} + B^{\mathrm{s}}_{12} * \varepsilon_{22} + B^{\mathrm{s}}_{13} * \varepsilon_{33}, \quad & \sigma_{23} &= 2B^{\mathrm{s}}_{44} * \varepsilon_{23},\\
\sigma_{22} &= -p + B^{\mathrm{s}}_{12} * \varepsilon_{11} + B^{\mathrm{s}}_{11} * \varepsilon_{22} + B^{\mathrm{s}}_{13} * \varepsilon_{33}, \quad & \sigma_{13} &= 2B^{\mathrm{s}}_{44} * \varepsilon_{13},\\
\sigma_{33} &= -p + B^{\mathrm{s}}_{13} * \varepsilon_{11} + B^{\mathrm{s}}_{13} * \varepsilon_{22} + B^{\mathrm{s}}_{33} * \varepsilon_{33}, \quad & \sigma_{12} &= 2B^{\mathrm{s}}_{66} * \varepsilon_{12},
\end{aligned} \tag{6.34}$$

where p is the pressure in the fluid phase, $B^{\mathrm{s}}_{11}(t)$, $B^{\mathrm{s}}_{12}(t)$, $B^{\mathrm{s}}_{13}(t)$, $B^{\mathrm{s}}_{33}(t)$, and $B^{\mathrm{s}}_{44}(t)$ are independent stress-relaxation functions of the solid phase, $B^{\mathrm{s}}_{66}(t) = \big(B^{\mathrm{s}}_{11}(t) - B^{\mathrm{s}}_{12}(t)\big)/2$, and the symbol $*$ denotes the Stieltjes integral, i.e.,

$$B^{\mathrm{s}}_{kl} * \varepsilon_{ij} = \int_{-\infty}^{t} B^{\mathrm{s}}_{kl}(t-\tau)\, d\varepsilon_{ij}(\tau).$$

Correspondingly, the equilibrium equations of the solid matrix take the form

$$B^{\mathrm{s}}_{66} * \Delta_y \mathbf{v} + (B^{\mathrm{s}}_{11} - B^{\mathrm{s}}_{66}) * \nabla_y \nabla_y \cdot \mathbf{v} + B^{\mathrm{s}}_{44} * \frac{\partial^2 \mathbf{v}}{\partial z^2} + (B^{\mathrm{s}}_{13} + B^{\mathrm{s}}_{44}) * \frac{\partial}{\partial z} \nabla_y w = \nabla_y p, \quad (6.35)$$

$$B^{\mathrm{s}}_{44} * \Delta_y w + B^{\mathrm{s}}_{33} * \frac{\partial^2 w}{\partial z^2} + (B^{\mathrm{s}}_{13} + B^{\mathrm{s}}_{44}) * \frac{\partial}{\partial z} \nabla_y \cdot \mathbf{v} = \frac{\partial p}{\partial z}, \quad (6.36)$$

where $\mathbf{v}$ and w are the in-plane displacement vector and the normal displacement of the solid matrix, respectively.

The continuity equation for the BPVE medium has the same form as for biphasic mixtures, i.e.,

$$\frac{\partial}{\partial t}\left(\nabla_y \cdot \mathbf{v} + \frac{\partial w}{\partial z}\right) = k_1 \Delta_y p + k_3 \frac{\partial^2 p}{\partial z^2}. \quad (6.37)$$

The boundary conditions at the bottom surface of the layer, $z = h$, and at the top surface, $z = 0$, can be written as follows:

$$\mathbf{v}\big|_{z=h} = \mathbf{0}, \quad w\big|_{z=h} = 0, \quad \left.\frac{\partial p}{\partial z}\right|_{z=h} = 0;$$

$$-p + B^{\mathrm{s}}_{13} * \nabla_y \cdot \mathbf{v} + B^{\mathrm{s}}_{33} * \left.\frac{\partial w}{\partial z}\right|_{z=0} = -q, \quad (6.38)$$

$$B^{\mathrm{s}}_{44} * \left.\left(\nabla_y w + \frac{\partial \mathbf{v}}{\partial z}\right)\right|_{z=0} = \mathbf{0}, \quad \left.\frac{\partial p}{\partial z}\right|_{z=0} = 0.$$

Equations (6.35)–(6.37) with the given above boundary conditions and the initial conditions

$$\mathbf{v} = \mathbf{0}, \quad w = 0, \quad p = 0, \quad -\infty < t < 0,$$

constitute the deformation problem for a bonded BPVE layer.

Here, following Argatov and Mishuris [4], we construct a leading-order asymptotic solution to the deformation problem (6.35)–(6.37).

6.2.2 Short-Time Asymptotic Analysis of the Deformation Problem

Introducing a characteristic length, h_*, and a small parameter, ε, we require that

$$h = \varepsilon h_*.$$

Moreover, as usual, we introduce the dimensionless in-plane coordinates

$$\boldsymbol{\eta} = (\eta_1, \eta_2), \quad \eta_i = \frac{y_i}{h_*}, \quad i = 1, 2,$$

and stretch the normal coordinate as follows:

$$\zeta = \varepsilon^{-1} \frac{z}{h_*}.$$

The governing equations will be non-dimensionalized using the following non-dimensional variables (cf. Eq. (6.8)):

$$\tau = \frac{k_3 B_{44}^{\mathrm{s}0}}{h^2} t, \quad \mathbf{V} = \frac{\mathbf{v}}{h}, \quad W = \frac{w}{h}, \quad P = \frac{p}{B_{44}^{\mathrm{s}0}}, \quad Q = \frac{q}{B_{44}^{\mathrm{s}0}}. \tag{6.39}$$

Here, $B_{44}^{\mathrm{s}0} = B_{44}^{\mathrm{s}}(0)$ is the instantaneous shear modulus.

Following non-dimensionalisation, we apply the Laplace transformation to the obtained system and arrive at the following problem:

$$\bar{b}_{44}^{\mathrm{s}} \frac{\partial^2 \tilde{\mathbf{V}}}{\partial \zeta^2} + \varepsilon(\bar{b}_{13}^{\mathrm{s}} + \bar{b}_{44}^{\mathrm{s}}) \nabla_\eta \frac{\partial \tilde{W}}{\partial \zeta} + \varepsilon^2 \big(\bar{b}_{66}^{\mathrm{s}} \Delta_\eta \tilde{\mathbf{V}} + (\bar{b}_{11}^{\mathrm{s}} - \bar{b}_{66}^{\mathrm{s}}) \nabla_\eta \nabla_\eta \cdot \tilde{\mathbf{V}} \big) = \varepsilon \nabla_\eta \tilde{P}, \tag{6.40}$$

$$\bar{b}_{33}^{\mathrm{s}} \frac{\partial^2 \tilde{W}}{\partial \zeta^2} + \varepsilon(\bar{b}_{13}^{\mathrm{s}} + \bar{b}_{44}^{\mathrm{s}}) \nabla_\eta \cdot \frac{\partial \tilde{\mathbf{V}}}{\partial \zeta} + \varepsilon^2 \bar{b}_{44}^{\mathrm{s}} \Delta_\eta \tilde{W} = \frac{\partial \tilde{P}}{\partial \zeta}, \tag{6.41}$$

$$s \Big(\frac{\partial \tilde{W}}{\partial \zeta} + \varepsilon \nabla_\eta \cdot \tilde{\mathbf{V}} \Big) = \frac{\partial^2 \tilde{P}}{\partial \zeta^2} + \varepsilon^2 \kappa_1 \Delta_\eta \tilde{P}, \tag{6.42}$$

$$\tilde{\mathbf{V}}\big|_{\zeta=1} = \mathbf{0}, \quad \tilde{W}\big|_{\zeta=1} = 0, \quad \frac{\partial \tilde{P}}{\partial \zeta}\bigg|_{\zeta=1} = 0,$$

$$-\tilde{P} + \bar{b}_{13}^{\mathrm{s}} \nabla_\eta \cdot \tilde{\mathbf{V}} + \bar{b}_{33}^{\mathrm{s}} \frac{\partial \tilde{W}}{\partial \zeta}\bigg|_{\zeta=0} = -\tilde{Q}, \tag{6.43}$$

$$\nabla_\eta \tilde{W} + \frac{\partial \tilde{\mathbf{V}}}{\partial \zeta}\bigg|_{\zeta=0} = \mathbf{0}, \quad \frac{\partial \tilde{P}}{\partial \zeta}\bigg|_{\zeta=0} = 0.$$

The Laplace transforms are denoted by a tilde, $\kappa_1 = k_1/k_3$, and $\bar{b}_{kl}^{\mathrm{s}} = s\tilde{B}_{kl}^{\mathrm{s}}/B_{44}^{\mathrm{s}0}$, where $\tilde{B}_{kl}^{\mathrm{s}}$ is the Laplace transform of $B_{kl}^{\mathrm{s}}\big(h^2\tau/(B_{44}^{\mathrm{s}0}k_3)\big)$ with respect to the dimensionless time variable τ.

Following Ateshian et al. [7], we represent the asymptotic ansatz for the solution to the system (6.40)–(6.43) in the form

$$\tilde{P} \simeq \tilde{Q} + \varepsilon^2 \tilde{P}^1, \quad \tilde{\mathbf{V}} \simeq \varepsilon \tilde{\mathbf{V}}^0, \quad \tilde{W} \simeq \varepsilon^2 \tilde{W}^0. \tag{6.44}$$

Substituting the asymptotic expressions into Eqs. (6.40)–(6.42) and the boundary conditions (6.43), we find after some simple calculations

$$\tilde{\mathbf{V}}^0 = -\frac{1}{2\bar{b}^{\mathrm{s}}_{44}}(1-\zeta^2)\nabla_\eta \tilde{Q}, \tag{6.45}$$

where the pair $\tilde{W}^0$ and $\tilde{P}^1$ should be determined as the solution of the problem

$$\begin{aligned} \bar{b}^{\mathrm{s}}_{33}\frac{\partial^2 \tilde{W}^0}{\partial \zeta^2} - \frac{\partial \tilde{P}^1}{\partial \zeta} &= -(\bar{b}^{\mathrm{s}}_{44} + \bar{b}^{\mathrm{s}}_{13})\nabla_\eta \cdot \frac{\partial \tilde{\mathbf{V}}^0}{\partial \zeta}, \\ s\frac{\partial \tilde{W}^0}{\partial \zeta} - \frac{\partial^2 \tilde{P}^1}{\partial \zeta^2} &= \kappa_1 \Delta_\eta \tilde{Q} - s\nabla_\eta \cdot \tilde{\mathbf{V}}^0, \end{aligned} \tag{6.46}$$

$$\begin{aligned} \tilde{W}^0\big|_{\zeta=1} = 0, \quad \left.\frac{\partial \tilde{P}^1}{\partial \zeta}\right|_{\zeta=1} = 0, \\ -\tilde{P}^1 + \bar{b}^{\mathrm{s}}_{33}\left.\frac{\partial \tilde{W}^0}{\partial \zeta}\right|_{\zeta=0} = -\bar{b}^{\mathrm{s}}_{13}\nabla_\eta \cdot \tilde{\mathbf{V}}^0\big|_{\zeta=0}, \quad \left.\frac{\partial \tilde{P}^1}{\partial \zeta}\right|_{\zeta=0} = 0. \end{aligned} \tag{6.47}$$

The general solution of the homogeneous differential system corresponding to Eq. (6.46) is given by

$$\begin{aligned} \tilde{W}^0_0 &= C_0 + C_1 \cosh\sqrt{f(s)}\zeta + C_2 \sinh\sqrt{f(s)}\zeta, \\ \tilde{P}^1_0 &= C_3 + \frac{s}{\sqrt{f(s)}}\left(C_1 \sinh\sqrt{f(s)}\zeta + C_2 \cosh\sqrt{f(s)}\zeta\right), \end{aligned}$$

where we have introduced the notation

$$f(s) = \frac{s}{\bar{b}^{\mathrm{s}}_{33}}.$$

It can be shown that, in light of (6.45), the following pair represents a particular solution of the system (6.46):

$$\begin{aligned} \tilde{W}^0_1 &= \left(\frac{2}{s}\left[\bar{b}^{\mathrm{s}}_{44} + \bar{b}^{\mathrm{s}}_{13} - \bar{b}^{\mathrm{s}}_{33} + \kappa_1 \bar{b}^{\mathrm{s}}_{44}\right] + 1 - \frac{\zeta^2}{6}\right)\frac{\zeta}{2\bar{b}^{\mathrm{s}}_{44}}\Delta_\eta \tilde{Q}, \\ \tilde{P}^1_1 &= \frac{(\bar{b}^{\mathrm{s}}_{44} + \bar{b}^{\mathrm{s}}_{13} - \bar{b}^{\mathrm{s}}_{33})}{2\bar{b}^{\mathrm{s}}_{44}}\zeta^2 \Delta_\eta \tilde{Q}. \end{aligned}$$

Substituting the expressions

$$\tilde{W}^0 = \tilde{W}_0^0 + \tilde{W}_1^0, \quad \tilde{P}^1 = \tilde{P}_0^1 + \tilde{P}_1^1 \tag{6.48}$$

into the system of boundary conditions (6.47) and taking into account Eq. (6.45), we evaluate the integration constants C_0, C_1, C_2, and C_3 as follows:

$$C_0 = -\Big(\frac{1}{3\bar{b}_{44}^{\mathrm{s}}} + \frac{\kappa_1}{s}\Big)\Delta_\eta \tilde{Q}, \quad C_1 = 0, \quad C_2 = -\frac{(\bar{b}_{44}^{\mathrm{s}} + \bar{b}_{13}^{\mathrm{s}} - \bar{b}_{33}^{\mathrm{s}})}{s\bar{b}_{44}^{\mathrm{s}}} \frac{\Delta_\eta \tilde{Q}}{\sinh\sqrt{f(s)}},$$

$$C_3 = \frac{\bar{b}_{33}^{\mathrm{s}}}{2\bar{b}_{44}^{\mathrm{s}}}\Big(\frac{2}{s}(\bar{b}_{44}^{\mathrm{s}} + \bar{b}_{13}^{\mathrm{s}} - \bar{b}_{33}^{\mathrm{s}} + \kappa_1 \bar{b}_{44}^{\mathrm{s}}) + 1 - \frac{\bar{b}_{13}^{\mathrm{s}}}{\bar{b}_{33}^{\mathrm{s}}}\Big)\Delta_\eta \tilde{Q}.$$

The functions W, $\mathbf{V}$, and P can thus be obtained by performing the inverse Laplace transform.

6.2.3 Local Indentation of a Thin BPVE Layer

Recall that $B_{44}^{\mathrm{s}}(t)$ represents the out-of-plane relaxation modulus in shear so that, in light of the zero initial conditions, Eqs. $(6.34)_2$ and $(6.34)_4$ take the form

$$\sigma_{3i}(t) = 2\int_{0^-}^{t} B_{44}^{\mathrm{s}}(t-\tau)\dot{\varepsilon}_{3i}(\tau)\,d\tau, \quad i = 1, 2. \tag{6.49}$$

Let us introduce the out-of-plane creep compliance in shear of the solid matrix, $J_{44}^{\mathrm{s}}(t)$, which governs the deformation response of the solid phase under application of a step out-of-plane shear stress of unit magnitude. Hence, the inverse relations for (6.49) are given by

$$2\varepsilon_{3i}(t) = \int_{0^-}^{t} J_{44}^{\mathrm{s}}(t-\tau)\dot{\sigma}_{3i}(\tau)\,d\tau, \quad i = 1, 2.$$

For a given relaxation modulus $B_{44}^{\mathrm{s}}(t)$ and its Laplace transform $\tilde{B}_{44}^{\mathrm{s}}(s)$ (with respect to the time variable t), the corresponding creep compliance can be evaluated through its Laplace transform

$$\tilde{J}_{44}^{\mathrm{s}}(s) = \frac{1}{s^2\tilde{B}_{44}^{\mathrm{s}}(s)}. \tag{6.50}$$

Thus, collecting formulas (6.39), (6.44), (6.45), (6.48) and taking account of (6.50), we obtain the following asymptotic representations for the displacements of the surface points of the thin bonded BPVE layer:

$$\mathbf{v}\big|_{z=0} \simeq -\frac{h^2}{2}\int\limits_{0^-}^{t} J_{44}^{\mathrm{s}}(t-\tau)\frac{\partial}{\partial\tau}\nabla_y q(\tau,\mathbf{y})\,d\tau, \tag{6.51}$$

$$w\big|_{z=0} \simeq -\frac{h^3}{3}\int\limits_{0^-}^{t} J_{44}^{\mathrm{s}}(t-\tau)\frac{\partial}{\partial\tau}\Delta_y q(\tau,\mathbf{y})\,d\tau - hk_1\int\limits_{0}^{t}\Delta_y q(\tau,\mathbf{y})\,d\tau. \tag{6.52}$$

Observe that the derived asymptotic formula (6.52) reflects two types of mechanisms, which are responsible for time-dependent effects in articular cartilage: the flow independent and the flow dependent, characterized by the first and second terms on the right-hand side of (6.52), respectively.

The asymptotic relations (6.51) and (6.52) will be used to formulate asymptotic models for the frictionless contact interaction between thin bonded BPVE layers.

6.2.4 Reduced Relaxation and Creep Function for the Fung Model

Recall (see Sect. 5.4.1) that the so-called reduced stress-relaxation function, $\psi(t)$, is defined by

$$B_{44}^{\mathrm{s}}(t) = B_{44}^{\mathrm{s}\infty}\psi(t),$$

where $B_{44}^{\mathrm{s}\infty} = B_{44}^{\mathrm{s}}(+\infty)$ is the equilibrium modulus.

Let us now consider the reduced creep function, $\varphi(t)$, defined by the formula

$$J_{44}^{\mathrm{s}}(t) = J_{44}^{\mathrm{s}\infty}\varphi(t).$$

Here, $J_{44}^{\mathrm{s}\infty} = J_{44}^{\mathrm{s}}(+\infty)$ is the equilibrium compliance such that $J_{44}^{\mathrm{s}\infty} = 1/B_{44}^{\mathrm{s}\infty}$.

The following normalization conditions then hold:

$$\psi(+\infty) = 1, \quad \varphi(+\infty) = 1.$$

The reduced relaxation function can be represented in terms of a relaxation spectrum $S(\tau)$ as follows:

$$\psi(t) = 1 + \int\limits_{0}^{\infty} S(\tau)e^{-t/\tau}d\tau.$$

According to Fung [13], in order to account for the weakly frequency dependent behavior of soft biological tissues, the relaxation spectrum is taken in the form

$$S(\tau) = \begin{cases} \dfrac{c}{\tau}, & \tau_1 \le \tau \le \tau_2, \\ 0, & \tau < \tau_1, \quad \tau > \tau_2, \end{cases}$$

where τ_1 and τ_2 have the dimension of time, and c is dimensionless.

The Fung reduced relaxation function can be evaluated as

$$\psi(t) = 1 + c\Big[E_1\Big(\frac{t}{\tau_2}\Big) - E_1\Big(\frac{t}{\tau_1}\Big)\Big], \tag{6.53}$$

where $E_1(x) = \int_x^\infty e^{-\xi}/\xi \, d\xi$ is the exponential integral function.

The Fung reduced creep function $\varphi(t)$ corresponding to the reduced relaxation function $\psi(t)$ given by Eq. (6.53) can be obtained by employment of the Laplace transform and Eq. (6.50), that is

$$\tilde{\psi}(s)\tilde{\varphi}(s) = \frac{1}{s^2},$$

where the Laplace transform $\tilde{\psi}(s)$ is given by formula (5.197). Note also that the above relation immediately implies that

$$\int_0^t \psi(t-\tau)\varphi(\tau)\, d\tau = t.$$

According to Dortmans et al. [10], the following formula holds:

$$\begin{aligned} \varphi(t) = 1 &- \frac{(\tau_c - \tau_2)(\tau_c - \tau_1)}{c\tau_c(\tau_2 - \tau_1)} e^{-t/\tau_c} \\ &- c\int_{\tau_1}^{\tau_2} e^{-t/\tau} \frac{1}{\tau} \frac{1}{\Big(1 + c\ln\dfrac{\tau_2 - \tau}{\tau - \tau_1}\Big)^2 + \pi^2 c^2}\, d\tau, \end{aligned} \tag{6.54}$$

where we have used the notation

$$\tau_c = \frac{\tau_2 e^{1/c} - \tau_1}{e^{1/c} - 1}.$$

From (6.53) and (6.54), we find

$$\psi(0) = 1 + c\ln\frac{\tau_2}{\tau_1},$$

$$\varphi(0) = 1 - \frac{(\tau_c - \tau_2)(\tau_c - \tau_1)}{c\tau_c(\tau_2 - \tau_1)} - c\int_{\tau_1}^{\tau_2} \frac{1}{\tau} \frac{1}{\left(1 + c\ln\dfrac{\tau_2 - \tau}{\tau - \tau_1}\right)^2 + \pi^2 c^2}\, d\tau.$$

It can be numerically verified that $\psi(0)\varphi(0) = 1$. We conclude this case by noting that the creep spectrum corresponding to (6.54) was discussed in [10].

6.3 Contact of Thin Bonded Transversely Isotropic BPVE Layers

In this section, the leading-order asymptotic models have been developed for the short-time frictionless contact interaction between thin biphasic poroviscoelastic layers bonded to rigid impermeable substrates shaped like elliptic paraboloids.

6.3.1 Contact Problem Formulation for BPVE Cartilage Layers

When studying contact problems for real joint geometries, a numerical analysis, such as the finite element method, is necessary [6, 14, 27], since exact analytical solutions were obtained only for two-dimensional [5, 16], or axisymmetric and simple geometries [11, 12, 21]. In particular, the two-dimensional contact creep problem between two cylindrical biphasic layers bonded to rigid impermeable substrates was solved by Kelkar and Ateshian [18] for all times and arbitrary layer thicknesses using the integral transform method. The frictionless rolling contact problem for cylindrical biphasic layers was analytically studied by Ateshian and Wang [5].

An asymptotic solution for the contact problem of two identical isotropic biphasic cartilage layers attached to two rigid impermeable spherical bones of equal radii modeled as elliptic paraboloids was obtained by Ateshian et al. [7]. This solution was extended by Wu et al. [24] to a more general model by combining the assumption of the kinetic relationship from classical contact mechanics [17] with the joint contact model for the contact of two biphasic cartilage layers [7]. An improved solution for the contact of two biphasic cartilage layers which can be used for dynamic loading was obtained by Wu et al. [25]. These solutions have been widely used as the theoretical background in modeling articular contact mechanics.

Later, Mishuris and Argatov [1, 22] refined the analysis of [7, 24] by formulating the contact condition which takes into account the tangential displacements at the contact interface. Finally, the axisymmetric model of articular contact mechanics originally developed in [7, 24] was generalized in [2] in the case of elliptical contact.

In this section, the asymptotic model of articular contact for isotropic biphasic layers [2, 7, 24] is extended for the transversely isotropic BPVE case.

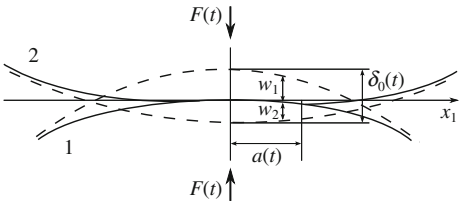

Fig. 6.3 Schematic diagram of the contact of articular cartilage surfaces *1* and *2* under the external load $F(t)$. The *dashed lines* imply the surfaces' profiles in the undeformed state

Consider two thin articular cartilage layers of uniform thicknesses h_1 and h_2 firmly attached to subchondral bones. Let $w_0^{(1)}(t, \mathbf{y})$ and $w_0^{(2)}(t, \mathbf{y})$ be the absolute values of the vertical displacements of the boundary points of the cartilage layers (see Fig. 6.3). Let also $\delta_0(t)$ denote the contact (vertical) approach of the rigid subchondral bones under a specified external vertical load, $F(t)$, which is assumed to be a function of the time variable t.

Further, let $\varphi(\mathbf{y})$ denote the gap between the layer surfaces before deformation. Here, following Argatov and Mishuris [2, 3], we consider a special case of the gap function represented by an elliptic paraboloid

$$\varphi(\mathbf{y}) = \frac{y_1^2}{2R_1} + \frac{y_2^2}{2R_2}, \tag{6.55}$$

where R_1 and R_2 are positive constants having dimensions of length.

Then, the linearized contact condition in the contact area $\omega(t)$ can be written as

$$w_0^{(1)}(t, \mathbf{y}) + w_0^{(2)}(t, \mathbf{y}) = \delta_0(t) - \varphi(\mathbf{y}), \quad \mathbf{y} \in \omega(t). \tag{6.56}$$

In the case of unilateral contact, the contact pressure between the cartilage layers, $p(\mathbf{y})$, is assumed to be positive inside the contact area $\omega(t)$ and satisfies the following boundary conditions [7] (see also [15, 23]):

$$p(t, \mathbf{y}) = 0, \quad \frac{\partial p}{\partial n}(t, \mathbf{y}) = 0, \quad \mathbf{y} \in \Gamma(t).$$

Here, $\partial/\partial n$ is the normal derivative at the contour $\Gamma(t)$ of the domain $\omega(t)$.

Moreover, the following equilibrium equation holds:

$$F(t) = \iint\limits_{\omega(t)} p(t, \mathbf{y})\, d\mathbf{y}.$$

Applying the leading-order asymptotic model (6.52) for the short-time deformation of a thin bonded biphasic poroviscoelastic (BPVE) layer, we approximate the vertical displacement of the surface points of the nth cartilage layer by the formula

$$w_0^{(n)}(t,\mathbf{y}) = -\frac{h_n^3}{3}\int\limits_{0^-}^{t} J_{44}^{\mathrm{s}(n)}(t-\tau)\frac{\partial}{\partial\tau}\Delta_y p(\tau,\mathbf{y})\,d\tau - h_n k_1^{(n)}\int\limits_{0}^{t}\Delta_y p(\tau,\mathbf{y})\,d\tau, \tag{6.57}$$

where $J_{44}^{\mathrm{s}(n)}(t)$ and $k_1^{(n)}$ are the out-of-plane creep compliance in shear of the solid matrix and the transverse (in-plane) permeability coefficient of the nth cartilage layer, respectively.

Let us simplify the mathematical formalism. First, by letting

$$G_0^{\prime\mathrm{s}(n)} = \frac{1}{J_{44}^{\mathrm{s}(n)}(0^+)}$$

we introduce the instantaneous out-of-plane shear elastic modulus of the solid matrix of the nth layer.

Second, using the integration by parts formula, we represent the second integral in (6.57) as follows:

$$\int\limits_{0}^{t}\Delta_y p(\tau,\mathbf{y})\,d\tau = \int\limits_{0^-}^{t}(t-\tau)\frac{\partial}{\partial\tau}\Delta_y p(\tau,\mathbf{y})\,d\tau.$$

Third, combining the fluid flow-independent viscoelasticity and the fluid flow-dependent viscous effects in articular cartilage, we introduce the following generalized normalized creep function of the nth thin BPVE layer:

$$\Phi^{(n)}(t) = G_0^{\prime\mathrm{s}(n)} J_{44}^{\mathrm{s}(n)}(t) + \frac{3G_0^{\prime\mathrm{s}(n)}}{h_n^2}k_1^{(n)}t. \tag{6.58}$$

Finally, the compound creep function, $\Phi_\beta(t)$, and the equivalent instantaneous shear elastic modulus, G_0', can be defined as follows (cf. Eqs. (4.102)–(4.105)):

$$\Phi_\beta(t) = \beta_1\Phi^{\prime(1)}(t) + \beta_2\Phi^{\prime(2)}(t),$$

$$G_0' = \frac{(h_1+h_2)^3 G_0^{\prime\mathrm{s}(1)} G_0^{\prime\mathrm{s}(2)}}{h_1^3 G_0^{\prime\mathrm{s}(2)} + h_2^3 G_0^{\prime\mathrm{s}(1)}}, \tag{6.59}$$

$$\beta_1 = \frac{h_1^3 G_0^{\prime\mathrm{s}(2)}}{h_1^3 G_0^{\prime\mathrm{s}(2)} + h_2^3 G_0^{\prime\mathrm{s}(1)}}, \quad \beta_2 = \frac{h_2^3 G_0^{\prime\mathrm{s}(1)}}{h_1^3 G_0^{\prime\mathrm{s}(2)} + h_2^3 G_0^{\prime\mathrm{s}(1)}}.$$

Thus, following the above relations, and after the substitution of the asymptotic approximations (6.57) into Eq. (6.56), we arrive at the governing integro-differential equation

$$-\int_{0-}^{t} \Phi_\beta(t-\tau)\Delta_y \frac{\partial p}{\partial \tau}(\tau,\mathbf{y})\,d\tau = m\big(\delta_0(t)-\varphi(\mathbf{y})\mathscr{H}(t)\big), \quad \mathbf{y}\in\omega(t). \tag{6.60}$$

where the Heaviside function factor $\mathscr{H}(t)$ takes into account the zero initial conditions for $t<0$, and m is given by (with $h=h_1+h_2$ being the joint thickness)

$$m=\frac{3G_0'}{h^3}.$$

Equation (6.60) can be used to determine the contact pressure distribution $p(t,\mathbf{y})$ between BPVE cartilage layers under the monotonicity condition $\omega(t_1)\subset\omega(t_2)$ for $t_1\le t_2$. The monotonicity condition that the contact zone increases for non-decreasing loads, when $dF(t)/dt\ge 0$, should be checked a posteriori.

6.3.2 Exact Solution for Monotonic Loading

As in the Hertz theory of elliptic contact between two elastic bodies, the contact area $\omega(t)$ between the cartilage layers with the initial gap determined by Eq. (6.55) is elliptic with the semi-axes $a(t)$ and $b(t)$ changing with time. The form of the ellipse $\Gamma(t)$ can be characterized by its aspect ratio $s=b(t)/a(t)$. Assuming, as usual, that $R_1\ge R_2$, we obtain $a(t)\ge b(t)$, and, generally, $0<s\le 1$ where the value $s=1$ corresponds to a circular contact area. We emphasize that the parameter s is constant during loading and depends only on the ratio R_2/R_1 via the following relation (see Sect. 4.5):

$$s=\sqrt{\sqrt{\left(\frac{R_1-R_2}{6R_1}\right)^2+\frac{R_2}{R_1}}-\frac{(R_1-R_2)}{6R_1}}.$$

The evolution of the major semi-axis of the contact area is governed by formula

$$a(t)=\left(\frac{96\sqrt{R_1R_2}}{\pi m}\right)^{1/6} c_a(s)\left(\int_{0-}^{t}\Phi_\beta(t-\tau)\frac{dF(\tau)}{d\tau}\,d\tau\right)^{1/6}. \tag{6.61}$$

Here, $\sqrt{R_1R_2}$ is a geometric mean of the radii R_1 and R_2, while $c_a(s)$ is a dimensionless factor given by (see Fig. 6.4)

$$c_a(s)=\left(\frac{\sqrt{(3s^2+1)(s^2+3)}}{4s^4}\right)^{1/6}.$$

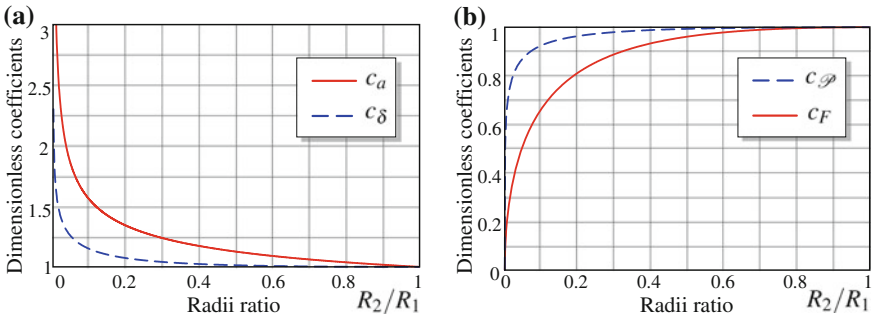

Fig. 6.4 Dimensionless scaling factors: **a** Coefficients c_a and c_δ; **b** Coefficients $c_{\mathscr{P}}$ and c_F. It is interesting that this behavior for the different scaling factors is overall substantially similar.

The contact approach between the subchondral bones is given by

$$\delta_0(t) = \left(\frac{3}{2\pi m R_1 R_2}\right)^{1/3} c_\delta(s) \left(\int_{0-}^{t} \Phi_\beta(t-\tau)\frac{dF(\tau)}{d\tau}\,d\tau\right)^{1/3}, \tag{6.62}$$

where we have introduced the notation

$$c_\delta(s) = \left(\frac{2(s^2+1)^3}{s(3s^2+1)(s^2+3)}\right)^{1/3}.$$

Now, if the contact load $F(t)$ is known, then Eqs. (6.61) and (6.62) allow us to determine the quantities $a(t)$ and $\delta_0(t)$, respectively.

The contact pressure is calculated by means of the formula

$$p(t,\mathbf{y}) = \mathscr{P}_0(t)\left(1 - \frac{y_1^2}{a(t)^2} - \frac{y_2^2}{s^2 a(t)^2}\right)^2 - \int_{t_*(\mathbf{y})}^{t} \frac{\partial \Psi_\beta}{\partial \tau}(t-\tau)\mathscr{P}_0(\tau)\left(1 - \frac{y_1^2}{a(\tau)^2} - \frac{y_2^2}{s^2 a(\tau)^2}\right)^2 d\tau. \tag{6.63}$$

Here, $\Psi_\beta(t)$ is the corresponding generalized normalized relaxation function determined by its Laplace transform $\tilde{\Psi}_\beta(s) = 1/[s^2\tilde{\Phi}_\beta(s)]$, s is the Laplace transform parameter, and $\mathscr{P}_0(t)$ is an auxiliary function given by

$$\mathscr{P}_0(t) = \left(\frac{27m}{96\pi^2\sqrt{R_1 R_2}}\right)^{1/3} c_{\mathscr{P}}(s) \left(\int_{0-}^{t} \Phi_\beta(t-\tau)\frac{dF(\tau)}{d\tau}\,d\tau\right)^{2/3},$$

where we have introduced the notation

$$c_{\mathscr{P}}(s) = \left(\frac{4s}{\sqrt{(3s^2+1)(s^2+3)}} \right)^{1/3}.$$

The quantity $t_*(\mathbf{y})$, which enters the lower limit in the integral (6.63), is the time when the contour of the contact area $\omega(t)$ first reaches the point $\mathbf{y}$. If, however, the point under consideration lies inside the instantaneous contact area, i.e., $\mathbf{y} \in \omega(0^+)$, then $t_*(\mathbf{y}) \equiv 0$. The quantity $t_*(\mathbf{y})$ is called the time-to-contact for the point $\mathbf{y}$. When the point $\mathbf{y}$ is located outside of $\omega(0^+)$, the nonzero quantity of $t_*(\mathbf{y})$ is determined by the equation $a(t_*)^2 = y_1^2 + y_2^2/s^2$, or in accordance with Eq. (6.61) by the following:

$$\int_{0-}^{t_*} \Phi_\beta(t_* - \tau) \frac{dF(\tau)}{d\tau}\, d\tau = \frac{\pi m}{96\sqrt{R_1 R_2}\, c_a(s)^6} \left(y_1^2 + \frac{y_2^2}{s^2} \right)^3.$$

In the case of a stepwise loading, we have $F(t) = F_0 \mathscr{H}(t)$, and the above equation reduces to

$$\Phi_\beta(t_*) = \frac{1}{a_0^6} \left(y_1^2 + \frac{y_2^2}{s^2} \right)^3, \tag{6.64}$$

where $a_0 = a(0^+)$ is the instantaneous value of the major semi-axis, which is given by

$$a_0 = \left(\frac{96\sqrt{R_1 R_2}}{\pi m} \right)^{1/6} c_a(s) F_0^{1/6}.$$

We note that the asymptotic model (6.57), $n = 1, 2$, holds true only when the cartilage thicknesses are small compared with the characteristic size of the contact area, i.e., $\max\{h_1, h_2\} \ll a_0$. For this reason the contact force F_0, and $F(0^+)$ generally, should not take too small values.

Table 6.1 Isotropic and transversely isotropic biphasic material properties of human articular cartilage. The highlighted values are used in the asymptotic models [9]

Material property	Isotropic	Transversely isotropic
Young's modulus E_3^s (MPa)	0.69	0.46
Young's modulus E_1^s (MPa)	0.69	5.8
Poisson's ratio ν_{12}^s	0.0	0.0
Poisson's ratio ν_{31}^s	0.0	0.0
Shear modulus G_{13}^s (MPa)	0.345	0.37
Shear modulus $G_{12}^s = E_1^s/[2(1+\nu_{12}^s)]$ (MPa)	0.345	0.23
Permeability $k_1 = k_3$ ($\times 10^{-15}$m^4/Ns)	3.0	5.1
Solid volume fraction ϕ^s	0.25	0.25

Thus, in the case of a stepwise loading, formula (6.63), where quantity $t_*(\mathbf{y})$ is determined by Eq. (6.64), represents the sought for solution of Eq. (6.60). Note that in the case of the biphasic layers the derived expression for the contact pressure coincides with the result obtained previously in [2].

Table 6.1 shows some typical values for biphasic material properties of human articular cartilage in the isotropic and transversely isotropic cases. It is known that the mechanical properties of cartilage may change with disease. In particular, the early stages of osteoarthritis are characterized [26] by increased permeability, increased thickness of the cartilage layers, reduced shear modulus, increased Poisson's ratio, and/or a combination of these effects.

To conclude, we emphasize (see, e.g., [7, 25]) that specifically in regard to articular cartilage, the constructed asymptotic model, which is based on the short-time asymptotic solution of the deformation problem for a thin BPVE layer and assumes that most of the contact load is carried by the interstitial fluid, can be used for time periods of several thousand seconds, when the articular joint is biologically functional, and becomes invalid for time $t \to \infty$, when the interstitial fluid is pushed out of the cartilage layer underlying the contact area and the total contact pressure is carried only by the solid phase of the cartilage.

References

1. Argatov, I., Mishuris, G.: Axisymmetric contact problem for a biphasic cartilage layer with allowance for tangential displacements on the contact surface. Eur. J. Mech. A/Solids **29**, 1051–1064 (2010)
2. Argatov, I., Mishuris, G.: Elliptical contact of thin biphasic cartilage layers: exact solution for monotonic loading. J. Biomech. **44**, 759–761 (2011)
3. Argatov, I., Mishuris, G.: Frictionless elliptical contact of thin viscoelastic layers bonded to rigid substrates. Appl. Math. Model. **35**, 3201–3212 (2011)
4. Argatov, I.I., Mishuris, G.S.: An asymptotic model for a thin biphasic poroviscoelastic layer. Quart. J. Mech. Appl. Math. (2015). doi:10.1093/qjmam/hbv008
5. Ateshian, G.A., Wang, H.: A theoretical solution for the frictionless rolling contact of cylindrical biphasic articular cartilage layers. J. Biomech. **28**, 1341–1355 (1995)
6. Ateshian, G.A., Maas, S., Weiss, J.A.: Finite element algorithm for frictionless contact of porous permeable media under finite deformation and sliding. J. Biomech. Eng. **132**, 061006 (13 pages) (2010)
7. Ateshian, G.A., Lai, W.M., Zhu, W.B., Mow, V.C.: An asymptotic solution for the contact of two biphasic cartilage layers. J. Biomech. **27**, 1347–1360 (1994)
8. Barry, S.I., Holmes, M.: Asymptotic behaviour of thin poroelastic layers. IMA J. Appl. Math. **66**, 175–194 (2001)
9. Donzelli, P.S., Spilker, R.L., Ateshian, G.A., Mow, V.C.: Contact analysis of biphasic transversely isotropic cartilage layers and correlations with tissue failure. J. Biomech. **32**, 1037–1047 (1999)
10. Dortmans, L.J.M.G., van de Ven, A.A.F., Sauren, A.A.H.J.: A note on the reduced creep function corresponding to the quasi-linear visco-elastic model proposed by Fung. J. Biomech. Eng. **116**, 373–375 (1994)
11. Eberhardt, A.W., Keer, L.M., Lewis, J.L., Vithoontien, V.: An analytical model of joint contact. J. Biomech. Eng. **112**, 407–413 (1990)

12. Eberhardt, A.W., Keer, L.M., Lewis, J.L.: Normal contact of elastic spheres with two elastic layers as a model of joint articulation. J. Biomech. Eng. **113**, 410–417 (1991)
13. Fung, Y.C.: Biomechanics: Mechanical Properties of Living Tissues. Springer, New York (1981)
14. Han, S.K., Federico, S., Epstein, M., Herzog, W.: An articular cartilage contact model based on real surface geometry. J. Biomech. **38**, 179–184 (2005)
15. Hlaváček, M.: A note on an asymptotic solution for the contact of two biphasic cartilage layers in a loaded synovial joint at rest. J. Biomech. **32**, 987–991 (1999)
16. Hlaváček, M.: Frictionless contact of two parallel congruent rigid cylindrical surfaces coated with thin elastic incompressible transversely isotropic layers: an analytic solution. Eur. J. Mech. A/Solids **25**, 497–508 (2006)
17. Johnson, K.L.: Contact Mechanics. Cambridge University Press, Cambridge (1985)
18. Kelkar, R., Ateshian, G.A.: Contact creep of biphasic cartilage layers. J. Appl. Mech. **66**, 137–145 (1999)
19. Lavrentyev, M.A., Shabat, B.V.: Methods of Complex Variable Functions. Nauka, Moscow (1987) (in Russian)
20. LePage, W.R.: Complex Variables and the Laplace Transform for Engineers. McGraw-Hill, New York (1961)
21. Li, G., Sakamoto, M., Chao, E.Y.S.: A comparison of different methods in predicting static pressure distribution in articulating joints. J. Biomech. **30**, 635–638 (1997)
22. Mishuris, G., Argatov, I.: Exact solution to a refined contact problem for biphasic cartilage layers. In: Nithiarasu, P., Löhner, R. (eds.) Proceedings of the 1st International Conference on Mathematical and Computational Biomedical Engineering—CMBE2009, pp. 151–154. Swansea, June 29–July 1 2009
23. Wu, J.Z., Herzog, W.: On the pressure gradient boundary condition for the contact of two biphasic cartilage layers. J. Biomech. **33**, 1331–1332 (2000)
24. Wu, J.Z., Herzog, W., Ronsky, J.: Modeling axi-symmetrical joint contact with biphasic cartilage layers—an asymptotic solution. J. Biomech. **29**, 1263–1281 (1996)
25. Wu, J.Z., Herzog, W., Epstein, M.: An improved solution for the contact of two biphasic cartilage layers. J. Biomech. **30**, 371–375 (1997)
26. Wu, J.Z., Herzog, W., Epstein, M.: Joint contact mechanics in the early stages of osteoarthritis. Med. Eng. Phys. **22**, 1–12 (2000)
27. Yang, T., Spilker, R.L.: A Lagrange multiplier mixed finite element formulation for three-dimensional contact of biphasic tissues. J. Biomech. Eng. **129**, 457–471 (2007)

Chapter 7
Articular Contact Mechanics

Abstract In this chapter, an asymptotic modeling methodology for tibio-femoral contact is developed, based on the asymptotic models of frictionless unilateral contact interaction between thin cartilage layers. In Sect. 7.1, the normal contact forces, which are needed for multibody dynamics simulations, are determined analytically based on the exact solution for elliptical contact between thin cartilage layers generally modeled as viscoelastic incompressible layers. In Sect. 7.2, the equivalent Hunt–Crossley model for articular contact is developed in the framework of the short-time contact model for thin bonded biphasic layers.

7.1 Asymptotic Modeling Methodology for Tibio-Femoral Contact

In Sects. 7.1.1 and 7.1.2, we present a brief overview of the principal models used in multibody dynamics simulations of human-body locomotion. The asymptotic modeling approach outlined in Sects. 7.1.3–7.1.5 requires use of the smooth contact surface geometry and efficient contact points detection methods, while in Sect. 7.1.6, the articulating femur and tibia geometries are approximated by elliptic paraboloids. In Sect. 7.1.7, the effective geometric characteristics of articular surfaces are introduced for use in the developed asymptotic models of elliptical contact between articular surfaces.

7.1.1 Articular Contact in Multibody Dynamics

Mathematical modeling of the distributed forces generated by articular contact in joints is required for multibody dynamic simulations of physical exercise of a human skeleton based on the rigid multibody approach [34] as well as on the flexible multibody approach [59]. It is believed that dynamic and impact patterns of the contact pressures play an important role in the development and progression of knee joint osteoarthritis [46]. Therefore, multibody dynamic models of the knee joint capable

I. Argatov and G. Mishuris, *Contact Mechanics of Articular Cartilage Layers*,
Advanced Structured Materials 50, DOI 10.1007/978-3-319-20083-5_7

of predicting contact pressures between the articular cartilage layers would be also useful for studying the mechanical aspects of this degenerative disease.

In a number of multibody dynamic models for the tibio-femoral joint [2, 69, 86], the problem of articular contact is resolved under the assumption of a rigid contact formulation, where the contact interaction between the surface of each femoral condyle and the surface of the tibia is realized at a single point and no deformation is considered in the articular cartilage layers due to the contact loading. In contrast to the rigid contact model, the deformable contact models, which take into account deformation of the articular cartilage layers, require not only a description of the articular surface geometry, but also additional information about the deformation behavior of articular cartilage. As was pointed out [24], the advantage of the deformable articular contact models over the rigid contact model is two-fold: firstly, they are not restricted to contraform contact and conforming surfaces can also be considered, and secondly the knee multibody dynamic models with deformable contact have higher numerical stability.

We observe (see, e.g., [22, 70]) that a multibody knee contact modeling methodology based on the deformable contact model should include the implementation of an efficient mathematical model for calculating contact pressures and the resulting contact forces. A number of models of the knee joint employ different forms of the elastic Winkler foundation model [24]. We recall (see Sect. 1.5.1) that the deformation response of a thin transversely isotropic compressible layer of thickness h resembles that of a Winkler elastic foundation with the modulus

$$k = \frac{h}{A_{33}},$$

where, with E, ν and E', ν' being respectively the in-plane and out-of-plane Young's modulus and Poisson's ratio,

$$A_{33} = E'(1-\nu)\left(1-\nu-\frac{2E}{E'}\,\nu'^2\right)^{-1}.$$

For two thin compressible layers in contact, the joint Winkler foundation modulus is defined as $k = (k_1^{-1} + k_2^{-1})^{-1}$, and in the isotropic case is given by

$$k = \left(\frac{(1+\nu_1)(1-2\nu_1)h_1}{(1-\nu_1)E_1} + \frac{(1+\nu_2)(1-2\nu_2)h_2}{(1-\nu_2)E_2}\right)^{-1}. \tag{7.1}$$

Furthermore, if the layers' materials are similar (i.e., $E_1 = E_2 = E$ and $\nu_1 = \nu_2 = \nu$), formula (7.1) simplifies to

$$k = \frac{(1-\nu)E}{(1+\nu)(1-2\nu)h}, \tag{7.2}$$

where $h = h_1 + h_2$ is the joint thickness. It is readily seen that the denominator in formula (7.2) vanishes in the incompressibility limit as $\nu \to 0.5$, and consequently the Winkler foundation modulus k tends to infinity.

The fact that a thin isotropic elastic layer, with a Poisson's ratio sufficiently different to 0.5, behaves like a Winkler elastic foundation was first rigorously established in [3]. The case of elliptical contact in the framework of Winkler's foundation model was considered in detail in [54]. The elastic foundation model based on Eq. (7.2) was used for multibody dynamic simulation of knee contact mechanics in a number of papers [24, 77]. Formula (7.1) was considered in [79] within a discussion of the analytical models employed for describing articular contact.

It is known [21] that the Winkler elastic foundation model is appropriate for describing the stress-deformation behavior of thin compressible elastic coating layers, and that it fails to represent the contact interaction of incompressible layers. At the same time, it has been shown [19] that the instantaneous response of a biphasic cartilage layer under distributed normal forces is in perfect agreement with the corresponding solution for a bonded thin incompressible elastic layer.

In recent years, finite-element (FE) models have been increasingly developed to simulate articular contact [85, 88]. In particular, a mathematical model of distributed contact using a number of contacting patches was employed in [27] with a uniform stress distribution assumed over each contact patch. The advantage of FE models over the elastic foundation model is based on their ability to evaluate the sub-surface stresses. Moreover, FE models are not confined to simple geometrical configurations, which are necessary for deriving analytical solutions like those used in the rigid contact model. However, in comparison [79] with simple deformable contact models, FE models are expensive in time and resources for the simulation of the knee joint dynamics in real activities such as the gait cycle.

To lower the high computational cost of repeated contact analysis within multibody dynamic simulation, the so-called surrogate modeling approach for performing computationally efficient three-dimensional elastic contact with general surface geometry was proposed [68]. The surrogate modeling method [68] fits a computationally cheap surrogate contact model to data points sampled from a computationally expensive FE elastic contact model.

7.1.2 Articular Cartilage Structure and Models

Articular cartilage is typically 2–4 mm thick and is composed of a dense extracellular matrix (ECM) with a sparse distribution of cells called chondrocytes. The ECM primarily consists of water, collagen, and proteoglycans. It is estimated [35] that the average pore size within the ECM is approximately 6.0 mm.

The structure of articular cartilage is often described in terms of the following four zones between the articular surface and the subchondral bone [35, 51, 72, 75]: the surface (or superficial/tangential) zone, the transitional (or middle) zone, the deep zone, and the calcified zone.

Tangential/superficial zone. The thin superficial zone protects deeper layers from shear stresses and makes up approximately 10 to 20 % of articular cartilage thickness. This zone is characterised by the tight parallel alignment of both the collagen fibers and the chondrocytes to the articular surface.

Middle/transitional zone. The middle zone represents 40 to 60 % of the total cartilage volume. In the transitional zone, the ECM and cells arch over from the perpendicular alignment with respect to the articular surface, seen in the deep zone, to the parallel alignment of the superficial zone, whereas the collagen fibrils are isotropically arranged.

Deep zone. The deep zone represents approximately 30 % of the articular cartilage volume. The chondrocytes are typically arranged in a columnar orientation perpendicular to the articular surface, this alignment being replicated in fibrils of the collagen matrix. It was experimentally observed [4, 5] that the commonly described deep zone longitudinal fibres were found to be tubular structures filled with fluid. We also note that in the deformation analysis of articular cartilage, this phenomenon can be described by microstructural models [25].

Calcified zone. The calcified layer plays an integral role in securing the cartilage to subchondral bone. The tide mark, the calcification front, is used to distinguish the deep zone from the calcified zone. The calcification of the collagen fibrils is found at the base of the deep zone.

We observe (see, e.g., [26]) that articular cartilage tissue in vivo is exposed to extremely complicated loading histories throughout life and even the period of a day. It is the cumulative influence of these loading histories that governs the biology of the tissue. At the same time articular cartilage is avascular and the movement of fluid into and out of cartilage (by 'pumping' solutes through the matrix under cyclic loading) aids nutrition and removal of the by-products of metabolism [76]. It is known [58] that mechanical forces can modulate synthesis and degradation of articular cartilage matrix, and can influence structural and functional adaptation of the tissue [55]. It is also known [57] that due to its avascular nature, articular cartilage has a very limited capacity to regenerate or repair. Phenomenological damage models for fibrous tissues like articular cartilage were developed in [53, 63].

A number of elastic analytical models for articular contact were developed by Eberhardt et al. [33]. It was shown that in conditions where the load times are short (i.e., running, jumping, or impact) it should often be sufficient to consider only elastic response. At the same time, the instantaneous response of the articular cartilage layers to impulsive compressive loads (see Fig. 7.1) corresponds to that of an incompressible elastic material [18, 36].

The effect of energy dissipation due to internal damping in articular cartilage can be taken into account in the framework of the theory of viscoelasticity. However, viscoelastic models [67, 75] have limited capabilities in describing the known viscous effects associated with the interstitial fluid flow. Previous studies have shown [17] that interstitial fluid pressurization plays an important role in the load support mechanics of articular cartilage.

It has been long known that articular cartilage is anisotropic and inhomogeneous, although it has been difficult to incorporate these complexities into engineering

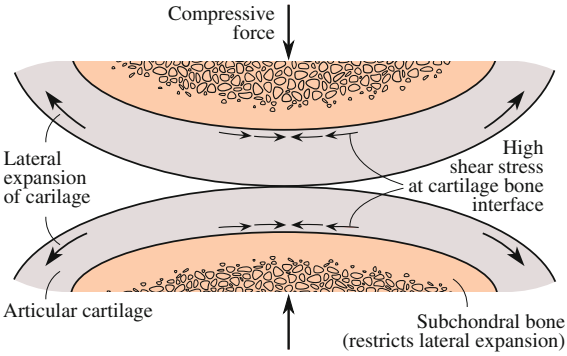

Fig. 7.1 Schematic of the articular cartilage deformation under impulsive compressive loads. The cartilage experiences a relatively large lateral displacement due to its high Poisson's ratio. This expansion is restrained by the subchondral bone, causing a high shear stress at the cartilage bone interface [72]

analysis [31]. Finite element models incorporating the inhomogeneity of articular cartilage were developed in [23]. The combined role of menisci and ligaments in load transmission and stability of the human knee was analyzed by a three-dimensional FE model [78]. Note also [20] that articular cartilage exhibits remarkable frictional properties, and pressurization of its interstitial fluid may contribute predominantly to reducing the friction coefficient at the contact interface [17].

An asymptotic modeling methodology for simulating tibio-femoral contact [8], which is further developed in this study, is based on the asymptotic models of frictionless unilateral contact interaction between thin biphasic [13] and viscoelastic [14] layers. The approach requires use of the smooth contact surface geometry and efficient contact points detection methods. While the subchondral bone is assumed to be rigid, the articular cartilage is considered to be a thin layer of transversely isotropic linear-elastic or viscoelastic incompressible material. The normal contact forces are determined analytically based on the exact solution for elliptical contact between thin viscoelastic incompressible cartilage layers bonded to rigid substrates.

7.1.3 Articular Surface Geometry

Observe [27] that an anatomically-based multibody dynamics model requires an accurate description of the articular surfaces in order to solve the articular contact problem. In this section, following [8], we present a generalization of the method [84] for approximating articular surfaces from the unstructured experimental surface data, which can be used for regularization of noisy surface data.

Let us assume that the geometrical data of the tibia and femur are given in the Cartesian coordinate systems (x_1, x_2, x_3) and $(\hat{x}_1, \hat{x}_2, \hat{x}_3)$, respectively. Following [24], the positive x_1-axis is directed anteriorly, the positive x_2-axis is pointed medially, and the positive x_3-axis is directed proximally (see Fig. 7.2). To describe the relative position of the femur with respect to the tibia, we assume that the tibia is considered to be rigidly fixed. In such a case, the coordinates $\mathbf{x}$ and $\hat{\mathbf{x}}$ can be referred to

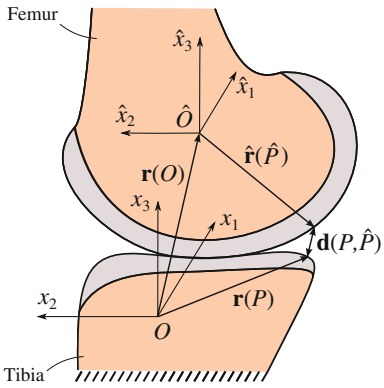

Fig. 7.2 Knee joint Cartesian coordinate systems: "space-fixed" $Ox_1x_2x_3$ and "body-fixed" $\hat{O}\hat{x}_1\hat{x}_2\hat{x}_3$. The tibia is considered to be rigidly fixed

as the "space-fixed" and "body-fixed" [50]. It is assumed that in the fully extended position of the joint, the directions of the corresponding coordinate axes of both coordinate systems coincide.

Let the position of an arbitrary point $\hat{P}$ on the femoral surface be represented by the vector $\hat{\mathbf{r}}(\hat{P})$ in the body-fixed coordinate system. To describe the position vector $\mathbf{r}(\hat{P})$ of the same point in the space-fixed system (x_1, x_2, x_3), one needs to determine the transition vector $\mathbf{r}(\hat{O})$ from the origin of the tibial coordinate system (point O) to the origin of the femoral coordinate system (point $\hat{O}$) as well as the rotation transformation matrix $\mathscr{R}$ (for its description, we refer to [24]). According to these definitions, the following relation holds [24, 50]:

$$\mathbf{r}(\hat{P}) = \mathbf{r}(\hat{O}) + \mathscr{R}\hat{\mathbf{r}}(\hat{P}). \tag{7.3}$$

Consider now an arbitrary point P on the tibial surface and a distance vector between the points P and $\hat{P}$ (see Fig. 7.2), i.e.,

$$\mathbf{d}(P, \hat{P}) = \mathbf{r}(\hat{P}) - \mathbf{r}(P). \tag{7.4}$$

Following [38, 70], we introduce the normal contact distance vector, $\mathbf{d}_0$, between the articular surfaces in such a way that it is parallel to each of the surface normals. The corresponding points P^0 and $\hat{P}^0$ are called the potential contact points. As a result, we have $\mathbf{d}_0 = \mathbf{d}(P^0, \hat{P}^0)$.

The length of vector $\mathbf{d}_0$ with the proper sign taken into account will be called the pseudo-penetration and will be denoted as follows:

$$\delta_0 = -\mathbf{d}_0 \cdot \mathbf{n}^0. \tag{7.5}$$

Here, $\mathbf{n}^0$ is the outer normal to the tibial surface at the point P^0, and the dot denotes the scalar product of vectors.

In the following, we will assume that for any admissible position of the femur relative to the tibia, there is only a pair of potential contact points P^0 and $\hat{P}^0$ for

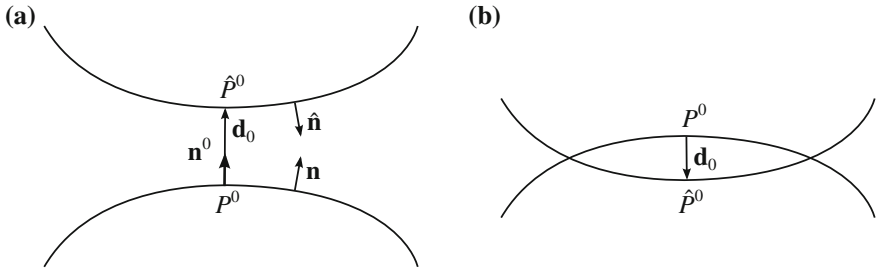

Fig. 7.3 Pseudo-penetration of the contacting bodies: **a** there is no contact interaction between the articular surfaces; **b** the contact between the articular surfaces exists

each pair of femoral and tibial condyles. Note that this assumption is in agreement with the geometric compatibility of rigid bodies condition used in [2, 69, 86].

Therefore, if $\delta_0 = 0$, then the articular surfaces contact each other at a single point. In this case a single tangent plane exists to both femoral and tibial surfaces. If $\mathbf{d}_0 \cdot \mathbf{n}^0 > 0$ (and $\mathbf{d}_0 \cdot \hat{\mathbf{n}}^0 < 0$, where $\hat{\mathbf{n}}^0$ is the outer normal to the femoral surface at the point $\hat{P}^0$), then there is no contact between the surfaces and $\delta_0 < 0$ (see, Fig. 7.3a). Finally, the penetration condition states that if $\mathbf{d}_0 \cdot \mathbf{n}^0 < 0$ (and $\mathbf{d}_0 \cdot \hat{\mathbf{n}}^0 > 0$), then the contact between the articular surfaces exists and $\delta_0 > 0$ (see, Fig. 7.3b).

Let us now introduce a local Cartesian coordinate system (ξ_1, ξ_2, ζ) with its center at the point P^0, in such a way that the positive ζ-axis is directed along the normal vector $\mathbf{n}^0$. Thus, in the vicinity of points P^0 and $\hat{P}^0$, the equations of both articular surfaces can be written as follows:

$$\zeta = -\phi_0(\boldsymbol{\xi}), \quad \zeta = -\delta_0 + \hat{\phi}_0(\boldsymbol{\xi}). \tag{7.6}$$

It is assumed that locally the tibia and femur occupy the domains $\zeta \le -\phi_0(\boldsymbol{\xi})$ and $\zeta \ge -\delta_0 + \hat{\phi}_0(\boldsymbol{\xi})$, respectively.

In light of Eq. (7.6), we define the local gap function as follows:

$$\phi(\boldsymbol{\xi}) = \phi_0(\boldsymbol{\xi}) + \hat{\phi}_0(\boldsymbol{\xi}). \tag{7.7}$$

In the next section, following [86], we may assume that the functions $\phi_0(\boldsymbol{\xi})$ and $\hat{\phi}_0(\boldsymbol{\xi})$ can be approximated by polynomials in ξ_1 and ξ_2 of degrees n and $\hat{n}$ as

$$\phi_0(\boldsymbol{\xi}) = \sum_{p=2}^{n}\sum_{q=0}^{p} a_{pq}\xi_1^{p-q}\xi_2^{q}, \quad \hat{\phi}_0(\boldsymbol{\xi}) = \sum_{p=2}^{\hat{n}}\sum_{q=0}^{p} \hat{a}_{pq}\xi_1^{p-q}\xi_2^{q}. \tag{7.8}$$

The coefficients a_{pq} and $\hat{a}_{pq}$ are calculated by minimizing the functions

$$\sum_{j=1}^{N}\Big(\zeta^j - \sum_{p=2}^{n}\sum_{q=0}^{p} a_{pq}(\xi_1^j)^{p-q}(\xi_2^j)^q\Big)^2, \quad \sum_{j=1}^{\hat{N}}\Big(\hat{\zeta}^j - \sum_{p=2}^{\hat{n}}\sum_{q=0}^{p} \hat{a}_{pq}(\hat{\xi}_1^j)^{p-q}(\hat{\xi}_2^j)^q\Big)^2, \tag{7.9}$$

where N and $\hat{N}$ are the numbers of measured surface points, and $(\xi_1^j, \xi_2^j, \zeta^j)$ and $(\hat{\xi}_1^j, \hat{\xi}_2^j, \hat{\zeta}^j)$ are the measured coordinates of the jth point on the tibial surface ($j = 1, \ldots, N$) and on the femoral surface ($j = 1, \ldots, \hat{N}$), respectively.

7.1.4 Contact Constitutive Relation. Elliptical Contact of Thin Incompressible Elastic Layers

We now consider analytical models of deformable tibio-femoral contact under the assumption that the local gap function can be approximated by an elliptical paraboloid. The articular cartilages are modeled as thin incompressible elastic or viscoelastic layers.

Consider the frictionless contact between two thin linear elastic layers of constant thicknesses, h_1 and h_2, firmly attached to rigid substrates with continuously varying curvatures. Let us assume that in the undeformed state, the surfaces of the layers touch at a single point denoted by P^0. Introducing a Cartesian coordinate system (η_1, η_2, ζ), with the center at the point P^0 such that the coordinate plane $\zeta = 0$ coincides with the common tangent plane to the layer surfaces, we may assume without loss of generality that with accuracy up to terms of order $|\boldsymbol{\eta}|^3$ the gap function, $\varphi(\boldsymbol{\eta})$, defined as the distance between the layer surfaces along the ζ-axis, is represented by an elliptic paraboloid

$$\varphi(\boldsymbol{\eta}) = \frac{\eta_1^2}{2R_1} + \frac{\eta_2^2}{2R_2}. \tag{7.10}$$

Now, let $-w_0(\boldsymbol{\eta})$ and $\hat{w}_0(\boldsymbol{\eta})$ be the vertical displacement functions for the surface points of the layers representing the tibial and femoral articular cartilages, respectively, due to the action of the surface pressures with the density $p(\boldsymbol{\eta})$. Given that the materials of the layers are elastic, incompressible and transversely isotropic with out-of-plane shear moduli G_1' and G_2', and based on the asymptotic analysis of the frictionless contact problem for a thin elastic layer bonded to a rigid substrate in the thin-layer limit (see Sect. 2.5), the following contact constitutive relation for thin incompressible layers can be established:

$$w_0(\boldsymbol{\eta}) = -\frac{h_1^3}{3G_1'}\Delta_\eta p(\boldsymbol{\eta}), \quad \hat{w}_0(\boldsymbol{\eta}) = -\frac{h_2^3}{3G_2'}\Delta_\eta p(\boldsymbol{\eta}). \tag{7.11}$$

Here, $\Delta_\eta = \partial^2/\partial\eta_1^2 + \partial^2/\partial\eta_2^2$ is the Laplace differential operator, and the index "1" refers to the tibia, while "2" refers to the femur.

Let δ_0 be the normal approach of the rigid substrates, which model the subchondral bones. Then, the following equation should hold in the contact region, ω, where the contact pressure is positive:

$$\hat{w}_0(\boldsymbol{\eta}) + w_0(\boldsymbol{\eta}) = \delta_0 - \varphi(\boldsymbol{\eta}), \quad \boldsymbol{\eta} \in \omega. \tag{7.12}$$

Substituting the expressions (7.11) into Eq. (7.12), we obtain the contact condition in the form of a differential equation

$$-\left(\frac{h_1^3}{3G_1'}+\frac{h_2^3}{3G_2'}\right)\Delta_\eta p(\boldsymbol{\eta})=\delta_0-\varphi(\boldsymbol{\eta}),\quad \boldsymbol{\eta}\in\omega. \tag{7.13}$$

We emphasize that Eq. (7.13) should hold over the whole contact region ω, which is not given a priori. As this differential equation is of the second order, it is necessary to formulate appropriate boundary conditions on the contour Γ of the contact region ω. According to [21, 28] (see also Sect. 2.7.3), we impose the two boundary conditions

$$p(\boldsymbol{\eta})=0,\quad \frac{\partial p}{\partial n}(\boldsymbol{\eta})=0,\quad \boldsymbol{\eta}\in\Gamma, \tag{7.14}$$

where $\partial/\partial n$ is the normal derivative.

In the case of the parabolic gap function (7.10), the exact solution to the problem (7.13), (7.14) was obtained in [21] in the form

$$p(\boldsymbol{\eta})=p_0\left(1-\frac{\eta_1^2}{a^2}-\frac{\eta_2^2}{b^2}\right)^2. \tag{7.15}$$

The maximum contact pressure p_0 and the semi-axes a and b of the elliptical contact area ω satisfy the following system of algebraic equation [21]:

$$\delta_0=\frac{4p_0}{ma^2}\left(1+\frac{1}{s^2}\right), \tag{7.16}$$

$$\frac{1}{2R_1}=\frac{4p_0}{ma^4}\left(3+\frac{1}{s^2}\right),\quad \frac{1}{2R_2}=\frac{4p_0}{ma^4s^2}\left(1+\frac{3}{s^2}\right). \tag{7.17}$$

Here, $s=b/a$ is the aspect ratio of the contact area, and

$$m=\left(\frac{h_1^3}{3G_1'}+\frac{h_2^3}{3G_2'}\right)^{-1}.$$

Integrating the contact pressure distribution (7.15) over the contact area and taking into account (7.16) and (7.17), we obtain

$$F=2\pi c_F(s)\frac{G_1'G_2'}{h_1^3G_2'+h_2^3G_1'}R_1R_2\delta_0^3, \tag{7.18}$$

where $c_F(s)$ is a dimensionless factor given by (see also Sect. 3.1.2)

$$s^2 = \sqrt{\left(\frac{R_1 - R_2}{6R_1}\right)^2 + \frac{R_2}{R_1}} - \frac{(R_1 - R_2)}{6R_1}, \tag{7.19}$$

$$c_F(s) = \frac{s(3s^2+1)(s^2+3)}{2(s^2+1)^3}. \tag{7.20}$$

Equation (7.18) represents the force-displacement relationship for the case of elliptical contact of thin incompressible coatings.

7.1.5 Asymptotic Model for Elliptical Contact of Thin Incompressible Viscoelastic Layers

Applying the viscoelastic correspondence principle to the elastic equation (7.13) (see Sect. 3.1.2), we arrive at the governing integro-differential equation

$$-\sum_{n=1}^{2} \frac{h_n^3}{3} \int_{0-}^{t} J'^{(n)}(t-\tau) \Delta_\eta \frac{\partial p}{\partial \tau}(\boldsymbol{\eta}, \tau)\, d\tau = \delta_0(t) - \varphi(\boldsymbol{\eta}) \mathscr{H}(t). \tag{7.21}$$

Here, $J'^{(n)}(t)$ is the out-of-plane creep compliance in shear for the nth viscoelastic layer, t is a time variable, $\delta_0(t)$ is the variable normal contact approach of the rigid substrates, $\mathscr{H}(t)$ is the Heaviside step function such that $\mathscr{H}(t) = 1$ for $t \geq 0$ and $\mathscr{H}(t) = 0$ for $t < 0$.

Let us introduce the normalized creep function $\Phi'^{(n)}(t)$ of the nth layer by letting

$$\Phi'^{(n)}(t) = G_0'^{(n)} J'^{(n)}(t), \tag{7.22}$$

where $G_0'^{(n)} = 1/J'^{(n)}(0^+)$ is the instantaneous out-of-plane shear elastic modulus of the nth layer, so that $\Phi'^{(n)}(0) = 1$.

Then, Eq. (7.21) can be represented in the form

$$-\frac{h^3}{3G_0'} \int_{0-}^{t} \Phi_\beta(t-\tau) \Delta_\eta \frac{\partial p}{\partial \tau}(\boldsymbol{\eta}, \tau)\, d\tau = \delta_0(t) - \varphi(\boldsymbol{\eta}) \mathscr{H}(t), \tag{7.23}$$

where $\Phi_\beta(t) = \beta_1 \Phi'^{(1)}(t) + \beta_2 \Phi'^{(2)}(t)$ is the compound creep function, β_1 and β_2 are weighted coefficients such that $\beta_1 + \beta_2 = 1$,

$$\beta_1 = \frac{h_1^3 G_0'^{(2)}}{h_1^3 G_0'^{(2)} + h_2^3 G_0'^{(1)}}, \quad \beta_2 = \frac{h_2^3 G_0'^{(1)}}{h_1^3 G_0'^{(2)} + h_2^3 G_0'^{(1)}}, \tag{7.24}$$

whereas h and G_0' are the joint thickness and the equivalent instantaneous out-of-plane shear elastic modulus given by

$$G_0' = \frac{h^3 G_0'^{(1)} G_0'^{(2)}}{h_1^3 G_0'^{(2)} + h_2^3 G_0'^{(1)}}, \quad h = h_1 + h_2. \tag{7.25}$$

As before, following [19], we require that the contact pressure distribution $p(\boldsymbol{\eta}, t)$ should satisfy the boundary conditions (7.14).

The general solution of Eq. (7.23) in the case of the parabolic gap function (7.10) was derived in [14]. Integrating the obtained contact pressures over the elliptical contact area, we arrive at the following force-displacement relationship:

$$F(t) = 2\pi c_F(s) \frac{G_0'^{(1)} G_0'^{(2)}}{h_1^3 G_0'^{(2)} + h_2^3 G_0'^{(1)}} R_1 R_2 \int_{0-}^{t} \Psi_\beta(t-\tau) \frac{d}{d\tau} \left(\delta_0(\tau)^3\right) d\tau. \tag{7.26}$$

Here, $c_F(s)$ is the factor introduced by formula (7.20), and $\Psi_\beta(t)$ is the corresponding normalized compound relaxation function determined by its Laplace transform $\tilde{\Psi}_\beta(s) = (s^2 \tilde{\Phi}_\beta(s))^{-1}$, where $\tilde{\Phi}_\beta(s)$ is the Laplace transform of $\Phi_\beta(t)$.

It is noteworthy that Eq. (7.26) is valid for the case of contact interaction under monotonic loading and can be applied for modeling contact forces in impact situations, and underline that the case of repetitive loading requires a special treatment.

We also emphasize that Eqs. (7.18) and (7.26) do not exactly describe the initial short time interval of contact interaction, while the contact zone does not exceed the joint thickness of the layers. However, if the maximum characteristic size of the contact zone achieved during the loading phase is much greater than each thickness of the layers, then the overall error introduced by this initial interval will be relatively small, just as was shown in [7] with respect to the influence of the superseismic stage of contact on the Hertzian impact theory.

7.1.6 Approximation of the Articular Femur and Tibia Geometries by Elliptic Paraboloids

To model the articular contact, one needs to describe the articular surface geometry in the framework of a mathematical model. A number of surface-fitting methods for representing the three-dimensional topography of articular surfaces, in particular the B-spline method [16, 30], use a structured data set and provide a limited continuity of the fitted articular surface. Methods to represent articular surfaces from the unstructured data were suggested in [44, 83] and are based on a parametric polynomial representation. In order to effectively deal with non-ordered data points, a method for the representation of articular surfaces was introduced in [84], based on the influence surface theory of elastic plates.

Since experimental measurements of surface data always contain a degree of measurement uncertainty, it was observed in [16] that a surface-fitting method which consists of interpolating the measured surface data may result in some degree of surface roughness. It was also noted that one limitation of the fitting method [84] is that it requires the fitting surface to pass through all measured surface points. This means that the fitting accuracy of the method [84] is partially controlled by the accuracy of the measurement instrument. Consequently, due to the noisy nature of measured data, forcing the fitting surface to pass through all measured surface data points may not produce an optimal fitting surface [84]. A regularization of the method [84] was proposed in [8], and spline smoothing methods for regularization of noisy data were considered in [16].

Due to the complexity of human knee joint geometry, it is difficult to obtain analytical solutions for the contact pressure distribution in the knee joint under physiological loading conditions, even under simplifying assumptions about the articular cartilage mechanical behavior. In [66], different analytical models for articular contact were compared with a finite element method solution in the case of an axisymmetric articular joint idealized as a system of a rigid ball covered with a cartilage layer in frictionless contact with a hemispherical layer of cartilage attached to a rigid base. Note that spherical surfaces were used for representing the medial and lateral femoral condyles in a number of papers [2, 62]. Also, in two-dimensional models [1, 62], the tibia surface is generally represented as a parabolic profile. In [79], a toroidal geometry was selected to represent the geometry of the medial (or the lateral) femoral and tibial components in a total knee replacement.

Elliptic paraboloids are widely used in contact mechanics for approximating the interacting non-axisymmetric surfaces. Based on high-resolution MRI (Magnetic resonance imaging), it was shown [47] that all articular surfaces of the knee joints of healthy volunteers displayed predominantly convex ovoid shapes, except for the central aspect of the medial tibia (with the highest degree of concavity), while none of the articulating surfaces displayed saddle-like properties.

In [60], the principal curvature radii of the femoral and tibial cartilage surfaces were measured in the weight-bearing regions of the medial and lateral compartments of three-dimensional models from the MP images obtained from 11 young healthy male individuals (age 30.5 ± 5.1 years). In particular, in the lateral condyle of the femur, the average radii were 22 ± 4 and 25 ± 4 mm in AP and ML directions, respectively. In the medial condyle of the femur, the average radii were 34 ± 5 and 21 ± 3 mm in AP and ML directions, respectively. In the lateral (medial) plateau of the tibia, the average radii were 37 ± 10 and -43 ± 11 mm (-95 ± 38 and -29 ± 7 mm), respectively. Here, positive and negative values represent convex and concave surfaces, respectively.

According to the measured data from [60], the shape functions $\phi_0(\boldsymbol{\xi})$ and $\hat{\phi}_0(\boldsymbol{\xi})$ in Eq. (7.6) are specified as follows:

$$\phi_0^{\mathrm{L}}(\boldsymbol{\xi}) = -\left(\frac{\xi_1^2}{37} - \frac{\xi_2^2}{43}\right), \quad \phi_0^{\mathrm{M}}(\boldsymbol{\xi}) = -\left(\frac{-\xi_1^2}{95} - \frac{\xi_2^2}{29}\right), \tag{7.27}$$

$$\hat{\phi}_0^{\mathrm{L}}(\boldsymbol{\xi}) = \frac{\xi_1^2}{22} + \frac{\xi_2^2}{25}, \quad \hat{\phi}_0^{\mathrm{M}}(\boldsymbol{\xi}) = \frac{\xi_1^2}{34} + \frac{\xi_2^2}{21}. \tag{7.28}$$

The coordinates ξ_1 and ξ_2 are assumed to be measured in millimeters, whereas the indexes "L" and "M" denote the quantities referring to the lateral and medial compartments, respectively.

Substituting (7.27) and (7.28) into Eq. (7.7), we obtain

$$\phi^{\mathrm{L}}(\boldsymbol{\xi}) = \Big(\frac{1}{22} + \frac{1}{37}\Big)\xi_1^2 + \Big(\frac{1}{25} - \frac{1}{43}\Big)\xi_2^2,$$

$$\phi^{\mathrm{M}}(\boldsymbol{\xi}) = \Big(\frac{1}{34} - \frac{1}{95}\Big)\xi_1^2 + \Big(\frac{1}{21} - \frac{1}{29}\Big)\xi_2^2.$$

From here it immediately follows that $R_1^{\mathrm{L}} = 30$ mm, $R_2^{\mathrm{L}} = 7$ mm, $R_1^{\mathrm{M}} = 38$ mm, and $R_2^{\mathrm{M}} = 26$ mm (recall that the inequality $R_1 \geq R_2$ is assumed in the choice of the radii R_1 and R_2). Therefore, we have

$$\overset{\mathrm{L}}{\varphi}(\boldsymbol{\eta}) = \frac{\eta_1^2}{60} + \frac{\eta_2^2}{14}, \quad \overset{\mathrm{M}}{\varphi}(\boldsymbol{\eta}) = \frac{\eta_1^2}{76} + \frac{\eta_2^2}{53}.$$

Further, formula (7.19) yields $s^{\mathrm{L}} = 0.61$ and $s^{\mathrm{M}} = 0.89$. Now, substituting these values into formula (7.20), we obtain $c_F(s^{\mathrm{L}}) = 0.84$, $c_F(s^{\mathrm{M}}) = 0.99$.

Thus, as a first approximation, the actual articulating surfaces in tibio-femoral contact can be represented by elliptic paraboloids. The parameters of such an approximation (i.e., the principal radii of curvature) generally depend on the position of the central contact point (point P^0 in Fig. 7.3).

The difference between the actual articulating surfaces and the idealized elliptic paraboloid surfaces influences the articular contact and especially the distribution of contact pressures. This question is explored in [12], where a perturbation solution is obtained under the assumption that the subchondral bones are rigid and shaped closely to elliptic paraboloids.

7.1.7 *Determining the Effective Geometrical Characteristics from Experimental Surface Data*

In order to apply the force displacement relationship (7.18) or (7.26), one needs to evaluate the geometric parameters R_1 and R_2 appearing in the paraboloid approximation (7.10) of the local gap function (7.7). In other words, the local gap function (7.7) must be approximated as follows:

$$\phi(\boldsymbol{\xi}) = \varphi(\boldsymbol{\xi}) + \tilde{\varphi}(\boldsymbol{\xi}). \tag{7.29}$$

Here, $\tilde{\varphi}(\boldsymbol{\xi})$ can be interpreted as a small discrepancy, while $\varphi(\boldsymbol{\xi})$, according to (7.10), should be taken in the form of an elliptic paraboloid

$$\varphi(\boldsymbol{\xi}) = \xi_1^2\left(\frac{\cos^2\theta}{2R_1} + \frac{\sin^2\theta}{2R_2}\right) + \xi_2^2\left(\frac{\sin^2\theta}{2R_1} + \frac{\cos^2\theta}{2R_2}\right) + \xi_1\xi_2 \sin 2\theta\left(\frac{1}{2R_1} - \frac{1}{2R_2}\right). \tag{7.30}$$

Observe that the parameter θ introduced in (7.30) represents the angle between the positive ξ_1-axis and the positive η_1-axis.

Under the assumption that the gap variation $\tilde{\varphi}(\boldsymbol{\xi})$ introduces a small perturbation into the contact region ω and the contact force F, we arrive at the following optimization criterion [8, 10]:

$$\min_{R_1,R_2,\theta} \iint\limits_{\omega_*} |\phi(\boldsymbol{\xi}) - \varphi(\boldsymbol{\xi})|^2 \rho_*(\boldsymbol{\xi})\, d\boldsymbol{\xi}. \tag{7.31}$$

Here, ω_* is an characteristic elliptic domain with the semi-axes a_* and b_*, while $\rho_*(\boldsymbol{\xi}) = 1 - a_*^{-2}\xi_1^2 - b_*^{-2}\xi_2^2$ is a weight function.

The optimization criterion (7.31) requires a continuous representation of the gap function $\phi(\boldsymbol{\xi})$, whereas originally only the coordinates of experimental surface data points $(\xi_1^j, \xi_2^j, \zeta^j)$ $(j = 1, \ldots, N)$ and $(\hat{\xi}_1^j, \hat{\xi}_2^j, \hat{\zeta}^j)$ $(j = 1, \ldots, \hat{N})$ were provided from the measurement experiment (see, Eq. (7.9)). It would be useful, however, to determine the parameters R_1 and R_2 directly from the experimental surface data. Consequently, the following discrete variant of the optimization criterion (7.31) is relevant and useful.

Given the measured surface data points $(\xi_1^j, \xi_2^j, \zeta^j)$ $(j = 1, \ldots, N)$ and $(\hat{\xi}_1^j, \hat{\xi}_2^j, \hat{\zeta}^j)$ $(j = 1, \ldots, \hat{N})$, the two sets of effective geometrical parameters R_1^0, R_2^0, θ_0 and $\hat{R}_1^0$, $\hat{R}_2^0$, $\hat{\theta}_0$ must satisfy the criteria

$$\min_{R_1^0,R_2^0,\theta_0} \sum_{\boldsymbol{\xi}^j \in \omega_*} |\zeta^j - \overset{0}{\varphi}(\boldsymbol{\xi}^j)|^2 \rho_*(\boldsymbol{\xi}^j), \tag{7.32}$$

$$\min_{\hat{R}_1^0,\hat{R}_2^0,\hat{\theta}_0} \sum_{\hat{\boldsymbol{\xi}}^j \in \omega_*} |\hat{\zeta}^j - \hat{\varphi}^0(\hat{\boldsymbol{\xi}}^j)|^2 \rho_*(\hat{\boldsymbol{\xi}}^j), \tag{7.33}$$

where $\varphi^0(\boldsymbol{\xi})$ and $\hat{\varphi}^0(\boldsymbol{\xi})$ are given by

$$\overset{0}{\varphi}(\boldsymbol{\xi}) = \xi_1^2\left(\frac{\cos^2\theta_0}{2R_1^0} + \frac{\sin^2\theta_0}{2R_2^0}\right) + \xi_2^2\left(\frac{\sin^2\theta_0}{2R_1^0} + \frac{\cos^2\theta_0}{2R_2^0}\right) + \xi_1\xi_2 \sin 2\theta_0\left(\frac{1}{2R_1^0} - \frac{1}{2R_2^0}\right), \tag{7.34}$$

$$\hat{\varphi}^0(\boldsymbol{\xi}) = \xi_1^2\left(\frac{\cos^2\hat{\theta}_0}{2\hat{R}_1^0} + \frac{\sin^2\hat{\theta}_0}{2\hat{R}_2^0}\right) + \xi_2^2\left(\frac{\sin^2\hat{\theta}_0}{2\hat{R}_1^0} + \frac{\cos^2\hat{\theta}_0}{2\hat{R}_2^0}\right) + \xi_1\xi_2 \sin 2\hat{\theta}_0\left(\frac{1}{2\hat{R}_1^0} - \frac{1}{2\hat{R}_2^0}\right). \tag{7.35}$$

According to (7.32) and (7.33), the tibial and femoral surfaces are represented locally by the effective elliptic paraboloids (7.34) and (7.35), whose orientations with respect to the positive ξ_1-axis are determined by the angles θ_0 and $\hat{\theta}_0$, respectively. The effective geometrical parameters R_1 and R_2 appearing in the elliptic paraboloidal approximation (7.10) can now be determined from R_1^0, R_2^0, θ_0 and $\hat{R}_1^0$, $\hat{R}_2^0$, $\hat{\theta}_0$ following a standard procedure used in Hertzian contact mechanics [54].

It is interesting to observe that, following [24] where the effects of different mathematical descriptions of articular contact and articular surface geometry on the kinematic characteristics of the knee model were investigated, close approximations of the articular surfaces by polynomials are not necessary, since the motion characteristics were not influenced greatly by the degree of the polynomial approximations for the curved tibial surfaces. This was a result of the size of the contact area, which covered small surface irregularities and made the contribution of the contact pressure distribution to the net contact force less dependent on the irregularities. This observation supports the necessity of operating with the effective geometrical characteristics of articular surfaces.

We also emphasize that the analytical models for the contact force using the local geometrical characteristics (principal radii of curvature of the articular surfaces at the potential contact points P^0 and $\hat{P}^0$) in contrast to the effective geometrical characteristics are restricted to simple geometries, and therefore their applicability to real articular contact geometries is limited.

7.1.8 Generalization of the Contact Constitutive Relation

The asymptotic methodology for tibio-femoral articular contact developed in [8] and outlined above is based on the leading-order asymptotic theory for a thin incompressible viscoelastic layer attached to a rigid substrate. As was shown in [14], the viscoelastic contact model for incompressible layers incorporates the asymptotic model [13, 19, 87] for short-time response of biphasic layers as a special case, corresponding to the Maxwell model of viscoelastic material.

In the elastic case, the force-displacement relationship for incompressible layers (7.18) can be generalized as

$$F = E M_n R^l \delta_0^n. \tag{7.36}$$

Here, E is a characteristic elastic modulus, $R = \sqrt{R_1 R_2}$ is a geometric mean of the curvature radii R_1 and R_2, the factor M_n is a function of the thicknesses of the

layers (h_1 and h_2) and the aspect ratio s of the elliptical contact region, which in turn depends on the ratio R_2/R_1. For incompressible layers, $n = 3$ and $l = 2$, while for compressible layers, $n = 2$ and $l = 1$. Note that the dimension of M is L^{2-n-l}, where L is the dimension of length.

We point out that Eq. (7.36) incorporates the Hertzian force-displacement relationship with $n = 3/2$ and $l = 1/2$. The contact constitutive relation in the form (7.36) was used in a number of publications on multibody simulations [37].

From Eq. (7.36), it is readily seen that in the case of incompressible layers, the contact force, F, is inversely proportional to the joint thickness cubed, h^3, while in the case of thin compressible coatings, the contact force is simply inversely proportional to the joint thickness h. This obvious implication is very important from the viewpoint of the articular contact modeling of osteoarthritic joints, as the change of the articular cartilage thickness has been widely used as an indicator of its degenerative status [15, 56].

In the case of viscoelastic layers, according to Eqs. (7.26) and (7.36), the contact constitutive relations can be represented as follows:

$$F(t) = E_0 M_n R^l \int_{0-}^{t} \Psi(t-\tau) \frac{d}{d\tau} \left(\delta_0(\tau)^n\right) d\tau. \tag{7.37}$$

Here, E_0 is a characteristic instantaneous elastic modulus, $\Psi(t)$ is the normalized compound relaxation function, and M_n is the same factor as shown in Eq. (7.36), with the dimension L^{2-n-l}.

Alternatively, in order to take into account the effect of energy dissipation during the elasto-plastic contact interaction, the following general Hunt–Crossley model [52] has been widely employed for modeling impact situations:

$$F(t) = b\delta_0(t)^p \dot{\delta}_0(t)^q + k\delta_0(t)^n. \tag{7.38}$$

The stiffness parameter k and the damping parameter b depend on material and geometric properties of colliding bodies. As was observed in [37], an important aspect of Eq. (7.38) is that damping depends on the indentation, which is physically sound in the impact of metal balls, since the contact area increases with deformation and a plastic region is more likely to develop for larger contact displacements.

For biomechanical applications, the general Hunt–Crossley model (7.38) was used in a number of papers [42, 70, 81]. Note also that the consideration of viscous effects in quasistatic or dynamic simulations could be important, in particular, in the simulation of total knee replacement [79].

Additionally, Eq. (7.38) incorporates the so-called Lankarani–Nikravesh contact-impact force model (with $p = n$ and the coefficient b inversely proportional to the initial impact velocity). In biomechanical applications, the Lankarani–Nikravesh model was used in [74] for describing articular contact between intervertebral discs in the study of cervical spine dynamics.

We observe that in contrast to Eq. (7.38), the force-displacement relationship (7.37) introduces the viscous mechanism of energy dissipation and is likely to be more physically sound in view of the biphasic nature of articular cartilage.

7.1.9 Modified Incomplete Storage Shear Modulus and Loss Angle

Let $D'_\beta(t)$ be the equivalent out-of-plane shear relaxation modulus defined as

$$D'_\beta(t) = G'_0 \Psi_\beta(t), \tag{7.39}$$

where G'_0 and $\Psi_\beta(t)$ are the equivalent instantaneous out-of-plane shear elastic modulus and the corresponding normalized compound relaxation function.

Then, in light of (7.25) and (7.37), Eq. (7.26) can be rewritten in the form

$$F(t) = M_n R^l \int_{0-}^{t} D'_\beta(t-\tau) \frac{d}{d\tau}\left(\delta_0(\tau)^n\right) d\tau, \tag{7.40}$$

where (with $c_F(s)$ and h being defined by formulas (7.20) and $(7.25)_2$)

$$n = 3, \quad l = 2, \quad R = \sqrt{R_1 R_2}, \quad M_3 = \frac{2\pi c_F(s)}{h^3}. \tag{7.41}$$

Let us now consider a sinusoidal loading with a prescribed contact approach according to the law

$$\delta_0(t) = \delta_m \sin \omega t, \quad t \in (0, t_m). \tag{7.42}$$

Here, δ_m is the maximum contact approach, and ω is a given quantity having the dimension of reciprocal time. The quantity

$$t_m = \frac{\pi}{2\omega} \tag{7.43}$$

has a physical interpretation as the time moment when the contact approach $\delta_0(t)$ reaches its maximum δ_m. We emphasize that one may use Eq. (7.40) in the time interval $(0, t_m)$, that is up to the moment when the monotonically increasing contact area attains its maximum.

Following [11], we consider the quantity

$$\frac{1}{M_n R^l} \frac{F(t_m)}{\delta_m^n} = \int_0^{t_m} D'_\beta(t_m - \tau) \frac{d}{d\tau}\left(\frac{\delta_0(\tau)}{\delta_m}\right)^n d\tau, \tag{7.44}$$

and note that the quantity on the right-hand side of Eq. (7.44) was previously considered in a number of studies on indentation of viscoelastic materials [49, 61].

Substituting the expression (7.42) into the right-hand side of Eq. (7.44), we arrive at the following integral:

$$\tilde{G}'_n(\omega) = \int_0^{\pi/(2\omega)} D'_\beta\Big(\frac{\pi}{2\omega} - \tau\Big)\frac{d}{d\tau}(\sin\omega\tau)^n d\tau. \tag{7.45}$$

As shown in [11], the notation $\tilde{G}'_n(\omega)$ has distinct interpretations for different values of the subscript n.

By changing the integration variable, the integral (7.45) may be recast in the form

$$\tilde{G}'_n(\omega) = \omega \int_0^{\pi/(2\omega)} D'_\beta(s) n \cos^{n-1}\omega s \ \sin\omega s \, ds. \tag{7.46}$$

Comparing the above integral with the storage shear modulus (see, [80])

$$G'_1(\omega) = \omega \int_0^{\infty} D'_\beta(s)\sin\omega s \, ds, \tag{7.47}$$

we see that in the case $n = 1$, formulas (7.46) and (7.47) coincide up to the upper limits of integration. This explains why the quantity $\tilde{G}'_n(\omega)$ will be called the modified incomplete storage shear modulus.

We now let $\tilde{t}_M$ be the time moment when the contact force (7.40) reaches its maximum, i.e., $\dot{F}(\tilde{t}_M) = 0$, for the loading protocol (7.42). Then, by analogy with the case of linear harmonic vibrations, we set

$$\tilde{\delta}_n(\omega) = \frac{\pi}{2} - \omega\tilde{t}_M. \tag{7.48}$$

As a consequence of (7.43), formula (7.48) can be rewritten in the form

$$\tilde{\delta}_n(\omega) = \frac{\pi}{2}\frac{(t_m - \tilde{t}_M)}{t_m},$$

where we call the quantity $\tilde{\delta}_n(\omega)$ the modified incomplete loss angle.

7.2 Hunt–Crossley Contact Model

In this section, we study the Hunt–Crossley model of nonlinear impact, which is widely employed in biomechanical applications. The equivalent Hunt–Crossley model for articular contact is introduced based on the coincidence of the corresponding modified incomplete storage moduli, in one instance, and of the so-called modified incomplete loss angle of viscoelastic (short-time biphasic) model with the corresponding loss angle for the Hunt–Crossley contact model, in the other.

7.2.1 Nonlinear Viscoelastic Hunt–Crossley Model of Impact

We now consider the impact of a rigid body of mass m against a deformable obstacle with the following contact force [52]:

$$F(x, \dot{x}) = bkx^n\dot{x} + kx^n. \tag{7.49}$$

Here, n is a real constant, k is a stiffness coefficient, and b is a damping parameter.

According to Newton's second law, the differential equation of the impact process has the form

$$m\ddot{x} = -F(x, \dot{x}), \quad t \in [0, t_c], \tag{7.50}$$

where t_c is the duration of contact interaction.

The initial conditions for Eq. (7.50) are formulated as follows:

$$x(0) = 0, \quad \dot{x}(0) = v_0, \tag{7.51}$$

where v_0 is the body velocity before impact.

The contact duration t_c is determined as the instant $t = t_c$, when the reaction force $-F(x, \dot{x})$, or the body's acceleration $\ddot{x}$, vanishes. It can be proven [32] that if at the initial time moment, $t = 0$, the before-collision velocity v_0 and the damping parameter b are positive, then at any subsequent time moment t during the impact the following inequality holds:

$$\dot{x}(t) > -\frac{1}{b}. \tag{7.52}$$

Since the penetration $x > 0$ for $t \in (0, t_c)$, the contact force (7.49) vanishes as a consequence of (7.52), when

$$x(t_c) = 0. \tag{7.53}$$

In other words, there is no residual penetration left as a result of the contact interaction in the Hunt–Crossley impact model (7.49)–(7.51).

7.2.2 Maximum Displacement

According to (7.49) and (7.50), the governing differential equation is

$$\ddot{x} + \frac{k}{m} x^n (1 + b\dot{x}) = 0. \tag{7.54}$$

We can eliminate the time variable from this equation by making use of the differential relation

$$\ddot{x} = \frac{dv}{dt} = \frac{dv}{dx}\frac{dx}{dt} = v\frac{dv}{dx}.$$

In this way, Eq. (7.54) is transformed to the form

$$v\frac{dv}{dx} + \frac{k}{m} x^n (1 + bv) = 0,$$

which can be integrated by separating variables as follows:

$$\int_{v_0}^{v} \frac{v\, dv}{1 + bv} = -\frac{1}{m} \Pi(x). \tag{7.55}$$

Here, $\Pi(x)$ is the potential energy of elastic deformation, i.e.,

$$\Pi(x) = k \int_0^x \xi^n d\xi = \frac{k x^{n+1}}{n+1}. \tag{7.56}$$

Evaluating the integral on the left-hand side of Eq. (7.55), in light of the inequality (7.52), we arrive at the following first integral [32, 48, 73]:

$$\ln(1 + bv) - bv = \ln(1 + bv_0) - bv_0 + \frac{b^2}{m} \Pi(x). \tag{7.57}$$

Let x_m denote the maximum displacement of the body during the impact, which occurs at the instant $t = t_m$, when the velocity vanishes, i.e., $\dot{x}(t_m) = 0$. So, substituting the value $v = 0$ into Eq. (7.57), we obtain

$$x_m = \left\{ \frac{(n+1)m}{kb^2} \left[bv_0 - \ln(1 + bv_0) \right] \right\}^{1/(n+1)}. \tag{7.58}$$

We now see that the peak penetration monotonically increases with increasing v_0 and decreases with increasing b.

7.2.3 Coefficient of Restitution

Since displacement $x = 0$ at the beginning and at the end of the impact (see Eqs. (7.51)$_1$ and (7.53)), the post-collision velocity v_1 is related to the pre-collision velocity v_0 by the equation

$$\ln(1 + bv_1) - bv_1 = \ln(1 + bv_0) - bv_0, \tag{7.59}$$

which follows from (7.57) due to the normalization $\Pi(0) = 0$ (see formula (7.56)). We note that $v_1 < 0$.

Following Dyagel and Lapshin [32], we solve Eq. (7.59) for v_1 using the Lambert W-function. Recall [29] that the Lambert function $W(z)$ is defined implicitly as the function satisfying

$$W(z)e^{W(z)} = z, \tag{7.60}$$

or, equivalently, for a given z, the corresponding value $W(z)$ (possibly non-unique) can be found as the solution of the equation $We^W = z$. Over the field of real numbers, the Lambert function has two branches $W_0(x)$, $x \in (-1/e, +\infty)$, and $W_{-1}(x)$, $x \in (-1/e, 0)$, shown in Fig. 7.4. Note that $W_0(-1/e) = W_{-1}(-1/e) = -1$.

Reducing the equation

$$\ln \varphi - \varphi = \xi$$

to the equation of the type (7.60)

$$-\varphi e^{-\varphi} = -e^{\xi},$$

we arrive at the following formula [32]:

$$v_1 = -\frac{1}{b}\left\{1 + W_0\left(-\frac{1 + bv_0}{\exp(1 + bv_0)}\right)\right\}. \tag{7.61}$$

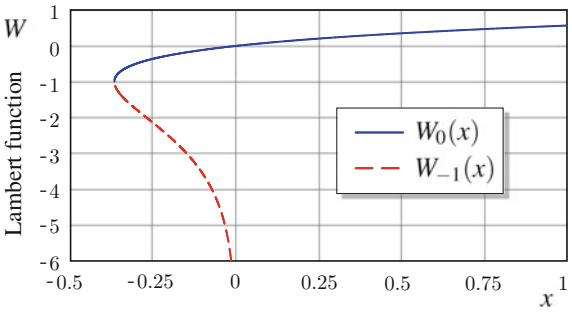

Fig. 7.4 Branches of the Lambert function $W(x)$: $W_0(x)$ is the principal real branch (*solid line*), $W_{-1}(x)$ is the second real branch (*dashed line*)

Since the velocity at the end of the impact

$$v_1 = -e_* v_0, \tag{7.62}$$

where e_* is the coefficient of restitution, formula (7.61) yields

$$e_* = \frac{1}{bv_0}\left\{1 + W_0\left(-\frac{1+bv_0}{\exp(1+bv_0)}\right)\right\}. \tag{7.63}$$

Here, $W_0(x)$ is the principal real branch of the Lambert function.

7.2.4 Interpretation of the Damping Parameter in Terms of the Coefficient of Restitution

The kinetic energy loss in the impact is

$$\Delta T = \frac{mv_0^2}{2} - \frac{mv_1^2}{2} = \frac{mv_0^2}{2}(1 - e_*^2),$$

where we have taken (7.62) into account.

The experimental data on collisions of balls [39] show that for most linear materials with an elastic range at low collision velocities v_0, the kinetic energy loss is proportional to the collision velocity cubed, i.e., $\Delta T \approx \alpha m v_0^3$, while the coefficient of restitution decreases proportionally to v_0, i.e.,

$$e_* \approx 1 - \alpha v_0. \tag{7.64}$$

Here, α is an empirical constant, which can be obtained as a linear fit (see formula (7.64)) of the experimental data for the coefficient of restitution e_* regarded as a function of the collision velocity v_0.

In the framework of the Hunt–Crossley model, by the substitution of (7.62) into Eq. (7.59), we arrive at the following equation for e_*:

$$\ln(1 - e_* b v_0) + e_* b v_0 - \ln(1 + bv_0) + bv_0 = 0. \tag{7.65}$$

For relatively small values of the impact velocity (i.e., assuming that $bv_0 \ll 1$), we can expand the left-hand side of Eq. (7.65) in a series of ascending powers of a small dimensionless parameter

$$\beta = bv_0.$$

In this way, Eq. (7.65) reduces to the following equation:

$$\frac{\beta^2}{2}(1 - e_*^2) - \frac{\beta^3}{3}(1 + e_*^3) + \frac{\beta^4}{4}(1 - e_*^4) - \cdots = 0.$$

We can derive useful formulas by keeping only two terms in the above expansion, as follows:

$$\beta \simeq \frac{3}{2}\frac{(1-e_*^2)}{(1+e_*^3)}. \tag{7.66}$$

By factoring the right-hand side of (7.66), we obtain the following formula [45]:

$$b \simeq \frac{3}{2v_0}\frac{(1-e_*)}{(1-e_*+e_*^2)}. \tag{7.67}$$

Since for $bv_0 \ll 1$, the coefficient of restitution is close to 1, and therefore we can simplify the denominator in formula (7.67) by putting $1-e_*+e_*^2 \approx 1$, we arrive at the following asymptotic formula [52]:

$$b \simeq \frac{3}{2v_0}(1-e_*). \tag{7.68}$$

Now, performing the same procedure for (7.66), we derive the following approximate formula [64, 65]:

$$b \simeq \frac{3}{4v_0}(1-e_*^2).$$

Other approximate relations connecting the damping parameter b and the coefficient of restitution e_* are discussed in [37, 43, 71, 82, 89] along with the applications of the Hunt–Crossley model in multibody dynamics simulations. Observe that the coefficient of restitution in the linear viscoelastic impact models [9, 73] depends on the impactor mass and does not depend on the impact velocity. An advantage of the Hunt–Crossley impact model is the lack of dependence of the coefficient of restitution on the mass of the colliding bodies, and thus it can be regarded as an intrinsic property of the material [73].

We point out that in [40, 89] it was recommended to evaluate the value of the damping parameter b from the exact Eq. (7.65), provided the value of e_* is known from experimental measurements.

7.2.5 *Interpretation of the Damping Parameter in Terms of the Loss Angle in the Hunt–Crossley Model*

Let us consider the variation of the Hunt–Crossley contact force (7.49) for a sinusoidal displacement

$$x(t) = A\sin\omega t, \quad t \in (0, \pi/\omega), \tag{7.69}$$

with an amplitude A and an angular frequency ω.

Substituting (7.69) into formula (7.49), we obtain

$$F(t) = kA^n \sin^n \omega t (1 + bA\omega \cos \omega t). \tag{7.70}$$

Let t_M be the time moment when the contact force (7.70) reaches its maximum. Then, following [11], by analogy with the case of harmonic vibrations, we set

$$\delta_n(\omega) = \frac{\pi}{2} - \omega t_M. \tag{7.71}$$

Differentiating Eq. (7.70), we derive the equation $\dot{F}(t_M) = 0$, which after the substitution $x = \cos \omega t_M$ can be reduced to the following form:

$$(n + 1)\beta x^2 + nx - \beta = 0. \tag{7.72}$$

Here we have introduced the notation

$$\beta = bA\omega. \tag{7.73}$$

Further, according to (7.71), we have

$$\cos \omega t_M = \sin \delta_n(\omega),$$

and, therefore, Eq. (7.72) yields

$$\sin \delta_n(\omega) = \frac{2\beta}{\sqrt{n^2 + 4(n + 1)\beta^2} + n}. \tag{7.74}$$

Alternatively, from (7.72) it follows that

$$\beta = \frac{n \sin \delta_n(\omega)}{1 - (n + 1) \sin^2 \delta_n(\omega)}. \tag{7.75}$$

Finally, taking into account that $\dot{x}(0) = A\omega$ and introducing the notation

$$v_0 = A\omega, \tag{7.76}$$

we can rewrite formula (7.75) as follows:

$$b = \frac{n \sin \delta_n(\omega)}{v_0\left[1 - (n + 1) \sin^2 \delta_n(\omega)\right]}. \tag{7.77}$$

Note that in writing the above formula, we used relations (7.73) and (7.76).

The quantity $\delta_n(\omega)$ will be called the loss angle for the Hunt–Crossley contact model. If this quantity is measured experimentally, the damping parameter can be recovered from (7.77) with (7.76) taken into account.

7.2.6 Equivalent Hunt–Crossley Model for Articular Contact

Based on the viscoelastic constitutive relation (7.26), we strightforwardly determine two parameters n and k from the three parameters of Eq. (7.49) as follows:

$$n = 3, \tag{7.78}$$

$$k = 2\pi c_F(s)\frac{G_0'}{h^3}R_1R_2, \tag{7.79}$$

where $c_F(s)$ is a dimensionless factor (see formulas (7.19) and (7.20)), which is close to 1 when the geometrical parameters R_1 and R_2 do not differ significantly, $h = h_1+h_2$ is the joint thickness of articular cartilage layers, and G_0' is the equivalent instantaneous out-of-plane shear elastic modulus given by (7.25).

A greater difficulty is encountered in determining the damping parameter b. In a number of papers (see, e.g., a review by Machado et al. [71]), the Hunt–Crossley model was employed in multibody dynamics simulations with the parameter b expressed in terms of the coefficient of restitution e_*, which concept is difficult to interpret in the context of articular contact.

We suggest the following approximate relation, based on Eq. (7.77), regarding the loss angle as an intrinsic property of both the viscoelastic and the Hunt–Crossley models:

$$b = \frac{3\sin\tilde{\delta}_3(\omega)}{v_0\left[1-4\sin^2\tilde{\delta}_3(\omega)\right]}. \tag{7.80}$$

Here, $\tilde{\delta}(\omega)$ is the so-called modified incomplete loss angle introduced by Argatov et al. [11] for the viscoelastic model (see formula (7.48)).

We recommend replacement of the straightforward formula (7.79) with a new relation, based on the coincidence of the corresponding modified incomplete storage moduli. Since

$$\frac{F(t_m)}{A^n} = k, \quad t_m = \frac{\pi}{2\omega},$$

and taking into account Eqs. (7.44) and (7.45), we obtain $k = M_n R^l \tilde{G}_n'(\omega)$. Alternatively, as a result of (7.41), we find

$$k = 2\pi c_F(s)\frac{\tilde{G}_3'(\omega)}{h^3}R_1R_2, \tag{7.81}$$

where $\tilde{G}_n'(\omega)$ is the modified incomplete storage shear modulus (7.47).

In the framework of the short-time contact model for thin bonded biphasic poro-viscoelastic layers (see Sect. 6.3), the corresponding normalized relaxation function $\Psi_\beta(t)$ is determined by its Laplace transform $\tilde{\Psi}_\beta(s) = 1/[s^2\tilde{\Phi}_\beta(s)]$, where $\Phi_\beta(t)$ is given by Eqs. (6.58) and (6.59).

In the framework of the short-time contact model for thin bonded biphasic layers (see [9, 14]), the corresponding equivalent instantaneous out-of-plane shear elastic modulus is

$$G_0' = \frac{(h_1+h_2)^3 A_{44}^{\mathrm{s}(1)} A_{44}^{\mathrm{s}(2)}}{h_1^3 A_{44}^{\mathrm{s}(2)} + h_2^3 A_{44}^{\mathrm{s}(1)}}, \tag{7.82}$$

where $A_{44}^{\mathrm{s}(1)}$ and $A_{44}^{\mathrm{s}(2)}$ are the out-of-plane shear elastic moduli of the solid matrices of the biphasic layers, h_1 and h_2 are the layer thicknesses.

Further, the equivalent (normalized) relaxation function is given by

$$\Psi_\beta(t) = \exp\Big(-\frac{t}{\tau_0}\Big), \tag{7.83}$$

where the equivalent relaxation time τ_0 is defined by the formula

$$\tau_0 = \frac{\tau_0^{(1)}\tau_0^{(2)}}{\beta_1\tau_0^{(2)} + \beta_2\tau_0^{(1)}}$$

with β_1 and β_2 being given by

$$\beta_1 = \frac{h_1^3 A_{44}^{\mathrm{s}(2)}}{h_1^3 A_{44}^{\mathrm{s}(2)} + h_2^3 A_{44}^{\mathrm{s}(1)}}, \quad \beta_2 = \frac{h_2^3 A_{44}^{\mathrm{s}(1)}}{h_1^3 A_{44}^{\mathrm{s}(2)} + h_2^3 A_{44}^{\mathrm{s}(1)}},$$

while $\tau_0^{(1)}$ and $\tau_0^{(2)}$ are the corresponding relaxation times of the biphasic layers, i.e.,

$$\tau_0^{(1)} = \frac{h_1^2}{3A_{44}^{\mathrm{s}(1)}k_1^{(1)}}, \quad \tau_0^{(2)} = \frac{h_2^2}{3A_{44}^{\mathrm{s}(2)}k_1^{(2)}}.$$

Here, $k_1^{(1)}$ and $k_1^{(1)}$ are the in-plane permeability coefficients of the biphasic layers.

The modified incomplete storage shear modulus (7.46) is given by

$$\tilde{G}_n'(\omega) = G_0'\omega \int_0^{\pi/(2\omega)} \Psi_\beta(s) n \cos^{n-1}\omega s \, \sin\omega s \, ds,$$

where G_0' and $\Psi_\beta(t)$ are defined by formulas (7.82) and (7.83).

In periodic activities like walking or running, we can put $\omega = 2\pi f$, where f is the corresponding frequency. Otherwise, we suggest a simple approximation

$\omega = \pi/(2t_m)$, where t_m is a characteristic time period of the loading phase up to the moment of peak contact approach. As in [37, 43, 71], the parameter v_0 in formula (7.80) is interpreted as the initial contact velocity.

Observe also that formulas (7.80) and (7.81) can be used in developing semi-analytical surrogate models for articular contact [41, 42], which, for instance, can also take into account the effect of menisci.

References

1. Abdel–Rahman, E.M., Hefzy, M.S.: A two-dimensional dynamic anatomical model of the human knee joint. J. Biomech. Eng. **115**, 357–365 (1993)
2. Abdel–Rahman, E.M., Hefzy, M.S.: Three-dimensional dynamic behaviour of the human knee joint under impact loading. Med. Eng. Phys. **20**, 276–290 (1998)
3. Aleksandrov, V.M., Vorovich, I.I.: Contact problems for the elastic layer of small thickness. J. Appl. Math. Mech. **28**, 425–427 (1964)
4. ap Gwynn, I., Wade, S., Ito, K., Richards, R.G.: Novel aspects to the structure of rabbit articular cartilage. Eur. Cell. Mater. **4**, 18–29 (2002)
5. ap Gwynn, I., Wade, S., Kaab, M.J., Owen, G.R., Richards, R.G.: Freeze-substitution of rabbit tibial articular cartilage reveals that radial zone collagen fibres are tubules. J. Microsc. **197**, 159–172 (2000)
6. Argatov, I.I.: The pressure of a punch in the form of an elliptic paraboloid on a thin elastic layer. Acta Mech. **180**, 221–232 (2005)
7. Argatov, I.I.: Asymptotic modeling of the impact of a spherical indenter on an elastic half-space. Int. J. Solids Struct. **45**, 5035–5048 (2008)
8. Argatov, I.I.: Development of an asymptotic modeling methodology for tibio-femoral contact in multibody dynamic simulations of the human knee joint. Multibody Syst. Dyn. **28**, 3–20 (2012)
9. Argatov, I.I.: Mathematical modeling of linear viscoelastic impact: Application to drop impact testing of articular cartilage. Trib. Int. **63**, 213–225 (2013)
10. Argatov, I.: Contact problem for a thin elastic layer with variable thickness: Application to sensitivity analysis of articular contact mechanics. Appl. Math. Model. **37**, 8383–8393 (2013)
11. Argatov, I., Daniels, A.U., Mishuris, G., Ronken, S., Wirz, D.: Accounting for the thickness effect in dynamic spherical indentation of a viscoelastic layer: Application to non-destructive testing of articular cartilage. Eur. J. Mech. A/Solids **37**, 304–317 (2013)
12. Argatov, I., Mishuris, G.: Contact problem for thin biphasic cartilage layers: Perturbation solution. Quart. J. Mech. Appl. Math. **64**, 297–318 (2011)
13. Argatov, I., Mishuris, G.: Elliptical contact of thin biphasic cartilage layers: exact solution for monotonic loading. J. Biomech. **44**, 759–761 (2011)
14. Argatov, I., Mishuris, G.: Frictionless elliptical contact of thin viscoelastic layers bonded to rigid substrates. Appl. Math. Model. **35**, 3201–3212 (2011)
15. Armstrong, C.G., Mow, V.C.: Variations in the intrinsic mechanical properties of human articular cartilage with age, degeneration, and water content. J Bone Joint Surg. Am. **64**, 88–94 (1982)
16. Ateshian, G.A.: A B-spline least-squares surface fitting method for articular surfaces of diarthrodial joints. J. Biomech. Eng. **115**, 366–373 (1993)
17. Ateshian, G.A.: The role of interstitial fluid pressurization in articular cartilage lubrication. J. Biomech. **42**, 1163–1176 (2009)
18. Ateshian, G.A., Ellis, B.J., Weiss, J.A.: Equivalence between short-time biphasic and incompressible elastic material responses. J. Biomech. Eng. **129**, 405–412 (2007)

19. Ateshian, G.A., Lai, W.M., Zhu, W.B., Mow, V.C.: An asymptotic solution for the contact of two biphasic cartilage layers. J. Biomech. **27**, 1347–1360 (1994)
20. Ateshian, G.A., Soltz, M.A., Mauck, R.L., Basalo, I.M., Hung, C.T., Lai, W.M.: The role of osmotic pressure and tension-compression nonlinearity in the frictional response of articular cartilage. Transp. Porous Med. **50**, 5–33 (2003)
21. Barber, J.R.: Contact problems for the thin elastic layer. Int. J. Mech. Sci. **32**, 129–132 (1990)
22. Bei, Y., Fregly, B.J.: Multibody dynamic simulation of knee contact mechanics. Med. Eng. Phys. **26**, 777–789 (2004)
23. Bell, J.S., Winlove, C.P., Smith, C.W., Dehghani, H.: Modeling the steady-state deformation of the solid phase of articular cartilage. Biomater **30**, 6394–6401 (2009)
24. Blankevoort, L., Kuiper, J.H., Huiskes, R., Grootenboer, H.J.: Articular contact in a three-dimensional model of the knee. J. Biomech. **24**, 1019–1031 (1991)
25. Bursać, P., McGrath, C.V., Eisenberg, S.R., Stamenović, D.: A microstructural model of elasto-static properties of articular cartilage in confined compression. J. Biomech. Eng. **122**, 347–353 (2000)
26. Carter, D.R., Wong, M.: Modelling cartilage mechanobiology. Phil. Trans. R. Soc. Lond. B **358**, 1461–1471 (2003)
27. Caruntu, D.I., Hefzy, M.S.: 3-D anatomically based dynamic modeling of the human knee to include tibio-femoral and patello-femoral joints. J. Biomech. Eng. **126**, 44–53 (2004)
28. Chadwick, R.S.: Axisymmetric indentation of a thin incompressible elastic layer. SIAM J. Appl. Math. **62**, 1520–1530 (2002)
29. Corless, R.M., Gonnet, G.H., Hare, D.E.G., Jeffrey, D.J., Knuth, D.E.: On the Lambert W function. Adv. Comput. Math. **5**, 329–359 (1996)
30. Dhaher, Y.Y., Delp, S.L., Rymer, W.Z.: The use of basis functions in modelling joint articular surfaces:application to the knee joint. J. Biomech. **33**, 901–907 (2000)
31. Donzelli, P.S., Spilker, R.L., Ateshian, G.A., Mow, V.C.: Contact analysis of biphasic transversely isotropic cartilage layers and correlations with tissue failure. J. Biomech. **32**, 1037–1047 (1999)
32. Dyagel, R.V., Lapshin, V.V.: On a nonlinear viscoelastic model of Hunt–Crossley impact. Mech. Solids **46**, 798–806 (2011)
33. Eberhardt, A.W., Keer, L.M., Lewis, J.L., Vithoontien, V.: An analytical model of joint contact. J. Biomech. Eng. **112**, 407–413 (1990)
34. Eberhard, P., Spägele, T., Gollhofer, A.: Investigations for the dynamical analysis of human motion. Multibody Syst. Dyn. **3**, 1–20 (1999)
35. Fox, A.J.S., Bedi, A., Rodeo, S.A.: The basic science of articular cartilage: structure, composition, and function. Sports Health **1**, 461–469 (2009)
36. Garcia, J.J., Altiero, N.J., Haut, R.C.: An approach for the stress analysis of transversely isotropic biphasic cartilage under impact load. J. Biomech. Eng. **120**, 608–613 (1998)
37. Gilardi, G., Sharf, I.: Literature survey of contact dynamics modelling. Mech. Mach. Theory **37**, 1213–1239 (2002)
38. Glocker, Ch.: Formulation of spatial contact situations in rigid multibody systems. Comput. Method. Appl. M. **177**, 199–214 (1999)
39. Goldsmith, W.: Impact: The Theory and Physical Behaviour of Colliding Solids. Edward Arnold Ltd, London (1960)
40. Gonthier, Y., McPhee, J., Lange, C., Piedbœuf, J.-C.: A regularized contact model with asymmetric damping and Dwell-time dependent friction multibody. Syst. Dyn. **11**, 209–233 (2004)
41. Guess, T.M.: Forward dynamics simulation using a natural knee with menisci in the multibody framework. Multibody Syst. Dyn. **28**, 37–53 (2012)
42. Guess, T.M., Thiagarajan, G., Kia, M., Mishra, M.: A subject specific multibody model of the knee with menisci. Med. Eng. Phys. **32**, 505–515 (2010)
43. Hanley, K., Collins, F., Cronin, K., Byrne, E., Moran, K., Brabazon, D.: Simulation of the impact response of a sliotar core with linear and non-linear contact models. Int. J. Impact Eng. **50**, 113–122 (2012)

44. Hirokawa, S., Ueki, T., Ohtsuki, A.: A new approach for surface fitting method of articular joint surfaces. J. Biomech. **37**, 1551–1559 (2004)
45. Herbert, R.G., McWhannell, D.C.: Shape and frequency composition of pulses from an impact pair. J. Eng. Ind. **99**, 513–518 (1977)
46. Herzog, W., Federico, S.: Considerations on joint and articular cartilage mechanics. Biomech. Model. Mechanobiol. **5**, 64–81 (2006)
47. Hohe, J., Ateshian, G., Reiser, M., Englmeier, K.-H., Eckstein, F.: Surface size, curvature analysis, and assessment of knee joint incongruity with MRI in vivo. Magn. Reson. Med. **47**, 554–561 (2002)
48. Horvay, G., Veluswami, M.A.: Hertzian impact of two elastic spheres in the presence of surface damping. Acta Mech. **35**, 285–290 (1980)
49. Hu, K., Radhakrishnan, P., Patel, R.V., Mao, J.J.: Regional structural and viscoelastic properties of fibrocartilage upon dynamic nanoindentation of the articular condyle. J. Struct. Biol. **136**, 46–52 (2001)
50. Huiskes, R., Van Dijk, R., de Lange, A., Woltring, H.J., Van Rens, Th.J.G.: Kinematics of the human knee joint. In: Berme, N., Engin, A.E., Correia da Silva, K.M. (eds.) Biomechanics of Normal and Pathological Human Articulating Joints, pp. 165–187. Martinus Nijhoff Publ., Dordrecht (1985)
51. Hughes, L.C., Archer, C.W., ap Gwynn, I.: The ultrastructure of mouse articular cartilage: collagen orientation and implications for tissue functionality. A polarised light and scanning electron microscope study and review. Eur. Cell. Mater. 9, 68–84 (2005)
52. Hunt, K.H., Crossley, F.R.E.: Coefficient of restitution interpreted as damping in vibroimpact. ASME J. Appl. Mech. **42**, 440–445 (1975)
53. Iatridis, J.C., ap Gwynn, I.: Mechanisms for mechanical damage in the intervertebral disc annulus brosus. J. Biomech. **37**, 1165–1175 (2004)
54. Johnson, K.L.: Contact Mechanics. Cambridge Univ. Press, Cambridge, UK (1985)
55. Jurvelin, J.S.: Biomechanical properties of the knee articular cartilage under various loading conditions. Ph.D. thesis, University of Kuopio, Kuopio, Finland (1991)
56. Karvonen, R.L., Negendank, W.G., Teitge, R.A., Reed, A.H., Miller, P.R., Fernandez-Madrid, F.: Factors affecting articular cartilage thickness in osteoarthritis and aging. J. Rheumatol. **21**, 1310–1318 (1994)
57. Khan, I.M., Gilbert, S.J., Singhrao, S.K., Duance, V.C., Archer, C.W.: Cartilage integration: evaluation of the reasons for failure of integration during cartilage repair. Rev. Eur. Cell. Mater. **16**, 26–39 (2008)
58. Kim, Y.J., Bonassar, L.J., Grodzinsky, A.J.: The role of cartilage streaming potential, fluid flow and pressure in the stimulation of chondrocyte biosynthesis during dynamic compression. J. Biomech. **28**, 1055–1066 (1995)
59. Kłodowski, A., Rantalainen, T., Mikkola, A., Heinonen, A., Sievänen, H.: Flexible multibody approach in forward dynamic simulation of locomotive strains in human skeleton with flexible lower body bones. Multibody Syst. Dyn. **25**, 395–409 (2011)
60. Koo, S., Andriacchi, T.P.: A comparison of the influence of global functional loads vs. local contact anatomy on articular cartilage thickness at the knee. J. Biomech. **40**, 2961–2966 (2007)
61. Kren, A.P., Naumov, A.O.: Determination of the relaxation function for viscoelastic materials at low velocity impact. Int. J. Impact Eng. **37**, 170–176 (2010)
62. Kücük, H.: The effect of modeling cartilage on predicted ligament and contact forces at the knee. Comput. Biol. Med. **36**, 363–375 (2006)
63. Landinez-Parra, N.S., Garzón-Alvarado, D.A., Vanegas-Acosta, J.C.: A phenomenological mathematical model of the articular cartilage damage. Comput. Meth. Prog. Bio. **104**, e58–e74 (2011)
64. Lankarani, H.M., Nikravesh, P.E.: A contact force model with hysteresis damping for impact analysis of multibody systems. J. Mech. Des. **112**, 369–376 (1990)
65. Lankarani, H.M., Nikravesh, P.E.: Continuous contact force models for impact analysis in multibody systems. Nonlinear Dyn. **5**, 193–207 (1994)

66. Li, G., Sakamoto, M., Chao, E.Y.S.: A comparison of different methods in predicting static pressure distribution in articulating joints. J. Biomech. **30**, 635–638 (1997)
67. Li, S., Patwardhan, A.G., Amirouche, F.M.L., Havey, R., Meade, K.P.: Limitations of the standard linear solid model of intervertebral discs subject to prolonged loading and low-frequency vibration in axial compression. J. Biomech. **28**, 779–790 (1995)
68. Lin, Y-Ch., Haftka, R.T., Queipo, N.V., Fregly, B.J.: Surrogate articular contact models for computationally efficient multibody dynamic simulations. Med. Eng. Phys. **32**, 584–594 (2010)
69. Ling, Z.-K., Guo, H.-Q., Boersma, S.: Analytical study on the kinematic and dynamic behaviors of a knee joint. Med. Eng. Phys. **19**, 29–36 (1997)
70. Machado, M., Flores, P., Claro, J.C.P., Ambrósio, J., Silva, M., Completo, A., Lankarani, H.M.: Development of a planar multibody model of the human knee joint. Nonlinear Dyn. **60**, 459–478 (2010)
71. Machado, M., Moreira, P., Flores, P., Lankarani, H.M.: Compliant contact force models in multibody dynamics: evolution of the Hertz contact theory. Mech. Mach. Theory **53**, 99–121 (2012)
72. Mansour, J.M.: Biomechanics of cartilage. In: Oatis, C.A. (ed.) Kinesiology: the mechanics and pathomechanics of human movement, 2nd edn, pp. 66–79. Lippincott Williams and Wilkins, Philadelphia, PA (2008)
73. Marhefka, D.W., Orin, D.E.: Simulation of contact using a nonlinear damping model. In: Proceedings of the 1996 IEEE International Conference on Robotics and Automation. pp. 16621–6628. Minneapolis, Minnesota (1996)
74. Monteiro, N.M.B., da Silva, M.P.T., Folgado, J.O.M.G., Melancia, J.P.L.: Structural analysis of the intervertebral discs adjacent to an interbody fusion using multibody dynamics and finite element cosimulation. Multibody Syst. Dyn. **25**, 245–270 (2011)
75. Mow, V.C., Gu, W.Y., Chen, F.H.: Structure and function of articular cartilage and meniscus. In: Mow, V.C., Huiskes, R. (eds.) Basic orthopaedic biomechanics and mechano-biology, 3rd edn, pp. 181–258. Lippincott Williams and Wilkins, Philadelphia, PA (2005)
76. O'Hara, B.P., Urban, J.P.G., Maroudas, A.: Influence of cyclic loading on the nutrition of articular cartilage. Ann. Rheum. Dis. **49**, 536–539 (1990)
77. Pandy, M.G., Sasaki, K., Kim, S.: A three-dimensional musculoskeletal model of the human knee joint. Part 1: Theoretical construction. Comput. Method. Biomec. **1**, 87–108 (1997)
78. Peña, E., Calvo, B., Martínez, M.A., Doblaré, M.: A three-dimensional finite element analysis of the combined behavior of ligaments and menisci in the healthy humen knee joint. J. Biomech. **39**, 1686–1701 (2006)
79. Pérez-González, A., Fenollosa-Esteve, C., Sancho-Bru, J.L., Sánchez-Marín, F.T., Vergara, M., Rodríguez-Cervantes, P.J.: A modified elastic foundation contact model for application in 3D models of the prosthetic knee. Med. Eng. Phys. **30**, 387–398 (2008)
80. Pipkin, A.C.: Lectures on Viscoelastic Theory. Springer Verlag, New York (1986)
81. Silva, M.P.T., Ambrósio, J.A.C., Pereira, M.S.: Biomechanical model with joint resistance for impact simulation. Multibody Syst. Dyn. **1**, 65–84 (1997)
82. Sørensen, S.E., Hansen, M.R., Ebbesen, M.K., Mouritsen, O.Ø.: Implicit identification of contact parameters in a continuous chain model. Model. Ident. Control **32**, 1–15 (2011)
83. van Ruijven, L.J., Beek, M., van Eijden, T.M.G.J.: Fitting parametrized polynomials with scattered surface data. J. Biomech. **32**, 715–720 (1999)
84. Wang, J.H-C., Ryu, J., Han, J.-S., Rowen, B.: A new method for the representation of articular surfaces using the influence surface theory of plates. J. Biomech. **33**, 629–633 (2000)
85. Wilson, W., van Donkelaar, C.C., van Rietberger, R., Huiskes, R.: The role of computational models in the search for the mechanical behaviour and damage mechanisms of articular cartilage. Med. Eng. Phys. **27**, 810–826 (2005)
86. Wismans, J., Veldpaus, F., Janssen, J., Huson, A., Struben, P.: A three-dimensional mathematical model of the knee-joint. J. Biomech. **13**(677–679), 681–685 (1980)
87. Wu, J.Z., Herzog, W., Epstein, M.: An improved solution for the contact of two biphasic cartilage layers. J. Biomech. **30**, 371–375 (1997)

88. Wu, J.Z., Herzog, W., Epstein, M.: Evaluation of the finite element software ABAQUS for biomechanical modelling of biphasic tissues. J. Biomech. **31**, 165–169 (1997)
89. Zhang, Y., Sharf, I.: Validation of nonlinear viscoelastic contact force models for low speed impact. J. Appl. Mech. 76, 051002 (12 pages) (2009)

Chapter 8
Contact of Thin Inhomogeneous Transversely Isotropic Elastic Layers

Abstract In this chapter we consider contact problems for thin bonded inhomogeneous transversely isotropic elastic layers. In particular, in Sects. 8.1 and 8.2, the deformation problems are studied for the cases of elastic layers with the out-of-plane and thickness-variable inhomogeneous properties, respectively. In Sect. 8.3, the axisymmetric frictionless contact problems for thin incompressible inhomogeneous elastic layers are studied in detail in the framework of the leading-order asymptotic model. Finally, the deformation problem for a transversely isotropic elastic layer bonded to a rigid substrate, and coated with a very thin elastic layer made of another transversely isotropic material is analyzed in Sect. 8.4.

8.1 Deformation of an In-Plane Inhomogeneous Elastic Layer

In the present section, the leading-order asymptotic models for the local indentation of compressible and incompressible elastic layers developed in Chaps. 1 and 2 are generalized for elastic layers with in-plane inhomogeneous material properties.

8.1.1 Deformation Problem Formulation

Recall that the constitutive relationship for a transversely isotropic media based in the Cartesian coordinates (y_1, y_2, z), where the Oy_1y_2 plane coincides with the plane of elastic symmetry, has the following form [9]:

$$\begin{pmatrix} \sigma_{11} \\ \sigma_{22} \\ \sigma_{33} \\ \sigma_{23} \\ \sigma_{13} \\ \sigma_{12} \end{pmatrix} = \begin{bmatrix} A_{11} & A_{12} & A_{13} & 0 & 0 & 0 \\ A_{12} & A_{11} & A_{13} & 0 & 0 & 0 \\ A_{13} & A_{13} & A_{33} & 0 & 0 & 0 \\ 0 & 0 & 0 & 2A_{44} & 0 & 0 \\ 0 & 0 & 0 & 0 & 2A_{44} & 0 \\ 0 & 0 & 0 & 0 & 0 & 2A_{66} \end{bmatrix} \begin{pmatrix} \varepsilon_{11} \\ \varepsilon_{22} \\ \varepsilon_{33} \\ \varepsilon_{23} \\ \varepsilon_{13} \\ \varepsilon_{12} \end{pmatrix}. \tag{8.1}$$

I. Argatov and G. Mishuris, *Contact Mechanics of Articular Cartilage Layers*,
Advanced Structured Materials 50, DOI 10.1007/978-3-319-20083-5_8

In this section, we assume that the elastic constants A_{kl} are functions of the in-plane coordinates $\mathbf{y} = (y_1, y_2)$, so that the layer possesses an in-plane inhomogeneity.

By substituting the components of strain

$$\varepsilon_{\alpha\beta} = \frac{1}{2}\Big(\frac{\partial v_\alpha}{\partial y_\beta} + \frac{\partial v_\beta}{\partial y_\alpha}\Big), \quad \alpha, \beta = 1, 2,$$

$$\varepsilon_{3\alpha} = \frac{1}{2}\Big(\frac{\partial w}{\partial y_\alpha} + \frac{\partial v_\alpha}{\partial z}\Big), \quad \varepsilon_{33} = \frac{\partial w}{\partial z}$$

into Hooke's law (8.1), we obtain the stress-displacement relations

$$\begin{aligned}
\sigma_{11} &= A_{11}\frac{\partial v_1}{\partial y_1} + A_{12}\frac{\partial v_2}{\partial y_2} + A_{13}\frac{\partial w}{\partial z}, \quad \sigma_{23} = A_{44}\Big(\frac{\partial w}{\partial y_2} + \frac{\partial v_2}{\partial z}\Big),\\
\sigma_{22} &= A_{12}\frac{\partial v_1}{\partial y_1} + A_{11}\frac{\partial v_2}{\partial y_2} + A_{13}\frac{\partial w}{\partial z}, \quad \sigma_{13} = A_{44}\Big(\frac{\partial w}{\partial y_1} + \frac{\partial v_1}{\partial z}\Big),\\
\sigma_{33} &= A_{13}\frac{\partial v_1}{\partial y_1} + A_{13}\frac{\partial v_2}{\partial y_2} + A_{33}\frac{\partial w}{\partial z}, \quad \sigma_{12} = A_{66}\Big(\frac{\partial v_1}{\partial y_2} + \frac{\partial v_2}{\partial y_1}\Big),
\end{aligned} \tag{8.2}$$

where $A_{12} = A_{11} - 2A_{66}$ due to the in-plane symmetry properties.

The substitution of the above expressions into the equilibrium equations

$$\frac{\partial \sigma_{i1}}{\partial x_1} + \frac{\partial \sigma_{i2}}{\partial x_2} + \frac{\partial \sigma_{i3}}{\partial x_3} = 0, \quad i = 1, 2, 3,$$

yields the system of Lamé equations

$$\mathfrak{L}(\nabla_y)\mathbf{v} + \nabla_y\Big(A_{13}\frac{\partial w}{\partial z}\Big) + A_{44}\nabla_y\frac{\partial w}{\partial z} + A_{44}\frac{\partial^2 \mathbf{v}}{\partial z^2} = \mathbf{0}, \tag{8.3}$$

$$\nabla_y \cdot (A_{44}\nabla_y w) + \frac{\partial}{\partial z}\nabla_y \cdot (A_{44}\mathbf{v}) + \frac{\partial}{\partial z}A_{13}\nabla_y \cdot \mathbf{v} + A_{33}\frac{\partial^2 w}{\partial z^2} = 0, \tag{8.4}$$

where $\nabla_y = (\partial/\partial y_1, \partial/\partial y_2)$ is the in-plane Hamilton operator, the scalar product is denoted by a dot, and $\mathfrak{L}(\nabla_y)$ is a 2×2 matrix differential operator such that

$$\begin{aligned}
\mathfrak{L}_{\alpha\alpha}(\nabla_y) &= \frac{\partial}{\partial y_\alpha}\Big(A_{11}\frac{\partial}{\partial y_\alpha}\Big) + \frac{\partial}{\partial y_{3-\alpha}}\Big(A_{66}\frac{\partial}{\partial y_{3-\alpha}}\Big),\\
\mathfrak{L}_{\alpha\beta}(\nabla_y) &= \frac{\partial}{\partial y_\alpha}\Big(A_{12}\frac{\partial}{\partial y_\beta}\Big) + \frac{\partial}{\partial y_\beta}\Big(A_{66}\frac{\partial}{\partial y_\alpha}\Big), \quad \alpha, \beta = 1, 2, \quad \alpha \neq \beta.
\end{aligned}$$

We consider the deformation of a thin in-plane inhomogeneous elastic layer (with the elastic constants $A_{kl}(\mathbf{y})$) of uniform thickness, h, ideally bonded to a rigid

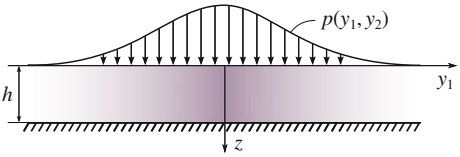

Fig. 8.1 An in-plane inhomogeneous elastic layer of uniform thickness bonded to a rigid substrate and supporting a distributed normal load

substrate (see Fig. 8.1). At the bottom surface of the layer, $z = h$, the following boundary conditions are imposed:

$$\mathbf{v}\big|_{z=h} = \mathbf{0}, \quad w\big|_{z=h} = 0. \tag{8.5}$$

On the upper surface of the elastic layer, we impose the boundary conditions of normal loading with no tangential tractions

$$\sigma_{13}\big|_{z=0} = \sigma_{23}\big|_{z=0} = 0, \quad \sigma_{33}\big|_{z=0} = -p, \tag{8.6}$$

where the normal load $p(\mathbf{y})$ is a given (sufficiently smooth) function of the in-plane coordinates $\mathbf{y} = (y_1, y_2)$.

The problem (8.3)–(8.6) generalizes the deformation problem studied in Chaps. 1 and 2 for the case of transversely isotropic elastic layers with in-plane inhomogeneous properties.

8.1.2 Perturbation Analysis of the Deformation Problem

Assuming that the elastic layer is relatively thin, we require that

$$h = \varepsilon h_*, \tag{8.7}$$

where ε is a small positive parameter, and h_* is a characteristic length, which is assumed to be independent of ε.

By introducing the so-called "stretched" *dimensional* normal coordinate

$$\zeta = \frac{z}{\varepsilon}, \tag{8.8}$$

we transform the Lamé equations (8.3), (8.4) into the following:

$$\frac{1}{\varepsilon^2} A_{44} \frac{\partial^2 \mathbf{v}}{\partial \zeta^2} + \frac{1}{\varepsilon} \frac{\partial}{\partial \zeta} \big(\nabla_y (A_{13} w) + A_{44} \nabla_y w \big) + \mathfrak{L}(\nabla_y) \mathbf{v} = \mathbf{0}, \tag{8.9}$$

$$\frac{1}{\varepsilon^2} A_{33} \frac{\partial^2 w}{\partial \zeta^2} + \frac{1}{\varepsilon} \frac{\partial}{\partial \zeta} \big(\nabla_y \cdot (A_{44} \mathbf{v}) + A_{13} \nabla_y \cdot \mathbf{v} \big) + \nabla_y \cdot (A_{44} \nabla_y w) = 0. \tag{8.10}$$

Correspondingly, the boundary conditions (8.6) become

$$\frac{1}{\varepsilon}\frac{\partial \mathbf{v}}{\partial \zeta} + \nabla_y w\Big|_{\zeta=0} = \mathbf{0}, \tag{8.11}$$

$$\frac{1}{\varepsilon}A_{33}\frac{\partial w}{\partial \zeta} + A_{13}\nabla_y \cdot \mathbf{v}\Big|_{\zeta=0} = -p. \tag{8.12}$$

As before, we apply the perturbation algorithm [14] to construct an approximate solution to the system (8.5), (8.9)–(8.12) in the form of asymptotic expansions

$$\mathbf{v} = \varepsilon \mathbf{v}^0(\mathbf{y}, \zeta) + \varepsilon^2 \mathbf{v}^1(\mathbf{y}, \zeta) + \cdots, \tag{8.13}$$

$$w = \varepsilon w^0(\mathbf{y}, \zeta) + \varepsilon^2 w^1(\mathbf{y}, \zeta) + \cdots, \tag{8.14}$$

where the successive coefficients of the powers of ε are independent of ε.

Following the standard procedure of the perturbation technique, we derive a set of equations for the terms of expansions (8.13) and (8.14). In particular, the leading terms of the asymptotic expansions are determined as solutions of the problems

$$A_{44}\frac{\partial^2 \mathbf{v}^0}{\partial \zeta^2} = \mathbf{0}, \quad \zeta \in (0, h_*), \quad \frac{\partial \mathbf{v}^0}{\partial \zeta}\Big|_{\zeta=0} = \mathbf{0}, \quad \mathbf{v}^0\big|_{\zeta=h_*} = \mathbf{0}; \tag{8.15}$$

$$A_{33}\frac{\partial^2 w^0}{\partial \zeta^2} = 0, \quad \zeta \in (0, h_*), \quad A_{33}\frac{\partial w^0}{\partial \zeta}\Big|_{\zeta=0} = -p, \quad w^0\big|_{\zeta=h_*} = 0, \tag{8.16}$$

from here it follows that

$$\mathbf{v}^0(\mathbf{y}, \zeta) \equiv \mathbf{0}, \quad w^0(\mathbf{y}, \zeta) = \frac{p(\mathbf{y})}{A_{33}}(h_* - \zeta). \tag{8.17}$$

The next two terms of the asymptotic expansions (8.13) and (8.14) satisfy the problems

$$A_{44}\frac{\partial^2 \mathbf{v}^1}{\partial \zeta^2} = -\nabla_y\Big(A_{13}\frac{\partial w^0}{\partial \zeta}\Big) - A_{44}\nabla_y \frac{\partial w^0}{\partial \zeta}, \quad \zeta \in (0, h_*),$$

$$\frac{\partial \mathbf{v}^1}{\partial \zeta}\Big|_{\zeta=0} = -\nabla_y w^0\big|_{\zeta=0}, \quad \mathbf{v}^1\big|_{\zeta=h_*} = \mathbf{0}; \tag{8.18}$$

$$A_{33}\frac{\partial^2 w^1}{\partial \zeta^2} = -\frac{\partial}{\partial \zeta}\nabla_y \cdot (A_{44}\mathbf{v}^0) - A_{13}\frac{\partial}{\partial \zeta}\nabla_y \cdot \mathbf{v}^0, \quad \zeta \in (0, h_*),$$

$$A_{33}\frac{\partial w^1}{\partial \zeta}\Big|_{\zeta=0} = -A_{13}\nabla_y \cdot \mathbf{v}^0\big|_{\zeta=0}, \quad w^1\big|_{\zeta=h_*} = 0. \tag{8.19}$$

In light of $(8.17)_1$, from (8.19), it immediately follows that

$$w^1(\mathbf{y},\zeta)\equiv 0, \tag{8.20}$$

while the substitution of $(8.17)_2$ into Eq. (8.18) leads to the problem

$$\begin{gathered} A_{44}\frac{\partial^2\mathbf{v}^1}{\partial\zeta^2}=\nabla_y\Big(\frac{A_{13}}{A_{33}}p\Big)+A_{44}\nabla_y\Big(\frac{p}{A_{33}}\Big),\quad \zeta\in(0,h_*),\\ \frac{\partial\mathbf{v}^1}{\partial\zeta}\Big|_{\zeta=0}=-h_*\nabla_y\Big(\frac{p}{A_{33}}\Big),\quad \mathbf{v}^1\big|_{\zeta=h_*}=\mathbf{0}. \end{gathered} \tag{8.21}$$

As the elastic constants and the normal load are functions of the in-plane coordinates only, the right-hand side of Eq. $(8.21)_1$ is independent of ζ. Thus, the double integration of Eq. $(8.21)_1$ with the boundary conditions $(8.21)_2$ and $(8.21)_3$ taken into account yields

$$\mathbf{v}^1(\mathbf{y},\zeta)=-\frac{(h_*^2-\zeta^2)}{2A_{44}}\nabla_y\Big(\frac{A_{13}}{A_{33}}p\Big)+\frac{(h_*-\zeta)^2}{2}\nabla_y\Big(\frac{p}{A_{33}}\Big). \tag{8.22}$$

The second non-trivial term of the asymptotic expansion satisfies the problem

$$\begin{gathered} A_{33}\frac{\partial^2 w^2}{\partial\zeta^2}=-\frac{\partial}{\partial\zeta}\big[\nabla_y\cdot(A_{44}\mathbf{v}^1)-A_{13}\nabla_y\cdot\mathbf{v}^1\big]-\nabla_y\cdot\big(A_{44}\nabla_y w^0\big),\\ A_{33}\frac{\partial w^2}{\partial\zeta}\Big|_{\zeta=0}=-A_{13}\nabla_y\cdot\mathbf{v}^1\big|_{\zeta=0},\quad w^2\big|_{\zeta=h_*}=0. \end{gathered}$$

In light of $(8.17)_2$ and (8.22), the above equations take the form

$$\begin{aligned} A_{33}\frac{\partial^2 w^2}{\partial\zeta^2}&=-\zeta\Delta_y\Big(\frac{A_{13}}{A_{33}}p\Big)-\zeta A_{13}\nabla_y\cdot\Big(\frac{1}{A_{44}}\nabla_y\Big(\frac{A_{13}}{A_{33}}p\Big)\Big)\\ &\quad+(h_*-\zeta)A_{13}\Delta_y\Big(\frac{p}{A_{33}}\Big),\quad \zeta\in(0,h_*), \end{aligned} \tag{8.23}$$

$$\frac{\partial w^2}{\partial\zeta}\Big|_{\zeta=0}=\frac{h_*^2A_{13}}{2A_{33}}\Big[\nabla_y\cdot\Big(\frac{1}{A_{44}}\nabla_y\Big(\frac{A_{13}}{A_{33}}p\Big)\Big)-\Delta_y\Big(\frac{p}{A_{33}}\Big)\Big],\quad w^2\big|_{\zeta=h_*}=0.$$

Integrating Eq. $(8.23)_1$ and taking into account the boundary condition $(8.23)_2$ at $\zeta=0$, we obtain

$$\begin{aligned} A_{33}\frac{\partial w^2}{\partial\zeta}&=-\frac{\zeta^2}{2}\Delta_y\Big(\frac{A_{13}}{A_{33}}p\Big)+\frac{(h_*^2-\zeta^2)}{2}A_{13}\nabla_y\cdot\Big(\frac{1}{A_{44}}\nabla_y\Big(\frac{A_{13}}{A_{33}}p\Big)\Big)\\ &\quad+\Big(h_*\zeta-\frac{\zeta^2}{2}-\frac{h_*^2}{2}\Big)A_{13}\Delta_y\Big(\frac{p}{A_{33}}\Big),\quad \zeta\in(0,h_*), \end{aligned}$$

By integrating the above equation and taking into account the boundary condition $(8.23)_3$ at $\zeta = h_*$, we arrive at the formula

$$w^2(\mathbf{y},\zeta) = \frac{1}{6A_{33}}(h_*^3 - \zeta^3)\Delta_y\Big(\frac{A_{13}}{A_{33}}p\Big) - \frac{A_{13}}{6A_{33}}(h_* - \zeta)^2(\zeta + 2h_*)\nabla_y\cdot\Big(\frac{1}{A_{44}}\nabla_y\Big(\frac{A_{13}}{A_{33}}p\Big)\Big) + \frac{A_{13}}{6A_{33}}(h_* - \zeta)^3\Delta_y\Big(\frac{p}{A_{33}}\Big), \tag{8.24}$$

where for brevity we do not show the argument $\mathbf{y}$ of the functions $p(\mathbf{y})$, $A_{13}(\mathbf{y})$, $A_{33}(\mathbf{y})$, and $A_{44}(\mathbf{y})$.

8.1.3 *Local Indentation of the In-Plane Inhomogeneous Layer: Leading-Order Asymptotics for the Compressible and Incompressible Cases*

Recall that the local indentation of an elastic layer is defined as

$$w_0(\mathbf{y}) \equiv w(\mathbf{y}, 0),$$

where $w(\mathbf{y}, 0)$ is the normal displacement of the layer surface.

In the case of the compressible layer, Eqs. (8.7), (8.8), (8.14), and $(8.17)_2$ yield

$$w_0(\mathbf{y}) \simeq \frac{h}{A_{33}(\mathbf{y})}p(\mathbf{y}), \tag{8.25}$$

so that the deformation response of the elastic layer is analogous to that of a Winkler elastic foundation with the variable modulus

$$k(\mathbf{y}) = \frac{A_{33}(\mathbf{y})}{h}. \tag{8.26}$$

We emphasize that formula (8.26) is valid for a thin bonded compressible transversely isotropic elastic layer with in-plane inhomogeneous properties.

When the material approaches the incompressible limit, the right-hand side of (8.26) increases unboundedly and the first term in the asymptotic expansion (8.14) disappears. Consequently, the ratios A_{44}/A_{33} and A_{13}/A_{33} tend to 0 and 1, respectively.

Therefore, in the limit situation, formula (8.24) reduces to

$$w^2(\mathbf{y},\zeta) = -\frac{1}{6}(h_* - \zeta)^2(\zeta + 2h_*)\nabla_y\cdot\Big(\frac{1}{A_{44}}\nabla_y p\Big). \tag{8.27}$$

In the case of an incompressible bonded elastic layer, formulas (8.7), (8.8), (8.14), and (8.27) give

$$w_0(\mathbf{y}) \simeq -\frac{h^3}{3}\nabla_y \cdot \left(\frac{1}{a_{44}(\mathbf{y})}\nabla_y p(\mathbf{y})\right), \tag{8.28}$$

where $a_{44} = A_{44}$ is the out-of-plane shear modulus.

8.2 Deformation of an Elastic Layer with Thickness-Variable Inhomogeneous Properties

In the present section, the leading-order asymptotic models for the local indentation of thin bonded compressible and incompressible elastic layers developed in Chaps. 1 and 2 are generalized for elastic layers with the so-called thickness-variable inhomogeneous material properties.

8.2.1 Deformation Problem Formulation

Let us consider the deformation of a thin transversely isotropic inhomogeneous elastic layer of uniform thickness, h, with variable properties across the layer thickness (see Fig. 8.2). If the plane of isotropy is parallel to the layer surface, the stress-displacement relations take the form

$$\begin{aligned}
\sigma_{11} &= A_{11}\frac{\partial v_1}{\partial y_1} + A_{12}\frac{\partial v_2}{\partial y_2} + A_{13}\frac{\partial w}{\partial z}, \quad \sigma_{23} = A_{44}\left(\frac{\partial w}{\partial y_2} + \frac{\partial v_2}{\partial z}\right),\\
\sigma_{22} &= A_{12}\frac{\partial v_1}{\partial y_1} + A_{11}\frac{\partial v_2}{\partial y_2} + A_{13}\frac{\partial w}{\partial z}, \quad \sigma_{13} = A_{44}\left(\frac{\partial w}{\partial y_1} + \frac{\partial v_1}{\partial z}\right),\\
\sigma_{33} &= A_{13}\frac{\partial v_1}{\partial y_1} + A_{13}\frac{\partial v_2}{\partial y_2} + A_{33}\frac{\partial w}{\partial z}, \quad \sigma_{12} = A_{66}\left(\frac{\partial v_1}{\partial y_2} + \frac{\partial v_2}{\partial y_1}\right).
\end{aligned} \tag{8.29}$$

Here, $\mathbf{u} = (\mathbf{u}, w)$ is the displacement vector, $\mathbf{v}$ and w are the in-plane and out-of-plane displacements, respectively, both of which are functions of three-dimensional Cartesian coordinates $(\mathbf{y}, z)$.

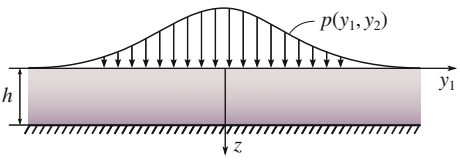

Fig. 8.2 A thickness-variable inhomogeneous elastic layer of uniform thickness bonded to a rigid substrate and supporting a distributed normal load

Let us assume that the elastic constants A_{kl} are represented in the form

$$A_{kl} = \alpha_{kl}\Big(\frac{z}{h}\Big), \tag{8.30}$$

or, equivalently, the material properties are expressed as functions of the normalized depth coordinate z/h. Note that according to the terminology introduced in [11, 12], we consider a transversely isotropic, transversely homogeneous (TITH) elastic model.

The substitution of the stress-displacement relations (8.29) into the equations of equilibrium

$$\frac{\partial \sigma_{i1}}{\partial x_1} + \frac{\partial \sigma_{i2}}{\partial x_2} + \frac{\partial \sigma_{i3}}{\partial x_3} = 0, \quad i = 1, 2, 3,$$

yields the Lamé equations

$$A_{66}\Delta_y \mathbf{v} + (A_{11} - A_{66})\nabla_y \nabla_y \cdot \mathbf{v} + A_{13}\frac{\partial}{\partial z}\nabla_y w + \frac{\partial}{\partial z}(A_{44}\nabla_y w) + \frac{\partial}{\partial z}\Big(A_{44}\frac{\partial \mathbf{v}}{\partial z}\Big) = \mathbf{0}, \tag{8.31}$$

$$\frac{\partial}{\partial z}(A_{13}\nabla_y \cdot \mathbf{v}) + A_{44}\frac{\partial}{\partial z}\nabla_y \cdot \mathbf{v} + A_{44}\Delta_y w + \frac{\partial}{\partial z}\Big(A_{33}\frac{\partial w}{\partial z}\Big) = 0, \tag{8.32}$$

where $\nabla_y = (\partial/\partial y_1, \partial/\partial y_2)$ and $\Delta_y = \nabla_y \cdot \nabla_y$ are the in-plane Hamilton and Laplace operators, respectively, and the scalar product is denoted by a dot.

Let us assume that the elastic layer is loaded on the upper surface, $z = 0$, with a normal load, p, without tangential tractions, and that it is perfectly attached to a rigid substrate at the bottom surface, $z = h$, so that the following boundary conditions take place:

$$\sigma_{13}\big|_{z=0} = \sigma_{23}\big|_{z=0} = 0, \quad \sigma_{33}\big|_{z=0} = -p, \tag{8.33}$$

$$\mathbf{v}\big|_{z=h} = \mathbf{0}, \quad w\big|_{z=h} = 0. \tag{8.34}$$

As before, we are interested in the case where the applied load p is specified on the whole upper surface of the layer, and is a sufficiently smooth function of the in-plane coordinates $\mathbf{y} = (y_1, y_2)$.

8.2.2 Perturbation Analysis of the Deformation Problem

We assume that the elastic layer is relatively thin and we set

$$h = \varepsilon h_*, \tag{8.35}$$

where ε is a small positive parameter, and h_* is a characteristic length, which is assumed to be independent of ε.

Let us also introduce the *dimensional* stretched normal coordinate

$$\zeta = \frac{z}{\varepsilon}, \tag{8.36}$$

so that in light of (8.30), (8.35), and (8.36), we obtain

$$A_{kl} = \alpha_{kl}\Big(\frac{\zeta}{h_*}\Big). \tag{8.37}$$

The substitution of the coordinate change (8.36) into the Lamé equations (8.31), (8.4) leads to the system

$$\frac{1}{\varepsilon^2}\frac{\partial}{\partial\zeta}\Big(A_{44}\frac{\partial \mathbf{v}}{\partial\zeta}\Big) + \frac{1}{\varepsilon}\Big(A_{13}\frac{\partial}{\partial\zeta}\nabla_y w + \frac{\partial}{\partial\zeta}(A_{44}\nabla_y w)\Big) + A_{66}\Delta_y \mathbf{v} + (A_{11} - A_{66})\nabla_y\nabla_y\cdot\mathbf{v} = \mathbf{0}, \tag{8.38}$$

$$\frac{1}{\varepsilon^2}\frac{\partial}{\partial\zeta}\Big(A_{33}\frac{\partial w}{\partial\zeta}\Big) + \frac{1}{\varepsilon}\Big(\frac{\partial}{\partial\zeta}(A_{13}\nabla_y\cdot\mathbf{v}) + A_{44}\frac{\partial}{\partial\zeta}\nabla_y\cdot\mathbf{v})\Big) + A_{44}\Delta_y w = 0. \tag{8.39}$$

Correspondingly, the boundary conditions (8.33) on the upper surface of the layer become

$$\frac{1}{\varepsilon}\frac{\partial \mathbf{v}}{\partial\zeta} + \nabla_y w\Big|_{\zeta=0} = \mathbf{0}, \tag{8.40}$$

$$\frac{1}{\varepsilon}A_{33}\frac{\partial w}{\partial\zeta} + A_{13}\nabla_y\cdot\mathbf{v}\Big|_{\zeta=0} = -p. \tag{8.41}$$

The boundary conditions (8.34) on the bottom surface then take the form

$$\mathbf{v}\big|_{\zeta=h_*} = \mathbf{0}, \quad w\big|_{\zeta=h_*} = 0. \tag{8.42}$$

Using the perturbation algorithm [14], we construct an approximate solution to the system (8.38)–(8.42) in the form of asymptotic expansions

$$\mathbf{v} = \varepsilon\mathbf{v}^0(\mathbf{y},\zeta) + \varepsilon^2\mathbf{v}^1(\mathbf{y},\zeta) + \cdots, \tag{8.43}$$

$$w = \varepsilon w^0(\mathbf{y},\zeta) + \varepsilon^2 w^1(\mathbf{y},\zeta) + \cdots, \tag{8.44}$$

where the successive coefficients of the powers of ε are assumed to be independent of the small parameter ε.

The substitution of the asymptotic expansions (8.43) and (8.44) into Eqs. (8.38)–(8.42) produces a set of differential equations that must be satisfied for arbitrary ε.

In particular, the leading terms of the asymptotic expansions (8.43) and (8.44) are determined as solutions of the following two problems:

$$\frac{\partial}{\partial\zeta}\left(A_{44}\frac{\partial\mathbf{v}^0}{\partial\zeta}\right)=\mathbf{0},\ \zeta\in(0,h_*),\quad \frac{\partial\mathbf{v}^0}{\partial\zeta}\bigg|_{\zeta=0}=\mathbf{0},\quad \mathbf{v}^0\big|_{\zeta=h_*}=\mathbf{0};\tag{8.45}$$

$$\frac{\partial}{\partial\zeta}\left(A_{33}\frac{\partial w^0}{\partial\zeta}\right)=0,\ \zeta\in(0,h_*),\quad A_{33}\frac{\partial w^0}{\partial\zeta}\bigg|_{\zeta=0}=-p,\quad w^0\big|_{\zeta=h_*}=0.\tag{8.46}$$

From (8.45), it immediately follows that

$$\mathbf{v}^0(\mathbf{y},\zeta)\equiv\mathbf{0},\tag{8.47}$$

while the non-trivial boundary-value problem (8.46) has the following solution:

$$w^0(\mathbf{y},\zeta)=p(\mathbf{y})\int\limits_{\zeta}^{h_*}\frac{d\zeta'}{A_{33}(\zeta')}.\tag{8.48}$$

As a result of (8.47), it can be easily seen that the problem

$$\frac{\partial}{\partial\zeta}\left(A_{33}\frac{\partial w^1}{\partial\zeta}\right)=-\frac{\partial}{\partial\zeta}(A_{13}\nabla_y\cdot\mathbf{v}^0)-A_{44}\frac{\partial}{\partial\zeta}\nabla_y\cdot\mathbf{v}^0,\quad \zeta\in(0,h_*),$$

$$A_{33}\frac{\partial w^1}{\partial\zeta}\bigg|_{\zeta=0}=-A_{13}\nabla_y\cdot\mathbf{v}^0\big|_{\zeta=0},\quad w^1\big|_{\zeta=h_*}=0$$

is homogeneous, and therefore its solution is trivial:

$$w^1(\mathbf{y},\zeta)\equiv 0.\tag{8.49}$$

Simultaneously, for the first non-trivial term of the asymptotic expansion (8.43), we have the problem

$$\begin{gathered}\frac{\partial}{\partial\zeta}\left(A_{44}\frac{\partial\mathbf{v}^1}{\partial\zeta}\right)=\frac{\partial A_{13}}{\partial\zeta}\nabla_y w^0-\frac{\partial}{\partial\zeta}\big((A_{13}+A_{44})\nabla_y w^0\big),\quad \zeta\in(0,h_*),\\ \frac{\partial\mathbf{v}^1}{\partial\zeta}\bigg|_{\zeta=0}=-\nabla_y w^0\big|_{\zeta=0},\quad \mathbf{v}^1\big|_{\zeta=h_*}=\mathbf{0}.\end{gathered}\tag{8.50}$$

To solve the above problem, we first rewrite formula (8.48) in the form

$$w^0(\mathbf{y},\zeta)=p(\mathbf{y})\mathscr{W}^0(\zeta),\tag{8.51}$$

where we have introduced the notation

$$\mathscr{W}^0(\zeta) = \int_{\zeta}^{h_*} \frac{d\zeta'}{A_{33}(\zeta')}. \tag{8.52}$$

Observe that we employ the notation $A_{33}(\zeta)$ for brevity, and that as a result of (8.37), Eq. (8.52) can be written as

$$\mathscr{W}^0(\zeta) = \int_{\zeta}^{h_*} \frac{1}{\alpha_{33}(\zeta'/h_*)}\, d\zeta'.$$

Thus, according to (8.51), the solution of the system (8.50) can be represented in the form

$$\mathbf{v}^1(\mathbf{y}, \zeta) = \nabla_y p(\mathbf{y}) \mathscr{V}^1(\zeta), \tag{8.53}$$

where $\mathscr{V}^1(\zeta)$ is a scalar function satisfying the problem

$$\begin{gathered} \frac{d}{d\zeta}\left(A_{44}\frac{d\mathscr{V}^1}{d\zeta}\right) = -A_{13}\frac{d\mathscr{W}^0}{d\zeta} - \frac{d}{d\zeta}\left(A_{44}\mathscr{W}^0\right), \quad \zeta \in (0, h_*), \\ \left.\frac{d\mathscr{V}^1}{d\zeta}\right|_{\zeta=0} = -\mathscr{W}^0(0), \quad \mathscr{V}^1\big|_{\zeta=h_*} = 0. \end{gathered} \tag{8.54}$$

Integrating the differential equation $(8.54)_1$, we obtain

$$\frac{d\mathscr{V}^1}{d\zeta} = \frac{1}{A_{44}(\zeta)} \int_0^{\zeta} \frac{A_{13}(\zeta')}{A_{33}(\zeta')}\, d\zeta' - \mathscr{W}^0(\zeta) + \frac{C_1}{A_{44}(\zeta)},$$

where C_1 is an integration constant. In light of the first boundary condition (8.54), we readily find that $C_1 = 0$.

Upon integration of the above equation, we arrive at the formula

$$\mathscr{V}^1(\zeta) = -\int_{\zeta}^{h_*} \left(\frac{1}{A_{44}(\xi)} \int_0^{\xi} \frac{A_{13}(\zeta')}{A_{33}(\zeta')}\, d\zeta' - \mathscr{W}^0(\xi) \right) d\xi,$$

which after recalling the definition of the function $\mathscr{W}^0(\zeta)$ (see Eq. (8.52)) can be rewritten as

$$\mathscr{V}^1(\zeta) = -\int_{\zeta}^{h_*} \frac{1}{A_{44}(\xi)} \int_0^{\xi} \frac{A_{13}(\zeta')}{A_{33}(\zeta')}\, d\zeta' d\xi + \int_{\zeta}^{h_*} \frac{\xi - \zeta}{A_{33}(\xi)}\, d\xi. \tag{8.55}$$

We now return to the problem for the second non-trivial term of the asymptotic expansion (8.44), that is

$$\begin{gathered} \frac{\partial}{\partial \zeta}\left(A_{33}\frac{\partial w^2}{\partial \zeta}\right) = -\frac{\partial}{\partial \zeta}(A_{13}\nabla_y \cdot \mathbf{v}^1) - A_{44}\frac{\partial}{\partial \zeta}\nabla_y \cdot \mathbf{v}^1 - A_{44}\Delta_y w^0, \\ A_{33}\frac{\partial w^2}{\partial \zeta}\bigg|_{\zeta=0} = -A_{13}\nabla_y \cdot \mathbf{v}^1\,\big|_{\zeta=0}, \quad w^2\big|_{\zeta=h_*} = 0. \end{gathered} \tag{8.56}$$

According to (8.51) and (8.53), the solution to the problem (8.56) can be represented in the form

$$w^1(\mathbf{y}, \zeta) = \Delta_y p(\mathbf{y}) \mathscr{W}^2(\zeta), \tag{8.57}$$

where $\mathscr{W}^2(\zeta)$ is a scalar function satisfying the problem

$$\begin{gathered} \frac{d}{d\zeta}\left(A_{33}\frac{d\mathscr{W}^2}{d\zeta}\right) = -\frac{d}{d\zeta}(A_{13}\mathscr{V}^1) - A_{44}\frac{d\mathscr{V}^1}{d\zeta} - A_{44}\mathscr{W}^0, \quad \zeta \in (0, h_*), \\ A_{33}\frac{d\mathscr{W}^2}{d\zeta}\bigg|_{\zeta=0} = -A_{13}\mathscr{V}^1\,\big|_{\zeta=0}, \quad \mathscr{W}^2\big|_{\zeta=h_*} = 0. \end{gathered} \tag{8.58}$$

By integrating Eq. $(8.58)_1$ with boundary condition $(8.58)_2$ taken into account, we find

$$\frac{d\mathscr{W}^2}{d\zeta} = -\frac{A_{13}}{A_{33}}\mathscr{V}^1 - \frac{1}{A_{33}}\int_0^{\zeta} (\zeta - \zeta')\frac{A_{13}(\zeta')}{A_{33}(\zeta')}\, d\zeta'.$$

A final integration reveals

$$\mathscr{W}^2(\zeta) = \int_{\zeta}^{h_*} \frac{A_{13}(\eta)}{A_{33}(\eta)}\mathscr{V}^1(\eta)\, d\eta + \int_{\zeta}^{h_*} \frac{1}{A_{33}(\xi)} \int_0^{\xi} (\xi - \zeta')\frac{A_{13}(\zeta')}{A_{33}(\zeta')}\, d\zeta' d\xi. \tag{8.59}$$

By collecting formulas (8.57) and (8.59), we can write out a closed-form representation for the function $w^2(\mathbf{y}, \zeta)$.

8.2.3 *Local Indentation of the Inhomogeneous Layer: Leading-Order Asymptotics for the Compressible and Incompressible Cases*

In the case of the compressible layer, formulas (8.44), (8.51), and (8.52) yield for the local indentation

$$w_0(\mathbf{y}) \equiv w(\mathbf{y}, 0)$$

the following leading-order asymptotic approximation:

$$w_0(\mathbf{y}) \simeq \varepsilon p(\mathbf{y}) \int_0^{h_*} \frac{d\zeta}{A_{33}(\zeta)}.$$

Following (8.30), (8.35)–(8.37), the above formula can be transformed to

$$w_0(\mathbf{y}) \simeq p(\mathbf{y}) \int_0^{h} \frac{dz}{A_{33}(z)}. \tag{8.60}$$

In other words, the deformation response of a thin bonded compressible inhomogeneous elastic layer resembles that of a Winkler elastic foundation with the modulus

$$k = \left(\int_0^{h} \frac{dz}{A_{33}(z)} \right)^{-1}. \tag{8.61}$$

It is clear that in the case of a thin compressible homogeneous elastic layer formula (8.61) reduces to (1.65).

When the layer material approaches the incompressibility limit, the ratio A_{44}/A_{33} vanishes, while the ratio A_{13}/A_{33} tends to 1. At the same time, the Winkler foundation modulus k defined by (8.61) tends to infinity. Thus, in the case of the incompressible layer, formula (8.55) results in the following:

$$\mathscr{V}^1(\zeta) = -\int_{\zeta}^{h_*} \frac{\xi \, d\xi}{a_{44}(\xi)}. \tag{8.62}$$

Here, $a_{44} = A_{44}$ is the out-of-plane shear modulus.

Correspondingly, Eq. (8.59) reduces to

$$\mathscr{W}^2(\zeta) = \int_{\zeta}^{h_*} \mathscr{V}^1(\eta)\, d\eta. \tag{8.63}$$

The substitution of (8.62) into (8.63) reveals

$$\begin{aligned} \mathscr{W}^2(0) &= \zeta \mathscr{V}^1(\zeta)\Big|_0^{h_*} - \int_0^{h_*} \zeta \frac{d\mathscr{V}^1}{d\zeta}(\zeta)\, d\zeta \\ &= -\int_0^{h_*} \frac{\zeta^2}{a_{44}(\zeta)}\, d\zeta. \end{aligned} \tag{8.64}$$

Collecting formulas (8.44), (8.57), (8.64), and taking into account Eqs. (8.35)–(8.37), we obtain

$$w_0(\mathbf{y}) \simeq -\Delta_y p(\mathbf{y}) \int_0^h \frac{z^2 dz}{a_{44}(z)}. \tag{8.65}$$

We emphasize that formula (8.65) is derived for a thin bonded incompressible transversely isotropic, transversely homogeneous elastic layer.

8.3 Contact of Thin Bonded Incompressible Inhomogeneous Layers

In this section we briefly consider the axisymmetric frictionless contact problems for thin inhomogeneous transversely isotropic elastic layers bonded to slightly curved rigid substrates. The developed leading-order asymptotic models are validated by comparison with available published results.

8.3.1 Contact Problem Formulation

We consider two thin uniform inhomogeneous elastic layers firmly attached to rigid substrates. In the undeformed configuration the layers are in contact at a single point, O, chosen as the center of the Cartesian coordinate system Oy_2y_2z (see Fig. 3.1). We write the equations of the layer surfaces in the form $z = (-1)^n \varphi_n(\mathbf{y})$ $(n = 1, 2)$, so that the gap between the contacting surfaces is

$$\varphi(\mathbf{y}) = \varphi_1(\mathbf{y}) + \varphi_2(\mathbf{y}). \tag{8.66}$$

Denoting the vertical contact approach of the substrates—as usual—by δ_0, we formulate the linearized unilateral non-penetration condition as follows:

$$\delta_0 - \left(w_0^{(1)}(\mathbf{y}) + w_0^{(2)}(\mathbf{y})\right) \le \varphi(\mathbf{y}). \tag{8.67}$$

Here, $w_0^{(n)}(\mathbf{y})$ is the local indentation of the nth elastic layer.

Generalizing the results of the previous two sections, we arrive at the approximate formula for the local indentation of the nth layer

$$w_0^{(n)}(\mathbf{y}) = -\nabla_y \cdot \left(\int_0^{h_n} \frac{z^2 dz}{G_n'(\mathbf{y}, z)} \nabla_y p(\mathbf{y}) \right), \tag{8.68}$$

where $p(\mathbf{y})$ is the contact pressure density, h_n is the thickness of the nth layer, and $G_n'(\mathbf{y}, z)$ is the out-of-plane shear modulus as it measured from the layer surface.

The contour Γ of the contact area ω is determined from the condition that the contact pressure is positive inside ω and vanishes at Γ, so that

$$p(\mathbf{y}) > 0, \quad \mathbf{y} \in \omega, \quad p(\mathbf{y}) = 0, \quad \mathbf{y} \in \Gamma. \tag{8.69}$$

Moreover, in the case of incompressible layers, we additionally assume a smooth transition of the pressure density $p(\mathbf{y})$ from the contact region ω to the outside region $\mathbf{y} \notin \omega$, where $p(\mathbf{y}) \equiv 0$. Thus, in addition to $(8.69)_2$, we impose the following zero-pressure-gradient boundary condition (see Sect. 2.7.3 and [5, 7, 8]):

$$\frac{\partial p}{\partial n}(\mathbf{y}) = 0, \quad \mathbf{y} \in \Gamma. \tag{8.70}$$

Here, $\partial/\partial n$ is the normal derivative directed outward from ω.

By substituting the expressions for the local indentations $w_0^{(1)}(\mathbf{y})$ and $w_0^{(2)}(\mathbf{y})$ provided by formula (8.68) into the contact condition (8.67) and taking into account $(8.69)_1$, we derive the governing differential equation

$$-\nabla_y \cdot \left(\gamma(\mathbf{y}) \nabla_y p(\mathbf{y})\right) = \delta_0 - \varphi(\mathbf{y}), \quad \mathbf{y} \in \omega, \tag{8.71}$$

where we have introduced the notation

$$\gamma(\mathbf{y}) = \int_0^{h_1} \frac{z^2 dz}{G_1'(\mathbf{y}, z)} + \int_0^{h_1} \frac{z^2 dz}{G_1'(\mathbf{y}, z)}. \tag{8.72}$$

Finally, the equilibrium equation for the whole system is

$$\iint\limits_{\omega} p(\mathbf{y})\, d\mathbf{y} = F, \tag{8.73}$$

where F is the external load compressing the elastic layers.

The boundary-value problem (8.69)–(8.71) will be used to find both the contact area ω and the contact pressure $p(\mathbf{y})$, while the equilibrium equation (8.73) will allow determination of the contact approach δ_0, provided that the contact force F is given in advance.

8.3.2 Axisymmetric Unilateral Contact Problem

Introducing the cylindrical coordinate system (r, θ, z), we can write equations of the undeformed layer surfaces in the form $z = (-1)^n \varphi_n(r)$ $(n = 1, 2)$, so that the gap function (8.66) becomes (see Fig. 8.3)

$$\varphi(r) = \varphi_1(r) + \varphi_2(r). \tag{8.74}$$

For the sake of simplicity, we assume that the gap $\varphi(r)$ is a smooth increasing function and thus that the contact area ω is a circle of some radius a.

Due to the chain rule of differentiation, we have

$$\frac{\partial}{\partial y_1} = \cos\theta \frac{\partial}{\partial r} - \frac{\sin\theta}{r} \frac{\partial}{\partial \theta}, \quad \frac{\partial}{\partial y_2} = \sin\theta \frac{\partial}{\partial r} + \frac{\cos\theta}{r} \frac{\partial}{\partial \theta},$$

so that the in-plane Hamilton operator is

$$\nabla_y = \Big(\cos\theta \frac{\partial}{\partial r} - \frac{\sin\theta}{r} \frac{\partial}{\partial \theta}\Big)\mathbf{e}_1 + \Big(\sin\theta \frac{\partial}{\partial r} + \frac{\cos\theta}{r} \frac{\partial}{\partial \theta}\Big)\mathbf{e}_2,$$

where $\mathbf{e}_1$ and $\mathbf{e}_2$ are the basis vectors of the Cartesian coordinate system.

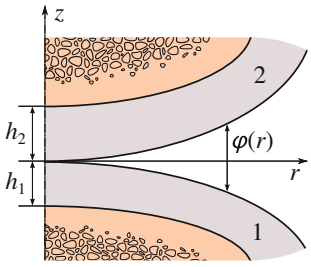

Fig. 8.3 Two inhomogeneous incompressible elastic layers bonded to axisymmetric rigid substrates in the undeformed configuration

For an axisymmetric density $p(r)$, we have

$$\nabla_y p(r) = \cos\theta \frac{dp}{dr}(r)\,\mathbf{e}_1 + \sin\theta \frac{dp}{dr}(r)\,\mathbf{e}_2$$

and correspondingly

$$\begin{aligned}\nabla_y \cdot \big(\gamma(r)\nabla_y p(r)\big) &= \frac{d}{dr}\Big(\gamma(r)\frac{dp}{dr}(r)\Big) + \frac{1}{r}\gamma(r)\frac{dp}{dr}(r)\\ &= \frac{1}{r}\frac{d}{dr}\Big(r\gamma(r)\frac{dp}{dr}(r)\Big),\end{aligned} \tag{8.75}$$

while, as a result of (8.72), the function $\gamma(r)$ is given by

$$\gamma(r) = \int_0^{h_1} \frac{z^2 dz}{G_1'(r,z)} + \int_0^{h_1} \frac{z^2 dz}{G_1'(r,z)}.$$

Further, Eq. (8.71) takes the form

$$-\frac{1}{r}\frac{d}{dr}\Big(r\gamma(r)\frac{dp}{dr}(r)\Big) = \delta_0 - \varphi(r), \quad r \in (0,a), \tag{8.76}$$

whereas the boundary conditions $(8.69)_2$ and (8.70) become

$$p(a) = 0, \quad \frac{dp}{dr}(a) = 0. \tag{8.77}$$

Integrating Eq. (8.76), we find

$$\frac{dp}{dr}(r) = -\frac{\delta_0}{2}\frac{r}{\gamma(r)} + \frac{1}{r\gamma(r)}\int_0^r \varphi(\rho)\rho\, d\rho, \tag{8.78}$$

where the integration constant vanishes due to the regularity condition for the solution of the problem (8.76), (8.77) at the center of the contact area $r = 0$.

By substituting $r = a$ into the above equation and taking into account the boundary condition $(8.77)_2$, we derive the following equation:

$$\delta_0 = \frac{2}{a^2}\int_0^r \varphi(\rho)\rho\, d\rho. \tag{8.79}$$

By integrating Eq. (8.78) and employing the boundary condition $(8.77)_1$, we obtain

$$p(r) = \frac{\delta_0}{2} \int_r^a \frac{\rho\, d\rho}{\gamma(\rho)} - \int_r^a \frac{1}{\rho\gamma(\rho)} \int_0^\rho \varphi(\xi)\xi\, d\xi d\rho. \tag{8.80}$$

Formula (8.80) presents the contact pressure in terms of the gap function $\varphi(r)$, given by (8.74), the elastic compliance function $\gamma(r)$, defined by (8.72), and two a priori unknown parameters δ_0 and a, which are related by Eq. (8.79).

An additional equation for determining the contact approach δ_0 and the contact radius a is provided by the equilibrium equation (8.73). Specifically, the substitution of (8.80) into Eq. (8.73) yields

$$F = \frac{\pi}{2}\delta_0 \int_0^a \frac{\rho^3 d\rho}{\gamma(\rho)} - \pi \int_0^a \frac{r}{\gamma(r)} \int_0^r \varphi(\rho)\rho\, d\rho dr. \tag{8.81}$$

In the case of in-plane homogeneous elastic layers, where $\gamma(r)$ is constant, formulas (8.80) and (8.81) reduce to the following:

$$p(r) = \frac{\delta_0}{4\gamma}(a^2 - r^2) - \frac{1}{\gamma}\Theta(a, r), \tag{8.82}$$

$$F = \frac{\pi}{4\gamma} \int_0^a \varphi(\rho)(2\rho^2 - a^2)\rho\, d\rho. \tag{8.83}$$

Here we have introduced the notation

$$\Theta(a, r) = \int_r^a \varphi(\rho)\rho \ln\frac{a}{\rho}\, d\rho - \int_0^r \varphi(\rho)\rho \ln\frac{r}{\rho}\, d\rho. \tag{8.84}$$

Observe that in writing formula (8.83) we have taken into account Eq. (8.79). We also note that the contact radius is determined as a solution of Eq. (8.79).

8.3.3 Contact Problem for a Thin Bonded Non-homogeneous Incompressible Elastic Layer with Fixed Contact Area

Let us now consider contact interaction between a thin elastic layer bonded to a rigid substrate and a punch, under the assumption that the contact area, ω, does not change if the contact load, F, varies. In this case, the contact condition is

$$w_0(\mathbf{y}) = \delta_0 - \varphi(\mathbf{y}), \quad \mathbf{y} \in \omega, \tag{8.85}$$

where δ_0 and $\varphi(\mathbf{y})$ are the punch's normal displacement and the punch shape function, and $w_0(\mathbf{y})$ is the local indentation of the elastic layer.

For a thin incompressible elastic layer, according to the asymptotic analysis performed in Sects. 8.1 and 8.2, we have

$$w_0(\mathbf{y}) = -\nabla_y \cdot \left(\int_0^h \frac{z^2 dz}{G'(\mathbf{y}, z)} \nabla_y p(\mathbf{y}) \right), \tag{8.86}$$

where $p(\mathbf{y})$ is the contact pressure distribution, h_n and $G'(\mathbf{y}, z)$ are the elastic layer's thickness and out-of-plane shear modulus measured in the z-direction from the layer surface, respectively.

Substituting (8.86) into Eq. (8.85), we arrive at the equation

$$-\nabla_y \cdot \left(\gamma(\mathbf{y}) \nabla_y p(\mathbf{y}) \right) = \delta_0 - \varphi(\mathbf{y}), \quad \mathbf{y} \in \omega, \tag{8.87}$$

where we have introduced the notation

$$\gamma(\mathbf{y}) = \int_0^h \frac{z^2 dz}{G'(\mathbf{y}, z)}. \tag{8.88}$$

The second-order differential equation (8.87) requires some boundary conditions at the contour Γ of the domain ω. As was shown by Aleksandrov [1] (see also Sect. 2.7.2) in the axisymmetric contact problem for a thin incompressible isotropic elastic layer, in order to construct the leading-order inner asymptotic solution for the contact pressure under a flat-ended punch, the differential equation (8.87) should be supplemented with the following boundary condition:

$$p(\mathbf{y}) = 0, \quad \mathbf{y} \in \Gamma. \tag{8.89}$$

In the case of a thin bonded homogeneous incompressible elastic layer (when $\gamma(\mathbf{y}) \equiv \text{const}$), Barber [7] has shown that the problem (8.87), (8.89) is formally equivalent to the Saint-Venant torsion problem (see, e.g., [19], Chap. 10), and hence the analytical solutions to many contact problems can be written down.

We emphasize that in the case of an elastic layer indented by a rigid punch with a sharp edge, the contact pressure has a square-root singularity at the contour Γ (see, e.g., [3, 13, 15]). For a thin elastic layer this effect is taken into account by the additional asymptotic solution of the boundary-layer type (see, in particular, [1]).

Finally, the punch's displacement δ_0 and the contact force F are related through the equilibrium equation

$$\iint\limits_{\omega} p(\mathbf{y})\, d\mathbf{y} = F. \tag{8.90}$$

Observe that, from a physical point of view, there exists a constant γ_0 such that the function (8.88) satisfies the condition

$$\gamma(\mathbf{y}) \geq \gamma_0, \quad \mathbf{y} \in \bar{\omega} = \omega \cup \Gamma.$$

According to the weak maximum principle (see, e.g., [10]), if the right-hand side of Eq. (8.87) satisfies the condition

$$\delta_0 - \varphi(\mathbf{y}) \geq 0, \quad \mathbf{y} \in \omega, \tag{8.91}$$

then the minimum of the contact pressure $p(\mathbf{y})$ in $\bar{\omega}$ is achieved on Γ, i.e.,

$$\min_{\mathbf{y}\in\bar{\omega}} p(\mathbf{y}) = \min_{\mathbf{y}\in\Gamma} p(\mathbf{y}). \tag{8.92}$$

Hence, from (8.89) and (8.92), it follows that in the case (8.91), we have throughout the contact area

$$p(\mathbf{y}) \geq 0, \quad \mathbf{y} \in \omega. \tag{8.93}$$

We note that under some assumptions on the domain ω (e.g., for a simply connected domain ω bounded by a smooth contour Γ of class C^2), the strict inequality in (8.91) implies the strict inequality in (8.93). Equivalently, if the local indentation of a thin incompressible elastic layer is positive over the whole contact area, then the contact pressure under the punch is positive, which is generally not the case.

8.3.4 Axisymmetric Contact Problem with Fixed Contact Area

We now consider the following linear contact problem (see Fig. 8.4):

$$-\frac{1}{r}\frac{d}{dr}\left(r\gamma(r)\frac{dp}{dr}(r)\right) = \delta_0 - \varphi(r), \quad r \in (0, a), \tag{8.94}$$

$$p(a) = 0, \tag{8.95}$$

$$2\pi \int_0^a p(r) r\, dr = F. \tag{8.96}$$

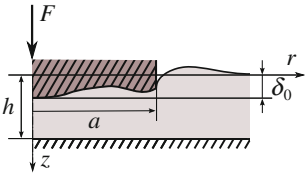

Fig. 8.4 An inhomogeneous incompressible elastic layer bonded to a rigid substrate in full contact with an axisymmetric rigid punch

As a result of (8.88), we have

$$\gamma(r) = \int_0^h \frac{z^2 dz}{G'(r,z)}.$$

The solution to Eqs. (8.94)–(8.96) is given by the formulas (see Sect. 8.3.2):

$$p(r) = \frac{\delta_0}{2} \int_r^a \frac{\rho\, d\rho}{\gamma(\rho)} - \int_r^a \frac{1}{\rho\gamma(\rho)} \int_0^\rho \varphi(\xi)\xi\, d\xi d\rho, \tag{8.97}$$

$$F = \frac{\pi}{2}\delta_0 \int_0^a \frac{\rho^3 d\rho}{\gamma(\rho)} - \pi \int_0^a \frac{r}{\gamma(r)} \int_0^r \varphi(\rho)\rho\, d\rho dr. \tag{8.98}$$

In the case of the in-plane homogeneous elastic layer, where the shear modulus G' does not depend on r and $\gamma(r)$ is constant, Eqs. (8.97) and (8.98) yield simply

$$p(r) = \frac{\delta_0}{4\gamma}(a^2 - r^2) - \frac{1}{\gamma}\Theta(a,r), \tag{8.99}$$

$$F = \frac{\pi}{8\gamma}\delta_0 a^4 - \frac{\pi}{2\gamma} \int_0^a \varphi(\rho)(a^2 - \rho^2)\rho\, d\rho, \tag{8.100}$$

where the factor $\Theta(a,r)$ is given by formula (8.84).

The obtained solution and, in particular, formula (8.99) agree with the so-called degenerate asymptotic solution obtained by Aleksandrov [1] in the isotropic and homogeneous case. The contact problem for an incompressible inhomogeneous isotropic elastic layer bonded to a rigid substrate, and indented without friction by a rigid punch, was studied by Malits [16], who, in particular, constructed the leading-order asymptotic solution in the case of a circular punch of three-dimensional profile, where formula (8.100) takes the following form:

$$F = \frac{\pi}{8\gamma}\delta_0 a^4 - \frac{1}{4\gamma}\int_0^{2\pi} d\theta \int_0^a \varphi(\rho,\theta)(a^2-\rho^2)\rho\, d\rho.$$

For the flat-ended punch, when $\varphi(r) \equiv 0$, Eqs. (8.99) and (8.100) further simplify to

$$p(r) = \frac{\delta_0}{4\gamma}(a^2 - r^2), \tag{8.101}$$

$$F = \frac{\pi}{8\gamma}\delta_0 a^4. \tag{8.102}$$

In the case of the homogeneous isotropic incompressible elastic layer, we have

$$\gamma = \frac{h^3}{3G}, \tag{8.103}$$

where G is the shear modulus, and formula (8.101) coincides with the solution obtained by Aleksandrov [1], while Eq. (8.102), apart from notation, coincides with the corresponding equation obtained by Malits [16].

8.4 Deformation of a Thin Elastic Layer Coated with an Elastic Membrane

In this section we consider the deformation problem for a transversely isotropic elastic layer bonded to a rigid substrate and coated with a very thin elastic layer made of another transversely isotropic material. The leading-order asymptotic model is based on the simplifying assumptions that the generalized plane stress conditions apply to the coating layer, and the flexural stiffness of the coating layer is negligible compared to its tensile stiffness.

8.4.1 Boundary Conditions for a Coated Elastic Layer

We consider a very thin transversely isotropic elastic coating layer (of uniform thickness $\hat{h}$) bonded to an elastic layer (of thickness h) made of another transversely isotropic material (see Fig. 8.5).

Let the five independent elastic constants of the elastic layer and its coating are denoted by A_{11}, A_{12}, A_{13}, A_{33}, A_{44} and $\hat{A}_{11}$, $\hat{A}_{12}$, $\hat{A}_{13}$, $\hat{A}_{33}$, $\hat{A}_{44}$, respectively.

Under the assumption that the two layers are in perfect contact with one another along their common interface, $z = 0$, the following boundary conditions of continuity (interface conditions of perfect bonding) should be satisfied:

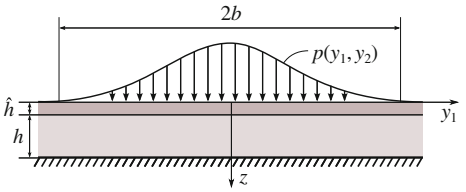

Fig. 8.5 A two-layer elastic system (coated layer and coating layer in perfect bonding) bonded to a rigid substrate and loaded by a normal load

$$\hat{\mathbf{v}}(\mathbf{y}, 0) = \mathbf{v}(\mathbf{y}, 0), \quad \hat{w}(\mathbf{y}, 0) = w(\mathbf{y}, 0), \tag{8.104}$$

$$\hat{\sigma}_{3j}(\mathbf{y}, 0) = \sigma_{3j}(\mathbf{y}, 0), \quad j = 1, 2, 3. \tag{8.105}$$

Here, $(\hat{\mathbf{v}}, \hat{w})$ is the displacement vector of the elastic coating layer, and $\hat{\sigma}_{ij}$ are the corresponding components of stress.

On the upper surface of the two-layer system, $z = -\hat{h}$, we impose the boundary conditions of normal loading with no tangential tractions

$$\hat{\sigma}_{31}(\mathbf{y}, -\hat{h}) = \sigma_{32}(\mathbf{y}, -\hat{h}) = 0, \quad \hat{\sigma}_{33}(\mathbf{y}, -\hat{h}) = -p(\mathbf{y}), \tag{8.106}$$

where $p(\mathbf{y})$ is a specified function.

Following Rahman and Newaz [18], we simplify the deformation analysis of the elastic coating layer based on the following two assumptions: (1) the coating layer is assumed to be very thin, so that the generalized plane stress conditions apply; (2) the flexural stiffness of the coating layer in the z-direction is negligible compared to its tensile stiffness.

In the absence of body forces, the equilibrium equations for an infinitesimal element of the coating layer are

$$\frac{\partial \hat{\sigma}_{11}}{\partial y_1} + \frac{\partial \hat{\sigma}_{12}}{\partial y_2} + \frac{\partial \hat{\sigma}_{13}}{\partial z} = 0, \quad \frac{\partial \hat{\sigma}_{21}}{\partial y_1} + \frac{\partial \hat{\sigma}_{22}}{\partial y_2} + \frac{\partial \hat{\sigma}_{23}}{\partial z} = 0, \tag{8.107}$$

$$\frac{\partial \hat{\sigma}_{31}}{\partial y_1} + \frac{\partial \hat{\sigma}_{32}}{\partial y_2} + \frac{\partial \hat{\sigma}_{33}}{\partial z} = 0. \tag{8.108}$$

The stress-strain relationship for the transversely isotropic elastic coating layer is given by

$$\begin{pmatrix} \hat{\sigma}_{11} \\ \hat{\sigma}_{22} \\ \hat{\sigma}_{33} \\ \hat{\sigma}_{23} \\ \hat{\sigma}_{13} \\ \hat{\sigma}_{12} \end{pmatrix} = \begin{bmatrix} \hat{A}_{11} & \hat{A}_{12} & \hat{A}_{13} & 0 & 0 & 0 \\ \hat{A}_{12} & \hat{A}_{11} & \hat{A}_{13} & 0 & 0 & 0 \\ \hat{A}_{13} & \hat{A}_{13} & \hat{A}_{33} & 0 & 0 & 0 \\ 0 & 0 & 0 & 2\hat{A}_{44} & 0 & 0 \\ 0 & 0 & 0 & 0 & 2\hat{A}_{44} & 0 \\ 0 & 0 & 0 & 0 & 0 & 2\hat{A}_{66} \end{bmatrix} \begin{pmatrix} \hat{\varepsilon}_{11} \\ \hat{\varepsilon}_{22} \\ \hat{\varepsilon}_{33} \\ \hat{\varepsilon}_{23} \\ \hat{\varepsilon}_{13} \\ \hat{\varepsilon}_{12} \end{pmatrix}, \tag{8.109}$$

where $2\hat{A}_{66} = \hat{A}_{11} - \hat{A}_{12}$.

Integrating Eqs. (8.107), (8.108) through the thickness of the coating layer and taking into account the interface and boundary conditions (8.105) and (8.106), we find

$$\hat{h}\left(\frac{\partial\hat{\tilde{\sigma}}_{11}}{\partial y_1}+\frac{\partial\hat{\tilde{\sigma}}_{12}}{\partial y_2}\right)=-\sigma_{13}\big|_{z=0},\quad \hat{h}\left(\frac{\partial\hat{\tilde{\sigma}}_{12}}{\partial y_1}+\frac{\partial\hat{\tilde{\sigma}}_{22}}{\partial y_2}\right)=-\sigma_{23}\big|_{z=0}, \tag{8.110}$$

$$\hat{h}\left(\frac{\partial\hat{\tilde{\sigma}}_{13}}{\partial y_1}+\frac{\partial\hat{\tilde{\sigma}}_{23}}{\partial y_2}\right)=-\sigma_{33}\big|_{z=0}-p. \tag{8.111}$$

Here, $\hat{\tilde{\sigma}}_{ij}$ are the averaged stresses, i.e.,

$$\hat{\tilde{\sigma}}_{ij}(\mathbf{y})=\frac{1}{\hat{h}}\int\limits_{-\hat{h}}^{0}\hat{\sigma}_{ij}(\mathbf{y},z)\,dz.$$

Under the simplifying assumptions made above, we have

$$\hat{\tilde{\sigma}}_{13}=\hat{\tilde{\sigma}}_{23}=\hat{\tilde{\sigma}}_{33}=0. \tag{8.112}$$

Hence, Eq. (8.111) immediately implies that

$$\sigma_{33}\big|_{z=0}=-p. \tag{8.113}$$

Moreover, in light of (8.112), the averaged strain $\hat{\tilde{\varepsilon}}_{33}$ must satisfy the equation

$$\hat{A}_{13}\hat{\tilde{\varepsilon}}_{11}+\hat{A}_{13}\hat{\tilde{\varepsilon}}_{22}+\hat{A}_{33}\hat{\tilde{\varepsilon}}_{33}=0,$$

and, therefore, the in-plane averaged stress-strain relationship takes the form

$$\begin{pmatrix}\hat{\tilde{\sigma}}_{11}\\ \hat{\tilde{\sigma}}_{22}\\ \hat{\tilde{\sigma}}_{12}\end{pmatrix}=\begin{bmatrix}\hat{\tilde{A}}_{11} & \hat{\tilde{A}}_{12} & 0\\ \hat{\tilde{A}}_{12} & \hat{\tilde{A}}_{11} & 0\\ 0 & 0 & 2\hat{\tilde{A}}_{66}\end{bmatrix}\begin{pmatrix}\hat{\tilde{\varepsilon}}_{11}\\ \hat{\tilde{\varepsilon}}_{22}\\ \hat{\tilde{\varepsilon}}_{12}\end{pmatrix}, \tag{8.114}$$

where we have introduced the notation

$$\hat{\tilde{A}}_{11}=\hat{A}_{11}-\frac{\hat{A}_{13}^2}{\hat{A}_{33}},\quad \hat{\tilde{A}}_{12}=\hat{A}_{12}-\frac{\hat{A}_{13}^2}{\hat{A}_{33}},\quad 2\hat{\tilde{A}}_{66}=\hat{\tilde{A}}_{11}-\hat{\tilde{A}}_{12}. \tag{8.115}$$

On the other hand, in light of the interface conditions (8.104), we have

$$\hat{\tilde{\varepsilon}}_{11}=\varepsilon_{11}\big|_{z=0},\quad \hat{\tilde{\varepsilon}}_{22}=\varepsilon_{22}\big|_{z=0},\quad \hat{\tilde{\varepsilon}}_{12}=\varepsilon_{12}\big|_{z=0}, \tag{8.116}$$

where ε_{11}, ε_{22}, and ε_{12} are the in-plane strains in the coated elastic layer $z \in (0, h)$.

Taking Eqs. (8.114) and (8.116) into account, we transform the boundary conditions (8.110) into the following:

$$-\frac{1}{\hat{h}}\sigma_{31}\big|_{z=0} = \frac{\partial}{\partial y_1}\left(\hat{\hat{A}}_{11}\frac{\partial v_1}{\partial y_1} + \hat{\hat{A}}_{12}\frac{\partial v_2}{\partial y_2}\right) + \hat{\hat{A}}_{66}\frac{\partial}{\partial y_2}\left(\frac{\partial v_1}{\partial y_2} + \frac{\partial v_2}{\partial y_1}\right),$$

$$-\frac{1}{\hat{h}}\sigma_{32}\big|_{z=0} = \hat{\hat{A}}_{66}\frac{\partial}{\partial y_1}\left(\frac{\partial v_1}{\partial y_2} + \frac{\partial v_2}{\partial y_1}\right) + \frac{\partial}{\partial y_2}\left(\hat{\hat{A}}_{12}\frac{\partial v_1}{\partial y_1} + \hat{\hat{A}}_{11}\frac{\partial v_2}{\partial y_2}\right).$$

The above boundary conditions can be rewritten in the matrix form as

$$\sigma_{31}\mathbf{e}_1 + \sigma_{32}\mathbf{e}_2\big|_{z=0} = -\hat{\mathfrak{L}}(\nabla_y)\mathbf{v}\big|_{z=0}, \tag{8.117}$$

where $\hat{\mathfrak{L}}(\nabla_y)$ is a 2×2 matrix differential operator such that

$$\begin{aligned}
\hat{\mathfrak{L}}_{\alpha\alpha}(\nabla_y) &= \hat{h}\hat{\hat{A}}_{11}\frac{\partial^2}{\partial y_\alpha^2} + \hat{h}\hat{\hat{A}}_{66}\frac{\partial^2}{\partial y_{3-\alpha}^2} \\
\hat{\mathfrak{L}}_{\alpha\beta}(\nabla_y) &= \hat{h}\big(\hat{\hat{A}}_{12} + \hat{\hat{A}}_{66}\big)\frac{\partial^2}{\partial y_\alpha \partial y_\beta}, \quad \alpha, \beta = 1, 2, \quad \alpha \neq \beta.
\end{aligned} \tag{8.118}$$

Thus, the deformation problem for an elastic layer coated with a very thin flexible elastic layer is reduced to that for the elastic layer without coating, but subjected to a different set of boundary conditions (8.113) and (8.117) on the surface $z = 0$.

Observe that in the axisymmetric case, as a result of (8.116), we have

$$\hat{\hat{\sigma}}_{rr} = \hat{\hat{A}}_{11}\varepsilon_{rr} + \hat{\hat{A}}_{12}\varepsilon_{\theta\theta}, \quad \hat{\hat{\sigma}}_{\theta\theta} = \hat{\hat{A}}_{12}\varepsilon_{rr} + \hat{\hat{A}}_{11}\varepsilon_{\theta\theta}, \quad \hat{\hat{\sigma}}_{r\theta} = 0,$$

where

$$\varepsilon_{rr} = \frac{\partial v_r}{\partial r}, \quad \varepsilon_{\theta\theta} = \frac{v_r}{r},$$

and Eqs. (8.110) should be replaced with the following:

$$\frac{\hat{h}}{r}\left(\frac{\partial(r\hat{\hat{\sigma}}_{rr})}{\partial r} - \hat{\hat{\sigma}}_{\theta\theta}\right) = -\sigma_{zr}\big|_{z=0}.$$

Correspondingly, the boundary condition (8.117) takes the following form:

$$\sigma_{zr}\big|_{z=0} = -\hat{h}\hat{\hat{A}}_{11}\left(\frac{\partial^2 v_r}{\partial r^2} + \frac{1}{r}\frac{\partial v_r}{\partial r} - \frac{v_r}{r^2}\right). \tag{8.119}$$

We note here that the axisymmetric boundary condition (8.119) was previously derived in a number of papers [2, 6, 17, 18].

8.4.2 Deformation Problem Formulation

We now consider a relatively thin transversely isotropic elastic layer of uniform thickness, h, coated with an infinitesimally thin elastic membrane and bonded to a rigid substrate (see Fig. 8.6), so that

$$\mathbf{v}\big|_{z=h} = \mathbf{0}, \quad w\big|_{z=h} = 0. \tag{8.120}$$

In the absence of body forces, the vector $(\mathbf{v}, w)$ of displacements in the elastic layer satisfies the Lamé system

$$\begin{aligned} A_{66}\Delta_y\mathbf{v} + (A_{11} - A_{66})\nabla_y\nabla_y\cdot\mathbf{v} + A_{44}\frac{\partial^2\mathbf{v}}{\partial z^2} + (A_{13} + A_{44})\frac{\partial}{\partial z}\nabla_y w = \mathbf{0}, \\ A_{44}\Delta_y w + A_{33}\frac{\partial^2 w}{\partial z^2} + (A_{13} + A_{44})\frac{\partial}{\partial z}\nabla_y\cdot\mathbf{v} = 0. \end{aligned} \tag{8.121}$$

Assuming that the coated layer is supporting a normal load and denoting the load density by p, we require that

$$\sigma_{33}\big|_{z=0} = -p. \tag{8.122}$$

Based on the analysis performed in Sect. 8.4.1, the influence of the elastic membrane is represented by the boundary condition

$$\sigma_{31}\mathbf{e}_1 + \sigma_{32}\mathbf{e}_2\big|_{z=0} = -\hat{\mathfrak{L}}(\nabla_y)\mathbf{v}\big|_{z=0}, \tag{8.123}$$

where $\hat{\mathfrak{L}}(\nabla_y)$ is the matrix differential operator defined by formulas (8.118).

Taking into account the stress-strain relationship

$$\begin{pmatrix} \sigma_{11} \\ \sigma_{22} \\ \sigma_{33} \\ \sigma_{23} \\ \sigma_{13} \\ \sigma_{12} \end{pmatrix} = \begin{bmatrix} A_{11} & A_{12} & A_{13} & 0 & 0 & 0 \\ A_{12} & A_{11} & A_{13} & 0 & 0 & 0 \\ A_{13} & A_{13} & A_{33} & 0 & 0 & 0 \\ 0 & 0 & 0 & 2A_{44} & 0 & 0 \\ 0 & 0 & 0 & 0 & 2A_{44} & 0 \\ 0 & 0 & 0 & 0 & 0 & 2A_{66} \end{bmatrix} \begin{pmatrix} \varepsilon_{11} \\ \varepsilon_{22} \\ \varepsilon_{33} \\ \varepsilon_{23} \\ \varepsilon_{13} \\ \varepsilon_{12} \end{pmatrix},$$

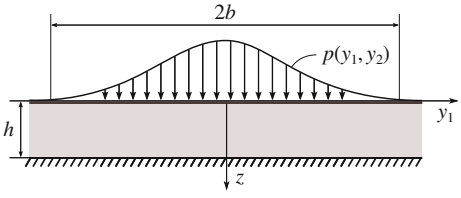

Fig. 8.6 A coated elastic layer of uniform thickness bonded to a rigid substrate and loaded by a normal load

we rewrite Eqs. (8.122), (8.123) as follows:

$$A_{13}\frac{\partial v_1}{\partial y_1} + A_{13}\frac{\partial v_2}{\partial y_2} + A_{33}\frac{\partial w}{\partial z}\bigg|_{z=0} = -p, \tag{8.124}$$

$$A_{44}\left(\nabla_y w + \frac{\partial \mathbf{v}}{\partial z}\right)\bigg|_{z=0} = -\hat{\mathfrak{L}}(\nabla_y)\mathbf{v}\big|_{z=0}. \tag{8.125}$$

Equations (8.120), (8.121), (8.124), and (8.125) comprise the deformation problem for the coated transversely isotropic elastic layer.

Here, following Argatov and Mishuris [4], we construct a leading-order asymptotic solution to the deformation problem (8.120)–(8.125).

8.4.3 Asymptotic Analysis of the Deformation Problem

Let h_* be a characteristic length of the external load distribution. Denoting by ε a small positive parameter, we require that

$$h = \varepsilon h_* \tag{8.126}$$

and introduce the stretched dimensionless normal coordinate

$$\zeta = \frac{z}{\varepsilon h_*}.$$

In addition, we non-dimensionalize the in-plane coordinates by the formulas

$$\eta_i = \frac{y_i}{h_*}, \quad i = 1, 2, \quad \boldsymbol{\eta} = (\eta_1, \eta_2),$$

so that

$$\frac{\partial}{\partial z} = \frac{1}{\varepsilon h_*}\frac{\partial}{\partial \zeta}, \quad \nabla_y = \frac{1}{h_*}\nabla_\eta.$$

Moreover, we assume that the tensile stiffness of the coating layer is relatively high, i.e., $\hat{\hat{A}}_{11} \gg A_{11}$, and so on. Continuing, we consider the situation when

$$\hat{\mathfrak{L}}(\nabla_y) = \varepsilon^{-1}\hat{\mathfrak{L}}^*(\nabla_y), \tag{8.127}$$

so that, in particular, the ratio $A_{11}/\hat{\hat{A}}_{11}$ is of the order of ε.

Following the perturbation algorithm [14], the solution to the deformation problem (8.120), (8.121), (8.124), (8.125) is represented as follows:

$$\mathbf{v} = \varepsilon^2 \mathbf{v}^1(\boldsymbol{\eta}, \zeta) + \cdots, \tag{8.128}$$

$$w = \varepsilon w^0(\boldsymbol{\eta}, \zeta) + \varepsilon^3 w^2(\boldsymbol{\eta}, \zeta) + \cdots . \tag{8.129}$$

For the sake of brevity, we include here only the non-vanishing terms (for details see Sect. 1.2).

It can be shown that the leading-order term in (8.129) is given by

$$w^0(\boldsymbol{\eta}, \zeta) = \frac{h_* p}{A_{33}}(1 - \zeta), \tag{8.130}$$

whereas the first non-trivial term of the expansion (8.128) satisfies the problem

$$A_{44}\frac{\partial^2 \mathbf{v}^1}{\partial \zeta^2} = -(A_{13} + A_{44})\nabla_\eta \frac{\partial w^0}{\partial \zeta}, \quad \zeta \in (0, 1),$$

$$A_{44}\frac{\partial \mathbf{v}^1}{\partial \zeta} + \frac{1}{h_*}\hat{\mathfrak{L}}^*(\nabla_\eta)\mathbf{v}^1\Big|_{\zeta=0} = -A_{44}\nabla_\eta w^0\big|_{\zeta=0}, \quad \mathbf{v}^1\big|_{\zeta=1} = \mathbf{0}.$$

Substituting the expansion (8.130) for w^0 into the above equations, we obtain

$$\begin{aligned} A_{44}\frac{\partial^2 \mathbf{v}^1}{\partial \zeta^2} &= \frac{A_{13} + A_{44}}{A_{33}} h_* \nabla_\eta p, \quad \zeta \in (0, 1), \\ A_{44}\frac{\partial \mathbf{v}^1}{\partial \zeta} + \frac{1}{h_*}\hat{\mathfrak{L}}^*(\nabla_\eta)\mathbf{v}^1\Big|_{\zeta=0} &= -\frac{A_{44}}{A_{33}} h_* \nabla_\eta p, \quad \mathbf{v}^1\big|_{\zeta=1} = \mathbf{0}. \end{aligned} \tag{8.131}$$

The solution to the boundary-value problem (8.131) is represented in the form

$$\mathbf{v}^1 = -\frac{A_{13} + A_{44}}{2A_{33}A_{44}}\zeta(1 - \zeta)h_* \nabla_\eta p + (1 - \zeta)\mathbf{V}^1(\boldsymbol{\eta}), \tag{8.132}$$

where $\mathbf{V}^1(\boldsymbol{\eta})$ satisfies the equation

$$\frac{1}{h_*}\hat{\mathfrak{L}}^*(\nabla_\eta)\mathbf{V}^1 - A_{44}\mathbf{V}^1 = \frac{A_{13} - A_{44}}{2A_{33}} h_* \nabla_\eta p \tag{8.133}$$

on the entire plane $\zeta = 0$.

For the second non-trivial term of the expansion (8.129), we derive the problem

$$A_{33}\frac{\partial^2 w^2}{\partial \zeta^2} = -(A_{13} + A_{44})\nabla_\eta \cdot \frac{\partial \mathbf{v}^1}{\partial \zeta} - A_{44}\Delta_\eta w^0, \quad \zeta \in (0, 1),$$

$$A_{33}\frac{\partial w^2}{\partial \zeta}\Big|_{\zeta=0} = -A_{13}\nabla_\eta \cdot \mathbf{v}^1\big|_{\zeta=0}, \quad w^2\big|_{\zeta=1} = 0.$$

Substituting the expressions (8.130) and (8.132) for w^0 and $\mathbf{v}^1$, respectively, into the above equations, we arrive at the problem

$$\frac{\partial^2 w^2}{\partial \zeta^2} = -\left[(A_{13}+A_{44})^2(2\zeta-1)+2A_{44}^2(1-\zeta)\right]\frac{h_*\Delta_\eta p}{2A_{33}^2A_{44}} + \frac{A_{13}+A_{44}}{A_{33}}\nabla_\eta\cdot\mathbf{V}^1, \quad \zeta\in(0,1), \tag{8.134}$$

$$\left.\frac{\partial w^2}{\partial \zeta}\right|_{\zeta=0} = -\frac{A_{13}}{A_{33}}\nabla_\eta\cdot\mathbf{V}^1, \quad w^2\big|_{\zeta=1}=0. \tag{8.135}$$

Integrating Eq. (8.134) twice with respect to ζ and taking into account the boundary condition $(8.135)_2$, we obtain

$$w^2 = -\left[(A_{13}+A_{44})^2\left(2\zeta^3-3\zeta^2+1\right)+2A_{44}^2(1-\zeta)^3\right]\frac{h_*\Delta_\eta p}{12A_{33}^2A_{44}} + \frac{A_{13}+A_{44}}{2A_{33}}(1-\zeta)^2\nabla_\eta\cdot\mathbf{V}^1(\boldsymbol{\eta})+C_2(\boldsymbol{\eta})(1-\zeta), \tag{8.136}$$

where $C_2(\boldsymbol{\eta})$ is an arbitrary function.

The substitution of (8.136) into the boundary condition $(8.135)_1$ yields

$$C_2 = \frac{A_{44}}{2A_{33}^2}h_*\Delta_\eta p - \frac{A_{44}}{A_{33}}\nabla_\eta\cdot\mathbf{V}^1,$$

and thus, in light of this relation, formula (8.136) implies

$$w^2\big|_{\zeta=0} = -\left[(A_{13}+A_{44})^2-4A_{44}^2\right]\frac{h_*\Delta_\eta p}{12A_{33}^2A_{44}} + \frac{A_{13}-A_{44}}{2A_{33}}\nabla_\eta\cdot\mathbf{V}^1, \tag{8.137}$$

where $\mathbf{V}^1$ is the solution of Eq. (8.133).

8.4.4 *Local Indentation of the Coated Elastic Layer: Leading-Order Asymptotics for the Compressible and Incompressible Cases*

In the case of the compressible layer, Eqs. (8.129) and (8.130) yield

$$w_0(\mathbf{y}) \simeq \frac{h}{A_{33}}p(\mathbf{y}), \tag{8.138}$$

so that the deformation response of the coated elastic layer is analogous to that of a Winkler elastic foundation with the foundation modulus $k = A_{33}/h$. In other words, the deformation of the elastic coating does not contribute substantially to the deformation of a thin compressible layer.

When the material approaches the incompressible limit, the right-hand side of (8.138) decreases to zero and the first term in the asymptotic expansion (8.129) disappears. Hence, the ratios A_{13}/A_{33} and A_{44}/A_{33} tend to 1 and 0, respectively.

Therefore, in the limit situation formula (8.137) reduces to

$$w^2\big|_{\zeta=0} = -\frac{h_*}{12a_{44}}\Delta_\eta p(\boldsymbol{\eta}) + \frac{1}{2}\nabla_\eta \cdot \mathbf{V}^1(\boldsymbol{\eta}), \tag{8.139}$$

where $a_{44} = A_{44}$ is the out-of-plane shear modulus of the elastic layer, and $\mathbf{V}^1(\boldsymbol{\eta})$ satisfies the equation

$$\frac{1}{h_*}\hat{\mathfrak{L}}^*(\nabla_\eta)\mathbf{V}^1(\boldsymbol{\eta}) - a_{44}\mathbf{V}^1(\boldsymbol{\eta}) = \frac{h_*}{2}\nabla_\eta p(\boldsymbol{\eta}), \quad \boldsymbol{\eta} \in \mathbb{R}^2. \tag{8.140}$$

Thus, in the case of the incompressible bonded elastic layer, formulas (8.127)–(8.129), (8.139), and (8.140) produce

$$w_0(\mathbf{y}) \simeq -\frac{h^3}{12a_{44}}\Delta_y p(\mathbf{y}) + \frac{h}{2}\nabla_y \cdot \mathbf{v}_0(\mathbf{y}), \tag{8.141}$$

where the vector $\mathbf{v}_0(\mathbf{y})$ satisfies the equation

$$h\hat{\mathfrak{L}}(\nabla_y)\mathbf{v}_0(\mathbf{y}) - a_{44}\mathbf{v}_0(\mathbf{y}) = \frac{h^2}{2}\nabla_y p(\mathbf{y}), \quad \mathbf{y} \in \mathbb{R}^2. \tag{8.142}$$

Here, $\hat{\mathfrak{L}}(\nabla_y)$ is the matrix differential operator defined by formulas (8.118).

Observe that, as a consequence of (8.132), the vector-function $\mathbf{v}_0(\mathbf{y})$ can be interpreted as the tangential displacement of the surface point $(\mathbf{y}, 0)$ of the elastic layer.

Finally, let us consider two opposite limit situations. First, when the coating is absent and $\hat{\mathfrak{L}}(\nabla_y) \equiv 0$, Eq. (8.142) implies

$$\mathbf{v}_0(\mathbf{y}) = -\frac{h^2}{2a_{44}}\nabla_y p(\mathbf{y}).$$

The substitution of this expression into formula (8.141) leads to

$$w_0(\mathbf{y}) \simeq -\frac{h^3}{3a_{44}}\Delta_y p(\mathbf{y}), \tag{8.143}$$

which agrees completely with the asymptotic model developed in Sect. 2.7.1.

Second, in the case of a very stiff coating we have $\mathbf{v}_0(\mathbf{y}) \equiv \mathbf{0}$, and formula (8.141) reduces to

$$w_0(\mathbf{y}) \simeq -\frac{h^3}{12a_{44}} \Delta_y p(\mathbf{y}). \tag{8.144}$$

In other words, comparing (8.143) and (8.144), we conclude that the inextensible membrane coating attached to the surface of a thin bonded incompressible elastic layer reduces the out-of-plane shear compliance of the layer by a factor of four.

References

1. Aleksandrov, V.M.: Asymptotic solution of the axisymmetric contact problem for an elastic layer of incompressible material. J. Apll. Math. Mech. **67**, 589–593 (2003)
2. Alexandrov, V.M., Mkhitaryan, S.M.: Contact Problems for Solids with Thin Coatings and Layers [in Russian]. Nauka, Moscow (1985)
3. Alexandrov, V.M., Pozharskii, D.A.: Three-Dimensional Contact Problems. Kluwer, Dordrecht (2001)
4. Argatov, I., Mishuris, G.: An asymptotic model for a thin bonded elastic layer coated with an elastic membrane. arXiv preprint arXiv:1504.06792 (2015)
5. Ateshian, G.A., Lai, W.M., Zhu, W.B., Mow, V.C.: An asymptotic solution for the contact of two biphasic cartilage layers. J. Biomech. **27**, 1347–1360 (1994)
6. Avilkin, V.I., Alexandrov, V.M., Kovalenko, E.V.: On using the more-accurate equations of thin coatings in the theory of axisymmetric contact problems for composite foundations. J. Appl. Math. Mech. **49**, 770–777 (1985)
7. Barber, J.R.: Contact problems for the thin elastic layer. Int. J. Mech. Sci. **32**, 129–132 (1990)
8. Chadwick, R.S.: Axisymmetric indentation of a thin incompressible elastic layer. SIAM J. Appl. Math. **62**, 1520–1530 (2002)
9. Elliott, H.A.: Three-dimensional stress distributions in hexagonal aeolotropic crystals. Math. Proc. Camb. Phil. Soc. **44**, 522–533 (1948)
10. Evans, L.C.: Partial Differential Equations. AMS, Providence (2010)
11. Federico, F., Herzog, W.: Towards an analytical model of soft biological tissues. J. Biomech. **41**, 3309–3313 (2008)
12. Federico, S., Grillo, A., La Rosa, G., Giaquinta, G., Herzog, W.: A transversely isotropic, transversely homogeneous microstructural-statistical model of articular cartilage. J. Biomech. **38**, 2008–2018 (2005)
13. Gladwell, G.M.L.: Contact Problems in the Classical Theory of Elasticity. Sijthoff and Noordho, Alphen aan den Rijn (1980)
14. Gol'denveizer, A.L.: Derivation of an approximate theory of bending of a plate by the method of asymptotic integration of the equations of the theory of elasticity. J. Appl. Math. Mech. **26**, 1000–1025 (1962)
15. Johnson, K.L.: Contact Mechanics. Cambridge University Press, Cambridge (1985)
16. Malits, P.: Indentation of an incompressible inhomogeneous layer by a rigid circular indenter. Q. J. Mech. Appl. Math. **59**, 343–358 (2006)
17. Rahman, M., Newaz, G.: Elastostatic surface displacements of a half-space reinforced by a thin film due to an axial ring load. Int. J. Eng. Sci. **35**, 603–611 (1997)
18. Rahman, M., Newaz, G.: Boussinesq type solution for a transversely isotropic half-space coated with a thin film. Int. J. Eng. Sci. **38**, 807–822 (2000)
19. Timoshenko, S.P., Goodier, J.N.: Theory of Elasticity. McGraw-Hill, New York (1970)

Chapter 9
Sensitivity Analysis of Articular Contact Mechanics

Abstract Asymptotic models of articular contact developed in the previous chapters assume, in particular, that the cartilage layers are of uniform thickness and are bonded to rigid substrates shaped like elliptic paraboloids. In this final chapter, treating the term "sensitivity" in a broad sense, we study the effects of deviation of the substrate's shape from the elliptic (Sect. 9.1) and of nonuniform thicknesses of the contacting incompressible layers (Sect. 9.2). It is shown that these effects in multibody dynamics simulations can be minimized if the geometric parameters in question (in particular, the layer thicknesses) are determined in a specific way to minimize the corresponding error in the force-displacement relationship.

9.1 Non-elliptical Contact of Thin Incompressible Viscoelastic Layers: Perturbation Solution

In this section, a more general three-dimensional unilateral contact problem for thin incompressible transversely isotropic viscoelastic layers bonded to rigid substrates, whose shapes are close to those of elliptic paraboloids, is considered and approximately solved by the perturbation technique.

9.1.1 Formulation of the Contact Problem

Consider the frictionless unilateral contact between two thin linear incompressible transversely isotropic viscoelastic layers firmly attached to rigid substrates. Introducing the Cartesian coordinate system (y_1, y_2, z), we write the equations of the layer surfaces $(n = 1, 2)$ in the form $z = (-1)^n \varphi_\varepsilon^{(n)}(\mathbf{y})$, where $\mathbf{y} = (y_1, y_2)$. In the undeformed state, the two layer/substrate systems occupy convex domains $z \le -\varphi_\varepsilon^{(1)}(\mathbf{y})$ and $z \ge \varphi_\varepsilon^{(2)}(\mathbf{y})$ in contact with the plane $z = 0$ at a single point chosen as the coordinate origin. Let us assume that

$$\varphi_\varepsilon^{(n)}(\mathbf{y}) = \varphi_0^{(n)}(\mathbf{y}) + \varepsilon\phi_n(\mathbf{y}), \tag{9.1}$$

I. Argatov and G. Mishuris, *Contact Mechanics of Articular Cartilage Layers*,
Advanced Structured Materials 50, DOI 10.1007/978-3-319-20083-5_9

where $\varphi_0^{(n)}(\mathbf{y})$ is an elliptic paraboloid, ε is a small positive dimensionless parameter, and the function $\varepsilon\phi_n(\mathbf{y})$ describes a small deviation of the nth substrate surface from the paraboloid shape ($n = 1, 2$).

We denote the normal approach of the substrates by $\delta_\varepsilon(t)$. The linearized unilateral contact condition that the surface points of the viscoelastic layers do not penetrate one into another can then be written as follows:

$$\delta_\varepsilon(t) - w_0^{(1)}(t, \mathbf{y}) - w_0^{(2)}(t, \mathbf{y}) \le \varphi_\varepsilon^{(1)}(\mathbf{y}) + \varphi_\varepsilon^{(2)}(\mathbf{y}). \tag{9.2}$$

Here, $w_0^{(n)}(t, \mathbf{y})$ is the local indentation (i.e., the normal displacement of the surface points) of the nth layer ($n = 1, 2$).

According to the perturbation analysis performed in Sect. 2.5 (see, in particular, formula (2.152)), the leading-order asymptotic solution for the local indentation of an incompressible viscoelastic layer of thickness h_n is given by

$$w_0^{(n)}(t, \mathbf{y}) = -\frac{h_n^3}{3} \int_{0^-}^{t} J'^{(n)}(t - \tau) \Delta_y \frac{\partial p_\varepsilon}{\partial \tau}(\tau, \mathbf{y})\, d\tau. \tag{9.3}$$

Here, $J'^{(n)}(t)$ is the out-of-plane shear creep compliance of the nth layer ($n = 1, 2$), $p_\varepsilon(t, \mathbf{y})$ is the contact pressure, and $\Delta_y = \partial^2/\partial y_1^2 + \partial^2/\partial y_2^2$ is the Laplace operator.

The equality in relation (9.2) determines the contact region $\omega_\varepsilon(t)$. In other words, the following equation holds within the contact area

$$w_0^{(1)}(t, \mathbf{y}) + w_0^{(2)}(t, \mathbf{y}) = \delta_\varepsilon(t) - \varphi_\varepsilon(\mathbf{y}), \quad \mathbf{y} \in \omega_\varepsilon(t), \tag{9.4}$$

where we have introduced the notation $\varphi_\varepsilon(\mathbf{y}) = \varphi_\varepsilon^{(1)}(\mathbf{y}) + \varphi_\varepsilon^{(2)}(\mathbf{y})$.

According to (9.1), we have

$$\varphi_\varepsilon(\mathbf{y}) = \varphi_0(\mathbf{y}) + \varepsilon\phi(\mathbf{y}), \tag{9.5}$$

where $\varphi_0(\mathbf{y}) = \varphi_0^{(1)}(\mathbf{y}) + \varphi_0^{(2)}(\mathbf{y})$ and $\phi(\mathbf{y}) = \phi_1(\mathbf{y}) + \phi_2(\mathbf{y})$. The function $\varepsilon\phi(\mathbf{y})$ will be called the gap function variation.

Without any loss of generality we may assume that

$$\varphi_0(\mathbf{y}) = \frac{y_1^2}{2R_1} + \frac{y_2^2}{2R_2}, \tag{9.6}$$

where the parameters R_1 and R_2 are positive and can be related to the coefficients of the paraboloids $\varphi_0^{(1)}(\mathbf{y})$ and $\varphi_0^{(2)}(\mathbf{y})$ by known formulas (see Sect. 2.1.1).

Substituting the expressions for displacements $w_0^{(1)}(t, \mathbf{y})$ and $w_0^{(2)}(t, \mathbf{y})$ given by formula (9.3) into Eq. (9.4), we obtain the contact condition in the following form:

$$-\sum_{n=1}^{2}\frac{h_n^3}{3}\int_{0^-}^{t}J'^{(n)}(t-\tau)\Delta_y\frac{\partial p_\varepsilon}{\partial\tau}(\tau,\mathbf{y})\,d\tau=\delta_\varepsilon(t)-\varphi_\varepsilon(\mathbf{y})\mathscr{H}(t). \tag{9.7}$$

Here, we assume that $\mathbf{y}\in\omega_\varepsilon(t)$, and $\mathscr{H}(t)$ is Heaviside's function introduced in a standard way, namely $\mathscr{H}(t)=0$ for $t<0$ and $\mathscr{H}(t)=1$ for $t\geq 0$.

Let $G_0'^{(n)}=1/J'^{(n)}(0^+)$ be the instantaneous out-of-plane shear elastic modulus of the nth layer. Then, the normalized creep function $\Phi'^{(n)}(t)$ is introduced by

$$J'^{(n)}(t)=\frac{1}{G_0'^{(n)}}\Phi'^{(n)}(t). \tag{9.8}$$

Let us rewrite Eq. (9.7) in the form corresponding to one layer by introducing the compound creep function, $\Phi_\beta(t)$, and the equivalent instantaneous shear elastic modulus, G_0', as follows:

$$\Phi_\beta(t)=\beta_1\Phi'^{(1)}(t)+\beta_2\Phi'^{(2)}(t), \tag{9.9}$$

$$G_0'=\frac{(h_1+h_2)^3G_0'^{(1)}G_0'^{(2)}}{h_1^3G_0'^{(2)}+h_2^3G_0'^{(1)}}, \tag{9.10}$$

$$\beta_1=\frac{h_1^3G_0'^{(2)}}{h_1^3G_0'^{(2)}+h_2^3G_0'^{(1)}},\quad \beta_2=\frac{h_2^3G_0'^{(1)}}{h_1^3G_0'^{(2)}+h_2^3G_0'^{(1)}}. \tag{9.11}$$

Moreover, let us introduce an auxiliary notation

$$m=\frac{3G_0'}{h^3}, \tag{9.12}$$

where $h=h_1+h_2$ is the joint thickness. Recall that formula (9.10) determines the equivalent modulus in such a way that $\beta_1+\beta_2=1$ and thus, $\Phi_\beta(0)=1$.

Thus, taking into account (9.8)–(9.12), we rewrite Eq. (9.7) as

$$\int_{0^-}^{t}\Phi_\beta(t-\tau)\Delta_y\frac{\partial p_\varepsilon}{\partial\tau}(\tau,\mathbf{y})\,d\tau=m\big(\varphi_\varepsilon(\mathbf{y})\mathscr{H}(t)-\delta_\varepsilon(t)\big). \tag{9.13}$$

Equation (9.13) will be used to find the contact pressure density $p_\varepsilon(t,\mathbf{y})$. The contour $\Gamma_\varepsilon(t)$ of the contact area $\omega_\varepsilon(t)$ is determined from the condition that the contact pressure is positive and vanishes at the contour of the contact area:

$$p_\varepsilon(t,\mathbf{y})>0,\quad \mathbf{y}\in\omega_\varepsilon(t), \tag{9.14}$$

$$p_\varepsilon(t,\mathbf{y})=0,\quad \mathbf{y}\in\Gamma_\varepsilon(t). \tag{9.15}$$

In the case of the contact problem for an incompressible layer (see, in particular, Sect. 2.7.3), we additionally assume a smooth transition of the surface normal stresses from the contact region $\mathbf{y} \in \omega_\varepsilon(t)$ to the outside region $\mathbf{y} \notin \omega_\varepsilon(t)$. Hence, we impose the following zero-pressure-gradient boundary condition [9, 10, 13, 17]:

$$\frac{\partial p_\varepsilon}{\partial n}(t, \mathbf{y}) = 0, \quad \mathbf{y} \in \Gamma_\varepsilon(t). \tag{9.16}$$

Here, $\partial/\partial n$ is the normal derivative directed outward from $\omega_\varepsilon(t)$.

We assume that the density $p_\varepsilon(t, \mathbf{y})$ is defined on the entire plane such that

$$p_\varepsilon(t, \mathbf{y}) = 0, \quad \mathbf{y} \notin \omega_\varepsilon(t). \tag{9.17}$$

From the physical point of view, the contact pressure between the smooth surfaces should satisfy the regularity condition, i.e., in the case (9.5), the function $p_\varepsilon(t, \mathbf{y})$ is assumed to be analytical in the domain $\omega_\varepsilon(t)$.

The equilibrium equation for the whole system is

$$\iint\limits_{\omega_\varepsilon(t)} p_\varepsilon(t, \mathbf{y})\, d\mathbf{y} = F(t), \tag{9.18}$$

where $F(t)$ denotes the external load, which is assumed to be known a priori.

For non-decreasing loads, when $dF(t)/dt \geq 0$, the contact zone should increase. Thus, we assume that the following monotonicity condition holds:

$$\omega_\varepsilon(t_1) \subset \omega_\varepsilon(t_2), \quad t_1 \leq t_2. \tag{9.19}$$

Following Argatov and Mishuris [8], we construct an asymptotic solution for the three-dimensional contact problem formulated by Eq. (9.13), under the monotonicity condition (9.19). We will first consider the problem in its general formulation transforming it to a set of equations more suitable for further analysis.

9.1.2 Equation for the Contact Approach

Integrating Eq. (9.13) over the contact domain $\omega_\varepsilon(t)$, we find

$$\iint\limits_{\omega_\varepsilon(t)} \int\limits_{0^-}^{t} \Phi_\beta(t-\tau) \Delta_y \frac{\partial p_\varepsilon}{\partial \tau}(\tau, \mathbf{y})\, d\tau d\mathbf{y} = m \iint\limits_{\omega_\varepsilon(t)} \big(\varphi_\varepsilon(\mathbf{y}) \mathscr{H}(t) - \delta_\varepsilon(t)\big)\, d\mathbf{y}. \tag{9.20}$$

In light of (9.17) and (9.19), we have $\omega_\varepsilon(\tau) \subset \omega_\varepsilon(t)$ for $\tau \in (0, t)$, as well as $p_\varepsilon(\tau, \mathbf{y}) \equiv 0$ for $\mathbf{y} \notin \omega_\varepsilon(\tau)$. Therefore, the integral on the left-hand side of (9.20),

which is denoted by $\mathscr{I}(t)$, can be transformed into

$$\begin{aligned}\mathscr{I}(t) &= \iint\limits_{\omega_\varepsilon(t)} \int\limits_{0^-}^{t} \Phi_\beta(t-\tau)\Delta_y \frac{\partial p_\varepsilon}{\partial \tau}(\tau,\mathbf{y})\, d\tau d\mathbf{y} \\ &= \int\limits_{0^-}^{t} \Phi_\beta(t-\tau) \iint\limits_{\omega_\varepsilon(t)} \Delta_y \frac{\partial p_\varepsilon}{\partial \tau}(\tau,\mathbf{y})\, d\mathbf{y} d\tau \\ &= \int\limits_{0^-}^{t} \Phi_\beta(t-\tau) \frac{\partial}{\partial \tau} \iint\limits_{\omega_\varepsilon(t)} \Delta_y p_\varepsilon(\tau,\mathbf{y})\, d\mathbf{y} d\tau. \end{aligned} \tag{9.21}$$

We note that, as a consequence of (9.15)–(9.17), the density $p_\varepsilon(t,\mathbf{y})$ is a smooth function of the variables y_1 and y_2 on the entire plane.

Further, by employing the second Green's formula

$$\iint\limits_{\omega} \big(u(\mathbf{y})\Delta v(\mathbf{y}) - v(\mathbf{y})\Delta u(\mathbf{y})\big)\, d\mathbf{y} = \int\limits_{\Gamma} \left(u(\mathbf{y})\frac{\partial v}{\partial n}(\mathbf{y}) - v(\mathbf{y})\frac{\partial u}{\partial n}(\mathbf{y})\right) ds, \tag{9.22}$$

where ds is the element of the arc length, we obtain

$$\iint\limits_{\omega_\varepsilon(t)} \Delta_y p_\varepsilon(\tau,\mathbf{y})\, d\mathbf{y} = \int\limits_{\Gamma_\varepsilon(t)} \frac{\partial p_\varepsilon}{\partial n}(\tau,\mathbf{y})\, ds. \tag{9.23}$$

In light of the boundary condition (9.16) and the monotonicity condition (9.19), the right-hand side of Eq. (9.23) vanishes for $t > 0$ and, therefore, Eq. (9.20) reduces to

$$\iint\limits_{\omega_\varepsilon(t)} \big(\varphi_\varepsilon(\mathbf{y})\mathscr{H}(t) - \delta_\varepsilon(t)\big)\, d\mathbf{y} = 0.$$

From here it immediately follows that

$$\delta_\varepsilon(t) = \frac{\mathscr{H}(t)}{A_\varepsilon(t)} \iint\limits_{\omega_\varepsilon(t)} \varphi_\varepsilon(\mathbf{y})\, d\mathbf{y}, \tag{9.24}$$

where $A_\varepsilon(t)$ is the area of $\omega_\varepsilon(t)$ given by the integral

$$A_\varepsilon(t) = \iint\limits_{\omega_\varepsilon(t)} d\mathbf{y}. \tag{9.25}$$

Equation (9.24) connects the unknown contact approach $\delta_\varepsilon(t)$ with some integral characteristics of the contact domain $\omega_\varepsilon(t)$.

9.1.3 Equation for the Integral Characteristics the Contact Area

Substituting the functions $u(\mathbf{y}) = p_\varepsilon(\tau, \mathbf{y})$ and $v(\mathbf{y}) = (y_1^2 + y_2^2)/4$ into Green's formula (9.22) for the domain $\omega_\varepsilon(t)$, assuming that $\tau < t$, and taking into account the boundary conditions (9.15), (9.16) and the monotonicity condition (9.19), we obtain the relation

$$\frac{1}{4}\iint\limits_{\omega_\varepsilon(t)} |\mathbf{y}|^2 \Delta p_\varepsilon(\tau, \mathbf{y})\, d\mathbf{y} = \iint\limits_{\omega_\varepsilon(\tau)} p_\varepsilon(\tau, \mathbf{y})\, d\mathbf{y}. \tag{9.26}$$

Using formula (9.26), we can evaluate the contact load (9.18). Indeed, by multiplying both sides of (9.13) by $(y_1^2 + y_2^2)/4$ and integrating the obtained equation over the contact domain $\omega_\varepsilon(t)$, we obtain

$$\int\limits_{0^-}^{t} \Phi_\beta(t-\tau)\frac{\partial}{\partial\tau}\iint\limits_{\omega_\varepsilon(\tau)} p_\varepsilon(\tau, \mathbf{y})\, d\mathbf{y} d\tau = \frac{m}{4}\iint\limits_{\omega_\varepsilon(t)} |\mathbf{y}|^2 \big(\mathscr{H}(t)\varphi_\varepsilon(\mathbf{y}) - \delta_\varepsilon(t)\big)\, d\mathbf{y}. \tag{9.27}$$

Taking into account the notation (9.18) for the contact force, we rewrite (9.27) as

$$\int\limits_{0^-}^{t} \Phi_\beta(t-\tau)\dot{F}(\tau)\, d\tau = \frac{m}{4}\mathscr{H}(t)\iint\limits_{\omega_\varepsilon(t)} |\mathbf{y}|^2\varphi_\varepsilon(\mathbf{y})\, d\mathbf{y} - \delta_\varepsilon(t)\frac{m}{4}\iint\limits_{\omega_\varepsilon(t)} |\mathbf{y}|^2 d\mathbf{y}, \tag{9.28}$$

where the dot denotes the differentiation with respect to time, i.e., $\dot{F}(t) = dF(t)/dt$.

Then, excluding the quantity $\delta_\varepsilon(t)$ from (9.28) by means of Eq. (9.24), we arrive at the following equation:

$$\int\limits_{0^-}^{t} \Phi_\beta(t-\tau)\dot{F}(\tau)\, d\tau = \frac{m}{4}\mathscr{H}(t)\iint\limits_{\omega_\varepsilon(t)} \left(|\mathbf{y}|^2 - \frac{I_\varepsilon(t)}{A_\varepsilon(t)}\right)\varphi_\varepsilon(\mathbf{y})\, d\mathbf{y}. \tag{9.29}$$

Here, $I_\varepsilon(t)$ is the polar moment of inertia of $\omega_\varepsilon(t)$ given by the integral

$$I_\varepsilon(t) = \iint\limits_{\omega_\varepsilon(t)} |\mathbf{y}|^2 d\mathbf{y}. \tag{9.30}$$

Equation (9.29) connects the known contact force $F(t)$ with some integral characteristics of the unknown contact area $\omega_\varepsilon(t)$.

9.1.4 Equation for the Contact Pressure

Let us rewrite Eq. (9.13) in the form

$$\Delta_y P_\varepsilon(t, \mathbf{y}) = m\big(\varphi_\varepsilon(\mathbf{y}) - \delta_\varepsilon(t)\big), \quad \mathbf{y} \in \omega_\varepsilon(t), \tag{9.31}$$

where we have introduced the notation

$$P_\varepsilon(t, \mathbf{y}) = \int_{0^-}^{t} \Phi_\beta(t-\tau)\frac{\partial p_\varepsilon}{\partial \tau}(\tau, \mathbf{y})\, d\tau. \tag{9.32}$$

By denoting the integral operator on the right-hand side of the previous equation by $\mathscr{K}$, we have

$$\mathscr{K} y(\tau) = \int_{0^-}^{t} \Phi_\beta(t-\tau)\dot{y}(\tau)\, d\tau, \tag{9.33}$$

so that formula (9.32) can be represented as

$$P_\varepsilon(t, \mathbf{y}) = \mathscr{K} p_\varepsilon(\tau, \mathbf{y}). \tag{9.34}$$

The inverse operator to $\mathscr{K}$ denoted by $\mathscr{K}^{-1}$ is defined by the formula

$$\mathscr{K}^{-1} Y(\tau) = \int_{0^-}^{t} \Psi_\beta(t-\tau)\dot{Y}(\tau)\, d\tau, \tag{9.35}$$

where $\Psi_\beta(t)$ is the compound relaxation function defined by its Laplace transform

$$\tilde{\Psi}_\beta(s) = \frac{1}{s^2\tilde{\Phi}_\beta(s)}. \tag{9.36}$$

Note that since

$$\tilde{\Phi}_\beta(s) = \beta_1\tilde{\Phi}'^{(1)}(s) + \beta_2\tilde{\Phi}'^{(2)}(s),$$

and

$$\tilde{\Phi}'^{(n)}(s) = \frac{1}{s^2\tilde{\Psi}'^{(n)}(s)},$$

where $\tilde{\Psi}'^{(n)}(s)$ is the Laplace transform of the relaxation function in out-of-plane shear for the nth layer, formula (9.36) can be reduced to the following:

$$\tilde{\Psi}_\beta(s) = \frac{\tilde{\Psi}'^{(1)}(s)\tilde{\Psi}'^{(2)}(s)}{\beta_1\tilde{\Psi}'^{(2)}(s) + \beta_2\tilde{\Psi}'^{(1)}(s)}. \tag{9.37}$$

Recall also that the coefficients β_1 and β_2 are introduced by formulas (9.11) in such a way that $\Psi_\beta(0) = 1$.

As a result of the boundary conditions (9.15) and (9.16), the function $P_\varepsilon(t, \mathbf{y})$ must satisfy the following boundary conditions:

$$P_\varepsilon(t, \mathbf{y}) = 0, \quad \mathbf{y} \in \Gamma_\varepsilon(t), \tag{9.38}$$

$$\frac{\partial P_\varepsilon}{\partial n}(t, \mathbf{y}) = 0, \quad \mathbf{y} \in \Gamma_\varepsilon(t). \tag{9.39}$$

Thus, in the case of monotonically increasing contact area $\omega_\varepsilon(t)$, the problem (9.31), (9.38), (9.39) allows us to determine the domain $\omega_\varepsilon(t)$ based on the positivity condition for the contact pressure (9.14). Then, from Eq. (9.24) we can determine the contact approach $\delta_\varepsilon(t)$. Finally, by applying the inverse operator (9.35), we obtain a complete solution to the problem.

9.1.5 Limiting Case Problem: Elliptical Contact Area

We now consider the problem for the limiting case $\varepsilon = 0$, when the function $\varphi_0(\mathbf{y})$ represents an elliptic paraboloid. In a special case of the integral operator $\mathscr{K}$, the solution to this problem has previously been presented in [6]. Here we adopt it in the necessary form for the further asymptotic analysis, in order to construct a more general solution to the problem with the slightly perturbed boundary of an arbitrary shape.

In this case the right-hand side of (9.31) takes the form $m\big(\varphi_0(\mathbf{y}) - \delta_0(t)\big)$. This suggests that we assume the domain $\omega_0(t)$ to be elliptical and so we set

$$P_0(t, \mathbf{y}) = Q_0(t)\left(1 - \frac{y_1^2}{a(t)^2} - \frac{y_2^2}{b(t)^2}\right)^2. \tag{9.40}$$

In other words, the contour $\Gamma_0(t)$ is an ellipse with the semi-axises $a(t)$ and $b(t)$. It is simple to verify that the function $P_0(t, \mathbf{y})$ satisfies the boundary conditions (9.38) and (9.39) exactly.

Substituting (9.40) into Eq. (9.31), we obtain after some algebra the following system of algebraic equations:

$$\delta_0(t) = \frac{4Q_0(t)}{m}\left(\frac{1}{a(t)^2} + \frac{1}{b(t)^2}\right), \tag{9.41}$$

$$\frac{1}{R_1} = \frac{8Q_0(t)}{ma(t)^2}\left(\frac{3}{a(t)^2} + \frac{1}{b(t)^2}\right), \quad \frac{1}{R_2} = \frac{8Q_0(t)}{mb(t)^2}\left(\frac{1}{a(t)^2} + \frac{3}{b(t)^2}\right). \tag{9.42}$$

The form of the ellipse $\Gamma_0(t)$ can be characterized by its aspect ratio s defined as

$$s = \frac{b(t)}{a(t)}, \tag{9.43}$$

and from (9.42), it immediately follows that s is constant with time and is determined as a positive root of the equation

$$\frac{R_2}{R_1} = \frac{s^2(3s^2+1)}{3+s^2}. \tag{9.44}$$

In turn, Eq. (9.44) can be reduced to a quadratic equation for s^2, so that

$$s^2 = \sqrt{\left(\frac{R_1 - R_2}{6R_1}\right)^2 + \frac{R_2}{R_1}} - \frac{(R_1 - R_2)}{6R_1}. \tag{9.45}$$

Recall that, along with Eqs. (9.41) and (9.42), we have Eqs. (9.24) and (9.29), which connect the contact approach $\delta_\varepsilon(t)$ and the known contact force $F(t)$ with some integral characteristics of the contact domain $\omega_\varepsilon(t)$.

By taking into account (9.45), we transform Eq. (9.24) into

$$\delta_0(t) = \frac{1}{8}\left(\frac{1}{R_1} + \frac{s^2}{R_2}\right)a(t)^2. \tag{9.46}$$

Then, by excluding the quantity $\delta_0(t)$ from Eqs. (9.41) and (9.46), we obtain

$$Q_0(t) = \frac{m}{32}\frac{s^2}{(s^2+1)}\left(\frac{1}{R_1} + \frac{s^2}{R_2}\right)a(t)^4. \tag{9.47}$$

By application of the same method, Eq. (9.29) becomes

$$\mathscr{K}F(\tau) = \frac{\pi m}{384}\left(\frac{3s - s^3}{R_1} + \frac{3s^5 - s^3}{R_2}\right)a(t)^6. \tag{9.48}$$

This allows us to determine the major semi-axis $a(t)$ of the contact area $\omega_0(t)$ as a function of time t in the form

$$a(t) = \left[\frac{\pi m}{384}\left(\frac{3s - s^3}{R_1} + \frac{3s^5 - s^3}{R_2}\right)\right]^{-1/6}\left(\mathscr{K}F(\tau)\right)^{1/6}. \tag{9.49}$$

As a consequence of (9.49), formulas (9.46) and (9.47) determine the quantities $\delta_0(t)$ and $Q_0(t)$, respectively.

We now turn to evaluating the contact pressure in the case of elliptical contact. In light of (9.33) and (9.40), we obtain the following operator equation for the contact

pressure density $p_0(t, \mathbf{y})$:

$$\mathscr{K}\, p_0(\tau, \mathbf{y}) = Q_0(t)\left(1 - \frac{y_1^2}{a(t)^2} - \frac{y_2^2}{b(t)^2}\right)^2, \quad \mathbf{y} \in \omega_0(t). \tag{9.50}$$

By inverting Eq. (9.50) with the help of (9.35), we obtain

$$p_0(t, \mathbf{y}) = \mathscr{K}^{-1}\left\{ Q_0(\tau)\left(1 - \frac{y_1^2}{a(\tau)^2} - \frac{y_2^2}{b(\tau)^2}\right)^2 \mathscr{H}\left(1 - \frac{y_1^2}{a(\tau)^2} - \frac{y_2^2}{b(\tau)^2}\right)\right\}, \tag{9.51}$$

where the Heaviside factor indicates the contact domain $\omega_0(\tau)$.

Following the notation (9.35), Eq. (9.51) can be transformed into

$$p_0(t, \mathbf{y}) = \int_{0^-}^{t} \Psi_\beta(t - \tau) Q_0(\tau)\left(1 - \frac{y_1^2}{a(\tau)^2} - \frac{y_2^2}{b(\tau)^2}\right)_+^2 d\tau. \tag{9.52}$$

Here the positive part function $(x)_+ = (x + |x|)/2$ is used as an indicator of the current contact area $\omega_0(\tau)$.

9.1.6 Slightly Perturbed Elliptical Contact Area

We now consider the gap function $\varphi_\varepsilon(\mathbf{y})$, given in a general form (9.5) with small $\varepsilon > 0$. The solution corresponding to the limiting case $\varepsilon = 0$ was defined above and is denoted by $p_0(t, \mathbf{y})$ and $\delta_0(t)$, where the contact domain $\omega_0(t)$ is bounded by an ellipse $\Gamma_0(t)$. Then, the function $P_0(t, \mathbf{y}) = \mathscr{K}\, p_0(\tau, \mathbf{y})$ satisfies the problem

$$\Delta_y p_0(t, \mathbf{y}) = m\big(\varphi_0(\mathbf{y}) - \delta_0(t)\big), \quad \mathbf{y} \in \omega_0(t), \tag{9.53}$$

$$p_0(t, \mathbf{y}) = 0, \quad \frac{\partial p_0}{\partial n}(t, \mathbf{y}) = 0, \quad \mathbf{y} \in \Gamma_0(t). \tag{9.54}$$

Recall also that in accordance with (9.24), the contact approach $\delta_0(t)$ is given by

$$\delta_0(t) = \frac{1}{A_0(t)} \iint_{\omega_0(t)} \varphi_0(\mathbf{y})\, d\mathbf{y}, \tag{9.55}$$

where $A_0(t)$ is the area of $\omega_0(t)$. Moreover, in light of (9.29), we have

$$\mathscr{K} F(\tau) = \frac{m}{4} \iint_{\omega_0(t)} B_0(t, \mathbf{y}) \varphi_0(\mathbf{y})\, d\mathbf{y}, \tag{9.56}$$

where, with $I_0(t)$ being the polar moment of inertia of $\omega_0(t)$,

$$B_0(t, \mathbf{y}) = |\mathbf{y}|^2 - \frac{I_0(t)}{A_0(t)}. \tag{9.57}$$

We represent the solution to the perturbed auxiliary contact problem (9.31), (9.38), (9.39) as

$$P_\varepsilon(t, \mathbf{y}) = P_0(t, \mathbf{y}) + \varepsilon P_1(t, \mathbf{y}) + O(\varepsilon^2), \tag{9.58}$$

$$\delta_\varepsilon(t) = \delta_0(t) + \varepsilon\delta_1(t) + O(\varepsilon^2), \tag{9.59}$$

and recall that the contact load $F(t)$ is assumed to be specified, while the contact approach $\delta_\varepsilon(t)$ is unknown a priori.

By substituting (9.58) and (9.59) into Eq. (9.31), we arrive at the equation

$$\Delta_y P_1(t, \mathbf{y}) = m\big(\varphi(\mathbf{y}) - \delta_1(t)\big), \quad \mathbf{y} \in \omega_0(t). \tag{9.60}$$

Let us assume that the unknown boundary $\Gamma_\varepsilon(t)$ of the contact area $\omega_\varepsilon(t)$ (see Fig. 9.1) is described by the equation

$$n = h_\varepsilon(t, \sigma), \quad s \in \Gamma_0(t). \tag{9.61}$$

Here, σ is the arc length along $\Gamma_0(t)$, and n is the distance (taking the sign into account) measured along the outward (with respect to the domain $\omega_0(t)$) normal to the curve $\Gamma_0(t)$. The function $h_\varepsilon(t, \sigma)$ describes the variation of the contact area and should be determined by considering the boundary conditions for Eq. (9.60).

In light of (9.58) and (9.59), we set

$$h_\varepsilon(t, \sigma) = \varepsilon h(t, \sigma), \tag{9.62}$$

where the function $h(t, \sigma)$ is assumed to be independent of ε.

Applying the perturbation technique (see, for example, [20]), we have

$$P_\varepsilon\big|_\Gamma = P_\varepsilon\big|_{\Gamma_0} + h_\varepsilon \frac{\partial P_\varepsilon}{\partial n}\Big|_{\Gamma_0} + O(\varepsilon^2). \tag{9.63}$$

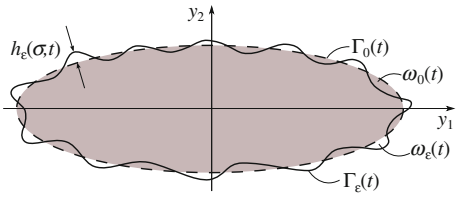

Fig. 9.1 Schematic representation of the contact domain $\omega_\varepsilon(t)$ with the boundary $\Gamma_\varepsilon(t)$, and the limit domain $\omega_0(t)$ with the boundary $\Gamma_0(t)$

Let $\mathbf{n}_\varepsilon$ be the unit outward normal vector to the curve $\Gamma_\varepsilon(t)$. Then, the following formula holds:

$$\mathbf{n}_\varepsilon = \frac{\big(1-\kappa(t,\sigma)h_\varepsilon(t,\sigma)\big)\mathbf{n}_0 - h'_\varepsilon(t,\sigma)\mathbf{t}_0}{\sqrt{\big(1-\kappa(t,\sigma)h_\varepsilon(t,\sigma)\big)^2 + h'_\varepsilon(t,\sigma)^2}}. \tag{9.64}$$

Here, $\mathbf{t}_0$ and $\mathbf{n}_0$ are the unit tangential and outward normal vectors to the curve $\Gamma_0(t)$, $\kappa(t,\sigma)$ is the curvature of $\Gamma_0(t)$, and the prime denotes the derivative with respect to the arc length σ.

Taking into account formula (9.64), we obtain

$$\frac{\partial p_\varepsilon}{\partial n}\Big|_\Gamma = \frac{\partial p_\varepsilon}{\partial n}\Big|_{\Gamma_0} - h'_\varepsilon \frac{\partial p_\varepsilon}{\partial \sigma}\Big|_{\Gamma_0} + O(\varepsilon^2), \tag{9.65}$$

and by substituting the expansion (9.58) into Eqs. (9.63), (9.65) and taking into account the boundary conditions (9.54) for the function $P_0(t,\mathbf{y})$, we derive the following boundary conditions at the unperturbed contact boundary:

$$P_1(t,\mathbf{y}) = 0, \quad \mathbf{y} \in \Gamma_0(t), \tag{9.66}$$

$$\frac{\partial P_1}{\partial n}(t,\mathbf{y}) = -h(t,\sigma)\frac{\partial^2 P_0}{\partial n^2}(t,\mathbf{y}), \quad \mathbf{y} \in \Gamma_0(t). \tag{9.67}$$

Here, in accordance with Eq. (9.53), we have

$$\frac{\partial^2 P_0}{\partial n^2}(t,\mathbf{y}) = m\big(\varphi_0(\mathbf{y}) - \delta_0(t)\big), \quad \mathbf{y} \in \Gamma_0(t). \tag{9.68}$$

Note that the right-hand side of (9.68) is strictly positive. This can be verified by employing the explicit formula obtained in Sect. 9.1.5, or proved by using the maximum principle for harmonic functions.

Finally, Eqs. (9.24) and (9.29) yield

$$A_0(t)\delta_1(t) = \iint\limits_{\omega_0(t)} \phi(\mathbf{y})\,d\mathbf{y} + \int\limits_{\Gamma_0(t)} \varphi_0(\mathbf{y})h(t,\sigma)\,d\sigma_y - A_1(t)\delta_0(t), \tag{9.69}$$

from which it follows that, for $B_0(t,\mathbf{y})$ defined by (9.56),

$$\begin{aligned} 0 = \iint\limits_{\omega_0(t)} B_0(t,\mathbf{y})\phi(\mathbf{y})\,d\mathbf{y} - \delta_0(t)\left(I_1(t) - \frac{I_0(t)}{A_0(t)}A_1(t)\right) \\ + \int\limits_{\Gamma_0(t)} B_0(t,\mathbf{y})\varphi_0(\mathbf{y})h(t,\sigma)\,d\sigma_y. \end{aligned} \tag{9.70}$$

Here, $A_1(t)$ and $I_1(t)$ are the first-order perturbation coefficients of $A_\varepsilon(t)$ and $I_\varepsilon(t)$, respectively, given by

$$A_1(t) = \int\limits_{\Gamma_0(t)} h(t,\sigma)\, d\sigma_y, \tag{9.71}$$

$$I_1(t) = \int\limits_{\Gamma_0(t)} |\mathbf{y}|^2 h(t,\sigma)\, d\sigma_y. \tag{9.72}$$

Equations (9.60), (9.66), (9.67), (9.69) and (9.70) constitute the first-order perturbation problem. By employing the relations (9.68) and (9.71), it is not hard to check that Eq. (9.69) coincides with the solvability condition (see, for instance, (9.23)) of the boundary-value problem (9.60), (9.66), (9.67).

9.1.7 Determination of the Contour of the Contact Area

First, let us express the solution to Eq. (9.60) in the form

$$P_1(t,\mathbf{y}) = m\big(P_1^{[0]}(t,\mathbf{y}) + P_1^{[1]}(t,\mathbf{y})\big), \tag{9.73}$$

where we have introduced the notation

$$P_1^{[0]}(t,\mathbf{y}) = Y_\phi^{[0]}(\mathbf{y}) - \delta_1(t) Y_1^{[0]}(\mathbf{y}), \tag{9.74}$$

$$Y_\phi^{[0]}(\mathbf{y}) = \frac{1}{2\pi} \iint\limits_{\omega_0(t)} \phi(\mathbf{y}) \ln|\mathbf{y}-\mathbf{y}|\, d\mathbf{y}, \quad Y_1^{[0]}(\mathbf{y}) = \frac{1}{2\pi} \iint\limits_{\omega_0(t)} \ln|\mathbf{y}-\mathbf{y}|\, d\mathbf{y}. \tag{9.75}$$

Substituting the form (9.73) into Eqs. (9.60), (9.66) and (9.67), we obtain the following boundary value problem for the function $P_1^{[1]}(t,\mathbf{y})$:

$$\Delta_y P_1^{[1]}(t,\mathbf{y}) = 0, \quad \mathbf{y} \in \omega_0(t), \tag{9.76}$$

$$P_1^{[1]}(t,\mathbf{y}) = -Y_\phi^{[0]}(\mathbf{y}) + \delta_1(t) Y_1^{[0]}(\mathbf{y}), \quad \mathbf{y} \in \Gamma_0(t), \tag{9.77}$$

$$\begin{aligned} \frac{\partial P_1^{[1]}}{\partial n}(t,\mathbf{y}) = {} & -h(t,\sigma)\big(\varphi_0(\mathbf{y}) - \delta_0(t)\big) \\ & - \frac{\partial Y_\phi^{[0]}}{\partial n}(t,\mathbf{y}) + \delta_1(t) \frac{\partial Y_1^{[0]}}{\partial n}(t,\mathbf{y}), \quad \mathbf{y} \in \Gamma_0(t). \end{aligned} \tag{9.78}$$

Here we have used relations (9.68) and (9.74).

Let us denote the first term on the right-hand side of (9.78) by $-\hat{h}(t,\sigma)$, so that

$$h(t,\sigma) = \frac{\hat{h}(t,\sigma)}{\varphi_0(\mathbf{y}) - \delta_0(t)}, \quad \mathbf{y} \in \Gamma_0(t). \tag{9.79}$$

As a result of (9.71), (9.72) and (9.79), Eqs. (9.69), (9.70) and (9.78) respectively take the forms

$$\delta_1(t) = \frac{1}{A_0(t)} \iint\limits_{\omega_0(t)} \phi(\mathbf{y})\, d\mathbf{y} + \frac{1}{A_0(t)} \int\limits_{\Gamma_0(t)} \hat{h}(t,\sigma)\, d\sigma_y, \tag{9.80}$$

$$0 = \iint\limits_{\omega_0(t)} B_0(t,\mathbf{y})\phi(\mathbf{y})\, d\mathbf{y} + \int\limits_{\Gamma_0(t)} B_0(t,\mathbf{y})\hat{h}(t,\sigma)\, d\sigma_y. \tag{9.81}$$

$$\frac{\partial P_1^{[1]}}{\partial n}(t,\mathbf{y}) = -\hat{h}(t,\sigma) - \frac{\partial Y_\phi^{[0]}}{\partial n}(t,\mathbf{y}) + \delta_1(t)\frac{\partial Y_1^{[0]}}{\partial n}(t,\mathbf{y}), \quad \mathbf{y} \in \Gamma_0(t). \tag{9.82}$$

Second, to proceed further with the computation of the contour of the contact area, we now define the Steklov—Poincaré (Dirichlet-to-Neumann) operator $\mathfrak{S} : H^{1/2}(\Gamma_0(t)) \to H^{-1/2}(\Gamma_0(t))$ by

$$\big(\mathfrak{S}g\big)(\mathbf{y}) = \frac{\partial w}{\partial n}(\mathbf{y}), \quad \mathbf{y} \in \Gamma_0(t), \tag{9.83}$$

where $w(\mathbf{y})$ is the unique solution of the Dirichlet problem

$$\Delta_y w(\mathbf{y}) = 0, \quad \mathbf{y} \in \omega_0(t); \qquad w(\mathbf{y}) = g(\mathbf{y}), \quad \mathbf{y} \in \Gamma_0(t). \tag{9.84}$$

The operator $\mathfrak{S}$ for a circular domain is well known, and we will use the above form later in Sect. 9.1.9. To the authors' best knowledge there is no closed form representation for $\mathfrak{S}$ in the case of an elliptic domain. However, the finite element Steklov—Poincaré operator can be computed by standard FEM packages (see for details [15]). In [8], an alternative approach for constructing the operator numerically in terms of conformal mappings was presented.

In terms of the Steklov—Poincaré operator, Eqs. (9.77) and (9.82) yield

$$\begin{aligned}\hat{h}(t,\sigma) = {} & \big(\mathfrak{S}Y_\phi^{[0]}\big)(\mathbf{y}) - \frac{\partial Y_\phi^{[0]}}{\partial n}(t,\mathbf{y}) \\ & - \delta_1(t)\left(\big(\mathfrak{S}Y_1^{[0]}\big)(\mathbf{y}) - \frac{\partial Y_1^{[0]}}{\partial n}(t,\mathbf{y})\right), \quad \mathbf{y} \in \Gamma_0(t).\end{aligned} \tag{9.85}$$

Note that the substitution of (9.85) into (9.80) results in an identity, which we check by verifying the following properties:

$$\int\limits_{\Gamma_0(t)} \big(\mathfrak{S}g\big)(\mathbf{y})\, d\sigma_y = 0, \quad \forall g \in H^{1/2}(\Gamma_0(t)),$$

$$\iint\limits_{\omega_0(t)} \phi(\mathbf{y})\, d\mathbf{y} = \int\limits_{\Gamma_0(t)} \frac{\partial Y_\phi^{[0]}}{\partial n}(t, \mathbf{y})\, d\sigma_y, \quad \forall \varphi \in L^2(\omega_0(t)).$$

Now, excluding the variable $\delta_1(t)$ from (9.85) by means of (9.80), we obtain

$$\hat{h}(t,\sigma) = -\left(\frac{1}{A_0(t)} \iint\limits_{\omega_0(t)} \phi(\mathbf{y})\, d\mathbf{y} + \hat{H}_0(t)\right)\left(\big(\mathfrak{S}Y_1^{[0]}\big)(\mathbf{y}) - \frac{\partial Y_1^{[0]}}{\partial n}(t, \mathbf{y})\right)$$
$$+ \big(\mathfrak{S}Y_\phi^{[0]}\big)(\mathbf{y}) - \frac{\partial Y_\phi^{[0]}}{\partial n}(t, \mathbf{y}), \quad \mathbf{y} \in \Gamma_0(t), \tag{9.86}$$

where $\hat{H}_0(t)$ is the relative weighted increment of the contact area defined as

$$\hat{H}_0(t) = \frac{1}{A_0(t)} \int\limits_{\Gamma_0(t)} \hat{h}(t,\sigma)\, d\sigma. \tag{9.87}$$

At this point, the function $\hat{h}(t,\sigma)$ is determined by Eq. (9.86) with an accuracy up to its integral characteristics $\hat{H}_0(t)$.

By substitution of the expression (9.86) into Eq. (9.81), we arrive at the following simple equation to determine $\hat{H}_0(t)$:

$$\Xi_1^{[0]}(t)\hat{H}_0(t) = \Xi_\phi^{[0]}(t) + \iint\limits_{\omega_0(t)} \left(B_0(t,\mathbf{y}) - \frac{\Xi_1^{[0]}(t)}{A_0(t)}\right)\phi(\mathbf{y})\, d\mathbf{y}. \tag{9.88}$$

Here, both functions $\Xi_1^{[0]}(t)$ nd $\Xi_\phi^{[0]}(t)$ are determined by the formula

$$\Xi_{\phi;1}^{[0]}(t) = \int\limits_{\Gamma_0(t)} B_0(t,\mathbf{y})\left(\big(\mathfrak{S}Y_{\phi;1}^{[0]}\big)(\mathbf{y}) - \frac{\partial Y_{\phi;1}^{[0]}}{\partial n}(t,\mathbf{y})\right) d\mathbf{y}. \tag{9.89}$$

It is clear that the solvability of Eq. (9.86) depends crucially on the property of having fixed sign for $\Xi_1^{[0]}(t)$. In [8], it was proven that $\Xi_1^{[0]}(t) < 0$.

Thus, determining the function $\hat{H}_0(t)$ by dividing both sides of (9.88) by $\Xi_1^{[0]}(t)$ and substituting the obtained result into Eq. (9.86), we find $\hat{h}(t,\sigma)$ and, as a consequence of (9.79), uniquely determine the function $h(t,\sigma)$, which describes the variation of the contact domain $\omega_0(t)$.

9.1.8 Asymptotics of the Contact Pressure

In accordance with (9.34), the contact pressure is given by

$$p_\varepsilon(t,\mathbf{y}) = \mathscr{K}^{-1}\big(P_\varepsilon(\mathbf{y},\tau)\mathscr{I}_{\omega_\varepsilon(\tau)}(\mathbf{y})\big), \tag{9.90}$$

where the integral operator $\mathscr{K}^{-1}$ is defined by formula (9.35), and $\mathscr{I}_{\omega_\varepsilon(t)}(\mathbf{y})$ is the indicator function of the domain $\omega_\varepsilon(t)$ defined by

$$\mathscr{I}_{\omega_\varepsilon(t)}(\mathbf{y}) = \begin{cases} 1, & \mathbf{y} \in \omega_\varepsilon(t), \\ 0, & \mathbf{y} \notin \omega_\varepsilon(t). \end{cases}$$

In the interior of the contact area $\omega_\varepsilon(t)$, Eqs. (9.58) and (9.90) yield the asymptotic representation

$$p_\varepsilon(t,\mathbf{y}) = p_0(t,\mathbf{y}) + \varepsilon p_1(t,\mathbf{y}) + O(\varepsilon^2), \tag{9.91}$$

where

$$p_i(t,\mathbf{y}) = \mathscr{K}^{-1}\big(P_i(t,\mathbf{y})\mathscr{I}_{\omega_0(t)}(\mathbf{y})\big), \quad i = 0, 1. \tag{9.92}$$

In the boundary-layer region near the contour $\Gamma_\varepsilon(t)$, the so-called outer asymptotic representation (9.91) does not work, and the so-called inner asymptotic representation should be constructed. Here we employ the terminology from the method of matched asymptotic expansions [20].

The inner asymptotic representation

$$p_\varepsilon(t,\mathbf{y}) = \varepsilon^2 \mathscr{K}^{-1}\mathscr{P}(\tau, s, \nu) + O(\varepsilon^3) \tag{9.93}$$

will be constructed by making use of the stretched coordinate

$$\nu = \varepsilon^{-1} n. \tag{9.94}$$

In light of (9.73)–(9.75), the function $P_1(t,\mathbf{y})$ will be determined completely as soon as we know the function $P_1^{[1]}(t,\mathbf{y})$ which satisfies the following Dirichlet problem (see (9.76) and (9.77)):

$$\Delta P_1^{[1]}(t,\mathbf{y}) = 0, \quad \mathbf{y} \in \omega_0(t); \quad P_1^{[1]}(t,\mathbf{y}) = g_\phi^{[0]}(t,\mathbf{y}), \quad \mathbf{y} \in \Gamma_0(t).$$

Here we have introduced the following notation (see Eqs. (9.80), (9.87) and (9.88)):

$$g_\phi^{[0]}(t,\mathbf{y}) = -Y_\phi^{[0]}(\mathbf{y}) + \delta_1(t) Y_1^{[0]}(\mathbf{y}), \tag{9.95}$$

and as a consequence of said relations, we have

$$\delta_1(t) = \frac{\Xi_\phi^{[0]}(t)}{\Xi_1^{[0]}(t)} + \frac{1}{\Xi_1^{[0]}(t)} \iint\limits_{\omega_0(t)} B_0(t,\mathbf{y})\phi(\mathbf{y})\, d\mathbf{y}. \tag{9.96}$$

Near the boundary of the domain $\omega_0(t)$, we may use the Taylor expansions

$$P_0(t,\mathbf{y}) = \frac{m}{2}\big[\varphi_0(\mathbf{y}_0(\sigma)) - \delta_0(t)\big]n^2 + O(n^3), \tag{9.97}$$

$$P_1(t,\mathbf{y}) = \frac{m}{2}\big[\phi(\mathbf{y}_0(\sigma)) - \delta_1(t)\big]n^2 - m\hat{h}(t,\sigma)n + O(n^3), \tag{9.98}$$

where $\mathbf{y}_0(\sigma)$ is the point of the curve $\Gamma_0(t)$ with the natural coordinate σ.

Applying the perturbation method developed by Nazarov [18], we construct the auxiliary function of the inner asymptotic representation (9.93) in the form

$$\mathscr{P}(t,\sigma,\nu) = \frac{m}{2}\big[\varphi_0(\mathbf{y}_0(\sigma)) - \delta_0(t)\big](\nu - h(t,\sigma))^2. \tag{9.99}$$

The function (9.99) exactly satisfies the relations (9.15), while the boundary condition (9.16) is satisfied asymptotically. We note that the normals $\mathbf{n}_0$ and $\mathbf{n}_\varepsilon$ to the contours $\Gamma_0(t)$ and $\Gamma_\varepsilon(t)$ are, generally speaking, different (see formula (9.64)).

Finally, taking account of the relations (9.79), (9.94), (9.97)–(9.99), it is not hard to verify verify that the matching asymptotic condition for the outer (9.91) and inner (9.93) asymptotic representations is fulfilled.

9.1.9 Slightly Perturbed Circular Contact Area

Let us assume that a circular domain can be taken as a zero approximation in the form (9.5), where the function $\varphi(\mathbf{y})$ defining the perturbed boundary is given by the polynomials

$$\varphi_0(\mathbf{y}) = \frac{1}{2R}(y_1^2 + y_2^2), \quad \phi(\mathbf{y}) = \sum_{n=0}^{N}\sum_{j=0}^{n} c_{nj}\, y_1^j\, y_2^{n-j}, \tag{9.100}$$

where c_{nj} are given dimensional coefficients.

In this case, the limit ($\varepsilon = 0$) auxiliary contact problem (9.31), (9.38), (9.39) has the following solution:

$$P_0(t,\mathbf{y}) = Q_0(t)\left(1 - \frac{y_1^2 + y_2^2}{a_0(t)^2}\right)^2.$$

Correspondingly, Eqs. (9.46), (9.47) and (9.49) take the form

$$\delta_0(t) = \frac{a_0(t)^2}{4R}, \quad Q_0(t) = \frac{m}{32}\frac{a_0(t)^4}{R}, \tag{9.101}$$

$$a_0(t) = \left(\frac{m\pi}{96R}\right)^{-1/6} \left(\int_{0^-}^{t} \Phi_\beta(t-\tau)\dot{F}(\tau)\, d\tau \right)^{1/6}. \tag{9.102}$$

The first-oder perturbation problem (9.60), (9.66), (9.67), (9.69) and (9.70) now can be written as follows:

$$\Delta_y P_1(t, \mathbf{y}) = m\left(\sum_{n=0}^{N} \sum_{j=0}^{n} c_{nj} y_1^j y_2^{n-j} - \delta_1(t) \right), \quad \mathbf{y} \in \omega_0(t), \tag{9.103}$$

$$P_1(t, \mathbf{y}) = 0, \quad \mathbf{y} \in \Gamma_0(t), \tag{9.104}$$

$$\frac{\partial P_1}{\partial n}(t, \mathbf{y}) = -mh(t, \sigma)\frac{a_0(t)^2}{4R}, \quad \mathbf{y} \in \Gamma_0(t), \tag{9.105}$$

$$\pi a_0(t)^2 \delta_1(t) = \sum_{n=0}^{N} \frac{a_0(t)^{n+2}}{n+2} \sum_{j=0}^{n} c_{nj} K_{nj} + \frac{a_0(t)^3}{4R} H_0(t), \tag{9.106}$$

$$0 = \frac{a_0(t)^5}{8R} H_0(t) + \sum_{n=0}^{N} \frac{n a_0(t)^{n+4}}{2(n+2)(n+4)} \sum_{j=0}^{n} c_{nj} K_{nj}. \tag{9.107}$$

Here, $\omega_0(t)$ and $\Gamma_0(t)$ are the disc and the circle of the radius $a_0(t)$, $K_{nj} = 0$ for odd n and j, while $K_{nj} = 2B\big((n+1-j)/2, (j+1)/2\big)$ for even values of n and j, and $B(\zeta, \xi)$ is the Beta function defined by

$$B(\zeta, \xi) = \int_0^1 t^{\zeta-1}(1-t)^{\xi-1} dt.$$

Moreover, $H_0(t)$ is an integral characteristics of the contour variation $h(t, \sigma)$ which can be described by the contour variation in polar coordinates as

$$H_0(t) = \int_0^{2\pi} h(\theta, t)\, d\theta.$$

From (9.106) and (9.107), it immediately follows that

$$H_0(t) = -\sum_{n=0}^{N} \frac{4R a_0(t)^{n-1}}{(n+2)(n+4)} \sum_{j=0}^{n} c_{nj} K_{nj},$$

$$\delta_1(t) = \sum_{n=0}^{N} \frac{(n+3)a_0(t)^n}{\pi(n+2)(n+4)} \sum_{j=0}^{n} c_{nj} K_{nj}. \tag{9.108}$$

Using Green's function $\mathcal{G}(t, \mathbf{y}, \mathbf{y}')$ of the Dirichlet problem for the domain $\omega_0(t)$, we express the solution to the Dirichlet problem (9.103), (9.104) in the form

$$P_1(t, \mathbf{y}) = m \iint\limits_{\omega_0(t)} \phi(\mathbf{y}') \mathcal{G}(t, \mathbf{y}, \mathbf{y}')\, d\mathbf{y}' - \frac{m}{4} \delta_1(t)(|\mathbf{y}|^2 - a_0(t)^2). \tag{9.109}$$

Recall that for a circular domain $\omega_0(t)$ of radius $a_0(t)$, Green's function is

$$\mathcal{G}(t, \mathbf{y}, \mathbf{y}') = \frac{1}{2\pi} \ln \frac{a_0(t)|\mathbf{y}'||\mathbf{y} - \mathbf{y}'|}{\big||\mathbf{y}'|\mathbf{y} - a_0(t)^2\mathbf{x}'\big|},$$

whereas, in polar coordinates, we have

$$\mathcal{G}(t, \mathbf{y}, \mathbf{y}') = \frac{1}{4\pi} \ln \frac{a_0(t)^2\big(r^2 + r'^2 - 2r'r\cos(\theta - \theta')\big)}{a_0(t)^4 + r'^2 r^2 - 2r'r a_0(t)^2 \cos(\theta - \theta')}.$$

Calculating the normal derivative of the function (9.109), we obtain

$$\frac{\partial P_1}{\partial n}(t, \mathbf{y}) = m \iint\limits_{\omega_0(t)} \phi(\mathbf{y}') \frac{\partial \mathcal{G}}{\partial n}(t, \mathbf{y}, \mathbf{y}')\, d\mathbf{y}' - \frac{m}{2} \delta_1(t)|\mathbf{y}|, \tag{9.110}$$

where

$$\frac{\partial}{\partial n}\mathcal{G}(t, \mathbf{y}, \mathbf{y}') = \frac{1}{2\pi} \frac{a_0(t)^2 - r'^2}{a_0(t)\big(a_0(t)^2 + r'^2 - 2r'a_0(t)\cos(\theta - \theta')\big)}.$$

By substitution of the expression (9.110) into the boundary condition (9.105) and taking into account (9.108), we obtain the function $h(t, \theta)$ describing variation of the contact domain in the following form:

$$\begin{aligned} h(t, \theta) = {} & \frac{2R}{\pi a_0(t)} \sum_{n=0}^{N} \frac{(n+3)a_0(t)^n}{(n+2)(n+4)} \sum_{j=0}^{n} c_{nj} K_{nj} \\ & - \frac{2R}{\pi a_0(t)^3} \int_0^{2\pi} d\theta' \int_0^{a_0(t)} \Bigg(\sum_{n=0}^{N} r'^n \sum_{j=0}^{n} c_{nj} \cos^j \theta' \sin^{n-j} \theta' \Bigg) \\ & \times \frac{a_0(t)^2 - r'^2}{a_0(t)^2 + r'^2 - 2r'a_0(t)\cos(\theta - \theta')} r'\, dr'. \end{aligned} \tag{9.111}$$

Note that the integral with respect to θ' on the right-hand side of (9.111) can be evaluated with the help of the following relation (see, e.g., [14]):

$$\int_0^{\pi} \frac{\cos nx dx}{1 - 2\rho \cos x + \rho^2} = \frac{\pi \rho^n}{1 - \rho^2}, \quad \rho^2 < 1.$$

It was shown [8] that formula (9.111) asymptotically coincides with the exact solution for the ellipse presented in Sect. 9.1.5 in the case of small eccentricity.

9.2 Contact of Two Bonded Thin Transversely Isotropic Elastic Layers with Variable Thicknesses

In this section, a three-dimensional unilateral contact problem for a thin transversely isotropic elastic layer with variable thickness bonded to a rigid substrate is considered. Two cases are studied sequentially: (a) the layer material is compressible; (b) the layer material is incompressible. It is well known that the asymptotic solution for a thin isotropic elastic layer undergoes a dramatic change in the limit as Poisson's ratio ν tends to 0.5, so that the formulas obtained in the case (a) are not applicable when the layer material approaches the incompressible limit. After developing a refined asymptotic model for the deformation of one elastic layer of variable thickness, we apply sensitivity analysis to determine how "sensitive" the mathematical model for contact interactions of two thin uniform layers of thicknesses h_1 and h_2 is to variations in the layer thicknesses. We will consider the term "sensitivity" in a broad sense by allowing variable layer thicknesses $H_1(\mathbf{y})$ and $H_2(\mathbf{y})$, whereas the original model deals with the scalar parameters h_1 and h_2.

9.2.1 Unperturbed Asymptotic Model

As a rule, analytical models of articular contact assume rigid bones and represent cartilage as a thin elastic layer of constant thickness resisting deformation like a Winkler foundation consisting of a series of discrete springs with constant length and stiffness [12]. However, a subject-specific approach to articular contact mechanics requires developing patient-specific models for accurate predictions. A sensitivity analysis of finite element models of hip cartilage mechanics with respect to varying degrees of simplified geometry was performed in [2].

Based on the asymptotic analysis of the frictionless contact problem for a thin elastic layer bonded to a rigid substrate in the thin-layer limit (see Chap. 2), the following asymptotic model for contact interaction of two thin incompressible transversely isotropic layers was established:

$$-\left(\frac{h_1^3}{3G_1'}+\frac{h_2^3}{3G_2'}\right)\Delta_y p(\mathbf{y})=\delta_0-\varphi(\mathbf{y}),\quad \mathbf{y}\in\omega, \tag{9.112}$$

$$p(\mathbf{y})=0,\quad \frac{\partial p}{\partial n}(\mathbf{y})=0,\quad \mathbf{y}\in\Gamma. \tag{9.113}$$

Here, $p(\mathbf{y})$ is the contact pressure density, h_n and G_n' are the thickness and out-of-plane shear modulus of the nth layer material, respectively, $n=1,2$, $\Delta_y=\partial^2/\partial y_1^2+\partial^2/\partial y_2^2$ is the Laplace differential operator, δ_0 is the vertical approach of the rigid substrates to which the layers are bonded, $\varphi(\mathbf{y})$ is the initial gap function defined as the distance between the layer surfaces in the vertical direction, ω is the contact area, and Γ is the contour of ω, $\partial/\partial n$ is the normal derivative.

In the isotropic case, the asymptotic model (9.112), (9.113) was developed in [4, 10]. It was shown [6, 9, 11] that this model describes the instantaneous response of thin biphasic layers to dynamic and impact loading. In [7], the isotropic elastic model (9.112), (9.113) was generalized for a general viscoelastic case.

With respect to articular contact, a case of special interest is when the subchondral bones are approximated by elliptic paraboloids, so that the gap function is given by

$$\varphi(\mathbf{y})=\frac{y_1^2}{2R_1}+\frac{y_2^2}{2R_2} \tag{9.114}$$

with positive curvature radii R_1 and R_2.

In the case (9.114), the exact solution to the problem (9.112), (9.113) has the following form [6, 10]:

$$p(\mathbf{y})=p_0\left(1-\frac{y_1^2}{a_1^2}-\frac{y_2^2}{a_2^2}\right)^2. \tag{9.115}$$

Integration of the contact pressure distribution (9.115) over the elliptical contact area ω with the semi-axes a_1 and a_2 results in the following force-displacement relationship [4]:

$$F=\frac{2\pi}{3}c_F(s)mR_1R_2\delta_0^3. \tag{9.116}$$

Here, $c_F(s)$ is a dimensionless factor depending on the aspect ratio $s=a_2/a_1$ (see Sect. 4.5.6), and the coefficient m is given by

$$m=3\left(\frac{h_1^3}{G_1'}+\frac{h_2^3}{G_2'}\right)^{-1}. \tag{9.117}$$

The asymptotic model (9.112)–(9.114) assumes that the cartilage layers have constant thicknesses, whereas it is well known [1] that articular cartilage has a variable thickness and that the surface of subchondral bone deviates from the ellipsoid shape [19]. A sensitivity analysis of the model (9.112), (9.113) with respect

to small perturbations of the gap function (9.114) was performed in [8]. In particular, it has been shown [4] that the influence of the gap function variation on the force-displacement relationship will be negligible if the effective geometrical characteristics R_1 and R_2 are determined by a least square method.

The two-dimensional contact problem for a thin isotropic elastic strip of variable thickness was solved by Vorovich and Peninin [21] using an asymptotic method, under the assumption that the Poisson's ratio of the strip material is not very close to 0.5. A three-dimensional unilateral contact problem for a thin isotropic elastic layer of variable thickness bonded to a rigid substrate was studied in [5]. Here, the results obtained in [5] are generalized for the transversely isotropic case.

9.2.2 *Contact Problem for a Thin Transversely Isotropic Elastic Layer with Variable Thickness*

We consider (see Fig. 9.2) a homogeneous, isotropic, linearly elastic layer with a planar contact interface, $x_3 = 0$, and a variable thickness, $H(x_1, x_2)$, firmly attached to an uneven rigid surface

$$x_3 = H(x_1, x_2). \tag{9.118}$$

In the absence of body forces, the equilibrium equations and the strain-displacement relations governing small deformations of the elastic layer are

$$\frac{\partial \sigma_{1j}}{\partial x_1} + \frac{\partial \sigma_{2j}}{\partial x_2} + \frac{\partial \sigma_{3j}}{\partial x_3} = 0, \quad j = 1, 2, 3, \tag{9.119}$$

$$\varepsilon_{ij} = \frac{1}{2}\left(\frac{\partial u_i}{\partial x_j} + \frac{\partial u_j}{\partial x_i}\right), \quad i, j = 1, 2, 3, \tag{9.120}$$

where σ_{ij} is the Cauchy stress tensor, ε_{ij} is the infinitesimal strain tensor, and u_j is the displacement component along the x_j-axis. Here the Cartesian coordinate system (y_1, y_2, z) will be used such that $y_1 = x_1$, $y_2 = x_2$, and $z = x_3$.

Moreover, a transversely isotropic elastic body is characterized by the following stress-strain relationships:

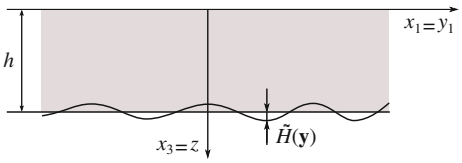

Fig. 9.2 Elastic layer with a variable thickness

$$\begin{pmatrix}\sigma_{11}\\ \sigma_{22}\\ \sigma_{33}\\ \sigma_{23}\\ \sigma_{13}\\ \sigma_{12}\end{pmatrix} = \begin{bmatrix} A_{11} & A_{12} & A_{13} & 0 & 0 & 0\\ A_{12} & A_{11} & A_{13} & 0 & 0 & 0\\ A_{13} & A_{13} & A_{33} & 0 & 0 & 0\\ 0 & 0 & 0 & 2A_{44} & 0 & 0\\ 0 & 0 & 0 & 0 & 2A_{44} & 0\\ 0 & 0 & 0 & 0 & 0 & 2A_{66}\end{bmatrix} \begin{pmatrix}\varepsilon_{11}\\ \varepsilon_{22}\\ \varepsilon_{33}\\ \varepsilon_{23}\\ \varepsilon_{13}\\ \varepsilon_{12}\end{pmatrix}. \tag{9.121}$$

Recall that $2A_{66} = A_{11} - A_{12}$, while $A_{11}, A_{12}, A_{13}, A_{33}$, and A_{44} are five independent elastic constants.

We assume that the elastic layer is indented by a smooth rigid punch in the form of an elliptic paraboloid

$$z = -\varphi(y_1, y_2),$$

where

$$\varphi(\mathbf{y}) = \frac{y_1^2}{2R_1} + \frac{y_2^2}{2R_2}. \tag{9.122}$$

Under the assumption of frictionless contact, we have

$$\sigma_{31}(\mathbf{y}, 0) = 0, \quad \sigma_{32}(\mathbf{y}, 0) = 0, \quad \mathbf{y} = (y_1, y_2) \in \mathbb{R}^2. \tag{9.123}$$

Denoting by δ_0 the indenter's displacement, we formulate the boundary condition on the contact interface as

$$\begin{gathered} u_3(\mathbf{y}, 0) \geq \delta_0 - \varphi(\mathbf{y}), \quad \sigma_{33}(\mathbf{y}, 0) \leq 0,\\ \big(u_3(\mathbf{y}, 0) - \delta_0 + \varphi(\mathbf{y})\big)\sigma_{33}(\mathbf{y}, 0) = 0, \quad \mathbf{y} \in \mathbb{R}^2, \end{gathered} \tag{9.124}$$

while on the rigid substrate surface defined by Eq. (9.118) we have

$$u_j(\mathbf{y}, H(\mathbf{y})) = 0, \quad \mathbf{y} \in \mathbb{R}^2 \quad (j = 1, 2, 3). \tag{9.125}$$

Assuming that the layer is relatively thin in comparison to the characteristic dimensions of ω, we introduce a small dimensionless parameter ε and require that

$$\delta_0 = \varepsilon\delta_0^*, \quad R_1 = \varepsilon^{-1}R_1^*, \quad R_2 = \varepsilon^{-1}R_2^*, \tag{9.126}$$

$$H(\mathbf{y}) = \varepsilon h_*(1 + \varepsilon\psi_*(\mathbf{y})), \tag{9.127}$$

where δ_0^*, R_1^*, and R_2^* are assumed to be comparable with h_*. Without loss of generality we can assume that $|\psi_*(\mathbf{y})| \leq h_*$ for any $\mathbf{y} \in \mathbb{R}^2$.

The problem is to calculate the contact pressure distribution

$$p(x_1, x_2) = -\sigma_{33}(x_1, x_2, 0), \quad (x_1, x_2) \in \omega, \tag{9.128}$$

and the contact force required to indent the punch into the elastic layer

$$F = \iint_{\omega} p(\mathbf{y})\, d\mathbf{y}. \tag{9.129}$$

We introduce the notation

$$h = \varepsilon h_*, \quad \tilde{H}(\mathbf{y}) = \varepsilon^2 \tilde{H}_*(\mathbf{y}), \tag{9.130}$$

where

$$\tilde{H}_*(\mathbf{y}) = h_* \psi_*(\mathbf{y}). \tag{9.131}$$

Hence, the following relation is evident:

$$H(\mathbf{y}) = h + \tilde{H}(\mathbf{y}), \tag{9.132}$$

where h is an average thickness, and $\tilde{H}(\mathbf{y})$ is a small variation such that $\tilde{H}(\mathbf{y}) \ll h$.

We note that as a consequence of (9.128), the unilateral contact condition (9.124) can be rewritten as follows:

$$p(\mathbf{y}) \geq 0, \quad \mathbf{y} \in \mathbb{R}^2,$$

$$p(\mathbf{y}) > 0 \;\; \Rightarrow \;\; u_3(\mathbf{y}, 0) = \delta_0 - \varphi(\mathbf{y}),$$

$$p(\mathbf{y}) = 0 \;\; \Rightarrow \;\; u_3(\mathbf{y}, 0) \geq \delta_0 - \varphi(\mathbf{y}).$$

We pose the following frictionless unilateral contact problem: for a given value of the punch displacement δ_0, find the contact pressure $p(\mathbf{y})$ such that the Signorini boundary condition (9.124) is satisfied both inside the contact area ω and outside (that is $p(\mathbf{y}) = 0$ for $\mathbf{y} \in \mathbb{R}^2 \setminus \bar{\omega}$).

9.2.3 Perturbation Solution

First, we introduce the so-called stretched coordinate

$$\zeta = \varepsilon^{-1} z. \tag{9.133}$$

Substituting (9.121) and (9.120) into Eqs. (9.119) and taking into account the variable transformation (9.133), we arrive at the following Lamé system for the displacement vector $\mathbf{u} = (\mathbf{v}, w)$:

$$\begin{aligned} \varepsilon^{-2} A_{44} \frac{\partial^2 \mathbf{v}}{\partial \zeta^2} + \;& \varepsilon^{-1} (A_{13} + A_{44}) \nabla_y \frac{\partial w}{\partial \zeta} \\ & + A_{66} \Delta_y \mathbf{v} + (A_{11} - A_{66}) \nabla_y \nabla_y \cdot \mathbf{v} = \mathbf{0}, \end{aligned} \tag{9.134}$$

$$\varepsilon^{-2}A_{33}\frac{\partial^2 w}{\partial\zeta^2}+\varepsilon^{-1}(A_{13}+A_{44})\nabla_y\cdot\frac{\partial\mathbf{v}}{\partial\zeta}+A_{44}\Delta_y w=0. \tag{9.135}$$

Here, $\nabla_y=(\partial/\partial y_1,\partial/\partial y_2)$ is the Hamilton differential operator, and the dot denotes the scalar product, so that $\nabla_y\cdot\nabla_y=\Delta_y$ is the Laplace operator.

Correspondingly, the boundary condition (9.123) takes the form

$$\varepsilon^{-1}\frac{\partial\mathbf{v}}{\partial\zeta}+\nabla_y w\Big|_{\zeta=0}=\mathbf{0}. \tag{9.136}$$

In light of (9.124) and (9.126), we have

$$w(\mathbf{y},0)=\varepsilon(\delta_0^*-\varphi^*(\mathbf{y})),\quad \mathbf{y}\in\omega, \tag{9.137}$$

where we have introduced the notation (see Eqs. (9.122) and (9.126))

$$\varphi^*(\mathbf{y})=\frac{y_1^2}{2R_1^*}+\frac{y_2^2}{2R_2^*}. \tag{9.138}$$

Furthermore, by stretching the normal coordinate, Eq. (9.128) is reduced to

$$-p(\mathbf{y})=\varepsilon^{-1}A_{33}\frac{\partial w}{\partial\zeta}+A_{13}\nabla_y\cdot\mathbf{v}\Big|_{\zeta=0},\quad \mathbf{y}\in\omega. \tag{9.139}$$

The boundary conditions (9.125) on the substrate surface (see Eqs. (9.118) and (9.127))

$$\zeta=h_*(1+\varepsilon\psi_*(\mathbf{y})) \tag{9.140}$$

take the following form:

$$\mathbf{v}\big(\mathbf{y},h_*+\varepsilon h_*\psi_*(\mathbf{y})\big)=\mathbf{0},\quad w\big(\mathbf{y},h_*+\varepsilon h_*\psi_*(\mathbf{y})\big)=0. \tag{9.141}$$

Observe that among Eqs. (9.134)–(9.137), (9.139) and (9.141), there are only two inhomogeneous equations, namely (9.137) and (9.139). The form of (9.137) suggests the asymptotic expansion

$$w(\mathbf{y},\zeta)=\varepsilon w^0(\mathbf{y},\zeta)+\varepsilon^2 w^1(\mathbf{y},\zeta)+\cdots. \tag{9.142}$$

In light of (9.139) and (9.142), we suggest that $p(\mathbf{y})=O(1)$ as $\varepsilon\to 0$. Taking into account the homogeneous conditions (9.136), (9.141), we set

$$\mathbf{v}(\mathbf{y},\zeta)=\varepsilon\mathbf{v}^0(\mathbf{y},\zeta)+\varepsilon^2\mathbf{v}^1(\mathbf{y},\zeta)+\cdots. \tag{9.143}$$

We emphasize that the asymptotic ansatz (9.142), (9.143) is valid only inside the contact region ω. In other words, a plane boundary layer should be constructed near the edge of the contact area. We refer to [3, 13] for more details.

9.2.4 Derivation of Asymptotic Expansions

Substituting (9.142) and (9.143) into Eqs. (9.134) and (9.135), we obtain

$$\begin{aligned}\varepsilon^{-2}A_{44}\frac{\partial^2\mathbf{v}^0}{\partial\zeta^2}+\varepsilon^{-1}\left((A_{13}+A_{44})\nabla_y\frac{\partial w^0}{\partial\zeta}+A_{44}\frac{\partial^2\mathbf{v}^1}{\partial\zeta^2}\right)\\+\varepsilon^0\left\{A_{66}\Delta_y\mathbf{v}^0+(A_{11}+A_{66})\nabla_y\nabla_y\cdot\mathbf{v}^0\right.\\\left.+(A_{13}+A_{44})\nabla_y\frac{\partial w^1}{\partial\zeta}+A_{44}\frac{\partial^2\mathbf{v}^2}{\partial\zeta^2}\right\}+\cdots=\mathbf{0},\end{aligned}\tag{9.144}$$

$$\begin{aligned}\varepsilon^{-2}A_{33}\frac{\partial^2 w^0}{\partial\zeta^2}+\varepsilon^{-1}\left(A_{33}\frac{\partial^2 w^1}{\partial\zeta^2}+(A_{13}+A_{44})\nabla_y\cdot\frac{\partial\mathbf{v}^0}{\partial\zeta}\right)+\varepsilon^0\left\{A_{33}\frac{\partial^2 w^2}{\partial\zeta^2}\right.\\\left.+(A_{13}+A_{44})\nabla_y\cdot\frac{\partial\mathbf{v}^1}{\partial\zeta}+A_{44}\Delta_y w^0\right\}+\cdots=0.\end{aligned}\tag{9.145}$$

Further, by substituting (9.142) and (9.143) into the boundary conditions (9.136) and (9.139) at the contact region, we find

$$\varepsilon^{-1}\frac{\partial\mathbf{v}^0}{\partial\zeta}+\varepsilon^0\left(\nabla_y w^0+\frac{\partial\mathbf{v}^1}{\partial\zeta}\right)+\varepsilon\left(\nabla_y w^1+\frac{\partial\mathbf{v}^2}{\partial\zeta}\right)+\cdots\Big|_{\zeta=0}=\mathbf{0},\tag{9.146}$$

$$\begin{aligned}A_{33}\frac{\partial w^0}{\partial\zeta}+\varepsilon\left(A_{13}\nabla_y\cdot\mathbf{v}^0+A_{33}\frac{\partial w^1}{\partial\zeta}\right)\\+\varepsilon^2\left(A_{13}\nabla_y\cdot\mathbf{v}^1+A_{33}\frac{\partial w^2}{\partial\zeta}\right)+\cdots\Big|_{\zeta=0}=-p(\mathbf{y}).\end{aligned}\tag{9.147}$$

The substitution of (9.142), (9.143) into Eqs. (9.141) then yields

$$\mathbf{v}^0+\varepsilon\left(\mathbf{v}^1+\tilde{H}_*\frac{\partial\mathbf{v}^0}{\partial\zeta}\right)+\varepsilon^2\left(\mathbf{v}^2+\tilde{H}_*\frac{\partial\mathbf{v}^1}{\partial\zeta}+\frac{\tilde{H}_*^2}{2}\frac{\partial^2\mathbf{v}^0}{\partial\zeta^2}\right)+\cdots\Big|_{\zeta=h_*}=\mathbf{0},\tag{9.148}$$

$$w^0+\varepsilon\left(w^1+\tilde{H}_*\frac{\partial w^0}{\partial\zeta}\right)+\varepsilon^2\left(w^2+\tilde{H}_*\frac{\partial w^1}{\partial\zeta}+\frac{\tilde{H}_*^2}{2}\frac{\partial^2 w^0}{\partial\zeta^2}\right)+\cdots\Big|_{\zeta=h_*}=0, \quad (9.149)$$

where we have used notation (9.131).

Thus, on the basis of Eqs. (9.144)–(9.149), we have arrived at a recurrence system of boundary-value problems for the functions $\mathbf{v}^k$ and w^k $(k = 0, 1, \ldots)$. Let us construct the first several terms of the asymptotic series (9.142) and (9.143).

9.2.5 Asymptotic Solution for a Thin Compressible Layer

According to (9.144)–(9.149), the first-order problem takes the form

$$\frac{\partial^2 w^0}{\partial\zeta^2}=0, \quad \zeta\in(0,h_*), \quad A_{33}\frac{\partial w^0}{\partial\zeta}\Big|_{\zeta=0}=-p(\mathbf{y}), \quad w^0\big|_{\zeta=h_*}=0; \quad (9.150)$$

$$\frac{\partial^2 \mathbf{v}^0}{\partial\zeta^2}=\mathbf{0}, \quad \zeta\in(0,h_*), \quad \frac{\partial \mathbf{v}^0}{\partial\zeta}\Big|_{\zeta=0}=\mathbf{0}, \quad \mathbf{v}^0\big|_{\zeta=h_*}=\mathbf{0}. \quad (9.151)$$

From (9.150) and (9.151), it immediately follows that

$$w^0(\mathbf{y},\zeta)=\frac{p(\mathbf{y})}{A_{33}}(h_*-\zeta), \quad (9.152)$$

$$\mathbf{v}^0(\mathbf{y},\zeta)\equiv\mathbf{0}. \quad (9.153)$$

As a consequence of (9.153), the second-order problem, derived from (9.144)–(9.149) is

$$\frac{\partial^2 w^1}{\partial\zeta^2}=0, \quad \zeta\in(0,h_*),$$

$$\frac{\partial w^1}{\partial\zeta}\Big|_{\zeta=0}=0, \quad w^1\big|_{\zeta=h_*}=-\tilde{H}_*(\mathbf{y})\frac{\partial w^0}{\partial\zeta}\Big|_{\zeta=h_*}; \quad (9.154)$$

$$A_{44}\frac{\partial^2 \mathbf{v}^1}{\partial\zeta^2}=-(A_{13}+A_{44})\nabla_y\frac{\partial w^0}{\partial\zeta}, \quad \zeta\in(0,h_*),$$

$$\frac{\partial \mathbf{v}^1}{\partial\zeta}\Big|_{\zeta=0}=-\nabla_y w^0\big|_{\zeta=0}, \quad \mathbf{v}^1\big|_{\zeta=h_*}=\mathbf{0}. \quad (9.155)$$

It is readily seen that the solution of the problem (9.154) is given by

$$w^1(\mathbf{y},\zeta)=\frac{p(\mathbf{y})}{A_{33}}\tilde{H}_*(\mathbf{y}). \tag{9.156}$$

On the other hand, the solution of the problem (9.155) is

$$\mathbf{v}^1(\mathbf{y},\zeta)=\Psi(\zeta)\nabla_y p(\mathbf{y}), \tag{9.157}$$

where we have introduced the notation

$$\Psi(\zeta)=\frac{(A_{13}+A_{44})}{2A_{33}A_{44}}(h_*-\zeta)^2-\frac{h_*A_{13}}{A_{33}A_{44}}(h_*-\zeta). \tag{9.158}$$

Collecting Eqs. (9.142), (9.152) and (9.156), we arrive at the two-term asymptotic approximation for the normal displacement

$$w(\mathbf{y},\zeta)\simeq\varepsilon\frac{p(\mathbf{y})}{A_{33}}(h_*-\zeta)+\varepsilon^2\frac{p(\mathbf{y})}{A_{33}}\tilde{H}_*(\mathbf{y}). \tag{9.159}$$

By taking into account the scaling relations (9.130), we rewrite (9.159) in the form

$$u_3(\mathbf{y},z)\simeq\frac{p(\mathbf{y})}{A_{33}}\big(h+\tilde{H}(\mathbf{y})-z\big). \tag{9.160}$$

By substituting the expression (9.160) into the contact condition

$$u_3(\mathbf{y},0)=\delta_0-\varphi(\mathbf{y}),\quad \mathbf{y}\in\omega, \tag{9.161}$$

we derive the following equation for the contact pressure density:

$$\frac{h+\tilde{H}(\mathbf{y})}{A_{33}}p(\mathbf{y})=\delta_0-\varphi(\mathbf{y}),\quad \mathbf{y}\in\omega. \tag{9.162}$$

In light of the condition $p(\mathbf{y})>0$ for $\mathbf{y}\in\omega$, we obtain

$$p(\mathbf{y})=\frac{A_{33}}{h+\tilde{H}(\mathbf{y})}\big(\delta_0-\varphi(\mathbf{y})\big)_+, \tag{9.163}$$

where $(x)_+=\max\{x,0\}$ is the positive-part function.

Invoking the notation (9.132) for the variable thickness of the elastic layer, we rewrite formula (9.163) as

$$p(\mathbf{y})=\frac{A_{33}}{H(\mathbf{y})}\big(\delta_0-\varphi(\mathbf{y})\big)_+. \tag{9.164}$$

Formula (9.164) shows that a thin compressible elastic layer deforms like a Winkler foundation with the variable foundation modulus

$$k(\mathbf{y}) = \frac{A_{33}}{H(\mathbf{y})}. \tag{9.165}$$

Let us recall that the elastic parameter A_{33} is related to Young's moduli, E and E', and Poisson's ratios, ν and ν', by the formulas

$$A_{33} = \frac{E'(1-\nu)}{1-\nu-\dfrac{2E}{E'}\,\nu'^2}, \tag{9.166}$$

Finally, according to [16] (see also Sect. 2.4), the denominator of (9.166) would approach zero if the layer material became more incompressible. It is readily seen from (9.165) that $k(\mathbf{y}) \to \infty$ in the incompressibility limit, implying that the case of an incompressible elastic layer requires special consideration.

9.2.6 Asymptotic Solution for a Thin Incompressible Layer

Let us continue the process of constructing terms of the asymptotic expansions (9.142) and (9.143). In light of (9.156), Eqs. (9.144)–(9.149) yield the following third-order problem:

$$A_{33}\frac{\partial^2 w^2}{\partial \zeta^2} = -(A_{13}+A_{44})\nabla_y\cdot\frac{\partial \mathbf{v}^1}{\partial \zeta} - A_{44}\Delta_y w^0, \quad \zeta\in(0,h_*),$$

$$A_{33}\frac{\partial w^2}{\partial \zeta}\bigg|_{\zeta=0} = -A_{13}\nabla_y\cdot\mathbf{v}^1\big|_{\zeta=0}, \quad w^2\big|_{\zeta=h_*}=0; \tag{9.167}$$

$$\frac{\partial^2 \mathbf{v}^2}{\partial \zeta^2} = \mathbf{0}, \quad \zeta\in(0,h_*),$$

$$\frac{\partial \mathbf{v}^2}{\partial \zeta}\bigg|_{\zeta=0} = -\nabla_y w^1\big|_{\zeta=0}, \quad \mathbf{v}^2\big|_{\zeta=h_*} = -\tilde{H}_*(\mathbf{y})\frac{\partial \mathbf{v}^1}{\partial \zeta}\bigg|_{\zeta=h_*}. \tag{9.168}$$

Substituting (9.152) and (9.157) into Eqs. (9.167), we derive the problem

$$\frac{\partial^2 w^2}{\partial \zeta^2} = \frac{A_{13}\Delta_y p(\mathbf{y})}{A_{33}^2 A_{44}}\big[(A_{13}+2A_{44})(h_*-\zeta)-(A_{13}+A_{44})h_*\big], \quad \zeta\in(0,h_*),$$

$$\frac{\partial w^2}{\partial \zeta}\Big|_{\zeta=0} = -\frac{A_{13}(A_{44}-A_{13})h_*^2}{2A_{33}^2 A_{44}}\Delta_y p(\mathbf{y}), \quad w^2\big|_{\zeta=h_*} = 0. \tag{9.169}$$

It can be verified that the solution to (9.169) condenses into the form

$$w^2(\mathbf{y},\zeta) = \frac{A_{13}\Delta_y p(\mathbf{y})}{A_{33}^2}\left\{\frac{A_{13}+2A_{44}}{6A_{44}}(h_*-\zeta)^3 - \frac{(A_{13}+A_{44})h_*}{2A_{44}}(h_*-\zeta)^2 + \frac{h_*^2}{2}(h_*-\zeta)\right\}. \tag{9.170}$$

Further, in light of (9.156) and (9.157), the problem (9.168) takes the form

$$\frac{\partial^2 \mathbf{v}^2}{\partial \zeta^2} = \mathbf{0}, \quad \zeta \in (0,h_*),$$

$$\frac{\partial \mathbf{v}^2}{\partial \zeta}\Big|_{\zeta=0} = -\frac{\nabla_y(p\tilde{H}_*)}{A_{33}}, \quad \mathbf{v}^2\big|_{\zeta=h_*} = -\frac{A_{13}h_*}{A_{33}A_{44}}\tilde{H}_*\nabla_y p, \tag{9.171}$$

where we have omitted the arguments of functions $p(\mathbf{y})$ and $\tilde{H}_*(\mathbf{y})$ for clarity.

It can be easily verified that the solution to (9.171) has the form

$$\mathbf{v}^2(\mathbf{y},\zeta) = \frac{h_*-\zeta}{A_{33}}\nabla_y(p\tilde{H}_*) - \frac{A_{13}h_*}{A_{33}A_{44}}\tilde{H}_*\nabla_y p. \tag{9.172}$$

We emphasize that in contrast to the two-term approximation (9.159), the third term (9.170) does not vanish at the contact interface in the limit as $\nu \to 0.5$. Indeed, formula (9.170) yields

$$w^2(\mathbf{y},0) = -\frac{h_*^3 A_{13}(A_{13}-A_{44})}{3A_{33}^2 A_{44}}\Delta_y p(\mathbf{y}). \tag{9.173}$$

In the incompressibility limit, we have

$$\frac{A_{13}(A_{13}-A_{44})}{A_{33}^2 A_{44}} \to \frac{1}{a_{44}}, \tag{9.174}$$

where $a_{44} = A_{44} = G'$ is the out-of-plane shear modulus.

In order to construct a correction for the leading asymptotic term (9.170), we consider the following problem:

$$A_{33}\frac{\partial^2 w^3}{\partial \zeta^2} = -(A_{13}+A_{44})\nabla_y \cdot \frac{\partial \mathbf{v}^2}{\partial \zeta} - A_{44}\Delta_y w^1, \quad \zeta \in (0,h_*),$$

$$A_{33}\frac{\partial w^3}{\partial \zeta}\Big|_{\zeta=0} = -A_{13}\nabla_y\cdot \mathbf{v}^2\big|_{\zeta=0}, \quad w^3\big|_{\zeta=h_*} = -\tilde{H}_*(\mathbf{y})\frac{\partial w^2}{\partial \zeta}\Big|_{\zeta=h_*}. \tag{9.175}$$

By substituting (9.156), (9.170) and (9.172) into Eqs. (9.175), we find

$$\frac{\partial^2 w^3}{\partial \zeta^2} = \frac{A_{13}}{A_{33}^2}\Delta_y(p\tilde{H}_*), \quad \zeta \in (0, h_*), \tag{9.176}$$

$$\frac{\partial w^3}{\partial \zeta}\Big|_{\zeta=0} = \frac{A_{13}h_*}{A_{33}^2A_{44}}\big(A_{13}\nabla_y\cdot(\tilde{H}_*\nabla_y p) - A_{44}\Delta_y(p\tilde{H}_*)\big), \tag{9.177}$$

$$w^3\big|_{\zeta=h_*} = \frac{A_{13}h_*^2}{2A_{33}^2}\tilde{H}_*\Delta_y p. \tag{9.178}$$

Integrating Eq. (9.176), we obtain

$$w^3(\mathbf{y}, 0) = \frac{A_{13}}{2A_{33}^2}\Delta_y(p\tilde{H}_*)\zeta^2 + C_1(\mathbf{y})\zeta + C_0(\mathbf{y}), \tag{9.179}$$

where the integration functions $C_1(\mathbf{y})$ and $C_0(\mathbf{y})$ are determined by the boundary conditions (9.177) and (9.178). It can be checked that

$$C_1(\mathbf{y}) = \frac{A_{13}h_*}{A_{33}^2A_{44}}\big(A_{13}\nabla_y\cdot(\tilde{H}_*\nabla_y p) - A_{44}\Delta_y(p\tilde{H}_*)\big), \tag{9.180}$$

$$C_0(\mathbf{y}) = \frac{A_{13}h_*^2}{2A_{33}^2}[\tilde{H}_*\Delta_y p + \Delta_y(p\tilde{H}_*)] - \frac{A_{13}^2h_*^2}{A_{33}^2A_{44}}\nabla_y\cdot(\tilde{H}_*\nabla_y p). \tag{9.181}$$

From (9.179), it immediately follows that

$$w^3(\mathbf{y}, 0) = C_0(\mathbf{y}), \tag{9.182}$$

and it can be shown that in the incompressibility limit (when $A_{13}/A_{33} \to 1$ and $A_{44}/A_{33} \to 0$), we arrive at the following result:

$$C_0(\mathbf{y}) = -\frac{h_*^2}{a_{44}}\nabla_y\cdot(\tilde{H}_*\nabla_y p). \tag{9.183}$$

Thus, collecting Eqs. (9.142), (9.173), (9.182) and (9.183), we obtain the following two-term asymptotic approximation for the normal displacement at the contact interface in the case of the incompressible elastic layer:

$$w(\mathbf{y}, 0) \simeq -\varepsilon^3\frac{h_*^3}{3a_{44}}\Delta_y p(\mathbf{y}) - \varepsilon^4\frac{h_*^2}{a_{44}}\nabla_y\cdot(\tilde{H}_*(\mathbf{y})\nabla_y p(\mathbf{y})). \tag{9.184}$$

Recalling the scaling relations (9.130) and the notation $a_{44} = G'$, we rewrite (9.184) in the form

$$u_3(\mathbf{y}, 0) \simeq -\frac{h^3}{3G'}\Delta_y p(\mathbf{y}) - \frac{h^2}{G'}\nabla_y \cdot (\tilde{H}(\mathbf{y})\nabla_y p(\mathbf{y})). \tag{9.185}$$

Now, substituting the expression (9.185) into the contact condition (9.161), we arrive at a partial differential equation in the domain ω with respect to the function $p(\mathbf{y})$. According to the asymptotic analysis [13] (see also Sect. 2.7.3), at the contour Γ of ω, we impose the following boundary conditions:

$$p(\mathbf{y}) = 0, \quad \frac{\partial p}{\partial n}(\mathbf{y}) = 0, \quad \mathbf{y} \in \Gamma. \tag{9.186}$$

Here, $\partial/\partial n$ is the normal derivative. We underline that the location of the contour Γ must be determined as part of the solution. For analytical evaluation of the contour Γ, a perturbation-based method was developed in [8].

9.2.7 Perturbation of the Contact Pressure in the Compressible Case

Collecting Eqs. (9.142), (9.152), (9.156), (9.170) and (9.179), we obtain

$$\begin{aligned} w(\mathbf{y}, 0) \simeq\ & \varepsilon\frac{h_*}{A_{33}}p(\mathbf{y}) + \varepsilon^2\frac{\tilde{H}_*(\mathbf{y})}{A_{33}}p(\mathbf{y}) - \varepsilon^3\frac{h_*^3 A_{13}(A_{13} - A_{44})}{3A_{33}^2 A_{44}}\Delta_y p(\mathbf{y}) \\ & + \varepsilon^4\left\{\frac{h_*^2 A_{13}}{2A_{33}^2}\left[\tilde{H}_*(\mathbf{y})\Delta_y p(\mathbf{y}) + \Delta_y\left(p(\mathbf{y})\tilde{H}_*(\mathbf{y})\right)\right]\right. \\ & \left. - \frac{h_*^2 A_{13}^2}{A_{33}^2 A_{44}}\nabla_y \cdot \left(\tilde{H}_*(\mathbf{y})\nabla_y p(\mathbf{y})\right)\right\}. \end{aligned} \tag{9.187}$$

By substitution of the asymptotic expansion (9.187) into the contact condition (9.137) and using the notation (9.131), we arrive at the equation

$$\begin{aligned} & p(\mathbf{y}) + \varepsilon\psi_*(\mathbf{y})p(\mathbf{y}) - \varepsilon^2\frac{h_*^3 A_{13}(A_{13} - A_{44})}{3A_{33}A_{44}}\Delta_y p(\mathbf{y}) \\ & + \varepsilon^3\frac{A_{13}h_*^2}{2A_{33}A_{44}}\left\{A_{44}\left[\psi_*(\mathbf{y})\Delta_y p(\mathbf{y}) + \Delta_y\left(p(\mathbf{y})\psi_*(\mathbf{y})\right)\right]\right. \\ & \left. - 2A_{13}\nabla_y \cdot \left(\psi_*(\mathbf{y})\nabla_y p(\mathbf{y})\right)\right\} = \frac{A_{33}}{h_*}f^*(\mathbf{y}), \end{aligned} \tag{9.188}$$

where we have introduced the shorthand notation

$$f^*(\mathbf{y}) = \delta_0^* - \varphi^*(\mathbf{y}). \tag{9.189}$$

It should be noted that Eq. (9.188) is applied in the case of compressible materials when its right-hand side makes sense.

By employing a perturbation method, the third-order asymptotic solution to Eq. (9.188) is expressed in the form

$$p(\mathbf{y}) \simeq \frac{A_{33}}{h_*}\big(\sigma_0(\mathbf{y}) + \varepsilon\sigma_1(\mathbf{y}) + \varepsilon^2\sigma_2(\mathbf{y}) + \varepsilon^3\sigma_3(\mathbf{y})\big). \tag{9.190}$$

Upon substitution of (9.195) into (9.188), we straightforwardly obtain

$$\sigma_0 = f^*, \quad \sigma_1 = -\psi_* f^*, \quad \sigma_2 = \psi_*^2 f^* + \frac{h_*^2 A_{13}(A_{13} - A_{44})}{3A_{33}A_{44}}\Delta_y f^*, \tag{9.191}$$

$$\begin{aligned}\sigma_3 = {} & -\psi_*^3 f^* - \frac{h_*^2 A_{13}(A_{13} - A_{44})}{3A_{33}A_{44}}\big(\psi_*\Delta_y f^* + \Delta_y(\psi_* f^*)\big) \\ & - \frac{h_*^2 A_{13}}{2A_{33}A_{44}}\big\{A_{44}\big[\psi_*\Delta_y f^* + \Delta_y(f^*\psi_*)\big] - 2A_{13}\nabla_y\cdot(\psi_*\nabla_y f^*)\big\},\end{aligned} \tag{9.192}$$

where, for the sake of brevity, the argument $\mathbf{y}$ is omitted.

Further, by making use of the differential identities

$$\nabla\cdot(\psi\nabla f) = \nabla\psi\cdot\nabla f + \psi\Delta f,$$

$$\Delta(f\psi) = \psi\Delta f + f\Delta\psi + 2\nabla f\cdot\nabla\psi,$$

we simplify formula (9.192) as follows:

$$\begin{aligned}\sigma_3 = {} & -\psi_*^3 f^* - \frac{h_*^2 A_{13}(2A_{13} + A_{44})}{6A_{33}A_{44}} f^*\Delta_y\psi_* \\ & + \frac{h_*^2 A_{13}(A_{13} - A_{44})}{3A_{33}A_{44}}\big(\nabla_y f^*\cdot\nabla_y\psi_* + \psi_*\Delta_y f^*\big).\end{aligned} \tag{9.193}$$

Observe also that formula (9.181) can be transformed to

$$C_0(\mathbf{y}) = -\frac{h_*^2 A_{13}(A_{13} - A_{44})}{A_{33}^2 A_{44}}\big[\nabla_y\tilde{H}_*\cdot\nabla_y p + \tilde{H}_*\Delta_y p\big] + \frac{h_*^2 A_{13}}{2A_{33}^2} p\Delta_y\tilde{H}_*, \tag{9.194}$$

where the expression in the brackets in (9.194) is equal to $\nabla_y\cdot(\tilde{H}_*\nabla_y p)$.

In the isotropic case, Eqs. (9.190)–(9.193) reduce to the following [5]:

$$p(\mathbf{y}) \simeq \frac{2\mu + \lambda}{h_*}\big(\sigma_0(\mathbf{y}) + \varepsilon\sigma_1(\mathbf{y}) + \varepsilon^2\sigma_2(\mathbf{y}) + \varepsilon^3\sigma_3(\mathbf{y})\big), \tag{9.195}$$

$$\sigma_0 = f^*, \quad \sigma_1 = -\psi_* f^*, \quad \sigma_2 = \psi_*^2 f^* + \frac{h_*^2 \lambda(\lambda-\mu)}{3\mu(2\mu+\lambda)} \Delta_y f^*, \tag{9.196}$$

$$\sigma_3 = -\psi_*^3 f^* - \frac{h_*^2 \lambda(2\lambda+\mu)}{6\mu(2\mu+\lambda)} f^* \Delta_y \psi_* + \frac{h_*^2 \lambda(\lambda-\mu)}{3\mu(2\mu+\lambda)} \big(\nabla_y f^* \cdot \nabla_y \psi_* + \psi_* \Delta_y f^*\big). \tag{9.197}$$

It can be easily checked that the four-term asymptotic expansion (9.195), with the coefficients given by (9.196) and (9.197) in the 2D case, recovers the corresponding solution obtained in [21], where the next asymptotic term for the contact pressure in (9.195) was given explicitly.

9.2.8 Application to Sensitivity Analysis of the Contact Interaction Between Two Thin Incompressible Layers

According to (9.185) and (9.186), the refined asymptotic model for contact interaction of thin incompressible layers bonded to rigid substrates takes the form

$$-m^{-1} \Delta_y p(\mathbf{y}) - \sum_{n=1}^{2} \frac{h_n^2}{G_n'} \nabla_y \cdot (\tilde{H}_n(\mathbf{y}) \nabla_y p(\mathbf{y})) = \delta_0 - \varphi(\mathbf{y}), \quad \mathbf{y} \in \tilde{\omega}, \tag{9.198}$$

$$p(\mathbf{y}) = 0, \quad \frac{\partial p}{\partial n}(\mathbf{y}) = 0, \quad \mathbf{y} \in \tilde{\Gamma}, \tag{9.199}$$

where $\tilde{\Gamma}$ is the contour of the contact region $\tilde{\omega}$, and m is given in (9.117).

Let us define

$$p(\mathbf{y}) = \bar{p}(\mathbf{y}) + \tilde{p}(\mathbf{y}), \tag{9.200}$$

where $\bar{p}(\mathbf{y})$ is the solution to the original asymptotic model (9.112), (9.113), and $\tilde{p}(\mathbf{y})$ represents a perturbation due to the variability of the layer thickness.

Then, under the assumption that the thickness variation functions $\tilde{H}_1(\mathbf{y})$ and $\tilde{H}_2(\mathbf{y})$ introduce a small variation into the elliptical contact region ω corresponding to the density $\bar{p}(\mathbf{y})$, we derive from (9.198)–(9.200) the following limit problem for the variation of the contact pressure density:

$$-m^{-1} \Delta_y \tilde{p}(\mathbf{y}) = \sum_{n=1}^{2} \frac{h_n^2}{G_n'} \nabla_y \cdot (\tilde{H}_n(\mathbf{y}) \nabla_y \bar{p}(\mathbf{y})), \quad \mathbf{y} \in \omega, \tag{9.201}$$

$$\tilde{p}(\mathbf{y}) = 0, \quad \mathbf{y} \in \Gamma. \tag{9.202}$$

Here, Γ is the contour corresponding to the contact pressure (9.115).

Moreover, the thickness variation functions $\tilde{H}_1(\mathbf{y})$ and $\tilde{H}_2(\mathbf{y})$ will not greatly influence the resulting force-displacement relationship, if

$$\iint\limits_{\omega} \tilde{p}(\mathbf{y})\, d\mathbf{y} = 0. \tag{9.203}$$

In this case, the contact force P is related to the displacement δ_0 by the same relation as that derived in framework of the original asymptotic model (9.112), (9.113).

Let us derive the conditions for $\tilde{H}_1(\mathbf{y})$ and $\tilde{H}_2(\mathbf{y})$ under which the equality (9.203) holds true. With this aim we consider an auxiliary problem

$$\Delta_y \Theta(\mathbf{y}) = 1, \quad \mathbf{y} \in \omega, \quad \Theta(\mathbf{y}) = 0, \quad \mathbf{y} \in \Gamma \tag{9.204}$$

with the solution

$$\Theta(\mathbf{y}) = -\frac{a_1^2 a_2^2}{2(a_1^2 + a_2^2)}\theta(\mathbf{y}),$$

where

$$\theta(\mathbf{y}) = 1 - \frac{y_1^2}{a_1^2} - \frac{y_2^2}{a_2^2}. \tag{9.205}$$

As a result of (9.204), we rewrite Eq. (9.203) as

$$\iint\limits_{\omega} \tilde{p}(\mathbf{y}) \Delta_y \Theta(\mathbf{y})\, d\mathbf{y} = 0. \tag{9.206}$$

Applying the second Green's formula and taking into account Eqs. (9.201), (9.202) and (9.204), we reduce Eq. (9.206) to

$$\iint\limits_{\omega} \theta(\mathbf{y}) \sum_{n=1}^{2} \frac{h_n^2}{G_n'} \nabla_y \cdot (\tilde{H}_n(\mathbf{y}) \nabla_y \bar{p}(\mathbf{y}))\, d\mathbf{y} = 0. \tag{9.207}$$

After rewriting Eq. (9.207) in the form

$$\iint\limits_{\omega} \theta(\mathbf{y}) \sum_{k=1}^{2} \frac{\partial}{\partial y_k} \left(\frac{\partial \bar{p}}{\partial y_k}(\mathbf{y}) \sum_{n=1}^{2} \frac{h_n^2}{G_n'} \tilde{H}_n(\mathbf{y}) \right) d\mathbf{y} = 0$$

and integrating by parts with (9.205) taken into account, we find

$$-\iint\limits_{\omega}\sum_{k=1}^{2}\frac{2y_k}{a_k^2}\frac{\partial\bar{p}}{\partial y_k}(\mathbf{y})\sum_{n=1}^{2}\frac{h_n^2}{G_n'}\tilde{H}_n(\mathbf{y})\,d\mathbf{y}$$
$$+\int\limits_{\Gamma}\theta(\mathbf{y})\sum_{k=1}^{2}\cos(n,y_k)\frac{\partial\bar{p}}{\partial y_k}(\mathbf{y})\sum_{n=1}^{2}\frac{h_n^2}{G_n'}\tilde{H}_n(\mathbf{y})\,ds_y=0. \tag{9.208}$$

It is clear that the line integral in (9.208) vanishes due to the boundary condition (9.205). Hence, taking into account the exact expression (9.115) for $\bar{p}(\mathbf{y})$, we finally transform Eq. (9.208) into

$$\sum_{n=1}^{2}\frac{h_n^2}{G_n'}\iint\limits_{\omega}\tilde{H}_n(\mathbf{y})\rho(\mathbf{y})\,d\mathbf{y}=0, \tag{9.209}$$

where we have introduced the notation

$$\rho(\mathbf{y})=\left(\frac{sy_1^2}{a_1^2}+\frac{y_2^2}{sa_2^2}\right)\left(1-\frac{y_1^2}{a_1^2}-\frac{y_2^2}{a_2^2}\right). \tag{9.210}$$

Based on the derived Eq. (9.209), we suggest the following optimization criterion for determining the average thicknesses h_1 and h_2:

$$\min_{h_n}\iint\limits_{\omega_*}(H_n(\mathbf{y})-h_n)^2\rho_*(\mathbf{y})\,d\mathbf{y}. \tag{9.211}$$

Here, ω_* is a characteristic elliptic domain with semi-axes a_1^* and a_2^*. In particular, in the capacity of ω_* we can take the average elliptic contact area for a class of admissible contact loadings, while $\rho_*(\mathbf{y})$ is given by

$$\rho_*(\mathbf{y})=\left(\frac{s^*y_1^2}{a_1^{*2}}+\frac{y_2^2}{s^*a_2^{*2}}\right)\left(1-\frac{y_1^2}{a_1^{*2}}-\frac{y_2^2}{a_2^{*2}}\right), \tag{9.212}$$

where $s^*=a_2^*/a_1^*$ is the aspect ratio of ω_*.

It is clear that the necessary optimality condition for (9.211) has the form

$$\iint\limits_{\omega_*}(H_n(\mathbf{y})-h_n)\rho_*(\mathbf{y})\,d\mathbf{y}=0, \tag{9.213}$$

from which it follows that

$$h_n = \frac{1}{R_*} \iint\limits_{\omega_*} H_n(\mathbf{y}) \rho_*(\mathbf{y})\, d\mathbf{y}, \tag{9.214}$$

where

$$R_* = \iint\limits_{\omega_*} \rho_*(\mathbf{y})\, d\mathbf{y} = \frac{\pi}{12}\left(a_1^{*2} + a_2^{*2}\right).$$

It remains to show that Eq. (9.209) follows from (9.213) if ω_* coincides with ω. Indeed, as a consequence of (9.132), Eq. (9.213) is equivalent to the following:

$$\iint\limits_{\omega_*} \tilde{H}_n(\mathbf{y}) \rho_*(\mathbf{y})\, d\mathbf{y} = 0, \quad n = 1, 2. \tag{9.215}$$

By adding the two equations above, multiplied by h_n^2/G_n', $n = 1, 2$, respectively, we arrive at Eq. (9.209).

It is interesting to observe that Eq. (9.214) indicates that, in order to obtain the optimal average thickness h_n, the corresponding variable thickness $H_n(\mathbf{y})$ has been averaged with the weight function $\rho_*(\mathbf{y})$ given by (9.212).

To conclude, we note that in the case of compressible layers, the optimal value of the average thickness h_n coincides with the simple average of $H_n(\mathbf{y})$.

References

1. Akiyama, K., Sakai, T., Sugimoto, N., Yoshikawa, H., Sugamoto, K.: Three-dimensional distribution of articular cartilage thickness in the elderly talus and calcaneus analyzing the subchondral bone plate density. Osteoarthritis Cartilage **20**, 296–304 (2012)
2. Anderson, A.E., Ellis, B.J., Maas, S.A., Weiss, J.A.: Effects of idealized joint geometry on finite element predictions of cartilage contact stresses in the hip. J. Biomech. **43**, 1351–1357 (2010)
3. Argatov, I.I.: Pressure of a punch in the form of an elliptic paraboloid on a thin elastic layer. Acta Mech. **180**, 221–232 (2005)
4. Argatov, I.: Development of an asymptotic modeling methodology for tibio-femoral contact in multibody dynamic simulations of the human knee joint. Multibody Syst. Dyn. **28**, 3–20 (2012)
5. Argatov, I.: Contact problem for a thin elastic layer with variable thickness: Application to sensitivity analysis of articular contact mechanics. Appl. Math. Model. **37**, 8383–8393 (2013)
6. Argatov, I., Mishuris, G.: Elliptical contact of thin biphasic cartilage layers: Exact solution for monotonic loading. J. Biomech. **44**, 759–761 (2011)
7. Argatov, I., Mishuris, G.: Frictionless elliptical contact of thin viscoelastic layers bonded to rigid substrates. Appl. Math. Model. **35**, 3201–3212 (2011)
8. Argatov, I.I., Mishuris, G.S.: Contact problem for thin biphasic cartilage layers: perturbation solution. Quart. J. Mech. Appl. Math. **64**, 297–318 (2011)
9. Ateshian, G.A., Lai, W.M., Zhu, W.B., Mow, V.C.: An asymptotic solution for the contact of two biphasic cartilage layers. J. Biomech. **27**, 1347–1360 (1994)

10. Barber, J.R.: Contact problems for the thin elastic layer. Int. J. Mech. Sci. **32**, 129–132 (1990)
11. Barry, S.I., Holmes, M.: Asymptotic behaviour of thin poroelastic layers. IMA J. Appl. Math. **66**, 175–194 (2001)
12. Bei, Y., Fregly, B.J.: Multibody dynamic simulation of knee contact mechanics. Med. Eng. Phys. **26**, 777–789 (2004)
13. Chadwick, R.S.: Axisymmetric indentation of a thin incompressible elastic layer. SIAM J. Appl. Math. **62**, 1520–1530 (2002)
14. Gradshteyn, I.S., Ryzhik, I.M.: Table of Integrals, Series, and Products. Academic, New York (1980)
15. Hsiao, G.C., Steinbach, O., Wendland, W.L.: Domain decomposition methods via boundary integral equations. J. Comput. Appl. Math. **125**, 521–537 (2000)
16. Itskov, M., Aksel, N.: Elastic constants and their admissible values for incompressible and slightly compressible anisotropic materials. Acta Mech. **157**, 81–96 (2002)
17. Jaffar, M.J.: Asymptotic behaviour of thin elastic layers bonded and unbonded to a rigid foundation. Int. J. Mech. Sci. **31**, 229–235 (1989)
18. Nazarov, S.A.: Perturbations of solutions of the Signorini problem for a second-order scalar equation. Math. Notes **47**, 115–126 (1990)
19. Siu, D., Rudan, J., Wevers, H.W., Griffiths, P.: Femoral articular shape and geometry: A three-dimensional computerized analysis of the knee. J. Arthroplasty **11**, 166–173 (1996)
20. Van Dyke, M.D.: Perturbation Methods in Fluid Mechanics. Academic Press, New York (1964)
21. Vorovich, I.I., Penin, O.M.: Contact problem for an infinite strip of variable height [in Russian]. Solid Mech. **5**, 112–121 (1971)

Index

I. Argatov and G. Mishuris, *Contact Mechanics of Articular Cartilage Layers*,
Advanced Structured Materials 50, DOI 10.1007/978-3-319-20083-5